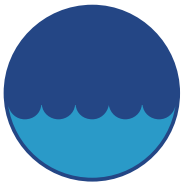

MIDDLE POMERANIAN SCIENTIFIC SOCIETY
OF THE ENVIRONMENT PROTECTION

Rocznik
Ochrona Środowiska
Volume 22. Year 2020

Part 1

ISSN 1506-218X

MIDDLE POMERANIAN SCIENTIFIC SOCIETY
OF THE ENVIRONMENT PROTECTION

Rocznik
Ochrona Środowiska
Volume 22. Year 2020

ISSN 1506-218X

Rocznik Ochrona Środowiska is covered by:
Polish Ministry of Science and Higher Education
Journal Rankings of Environmental Science
Master Journal List, Thomson Reuters

Publication of Middle Pomeranian Scientific Society
of The Environment Protection

Edition 130 copies, publishing sheets 68.3, format B-5
Printed by: INTRO-DRUK, Koszalin

Reviewers

Izabela Bartkowska, *Bialystok University of Technology*
Lilianna Bartoszek, *Rzeszow University of Technology*
Petr Besta, *VŠB - Technical University of Ostrava*
Miroslav Betuš, *Ministry of Interior of the Slovak Republic*
Stanisław Biedugnis, *The Main School of Fire Service*
Daniel Blaško, *Technical University of Kosice*
Andrzej Bogdał, *University of Agriculture in Krakow*
Tadeusz Borkowski, *Maritime University of Szczecin*
Klaudia Borowiak, *Poznań University of Life Sciences*
Tadeusz Borys, *University of Zielona Góra*
Anatolii Bovsunovsky, *National University of Food Technologies*
Tomasz Brzozowski, *Wroclaw University of Economics and Business*
Ewa Burszta-Adamiak, *Wrocław University of Environmental and Life Sciences*
Norbert Chamier-Gliszczyński, *Koszalin University of Technology*
Andrii A. Cheilytko, *Zaporizhzhia State Engineering Academy*
Aleksandr Chernykh, *Saint Petersburg State University of Architecture and Civil Engineering*
Dorota Chwieduk, *Warsaw University of Technology*
Aneta Czechowska-Kosacka, *Lublin University of Technology*
Krystian Czernek, *Opole University of Technology*
Jacek Dawidowicz, *Bialystok University of Technology*
Wojciech Dąbrowski, *Bialystok University of Technology*
Jacek Domski, *Koszalin University of Technology*
Stanisław Drozdowski, *Warsaw University of Life Sciences – SGGW*
Wojciech Drożdż, *University of Szczecin*
Mariusz Dudziak, *Silesian University of Technology*
Maxim A. Dulebenets, *Florida State University*
Vladimir Viktorovich Egorov, *Emperor Alexander I St. Petersburg State Transport University*
Gennadiy Farenyuk, *The State Research Institute Of Building Construction*
Christian Fritz, *HBLFA Raumberg-Gumpenstein*
Peter Gallo, *University of Prešov*
Maciej Gis, *Motor Transport Institute*
Piotr Gołos, *Forest Research Institute*
Valery Gorobets, *National University of Life and Environmental Sciences of Ukraine*
Kazimierz Górka, *Cracow University of Economics*
Wieslaw Grebski, *The Pennsylvania State University*
Bohuslava Gregorová, *Matej Bel University in Banska Bystrica*
Marek Gromiec, *University of Ecology and Management in Warsaw*
Antoni Grzywna, *University of Life Sciences in Lublin*
Edmund Hajduk, *University of Rzeszów*
Mateusz Hämmerling, *Poznań University of Life Sciences*

Table of Contents for Part 1

MIDDLE POMERANIAN SCIENTIFIC SOCIETY OF THE ENVIRONMENT PROTECTION

Rocznik Ochrona Środowiska

Volume 22. Year 2020 ISSN 1506-218X 11-23

Thermophysical-based Effect of Gas Hydrates Self-Preservation

Bohdan Kutnyi[1], Anatoliy Pavlenko[2], Hanna Koshlak[2]*

[1]Ivano-Frankivsk National Technical University of Oil and Gas, Ukraine

[2]Kielce University of Technology, Poland

[*]corresponding author's e-mail: apavlenko@tu.kielce.pl

1. Introduction

The industrial use of gas hydrates (GH) can play a large role in supplying humanity with energy. Gas hydrates are considered to be the best alternative fuel in many countries (Koh 2012). However, effective technologies for the gas hydrates production, storage and transportation are still under development (Kvenvolden 1994, Pavlenko et al. 2017). The production of methane from natural gas hydrates is closely related to studies of its dissociation under various conditions. At atmospheric pressure and positive ambient temperature, gas hydrates gradually dissosiate into gas and water. The study of the GH dissociation process enables to determine the optimal conditions for their transportation and storage, to minimize gas losses.

An important feature of gas hydrates is the possibility of a long stay in nonequilibrium conditions – the effect of self-preservation. It enables to simplify and reduce the cost of their storage and transportation significantly. However, under nonequilibrium conditions, hydrate dissociation, although it slows down, does not totally stop. Despite the fact that natural gas is a flammable and "greenhouse" gas, the problem of its release during transportation and storage is very important. That is why, the tasks associated with the gas hydrates dissociation are of great practical importance.

2. Review of the latest research sources and publications

Two ways of supplying heat for GH dissociation are possible: surface and bulk. In (Misyura 2016), methane hydrate dissociation at negative temperatures in porous medium was considered. The transportation hydrodynamics of a dissociating hydrate mixture with a liquid was studied in (Zerpa 2013). Several authors

investigated the behavior of natural gas hydrates under water (Sabodh K. Garg et al, 2008). The hydrate dissociation effect on the soil elastic properties is considered in (Jeffrey et al. 2011). In (Thomas et al. 2010), it was proposed to synthesize and store hydrate in sealed containers under pressure. Considering that the minimum pressure for the methane hydrate formation is 35-40 bar, such tanks have too much metal consumption. The basic design for the hydrates storage facilities in the form of a hemisphere has been studied in (Hailu & Thor 2010). The storage temperature regime depends on the thermal characteristics of its tent and base and determines hydrate shelf life and its dissociation intensity.

The study of heat and mass transfer during gas hydrates self-preservations is important not only on the practical side, but also from a theoretical perspective. dissociation of gas hydrates thermophysical parameters The problems of non-stationary thermal conductivity with moving boundary conditions are called Stefan problems. Ice melting, metal solidification, wood matuaring are just some examples of such tasks application. Analytical solutions of two-dimensional problems of nonlinear heat conduction are known only for separate, relatively simple cases (Pavlenko 2018, Pavlenko & Szkarowski 2018). The most universal way to solve them is the use of digital methods (Pavlenko 2020, Pavlenko et al. 2014), which can be easily implemented using computer technology. However, digital methods impose their limitations (Pavlenko 2019): the need to solve a system of a large number of linear algebraic equations is a small time step, which leads to cost increase of computer time for calculation (Dąbek et al. 2018). Using the method of grids dynamical adjustment (Dąbek et al. 2016) requires a complex algorithm to implement other problems.

Thus, an analysis of literature indicates an insufficient amount of information regarding the temperature regime of gas hydrate dissociation under nonequilibrium conditions and the absence of a mathematical model for its calculation.

3. The purpose and objectives of the study

The aim of this work is to study the thermophysical features of the gas hydrates dissociation under nonequilibrium conditions. For a quantitative assessment of the dissociating GH temperature regime, a number of experimental studies should be carried out. For this, a number of tasks have to be solved:

1. To develop an experimental setup for performing GH studies of the temperature regime of array dissociation.
2. To conduct a series of field experiments with propane hydrate of various concentrations to determine the temperature regime of dissociating GH under long-term storage.

3. To develop a mathematical model of thermal processes occurring during the gas hydrates dissociation.

4. Experimental studies of GH dissociation with surface heat input

The dissociation rate of gas hydrate depends on the heat flow brought to its surface. Therefore, the temperature on the gas hydrate surface is an important factor that needs to be clarified. To determine the temperature regime on the surface and in the deeper layers of a dissociating gas hydrate, experimental research methods are presented. In field experiments, propane gas hydrate is used. It has thermophysical characteristics similar to methane GH, however it does not require high pressures to get it.

To carry out experimental studies to determine the temperature on the dissociating gas hydrate surface, an experimental setup was constructed. Its scheme and general view are shown in Fig. 1. To simulate a large array of GH, it is necessary to avoid significant heat loss to the environment in all directions except one. Therefore, GH was inside the Dewar vessel, which was placed in 2 layers of thermal insulation (mineral wool 2 cm thick, and polystyrene foam 4 cm thick). For temperature measurement, ds18b20 electronic sensors with a measurement accuracy of ± 0.1°C and a control thermometer with a division value of 0.1°C were used.

Propane hydrate was loaded into the Dewar flask, electronic temperature sensors and a mercury thermometer were placed. To reduce the effect of external air circulation, the Dewar flask was covered with a polystyrene foam lid. Periodically, the position of the sensors relative to the hydrate was changed by rotation around a vertical axis.

As a result of the experimental studies analysis, it was found that due to the hydrate structure heterogeneity, its temperature in different parts of the surface can differ significantly. The results of the studies show that the temperature on the surface of the "dry" propane hydrate is in the range 0.3-3.0°C. Its average value is + 1.1°C. After partial dissociation, an ice crust forms on the hydrate surface and its melting temperature becomes equal to 0°C. To reduce the effect of hydrate heterogeneity in measuring average temperatures on the hydrate surface and in its depth, in the next series of experiments, sensors with a small surface area and high thermal conductivity, in particular thermocouples, were used. Unlike electronic sensors, thermocouples are not "afraid" of moisture and, after calibration, can measure temperature with an accuracy of ± 0.05°C. For measuring thermocouples EMF, a F136 microvoltammeter was used.

The aim of the second series of studies was to clarify the temperature distribution in the inner layers and on the surface of a large mass of propane hydrate. Thus, all temperature sensors (thermocouples) were located inside the GH

at different depths and only one was on its surface. For research, "dry" GH was used with a gas capacity of 40 ml of gas / ml of water. The scheme and appearance of the research facility are shown in Fig. 2.

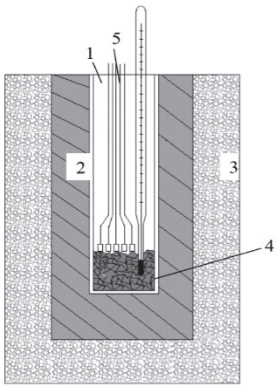

Fig. 1. Scheme of the research facility: 1 – Dewar vessel; 2 – layer of mineral wool; 3 – thermal insulation layer of expanded polystyrene; 4 – gas hydrate; 5 – electronic temperature sensors

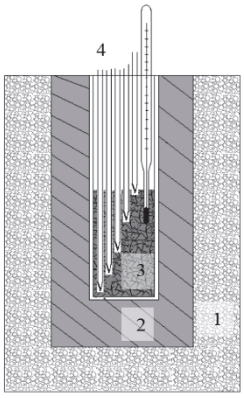

Fig. 2. Scheme of the pilot plant: 1 – a layer of expanded polystyrene; 2 – layer of mineral wool; 3 – gas hydrate inside the Dewar vessel; 4 – thermocouples

Research progress. Thermocouples were placed at different heights in the Dewar vessel, Fig. 2. After that, the propane hydrate was poured and rammed. The measured temperatures were recorded in a table. The results of temperature measurements are shown in Fig. 3. An analysis of the data obtained indicates that, at hydrate low gas capacity, the temperature curve always starts at 0°C (ice), and ends with the hydrate stable storage temperature, Fig. 3. The obtained results can be explained with the following physical explanation: on the hydrate surface there is ice that melts at a temperature of 0°C. Due to the elevated temperature, hydrate layers that come into contact with the surface dissociate faster. Gas is released through slots and cools hydrate inner layers. At a certain depth, the hydrate temperature stabilizes and the process of dissociation slows down.

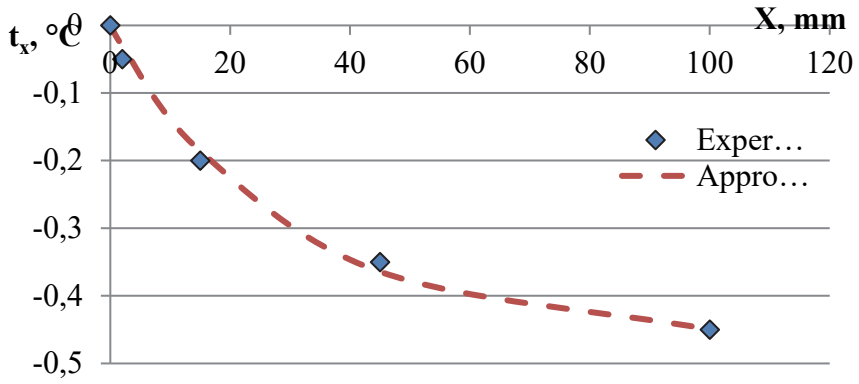

Fig. 3. Low-gas hydrate temperature regime

The obtained experimental data show that the temperature distribution in the surface layer of propane hydrate is well approximated by the dependence:

$$t_x = -0,47 + \left(0 - (-0,47)\right) \ell^{-35x}, \quad (1)$$

where: -0.47 – stable temperature of the deep layers, °C; 0 – temperature on the surface of the array, °C; 35 – approximation coefficient, m^{-1}; x is the distance from the array, m.

A number of experiments were conducted with hydrate, which has a high gas content (57 ml of gas / ml of water). The analysis of the obtained data indicates that the top layer of the "dry" not covered with ice crust, propane hydrate is in the range of positive temperatures 0.5-0.8°C. The deepest layer is in conditions close to thermodynamic stability at a temperature of – 0,9°C. There is a transition region approximately 50 mm thick, where a significant temperature gradient is observed, Fig. 4. The temperature distribution in the surface layer of propane hydrate is well approximated by the dependence:

$$t_x = -0,9 + \left(0,7 - (-0,9)\right) \ell^{-50x}, \quad (2)$$

where: -0,9 – stable temperature of the deep layers, °C; +0,7 – temperature on the array surface, °C; 50 – approximation coefficient, m^{-1}.

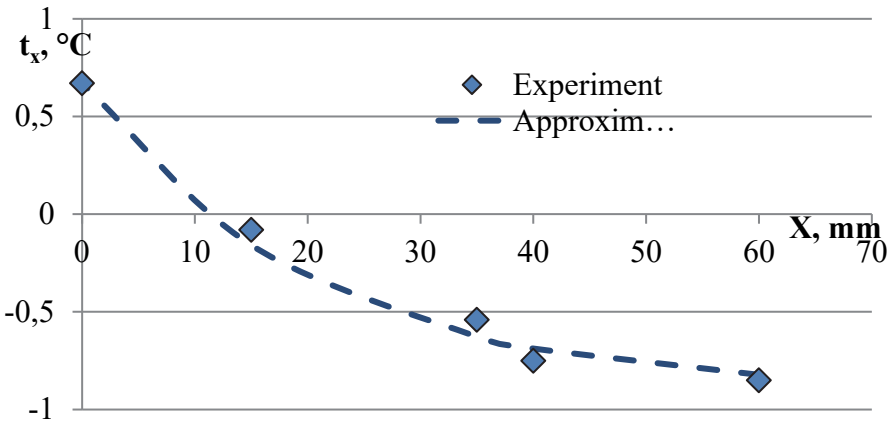

Fig. 4. Temperature distribution at the hydrate surface

Thus, the results of experimental studies show that the temperature distribution in the depth of the slowly dissociating GH is well approximated by the dependence:

$$t_x = t_\infty + (t_0 - t_\infty)\ell^{-kx}, \tag{3}$$

where: t_∞ – the temperature of the thermodynamically stable layer of the hydrate, °C; t_0 – temperature on the hydrate surface, °C; k – is the approximation coefficient, m^{-1}. The coefficient k reflects a change in the intensity of internal heat sources in the depth of GH.

5. The mathematical model of quasi-stationary gas hydrates dissociation

In a dissociating hydrate, the process of phase transition and heat removal with gas heating both occur simultaneously. Most of the heat flow, which is supplied to the inner layer by heat conduction, is absorbed by dissociatinging hydrate, and a smaller part is removed by heating the gas, which moves from the cold internal (deep) layers of the hydrate to the outside. The system of equations describing these processes is a mathematical model of the process of gas hydrates dissociation. For the most accurate reproduction of thermophysical processes in mathematical modeling, it should be focused on the experimental data as for the temperature distribution inside a dissociating gas hydrate.

It is supposed that there is a sufficiently GH large array so that the temperature field in it can be considered one-dimensional. Heat is supplied to the surface of this hydrate by heat exchange. To calculate the hydrate storage

conditions, the dissociation process can be considered long enough to establish a stationary temperature distribution in the hydrate mass.

The mathematical model of the hydrate dissociation thermal regime is based on the nonlinear Fourier heat equation with heat specific volume sources (or sinks). Considering the conditions for conducting experimental studies, it can be assumed that the temperature field varies along only one coordinate axis. The one-dimensional Fourier heat equation with volumetric heat sources (Lysak 2010) has the form:

$$\frac{\partial t_g}{\partial \tau} = \frac{\lambda_g}{c_g \rho_g} \frac{\partial^2 t_g}{\partial x^2} + \frac{q_{V(x)}}{c_g \rho_g}, \tag{4}$$

where: t_g – temperature, °C; λ_g – thermal conductivity of hydrate, W/(m·°C); c_g – its heat capacity, J/(kg·°C); ρ_g – hydrate density, kg/m^3; q_v – volumetric heat sources, W/m^3.

At the boundary of the hydrate mass, the boundary conditions of the third kind are valid:

$$-\lambda_g \frac{dt_{g(0)}}{dx} = \alpha_3 \left(t_3 - t_{g(0)} \right), \tag{5}$$

where: α_3 – GH surface heat transfer coefficient, W/(m^2·°C); t_3 – ambient air temperature, °C; $t_{g(0)}$ – GH surface temperature, °C.

Since the problem is stationary, the partial derivative of temperature with respect to time is zero, and the partial derivative of temperature with respect to spatial coordinate can be replaced by the full derivative. Thus, the capacity of volumetric heat sinks can be defined as a function of coordinate, W/m^3:

$$q_{V(x)} = -\lambda_g \frac{d^2 t_g}{dx^2}. \tag{6}$$

Substituting the second derivative of equation (3) into (6), it is obtained the distribution of the volume runoff of heat in hydrate, W/m^3.

$$q_{V(x)} = -\lambda_g k^2 \left(t_0 - t_\infty \right) \ell^{-kx}. \tag{7}$$

For experimental conditions: thermal conductivity of propane hydrate $\lambda_g = 0.5$ (W/(m°C)), surface temperature of hydrate $t_0 = 0.7$°C, stable temperature of deep layers of hydrate $t_\infty = -0.9$°C. Therefore, after substitution of the original data in equation (7), it is obtained the values of the volumetric heat sinks, W/m^3:

$$q_{V(x)} = -2000 \ell^{-50x}. \tag{8}$$

Equation (8) shows that heat sinks with a power of 2000 W/m^3 act on the surface of a dissociating propane hydrate. In the deep layers, their power decreases rapidly and at a depth of 50 mm it is only 164 W/m^3.

The temperature at the surface of the dissociating GH (t_0) plays a key role, since it determines how dissociation occurs. At $t_0 < 0$°C – hydrate recrystallization in ice occurs and the effect of self-preservation is observed, at $t_0 > 0$° C – the hydrate immediately dissociates into gas and water. The surface temperature of the dissociating GH is the result of the heat balance of the surface with the environment and can be found from the boundary conditions (5), where the first derivative from equation (3) with respect to x:

$$\frac{dt_0}{dx} = -k\left(t_0 - t_\infty\right)\ell^{-kx}. \tag{9}$$

Substitution of the obtained expression (9) into equation (5) enables to find the temperature on the hydrate surface:

$$t_0 = \frac{\lambda k t_\infty + \alpha_3 t_3}{\lambda k + \alpha_3}. \tag{10}$$

During the experiment, the ambient temperature was $t_3 = +11$°C. For a top-down heat flow in still air, the coefficient of heat exchange near the surface is $\alpha_3 = 4$ W/(m^2°C). Substituting the experimental data, the temperature value on the surface of the dissociating hydrate can be obtained, °C:

$$t_0 = \frac{0,5 \cdot 50 \cdot (-0,9) + 4 \cdot (+11)}{0,5 \cdot 50 + 4} = 0,74 \cdot$$

Since the temperature on the hydrate surface is above 0°C, the effect of self-preservation is not observed, and the hydrate dissosiates into gas and water.

6. Hydrate self-preservation

Another important parameter that determines the heat transfer processes in the gas hydrate array is the coefficient k. It reflects the intensity of change in internal heat sinks in the hydrate. It is checked at which k the effect of self-preservation on the open surface in the room by the formula (10). It is observed:

$$k = \frac{\alpha_3\left(t_3 - t_0\right)}{\lambda\left(t_0 - t_\infty\right)}. \tag{11}$$

Substitute the value for propane hydrate at t_0 = 0°C, room temperature +18°C, heat transfer coefficient near the vertical surface α_3 = 8.7 W/(m°C), it is obtained:

$$k = \frac{8,7\left(18-0\right)}{0,5\left(0-(-2,5)\right)} = 125 \cdot$$

Thus, theoretically, the effect of self-preservation for propane hydrate in "room conditions" can be expected at values of 125. However, the experimentally determined maximum value of *k* for does not exceed 50.

Similarly, the *k* value for methane hydrate can be calculated. The temperature on the ice surface is -2°C, and the equilibrium temperature inside the methane hydrate mass at atmospheric pressure is -33°C. Substituting these values for the methane hydrate of formula (11) gives m^{-1}

$$k = \frac{8,7\left(18-(-2)\right)}{0,5\left((-2)-(-33)\right)} = 11,2$$

Thus, for methane hydrate, self-preservation can be observed already at values k > 11.2. The intensity of internal heat sinks near the surface of GH, W/m^3

$$q_{V(0)} = -0,5 \cdot 11,2^2 \left(-2-(-33)\right) = 1944 \cdot$$

Similarly, this factor can be determined for other hydrating gases. The calculation results for the various gases are summarized in Table 1.

Table 1. Characteristics of hydrates under conditions of self-preservation

Gas - hydrating agent	t_0, °C	t_∞, °C	k, W	$q_{V(0)}$, W/m^3
Nitrogen	-1	-49	6,9	1142
Methan	-2	-33	11,2	1944
Carbon Dioxide	-2	-22	17,4	3027
Ethan	-1	-13	27,6	4570
Propan (for self-presevation)	0	-2,5	125	19531
Propan (by experiment)	0,7	-0,9	50	2000

Analyzing the results, it can be noted that in propane hydrate, the intensity of volumetric heat sinks is about ten times lower than it is required to obtain the self-preservation effect. Thus, at relatively high ambient temperatures, the self-preservation of propane hydrate is usually not observed.

From the formula (11) it is possible to obtain a dependence for determining the temperature of the outside air below which the effect of self-preservation can be obtained, °C:

$$t_{3c} = t_0 + \frac{k \cdot \lambda \left(t_0 - t_\infty \right)}{\alpha_3}. \tag{12}$$

For example, for propane GH, a self-preservation phenomenon can be expected if the ambient temperature drops below °C.

$$t_{3c} = \frac{50 \cdot 0,5 \left(0 - (-2,5) \right)}{8,7} = 7,1 \cdot$$

Thus, formula (12) is of great practical importance because it enables to calculate the conditions under which long-term storage of hydrates in a nonequilibrium state can be achieved.

In some scientific papers, the authors note the complexity, and even the inability to obtain the self-preservation effect for small pieces of hydrate. The physical explanation of this phenomenon has not been discovered by the authors. The results of our studies show that the transition temperature range is 50-100 mm deep in the GH array. Thus, the lack of self-preservation effect for small pieces of gas hydrate is explained by the inability to obtain the required temperature decrease in their depth.

A number of scientific papers by different authors (Tarko 2012) note the key role of the ice crust on the hydrate surface in obtaining the effect of self-preservation. To analyze the effect of the thermal resistance of the ice crust on the hydrate self-preservation, it is determine the effect that it can have on the heat exchange process on the GH surface. If the effect of self-preservation (as for methane) is observed, then the formed layer of ice on the surface can be considered as an additional resistance to heat transfer. The thickness of the ice crust on the surface of GH methane in the mode of self-preservation is approximately 0.3 mm. The calculation results show that such a thickness of the ice crust increases the thermal resistance by only 0.1% and is not able to significantly affect the thermal regime of GH. In such a case, the principle of ice crust application can only be to partially seal the GH and reduce the area of the heat exchange surface.

7. Conclusion

For the investigation of thermal modes of gas hydrate dissociation, an experimental setup has been developed, where a number of experimental studies with propane hydrate have been performed. Approximation dependences for determining the surface temperature and the depth of the dissociating gas hydrate

are obtained. Thus, it has been established that the temperature distribution in the depth of the hydrate is exponential. The results of the experimental studies show that hydrate dissociation occurs within a certain temperature range. Increasing the temperature leads to an intensification of this process.

The one-dimensional mathematical model of thermal processes occurring during the dissociation of a hydrate array is developed. It considers the functional dependence of heat sinks on the depth in the hydrate and enables to determine the temperature on the surface and in the depth of the gas hydrate array. The results of the studies show that the effect of the hydrate self-preservation is due to the decrease in the temperature of its deep layers due to partial dissociation. The freezing of supercooled water and the formation of an ice crust on the surface of the dissociating GH massif are only a consequence of this effect. The reason for the lack of self-preservation effect in small pieces of gas hydrate is established.

The practical significance of the research results is to determine the conditions under which the phenomenon of hydrate self-preservation is observed. The prospect of further scientific development in this direction is the study of the thermal insulation effect on the slowdown of GH dissociation, which is stored under nonequilibrium conditions.

The project is supported by the program of the Minister of Science and Higher Education under the name: "Regional Initiative of Excellence" in 2019-2022 project number 025 / RID / 2018/19 financing amount PLN 12,000,000.

References

Abay, H.K., Svartaas, T.M. (2010). Effect of Ultralow Concentration of Methanol on Methane Hydrate Formation, *Energy Fuels*, *24*(2), 752-757.

Brown, T.D., Taylor, Ch.E. & Bernardo, M.P. Rapid. (2010), Gas Hydrate Formation Processes: Will They Work? *Energies, 3*(6), 1154-1175.

Dąbek, L., Kapjor, A., Orman, Ł. (2016). *Ethyl alcohol boiling heat transfer on multilayer meshed surfaces*. Proc. of 20th Int. Scientific Conference on The Application of Experimental and Numerical Methods in Fluid Mechanics and Energy 2016, Terchova, Slovakia, AIP Conference Proceedings, 1745, 020005. DOI: 10.1063/ 1.4953699.

Dąbek, L., Kapjor, A., Orman, Ł. (2018). *Boiling heat transfer augmentation on surfaces covered with phosphor bronze meshes*. Proc. of 21st Int. Scientific Conference on The Application of Experimental and Numerical Methods in Fluid Mechanics and Energy 2018, Rajecke Teplice, Slovakia, MATEC Web of Conferences, 168, 07001. DOI: 10.1051/matecconf/201816807001

Garg, S.K., Pritchett, J.W., Katoh, A., Baba, K., Fuji, T. (2008). A mathematical model for the formation and dissociation of methane hydrates in the marine environment. *Journal of geophysical research. 113*, B01201. DOI: 10.1029/2006JB004768.

Koh, C.A., Sum, A.K., Sloan, E.D. (2012). State of the art: Natural gas hydrates as a natural resource. *J. Nat. Gas Sci. Eng*., *8*, 132-138.

Kvenvolden, K.A. (1994). Natural Gas Hydrate Occurrence and Issues. *Annals of the New York Academy of Sciences. 715*(1). Natural Gas H, 232-246.

Lysak, A. Reshenie uravneniya teploprovodnosti dlya nekotoryh zadach strojindustrii. [Solution of the heat equation for some problems of the construction industry.] Tomskij politekhnicheskij universitet. *Polzunovskij al'manah, 1*, 41-46. http://elib.altstu.ru/elib/books/Files/pa2011_1 /pdf/041lysak.pdf

Misyura, S.Y. (2016). The influence of porosity and structural parameters on different kinds of gas hydrate dissociation. *Scientific Reports, 11*. https://www.ncbi.nlm.nih.gov/pmc/articles/PMC4957226/.

Pavlenko, A. (2019). Change of emulsion structure during heating and boiling International *Journal of Energy for a Clean Environment, 20*(4), 291-302.

Pavlenko, A. (2020). Energy conversion in heat and mass transfer processes in boiling emulsions. *Thermal Science and Engineering Progress, 15*, 100439. DOI: https://doi.org/10.1016/j.tsep.2019.100439.

Pavlenko, A., Szkarowski, A. (2018). Thermal insulation materials with high-porous structure based on the soluble glass and technogenic mineral fillers. *Rocznik Ochrona Srodowiska, 20*, 725-740.

Pavlenko, A., Szkarowski, A., Janta-Lipińska, S. (2014). Research on burning of water black oil emulsions. *Rocznik Ochrona Srodowiska, 16*(1), 376-385.

Pavlenko, A.M., (2018). Dispersed Phase Breakup in Boiling of Emulsion. *Heat Transf. Res., 49*(7), 633-641. DOI: 10.1615/HeatTransRes. 2018020630.

Pavlenko, A., Kutnyi, B., Holik, Yu. (2017). Study of the effect of thermobaric conditions on the process of formation of propane hydrate. *Eastern-European Journal of Enterprise Technologies*. 5/5(89), 43-50.

Priest, J., Sultaniya, A. & Clayton, C. (2011). *Impact of hydrate formation and dissociation on the stiffness of a sand*. Proceedings of the 7th International Conference on Gas Hydrates (ICGH 2011), Edinburgh, Scotland, United Kingdom, July 17-21, http://www.pet.hw. ac.uk/icgh7/papers/icgh2011Final00742.pdf

Tarko, Ya.B. (2012). Perspektivi gazogIdratnoyi tehnologiyi na rinku morskih perevezen prirodnogo gazu / Ya.B. Tarko, L.O. Pedchenko, M.M. Pedchenko *Tehnika i tehnologiyi. Rozvidka ta rozrobka naftovih i gazovih rodovisch. 2*(43). http://irbis-nbuv.gov.ua/cgi-bin/opac/search.exe?C21COM=2&I21DBN=UJRN&P21DBN=UJRN&IMAGEFILE_DOWNLOAD=1&Image_file_name=PDF/rrngr%5F2012%5F2%5F8%2Epdf

Zerpa, L.E. (2013). A practical model to predict gas hydrate formation, dissociation and transportability in oil and gas flowlines. 193.

Abstract

To improve gas hydrates dissociation technology, studies of heat transfer processes on the interfacial surface are significant. In the work, experimental and theoretical studies of the gas hydrates dissociation are presented.

The scientific novelty is in establishing quantitative characteristics that describe the gas hydrates thermophysical parameters thermophysical characteristics influence on the heat transfer processes intensity on the interphase surface under conditions of gas

hydrates dissociation. Based on the results of experimental studies, approximation dependences for determining the temperature in the depths of a dissociating gas hydrate array have been obtained. Gas hydrates dissociation mathematical model is presented.

The practical significance of the research results is in determining quantitative indicators of the heat transfer processes intensity under the conditions of propane hydrate dissociation. The results of the work can be applied to designing equipment for gas hydrates storage and dissociation.

Keywords:
gas hydrates, self-preservation effect, experimental studies,
mathematical modeling, dissociation

Termofizyczny efekt samozachowawczy hydratów gazowych

Streszczenie

Badania procesów wymiany ciepła na powierzchni międzyfazowej mają ogromne znaczenie dla poprawy technologii dysocjacji hydratów gazowych. W pracy przedstawiono eksperymentalne i teoretyczne badania dysocjacji hydratów gazu.

Nowość polega na ustaleniu cech ilościowych, które opisują wpływ właściwości termofizycznych hydratów gazu na intensywność procesów wymiany ciepła na powierzchni międzyfazowej w warunkach dysocjacji hydratów gazu. Na podstawie wyników badań eksperymentalnych uzyskuje się zależności aproksymacyjne do określania temperatury na głębokościach dysocjującego układu hydratów gazu. Przedstawiono matematyczny model dysocjacji hydratów gazu.

Praktyczne znaczenie wyników badań polega na określeniu ilościowych wskaźników intensywności procesów wymiany ciepła w warunkach dysocjacji hydratu propanu. Wyniki można zastosować w projektowaniu urządzeń do magazynowania i dysocjacji hydratów gazu.

Słowa kluczowe:
hydraty gazu, efekt samozachowawczy, badania eksperymentalne,
modelowanie matematyczne, dysocjacja

MIDDLE POMERANIAN SCIENTIFIC SOCIETY OF THE ENVIRONMENT PROTECTION

Rocznik Ochrona Środowiska

Volume 22. Year 2020 ISSN 1506-218X 24-39

Safety Assessment of a Mineworking in Order to Use Its Cultural and Educational Potential and Ensure Environmental Sustainability

Oľga Végsöová, Martin Straka[*]*, Kamil Kyšeľa*

Technical University of Kosice, Slovakia

[*]*corresponding author's e-mail: martin.straka@tuke.sk*

1. Introduction

This paper presents a proposal for the revitalization of a mining operation and the surrounding environment, which may have a significant socio-economic impact on this micro-region of the Spiš region. The paper concerns the mining operation in Novoveská Huta, where its closure and a proposal for revitalization are being considered in the foreseeable future. Our proposal shows one of the possibilities of dealing with the mineworking in such a way that, in our opinion, contributes to the sustainable development of this micro-region, which has been associated with mining activities for decades so that it remains on today's mining map of Slovakia.

Alexandrowicz and Miskiewicz (2016) addressed the issue of revitalization of mining areas from the point of view of geoheritage, working with the idea of revitalization in the form of geoparks, designing them from the conceptual phase through implementation, with an emphasis on the Republic of Poland.

As reported by Novas et al. (2017), underground space can be remodelled for uses such as underground museums, car parks, an entertainment centre or new communities.

Szente et al. (2019) point out that information and spreading knowledge of environmental burdens in connection with mineworkings that are no longer in operation is of great importance to the local population.

Geological records are the result of processes lasting millions of years. They are considered valuable and require special care. Our main responsibility is to take care of this heritage so that it is not lost forever, according to Lopes et al. (2015), who also emphasized the need to pass on knowledge and geoheritage to

future generations. Also, Manyuk et al. (2020) focus on the protection of geological heritage. Similarly, Tlhapiso and Stephens (2020) share the view that geoheritage sites can be an excellent source of sustainable development. Gray and Gordon (2020) add to the view and argue that geodiversity as a concept has real value because it is the backbone of international and national geoheritage strategies and they present a document that explains e.g. the relationship between geology, geodiversity, geoheritage geoconservation.

Closed mines are becoming a suitable place for teaching.

Molokac et al. (2017) stated the reasons why education is a powerful tool not only for obtaining information and knowledge, but also for creating opinions and decision making. Education is capable of changing views and stereotypes associated with various industrial sectors. The aim of Alvarez (2020) was to highlight the educational activities that resulted from the UNESCO Villuercas global geopark, which provides resources to address the process of teaching cultural and natural values, including geology, while having a positive impact on environmental awareness and respect for the environment and cultural resources.

Meléndez et al. (2007) confirmed that museum mines, when properly selected and maintained, offer students good opportunities to teach geology. As Stefano and Paolo (2017) describe, abandoned mines often serve as valuable resources for education or as exhibits for museum purposes. At present, museums also offer digitized content, or virtual reality, which significantly increases the understanding of technology by visitors. Torres-Ruiz et al. (2020) address this area of visitor perception, which develops the technology of the Internet of Things and semantic analysis. More on this technology can be found in Glova et al. (2014), Tilabi et al. 2019, Grabara et al. (2020), which includes the creation of business models for various types of solutions, also applicable in the context of revitalization.

As expressed by Filocamo et al. 2020 Geotourism is a powerful and new form of sustainable tourism that has spread rapidly around the world in recent decades. Chrobak et al. (2020) define Geotourism as a type of qualified tourism promoting geosites related to geological backgrounds and relief elements.

Bento et al. (2020) present a study in which they attempted to understand the segmentation of tourism; reflect Geotourism in its historical context, relate the concepts of Geodiversity and Geotourism, understand and differentiate the approaches directed to the concepts of Ecotourism and Geotourism, evaluate issues related to geotourism products and types of geotourists.

Ruiz (2020) investigates the material and non-material remains of mining activities that have undergone a growing process of heritage enhancement that enables relevant cultural initiatives to be sustained, among them mining museums and mining parks. This paper examines mining heritage in the context of the

UNESCO Geoparks. The objective is to heighten the visibility of the mining heritage by taking advantage of the Geoparks "brand" when integrating mining tourism activities into geotourism.

Strba et al. (2016) and Klos, Trebuna (2017) pointed out that not only do geotourism and geoparks create a sustainable form of environmental protection, but the reopening of a mineworking also requires comprehensive safety for the entire operation and has a significant impact on the environment. Environmental awareness assessment for geotourism is also addressed by Mokhtari et al. (2019). Vukoicic et al. (2020) explain why abandoned mines can pose a major risk to the environment. At the beginning of the 21st century, significant steps were taken around the world to protect these historically valuable complexes, and mining heritage began to be seen as having potential for the development of alternative tourism. The main requirement for safely reconciling decommissioned mineworkings with the environment is, if necessary, their subsequent decontamination and reclamation (Kumar et al. 2013, Božek 2019).

Jeong et al. (2020) also considered the fact that if geologically and geomorphologically valuable resources are used for geotourism, then it can also be expected that there will be a positive impulse for the revitalization of the regional economy through diversification of attractive factors and job creation for local people. A perspective on the use of geological and geomorphological valuable resources in geotourism is also offered by Jeong et al. (2020), who emphasize that the revitalization of the regional economy through diversification is an attractive factor for job creation for local people. Shekhar et al. (2019) also argue that investing in the renewal of disused mining operations will help strengthen the local economy by developing infrastructure, health care and educational activities. Komoo (2010) also states that another advantage of a geopark so created lies in the creation of new job opportunities for local young people. Stemberk et al. (2018) present results that show that an increase in economic benefits in the field of geotourism results from the development of key areas.

Kravtcova (2014) states that in the process of implementing the main social functions, museums become centres for representing mining associations, forming professional culture, promoting patriotic education and increasing the prestige of the occupation of mining. Moradipour et al. (2020) emphasize the need to pay attention to the state of conservation of geomorphosites in order to preserve their scientific, educational and geotouristic values. Casale et al. (2008) state that examples of the use of unused mining space, such as mining museums, are essential for the revitalization of the mine.

Franco et al. (2020) point to the importance of projects related to the geomorphological and geological characteristics of land use for tourism. A sustainable development project was published by Meech et al. (2006), in which they

examine a specific project aimed at the transformation of an abandoned mineworking.

The aim of the presented paper is to provide information on the design for a comprehensive underground mining museum, the purpose of which is to increase the attractiveness of the entire region.

2. Theoretical base

The anhydrite and gypsum deposit in Novoveská Huta is located on the southeastern slopes of Tolstein. It is one of the most important mining deposits in Slovakia. The deposit stretches approximately 5 km, which ranks it among the largest deposits in Slovakia. The shape of the deposit is very varied. This mining deposit is located in the immediate vicinity of the protected area The National Park Slovak Paradise. The location of the Novoveská Huta deposit can be seen in Fig. 1.

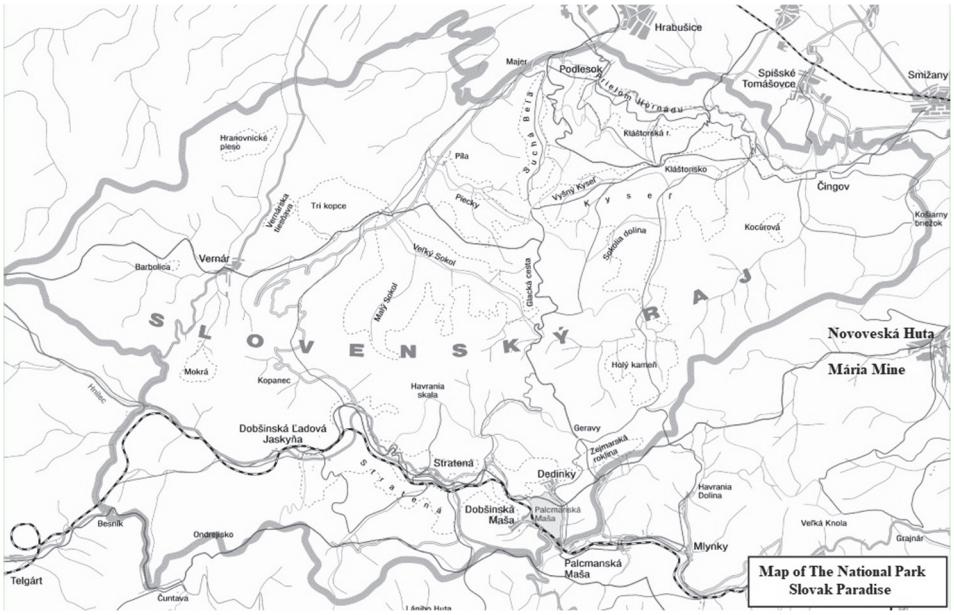

Fig. 1. Novoveská Huta deposit (Mária Mine)

Water infiltrates into the deposit along tectonic structures, causing serious complications of the body of the deposit. The thickness of the deposit ranges from 1 to 15 m. It reaches its maximum thickness at the surface. The current spatial limitations of the deposit give a fairly accurate picture of the original shape

and thickness of the sedimentation basin. More information on the chemical composition of the mined raw material is located in Table 1 and 2.

Table 1. Content of useful components in gypsum and anhydrite

Mineral	Sulfate content	SO_3 content
Gypsum	69.97%	30.03%
Anhydrite	65.04%	34.96%

Table 2. Chemical and physical-mechanical properties

Property	Gypsum	Anhydrite
Chemical composition	$CaSO_4 \cdot 2H_2O$	$CaSO_4$
Hardness	1.5-2.0	3.0-3.5
Bulk density	2.2-2.4 g/m^3	2.7-2.9 g cm^3
Density	2.3-2.4 g/cm^3	2.8-3.0 g/cm^3
Transparency	transparent to opaque	transparent to translucent
Lustre	glass, pearlescent	pearlescent, glassy
Cleavage	perfect	good
Solubility	soluble in acids; very slightly soluble in water	slightly soluble in acids and in water

Due to the fact that the deposit in Novoveská Huta has an important place among mining activities in Slovakia, it is necessary to make it accessible to the professional and general public. The current state of the deposit is that mining activity is still in progress. The condition of the mine meets the technical and safety regulations according to Slovak legislation. In the foreseeable future, the termination of mining activities here is being considered, and that poses the question of its subsequent use for the needs of society.

This represents a proposal for a way to revitalize a mineworking, which can have a positive effect on the socioeconomic impacts in the Spiš region. In the future, after the completion of mining, the Novoveská Huta mine would be environmentally sustainable and at the same time remain to serve the public as a mining exhibition and therefore keep its important place on the mining map of Slovakia.

3. Sustainability of the mining environment for the needs of the safety of the mining exhibition / Proposal of a mining exhibition, Novoveská Huta Case Study

The Novoveská Huta deposit includes the Mária mineworking, which has great potential for creating an extremely interesting mining exhibition. The mining exhibition at the Mária mine cannot be designed without examining the technical condition of the deposit, which is closely related to safety.

The Mária Mine consists of 4 levels. The underground exhibition proposed by us includes only part of the 0^{th} level (elevation 540 m above sea level) of the Mária mine. In the plan, all mining technology and equipment, lighting, rails, pumps and other mining materials are to be removed (or taken to the surface) from the first (elevation 520 m above sea level), the second (elevation 480 m above sea level) and the third (elevation (420 m above sea level) levels, and all three levels will be flooded. The main pumping station (level 2) will also be destroyed. Before opening the museum, it is necessary to perform safety work that would guarantee the construction of the open-air museum under our valid legislation.

Only part of the 0th horizon will remain available to the open-air museum. Drainage is solved by gravity. Excess, unnecessary water from the mine falls by gravity to the surface then comes out through the existing channel, into the nearest stream. An auxiliary CVE pump is placed on the surface (max. flow 4500 l / min). The auxiliary pump is only used in the event of an emergency in the mine.

We propose an artificial ventilation method, using the vacuum from a main APA 1120 fan. The ventilation system would therefore be diagonal. The ventilation network would consist of one ventilation area with one inlet and one vent for the mineworking.

The main inlet for the mineworking is the entrance adit, 950 metres long, which connects the 0th horizon with the surface. The up-cast shaft, which is located on the 0th horizon at a distance of 1700 metres from the entrance to the mine, will serve as the ventilation outlet for the mineworking. The main fan located in the ventilation chimney has an air output of 24.6 kW and the power of the electric motor of the fan is 30 kW. As mining will end in the mine, the air consumption will not be so high. Therefore, the new fan could have a power output of a few kW less than the current fan.

The mine is currently illuminated by rechargeable electric lamps along the entire length of the underground space. Initially, for economic reasons, the lights must be removed from the places that will not be accessible to the public. Subsequently, defective lights must be replaced with new, functional lights. The operation would be connected from a 22 kW overhead line, which is connected

to a surface transformer station. This transformer station would supply energy for the surface, but also for the underground. The lighting would be partly provided by the fact that the visitors and the guide are provided with their own lamps.

The total length of the underground exhibition is estimated at approximately 1700 metres, and therefore it is necessary from a safety point of view to determine where to place safety equipment.

We would suggest placing 5 fire extinguishers in the underground area, which will be marked with lights. Fire extinguishers will be placed every 500 metres, from the mine entrance to the ventilation chimney. The exception will be the 2 fire extinguishers, which will be located by the demonstration of wooden reinforcements and in the presentation hall. The reason for placing these fire extinguishers in this place is due to the risk of fire. These would be powder fire extinguishers.

In our technical-safety proposal we present 2 escape routes. One is designed with the intention of leading through the entrance adit and the other is located near the main ventilation chimney. Escape routes will also be lighted. First-aid kits can be found with every fire extinguisher, except for the one that is by the example of the wooden reinforcement. It is assumed that the guide will also carry a first aid kit. Before entering the mine, it is necessary for an authorized and responsible person to provide safety training.

From a safety point of view, it would be advisable to install sensors at the entrance to the mine. These sensors would sense the chips that would be placed on the mine lights that every visitor must have when entering the mine. In the lamp room, a lamp is given to a specific visitor, who is entered in the computer records. The sensors would automatically transfer this information from the chip to a computer, which would be able to use the given algorithm to immediately find out who entered and left the mine and when (duplicate system). Using these sensors and chips, the exact number of people underground would be determined.

This modern method would avoid any complications. Figure 2 is a graphical representation of the location of the sensors (sensor 1-4) at the entrance to the mine (4 units).

Subsequently, we would propose building a wooden platform with a railing from the entrance towards the mine. This wooden platform should serve as a place to board the mine train with a BND 30 type locomotive. This then transports visitors to the underground exhibition of the open-air museum. The dimensions of the platform would be 10 metres long and 1 metre wide, the railing would be 80 cm high.

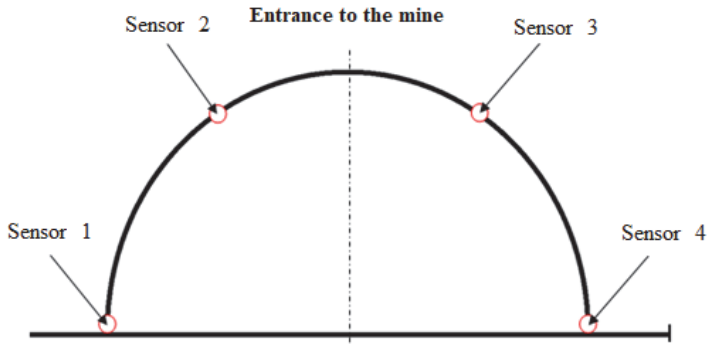

Fig. 2. Sensor placement diagram

The next step would be to renovate the rails. Locomotives and mining trucks intended for the transport of visitors would also have to be inspected.

Another important task would be to build a passing loop for locomotives. A locomotive with rolling stock could move with visitors in only one direction. Therefore, a passing loop would have to be built at a distance of about 800 metres from the entrance to the mine. This would be used to turn locomotives and rolling stock.

It is necessary to eliminate the mining areas where the mining pressures are so high that there could be a flood during the presence of visitors. These areas would either be flooded or made completely inaccessible (walled off). Conversely, mining areas where the pressures would not be so great would be reinforced with mesh and shotcrete (or wooden reinforcement) and would serve as underground areas for the guide's explanations and for storage of various pieces of mining equipment.

Fig. 3 shows the locations of the safety devices, the passing loop and the presentation room.

The Novoveská Huta mineworking, after the cessation of mining, would fulfil an environmental protection purpose. Several modifications and improvements need to be made in the area of the deposit. As can be seen in Fig. 3, a sample of wooden reinforcement will be located at a distance of 300 metres from the entrance to the mine. It would only be a 1 metre section so that people can imagine what it looks like and how wooden reinforcement is used.

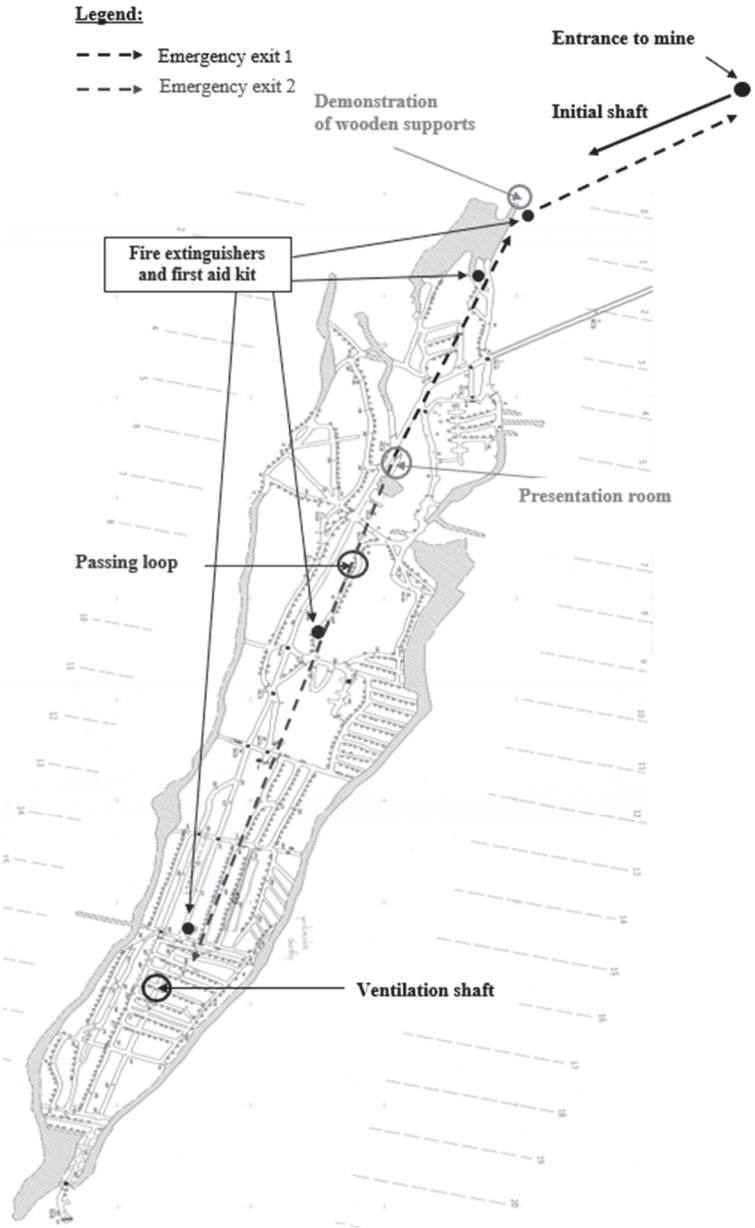

Fig. 3. Location of safety devices on the 0th level

An explosives warehouse is located 500 metres from the mine entrance. In the explosives warehouse, visitors could view dummies of rock and plastic explosives, various electric detonators (modern, old), old detonation equipment, etc. In the explosives warehouse, steel reinforcement would be built across the whole space. This is because the ceiling is in poor condition there. At present, this area is already excavated at a distance of 750 metres from the entrance to the mine. The dimensions are height: 4-5 metres, width: 8-9 metres and length: 20 metres. This room would function as a meeting room. A projector powered with electricity from the surface would be installed and wooden benches would be placed here. This space would be reinforced with mesh and shotcrete.

From a safety point of view, this would be very important. This space would be the only one in the mine where the floor would be modified. Gravel would be transported here, which would be compacted and levelled. There would always be the largest number of people there. This space would also include a mining telephone.

In the underground exhibition, 3 spaces would be set out together, in which there would be various items of mining equipment, tools, helmets, lamps, drilling rods, hammer drills, etc. The spaces would be created in a circular profile measuring 2x3 m and reinforced with circular steel reinforcement. In one of the rooms there would be a pulling machine – a Karlik's wheel with a loop of rope. A smaller part of a gallery would be dug out, to enable the visitors to see the method used. It would consist of a pair of vertical access shafts (entry and exit to the shaft) and discharge funnels. Visitors will have the opportunity to see the handling space for the mining method currently used on the deposit. They would use the first vertical access shaft to get to the handling area. At this point there would be a wooden bridge with a railing, as shown in Fig. 4, above the discharge system, along which visitors could safely access the other side of the handling area and then take the second vertical access shaft to return to the mining gallery.

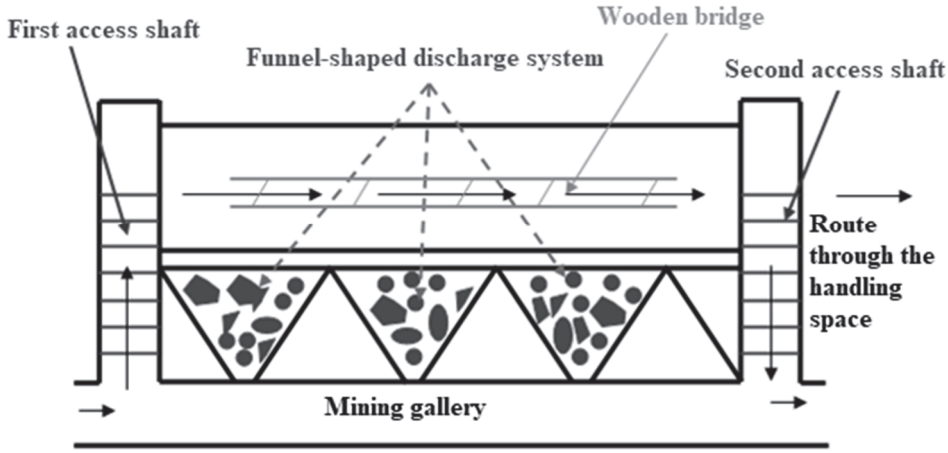

Fig. 4. Schematic drawing of the funnel-shaped discharge system and the route through the handling space

4. Conclusion

The construction of a museum would be very beneficial for the surrounding environment. Building it would increase awareness of mining as well as highlight the need for permanent care for the environment. The main vision of this proposal is not only the visit to the museum itself, but also the need for the visitor to realize that the place they have visited is a unique part of the environment and that making such an old mineworking accessible can have a great effect on environmental sustainability and safety. A visit to the museum forces the visitor to think about the seriousness of the environmental situation in mining operations. The creation of a mining museum in places that have been known for mining is the result of an ideal combination of environmental protection and the overall sustainability of the operation of the deposit even after mining has reduced.

All the safety, liquidation, renovation and other necessary work for the construction of the open-air museum represents a significant investment, which would ensure the maintenance of the mining tradition and history around the village of Novoveská Huta, and also of the Spiš region. The resulting investment could be covered by non-repayable grants from European Union funds. With the help of the investments made, the entire region of Eastern Slovakia would gain attractiveness and its economic potential would increase.

As it was already mentioned, this mining deposit is located in the immediate vicinity of the protected area The National Park Slovak Paradise. The daily attendance of the Slovak Paradise in the summer is in the number of approx. 4500 people a day. As the preliminary economic calculation of the sustainability of

a given geopark shows, it would be profitable and sustainable at least during the summer season. In addition, such a geopark could be one of the important attractions of the Slovak Paradise National Park, which would significantly increase the attractiveness of the area, which can also benefit from the vicinity of the High Tatras.

Another benefit of the proposed project is also the presentation and determination of the direction of development of the Spiš region, where after the end of mining operations the socio-economic level is likely to decrease, as happened in upper Nitra region in the mining area of the Nováky mine.

The mining museum is a unique project for this kind of local tourism within the whole region. It also brings a large number of economic benefits for the inhabitants of the Novoveská Huta mining area. The biggest economic positive can be considered to be the creation of new jobs, both direct and indirect. The opening of the mining museum would result in an increase in the number of domestic as well as foreign visitors, and with them, the needed economic revitalization of the entire region.

In our opinion, the proposed museum will significantly increase the positive awareness of mining, while still ensuring the continuous use of the deposit, taking into account its sustainability.

The layout of the individual parts of the underground exhibition during a visit to the mining museum are shown in Figure 5. The figure shows that the underground exhibition would start with entering the mine and subsequent boarding of transport trucks, mostly they would move about underground using mining transport. After entering the underground area, there would be samples of wooden and steel reinforcement. Subsequently, visitors will be able to view the explosives store. Then they will walk to the presentation room. At this point, the guide will show them a short film about the deposit and then they will move to the mining area. After viewing the mining (handling area), visitors will move on foot to another area with mining equipment. Next, they move to a third room, where there is a demonstration of a towing machine – a Karlik's wheel with a rope loop. The excursion would end at the place where the ventilation shaft is located. Subsequently, visitors would return to the passing loop, where they would board a locomotive and it would take them back to the wooden platform. The total duration of the tour would be 60 minutes, in which they would walk 1700 metres with the participation of a qualified guide giving expert explanations.

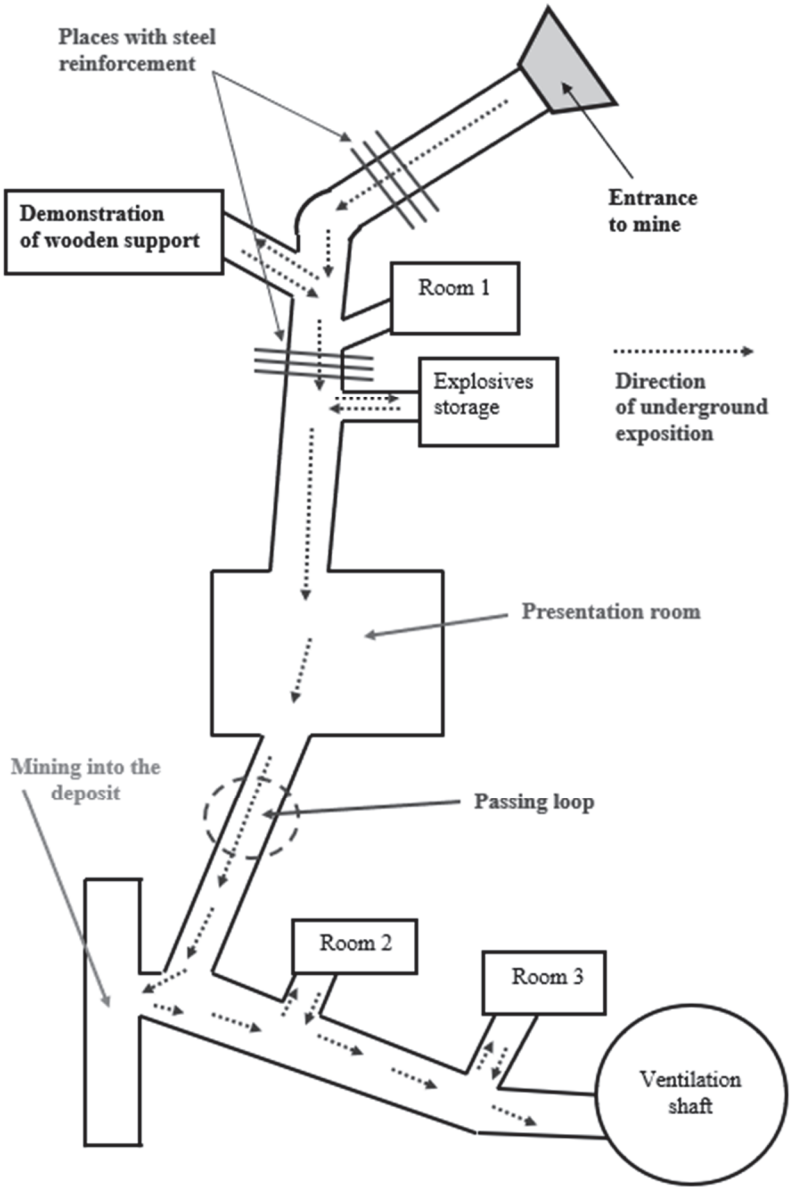

Fig. 5. Diagram of the underground exhibition

The submitted paper is a part of the projects "Projects of applied research as a means for development of new models of education in the study program of industrial logistics" KEGA 016TUKE-4/2020 and the project "Research and development of new smart solutions based on the principles of Industry 4.0, logistics, 3D modelling and simulation for streamlining production in the mining and building industry" VEGA 1/0317/19.

References

Alexandrowicz, Z., Miskiewicz, K. (2016). Geopark – from the concept to implementation, with special reference to Poland. *Chronmy Przyrode Ojczysta,* 72(4), *Instytut Ochrony Przyrody PAN,* 243-253.

Alvarez, R.F. (2020). Geoparks and Education: UNESCO Global Geopark Villuercas-Ibores-Jara as a Case Study in Spain. *Geosciences*, 10 (1), Article number 27.

Bento, L.C.M., de Farias, M.F., do Nascimento, M.A.L. (2020). Geotourism: A Tourism Segment? *Turismo-Estudos e Praticas (UERN)*, 9(1), 1-23.

Božek, P. (2019). Virtual production technology vs. environment. *Acta Tecnología, 5(4),* 109-114.

Casale, M., Oggeri, C., Peila, D. (2008). Imporovemnts of safety conditions of unstable rock slopes through the use of explosives. *Natural Hazards and Earth System Sciences, 8*, 473-481.

Filocamo, F., Di Paola, G., Mastrobuono, L., Rosskopf, C.M. (2020). MoGeo, a Mobile Application to Promote Geotourism in Molise Region (Southern Italy). *Resources-Basel, 9*(3), Article number 31.

Franco, L.J.N., Rojas, B.H.S., Cruz, C.S.S. (2020). Geotourism: Tourist Use of the Geological Potential in the San Benito and San Eugenio Streets in the Municipality of Sibate. *Anuario Turismo Y Sociedad, 27*, 187-215.

Glova, J., Sabol, T., Vajda, V. (2014). *Business models for the internet of things environment*. In: Procedia Economics and Finance: Emerging Markets Queries in Finance and Business: 24-27 October 2013, Tîrgu Mureş, Romania, 15, 1122-1129.

Grabara, J., Dabylova, M., Alibekova, G. (2020). Impact of legal standards on logistics management in the context of sustainable development. *Acta logistica, 7*(1), 31-37.

Gray, M., Gordon, J.E. (2020). Geodiversity and the '8Gs': a response to Brocx & Semeniuk (2019). *Australian Journal of Earth Sciences, 67*(3), 437-444.

Chrobak, A., Witkowski, K., Szmanda, J. (2020). Assessment of the Educational Values of Geomorphosites Based on the Expert Method, Case Study: the Bialka and Skawa Rivers, the Polish Carpathians. *Quaestiones Geographicae, 39*(1), 45-57.

Jeong, S.H., Gwon, O., Kim, T., Naik, S.P., Lee, J., Son, H., Kim, Y.S. (2020). Value of Geologic.Geomorphic Resources of Danyang-gun and Its Application from Geotourism Perspective. *Economic and Environmental Geology, 53*(1), 45-69.

Klos, S., Trebuna, P. (2017). The impact of the availability of resources, the allocation of buffers and number of workers on the effectiveness of an assembly manufacturing system. *Management and Production Engineering Review, 8*(3), 40-49.

Komoo, I. (2010). Geopark sebagai Peraga Pembangunan Lestari Wilayah (Geopark as a Model for Regional Sustainable Development). *Akademika, 80*(1), 9-18.

Kumar, S., Bansal, V.K. (2013). Construction Safety Knowledge for Practitioners in the Construction Industry. *Journal of Frontiers in Construction Engineering, 2*(2), 34-42.

Lopes, L., Martins, R. (2015). *Global Heritage Stone: Estremoz Marbles, Portugal*. In: Global Heritage stone: Towards International Recognition of Building and Ornamental Stones, Geological Society, London, Special Publications, 407(1), 57-74.

Manyuk, V.V., Bondar, O.V., Yaholnyk, O.V. (2020). Ukraine in the history of the movement for the conservation of geological heritage in Europe. *Journal of Geology Geography and Geoecology*, *29*(1), 111-134.

Meech, J.A., Mcphie, M., Clausen, K., Simpson, Y., Lang, B., Campbell, E., Johnstone, S., Condon, P. (2006). Transformation of a derelict mine site into a sustainable community: the Britannia project. *Journal of Cleaner Production*, *14*(3-4), 349-365.

Meléndez, G., Fermeli, G., Koutsouveli, A. (2007). *Analyzing Geology Textbooks for Secondary School Curricula in Greece and Spain: Educational use of Geological Heritage*. Conference: 11th International Conference of the Geological Society of Greece, Geoenvironment: Past-Present-Future At: Athens, Greece, 40(4), 1-14.

Mokhtari, D., Roostaei, S., Khodadadi, M., Ahmadi, M., Ebrahimi, O., Shahabi, H. (2019). Evaluation of the Role of Environmental Education in Manesht and Ghelarang Geotourism Destination, Iran. *Journal of Quality Assurance in Hospitality & Tourism, 20*(6), 681-708.

Molokac, M., Alexandrova, G., Kobylanska, M., Hlavnova, B., Hroncek, P., Tometzova, D. (2017). *Virtual Mine – educational model for Wider Society*. 15TH IEEE International Conference on Emerging Elearning Technologies and Applications (ICETA 2017), IEEE, 307-311.

Novas, N., Gazquez, J.A., MacLennan, J., García, R.M., Fernandez-Ros, M., Manzano-Agugliaro, F. (2017). A real-time underground environment monitoring system for sustainable tourism of caves. *Journal of Cleaner Production, 142*, 2707-2721.

Ruiz, M.D.C. (2020). Visibility and promotion of mining heritage in some Spanish geoparks. *Documents D Analisi Geografica*, *66*(1), 109-131.

Shekhar, S., Kumar, P., Chauhan, G., Thakkar, M.G. (2019). Conservation and Sustainable Development of Geoheritage, Geopark, and Geotourism: a Case Study of Cenozoic Successions of Western Kutch, India. *Geoheritage*, *11*(4),1475-1488.

Stefano, M., Paolo, S. (2017). Abandoned Quarries and Geotourism: An Opportunity for the Salento Quarry District (Apulia, Southern Italy). *Geoheritage*, *9*(4), 463-477.

Stemberk, J., Dolejs, J., Maresova, P., Kuca, K. (2018). Factors affecting the number of visitors in National Parks in the Czech Republic, Germany and Austria. *ISPRS International Journal of Geo-Information*, *7*(3), 1-10.

Strba, L., Krsak, B., Molokac, M., Adamkovic, J. (2016). *Geotourism and geoparks-a sustainable form of environmental protection*. Production management and Engineering Sciences, International Conference on Engineering Science and Production Management (ESPM), April, 279-284.

Szente, I., Takacs, B., Harman-Toth, E., Weiszburg, T.G. (2019). Managing and Surveying the Geological Garden at Tata (Northern Transdanubia, Hungary). *Geoheritage*, *11*(4), 1353-1365.

Tilabi, S., Tasmin, R., Takala, J., Palaniappan, R., Abd Hamid, N. A., Ngadiman, Y. (2019). Technology development process and managing uncertainties with sustainable competitive advantage approach. *Acta logistica, 6*(4), 131-140.

Tlhapiso, M., Stephens, M. (2020). Application of the Karst Disturbance Index (KDI) to Kobokwe Cave and Gorge, SE Botswana: Implications for the Management of a Nationally Important Geoheritage Site. *Geoheritage*, *12*(2), Article number 39, 1-13.

Torres-Ruiz, M., Mata, F., Zagal, R., Guzman, G., Quintero, R., Moreno-Ibarra, M. (2020). A recommender system to generate museum itineraries applying augmented reality and social-sensor mining techniques. *Virtual Reality*, *24*(1), 175-189.

Vukoicic, D., Ivanovic, R., Radovanovic, D., Dragojlovic, J., Martic-Bursac, N., Ivanovic, M., Ristic, D. (2020). Assessment of Geotourism Values and Ecological Status of Mines in Kopaonik Mountain (Serbia). *Minerals, 10*(3), Article number 269, 1-24.

Abstract

This paper addresses the protection of the environment and provides a design for the use of the deposit after the cessation of mining in the Novoveská Huta region. The area of interest of this case study describes the practical transformation of a functioning mining operation into a mining museum in order to reduce the pressures on the environment after mining. The resulting model of the functioning of the mining museum also deals in detail with the safety of a mining operation which is no longer used for mining, taking into account its further use. The article describes the proposed 1700-metre route which visitors will pass along, and also gives a detailed description of the proposed measures necessary for safety and long-term sustainable operation.

The aim was to design a use of the mining space, that would offer visitors the opportunity to see the handling space and mining methods of the deposit. An interesting element will also be the possibility of inspecting the explosives store, wall linings, steel and wooden reinforcements. The tour will also include a demonstration of storage facilities as well as a Karlik's wheel mining equipment with a rope loop. The open-air museum also offers the opportunity to get acquainted with transport around the entire deposit under strict safety conditions. It is assumed that devices such as a mining telephone or a siren placed on the walls of the tunnel will also arouse interest. An important element of the entire tour would also be a constant reminder of the safety rules during the tour.

The impacts of this solution on the environment are very acceptable and incomparably more beneficial than in the case of the termination of mining and subsequent non-use of the Novoveská Huta deposit.

Keywords:
mining, safety, environment, cultural heritage, safety

MIDDLE POMERANIAN SCIENTIFIC SOCIETY OF THE ENVIRONMENT PROTECTION

Rocznik Ochrona Środowiska

Volume 22. Year 2020 ISSN 1506-218X 40-50

Research of Aggregatic Stability and Bactericidal Activities of Nanosilver Colloidal Solutions

Anna Yushchishina[1], Maria Pasichnyk[1], Olena Mitryasova[2], Piotr Koszelnik[3], Renata Gruca-Rokosz[3], Małgorzata Kida[3]*

[1]Mykolaiv V.O., Sukhomlynskyi National University, Mykolaiv, Ukraine
[2]Petro Mohyla Black Sea National University, Mykolaiv, Ukraine
[3]Rzeszow University of Technology, Rzeszow, Poland
[*]corresponding author's e-mail: eco-terra@ukr.net

1. Introduction

The bactericidal properties of silver and its compounds are known for a long time. Argentum nitrate is indicated in the Pharmacopoeia of Pliny, issued back in 69 BC. Nevertheless, the active use of silver in medicine began only in the XIX century. Significant contribution in this regard was made by the American surgeon J.M. Sims, who in 1852 used silver threads as suture material during operations on vesicouvaginal fistulae. In addition, he also used catheters covered with silver for urine removal (Alexander 2009). At the same time, 1% solution of nitrate argentum in the treatment of neonatal ophthalmic infections was used in clinical practice. The efficiency of 0.25% and 0.1% solutions of argentum nitrate against typhoid sticks and anthrax was proved. However, with the discovery of antibiotics in the 40's. XX century the interest in the development of silver preparations has declined significantly.

Over time, with an increase in the number of antibiotics, most bacteria developed resistance to them, and researchers begin to look for other substances that have bactericidal properties. In many cases, previously forgotten, the important role belongs to silver preparations in the form of soluble and water-soluble salts (for example, argentum iodide), metallic silver in the form of nanoparticles with sizes ranging from several to hundreds of nanometers (Bernavsky 2006).

Thus, known works (Savchenko 2012, Litvinova 2016), where argentum nitrate was used as an antibacterial substance. The disadvantage of using silver salts as a bactericidal agent is their short-term effect, the instability of the solution, which manifests itself in the formation of a black color for the action of light,

as well as the restoration of nitrate to nitrite, which leads to oxidative stress of cells.

Compared with silver compounds, the mechanism of bactericidal action of silver nanoparticles remains unexplored until the end. Some researchers have discovered a greater toxic effect of silver nanoparticles related to gram-positive and gram-negative bacteria compared to its classical chemical compounds (Lok et al. 2007). The antibacterial activity of silver nanoparticles is mainly studied *in vitro* experiments. Their bactericidal action against ampicillin-resistant are established *Staphylococcus aureus* (MRSA) and *Escherichia inch* (Shahverdi 2007).

Antibacterial activity of silver nanoparticles depends on their size, shape, area, chemical composition and charge of the surface. Another factor in the toxicity of silver nanoparticles is the presence of ligands in aqueous solution, in particular, Cl^-, PO_4^{3-}, S^{2-}, SO_4^{2-}, which can interact with Ag^+ ion or with nanoparticles, causing aggregation (Choi et al. 2009). In addition, the presence of molecular oxygen contributes to the allocation of Ag^+ ions from the surface of the nanoparticle and increases their toxicity (Liu et al. 2011).

It is established (Xiu et al. 2011) that AgNPs (Ag nanoparticles) are covered with amorphous carbon in the size of 35.4±5.1 nm were in 20 times less toxic than Escherichia coli, than Ag^+ ions (EC 50: 2.04±0.07 vs. 0.10±0.01 μg/ml). However, their toxicity increased 2.3 times for the influence of air (EC 50: 0.87±0.03 mg/ml), which contributed to the allocation of Ag^+ ions from the surface of nanoparticles.

In the works (Baker et al. 2005, Kim et al. 2007) antimicrobial effect of silver nanoparticles at concentration of 0.35 ng/ml for *Escherichia coli* 3.5 ng/ml for *Staphylococcus aureus.* Also synergistic antimicrobial activity of silver nanoparticles with ampicillin, penicillin G, amoxicillin, kanamitsin, erythromycin, clindamycin, tetracycline, chloramphenicol and vancomycin have been established. In addition, the functional silver nanoparticles conjugated with ampicillin enhanced the bactericidal effect of cell wall lysis and interaction with DNA, resulting in the rapid death of bacteria.

Silver nanoparticles can directly interact with the proteins and phospholipids of the cell membrane, violating its integrity and permeability (Li et al. 2010). Unlike Ag^+ ions, silver nanoparticles, thanks to a larger surface area, provide better contact with bacteria. After attaching nanoparticles to the cell membrane, they pass inside the cells of the bacteria. Like the ions of the argentum, nanoparticles can interact with sulfur-containing proteins and phosphorus-containing components, in particular DNA, RNA, inhibiting their functions. In addition, silver nanoparticles violate the respiratory chain of mitochondria of bacteria, which inevitably leads to cell's death (Holt & Bard 2005).

Researchers have found that silver ions can produce free radicals, inducing oxidative stress (Danilczuk et al. 2006). However, there was no significant difference in the toxicity of silver nanoparticles between anaerobic and aerobic conditions, which undermines oxidative stress and the formation of active forms of oxygen (AFO) as an important antibacterial mechanism of Ag^{+}.

In (Lok et al. 2007), the resistance of strains of bacteria of the genus *Salmonella* to silver nanoparticles was discovered. It was established that the mechanisms of resistance are not related with chemical detoxification, but are the result of the membrane protein, which is ATP-azo and chemiososmotic cation: proton an anti-porter. This system, using the energy of ATP, removes silver ions from the cell.

It was also found in resistant to the action of silver *E coli* strains over expression of the Cus C, Cus F, Cus B and Cus A genes encoding the chemosmotic system involved in the transport of copper and silver ions from the cell (Lok et al. 2008).

It has been established that silver ions penetrate the ion channels into *E. coli* cells without damaging the membranes. Analysis revealed a reduction in the expression of genes coding forribosomal subunit S2, succinyl-CoA-synthetase, and maltose conveyor. An expression reduced of the ribosomal S2 gene. The subunits are critical to bacteria, as they lead to the suppression of other proteins, in particular those involved in the synthesis of ATP (Yamanaka et al. 2005). As a result, various metabolic pathways are violated and replication is inhibited.

Silver has antimicrobial properties against a wide range of microorganisms, not only bacteria, but also some fungi, as well as viruses. However, several mechanisms for the formation of resistance to silver in bacteria have been identified (Priskoka 2016).

1. *Salmonella* resistance *thyphimurium* can be formed due to plasmid pMG101, which is also responsible for the resistance to mercuric chloride, ampicillin, chloramphenicol, tetracycline, streptomycin and sulfanilamides. Plasmid pUPI199 in some strains *Acinetobacter baumannii* contains genes that are relevant for the resistance to argentum nitrogen.
2. Resistance to silver in the E. coli (*Escherichia coli*) are associated with the mechanisms of porous transport caused by porine proteins, which provide specific passive transport of sugars, ions and amino acids through the outer membrane, as well as mutations of the genes of proteinpores.
3. Resistance can be generated by applying silver in small concentrations, such as ½ MIC (half the maximum inhibitory concentration) or whole MIC, but not at the level of bactericidal concentrations.

Methods for obtaining such solutions are basically oxidation-reduction reactions in which cations Ag^+ recovered to metallic silver. In this case, the main problem of these methods, regardless of the reducing agent, is the aggregate stability of the solutions which were obtained.

Stabilizers are added in the lyophobic system to create a potential barrier of repulsion of colloidal particles and to provide the same aggregative stability. As stabilizers, inorganic and organic substances and also synthetic and natural polymers can be used (Shirokobokov 2009).

However, it is known that the stabilization of nanoparticles is more effective when using surfactants. They may contain various functional groups such as -SH, -CN, -COOH, $-NH_2$. One of the most commonly used stabilizers is cetyltrimethylammonium bromide (CTAB) and sodium dodecyl sulfate (SDS). In addition, surface-active substances may have their own bactericidal activity. Therefore, the purpose of this work was to investigate the effect of surfactants of different chemical nature on the aggregate stability of colloidal solutions of nanosilver and to determine the bactericidal activity of such multicomponent systems.

Purpose is study of the influence of various chemical nature SAS on the aggregate stability of nanosilver colloidal solutions and the determination of bactericidal activity of such multi-component systems.

2. Experiment methodology

Synthesis of colloidal solutions of silver nanoparticles was carried out by Ostwald's reaction, restoring 0,001 n. argentum nitrate solution (p.f.a.) 1% solution of tannin (chem.p.). The process was implemented in a practically neutral medium (pH from 5.7 to 6.8), which was provided by the addition of 1% sodium carbonate solution, by the reaction (1):

$$6AgNO_3 + C_{76}H_{52}O_{46} + 3Na_2CO_3 \rightarrow 6Ag + C_{76}H_{52}O_{49} + 3CO_2 + 6NaNO_3 \qquad (1)$$

To the obtained solutions of nanosilver surface-active substances of different chemical nature: cationic surfactant – alkamone (GOST 10106-75); anionic surfactants – sodium dodecyl sulfate (GOST 8748-2006) and sulfanol (TU 6-01-1001) and nonionic surfactants − OS-20 (GOST 10730-82) were added. The final concentration of surfactant in solutions was 0.1%.

The aggregate stability of the resulting colloidal solutions was determined by the spectral method (spectrophotometer SF-56, RF), measuring the spectra of the surface Plasmon resonance of silver nanoparticles immediately after their receipt and after 24 hours.

The bactericidal properties of solutions of silver nanoparticles were investigated using reference strains of the *Enterobacteriacea* family *Escherichia coli.* For the study of E.coli initial solution (10^8 units), a control sample was prepared by sequential dilution with a physiological solution: $1.5 \cdot 10^1$ units (maximum number of colonies-15). An experimental series of solutions was prepared for sowing according to Table 1. In this case, to each test tube, in addition to the control sample, added 0,1 ml of the studied solution. The test had 18-20-hour cultures of fresh test strains that did not pass more than three passages on nutrient media. Daily culture of test strains was washed off with a physiological solution and subjected to an optical turbidity standard corresponding to 1 billion cells in 1 ml.

With Densi La Meter determined the McFarlant's turbidity standard (unit) to the suspension concentration (Table 1).

Table 1. Turbidity standard

McFarland's Turbidity Standard (op.)	0.5	1	2	3	4
Number of International Turbidity Units (MO)	1.7	3.3	6.7	10	3.3
The appropriate concentration of the suspension x10^8 CFU/ml	1.5	3	6	9	12

Turbidity of the *E.coli* bacteria suspension was 0,5 (McFarland unit), corresponding to a concentration of $1.5 \cdot 10^8$ CFU/ml.

From the original standard suspension, ten times dilution was prepared by transfer of 0.5 ml of culture in 8 test tubes from 4.5 ml of physiological solution, mixing thoroughly, changing the pipette after each transfer. We received a series of serial dilutions from 10^8 to 10^0 *E. coli* cells at 1 ml. To each test tube with dilute suspension, 0.1 ml one of the studied solutions was added, namely:

Control sample (dilution $1.5 \cdot 10^1$),
Solution of argentum nitrate (0.001 n),
Solution of silver nanoparticles (NS),
0.1% alkamone solution for surfactant,
0.1% solution of surfactant: Sodium dodecyl sulfate,
0.1% solution of surfactant sulfanol,
0.1% solution of surfactant OS-20,
NS + alkamone solution,
Solution NS + Sodium dodecyl sulfate,
Solution of NS + sulfanol,
Solution NS + OS-20.

Control samples of dilutions were used for the study of bactericidal properties: $1.5 \cdot 10^1$ (maximum number of colonies − 15) and 10^o (no growth of bacteria).

Suspensions of microorganisms have been left at room temperature (22-23°C); in 24 and 48 hours. The hanging was carried out according to the standard method (Lok et. al. 2007) by the horizontal method. By 0.1 ml. from the investigated mixtures were placed *in the* center of the meat – pepper broth in Petri dishes, distributed by a spatula on the entire surface, after application, the material was placed in a thermostat at 36°C for 24 hours.

The total microbial number was determined by direct counting the number of bacteria. Colonies that grew both on the surface and in the depth of the agar were counted with a magnifying glass with an increase of 2-5 times. The number of viable cells of microorganisms was expressed by the number of colony-forming units (CFU), followed by a recount of 1 g sediment The results of bactericidal action were expressed as a percentage of the number of CSFs in the investigated solutions to the number of CFU in the control sample (the maximum number of CRU = 15).

3. Results and discussion

The aggregate stability of colloidal solutions of nanosilver was determined by using the phenomenon of the surface plasmon resonance inherent in nanoparticles of metals. Fig. 1 shows the spectra of colloidal solutions of nanosilver without the addition of surfactant and surfactants of different chemical nature, which were registered immediately upon receipt.

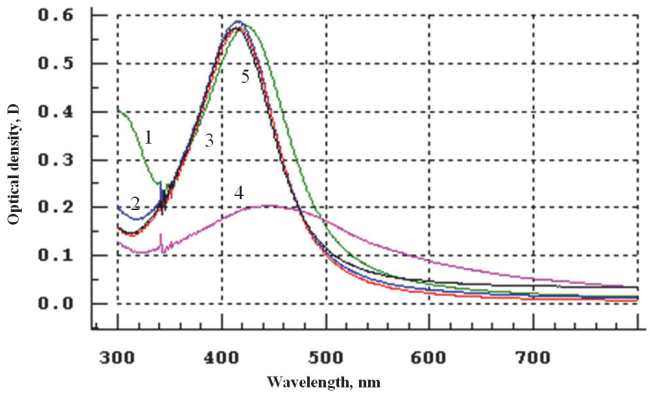

Fig. 1. Spectral characteristics of colloidal solutions of nanosilver with different surfactants immediately after preparation: (1 – without surfactants; 2 – Sulfanol; 3 – OC-20; 4 – Alcamone; 5 – Sodium dodecyl sulfate)

Fig. 2 shows the spectral characteristics of the same solutions that were recorded after 24 hours.

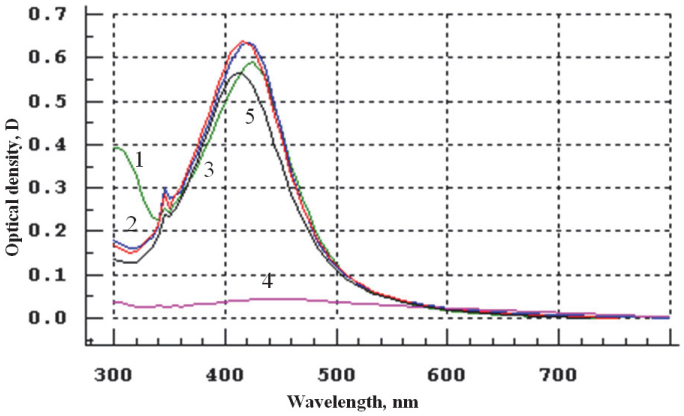

Fig. 2. Spectral characteristics of colloidal solutions of nanosilver with different surfactants immediately after after 24 hours: (1 – without surfactants; 2 – Sulfanol; 3 – OC-20; 4 – Alcamone; 5 – Sodium dodecyl sulfate)

It can be seen that anionic surfactants- sulfanol and sodium dodecyl sulfate and nonionic surfactants − OS-0 practically do not affect the spectra of surface plasmon resonance of silver nanoparticles. There is only a slight shift of maximum absorption from 420 nm for a solution of nanosilver without a surfactant up to 410 nm in the presence of surfactants. The high stability of silver nanoparticles without SAS can be explained by stabilizing properties of tannin, which has been used in exceed. At the same time, thecationic surfactant − Alcamone − greatly changes the spectral indices, also affecting the magnitude of the maximum absorption − its displacement occurs in the long wave region of 420 nm to 450 nm, which affects the optical density, which essentially decreases.

It is seen that the Alkamone solution does not actually contain nanoparticles of silver, which is characterized by a superficial Plasmon resonance. Their aggregation and precipitation dropped out. This fact is the actual proof of the negative charge presence on the surface of silver nanoparticles. The interaction of cationogenic SAS - Alkamone – with such particles leads to their electroneutrality and, consequently, to further aggregation. Spectral characteristics of other solutions have changed slightly. It should be noted that colloidal nanosilver solutions obtained with the use of tannin as a reducing agent, as opposed to other reducing agents investigated by us (ascorbic acid, hydrogen peroxide, hydroquinone with sodium citrate) exhibit high aggregate stability over a significant period of time (up to six months). Nevertheless, the study of bactericidal action of

nanosilver drugs (NS), stabilized by surfactants of different chemical nature has an independent interest, which was made at the second stage of our experimental study (Fig. 3).

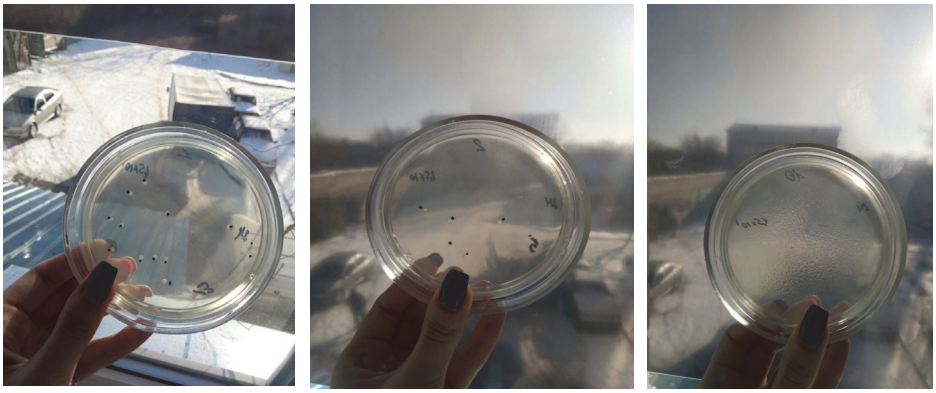

A B C

Fig. 3. Growth of bacteria on meat-peptone broth; A − control; B – SAS OS-20; C − solution NS+OS-20

Results of research on bactericidal action of nanosilver solutions in relation to the E.coli are presented in Table 2.

Table 2. Growth of the E.coli in solutions of nanosilver and surfactants

Sample number	Description of the sample	Percentage of CFU, (%)
1	Control sample (dilution $1.5 \cdot 10^{1}$)	100
2	Solution nitrate (0.001 n)	50
3	Solution of Silver Nanoparticles (NS)	not found
4	0.1% solution of surfactant: Alcamone	50
5	0.1% solution of surfactant: Sodium dodecyl sulfate	70
6	0.1% solution of surfactant: sulfanol	100
7	0.1% solution of surfactant: OS-20	40
8	Solution of NS + Alcamone	not found
9	Solution NS + Sodium dodecyl sulfate	10
10	Solution of NS + Sulfanol	20

11	Solution NS + OS-20	not found

One can see that solutions of silver nanoparticles without surfactant and in the presence of OS-20 and Alcamone completely inhibit the growth of the intestinal rod. Silver ions solutions (Ag^+) reduce the growth of E.coli colonies by half. Some of the surfactant agents negatively affect the growth of the E.coli, but do not have complete bactericidal action.

According to the results of the studies, it was found that compared with the control of Ag^+ partially suppresses the growth of bacteria, due to surface oxidation, thus exhibiting a toxicological effect in relation to *E. coli*.

Alkamone and OS-20 superficial substances independently partially inhibit the growth of bacteria (5 and 8 colonies). SAS Sodium dodecyl sulfate and Sulfanol alone and in the colloidal solution of silver nanoparticles do not exhibit bactericidal properties. Nevertheless, in the paper (Shulgina et al. 2012) using of *E.coli* as a test object, it was proved that the use of another anionic surfactant (such as Aerosol OT (AOT) is effective in terms of the bactericidal action of nanosilver-stabilized solutions of this substance.

Complete inhibition of growth of bacteria *E. coli* showing a colloidal solution of silver nanoparticles (Ag^o) that was synthesized without SAS, and also synthesized in the presence of cationic surfactant (Alcamone) and a colloidal solution synthesized in the presence of a nonionic surfactant (OS-20). The complete suppression of the growth of *E. coli* bacteria by the colloidal solution of silver nanoparticles is, in our opinion, related to the destruction of the surface of the cell wall, since nanosilver particles have an extremely large relative surface, thereby increasing their contact with bacteria and greatly improving their bactericidal effectiveness.

4. Conclusions

The influence of surface-active substances on the aggregate stability of colloidal solutions of nanosilver obtained by the restoration of the argentum nitrate by tanine in a neutral environment was studied. It has been proved that anionic surfactants – sulfanol and sodium dodecyl sulfate and nonionic surfactants − OS-20 can be used as stabilizers of colloidal solutions of nanosilver, whereas cationic surfactant alkalomone has a coagulating effect on the solutions of silver nanoparticles, reducing their aggregate resistance. It is proved that the solutions of nanoparticles are obtained silver exhibit bactericidal action against the E. coli and may be recommended as antiseptic agents for different purposes.

References

Alexander, J.W. (2009). History of the medical use of silver. *Surgical infections*, *10*(3), 289-299.

Baker, C., Pradhan, A., Pakstis, L. et al. (2005). Synthesis and antibacterial properties of silver nanoparticles. *J. Nanosci. Nanotechnol., 2*, 244-249.

Bernavsky, Z. (2006). *Colloidal silver. Natural antibiotic substitute*. RF, 24 (in rush.)

Choi, O. T. et al. (2009). Role of sulfide and ligand strength in controlling nanosilver toxicity. *Water Res*., *43*(7), 1879-1886.

Danilczuk, M., Lund, A., Saldo, J. et al. (2006). Conduction electron spin resonance of small silver particles. *Spectrochimaca Acta, 63*(A), 189-191.

Holt, K.B., Bard, A.J. (2005). Interaction of silver(I) ions with the respiratory chain of Escherichia coli: an electrochemical and scanning electrochemical microscopy study of the antimicrobial mechanism of micromolar Ag^{+}. *Biochemistry*, *44*(39), 13214-13223.

Kim, J. S., Kuk, E., Yu, K.N. et al. (2007). Antimicrobial effects of silver nanoparticles. *Nanomedicine*, *3*, 95-101.

Li, W.R., Xie, X.B., Shi, Q. S. et al. (2010). Antibacterial activity and mechanism of silver nanoparticles on Escherichia coli. *Appl. Microbiol. Biotechnol*., *85*(4), 1115-1122.

Litvinova, O.I. (2016). Development of the method of providing antibacterial properties to nonwoven fabrics using silver nanoparticles. *Scientific developments of youth at the present stage*.

Liu, J., Pennell, K., Hurt, R. (2011). Kinetics and mechanisms of nanosilver oxysulfidation. *Environ. Sci. Technol*., *45*, 7345-7353.

Lok, C.N., C. Ho, R. Chen. (2007). Silver nanoparticles: partial oxidation and antibacterial activities *J. Biol. Inorg. Chem*., *12*, 527-534.

Lok, C. N., Ho, C. M., Chen, R. et al. (2008). Proteomic identification of the Cus system as a major determinant of constitutive Escherichia coli silver resistance of chromosomal origin. *J. Proteome Res*., *7*(6), 2351-2356.

Medical microbiology, virology and immunology (2009). A textbook for the undergraduate and postgraduate students, edited by V.P. Shirokobokov, Vinnitsa: New Book, 952. (in ukr.).

Priskoka, A.O. (2016). Experimental Substantiation of Pharmacological Properties of Silver Nanoparticles: *Autoref. dis... Candidate pharmacy sciences*: 14.03.05, − Kh., 20. (in ukr.)

Savchenko, D.S. (2012). Investigation of antimicrobial properties of nanocomposite "Fine silica-clusters of silver", preparation "Silix" and silver nitrate. *Zaporozhye Medical Journal*, *4*, 124-128. Access mode: http://nbuv.gov.ua/UJRN/Zmzh_2012_4_40. (in ukr.)

Shahverdi, A.R. (2007). Synthesis and effect of silver nanoparticles on the antibacterial activity of different antibiotics against Staphylococcus aureus and Escherichia coli, *Nanomedicine*, *3*, 168-171.

Shulgina, T.A., Norkin, I.A., Puchinyan, D.M. (2012). Antibacterial Action of Water Dispersions of Silver Nanoparticles on Grammotric Micro-Organisms (on the example of Escherichia Coli). *Basic research, 7-2*, 424-426. (in rush).

Xiu, Z.M., Ma, J., Alvarez, P.J. (2011). Differential effect of common ligands and molecular oxygen on antimicrobial activity of silver nanoparticles versus silver ions. *Environ. Sci. Technol*., *45*, 9003-9008.

Yamanaka, M., Hara, K., Kudo, J. (2005). Bactericidal actions of a silver ion solution on Escherichia coli, studied by energy − filtering transmission electron microscopy and proteomic analysis. *Appl. Environ. Microbiol*., *71*, 7589-7593.

Abstract

The influence of SAS of different chemical nature on aggregate stability and bactericidal action of nano silver colloidal solutions is investigated. Colloidal solutions of silver were obtained by restoring the argentum nitrate agent in a neutral medium. With the help of spectrophotometric method, it has been proved that such solutions are characterized by high aggregate stability compared with the use of other traditional reducing agents. Anionic SAS (sodium dodecylsulfate and sulfanol) and nonionic SAS (OS-20) increase aggregate stability of nano silver solutions, while cationogenic SAS − alcamone promotes rapid coagulation and aggregation of nano silver particles. The study of bactericidal action of the solutions to the E.coli are showed that the nano silve colloidal solution with or without presence of OS-20 and alcamone completely inhibit the growth of colonies of E.coli, that is, it's have high bactericidal properties.

Keywords:
colloidal solutions of nanosilver, surface-active substances (SAS), aggregate resistance, bactericidal action

MIDDLE POMERANIAN SCIENTIFIC SOCIETY OF THE ENVIRONMENT PROTECTION

Rocznik Ochrona Środowiska

Volume 22. Year 2020 ISSN 1506-218X 51-59

Obtaining of Functional Product by Mechanical Processing of Secondary Fish Raw Materials

Yuriy Fatykhov[1], Oleg Ageev[1], Alexander Ivanov[2], Marek Jakubowski[3], Daniel Dutkievicz[3], Andrzej Dowgiallo[3]*

[1]Kaliningrad State Technical University, Russia

[2]Western Branch of the Federal State Budgetary Educational Institution of Higher Education "Russian Presidential Academy of National Economy and Public Administration", Russia

[3]Koszalin University of Technology, Poland

[*]corresponding author's e-mail: oleg.ageev@klgtu.ru

1. Introduction

The most competitive type of fish product that is in steady demand among the population is fresh or frozen fillets resulting from the deep cutting of raw materials. For the countries bordering the Baltic Sea, the raw materials for the production of fillets are cod, pike-perch, salmon, herring and others. Depending on the species composition of fish, the choice of cutting technology and equipment used, the output of the finished product (fillet) is 40...50%.

Remaining wastes (bones, fins, heads, scales, skin, insides) from the point of view of complex non-waste technology are rationally directed to fishmeal and hydrolysate production, however, the majority of fish processing enterprises do not have such production due to obvious economic, financial, industrial and technological difficulties. In practice, the easiest way is implemented by the enterprises: directing waste to cattle, birds, fur animals, etc. Disposal of fish waste is unacceptable for developed countries as it does not correspond to their environmental safety.

In fact, the components of fish produced by filleting are not wastes, but valuable secondary raw materials with rich biocapacity. Each of the components, individually or in combination, contains a rich spectrum of macro nutrients, minerals and vitamins, which determine the importance of their use in food, pharmacological, medical, fodder, technical purposes. One of the most modern directions

of rational use of secondary fish resources is obtaining on their basis food and therapeutic and preventive additives: biologically active additives (BAA).

The problem of processing secondary fish raw materials into healthy food products is of great importance. Suyue Song et al. (2020) describes the proposed method and the corresponding validation experiments with carp fillets. The differences in Raman spectra between fish bone and fish meat were investigated, and the optimal band information was selected using a fuzzy-rough set model based on the thermal-charge algorithm. Pınar Terzioğlu et al. (2018) summarizes the literature on the production of hydroxyapatite from fish bones and discusses their potential applications in biomedical field. The effect of processing conditions on the properties of final products including Ca/P ratio, crystal structure, particle shape, particle size and biological properties are presented in the light of X-ray diffraction, scanning electron microscopy, transmission electron microscopy, thermogravimetric-differential thermal analysis, bioactivity and biocompatibility investigations.

Albrektsen et al. (2018) suggests that hydrolysed compounds from fish bones may improve Ax utilization in salmon, and that they may have an impact on the functional properties of the muscle. Anindya Pal et al. (2017) presents aims at the synthesis of hydroxyapatite (HAp) from fish bone by simple heat treatment in the temperature ranging from 200 to 1200°C. The synthesized powders were characterized using X-ray diffraction and Fourier transform infrared spectroscopy to identify the phases and functional groups. Jin Zhang et al. (2016) investigates of effects of thermal treatments on breakage and calcium release of fish bone particles during high-energy wet ball milling. Heating temperature (55-130°C) showed much more obvious influences on the breakage and calcium release than heating time (20-60 min). Weeraphat Pon-On et al. (2018) fabricates composite scaffolds consisting of mineral ion-loaded hydroxyapatite derived from fish scale (mHAFS) in a poly (lactic acid) (PLA)/chitosan (Chi) matrix (mHAFS@PLA-Chi) by an *in situ* blending technique. Mineral ion loaded HAFS was successfully converted into mHAFS via the hydrothermal heating of HAFS in a SBF (simulated body fluid) solution.

We chose Baltic cod bone tissue as the object of research, which is a part of heads and fins when cutting on fillets, forms rib and ridge bones with muscle tissue incisions. Fish bone tissue is 6 to 20% of its muscle tissue. It is a source of protein and minerals. Protein is 73-95% represented by osseoalbumoids, which together with glucosaminoglycans form a glycoprotein that is more resistant to decomposition than collagen. Mineral substances are Ca, P, K, Na, Mn, Fe, Cu, Sn, Al. The contents of calcium in fish bone is 6.2 times higher than in muscle tissue, magnesium – 8 times higher, manganese – 1.1 times higher.

Substances included in the fish bone tissue have a positive effect on humans, stimulate the metabolism of proteins and carbohydrates. Complex of mineral salts and calcium has a positive effect on the treatment and prevention of caries, osteochondrosis, rickets. It is also known that the introduction of fish bone tissue in the diet leads to a decrease in the accumulation of radioactive isotopes in the human skeleton, reduces the risk of malignant tumors, prevents metastasis of already developed tumors and diseases of the hematopoietic and bone systems.

In this regard, the purpose of this study is to substantiate the developed technology of natural bone tissue supplement of hydrobionts (on the example of cod) and the development of recommendations for its use as a food and therapeutic additive in the production of dietary supplements.

2. Materials and methods

Determination of mass and chemical composition of the object of study was carried out in accordance with GOST of Russian Federation.

The mineral composition was determined by atomic-absorption spectroscopy on the device AA280Z of VARIAN company with graphite cell, sources of resonance radiation of the elements to be determined, prefix for generation of hydrates VARIAN VGA77. The method is based on the measurement of the absorption (optical density) of the atomic pair of a certain element, obtained by electrothermal atomization of the sample in the graphite cell of the spectrometer. To determine the contents of phosphorus, a two-beam spectrophotometer Hitachi 220A was used.

In the course of microbiological control in accordance with Russian Sanitary and Epidemiological Rules and Regulations, fish bone samples were examined by standard methods for the presence of: mesophilic aerobic and facultative anaerobic bacteria, the presence of Escherichia coli bacteria, Staphylococcus aureus, and the presence of pathogenic microflora, including the genus Salmonella.

Experimental studies of the fish bone drying process were carried out on a specially designed unit designed for vacuum drying of various moisture-containing food materials. Experiments were carried out at the temperature of heating plates on which the dried material was located, 70°C; 80°C; 90°C and absolute pressure inside the vacuum chamber of 1.6 kPa; 2.0 kPa; 2.4 kPa.

3. The results of the study

Hygiene assessment of radionuclide contents in fish raw materials is an integral part of a set of measures aimed at ensuring radiation safety of the population. Among the radioisotopes polluting water bodies the most important are 90Sr strontium and 137Cs cesium. For strontium, the critical organ is the bone

tissue, and for cesium – muscle tissue and internal organs. According to the data of the laboratory of radioecological researches of Atlant-NIRO in the bone tissue of cod extracted in the waters of the Baltic Sea, Curonian and Kaliningrad (Vistula) bays, strontium radioisotopes have not been found, which allows classifying such raw materials as safe in the radio-hygienic aspect.

The technological sequence of obtaining a food additive from fish bone tissue provides for cooking of the backbone with cuts in muscle tissue, upper and lower fins and tail fins (in this form, the raw material comes after filleting). In this process, the bone is cleaned, and after additional centrifugation is released from foreign inclusions and excessive moisture. Mass and chemical composition of cod bone before and after cooking is given in Table 1.

Table 1. Chemical composition of pike-perch and cod bone before and after cooking

	Factors												
	Mass fraction, %				Contents, %				Contents, mg/kg				
	Fat	Pr.*	Mo.*	Ash	K	P	Ca	Na	Mn	Fe	Cu	Al	Sn
Before boiling	0,3	13,0	71,0	15,6	0,10	1,90	2,40	0,10	5,7	8,0	1,5	< 0,1	< 0,01
After boiling	0,3	12,9	56,6	30,1	0,08	5,60	4,40	0,21	21,7	4,	3,8	< 0,1	< 0,01

* Pr. – Protein; Mo. – Moistur

Analysis of the data presented in Table 1 shows that the implementation of the thermal calculation of the boiling process does not lead to a reduction in the number of microelements in the bone tissue of fish and their content (in terms of dry matter) remains high.

As a parameter of process rationalize the rate of product dehydration (V) is chosen, it characterizes the rate of moisture removal per process:

$$V = (W_0^c - W_K^c)/\tau, \quad (1)$$

where:
W_0^c, W_K^c – Initial and final moisture content of the product,
in relation to dry matter, %;
τ – Drying time, min.

It is important at what rational parameters of the drying process of the object of study will be provided the minimum duration and maximum performance

of the plant for the finished product. The limitation is the moisture-containing of the final product and its quality, which determines the duration of storage.

In the process of vacuum drying of raw materials the influencing factors of the process are the temperature (T) of heating plates (heat exchangers) of the drying plant and the absolute pressure (P) inside the chamber of the device.

Implementation of experiments using the method of experiment planning allowed to obtain the following regression equations adequately describing the influence of factors on the rate of vacuum drying of cod bone (multiple determination factor $R^2 = 0{,}95$).

In the coded values of the factors:

$$y = 0{,}8019 + 0{,}0365x_1 + 0{,}115x_2 - 0{,}031x_1 \cdot x_2 - 1{,}583 \cdot 10^{-2}x_1^2 - 0{,}093x_2^2. \quad (2)$$

In the natural values of the factors:

$$V = -7{,}9098 + 1{,}1071T + 0{,}1763P - 7{,}750 \cdot 10^{-3}TP - 9{,}8958 \cdot 10^{-2}T^2 - 9{,}3333P^2. \quad (3)$$

The obtained regression equation allows not only to predict the value of the response function for the given conditions of implementation of the process of vacuum drying of the fish bone, but alsoprovide information on the shape of the response surface, which is presented in Fig. 1.

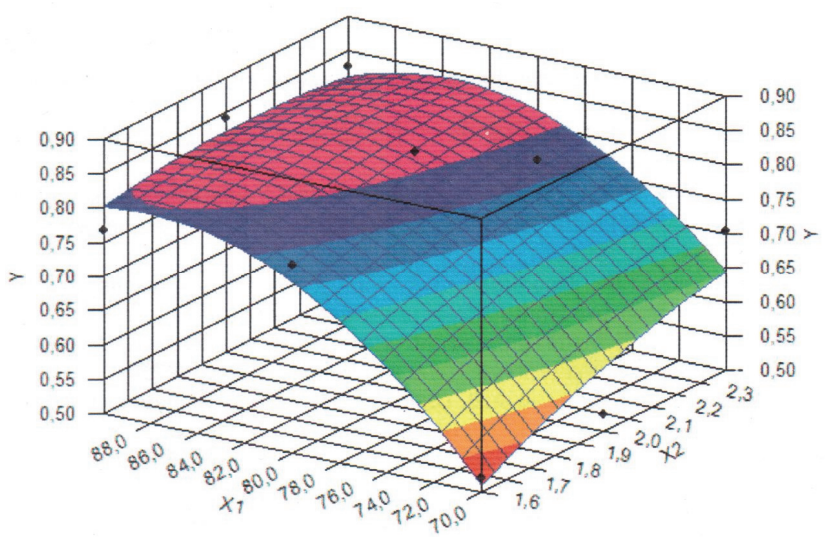

Fig. 1. Surfaces of the response function in the selected area of the factor space for cod bone

Rational parameters of the vacuum drying process of cod bone are:

$$P = 2{,}0 \text{ kPa}; T = 80°C; \tau = 155 \text{ min}; W_K^c = 3{,}09\% \quad (4)$$

After drying, the fish bone becomes brittle and changes colouration from white to light beige. In order to obtain a product in the form of a powder, it is subjected to fine grinding, and the rational process is when the final moisture content of the bone after drying corresponds to 3-5%. The finely grinded bone mass can be obtained with a hammer-type mill. The final product is an air-dry polydisperse substance consisting of 0.6 to 0.08 mm particles.

The shredded bone mass should be packaged in containers, which should have the least moisture and light permeability to ensure maximum preservation of the valuable properties of the finished product during storage. The best variant of packing containers: paper multilayered, jute or craft bags of different sizes.

The condition of storage of finely grinded fish bone is determined by its hygroscopic properties. The equilibrium moisture content of the bone mass (flour) W_p depends on the relative moisture content of the surrounding air (y), and within the range of 60-100% this dependence looks like:

$$W_p = 10^{(a+by)}, \quad (5)$$

where: a and b – constants depending on the properties of flour (for crumbly flour a = 0.072, b = 1.345).

Storage of flour in conditions of increasing moisture content and temperature contributes to the active absorption of moisture by the product, the breakdown of proteins, hydrolysis and oxidation of lipids, the destruction of vitamins, the development of residual microflora. Oxidative processes in the flour can lead to its self-heating and spontaneous combustion. The rational conditions for storing fishmeal are the air temperature 15…20°C at a relative moisture content of not more than 75%.

At determining the shelf life of the shredded fish bone in the specified rational conditions the actual moisture content of the product corresponds to the equilibrium moisture content and is 10-12%. The guaranteed minimum shelf life is 1 year from the date of manufacture.

Organoleptic evaluation of the product at the end of its shelf life. Appearance – finely grinded, finely dispersed and easily scattered powder. Colour – white. Smell – odorless. Taste – typical for this product. The presence of signs of oxidation – there are no signs of oxidation.

Lipid indicators of cod bone tissue are as follows. The acid number changed insignificantly from 1.2 to 1.5 mg KOH/g, which indicates that the degree of fat hydrolysis is insignificant. The peroxide number changed from 0.08

to 0.12%I during the same period, which shows that there is practically no oxidative process of fat.

It is interesting to compare the acceptability of the described technology for other fish species with high fat content in bone tissue. Despite the significant difference between this indicator for cod and pike-perch, the whole technological sequence of treatment is preserved and the parameters recommended in formula (4) are similar. However, during the storage of finely grinded pike-perch bone, the peroxide number increases significantly faster, which indicates a more intensive oxidation of fat, although it also does not reduce the final quality of the product. For fish bone raw materials with high fat content, storing the powder in vacuum packaging, which is known to slow down the oxidation process, is a recommended option.

Considering high biological value of a final product – fine-grained fish bone mass in the form of a flour or a powder is possible to use in industrial scales in following directions:

1. When preparing food for fish, birds and animals as an additive enriched with minerals and vitamin-enzymatic complex.
2. When added to wheat flour and meat products, sugar, confectionery and other products as a prophylactic component with easily assimilable protein and minerals of osteo-tropic and chondroprotective action. This practice exists in the USA, England and Canada.
3. As a component of biologically active substances containing easily digestible calcium, and recommended in medical practice as a general strengthening agent that helps reduce blood sugar levels, as well as with increased mental stress (powders "Tian Shan", "Calcium magnesium chelate", etc.).
4. As the main component of the dietary supplement, designed to improve the musculoskeletal system. In Russia, 44% are domestically produced dietary supplements, while the rest are imported dietary supplements (BAA "Calcimax", "Glucosamine", "Joint Flex" (USA), "Wise Dragon" (Vietnam), "Doholodan" (China),"Ortoosteo" (Germany) and etc.).
5. As an additive recommended for the prevention and treatment of radioactive threats to the human body.

Depending on the physiological needs of different population groups, a certain amount of fish powder supplement is calculated. Its application can be both in bulk form and in the form of bars, granules, tablets, capsules, etc. At the same time, the use of fish bone supplements to obtain the products recommended by us can be carried out on the basis of known traditional technologies.

4. Conclusion

1. Fish bone waste is a valuable secondary resource enriched with macro- and microelements and vitamins.
2. The technology of fish bone processing for obtaining mineralized food additive has been developed.
3. Rational mode of vacuum drying of fish bone with minimum moisture content is developed.
4. Conditions and guaranteed shelf life of the mineralized food additive are determined.
5. The recommendations on industrial use of the food mineralized additive are offered.

References

Albrektsen, S., Østbye, T. K., Pedersen, M., Ytteborg, E., Ruyter, B., Ytrestøyl, T. (2018). Dietary impacts of sulphuric acid extracted fish bone compounds on astaxanthin utilization and muscle quality in Atlantic salmon (Salmo salar). *Aquaculture, 495*, 255-266.

Anindya, Pal, Sudeep, Paul, Amit, Roy Choudhury, Vamsi, Krishna, Balla, Mitun, Das, Arijit, Sinha, (2017). Synthesis of hydroxyapatite from Lates calcarifer fish bone for biomedical applications. *Materials Letters, 203*, 89-92.

Jin, Zhang, TaoYin, Shanbai, Xiong, Yajie, Li, Ullah, Ikram, Ru, Liu, (2016). Thermal treatments affect breakage kinetics and calcium release of fish bone particles during high-energy wet ball milling. *Journal of Food Engineering, 183*, 74-80.

Pınar, Terzioğlu, Hamdi, Öğüt, Ayşe, Kalemtaş, (2018). Natural calcium phosphates from fish bones and their potential biomedical applications. *Materials Science and Engineering, 91*, 899-911.

Suyue, Song, Zhenfang, Liu, Min, Huang, Qibing, Zhu, Jianwei, Qin, Moon, S. Kim, (2020). Detection of fish bones in fillets by Raman hyperspectral imaging technology. *Journal of Food Engineering*, 272.

Weeraphat, Pon-On, Panan, Suntornsaratoon, Narattaphol, Charoenphandhu, Jirawan, Thongbunchoo, Nateetip, Krishnamra, I. Ming, Tang, (2018). Synthesis and investigations of mineral ions-loaded apatite from fish scale and PLA/chitosan composite for bone scaffolds. *Materials Letters, 221*, 143-146.

Abstract

The most competitive fish product is fresh or frozen fillets. The yield of the finished product is 40...50%. Waste from production is sent to livestock, birds for feeding and other purposes, as well as disposed of, which does not correspond to environmental safety. The bone components of fish are valuable secondary raw materials containing a wide range of macro nutrients and minerals. Their most rational use is to obtain biologically active additives on their basis. The object of research is cod bone tissue. The technology of obtaining a natural mineral additive from bone tissue is substantiated. After

boiling, the bone tissue is cleared of muscle tissue, while the content of minerals remains high. Vacuum drying of the grinded product allows it to be stored for a long time without compromising its quality. The rational values for vacuum drying of bone waste are given. The conditions of storage of finely grinded mineral bone additive are considered. The ways of its rational industrial use as a biologically active additive are determined.

Keywords:
cod, bone tissue, secondary raw materials, minerals, biologically active additive

Produkcja produktu funkcjonalnego przez obróbkę mechaniczną wtórnych surowców ryb

Streszczenie

Najbardziej konkurencyjnym rodzajem produktu rybnego jest świeży lub mrożony filet. W takim przypadku wydajność produktu końcowego wynosi 40...50%. Odpady z produkcji są kierowane na paszę dla zwierząt gospodarskich, ptaków i innych celów, a także są usuwane, co nie odpowiada bezpieczeństwu środowiska. Składniki kostne ryb są cennym surowcem wtórnym zawierającym bogate spektrum makroskładników i minerałów. Najbardziej racjonalnym zastosowaniem jest uzyskanie biologicznie aktywnych dodatków na ich bazie. Jako przedmiot badań wybrano tkankę kostną dorsza. Technologia uzyskiwania naturalnego suplementu mineralnego z tkanki kostnej jest uzasadniona. Po ugotowaniu tkanka kostna uwalnia się od tkanki mięśniowej, a zawartość minerałów pozostaje wysoka. Suszenie próżniowe pokruszonego produktu pozwala przechowywać go przez długi czas bez pogorszenia wskaźników jakości. Podano racjonalne wartości parametrów suszenia próżniowego odpadów kostnych. Uwzględniono warunki przechowywania drobno zmielonych mineralnych suplementów kostnych. Określono sposoby jego racjonalnego zastosowania przemysłowego jako biologicznie aktywnego dodatku.

Słowa kluczowe:
dorsz, tkanka kostna, surowce wtórne, minerały, suplement diety

MIDDLE POMERANIAN SCIENTIFIC SOCIETY OF THE ENVIRONMENT PROTECTION

Rocznik Ochrona Środowiska

Volume 22. Year 2020 ISSN 1506-218X 60-69

Immobilization of *Bacillus megaterium* in Carrageenan from Maluku Sea and Their Effect on Protease Production

Syarif Hamdani[1,2], Sri Nurlatifah[1], Dewi Astriany[1], Marlia Singgih W.[2], Slamet Ibrahim W.[2]*

[1] Sekolah Tinggi Farmasi Indonesia, Bandung, Indonesia

[2] School of Pharmacy, Bandung Institute of Technology, Bandung, Indonesia

[*]corresponding author's e-mail: syarifhamdani@stfi.ac.id

1. Introduction

Immobilization is a bacterial condition maintained in a matrix. Carrageenan, an isolate from red seaweed (Eucheuma cottoni) largely available in Indonesian waters, can be used as an immobilization matrix. There are three types of carrageenan: kappa-carrageenan, used as gelling agent, lambda-carrageenan, used as thickening agent or viscosity enhancer, and iota-carrageenan, used as gelling agent. Being a stronger gelling agent than other types of carrageenan, kappa-carrageenan is generally used in immobilization matrix (Rowe et al. 2009). Carrageenan used in this study was derived from the seaweed grown in West Seram, a district in Maluku known as the biggest producer of Eucheuma cottoni, which contains approximately 50% of kappa-carrageenan on its basic dry weight (Karyani 2013).

Microbes in immobilized form have advantages in industrial applications since they are easier to handle and they do not die easily. Bacteria as an enzyme resource has several advantages on its production scale; it is easier to increase if desired, the microbial cells are easier to grow with relatively faster growth, it takes lower production cost, it does not depend on seasonal changes and it takes shorter production time. Bacteria from the genus Bacillus are active producers of extracellular proteases which produce proteases with high pH and thermal stability (Chatterjee 2015). *Bacillus megaterium* was used in this study as it didn't produce toxins, didn't need expensive substrates, could survive in high temperature, had no metabolic side effect, was easy to grow and capable of producing a high number of extracellular protein (Poernomo 2003).

Protease enzymes produced from cellular immobilization have advantages such as easy-to-control immobilized cell and stable and non-toxic matrix.

Immobilization can also enhance productivity due to high cell density, the ease in cell isolation and continuable product purification (Riwayanti et al. 2012).

Immobilized *Bacillus megaterium* can produce higher protease enzymes as trapped cells in the matrix (immobilized cells) are reusable, have better stability, higher efficiency, and bigger resistance toward environmental disruption (Mrudula & Shyam 2012).

2. Materials and methods

2.1. Instrumental and apparatus

We used an analytical digital scale (Ohaus), UV-Visible spectrophotometer (Shimadzu), centrifugal (Tomy MX-305), centrifuge (PLC series), magnetic stirrer (Thermo scientific), shaker (Health H-SR-200H), vortex (Barnstead type 37600), Laminar Air Flow (ERSA Scientific), micropipette (Fisherbrand Elite), autoclave (GEA LS-50 LJ My Life MA 678GE), incubator (Memmert), colony counter (Rocker Galaxy 230), pH meter (Mettler Toledo), and general laboratory glassware.

2.2. Material and microorganisms

The material used is bacteria *Bacillus megaterium* ITBCC40, carrageenan isolated at Pharmaceutical Technology Laboratory STFI according to Ferdiansyah, 2017. Other materials used were nutrient broth (Oxoid); nutrient agar (Oxoid); 96% ethanol, distilled water, NaCl 0.9% (Wida R.); KCl 0.3 M (Merck); $CaCl_2$ 0.18 M (Merck); skim milk; peptone (Oxoid); yeast extract (Oxoid); casein; NaCl (Merck); KH_2PO_4 (Merck); $MgSO_4 \cdot 7H_2O$ (Merck); tyrosine; K_2HPO_4 (Merck); NaOH (Merck); and TCA (Trichloroacetic Acid) 0.1 M (Merck).

2.3. Determination of *Bacillus megaterium* growth curve

Determination of growth curves was carried out on *Bacillus megaterium* that had been incubated at 37°C for 24 hours. Bacteria was inoculated into 50 mL of sterile nutrient broth (NB) media and homogenized on a shaker at 100 rpm at room temperature for 24 hours. 10% of the culture was put into 100 mL of sterile NB and had its optical density value measured every hour (for 40 hours) at 600 nm wavelength by UV-Visible spectrophotometer (Shibata 1954).

2.4. Immobilization of *Bacillus megaterium*

Bacillus megaterium were cultured on nutrient agar (NA) media and incubated at 37°C for 24 hours, then made into suspension in 0.9% NaCl solution until 22% transmittance was obtained. Carrageenan matrix solution was made with different concentrations, i.e: 1, 1.5, and 2% (w/v) through a dilution process

in aquadest by shaking it on a magnetic stirrer at 80-100°C. Carrageenan solution was sterilized using an autoclave at 121°C at a pressure of 1.5 atm for 15 minutes. Sterile carrageenan solution was maintained in liquid form at around 40°C through heating and shaking on the magnetic stirrer, then a *Bacillus megaterium* suspension was added. The mixture was added drop by drop by using a pipette into a sterile 0.3 M KCl solution (10°C) while being shaken slowly for a few minutes to obtain beads, and let stand for 15-20 minutes. KCl solution was then decanted and the beads were immersed in a sterile 0.18 M $CaCl_2$ solution (10°C), let stand for 1 hour. $CaCl_2$ solution is decanted then beads containing immobilized bacteria were stored in a refrigerator at 4°C (Cassidy 1996).

2.5. Proteolytic test

Proteolytic assays were carried out on both of immobilized and not immobilized *Bacillus megaterium* by culturing it, using a toothpick, on nutrient agar (NA) which contain 2.8% (w/v) skim milk before incubating it for 48 hours at 30°C. Bacterial culture was observed visually; positive results were indicated by the presence of clear zones on media around bacteria colonies. Proteolytic indexes were calculated by comparing diameter of the clear zone with diameter of colony (Omer & Humadi 2013).

2.6. Calculation of total bacteria

Pour plate methods were used to calculate the total bacteria (total plate count) of immobilized *Bacillus megaterium* on different storage times: 4 months (K), 5 months (L), 7 months (M), and 9 months (N). A total of 0.1 gram beads containing immobilized bacteria were put into a tube filled with 10 mL of NaCl 0.9%, then the beads were dissolved by shaking by vortex. The solution was then diluted to 10^{-1}, 10^{-2} and 10^{-3} using 0.9% NaCl. A total of 100 µL of solution from each dilution was put into a Petri dish, then 10 mL NA was added and homogenized, incubated at 37°C for 24 hours. The growth of bacterial colonies was calculated using colony counter. The number of bacteria was calculated based on Bacteriological Analytical Manual (2011), with formula as follows:

$$N = \frac{\Sigma C}{[\![(1 \times n1) + (0{,}1 \times n2)]\!] \times d}$$

where:
C – the total number of colonies from all petri dish counted,
N – the number of colonies per ml/gram,
n1 – the number of petri dish on the first dilution,
n2 – the total of dilution on the second dilution,
d – the dilution level obtained from the first petri dish.

2.7. Production and isolation of rough protease

Enzyme production was done by inoculating beads containing immobilized bacteria as much as 100 mg into 50 mL of production media with the composition of casein 0.5% (w/v), peptone 0.01%, yeast extract 0.02%, NaCl 0.1%, K_2HPO_4 0.01%, $MgSO_4 \cdot 7H_2O$ 0.01% and $CaCl_2$ 0.01%, shaken at 150 rpm for 72 hours. The mixture was centrifuged at 6000 rpm at 4°C for 30 minutes. The resulting supernatant was a crude protease enzyme which would then be tested for activity test (Sevinc 2011).

2.8. Determination of activity value in protease enzymes

The Kunitz method was used to determine the activity value of the protease enzyme by extracting 1 ml of an enzyme (supernatant) into a centrifuge tube containing 1 ml of casein 1% (w/v) in dilution of phosphate buffer pH 7, then incubated 37°C for 30 minute. The hydrolysis reaction was stopped by adding 3 ml of TCA (trichloroacetic acid) 0.1 M then allowed to stand for 30 minutes at room temperature. Suspention centrifuged at a speed of 6000 rpm for 10 minutes, supernatant was taken carefully, then measured using a UV spectrophotometer at 288 nm. Enzyme activity was calculated based on the number of amino acids (simple peptides) formed by using a standard tyrosine curve. One unit of protease enzyme activity is defined as the amount of enzyme that liberates 1 μmol tyrosine under test conditions (Mrudula & Shyam 2012).

3. Results and discussion

3.1. Growth curve of *Bacillus megaterium*

The growth rate of *Bacillus megaterium* were measured three times repetation by turbidimetric method, based on the degree of turbidity during storage of bacteria grown on the inoculum medium. Turbidity measured the number of living cells as well as the dead cells (Maier 2008).

Bacillus megaterium underwent a relatively short lag phase (adaptation). This phase occurred at the first 0-2 hours of growth time, this condition similar as growth on peptone, glucose, and yeast extract media (Liu 2011). However, in the exponential phase there was quite difference, the results show that the exponential phase was reached at 15 hours, difference from Liu, 2011 which was reached at 36 hours. The maximum time in the exponential phase was closer to the growth curve under enriched media which was at 22 hours (Nguye 2018).

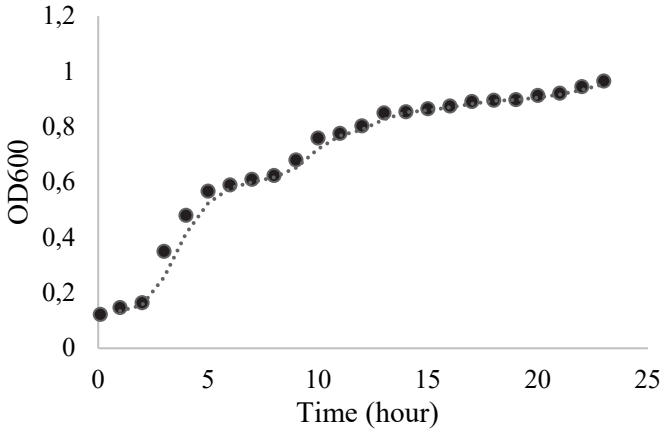

Fig. 1. Growth curve of *Bacillus megaterium*

3.2. Immobilization of *Bacillus megaterium*

The immobilization process was carried out by varying the concentrations of carrageenan to determine the optimal concentration to get the best beads. The concentrations of carrageenan commonly used were 0.2-2%. In this study the concentrations of 1%, 1.5% and 2% were used. The perfectly formed beads were produced in 1.5% concentration of carrageenan. Gel concentrations higher than 2% produced large lump because the matrix with high concentration would very quickly coagulate so that beads did not form. At lower concentrations, the beads produced were too soft and brittle, so the beads would leak easily. According to Kocher and Mishra (2012), the optimum bead diameter was 5.2 mm for protease production and optimum freezing time for protease production was 12 hours.

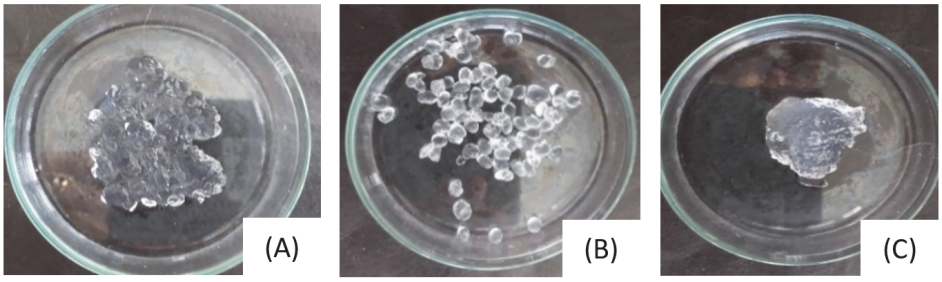

Fig. 2. *Bacillus megaterium* immobilized in Carrageenan. (A) Carrageenan 1%; (B) Carrageenan 1.5%; (C) 2% Carrageenan

The matrix dissolution process was carried out at thermal temperatures (80-100°C) as the matrix can be completely dissolved at this temperature. Under lower temperature, the only dissolved matrix was the salt form. Bacteria were integrated into carrageenan at 400C to prevent bacteria from dying. The use of 0.3 M KCl solution at 10°C in the process of forming beads is meant to induce the formation of 3-dimensional structure of the helical structure to form a strong and durable microcapsule, while immersion in $CaCl_2$ 0.18 M at 10°C was a gelatination stage to compact the beads (Cassidy 1996, Suzana 2013).

3.3. Proteolytic assay

Proteolytic indexing was carried out by culturing *Bacillus megaterium* immobilized into NA media contained skim milk, and positive result can be seen by the presence of clear zones around the colony, while observations can be seen in Figure 3. The addition of skim milk in the growth media functioned as an enzyme substrate. Casein hydrolysis reaction served to show proteolytic hydrolysis activity. Protease catalyzed casein degradation by breaking the peptide bonds in CO-NH as water entered the molecule; the hydrolysis reaction produced amino acids (Joseph 2006).

The results of proteoliytic index shown in Table 1 stated that *Bacillus megaterium* produced the same proteolytic index as K immobilized bacteria (4 months storage) which was 1.1 cm. Proteolytic index increased along the immobilization storage time, namely L (storage 5 months) 1.2 cm, M (storage 7 months) 1.8 cm, and N (storage 9 months) 2.7 cm. However, the clear area around the growth of bacteria did not represent the number of proteases produced by microorganisms as the clear area would grow larger along with the increased length of the incubation time (Figure 3). Therefore, the protease content in immobilized *Bacillus megaterium* had to be determined quantitatively.

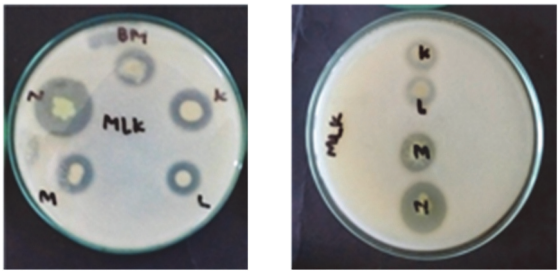

Fig. 3. Proteolytic tests of *Bacillus megaterium* unimmobilized and Immobilized. K (4 months), L (5 months), M (7 months), N (9 months), Bm (unimmobilized)

Table 1. Proteolytic index

Description	Clear zone diameter (mm)			
	Dish 1	Dish 2	Dish 3	Average
Bacillus megaterium	12	11	11	11
K (4 months)	11	11	11	11
L (5 months)	11	12	13	12
M (7 months)	11	16	25	18
N (9 months)	25	27	30	27

3.4. Calculation of total bacteria

Bacillus megaterium is an anaerobe facultative bacteria capable of growing on parts of the media that are indirectly exposed to the oxygen, therefore pour plate method is used to determine the number of bacteria on Total Plate Count. Dilution is a means to reduce the number of microbes to enable observation and determination of specific number of microorganism for accurate calculation. The study showed that the number of bacteria in storage were relatively stable, indicated by the number of bacteria increase that didn't go higher than 101 CFU/100 mg (Fig. 4).

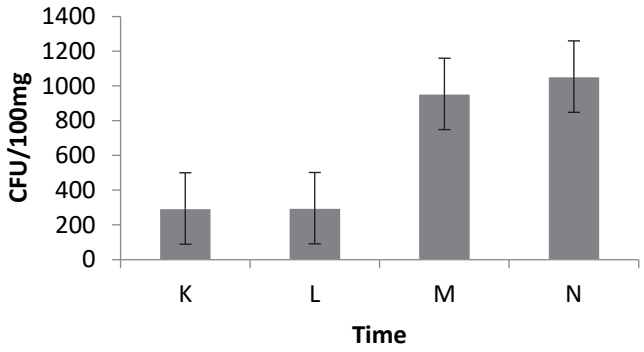

Fig. 4. Results of Total Plate Count (TPC) *Bacillus megaterium* immobilized
Description: K (4 months), L (5 months), M (7 months), and N (9 months)

3.5. Determination of protease activity enzymes

Determination of protease enzyme activity value was carried out by reacting 1 mL of casein solution dissolved in phosphate buffer pH 7 and 1 mL of enzyme solution from the sample. Casein was used to measure the size of enzyme

activity by measuring the amount of tyrosine in said protease. Phosphate buffer pH 7 used to dissolve casein was also used to maintain the stability of enzyme pH as pH changes can affect enzyme activity and extreme pH can ruin enzyme. Next, the solution was incubated at 37°C for 30 minutes to activate the protease enzyme in decomposing casein. The addition of TCA will denature the casein due to the formation of an acidic environment and form a white complex, tyrosine was then separated from other components by centrifugation. Casein with its high density would settle to form pellets, and tyrosine, enzymes, and buffers would be found in the supernatant. This supernatant was then measured at 288 nm wavelength, which is the maximum absorption of tyrosine (Kocher 2009).

Determination of protease activity was calculated based on the equation obtained from the standard tyrosine curve which was the line equation $y = 0.1595x + 0.0596$. The results of the observations shown in Figure 5 state that the increase of protease activity value is 0.0271 U/Gram for immobilization sample after being stored for 4 months (K), 0.0489 U/Gram for 5 months (L), and 0.1372 U/Gram for 7 months (M), and the activity decreases after being stored for 9 months (N) which is 0.0501 U/Gram immobilization.

Immobilized bacteria in carrageenan from Maluku sea are able to produce proteases with different activities influenced by storage time. The activity of the crude protease enzyme is shown in Figure 5, the immobilized bacteria stored provide higher enzyme activity compared to wild bacteria. Storage time that gave the highest effect on enzyme activity for storage up to 7 months but at 9 months storage the enzymes produced shown decrease activity, this condition is possible due to decreased physiological activity of bacteria due to growing environmental conditions that are increasingly unsupportive.

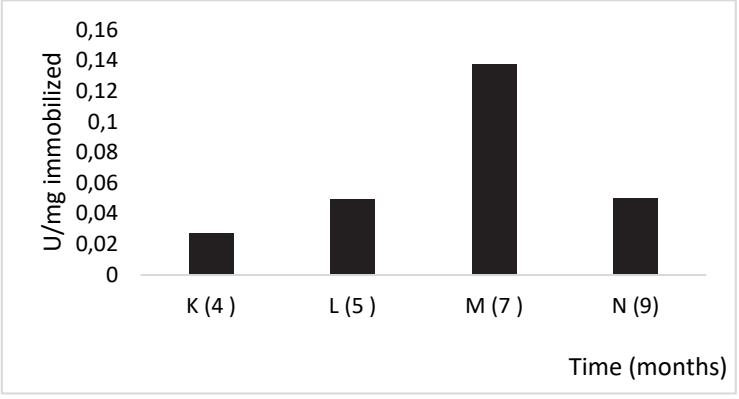

Fig. 5. Activity Value of Protease Enzyme

4. Conclusion

The study concluded that immobilized bacteria in carrageenan from Maluku sea are able to produce proteases with different activities influenced by storage time. The immobilized bacteria stored provide higher enzyme activity compared to wild bacteria. 7 months storage time gave the highest effect on enzyme activity with the activity value of 0.1372 U/Gram. Immobilized bacteria in storage for 9 months shows decreased activity of the enzymes produced, this condition was possible due to decreased physiological activity of bacteria at the environmental conditions that were increasingly unsupportive.

This research was funded by the Hibah Desertasi Doktor Ministry of Research, Technology and Higher Education of the Republic of Indonesia.

References

Cassidy, MB. et al. (1996). Enviromental applications of immobilized microbial cells. *Journal of Industrial Microbiologi, 16*, 79-101.

Chatterjee, Sh. (2015). Production and estimation of alkaline protease by immobilized *Bacillus licheniformis* isolated from poultry farm soil of 24 Parganas and its reusability. *Journal of Advanced Pharmaceutical Technology & Research*, *6*, 2-5.

Ferdiansyah, R., Yohana, A., and Abdassah, M. (2017). Karakteristik Kappa Karagenan dari Eucheuma Cottonii asal Perairan Kepulauan Natuna dan Aplikasinya sebagai Matrik Tablet Apung, *Jurnal Sains dan Teknologi Farmasi Indonesia*, *6*(1).

Fleming, Dara, L. (2004). *Evaluating bacterial cell immobilization matrices for use in a biosensor*. Blacksburg, Virginia USA: Virginia Polytechnic Institute and State University. 49.

Joseph, B. et al. (2006). Studies on the Enhanced Production of Extrasellular Lipase by Staphylococcus epidermidis. *Journal Gen. Appl. Microbiol,* 52.

Karyani, S. (2013). Analisis Kandungan *Foodgrade* pada Karagenan dari Ekstraksi Rumput Laut Hasil Budidaya Nelayan Seram Bagian Barat. *Journal.* Ambon : Politeknik Negeri.

Kocher, GS., and Mishra, S. (2009). Immobilization of *Bacillus circulans* MTCC 7906 for enhanced production of alkaline protease under batch and packed bed fermentation conditions. *International Journal Microbiology, 7*, 359-378.

Liu, C., Yuan, H., Yang, J.S., and Li, B.Z. (2011). Effective biosorption of reactive blue 5 by pHindependent lyophilized biomass of *Bacillus megaterium*. *African Journal of Biotechnology, 10*(73), 16626-16636.

Madigan, M.T., Martinko, J. (2006). *Brock Biology of Microorganism,* 10th ed. Pearson Education, Inc., New York.

Maier, Raina M. (2008). *Bacterial Growth.* Academic Press, Enviromental Microbiology.

McHugh, D.J. (2003). *A Guide to Seaweed Industry*. Food and Agric, Org. of the UN, Rome. 2.

Mrudula, Somda., Shyam, Nidhi. (2012). Immobilization of *Bacillus megaterium* MTCC 2444 by Ca-alginate Entrapment Method for Enhanced Alkaline Protease Production. *Brazil: Arch. Biol. Technol.,* 55, 136.

Nguyen, H.Y.T. and Trand, G.B. (2018). Optimization of Fermentation Conditions and Media for Production of Glucose Isomerase from *Bacillus megaterium* Using Response Surface Methodology. *Scientifica*.

Omer, Sind Shamel, Humadi, Hamid Gehad. (2013). Qualitative and Quantitative screening of alkaline protease production from some pathogenic bacteria. *Journal of Kerbala University, 11*(3), 311.

Poernomo. (2004). *Kitinase dalam Pengendalian Hayati.* Majalah Farmasi Airlangga, Jakarta. *42*, 24-27.

Riwayanti, I., et al. (2012). Teknologi Imobilisasi Sel Mikroorganisme Pada Produksi Enzim Lipase. *Prosiding SNST ke-3 Jurusan Teknik Kimia Fakultas Teknik.* Semarang : UNWAHAS. Hal. 55-59.

Rowe, Raymond, C. et al. (2009). *Handbook of Pharmaceutical Excipient.*6th Edition. Pharmaceutical Press, USA. 326-329.

Satyati, Wilis A. et al. (2015). Kinetika Pertumbuhan dan Aktivitas Protease Isolat 36k dari Sedimen Ekosistem Mangrove, Karimun Jawa, Jepara. *Ilmu Kelautan, 20*(3). 163-169.

Sevinc, Nihan and Demirkan, Elif. (2011). Production of Protease by *Bacillus megaterium sp.* N-40 Isolated from soil its Enzymatic Properties. *Journal Biology Environment Science.*Turkey: Uludag University. 96.

Shibata, K., Benson, A.A., & Calvin, M. (1954). *The Absorption Spectra Of Suspention Of Living Micro-Organisms*. https://escholarship.org/uc/item/9fp494sg. Lawrence Barkeley National Laboratory.

Susanti VH, Elfi. (2003). Isolasi dan Karakterisasi Protease dari *Baciluus subtilis 1012M15. Biodiversitas, 4*(1), 12-17.

Suzana, C.S.M. et al. (2013). Immobilization of Microbial Cells : A Promising Tool for Treatment of Toxic Pollutants in Industrial Wastewater. *African Journal of Biotechnology, 12,* 4412-4418.

Winarno, F.G. (1996). *Teknologi Pengolahan Rumput Laut*. Edisi I. Pustaka Sinar Harapan, Jakarta. 38.

Abstract

Bacteria immobilized in carrageenan are widely used in industry to facilitate bacterial handling and storage. Carrageenan is derived from seaweed and its nature is influenced by the condition of the origin of the sea where seaweed grows, one of the Indonesia sea territories that has seaweed that contains caraganen with good properties is Maluku. This study was conducted to determine the effect of storage time of bacteria immobilized in Maluku sea's carrageenan on proteolytic activity, the bacteria used were Bacillus megaterium. Bacterial immobilization of carrageenan was made at concentrations of 1%, 1.5%, and 2%, storage in cold conditions for up to 9 months. Protease activity was tested using Kunitz method by adding casein as a substrate. The optimal concentration of carrageenan for immobilization of Bacillus megaterium was obtained at a concentration of 1.5%. Protease isolated from immobilized Bacillus megaterium showed increased activity value from storage for 4 months (0.0489 Ug-1) to 7 months (0.1372 Ug-1), and decreased activity after being stored for 9 months (0.0501 Ug-1).

Keywords:
carrageenan, immobilization, protease activity, *Bacillus megaterium*

MIDDLE POMERANIAN SCIENTIFIC SOCIETY OF THE ENVIRONMENT PROTECTION

Rocznik Ochrona Środowiska

Volume 22. Year 2020 ISSN 1506-218X 70-81

Destruction of the Structure of Boiling Emulsions

Anatoliy Pavlenko[1], Viktor Melnyk[2]*

[1]Kielce University of Technology, Poland

[2]Ivano-Frankivsk National Technical University of Oil and Gas, Ukraine

[*]corresponding author's e-mail: apavlenko@tu.kielce.pl

1. Statement of the problem

Existing methods for calculating the processes of emulsification and homogenization of fluids are based on the dynamics of a single particle, which either boils with a sudden change in external parameters (Dolinsky et al. 2001, Dąbek et al. 2016, Dąbek et al. 2018), or is subjected to the action of dynamic impact during the acceleration (deceleration) of flow, as well as is subjected to mechanical effects (Dolinsky & Ivanitsky 1995, Ivanitsky 1997). The examination of the dynamic interaction of two particles while boiling of light boiling component of the emulsion is given in (Pavlenko & Koshlak 2017). Therefore, the study and development of the theoretical grounds of multitude drops breakup of discretely distributed phase is important for the determination of the optimal dispersion modes which results in a significant reduction in energy costs both during the grinding and crushing process, as well as reduction of the financial costs with repeated use of the same lubricating fluids, previously prepared before each cycle of use.

2. Identification of previously unsettled parts of the general problem

We research the droplets breakup of the dispersed phase, which is surrounded by other droplets during their boiling. As an object of our study we take an emulsion, shown in (Pavlenko 2018) and schematically presented in Fig. 1.

The diagram (Figure 1) shows a fragment of the structure of the fuel emulsion. It can be of any configuration. The main parameters that affect the homogenization process are the size of the dispersed phase droplets and the distance between the droplets. These parameters can determine the level of energy impact on the emulsion in order to reduce the size of the dispersed phase.

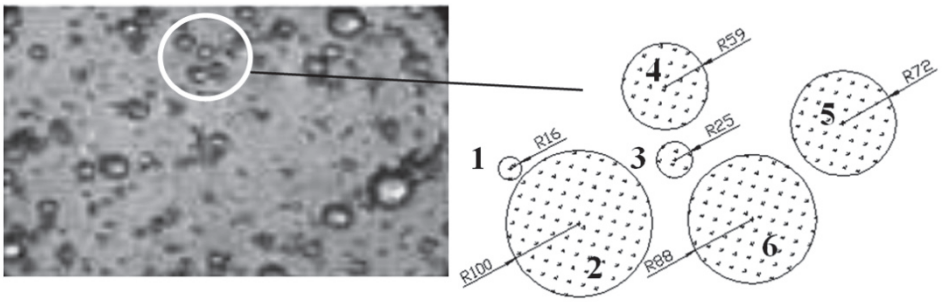

Fig. 1. To the calculated model of droplet breakup of the dispersed phase of the emulsion (characteristic dimensions in microns)

As can be seen from this figure, there are "small" drops between the "large" water drops, the small ones can serve as the sources of increased dynamic forces while boiling and thereby initiate the process of larger droplets breakup, because of the significant difference in accelerations and/or growth rates between them (Pavlenko 2018, Koshlak & Pavlenko 2019, Pavlenko & Koshlak 2019). The main types of instability are the Kelvin-Helmholtz instability caused by the speed difference, and the Rayleigh-Taylor instability, which is caused by the acceleration difference (Pavlenko 2018). Considering a drop of emulsion, it can be concluded that the main role in the processes of its breakup will be played by the forces acting on the normal component to the drop surface, i.e. forces directed either toward the drop center or from it. Acceleration and speed, as the exponents of forces acting on the drop surface from several sources are determined by equation:

$$g_{nr}(x_0, y_0) = \sum_{i=1}^{N-1} g_i(x_0, y_0) \cdot k_{nr_i} \tag{1}$$

$$w_{nr}(x_0, y_0) = \sum_{i=1}^{N-1} w_i(x_0, y_0) \cdot k_{nr_i}\ , \tag{1a}$$

where: x_0, y_0 – the point coordinates on the drop surface; g – acceleration at the desired point, acting from some source, m/s^2; w – speed, acting at a given point from the source, m/s; k_{nr} – correction for the normal component; N – total number of boiling drops of the dispersed phase.

The acceleration and speed acting on the drop surface are determined by equations (Pavlenko 2020):

$$g_i(d_i) = \left[p_{Ri} - p_\infty + 0.5 w_{Ri}^2 \rho_{oil} \left(1 - \frac{4R_i^3}{d_i^3} \right) \right] \frac{R_i}{\rho_{oil} d_i^2}; \tag{2}$$

$$w_i(d_i) = \frac{w_{Ri} R_i^2}{d_i^2}, \tag{2a}$$

where: $d_i(x_0,y_0)$ – the radius vector from the center of *i*-drop to the surface of the considered particle; where w_R – motion speed of the interface oil-vapor, m/s; p_∞ – the pressure in the oil volume at an infinitely large distance from the particle, Pa; R_i – the radius of the *i*-drop particle ($i = 1, 2, \ldots, n$), m; ρ_{oil} – oil density, kg/m^3.

It is important to consider the forces acting on opposite sides of inclusion. Taking a variable angle β, we can determine the coordinates of the unknown opposite points of the particle surface:

$$x_{s1} = x_n + \Delta x;\ y_{s1} = y_n + \Delta y; \tag{3}$$

$$x_{s2} = x_n - \Delta x;\ y_{s2} = y_n - \Delta y; \tag{3a}$$

$$\Delta x = R_n \sin\beta;\ \Delta y = R_n \cos\beta;\ 0 \le \beta < 180^\circ, \tag{3b}$$

where: x_0, y_0 – the coordinates of a given particle; x_{s1}, y_{s1} – coordinates of the surface of one side of the drop; x_{s2}, y_{s2} – coordinates of the opposite side.

Then the correction k_{nr} is determined by the equation

$$k_{nr_i} = \frac{(x_i - x_{s1,s2})\sin\beta + (y_i - y_{s1,s2})\cos\beta}{d_i(x_{s1,s2}, y_{s1,s2})}. \tag{4}$$

Using the equations (1)-(4), it is possible to determine the acceleration profile on the surface of the selected droplet. The results of calculations using the equations (1)-(4) for particle 2 (Figure 1) are shown in Fig. 2.

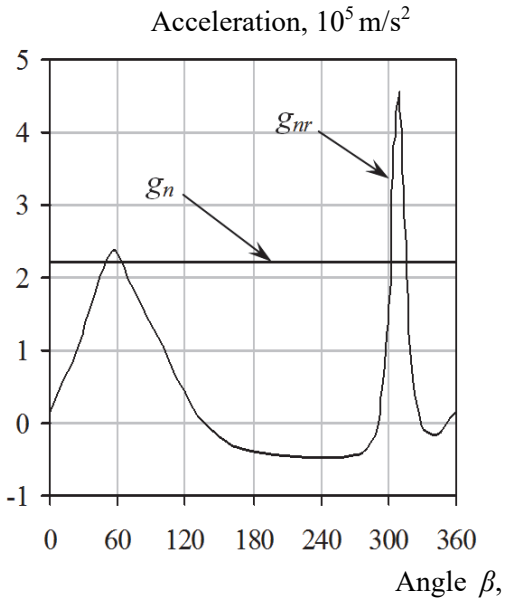

Fig. 2. Acceleration diagram acting on the drop surface No. 2 (Figure 1) from the neighboring boiling particles (g_{nr}) and counteracting acceleration of the particle itself (g_n)

It was assumed for the calculation that the considered system consisting of 6 particles at the initial time is under pressure, which corresponds to the saturation pressure of the thermolabile (water) phase of the emulsion at a temperature of $t_0 = 105$°C. At some timepoint, the pressure drops sharply to atmospheric pressure, as a result of which the water is superheated relative to the saturation temperature at atmospheric pressure, which leads to the appearance and intensive growth of the vapor phase. For the calculation, it was assumed the initial existence of a vapor interlayer (1 μm) on all selected particles at initial temperature and saturation pressure. The results of the calculations are given for the initial moment of pressure release.

Fig. 2 shows a clearly noticeable dependence between the angles of the droplet location relative to the selected one and the magnitude of the acceleration acting from them. There are at once two maxima of acceleration – angle $\beta \approx 57°$ and $\beta \approx 310°$, which corresponds to the angles of the nearest neighboring drops (No. 1 and No. 3, respectively, from Fig. 1). It is clear that the determining effect will have the force caused by the maximum acceleration, i.e. the maximum that is at an angle $\beta \approx 310°$. But in this case, we should also take into account the force that acts on the opposite side of the inclusion. Let us consider the principal

differences in determining the forces acting on the non-boiling and boiling inclusion of the dispersed phase of the emulsion.

Finding, for example, the acceleration and the force caused by it on one and the opposite drop side, we will assume that if two opposing forces are directed toward the center of the selected drop, then the total force acting on the drop is equal to the sum of these two forces. If both forces are directed from the center of the drop, then the total force is also equal to the sum of two vector forces. In case when both forces act in different directions in relation to the center of the drop, i.e. are in one-direction in space, we will consider the driving force the one that has a greater value of the two acting. Thus, the inclusion of a dispersed phase that does not boil (i.e. does not create any counteraction to the forces acting on it), the determining effect leading to possible breakup will be the maximum of two forces that act on opposite sides, under the conditions described above.

In the case where the drop of emulsion begins to boil, it has its own strength, which will counteract the external impact from other sources. Then the driving force can be the one that acts on one side of the inclusion and exceeds the counter-force. This is the main difference in consideration of the forces acting on the boiling drop unlike the non-boiling drop. This means that it is necessary to take into account the two given maxima and determine the main one from them. It is possible the coincidence of these forces maxima.

Taking into consideration the fact accepted in (Pavlenko 2018) that the force action of a drop cannot break this drop, it is possible to write down the equations that will determine the accelerations and speeds acting on the inclusion of the dispersed phase and leading to its breakup. Assuming that the resulting acceleration or speed are positive, then they are the cause of instability, and if they are negative, then there is no destabilizing effect, and we can write

$$g_{p1} = \begin{cases} g_{s1} - g_n; g_n \geq 0, g_{s1} \geq 0, \\ -g_{s1}; g_n > 0, g_{s1} < 0, \\ g_{s1}; g_n < 0, g_{s1} > 0, \\ g_n - g_{s1}; g_n \leq 0, g_{s1} \leq 0, \end{cases} \tag{5}$$

where: g_{p1} – resulting acceleration, acting on one side of the inclusion, m/s^2; g_n – acceleration of the oil-steam interface of the considered inclusion, m/s^2.

For the opposite side we can write an equation similar to (5), but, instead of g_{p1} and g_{s1}, substituting respectively g_{p2} and g_{p2}.

Then, the total acceleration acting on the drop is determined by the equation:

$$\Delta g = g_{p1} + g_{p2}, \tag{6}$$

with necessary conditions, taking the coefficient $Z = \frac{g_{s1}}{g_{s2}}$

$$g_{p1} = \begin{cases} 0; Z < 0, |g_{s1}| - |g_{s2}| < 0; \\ 0; Z > 0 : \begin{cases} g_n > 0, g_{s1} > 0, g_{s2} > 0, \\ g_{s1} - g_n < 0, g_{s2} - g_n > 0; \end{cases} \\ \qquad\qquad \begin{cases} g_n < 0, g_{s1} < 0, g_{s2} < 0, \\ g_{s1} - g_n > 0, g_{s2} - g_n < 0; \end{cases} \end{cases}$$

$$g_{p2} = \begin{cases} 0; Z < 0, |g_{s1}| - |g_{s2}| > 0; \\ 0; Z > 0 : \begin{cases} g_n > 0, g_{s1} > 0, g_{s2} > 0, \\ g_{s1} - g_n > 0, g_{s2} - g_n < 0; \end{cases} \\ \qquad\qquad \begin{cases} g_n < 0, g_{s1} < 0, g_{s2} < 0, \\ g_{s1} - g_n < 0, g_{s2} - g_n > 0. \end{cases} \end{cases} \tag{7}$$

If the maxima of the forces (accelerations, speeds) do not coincide, acting on the opposite sides of inclusion and on one side, we consider the driving force the one that is of greater value

$$g_d = \begin{cases} \Delta g_1, \Delta g_1 > \Delta g_2; \\ \Delta g_2, \Delta g_1 < \Delta g_2, \end{cases} \tag{8}$$

where: Δg_1, Δg_2 - the total acceleration acting on the drop, calculated on the maxima acting respectively on opposite sides and on the one side.

Similarly, we can obtain equations for the speed. In this case, in equations (5)-(8) it is necessary to change the acceleration « g » for speed « w », and equation (6) will be the following:

$$\Delta w = k\sqrt{|w_p|}, \tag{9}$$

where: $k = \begin{cases} +1, w_p \geq 0; \\ -1, w_p > 0, \end{cases}$ $w_p = w_{p1}\left|w_{p1}\right| + w_{p2}\left|w_{p2}\right|$.

Investigations have been carried out on how the forces, acting on the droplet, change as time passes, and also how the angle of maximum force impact changes. The forces caused by acceleration play a decisive role (in comparison with the forces of dynamic pressure), we calculate them by the equations. For these conditions, forces acting on different sides of the surface of the considered particle

$$F_{g1} = 4\pi R_n^3 \rho_{oil} g_{s1}, \tag{10}$$

$$F_{g2} = 4\pi R_n^3 \rho_{oil} g_{s2}. \tag{11}$$

The force of counteraction from the oil-vapor interface of the drop itself

$$F_g = 4\pi R_n^3 \rho_{oil} g_n. \tag{12}$$

The total force acting on the drop

$$F_{Bo} = 4\pi R_n^3 \rho_{oil} g_d. \tag{13}$$

Critical force causing instability according to Bond

$$F_{Bo}^{cr} = 40\pi\sigma R_n, \tag{14}$$

where σ is the surface tension at the oil-vapor interface, N/m.

The force that determines the deformation or displacement of a drop

$$\Delta F_{Bo} = F_{Bo} - 8\pi\sigma R_n. \tag{15}$$

The calculation is carried out either before the fulfillment of the condition

$$F_{Bo} \geq F_{Bo}^{cr}, \tag{16}$$

or before the mutual drops contact, determined by the condition

$$\Delta R_{i,j} \leq 0, \tag{17}$$

where: $\Delta R_{i,j} = d_{i,j} - \left(R_{ni} + R_{nj}\right)$, $d_{i,j} = \sqrt{\left(x_i - x_j\right)^2 + \left(y_i - y_j\right)^2}$; $i = 1,2...N$; $j = i+1, i+2...N$; i, j – the number of drops with the corresponding coordinates $x_i, y_i; x_j, y_j$.

3. Statement of assignment and methods of its solving

The results of calculations using equations (1)-(17) with the equations of the model (Pavlenko 2018) are presented in Fig. 3-4. The calculation was carried out for t_0 = 105°C.

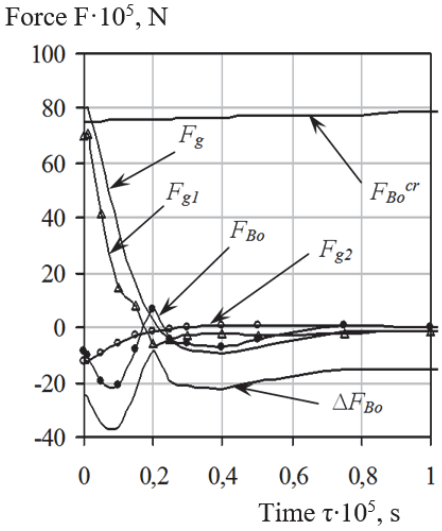

Fig. 3. The changes of forces acting on the drop No 4 over some time period (Fig. 1)

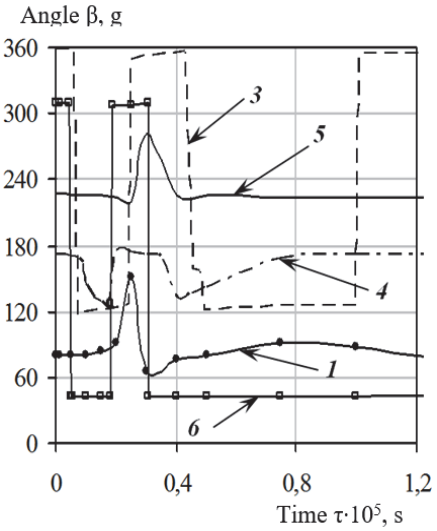

Fig. 4. The changes of the force angle of the maximum force for particles 1, 3-6 (Fig. 1) over some period of time

Fig. 3 shows that the critical force F_{Bo}^{cr} increases with time, which is associated with an increase in the radius of the selected droplet, and the values of forces acting on the drop tend to zero through time. Therefore, we can conclude that if we do not take into account the further interaction of the droplets when they contact, then at t_0 = 105°C if at the initial moments of pressure drop the systems of large drops breakup does not occur, then before the moment of contact they won't breakup. Change curves F_{g1}, F_{g2} show the maximum force that affects at a given time moment. These curves determine the predominance of these forces over the force of opposition F_g, or their insignificance over this force. They also do not determine the force acting at the same angle β, as they greatly depend on the given angle, which is shown in Fig. 4.

If we consider them together, this allows us to determine the force F_{B0}, which, in turn, plays a major role in this process. It can be seen that for the drop No. 4 (Figure 3) with a positive force value F_{B0} is possible only its displacement, which is indicated by a negative sign ΔF_{B0}.

We can also observe a sudden alteration of the force angle of the maximum force mostly for the drops No 3 and 6 (Fig. 4). At the same time particle No 2 was almost fractured at the initial time and, as a consequence, the graph of the force angle change of the maximum force in Fig. 4 for it is not given. As an example we consider the drop No 6. As can be seen from Fig. 4 with the change of the force angle of the maximum force, the dominant effect changes either of the fifth drop ($\beta \approx 40°$) or the third together with the fourth ($\beta \approx 300°$). The first peak of the angle change β at $\tau \approx 0.05 \cdot 10^{-5}$ s can be explained by a sharp decrease in the acceleration of the drop boundary No. 3 and the further predominant action from particle No. 5, after which at $\tau \approx 1.8 \cdot 10^{-6}$ s the third particle has the greatest force.

At the same time, despite the sharp change in the angle β of maximum force action for particles No 3 and 6, for No 5 this angle changes quite smoothly, most of the time is equal to ≈ 230°, i.e. near the action of the maximum force from the drop No 6.

It can be concluded that the angle β can sharply change only in those droplets that are surrounded by others, while for the droplets located quite far from the center the force angle of the maximum force will change by a small value. This can be explained by the fact that for droplets that are inside the emulsion, a maximum force can change quite rapidly both in value and in direction, due to the close position of neighboring droplets, which change their dominant impact on this particle. At the same time, the droplets in the outer layers have neighbors at a small part of their circle, which predetermines the small change value in the force angle of the maximum force.

Fig. 5 shows the changes of the angle of action of the maximum force acting on one side of the inclusion $F_{\Delta g2}$ and on the opposite sides $F_{\Delta g1}$.

It can be seen that there is no clear dependence between the force angles of these forces, they can both coincide and be very much different. Therefore, it is necessary to consider the possible maximum of the force and the angle of its action.

The calculations have been carried out for temperatures t_0 = 180°C and t_0 = 130°C, they showed that at the instant of instantaneous pressure drop, practically all large drops will be crushed, whereas at t_0 = 105°C only the largest drop will be crushed, because of the maximum approximation to its smallest particle.

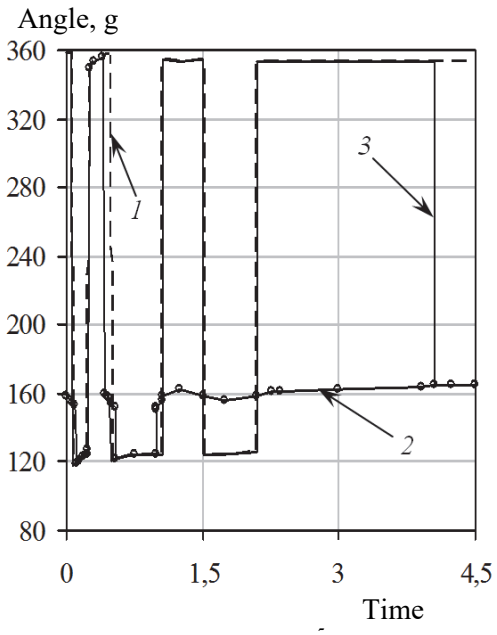

Fig. 5. The changes of the force angle of the maximum force for particle No 3 (Fig. 1), acting on one side (1) and on opposite sides of the inclusion (2), as well as the angle of action of the driving force (3) over some time period

4. Conclusion

A model for the fragmentation of large inclusions of the emulsion dispersed phase under the dynamic influence from boiling neighboring particles is considered. With the help of calculation we found out the force angles of the maximum forces, it can also be seen that the process of boiling inclusions breakup starts at different maximum forces (different angles β) in comparison with non-boiling particles. This indicates the need to find at least two maximal forces that can coincide with the angle of their action on the drop, or differ significantly in this force angle. Of course, it is necessary to take into account both the deformation of the inclusions surface and their displacement, as well as the boiling irregularity of droplets of various sizes. A large role is also played by surface active agents which allow to break up the particle with much less applied effort from other boiling inclusions. The behavior of two or more drops as they approach each other as well as the influence of neighboring drops on the growth of the selected one is still an open question. Taking these phenomena into account

will allow even more detailed and accurate consideration of the processes of growth and the dispersed phase inclusions breakup.

The project is supported by the program of the Minister of Science and Higher Education under the name: "Regional Initiative of Excellence" in 2019-2022 project number 025 / RID / 2018/19 financing amount PLN 12,000,000.

References

Dąbek, L., Kapjor, A., Orman, Ł. (2016). Ethyl alcohol boiling heat transfer on multilayer meshed surfaces. *Proc. of 20th Int. Scientific Conference on The Application of Experimental and Numerical Methods in Fluid Mechanics and Energy 2016, Terchova, Slovakia, AIP Conference Proceedings, 1745*, 020005. DOI: 10.1063/ 1.4953699.

Dąbek, L., Kapjor, A., Orman, Ł. (2018). Boiling heat transfer augmentation on surfaces covered with phosphor bronze meshes. *Proc. of 21st Int. Scientific Conference on The Application of Experimental and Numerical Methods in Fluid Mechanics and Energy 2018, Rajecke Teplice, Slovakia, MATEC Web of Conferences, 168*, 07001. DOI: 10.1051/matecconf/201816807001

Dolinsky, A.A., Basok, B.I., Nakorchevsky, A.I. (2001). *Adiabatically boiling flows*. Kiev, Publishing house: Naukova Dumka, 208.

Dolinsky, A.A., Ivanitsky, G.K. (1995). Theoretical justification of the discrete-pulse energy input. 1. Model of the dynamics of a single vapor bubble. *Heat-process engineering*, *17*(5), 3-29.

Ivanitsky, G.K. (1997). Modeling of the processes of deformation and droplets breakup when moving in liquid. *Heat-process engineering*, *19*(1), 9-16.

Ivanitsky, G.K. (1999). Destruction of emulsion droplets in adiabatically flashing flows. *Heat-process engineering, 21*(4-5), 10-15.

Koshlak, H., Pavlenko, A. (2019). Method of formation of thermophysical properties of porous materials | [Metoda formowania właściwości termofizycznych materiałów porowatych] *Rocznik Ochrona Środowiska, 21*(2), 1253-1262.

Pavlenko A. (2020). Energy conversion in heat and mass transfer processes in boiling emulsions. *Thermal Science and Engineering Progress, 15*, 100439. DOI: https://doi.org/10.1016/j.tsep.2019. 100439.

Pavlenko, A. (2018). Dispersed phase breakup in boiling of emulsion. *Heat Transfer Research, 49*(7), 633-641, DOI: 10.1615/HeatTransRes.2018020630.

Pavlenko, A., Koshlak, H. (2017). Design of the thermal insulation porous materials based on technogenic mineral fillers. *Eastern-European Journal of Enterprise Technologies, 5/12*(89), 58-64. DOI: 10.15587/1729-4061.2017.111996

Pavlenko, A., Koshlak, H. (2019). Heat and mass transfer during phase transitions in liquid mixtures | [Przenoszenie ciepła i masy podczas przemian fazowych w mieszaninach ciekłych], *Rocznik Ochrona Środowiska, 21*(1), 234-249.

Abstract

In this paper we consider the processes of dynamic interaction between the boiling particles of the dispersed phase of the emulsion leading to the large droplet breakup.

It is indicated the differences in the consideration of forces that determine the crushing of non-boiling and boiling drops. It is determined the possibility of using the model to define the processes of displacement, deformation or fragmentation of the inclusion of the dispersed phase under the influence of a set of neighboring particles.

The proposed method allows us to determine the main energy parameters of the homogenization process by boiling the emulsion.

Keywords:
crushing, desorption, force, speed, acceleration, pressure, dispersed phase

Niszczenie struktury wrzących emulsji

Streszczenie

W tym artykule rozważamy procesy dynamicznej interakcji między wrzącymi cząsteczkami zdyspergowanej fazy emulsji, prowadzące do rozpadu dużych kropel.

Wskazano na różnice w uwzględnianiu sił, które determinują kruszenie kropli niewrzących i wrzących. Określono możliwość wykorzystania modelu do zdefiniowania procesów przemieszczenia, deformacji lub fragmentacji włączenia fazy rozproszonej pod wpływem zestawu sąsiednich cząstek.

Proponowana metoda pozwala określić główne parametry energetyczne procesu homogenizacji podczas ogrzewania i wrzenia emulsji.

Słowa kluczowe:
kruszenie, desorpcja, siła, prędkość, przyspieszenie, ciśnienie, faza rozproszona.

MIDDLE POMERANIAN SCIENTIFIC SOCIETY OF THE ENVIRONMENT PROTECTION

Rocznik Ochrona Środowiska

Volume 22. Year 2020 ISSN 1506-218X 82-104

Integrated Approaches to Determination of CO_2 Concentration and Air Rate Exchange in Educational Institution

Valerii Deshko, Inna Bilous[*]*, Volodimer Vynogradov-Saltykov, Maryna Shovkaliuk, Hanna Hetmanchuk*

National Technical University of Ukraine "Igor Sikorsky Kyiv Polytechnic Institute", Ukraine

[*]*corresponding author's e-mail: biloys_inna@ukr.net*

1. Introduction

The effective use of energy resources occupies one of basic places of sustainable development. Having regard to the increase of standard of living, urbanization, part of buildings energy consumption grows. This range of problems touches public and housing building. Taking into account sourcing for coverage of building services, especially sharply the question of the effective use of power resources appeared in Ukrainian public sphere, that is related to wearing out of building stock and shortage of financing (Deshko et al. 2013). Providing of the prudent use of energy without the loss of terms of comfort is basic directions nowadays. IEA EBC Annex 53 (Yoshinoa et al. 2017) employed an interdisciplinary approach including physical and human-related factors to analyze and evaluate the real energy use in buildings. Building operation and maintenance, occupants' activities and behavior, and indoor environmental quality can have a significant influence (Yoshinoa et al. 2017).

In most cases, energy efficiency improvement starts with thermo- readjustment measures in the building (Dumała & Skwarczyński 2011, Siuta-Olcha et al. 2016). Reducing energy consumption and ensuring comfort conditions (Deshko et al. 2020) are important synergy effects in implementing energy saving measures.

At state and regional level one of the most guided segments there are public building, among them the special attention is paid to establishments of education.

Lately large consideration is spared to a vent constituent (to determination of air exchange rate) that can present 30-50% of general energy consumption (Younes et al. 2012, Jokisalo et al. 2008, Frączek et al. 2018). For providing of the proper terms of labour from the point of view of ventilation in a standard (EN 12831: 2003) regulated normative air exchange rate. In building the ventilation air exchange rate is provided in two ways: natural and mechanical. In most old Ukrainian educational building mechanical ventilation is not envisaged or not works. Thus through wearing out of main building stock the ventilation comes through air-channels, airing and leaks in windows, doors etc.

Features of energy-saving measures implementation in Ukraine follow the general trends in Central and Western Europe, where after the implementation of measures associated with improvement of building envelope thermophysical properties, the CO_2 concentration in premises with natural ventilation has increased significantly (Földváry et al. 2017). Reducing this component is the second step in implementing energy-saving measures in Ukraine. Therefore, in the context of widespread implementation of programs aimed at increasing the thermal protective properties of the building envelope, greater attention should be paid to factors influencing natural ventilation (free convection). Air exchange is affected by a large number of parameters which can be conventionally divided into internal and external (Fig. 1).

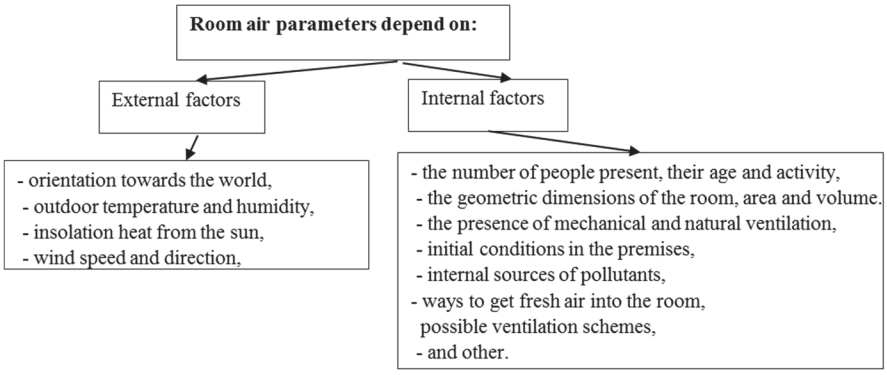

Fig. 1. Parameters affecting indoor air quality

The intensive use of educational buildings brings to the substantial increase of CO_2 concentration indoors, which needs an additional study. Carbon dioxide (CO_2) is one of the indicators of the human bioeffluents emission. There is a classification that is generally accepted and used in standards for premises occupied by people, where the main contamination is caused by human

metabolism (DBN V.2.2-3:2018, DBN V.2.5-67:2013, EN 15603:2008, DSTU B A.2.2-12:2015). At the same time, determining the carbon dioxide content by means of modern portable devices is a simple and convenient method to determine asthma and to carry out ventilation in school classrooms on the basis of these measurements.

Permissible values for the CO_2 content in classrooms compared to the requirements of standards of other countries and Ukraine are given in Table 1 (Kapalo 2018, DIN EN 15251), which are slightly different.

Considerable attention is paid by scientists to the determination of actual air exchange and the indoor CO_2 concentration (Földváry et al. 2017, Konig et al. 2018, Johnson et al. 2004, You et al. 2012, Stabile et al. 2017). There are various methods to measure air exchange rates, for example SF6 tests (Johnson et al. 2004), but usually they are quite complex and expensive. A number of studies have been carried out based on a field experiment to determine the natural air exchange for buildings in South China and Europe (Yongming et al. 2017, Almeida et al. 2017); the studies require special equipment and provide an average view on air exchange taking into account the variability of internal and external parameters affecting air exchange over time. Convenient air exchange rate monitoring method using continuous CO_2 sensors was developed through both laboratory experiments and field studies in classrooms in China (You et al. 2012). Similar approaches have been used in articles (Shi et al. 20015, Leivo et al. 2017, Salthammer 2019). The results obtained by such methods should be supplemented and analyzed by mathematical modeling. Similar approaches for determining the natural air exchange were used on animal farms in Germany (Konig et al. 2018); the peculiarity being that the buildings, where the animals were located, were single-storey, long-shaped and had large doorways.

The article (Földváry et al. 2017) notes that residential buildings in Central and Eastern Europe do not comply with modern energy efficiency requirements. In addition, indoor air quality is not given due attention. The authors (Földváry et al. 2017) conducted a study of the CO_2 concentrations in a residential building in Slovakia before and after renovation. It was found that after renovation the air exchange is significantly reduced and the indoor CO_2 level is increased, that is, the implementation of measures to improve the thermal protection properties of the building envelope should go together with measures for mechanical ventilation.

For schools in Central Spain with natural air exchange (Stabile et al. 2017) occurring through opening of windows, a study was conducted regarding the CO_2 concentration in classrooms for the heating and air conditioning period having the recommendations for airing the classrooms established, which can vary from 5 to 20 minutes, depending on a number of internal and external factors. Similar problems with high levels of CO_2 are typical for schools in Ukraine.

Table 1. Comparison of standards for the CO_2 content requirements in classrooms

	Country	Standard	CO_2 Level
1.	Finland	Ministry of Health and Social Development Standard, 2003	Air quality: high – 700 ppm; medium – 900 ppm; satisfactory – 1200 ppm.
2.	USA	US Department of Health Reference Guide on Indoor Air Quality in Schools	Limit: 1000 ppm
3.	USA	ASHRAE 62-1989 Standards "Ventilation for Acceptable Indoor Air Quality"	1000 ppm
4.	USA	The Occupational Safety and Health Administration (OSHA) Recommendations, 1994	800 ppm
5.	Poland	PL-EN 15251:2012	500 ppm+CO_2 concentration in the intake air
6.	Russia	GOST 30494-2011	Optimal values: 500-800 ppm. Acceptable limit: 1400 ppm.
7.	Great Britain	"Ventilation in School Buildings. Standards and Design Manual", 2006.	1500 ppm – limit value for a school day from 9.00 to 15.30
8.	Nether lands	"Overview of Indoor Air Quality Standards for Kindergartens in the Netherlands" Hygiene Standards	1000 ppm – hygienic standard for kindergartens; 1200 ppm – hygienic standard for schools;
9.	Estonia	Standards of the Ministry of Social Affairs	1000 ppm – hygienic standard for schools
10.	Germany	DIN EN 15251, Input parameters for indoor climate for design and energy performance evaluation of buildings - indoor air quality. Temperature, light and acoustics. 2007	Absolute concentration for energy efficiency calculations 750…1200 ppm
11.	Ukraine	DBN B.2.2-3:2018 with reference to DSTU B EN 15251:2011	750…1200 ppm

Simulation modeling based on physical and empirical calculation methods is widely used for the analysis of natural air exchange. Physical models for determining natural air exchange are quite complex and require a large number of output parameters, which significantly complicates the calculation for buildings with many zones. These approaches use algebraic equations that relate features of the building, such as height, orientation, air permeability of building envelope, and weather conditions. One of the first approaches was developed by Shaw and Tamura (Ng et al. 2015), which was based on a single equation that combined the stack and wind effect to calculate the natural air exchange rate.

An alternative variant is the use of empiric methods of determination of ventilation exchange rate on the basis of standards of ASHRAE and BLAST. Methods of the ASHRAE standards can be applied to low-rise buildings (Jokisalo et al. 2009, Chen et al. 2012, Nielsen & Drivsholm 2010). Ventilation is created on the basis of three mechanisms: the stack effect, wind effect and mechanical ventilation, first two touch the natural constituent of ventilation. Among these mechanisms a wind effect has the most difficult nature (Bilous et al. 2018) and depends on number of storeys, orientations of apartment speed and direction of wind et all. Empirical approaches have been reflected in software for calculating the energy performance of buildings. Among the most widely used software complexes for energy modeling of buildings are: eQuest, EnergyPlus, TRNSYS, DOE2, DesignBuilder, and Ecotect Analysis. More recently proposed a method of estimating infiltration in commercial buildings using EnergyPlus, which considers wind, not just temperature effects, but does not take into account the wind direction (Ng et al. 2013, Bilous et al. 2020).

One of the software used for the analysis of air flows in buildings is CONTAM (Ng et al. 2014, Ferdyn-Grygierek & Baranowski 2015). CONTAM is a multi-zone computer program for air quality and ventilation analysis that allows determining infiltration, exfiltration and airflows into rooms from controlled mechanical ventilation systems, wind pressures acting on the exterior surfaces of a building, the stack effect caused by the difference in indoor and outdoor air temperatures, concentrations of pollutants and their effects on humans. It should be noted that this software product is used at the design stage and has not found its application in the energy management of existing buildings.

It follows from the inspection that the study of the indoor air quality and air exchange parameters requires considerable attention both in low-efficiency buildings and in efficient buildings. A number of approaches are being used based on experimental, physical or empirical methods. The combination of methods will allow achieving best results that can be used in energy management, in implementing energy saving measures and ensuring adequate working/staying conditions in buildings.

The aim of the work is to apply integration of approaches for the determination of the CO_2 concentration and the air exchange rate in educational institutions of Ukraine on the basis of field and simulation modeling.

Tasks:

1) to investigate the factors that affect the change in the concentration of CO_2 in the premises of schools,
2) to explore the use of CO_2 concentration data to determine air exchange rates,
3) to create simulation models for determining natural air exchange based on empirical methods,
4) to compare of air exchange rates data from experiment and simulation.

2. Materials and methods

In this work, field and simulation modeling were conducted to determine changes in the indoor CO_2 concentration and natural air exchange in educational institutions, on the example of objects located in the city of Kyiv; the research scheme is presented in Fig. 2.

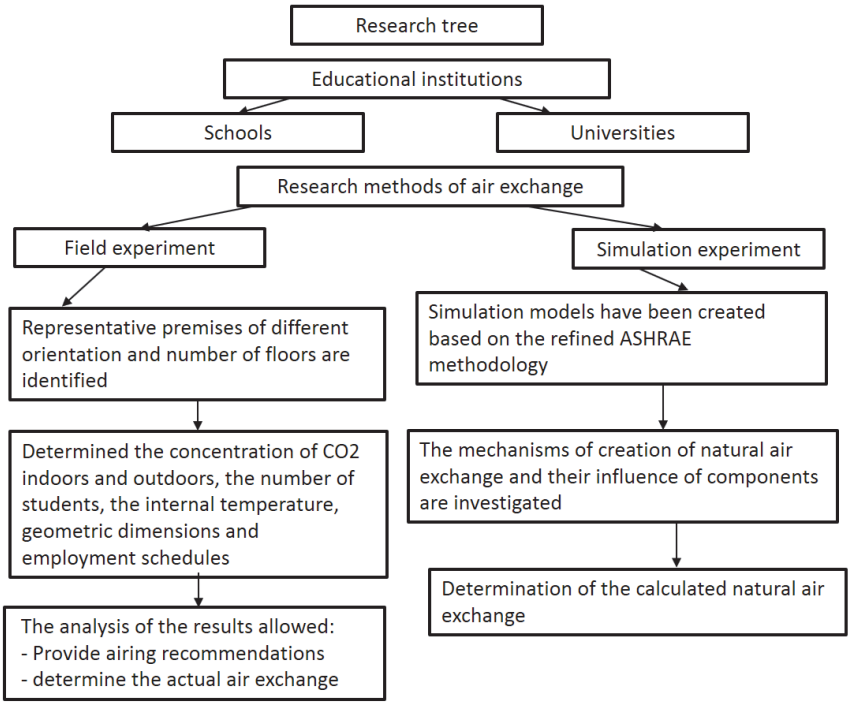

Fig. 2. Research scheme

2.1. Field experiment

The research was conducted consistently and developed in three schools and university. All schools are of typical H-shape, built in the years of mass development. On the basis of school 1 the substantiation of the representative rooms' definition was carried out, the local place of the sensors installation in premises for determination of the CO_2 concentration and other input parameters for calculation of the natural rate of air exchange were investigated. In school 2, the CO_2 concentrations in representative rooms were measured at the beginning and at the end of classes. In school 3, the CO_2 concentrations were measured for two options: 1) measurements of the CO_2 concentration in representative rooms at the beginning and at the end of classes; 2) recording of the dynamics of changes in the CO_2 concentration in representative rooms with 10 min. steps, taking into account changes in the number of students, physical activity and the schedule of the classroom occupancy. Experimental measurements of the concentration changes in representative rooms were carried out in the training building of Igor Sikorsky KPI. A local study of the background outdoor concentration of CO_2 was conducted near the examined objects during the day with different distances from them. Measured: outdoor temperature and relative humidity and in classes; speed and direction of wind on the street; CO_2 concentration on the street / background; schedule of stay of people and their number in classes; type of physical activity of people.

For the measurements were used:

- Complex device CO_2 logger TR-75Ui with CO_2 measurement range: 0…9999 ppm, temperature: 0… 55°C, relative humidity: 10… 95% RH.
- Thermistor electronic complex LM8000 device with temperature measurement range 20°C… + 65°C and relative humidity 10…95% RH was used for duplication of air temperatures and relative humidity.
- GM320 pyrometer with measurement range 50°C… + 380°C for wall surface temperatures measurements.
- The Eco Dist Plys laser rangefinder with the ability to measure up to 30 m and 1mm accuracy was used to measure the area and volume of the classes, as well as the built-in area and volume calculation function.

2.2. Methodology for analyzing the correlation between the CO_2 concentration data and air exchange, as well as methodology for processing experimental data

On the basis of balances of air flows and the indoor CO_2 concentrations (marking at Fig. 3) the following ratios were obtained.

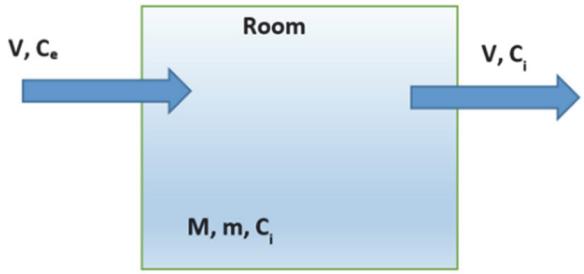

Fig. 3. Schematic representation of marking to CO_2 and air exchange values in the room V_r - rooms, m^3; V – air exchange, $м^3$/hour; m – indoor CO_2 emission, g/hour; M – indoor CO_2 mass, g; M_o – indoor CO_2 initial mass, g; C_e, C_i, C_{i0} – CO_2 concentration in the intake air, in the room at a given time and initial concentration, g/m^3

Indoor CO_2 concentration is determined as follows:

$$C_i = \frac{M}{V_r}, \tag{1}$$

Change in CO_2 amount over time:

$$\frac{dM}{d\tau} = m + V \cdot C_e - \frac{V}{V_r} M, \tag{2}$$

Amount of CO_2 in a time interval $\Delta\tau_j$:

$$M_j = M_{j-1} + \overline{m_j} \triangle \tau_j + \overline{V_j} \cdot \overline{C_{e.j}} \triangle \tau_j - \frac{\overline{V_j}}{V_r} \cdot \frac{M_{j-1}+M_j}{2} \triangle \tau_j, \tag{3}$$

In n time intervals $\Delta\tau_j$ formula (3) becomes as follows:

$$j = 1 \ldots n, \quad M_n = M_0 + \sum_{j=1}^{n} m_j \triangle \tau_j + \sum_{j=1}^{n} V_j \cdot C_{e.j} \triangle \tau_j - \sum_{j=1}^{n} \frac{V}{V_r} \cdot M_j, \tag{4}$$

Formula (4) can be used to determine the mass of CO_2 in the internal air through the values of C, V and m for each time interval $\Delta\tau_j$.

Integration of formula (2) at constant values C_e, V and m gives an expression for the mass of CO_2 in internal air at any point of time τ:

$$M = \frac{V_r}{V}\left\{ m + V \cdot C_e + \left[\frac{V}{V_r} \cdot M_0 - \left(m + V \cdot C_e \right) \right] \cdot e^{-\frac{V}{V_r}\tau} \right\}, \tag{5}$$

It follows from formula (5) that the internal concentration of CO_2 at constant values C_e, V and m is determined as follows:

$$C_i = \frac{m}{V} + C_e + \left[C_{i0} - \left(\frac{m}{V} + C_e \right) \right] \cdot e^{-\frac{V}{V_r}\tau}, \quad (6)$$

For boundary cases, formula (6) becomes as follows (7-8):

$$If \ \ m \to 0, C_i = C_e \left(1 - e^{-\frac{V}{V_r}\tau} \right) + C_{i0} \cdot e^{-\frac{V}{V_r}}, \quad (7)$$

$$If \ \ m \to 0 \ \ i \ \ C_i >> C_e, C_i = C_{i0} \cdot e^{-\frac{V}{V_r}\tau}. \quad (8)$$

Experimental data on changes in the indoor CO_2 concentration over time were processed by formula (6).

2.3. Simulation experiment

Air exchange is difficult to determine experimentally. Even with the same window designs in terms of air permeability, different amounts of air enter the room. Room air exchange depends on a number of factors, both external and internal ones. Simulation models were created for the representative rooms of the training building of Igor Sikorsky KPI to determine the natural air exchange of rooms based on the ASHRAE generalizing methodology. The use of simulation modeling allows to compare results and to verify the proposed methods of determining actual air exchange rate based on experimental data.

Methods

The methodological basis of the scientific research includes methods of mathematical modeling, systematic approach considering climatic and operational factors.

The generalization of the methods for air exchange rate determination based on the calculation of pressure differences given in the studies of Berge A. and others (Biler et al. 2018, Berge 2011) and according to the ASHRAE approaches (Jokisalo et al. 2009) is used in the paper, which allows to use the given technique for multi-story buildings. The pressure difference that determines the air exchange rate in a building is created by two different mechanisms: stack effect, wind pressure effect (Fig. 4) and is calculated as their sum (formula 9):

$$\Delta P_{tot} = \Delta P_s + \Delta P_w = \Delta P_{int}, \quad (9)$$

where:

ΔP_{tot} – total pressure difference, Pa,

ΔP_s – pressure difference from stack effect, Pa,

ΔP_w – the wind pressure difference, Pa,

ΔP_{inf} – infiltration pressure difference, Pa.

The stack effect is also called the buoyancy effect created by the difference in density between warm and cold air. Reduction of air pressure with the height determined by the formula (10):

$$\Delta P_s = z(\rho_e - \rho_i) \cdot g, \tag{10}$$

where:
z – height from the reference point, m
ρ_e, ρ_i – density of exterior and interior air, kg/m^3,
g – acceleration of gravity, m s^2.

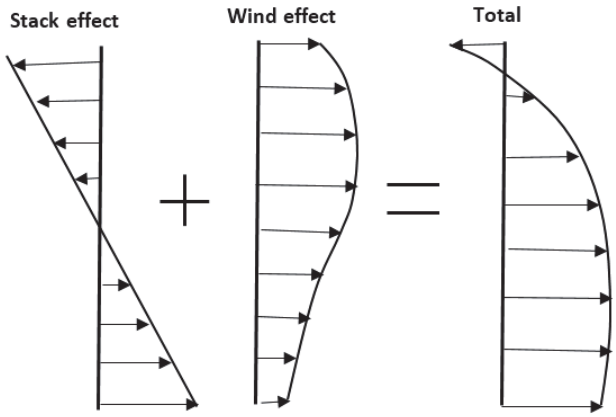

Fig. 4. Example of building height distribution and sum of pressure difference profiles

From the neutral pressure level towards the first floor, the pressure difference is positive, towards the last floor it is negative. Assuming that air is the perfect gas, formula (10) looks like:

$$\Delta P_s = 3456 \cdot z\left(\frac{1}{T_e} - \frac{1}{T_i}\right), \tag{11}$$

where:
T_e, T_i – exterior and interior air temperature, respectively, K.

Wind pressure is created when airflow hits an obstacle. The magnitude of the wind pressure depends on the wind speed and direction (windward, leeward side, etc.).

Most software products for modeling wind pressure, use the following formula (Biler et al. 2018, Berge 2011):

$$\Delta P_w = \frac{\rho U_{met}^2}{2} C_h C_p(\theta) \tag{12}$$

where:
ρ – density of the environment, kg/m^3,
U_{met} - wind speed according to the nearest weather station, m/s,
$C_p(\theta)$ – wind pressure factor considering wind direction through the angle of incidence θ,
θ – the magnitude of the wind angle relative to the normal drawn to the considered surface, degree,
C_h – wind pressure factor that considers the height.

The amount of air entering the room due to leakage under the specified conditions (without mechanical ventilation) is determined by the following formuls:

$$G_{\text{inf}} = C(\Delta P_{\text{inf}})^p \qquad \text{or} \qquad G_{\text{inf}} = \frac{\Delta P_{\text{inf}}^{\ p}}{R_b} F_w \tag{13}$$

where:
G_{inf} – the amount of air entering the room due to leakage, kg/h,
C, p – this coefficient and the degree index depend on the purpose of the building,
R_b – window air permeability resistance, (m^2·h·Pa$^{2/3}$)/kg
(DSTU B V.2.2-19:2007),
F_w – window area, m^2.

The space air exchange rate as a characteristic of the ventilation node in mathematical models is determined by the following formula (DSTU B V.2.2-19:2007):

$$n = \frac{G_{\text{inf}}}{\rho V} \tag{14}$$

where:
V – volume of the space, m^3,
n – air exchange rate, h^{-1}.

Determining the natural rate of air exchange based on ASHRAE advanced methodology does not take into account room-to-room airflows through ventilation ducts/extractors, but it does take into account wind speed and direction, but it takes

into account number of storeys, orientation, and so on. Determining the air exchange rate based on experimental methods does not give a clear idea of the infiltration or exfiltration component, and may be established during processing, and physical representations of the natural air exchange in buildings.

3. Results and discussion

On the basis of formula (6) a calculated study of the influence of air exchange, initial concentration and indoor CO_2 emissions, air flow by way of infiltration and exfiltration on the indoor CO_2 concentration was conducted.

Decreasing (Fig. 5, b) / increasing (Fig. 5, a) exponential curve at the same m/V ratio is due to different initial concentrations of CO_2 and indicates the time of airing / lack of airing respectively.

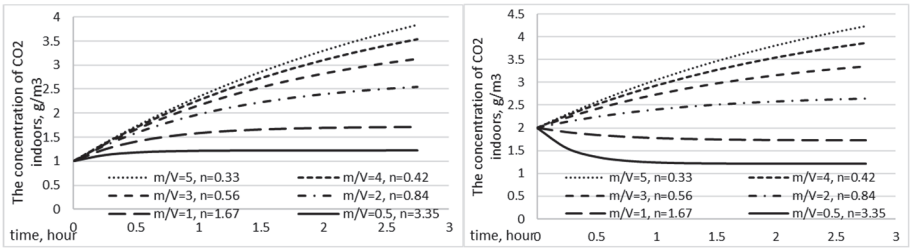

a) b)

Fig. 5. Change in the indoor CO_2 concentration over time provided that the number of present persons and different initial indoor CO_2 concentrations is constant

Fig. 6 shows the influence of the number of present persons on the indoor CO_2 concentration at a constant air exchange: 0.5 h^{-1} (Fig. 6, a) and 1 h^{-1} (Fig. 6, b) at the initial concentration: $C_{i0} = 2$ g/m^3.

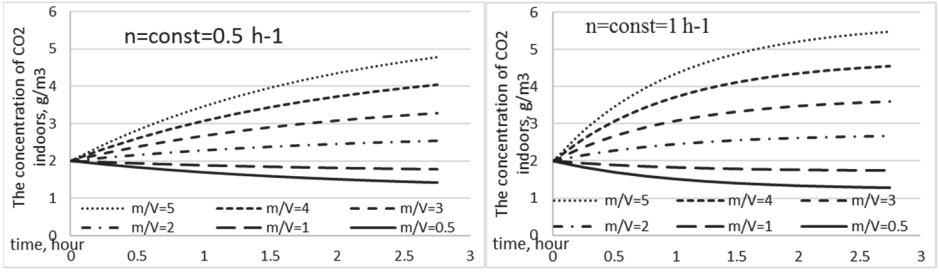

a) b)

Fig. 6. Change in the indoor CO_2 concentration over time under the condition of constant air exchange and different amount of present persons (indoor CO_2 emissions, m)

Reduction of the air exchange rate results in smaller degree of bend of the exponential dependence of CO_2 concentration over time. The number of present persons has a more significant impact on the indoor CO_2 concentration (Fig. 6) than on the air exchange rate (Fig. 5).

3.1. Experimental part

Experimental determination of the background concentration of CO_2 during the day locally next to the considered objects showed that the background concentration of CO_2 is in the range of 400-420 ppm. On the example of school 1 an experimental study was conducted to determine the local measurements of the indoor CO_2 concentration during and after classes. Measurements of the CO_2 concentration distribution were carried out after classes throughout the classroom area, and the difference between the values at the desks level was 30...180 ppm. Studies have shown that it is acceptable to use an integral characteristic of the CO_2 concentration in a representative room in the center of the room at an altitude of about one meter (the working area).

Measurements of the internal concentration of CO_2 results in school 2 during the vacation period were quite close to the background concentration, with the exception of classes where the project groups worked. Control measurements of the indoor CO_2 concentration were made at the beginning of classes, after classes and after a break.

It has been established that the CO_2 concentration is changed during the class to 700-1100 ppm and significantly exceeds the standard. During a break, the CO_2 concentration is reduced to 500-1000 ppm, depending on the type of ventilation.

At school 3, 10-minute measurements of the CO_2 concentration were made in representative rooms. Fig. 7 shows the determination of the air exchange rate on the example of high school students during three classes and two breaks.

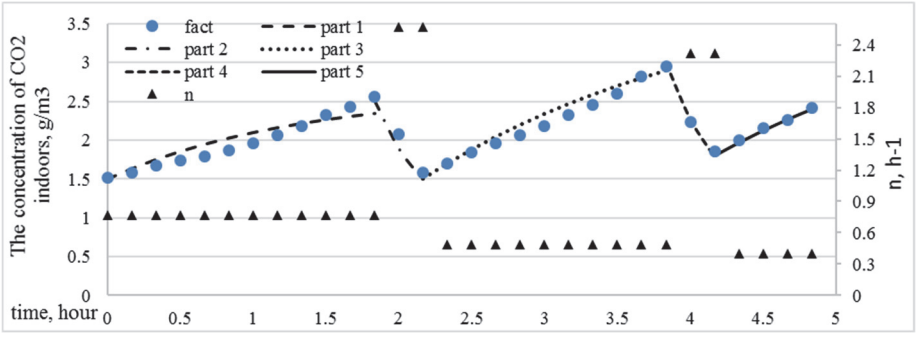

Fig. 7. Change in the indoor CO_2 concentration and air exchange rate in a classroom of school 3

The air exchange rate during classes (parts 1, 3, 5) is in the range of 0.4...0.75 h^{-1} (windows and doors are closed). During breaks, students leave the premises and the classrooms are ventilated through the opening of windows and doors. During this period (parts 2, 4), the air exchange rate is increased to 2.9-3.5 h^{-1}. For the range considered, the weighted average air exchange rate is 0.8 h^{-1} and even with forced airing, the air exchange rate is insufficient to ensure an adequate level of air exchange and the acceptable CO_2 concentration.

Similar studies of changes in the CO_2 concentration were conducted for the training building of Igor Sikorsky KPI. The building is long, 7-storey, with a technical floor, the main part of training classrooms and laboratories has one external S or N oriented envelope. Ventilation of the classrooms in the building is carried out by opening of doors to the corridors, mechanical ventilation is out of order. On the example of processing the experimental data on the change in the CO_2 concentration in classrooms, the calculation of natural rate of air exchange was performed (Fig. 8).

Decrease of the air exchange rate on the 3rd floor is explained by the reduction of the stack effect (according to the components of the air exchange mechanism Fig. 4).

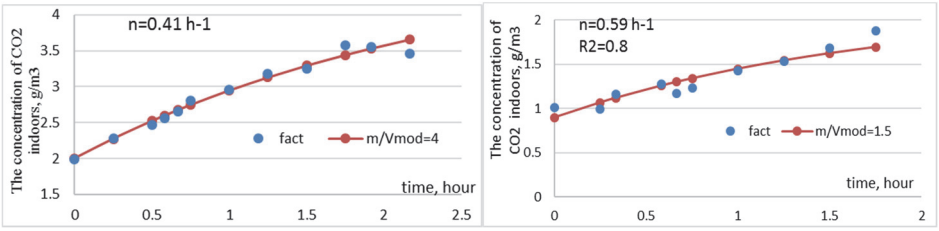

a) b)

Fig. 8. Air exchange in S oriented rooms on 3rd floor (a) and 1st floor (b)

Similar studies were conducted for large lecture halls, where the effect of ventilation during the break was more significant. Figure 9 provides determinations of air exchange rates based on the average air exchange (a) separating the periods where doors were opened (parts 2, 4) and closed (parts 1, 3) (b).

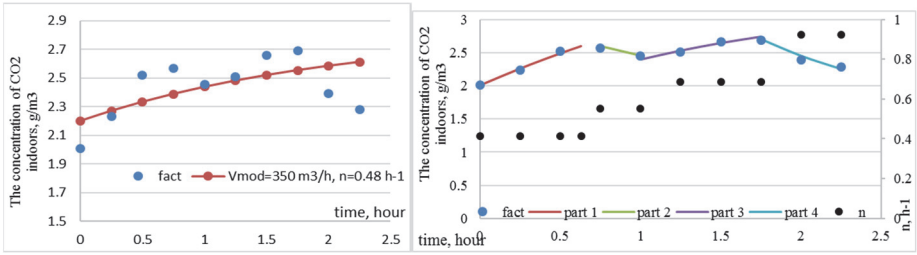

a) b)

Fig. 9. Changes in CO_2 concentration in the lecture hall (Igor Sikorsky KPI)

It follows from the analysis that the value of the average air exchange is 0.48 h^{-1} (processing of the graph with average values of *V*), after separate processing of parts 2, 4 and parts 1, 3 it is established that the air exchange rate during periods of the closed doors is 0.4-0.6 h^{-1}, and if the doors are open, it can reach 0.95 h^{-1}. The weighted average air exchange rate for the considered time period during partial analysis is 0.43 h^{-1}, as opposed to 0.48 h^{-1} for the average formula.

3.2. Simulation modeling

Simulation modeling of natural air exchange of N and S oriented rooms was carried out for the training building of Igor Sikorsky KPI.

Fig. 10 shows the change in climatic conditions during three days when experimental studies were conducted.

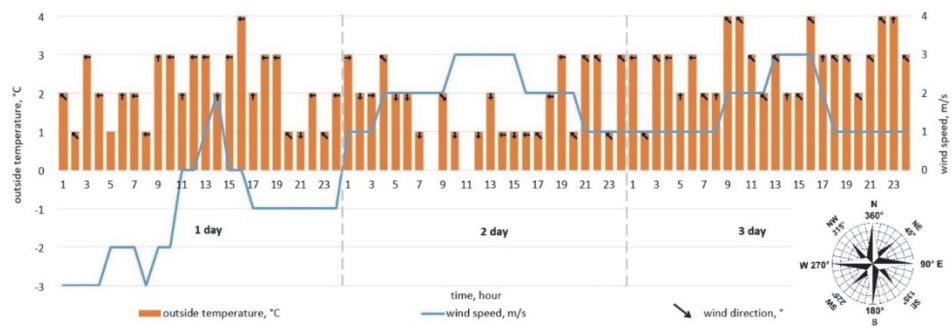

Fig. 10. Climatic conditions change

It follows from the meteorological data analysis (Fig. 11) that the dominant wind direction is SE (135°) (Fig. 11, a), wind speed is 3 m/s (Fig. 11, b), outside temperature is +1°C (Fig. 11, c).

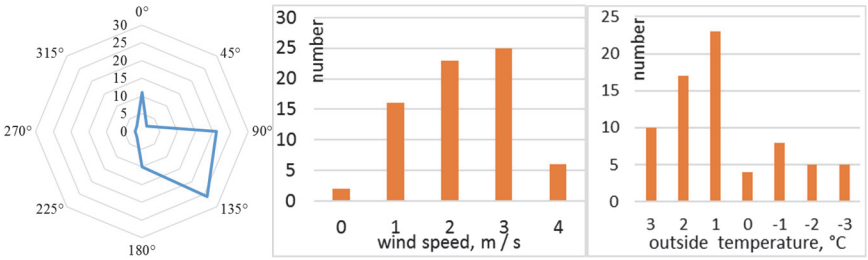

Fig. 11. Dominant parameters of the external weather conditions

A study of pressure changes under the influence of stacks and wind effect for dominant weather conditions was conducted. Fig. 12 shows the change in pressure difference of stack effect depending on the floor and outside temperature at a constant internal air temperature of 18°C.

Change in pressure due to the stack effect is directly proportional to the indoor and outdoor temperature difference. The negative value of ΔP_s is due to the starting point of the pressure difference from neutral pressure (NPL), which is on the middle floor of the building. The NPL level is the level at which the internal and external pressures are the same. The pressure difference is positive from the NPL level towards the ground floor; the pressure difference is negative from the NPL level towards the last floor.

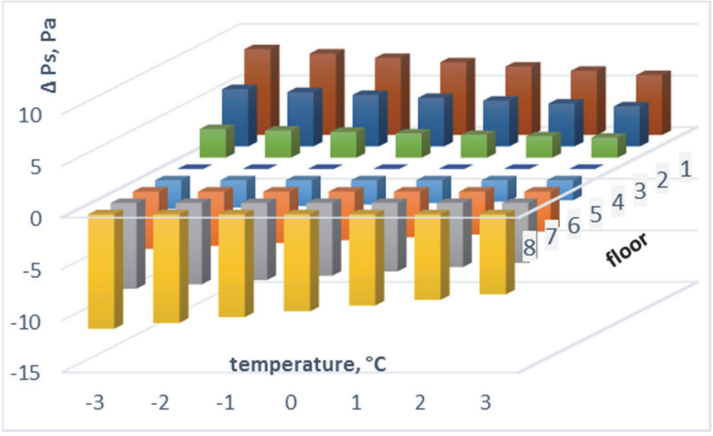

Fig. 12. Change in stack effect pressure depending on the outside temperature and floor number

Change in pressure due to the stack effect is directly proportional to the indoor and outdoor temperature difference. The negative value of ΔP_s is due to the starting point of the pressure difference from neutral pressure (NPL), which is on the middle floor of the building. The NPL level is the level at which the internal and external pressures are the same. The pressure difference is positive from the NPL level towards the ground floor; the pressure difference is negative from the NPL level towards the last floor.

Fig. 13 shows the profiles of the wind effect pressure changes for northern and southern orientation of the building for dominant wind direction and speed. For the southern orientation of premises, the wind pressure change profile has a positive sign, which is explained by the positive value of the $C_p(\theta)$ coefficient, which depends on the wind speed. At SE wind direction $C_p(\theta)$ is positive for premises of southern orientation, but it is negative for premises of northern orientation.

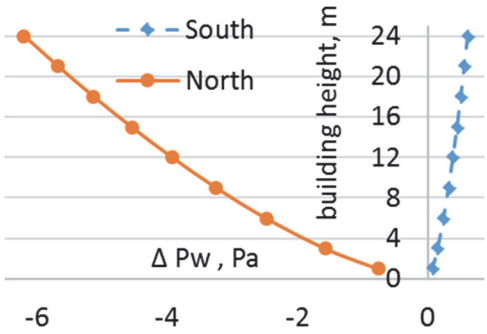

Fig. 13. Wind effect pressure change

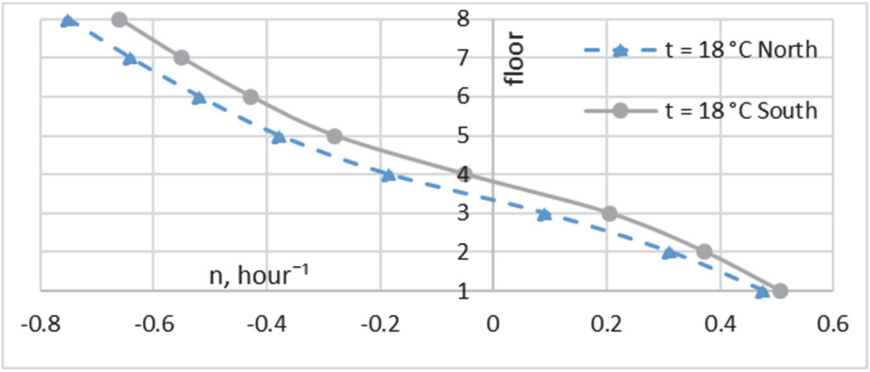

Fig. 14. Average change in the air exchange rate by height of a building for S and N oriented rooms

It follows from Figs. 12, 13 that the air exchange rate is more significantly affected by the difference in pressure caused by the stack effect rather than the wind effect. Fig. 14 shows the average change in the air exchange rate by height for N or S oriented premises. The difference of profiles of air exchange rate change by height for N or S oriented premises is explained by the predominant SE wind direction.

Figure 15 shows the hourly change in the air exchange rate for N or S oriented representative rooms. For the considered input parameters, the air exchange rate varied during three days in the range of 0.53-0.73 h^{-1}. Experimental determination of the air exchange rate (Fig. 8, b) showed that the air exchange rate for premises on the 1st floor is at the level of 0.6 h^{-1}. Simulation modeling with sufficient accuracy fits the experimental results.

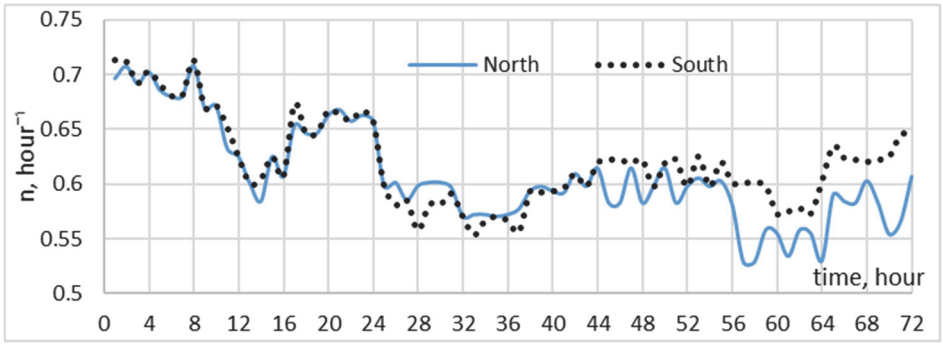

Fig. 15. Hourly change in the air exchange rate for S or N oriented rooms on the 1st floor

4. Conclusions

Studies of the air quality and air exchange were conducted in educational institutions of the city of Kyiv (Ukraine) based on field and simulation experiments. The work shows that CO_2 measurements are important not only for controlling the provision and regulation of the comfort conditions, but can also serve to determine the actual values of the air exchange rate in certain rooms.

On the example of the study in three schools in Kyiv it was found that:

1) Experimental study of the local background CO_2 concentration in the studied buildings is almost constant in time and is about 450 ppm.
2) The concentration of CO_2 in classrooms during classes increases almost twice and exceeds the norm by 700-1100 ppm. During the vacation period, the concentration of CO_2 in classrooms is close to the background concentration.
3) The model calculation showed that a decrease in the air exchange rate leads to a smaller degree of bend of the exponential dependence of the CO_2

concentration in time. The number of present persons has a more significant effect on the indoor CO_2 concentration than the air exchange rate.

4) The experiment has shown that the indoor CO_2 concentration increases significantly during classes, so it is necessary to do airing, but its available level is not always sufficient. The air exchange rate during the classes is in the range of 0.4...0.75 h^{-1} (windows and doors are closed); during airing of classes through the opening of windows and doors, the air exchange rate increases to 2.9-3.5 h^{-1}, the weighted average air exchange rate is 0.8 h^{-1}, and even with forced airing of classes the air exchange rate is not enough from the point of view of ensuring the proper level of air exchange and the permissible concentration of CO_2.

Similar studies were conducted for the training building of Igor Sikorsky KPI. The following was established:

1) Based on experimental data, the air exchange rate for the training building of the educational institution is in the range of 0.35-0.7 h^{-1} depending on the location of the classrooms. During the periods of airing (opening of doors to the corridor), the air exchange can increase by 0.45 h^{-1}, but this does not allow to reach the standard value.
2) In this work, a simulation model was created to determine the natural air exchange of the training building of the educational institution, based on the improved ASHRAE methodology and allows determining the air exchange rate under the conditions of variability of the environment, floor and orientation of premises.
3) It was found that air exchange is more sensitive to changes in pressure caused by the stack effect rather than wind effect.
4) The value of the natural air exchange based on a simulation experiment is in the range of -0.8...0.5 h^{-1}. Negative values are explained by exfiltration.
5) In the total energy balance of the building losses, the ventilation component is 30-60%. Not only comfort conditions depend on the actual level of the air exchange rate, but also the total energy consumption of the building that significantly affects the level of energy efficiency, and monitoring of the actual level of the air exchange rate should be taken into account during the complex modernization or implementation of the ventilation systems with heat recovery.

References

Almeida, R., Ramos, N., Pereira, P. (2017). A contribution for the quantification of the influence of windows onthe airtightness of Southern European buildings. *Energy and Buildings*, *139*, 174-185.

Berge, A. (2011). *Analysis of Methods to Calculate Air Infiltration for Use in Energy Calculations*. Sweden. 98.

Biler, A., Tavil, A., Su Y., Kha, N. (2018). A Review of Performance Specifications and Studies of Trickle. *Vent. Buildings*, *8*, 152-183.

Bilous, I., Deshko, V., Sukhodub, I. (2018). Parametric analysis of external and internal factors influence on building energy performance using non - linear multivariate regression models. *Journal of Building Engineering*, *20*, 327-336.

Bilous, I.Yu., Deshko, V.I., Sukhodub, I.O. (2020). Building energy modeling using hourly infiltration rate. *Magazine of Civil Engineering*, *96*(4), 27-41.

Chen, S., Levine, M.D., Li, H., Yowargana, P., Xie, L. (2012). Measured air tightness performance of residential buildings in North China and its influence on district space heating energy use. *Energy and Buildings*, *51*, 157-164.

DBN V.2.2-3:2018. Budynky i sporudi. Zaklady osvity. [Buildings and structures. Educational institutions]. K.: MinrehionUkrayiny. 2018. 61. (ukr)

DBN V.2.5-67:2013. Opalennia, ventyliatsiia ta kondytsionuvannia. [Heating, ventilation and air conditioning]. K.: MinrehionUkrayiny. 2018. 61. (ukr).

Deshko, V., Buyak, N., Bilous, I., Voloshchuk, V. (2020). Reference state and exergy based dynamics analysis of energy performance of the "heat source – human – building envelope" system". *Energy*, 200.

Deshko, V., Shevchenko, O. (2013). University campuses energy performance estimation in Ukraine based on measurable approach. *Energy and Buildings, 66*, 582-590.

DSTU B A.2.2-12:2015. Enerhetychna efektyvnist' budivel'. Metod rozrakhunku enerhospozhyvannya pry opalenni, okholodzhenni, ventylyatsiyi, osvitlenni ta haryachomu vodopostachanni [Energy efficiency of buildings. Method of calculation of energy heating, cooling, ventilation, lighting and hot water]. K.: MinrehionUkrayiny. 2015. 205 p. (ukr)

DSTU B V.2.2-19:2007. Metod vyznachennia povitropronyknosti ohorodzhuvalnykh konstruktsii v naturnykh umovakh [Method for determining the air permeability of enclosure structures in field conditions]. K.: Minrehion Ukrayiny. 2008. 20. (ukr)

Dumała, S., Skwarczyński, M. (2011) Influence of modernization activities on demand of thermal energy in buildings. *Rocznik Ochrona Srodowiska*, *13*(1), 1795-1808.

EN 12831: 2003 Heating of systems in buildings - Method of for calculation of the design heat load. (The heating systems in building are Calculation of the thermal loading). CEN, 2003. 76.

EN 15251:2007 Indoor environmental input parameters for design and assessment of energy performance of buildings addressing indoor air quality, thermal environment, lighting and acoustics. CEN, 2003. 64.

EN 15603:2008. Energy performance of buildings. Overall energy use and definition of energy ratings. CEN, 2003. 66.

Ferdyn-Grygierek, J., Baranowski, A. (2015). Internal environment in the museum building – Assessment andimprovement of air exchange and its impact on energy demandfor heating. *Energy and Buildings*, *92*, 45-54.

Földváry, V., Bekö, G., Langer, S., Arrhenius, K., Petráš, D. (2017). Effect of energy renovation on indoor air quality in multifamily residential buildings in Slovakia. Building and Environment, *122*, 363-372.

Frączek, K., Chmiel, M.J., Bulski, K. (2018). Bacterial aerosol at selected rooms of school bulidings of Malopolska province. *Rocznik Ochrona Srodowiska, 20*, 1583-1596.

Johnson, T., Myers, J., Kelly, T., Wisbith, A., Ollisonc, W. (2004). A pilot study using scripted ventilation conditions to identify key factors affecting indoor pollutant concentration and air exchange rate in a residence. *Journal of Exposure Analysis and Environmental Epidemiology*, *14*(1), 1-22.

Jokisalo, J., Kurnitski J., Korpi, M., Kalamees, T., Vinha, J. (2009). Building leakage, infiltration, and energy performance analyses for Finnish detached houses. *Building and Environment*, *44*, 377- 387.

Jokisalo, J., Kalamees, T., Kurnitski, J., Eskola, L., Jokiranta, K., Vinha, J. (2008). A comparison of measured and simulated air pressure conditions of a detached house in a cold climate. *Journal of Building Physics*, *32*(1), 67-89.

Kapalo, P., Voznyak, O., Yurkevych, Yu., Myroniuk, Kh. (2018). Ensuring comfort microclimate in the classrooms under condition of the required air exchange. *Eastern-European Journal of Enterprise Technologies, 95*, 6-14.

Konig, M., Hempel, S., Janke, D., Amon, B., Amon, T. (2018). Variabilities in determining air exchange rates in naturally ventilated dairy buildings using the CO_2 production model. *Biosystems eng ineering*, *174*, 249-259.

Leivo, V., Prasauskas, T., Du, L., Turunen, M., Kiviste, M., Aaltonen, A., Martuzevicius, D., Haverinen-Shaughnessy, U. (2018). Indoor thermal environment, air exchange rates, and carbon dioxide concentrations before and after energy retro fits in Finnish and Lithuanian multi-family buildings. *Science of the Total Environment, 621*, 398-406.

Ng, L., Musser, A., Persily, A., Emmerich, S. (2013). Multizone airflow models for calculating infiltration rates in commercial reference buildings. *Energy and Buildings*, *58*, 11-18.

Ng, L., Persily, A., Emmerich, S. (2014). Consideration of envelope airtightness in modelling commercial building energy consumption. *International Journal of Ventilation, 12*(4), 369-377.

Ng, L., Persily, A., Emmerich, S. (2015). Improving infiltration modeling in commercial building energy models. *Energy and Buildings, 88*, 316-323.

Nielsen, T., Drivsholm, C. (2010). Energy efficient demand controller ventilation in single family houses. *Energy and Buildings*, *42*(11), 1995-1998.

Salthammer, T. (2019). Formaldehyde sources, formaldehyde concentrations and air exchange rates in European housings. *Building and Environment*, 150, 219-232.

Shi, S., Chen, C., Zhao, B. (2015). Air infiltration rate distributions of residences in Beijing. *Building and Environment*, *92*, 528-537.

Siuta-Olcha, A., Cholewa, T., Syroka, M., Anasiewicz, R. (2016). Analysis of the influence of a glazed surface type and solar shading devices on the building energy balance. *Rocznik Ochrona Srodowiska*, *18*, 2, 259-270.

Stabile, L., Dell'Isola, M., Russi, A., Massimo, A., Buonanno, G. (2017). The effect of natural ventilation strategy on indoor air quality in schools. *Science of the Total Environment*, *595*, 894-902.

Yongming, J., Duanmu, L., Li, X. (2017). Building air leakage analysis for individual apartments in North China. *Building and Environment*, *122*, 105-115.

Yoshinoa H., Hongb T., Nord N. (2017). IEA EBC annex 53: Total energy use in buildings - Analysis andevaluation methods. *Energy and Buildings, 152*, 124-136.

You, Y., Niu, C., Zhou, J., Liu. Y., Bai, Z., Zhang, J., He, F., Zhang, N. (2012). Measurement of air exchange rates in different indoor environments using continuous CO_2 sensors. *Journal of Environmental Sciences*, *24*(4), 657-664.

Younes, C., Shdid, C., Bitsuamlak, G. (2012). Air infiltration through building envelopes: A review. *Journal of Building Physics, 35*(3), 267-302.

Abstract

Many old public buildings in Central and Eastern Europe are characterized by low energy efficiency and often lack of mechanical ventilation. The general trends are aimed to improve the energy efficiency of the building sector and to provide comfort conditions. The indoor air quality can be determined based on the CO_2 concentrations.

In the article, a complex approach to the definition and analysis of data on the indoor CO_2 concentration and the air exchange rate in educational institutions at natural air exchange and in the absence of mechanical air circulation was implemented. Educational institutions in Kyiv have been considered. The study of the CO_2 concentration of indoor and outdoor air of three typical schools of mass development in the 80 s, as well as the training building of Igor Sikorsky KPI, was carried out. Experimental determination of the background CO_2 concentration during the day next to the considered objects showed that the background concentration of CO_2 is in the range of 400-420 ppm. Measurements of the CO_2 concentration distribution were carried out after classes throughout the classroom area, according to which the difference between the values at the level of the working area was 30...180 ppm. It was found that the concentration of CO_2 varies during classes between 700-1100 ppm. During the break, the CO_2 concentration decreases to 500-1000 ppm, depending on the type of ventilation.

Experimental data on the dynamics of changes in the indoor CO_2 concentration are used to determine the air exchange rate based on balances of air flows and CO_2. It is shown that the number of present persons influences the indoor CO_2 concentration more significantly than the air exchange rate. On the example of an experimental study of the CO_2 concentration in the classrooms for high school students it was found that the air exchange rate during the classes is in the range of 0.4...0.75 h^{-1}. During breaks the air exchange rate increases to 2.9-3.5 h^{-1}. For the range considered, the weighted average air exchange rate is 0.8 h^{-1}, and even with forced airing, the air exchange rate is insufficient to ensure acceptable CO_2 concentration.

For the training building of Igor Sikorsky KPI a field experiment was carried out to determine the dynamics of changes in CO_2 concentration in time and on the basis of it the air exchange rates for representative classrooms were determined. The concentration of CO_2 ranged from 500 to 2000 ppm and increases by 350-850 ppm depending on the use and location of classrooms. Based on experimental data, the air exchange rate for the training building of the education institution is in the range of 0.35-0.7 h^{-1}. During the periods of airing the air exchange may increase by 0.45 h^{-1}, but this does not allow

reaching the standard value. When analyzing the obtained results, simulation models of natural air exchange of the examined classrooms were used on the basis of the improved ASHRAE method. The natural air exchange rate based on simulations is in the -0.8…0.5 h^{-1} range. Negative values are explained by exfiltration, which is typical for the upper floors.

Not only the comfort and condition of the building envelope, but also the total energy consumption of the building depend on the actual level of air exchange rate. In the total energy balance the ventilation component is 30-60%. Further use of the obtained results can be connected with monitoring of the actual level of air exchange rate and its consideration during complex modernization or implementation of the ventilation systems with heat recovery in the premises of educational institutions.

Keywords:
educational institutions, air quality, CO_2 concentration, air exchange,
simulation modeling, field experiment, comfort conditions

MIDDLE POMERANIAN SCIENTIFIC SOCIETY OF THE ENVIRONMENT PROTECTION

Rocznik Ochrona Środowiska

Volume 22. Year 2020 ISSN 1506-218X 105-116

Approach to Impact Assessment of the Rated Power Uprate of NPP Unit on the Service Life of the Turbine Critical Elements

Olga Chernousenko[1], Tetyana Nikulenkova[1], Vitaliy Peshko[1], Anatolii Nikulenkov[2]*

[1]National Technical University of Ukraine Igor Sikorsky Kyiv Polytechnic Institute, Ukraine

[2]The State Enterprise National Nuclear Energy Generating Company "Energoatom", Ukraine

[*]corresponding author's e-mail: tetyana.nikulenkova@gmail.com

1. Introduction

The practical exhaustion of the energy equipment life and fossil fuel shortage at thermal power plants determine significant contribution of NPPs to the energy sector of Ukraine. Therefore, utilization of power uprate margins of existing NPP (nuclear power plant) units is an urgent task which, if solved, would increase power generation at no significant cost (Rokicki et al. 2019).

There are objective preconditions for looking into and utilization of design basis margins of VVER units owing to accumulated VVER operating experience, as well as accuracy of thermal and neutron-physical calculations (Nikulenkov et al. 2018). When increasing NPP capacity to 104% there is a need to estimate the residual life of plant's typical elements and continue their operation.

The extension of NPPs lifetime subject to adherence to nuclear and radiation safety standards is one of the most effective ways for replacement of generating capacities. At the same time, specific financing costs for fulfilling requirements of normative documents allowing to obtain a license for NPP operation for an additional life period are much lower than costs of new nuclear builds. Revision of previously set operating life of NPP power equipment provides for an assessment of residual life of power equipment based on defining thermal and stress-strain states. However, reliability criteria for low-cycle fatigue and static damage require special consideration for steam turbines at NPPs (Nikulenkov et al. 2018).

2. Problem statement

Approaching the end of the established service life of NPP power equipment and the need to increase electricity generation due to ever-increasing consumer demands pose two major challenges for the nuclear industry (Chernousenko et al. 2018):

1) using the inherent design margins of operating power units in combination with increasing pace of science and technology development, as well as taking into account international experience backed by sufficient analytical justification to increase the installed capacity while ensuring the required safety for operating NPPs.
2) to carry out a set of works and modernizations to operate power units beyond the design period while ensuring the required safety.

To solve these challenges in the work is considered:

- impact assessment of the modification on the service life of high pressure cylinder (HPC) critical elements of the K-1000-60/3000 steam turbine using system one-dimensional and CFD-modeling codes;
- assessment of the possibility to continue high pressure rotor (HPR) operation of the K-1000-60/3000 steam turbine which includes calculated study of the residual life and acceptable number of start-ups from different thermal states under cyclic rotor loading.

3. Impact assessment of the modification on the service life of HPC critical elements of the K-1000-60/3000 steam turbine of 1000 MW NPP

When assessing impact of the modification on the service life of critical elements of the examined turbine it is suggested to use the pattern as follows (Nikulenkova et al. 2019):

1) building a 3-D model (3-D model of the high-pressure cylinder was developed, as well as CFD modelling to identify boundary conditions for subsequent determining of low-cycle loads for with and without modification cases),
2) calculation of initial and recalculation of boundary conditions (using CFD-codes or criteria equations),
3) determining a nonstationary temperature field in the solid critical element for further calculation of thermal load,
4) strength calculations (low-cycle fatigue, static loading, etc.) to determine a stress-strain state,

5) assessment of remaining service life (the remaining service life of a rotor is determined by assessing its accumulated damage and design service life, and the design remaining service life is a remainder between the design service life and its operating life at the time of forecasting,
6) assessing impact of the modification on remaining service life.

As previously specified, building a 3-D model is the first step in examining impact of the modification on the service life of the turbine's critical element. Figure 1 provides a 3-D model of the high-pressure rotor (Nikulenkova et al. 2019). The presented 3-D model was developed based on design and engineering documentation.

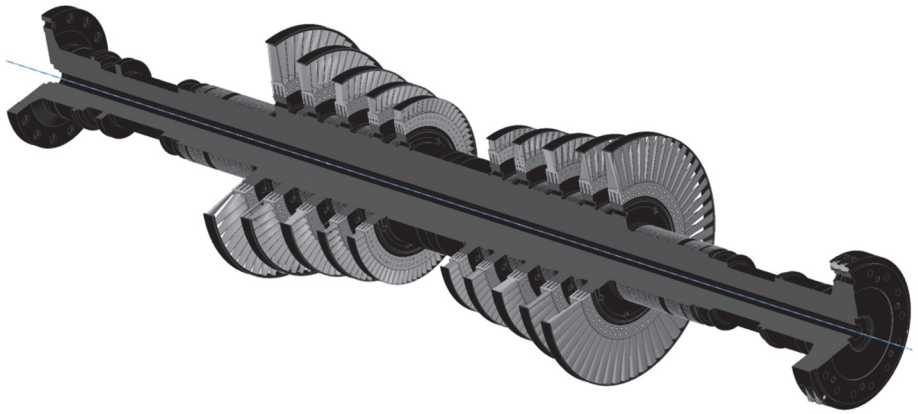

Fig. 1. 3-D model of the high-pressure rotor of the K-1000-60/3000 turbine

Since the high-pressure rotor of the K-1000-60/3000 turbine is geometrically symmetrical at the flow section and end seals and nature of the processes in the left and right parts are similar it was decided that for the purpose of estimate and in order to reduce the computational resources (scope and calculation time) the research area will be reduced from the first stage to the end seal last chamber of the right part of the rotor without operating blades (Figure 4).

The second step is to identify boundary conditions and determine temperature field in high-pressure rotor. It should be noted that calculation of boundary conditions of the third kind to solve a differential thermal conductivity equation in the works related with extension of service life of rotors (Bakhmutskaya et al. 2017), was performed primarily using criterion equations obtained by summarizing experimental data.

An alternative method would be using CFD modeling. To test this method considered nominal operation mode of the turbine set in a stationary

position for the 1st stage of the HPC flow section. The computational model (Figure 2) consists from one solid and three fluid domains. The first stationary fluid domain models the flow of wet steam through nozzle blades, the second rotating fluid domain models the flow of wet steam through working blades of the turbine, the third rotating fluid domain models air flow in the central opening of the rotor designed for handling operations related with package inspection. Wet steam is modeled as a homogeneous binary mixture based on IAPWS IF97 condition data for water and water steam.

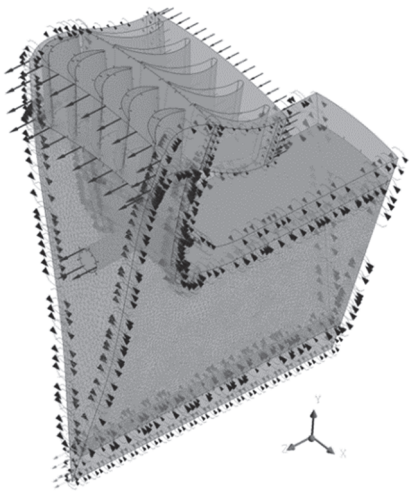

Fig. 2. Schematic diagram of the assigned boundary conditions in the ANSYS CFX computer environment

The boundary conditions at the inlet and outlet of the fluid domains were assigned as specified below.

Initial calculation parameters for Nominal value/Nominal value with modification:

- Mass steam flow rate per turbine, kg/s – 1622/1706 (Nikulenkova et al. 2018)
- Inlet static pressure, MPa – 5.839/5.839
- Inlet static temperature, K – 546.96/546.96
- Modelled medium (fluid 1 and fluid 2) – wet steam
- Modelled medium (fluid 3) – air
- Material of solid domain – steel
- Steam moisture content at the inlet – 0.002/0.002
- Rotor speed, rpm – 3000/3000

A boundary condition permitting flow reverse circulation is applied at the outlet of the domain modeling air flow. The side edges with Z as rotation axis received periodical boundary conditions. The obtained results specified correspond with controlled parameters during nominal operation mode.

The results are provided based on the calculations of boundary conditions of the third kind (Nikulenkov et al. 2018) and 3-D temperature field in the rotor (Figure 3).

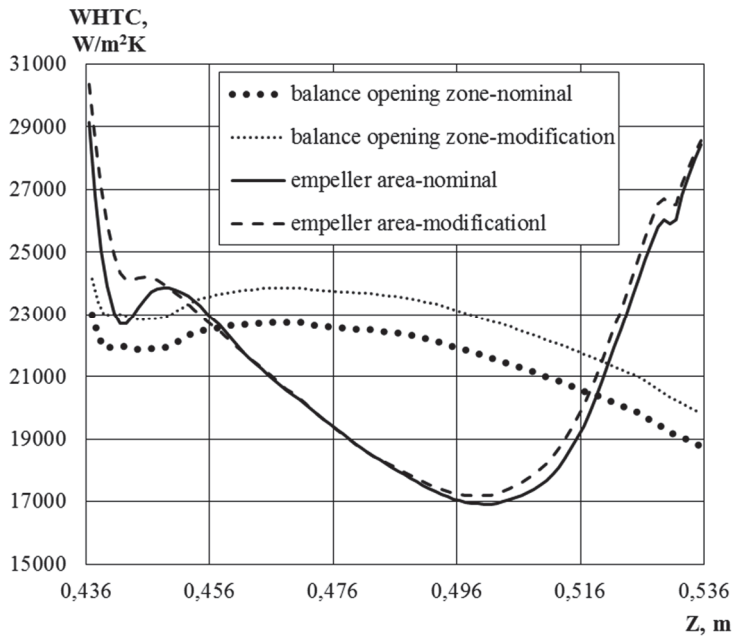

Fig. 3. Change in wall heat transfer coefficient along the flow section for either modification and rated power variants

The provided results show that increase in steam flow rate leads to increase of wall heat flux and wall heat transfer coefficient, and, consequently, to decrease of rotor wall temperature.

Further it is necessary to perform CFD modeling for all stages of the turbine in transient loads from cold, warm and cold shutdown to ensure possibility of strength calculations with subsequent impact assessment of the modification on the service life.

4. Calculation of the residual service lifetime of the high-pressure rotor of K-1000-60/3000 steam turbine

The residual life assessment of power equipment would require determining viability and damage of its base metal. Typical degradation mechanisms of steam turbine equipment include long-term strength reduction and low cycle fatigue accumulation. Intensity of their impact is determined by a numerical examination of equipment thermal (TS) and stress-strain states (SSS) for standard operation modes using integrated scheme provided in the study (Peshko et al. 2016, Chernousenko et al. 2018).

To perform a numerical examination of the stress-strain state would require solving a thermal conductivity boundary problem in quasi-stationary (for normal operation modes) and nonstationary models (for transients). It is convenient to solve such problems of mathematical physics through discretization of the calculation object using the finite element method.

For complex designs of a high-pressure rotor (HPR) the geometric model is built in the 3-D mode with account of the main elements (Figure 4). The model is build using specification drawing of the K-1000-60/3000 turbine. Typical HPR examination areas include areas which, usually, have maximum temperature gradients and stress intensities.

In solving the problem of thermal conductivity, the boundary conditions of heat exchange of the I-IV kind were set in all typical regions calculated by the authors earlier (Chernousenko et al. 2018). Based on the calculation of the basic thermo- and hydrodynamic parameters of the flow part for normal and transient operating modes, the values of temperatures, heat transfer coefficients and heat flux density were determined for all surfaces of the geometric model.

The results of examination of the HPR thermal state at nominal operation are presented in Figure 4a. The temperature of the first-stage pressure is 261-270°C, for areas from the second to the fifth stage – 166-255°C and for end seals area – 83-142°C.

The stress-strain state (Figure 4b) was obtained taking into account basic loads, namely: stresses from temperature expansions, irregularities of temperature fields, centrifugal forces and stresses from the steam pressure. The maximum stress intensity occurs in the axial orifice and in the unloading openings of the discs of all five stages σ_i = 158 MPa. In other HPR typical regions the stress intensity is 66-105 MPa.

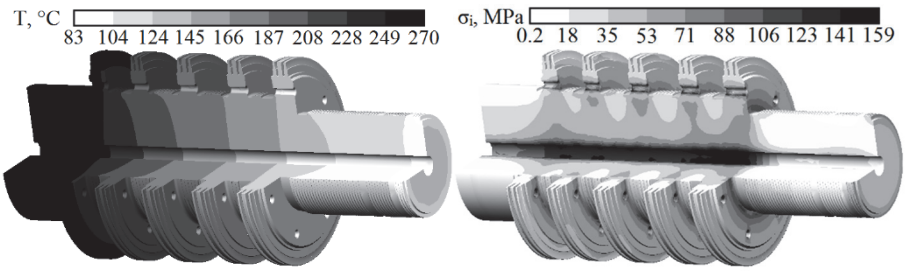

Fig. 4. Calculation results for nominal operation: a – thermal state; b – stress-strain state

The considerable level of stress intensity at axial orifice is explained by large values of centrifugal forces acting on the discs of the pressure stages and rotating blades. The highest level of stress under this condition is observed closer to the fifth stage, which is the most massive and is bladed by the longest blades.

Similar data were obtained for transient operating modes. It should be noted that variation of temperature gradients and stress intensity are of particular interest when examining non-stationary operation. For example, when start-up is performed from a hot state (temperature of the first stage metal t_m = 150°C) maximum values of the temperature gradient are observed at the rotor push (estimated time τ = 600 s) and for the front fillet of the first-stage pressure gradT = 1570 K/m (Figure 5). The following local maximums of the temperature gradient are observed at 400 MW of electrical power (time point τ = 3200 s) and at the end of start-up mode at power output of 1000 MW (time point τ = 14100 s). A significant temperature gradient is observed throughout the hot start-up gradT = 1310 K/m at the tail joint of the rotor disk and the first-stage operating blades.

The change in intensity of stresses during hot start-up is shown in Fig 6.

The highest values of stresses σ_i = 207 MPa are observed at the axial opening of the turbine (curve 5) at the time τ = 6600 s (holding the turbine at 750 MW capacity).

The highest compression stresses σ_i = -182 MPa are observed at the front fillet of the first stage at the time τ = 3200 s (ramping up 400 MW). At the end of the start-up period the intensity of stresses in all examined regions gradually decreases to the values corresponding to the nominal operation mode (Figure 4b).

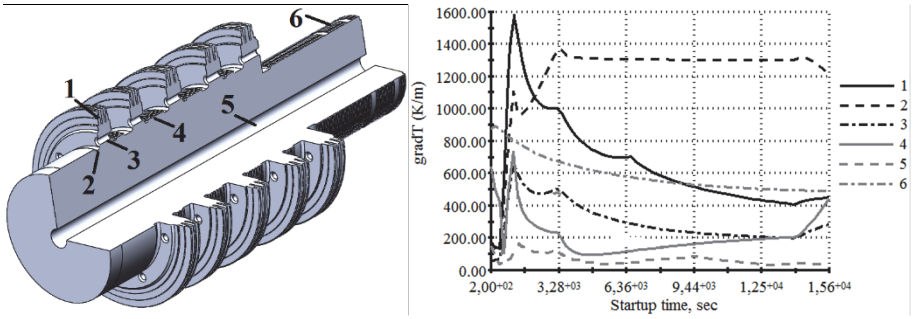

Fig. 5. Dynamics of variation of irregularity of the rotor temperature field at hot start-up: a – typical examination areas, b – temperature gradient during start-up

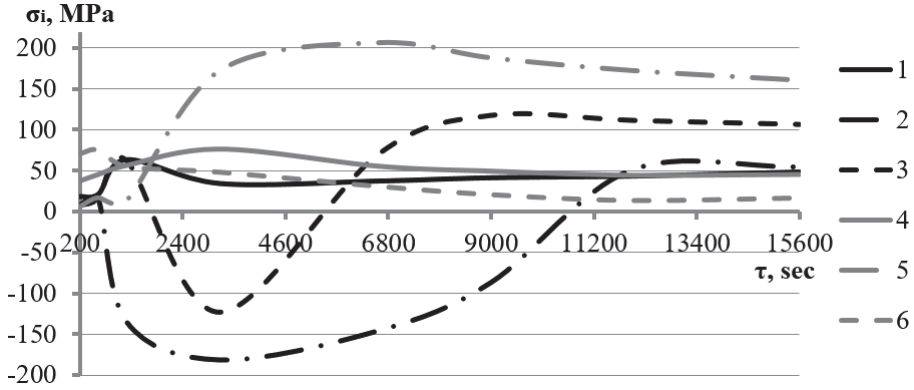

Fig. 6. Dynamics of variation of intensity of stresses in characteristic areas of research during start-up from hot state of metal

Similar data were obtained for other typical operating modes, which are presented in (Chernousenko et al. 2018, Chernousenko et al. 2019).

Calculation of damage from low-cycle fatigue involves setting the acceptable number of start-ups from different thermal states. Experimental curves of low-cycle fatigue are used for this purpose. However, for the 30CrNi3Mb1V steel from which the HPR is made, such curves are absent in the literature. Therefore, it is proposed to calculate the acceptable number of cycles using correlation dependencies of low-cycle fatigue:

$$N_{per} = \left[1 - \left|\frac{1{,}25\sigma^{s}}{\sigma_{l.s.}}\right|^{q}\right] min\left\{\frac{N_1}{n_N}; N_2\right\} \quad (1)$$

$$N_{1,2} = \left[\frac{\frac{1}{4} \ln \frac{100}{100 - \psi_{l.d.}}}{C\left(n_{1,2}\varepsilon_a + \frac{1-2\nu}{3E}\sigma_i \right) - \frac{\sigma_N}{E}} \right]^{\frac{1}{0,6}} \tag{2}$$

where:
σ^s – intensity of stresses in the steady creep state,
$\sigma_{l.s.}$ – long-term strength limit,
q – exponent in the long-term strength equation,
n_N – strength margin by number of cycles,
$\psi_{l.d.}$ – long-term ductility determined by the median values for each temperature level θ_1-θ_2,
θ_1 i θ_2 – temperatures corresponding to maximum and minimum strain rates in the load cycle,
C – coefficient of the current number of cycles,
$n_{1,2}$ – strength margin by strain rate,
ε_a – amplitude of the strain intensity in the cycle.

The calculated indicators of low-cycle fatigue and long-term strength are specified in Table 1.

To assess life performance of the K-1000-60/3000 turbine the Rivne NPP Unit 3 of the National Nuclear Energy Generating Company (NNEGC) Energoatom was selected. As of November 2019, the unit's operating time is 209 690 h, and the number of start-up from different thermal states is 271. At the same time, according to the normative documents of NNEGC Energoatom, the fleet life of the power unit with the K-1000-60/3000 turbine is 220,000 h with 600 start-ups.

The life performance calculation results of the K-1000-60/3000 high-pressure rotor at Rivne NPP Unit 3 are given in Table. 1. The strength factor in the calculations is accepted as 10 by the number of cycles and 1.5 by deformation in accordance with the normative documents.

Low-cycle fatigue is 11.2% estimated by the acceptable number of start-ups from different thermal states calculated using the correlation dependence of the fatigue of 30CrNi3Mb1V steel. The static damage component is 55.2%. In other words, for NPP turbines the low-cycle fatigue as a degradation mechanism has less significant impact than reduction of long-term strength of metals. The total damage of the high-pressure rotor is 66,4%. This determines its residual life at 106200 h while maintaining operating conditions which were typical until November 2019.

Table 1. Life performance indicators of the K-1000-60/3000 high-pressure rotor at Rivne NPP Unit 3

Life performance indicators		Values
Operating time		209,690 h
Total number of start-ups		271
Commercial operation year		1986
Current number of start-ups from different thermal states	Cold	58
	Hot	213
Stress intensity at nominal operation		158.5 MPa
Acceptable number of start-up cycles from different thermal states	Cold	1945
	Hot	2591
Cyclic damage		11.2%
Acceptable operation time		380,000 h
Static damage		55.2%
Total damage		66.4%
Residual life		106200 h

The above circumstances allow continuing operation of the HPR of the K-1000-60/3000 steam turbine for additional 50 thousand hours until the next preventive maintenance.

5. Conclusions

This paper describes an approach to impact assessment of the rated power uprate of NPP unit on the service life of the turbine critical elements.

1. Based on design and engineering documentation a 3-D model of the high pressure rotor of the K-1000-60/3000 high-speed turbine was developed which can be subsequently used for CFD modeling and strength calculations.
2. Calculations performed using CFD code show that the impact of the modification on the wall heat transfer coefficient is negligible.
3. The numerical studies of the stress-strain state of the K-1000-60/3000 turbine high pressure rotor allowed to establish that the most loaded areas are axial opening of the turbine, fillet rounding's and unloading openings of all pressure stages.
4. According to life performance indicators calculation results it was established that reduction of the long-term strength has a dominant effect as degradation mechanism compared to accumulation of low-cycle fatigue. For the high pressure rotor of Rivne NPP Unit 3 the total damage to the base metal is 66,4% which determines its residual life at 106,200 h.

5. Since the residual life exceeds twofold the value of the planned overhaul period, the possibility of increasing the installed capacity of the unit by 4% is justified in terms of maintaining the operation life of equipment.

References

Bakhmutskaya, Y., Goloshchapov, V. (2017). K-325-23,5 Steam Turbine High-Pressure Rotor Thermal and Thermo-structural State During Cold Start-up. *Journal of Mechanical Engineering*, *2*(20), 3-11.

Chernousenko, O., Nikulenkov, A., Nikulenkova, T., Butovskiy, L. & Bednarska, I. (2018). Calculating boundary conditions to determine the heat state of high pressure rotor of the turbine NPP K-1000-60/3000. *Bulletin of the National Technical University "KhPI"*, *12*(1288), 51-56. DOI: 10.20998/2078-774X.2019.03.01

Chernousenko, O., Rindyuk, D., & Peshko, V. (2017). Research on residual service life of automatic locking valve of turbine K-200-130. *Eastern-European Journal of Enterprise Technologies*, *5*(8-89), 39-44. DOI: 10.15587/1729-4061.2017.112284

Chernousenko, O., Rindyuk, D., & Peshko, V. (2018). Thermal and strain-stress state of high-pressure rotor of K-1000-60/3000 turbine of NPP unit. *Power Engineering: economics, technique, ecology*, 3, 135-141. DOI: 0.20535/1813-5420.3.2018. 163981

Chernousenko, O., Rindyuk, D., & Peshko, V. (2019). The strain-stress state of K-1000-60/3000 turbine rotor for typical operating modes. *Bulletin of the National Technical University "KhPI"*, *3*(1328), 4-10. DOI: 10.20998/2078-774X.2019.03.01

Chernousenko, O., Rindyuk, D., Peshko, V., & Goryazhenko, V. (2018). Development of a technological approach to the control of turbine casings resource for supercritical steam parameters. *Eastern-European Journal of Enterprise Technologies*, *2*(1-92), 51-56. DOI: 10.15587/1729-4061.2018.126042

Nikulenkov, A., Chernousenko, O., & Nikulenkova, T. (2018). Analysis of influence of heat power rate increase on beyond design basis accident for NPP unit. *Bulletin of the National Technical University "KhPI"*, *13*(1289), 37-45. DOI: 10.20998/2078-774X.2018.13.07

Nikulenkova, T., Nikulenkov, A. (2019). Calculation of boundary conditions using CFD modeling as part of a comprehensive approach to impact assessment of modifications on the service life of critical elements of a nuclear power plant turbine. *The 16th International Conference of Young Scientists on Energy Issues*, VII, 267-278.

Nikulenkov, A., Samoilenko, D., & Nikulenkova, T. (2018). Study of the impact of NPP rated thermal power uprate on process behaviour at different transient conditions. *Nuclear & Radiation safety*, *4*(80), 9-13.

Peshko, V., Chernousenko, O., Nikulenkova, T., & Nikulenkov, A. (2016). Comprehensive rotor service life study for high & intermediate pressure cylinders of high power steam turbines. *Propulsion and Power Research*, *5*(4), 302-309. DOI: 10.1016/j.jppr.2016.11.008

Rokicki, T., Ochnio, L., Koszela, G., Żak, A., Szczepaniuk, E., Szczepaniuk, H., Michalski, K., Perkowska, A. (2019). Public expenditure on environmental protection in the European union countries. *Rocznik Ochrona Srodowiska*, *21*(1), 364-377.

Abstract

Nuclear power plants play an important role in power systems of many countries. Ability to reasonable increase installed capacity of nuclear power units allow to reduce the cost for building of new power plants. When increasing NPP capacity to 104% there is a need to estimate the residual life of plant's typical elements and continue their operation. The mathematical model of estimation of service life indicators of steam turbine K-1000-60/3000 is developed. The effect of increasing the capacity of a nuclear reactor on the heat transfer coefficients of a steam in the nozzle segments of high-pressure cylinder was established by using CFD modeling. The thermal and stress-strain state of the high-pressure rotor for the most typical operating modes are calculated. Using the correlation dependences of low-cycle fatigue, the rate of accumulation of cyclic damage of the base metal is established. The resistance of the metal to the exhaustion of long-term strength is also determined. On the example of the high pressure rotor of the 3rd power unit of Rivne NPP the service life indicators are calculated. The validity of increasing the installed capacity of the power unit was also confirmed.

Keywords:
nuclear power plant, reliability, turbine, steam flow, computational fluid dynamics, high pressure rotor, service life, long-term strength, low cycle fatigue

MIDDLE POMERANIAN SCIENTIFIC SOCIETY OF THE ENVIRONMENT PROTECTION

Rocznik Ochrona Środowiska

Volume 22. Year 2020 ISSN 1506-218X 117-129

Internet of Things (IoT) and Artificial Neural Networks Towards Water Pollution Forecasting

Thaer Ibrahim[1,2], Alok Mishra[2,3]*

[1]Iraqi Federal Board of Supreme Audit, Baghdad, Iraq

[2]Atilim University, Ankara, Turkey

[3]Molde University College-Specialized University in Logistics, Norway

[*]corresponding author's e-mail: alok.mishra@atilim.edu.tr; alok.mishra@himolde.no

1. Introduction

The Tigris river originates from the Taurus mountains, the southeastern region of Anatolia in Turkey and passes through Syria 50 km from the outskirts of the city of Qamishli. The river contains a wide range of tributaries scattered in the lands of Turkey, Syria and Iraq, the most important of which are the Khabur, the Great Zab, the Small Zab, Al-Ethaim and Diyala. These tributaries contribute about two thirds of the river's total water volume. The other third comes from Turkey and takes the last tributary in the Tigris, the Diyala River south of Baghdad in a short distance. The Tigris branches further into two in the city of Kut, called Nahrgraf and Dujaila, respectively. The Tigris River meets the Euphrates River at Qurna in the south of Iraq, after which it passes through the territory of Iraq to Shatt al-Arab, finally flowing in the Arabian Gulf. The course of Tigris was changed and in the present times, it meets Euphrates in the area of Karma near Basra, so the length of the river is about 1,718 kilometers. It originates from Turkey and flows into Iraqi territory which is about 1,400 kilometers. Iraq's most fertile land is located in the region between Tigris and Euphrates rivers because of the irrigation water provided by them. In addition, most of Iraq's citizens lives in that region. Baghdad, the capital of Iraq and its largest city, is divided into two parts by Tigris river (FAO 2008) as shown on the map in Figure (1) (© Bible Study 2015).

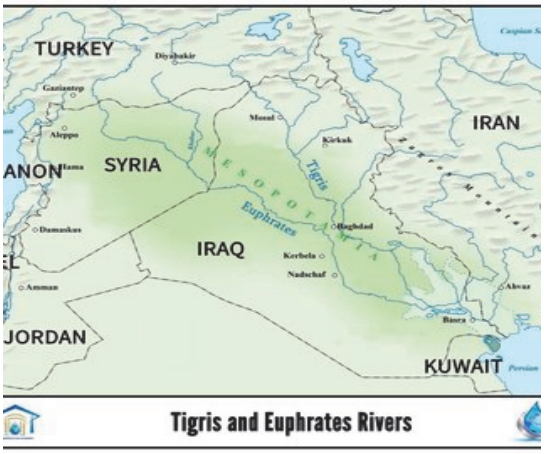

Fig. 1. The Tigris River on map

E-government refers to the use of Information and Communication Technology (ICT) in order to build an effective and efficient government to provide good services to citizens, as well as make these services available for citizens anywhere and at any time, on the other side, to make the governmental information accessible by public, finally to provide the citizens by the power to be a partner in all governmental decisions (Sarrayrih et al. 2015).

In order to make the definition of E-Government more clear, the word has been divided into two parts; the letter "E", which refers to the automation of government information and transactions, and government itself as an institution. E-government relies mainly on the services provided by ICT which has made communication between citizens and their government agents easier and faster. As a result, E-government has substantially reduced cases of bribery and administrative corruption in government institutions (Rajput et al. 2013). E-Government has four services channels which deliver the services from the government agency to the consumers. These are Government to Government (G2G), Government to Citizen (G2C), Government to Business (G2B), and Government to Employees (G2E) channels (Moon 2002).

The network of physical objects that contains of wireless sensors is called the Internet of Things (IoT), this network contains also actuators, Radio-Frequency Identification (RFID) tags, software, and connectivity to enable it to interact with people and other connected devices in achieving some common goals (Lopes et al. 2014). There is another definition for the Internet of Things (IOT), which is "IoT or smart object networking" which describes a situation whereby physical objects connected to the Internet are able to communicate with, and

identify themselves to, other devices (Thaler 2015). IoT has four types of communication models which are Device-to-Device Communications, Device-to-Cloud Communications, Device-to-Gateway, and Back-End Data-Sharing model (Internet society 2015).

Artificial Neural Network (ANN) is a network that has the ability to perform functions in a similar way to the functioning of the human brain if the problem is defined precisely. because the Artificial Neural Network (ANN) was inspired by the retinal system of the human brain. However, this system is sometimes not as accurate as in the human brain and attempts are still being made to obtain an artificial intelligence system with a similar problem solving capacity as our brains. Despite the variety of functions performed by ANNs, their structure is the same. The network consists of three layers, namely the input layer, hidden layer, and the output layer (Ostad Ali Askari et al. 2017). The type of problem determines the number of neurons in the input layer because this layer is an independent variable whose sole function is to receive the data. The hidden layer is the result of calculations performed within the network. The number of neurons constituting the output layer depends on the number of dependent variables in the network, therefore, the output layer represents the dependent variable (Keskin et al. 2015).

Water bodies, especially rivers and lakes are more susceptible to pollution than other water sources due to their direct contact with various human activities. The agricultural sector is one of the most water-consuming sectors, thus its wastewater volume is by necessity larger. Its pollutants contain not only salts dissolved in the soil, but also chemicals used in fertilizers and pesticides. Wastewater from the industrial sector also leaks into the riverbeds and because of its high toxicity, it causes serious health problems among humans. Water bodies are also affected by emissions from large plants that use fossil fuels as their source of power. These pollutants contribute indirectly to water pollution through their interaction with the rainwater, causing precipitation of acid rain that harms the physical and chemical characteristics of the water bodies, especially the lakes due to their weak water replenishment capacity, and as a result, reduced ability to self-purify (Alrobaiee 2014).

Pollution rates are calculated in the water bodies by calculating the values of the Biochemical Oxygen Demand (BOD) divided by Chemical Oxygen Demand (COD). If the values of the first are higher than those of the second, the water of the stream is polluted and unfit for human use, and often has unpleasant smell, color and taste. Water is free of pollution if the dissolved oxygen values range from 5-10 mg/l, depending on seasons of the year because of the variations in environmental temperatures (Northeast Georgia Regional Development Center 1998).

The impacts of natural disasters such as earthquakes, floods and volcanoes, and their effects such as air, water and soil pollution are considered life-threatening hazards on the Earth's surface. It is therefore essential to look for highly-sophisticated, practical and rapid methods to fill the many gaps in our lack of understanding on the changing nature of these disasters. These advanced methods can provide feasible ideal solutions for the scientific and practical analysis of the causes and transformations of these disasters before, during and after their occurrence, in order to understand their impact, dimensions and find better control and contain their effects. The best solutions for monitoring and mitigating disasters include the creation of an effective early warning system covering the geographical area of the disaster by providing the necessary information at the maximum speed, facilitating communications and movement processes, and providing accurate, real time monitoring of the changing circumstances in order to be up to date with all changes so as to contain its impact as best as possible (Saleh 2013).

2. Literature review

As we mentioned previously, the main objective of E-Government is to deliver high-quality services from the government to consumers (Nordfors et al. 2016). In the first generation of E-Government project, the consumers had to ask for the type of service they wanted and had to visit each E-Government agency website to get the service as well. Only after that, the government agency would provide them with the necessary services (Ibrahim 2014). Later, the service provision style has changed to what is called as the E-Government One-Stop-Shop, where the consumer can finish all the operations by using one government portal with a unique user name and password (Mustofa 2013). This type of service provision is called Reactive Services where the consumer has to ask for the service in order to get it. The next service provision style become known as the E-Government Zero-Stop-Shop. In this style, the government agency provides the service without any request on the consumer side by simply analyzing the consumer's profile as well as their social media information and predict the type of service needed, and then deliver the service at necessary time (Ayachi et al. 2015). One of the most important services provides by the governments to their citizens is security, whose aim is to preserve the life and property of citizens from damage whether it is due to human or the surrounding environment (Anthopoulos & Reddick 2016).

The risk of pollution is one of the most dangerous phenomena to the citizens' lives and property, therefore reason the government has to monitor this risk and try to find ways to protect its subjects by early detection and interference to control and minimize the damage caused by it (Mahmoud 2001). For effective

monitoring of aquatic environment, the remote sensing system can be used very effectively. This system is mainly composed of a Wireless Sensor Network (WSN), Cloud Computing, and Big Data in addition to many types of communication methods for data transfer (Maojing 2016). The cooperation of these technologies will produce reliable and useful data, which can helps the decision makers to take the right decision at the right time to keep citizens safe. The use of ICT in water environment monitoring has contributed significantly to reducing the risk of pollution and flooding (Wang & Tingtng 2015). In addition, it can be considered as one of the services provided by the E-Government to the citizen since government use ICT technology to provide security service to citizens. There are many types of water pollution parameters, however, those that have the most significant impact on the aquatic environment are seven (Al-Rubaiee 2014), and each one of them has its own acceptable ranges and influence in pollution.

2.1. Temperature

Air temperature, in addition to some other atmospheric elements such as sunlight, runoff speed, geographical location, the presence of groundwater, the proportion of rainfall and the proportion of the presence of aquatic plants and algae in the aquatic environment, directly effects the temperature of the aquatic environment. The ideal temperature for the aquatic environment is between 9-12°C. As the water temperature exceeds 12°C degrees drops below 9°C, the life of plants and aquatic animals gets shorter (Kale 2016).

2.2. PH

PH defined as the amount of acidity in water where some of the water molecules (H_2O) separated by the formation of positive hydrogen (H^+) and negative hydroxide (OH-) ions. Some other compounds may interact with these two ions, leading to an imbalance in the number of hydrogen and hydroxide ions in the solution. When the concentration of hydrogen ions is less, the dissolved hydroxide ions are left unpaired and then the water becomes basic. In contrast, when the concentration of hydroxide ions is less, hydrogen ions are left unpaired and the water becomes acidic. The acidity of the solution measured by counting the concentration of hydrogen ions and converting it into logarithmic scale of base 10 (Signs 2010).

2.3. Turbidity

Turbidity is the measurement of the visibility of water and it is calculated by measuring the amount of sediment and the degree of its impact on water. Rainfall leads to a significant increase in turbidity due to high amount of sediment in river water. High turbidity causes high water temperature low oxygen in addition to blocking sunlight from aquatic plants, which leads to reducing the ability of

these plants to complete photosynthesis. In addition, increasing turbidity will harm the fishes and their eggs. The minimum boundary of turbidity is between 3 NTU, and the maximum boundary is 30 NTU (Mc Caffrey 2010).

2.4. Conductivity

Conductivity is defined as the ability of water or other liquids to transmit electrical current. It is a measure of the concentration of electrolytes in water. Conductivity does not mean identifying certain types of ions in water and increased water ability to conduct electricity conductivity is an indicator of the increased amount of pollutants in water (Ramos et al. 2005).

2.5. Dissolved oxygen

Oxygen is one of the two components of water molecule, but it is also found in the dissolved form as gas (O_2). Fishes and plants living underwater require dissolved oxygen for their breathing process. There are two sources of supplying the aquatic environment with oxygen; that of the surrounding aquatic environment, and the oxygen produced by photosynthesis of aquatic plants. The higher the percentage of dissolved oxygen in water, the healthier the aquatic environment (Enderlein et al. 1990).

2.6. Total Dissolved Solids (TDS)

Solids dissolved in water are any substances other than water itself found in the aquatic environment that cannot seen by the naked eye. These include salts, minerals and water pollutants. Pure water is the water in which the concentration of solids is low. It is well-established that a small percentage of solids dissolved in water is beneficial for animals and plants living in the aquatic environment. However, the presence of large quantities of solids dissolved in water leads to damage to plants and animals living in the aquatic environment. Therefore, monitoring the proportion of solids dissolved in water on a continuous basis is very important. The maximum boundary of acceptable solid concentration is 1000 mg/l (WHO 1996).

2.7. Chlorophyll

Chlorophyll is the proportion of algae that grows in the aquatic environment. It is considered as one of the components of the fresh water system, but the presence of large amounts of algae leads to problems in the aquatic environment because they consume large amounts of dissolved oxygen in water. In addition, some types of algae produce toxic substances that affect the health of water inhabitants when they are in large quantities (Lailia et al. 2015).

3. Methodology

3.1. Data collection

In order to collect the historical data related to water pollution in Tigris river, Iraqi Environment and the Water Resources ministries were visited to conduct interviews with the employees who are experts in river water pollution and collect information related to water pollution of the river. In the Environment Ministry, there is a program called Remote Sensing Project (RSP) for detecting water pollution in Tigris River by using electronic sensors. The system consists of sensors which are installed directly on the waterway of the Tigris River and distributed on various locations along the route. These sensors can sense seven parameters to determine water quality, namely PH, Turbidity, Conductivity, Dissolved Oxygen, Total Dissolved Solids, Chlorophyll, and Water Temperature. In addition, these sensors can conduct a quality test every 15 minutes and send all the collected data to a central database using Global System for Mobile communications (GSM).

The data are then stored in a database in the form of Microsoft Excel sheets for later analysis. Unfortunately, this project was stopped after two years because of misuse. The sensors collected 85000 records for each of the seven parameters mentioned above during that period. After the remote sensing project was stopped, the Environment Ministry returned back to the traditional way of collecting samples once in 15 days. The manager of the project was contacted and the data from for the period of two years were collected, making a total number of 85000 reads for each of the seven parameters mentioned before.

3.2. Data normalization

The huge number of data points as well as the different measurement units of each one of pollution parameters makes the use of this data very difficult. Therefore, we tried to normalize the data in a different way. First of all, MS Excel was used to mark each one of parameter as Polluted or Not polluted depending on the pollution ranges for each one of parameters, as shown on the tables above. After that, a final result parameter was created and marked as "1" for polluted if there was at least one parameter outside the normal ranges, or "0" if all pollution parameters were within the accepted pollution boundaries. This classification was used to prepare the data for statistical analysis in Statistical Package for the Social Sciences (SPSS) software, version (18.0).

3.3. Pollution parameters correlation

In order to measure the effect of each of the pollution parameters on other parameter, correlation analysis between them was performed using the parametric

Pearson test on SPSS. These correlations showed the results presented on Table 2.

Table 2. The correlation between pollution parameters

1st parameter	2nd parameter	Pearson Correlation	R	R Square
CHLORO	DO	-.288	.288	0.83
CHLORO	COND	-.047	.047	.002
CHLORO	TDS	-.047	-.047	.002
COND	DO	.383	.383	.147
COND	PH	.172	.172	.030
COND	TDS	1.000	1.000	1.000
COND	TEMP	-.227	-.227	.051
COND	TUR	-.117	-.117	.014
PH	CHLORO	.059	.059	.003
PH	DO	.468	.468	.219
PH	TUR	-.166	-.166	.028
TDS	DO	.383	.383	.147
TDS	PH	.172	.172	.030
TDS	TUR	-.117	-.117	.014
TEMP	CHLORO	.290	.290	.084
TEMP	COND	-.227	-.227	.051
TEMP	DO	-.883	-.883	.780
TEMP	PH	-.255	-.255	.065
TEMP	TDS	-.227	-.227	.051
TEMP	TUR	.418	.418	.175
TUR	CHLORO	.206	.206	.043
TUR	DO	-.386	-.386	.149

- CHLORO refers to the Chlorophyll.
- COND refers to the Conductivity.
- PH refers to the amount of acidity in water.
- TDS refers to the Total Dissolved Solids.
- DO refers to the Dissolved Oxygen.
- TEMP refers to the Temperature.
- TUR refers to the Turbidity.
- R represents the Coefficient of correlation between parameters.
- R Square is used to know the Contrast Ratio of the dependent variable to predict the changes in the independent variable.
- Negative sign means an inverse relationship between parameters.

- Positive sign means a positive relationship between parameters.

It can be noted from the table that the strongest correlation is between COND (Conductivity) and TDS (Total Dissolved Solids), with very strong positive correlation values.

3.4. Water pollution prediction

The analysis was carried out in MATLAB© where an artificial neural network (ANN) was built for that purpose. In order to get the optimal type of ANN, Machine learning (ML) needs to undergo a series of trials and errors. Therefore, the network was trained for 150 times, and for each trial, one of the prediction functions, number of nodes, or number of hidden layers were changed until optimal results were obtained.

The Feed Forward Back Propagation network was used in the training. Backpropagation is an algorithm used for training and it contains of two steps; the first step is the feed forward of values to the next step, which calculates error and propagates it back to the previous layers. The training network consist of an input layer of 90 neurons, also there is one hidden layer, then the output layer. For training, 1000 epochs are used, which undergo 13 iterations. Many good results with low error rate were obtained during the network training, but the two best ones are shown on Table 3.

Table 3. Network Training Results

	Network 1	Network 2
Network Type	FEED.FW.BP	FEED.FW.BP
No. of layers	1	1
Performance function L1	MSEREG	MSEREG
No. of Neuron L1	90	90
Transfer function L1	PURLIN	PURLIN
Adoption function	GDM	GDM
Train function	LM	LM
Input Parameter	COND	TEMP
Output	POLUTED	POLUTED
Epochs	1000	1000
Iteration	13	16
Error Rate	1.58E-08	2.40E-08

4. Discussion

Water pollution is one of the human disasters. It can be caused either by nature or by human activities (Ibrahim et al. 2019). In the field of flooding and aquatic monitoring, (Shalini et al. 2016) devised a system to measure the level of water in the river. This system uses special sensors to measure water levels as the distance from the bottom of the river and send the data to the monitoring center using Wi-Fi technology, which then sends the information via smartphones using GSM technology to the decision-makers. The system provides forecasting using the Internet of Things, GSM and SMS.

In this research, after historical data obtained from a project to detect water pollution that was established on the banks of the Tigris River in the city of Baghdad in Iraq, seven types of water pollutants were identified, these parameters are (Temperature, PH, Turbidity, Conductivity, Dissolved Oxygen, Total Dissolved Solids, and Chlorophyll). Nghe et al. (2020) tried to forecast water quality by using (IoT). However, they use only four types of water pollution parameters (Salinity, PH, DO, Temperature). Ullo et al. (2020) found the relationships between elements of water pollution in order to understand the nature of the life of the aquatic environment.

The statistical analysis of the data was done using the statistical analysis program (SPSS) as shown in Table 2, the analysis results were as below:

1. Water temperature has an effect on all other pollution elements as discussed in (Boehm 2019).
2. The strongest correlation between pollution elements was (Conductivity) and (Total Dissolved Solids) by 100% correlation, which agrees with (Dennis et al. 2019).
3. The weakest correlation between pollution elements was between (Chlorophyll) and (Conductivity) and between (Chlorophyll) and (Total Dissolved Solids).

5. Conclusion

Prediction of water pollution is an important service that is provided by the government to consumers. The use of Information and Communication Technology (ICT) makes this service part of E-government services by predicting and alerting the consumers in order to reduce the damage caused by pollution or other natural disasters. Applying these services on prediction of water pollution will save a lot of time, besides budget and efforts on the side of the government in addition to people's lives and property. In this study, we tried to use Artificial Neural Networks (ANN) and Machine Learning (ML) for water pollution prediction. We used historical data from sensors installed on the Tigris River, which

generated huge amount of data as the measurements were made every 15 minutes, producing a total of 85000 measurements for each of the seven pollution parameters. The data were normalized in order to be used as input for the neural networks, which were trained to get the lowest error rate for reliable predictions.

6. Limitations and future work

Despite the amount and breadth of data that were used, there are a number of limitation of this study; the data used for analysis were somehow old because of the project of pollution sensing in Baghdad was stopped several years ago due to the misuse of devices and lack of maintenance of the system. Another important limitation is the use of old versions of the software because the new versions are under license, and therefore require investment. Future work should be focused on utilizing more recent data as well as new generation sensors to measure water pollution parameters in order to get more accurate data, and therefore better results in prediction of water pollution.

References

Ashram, M. (2001). *Water Economics in the Arab World and the World*. Beirut, Center for Arab Unity Studies, 30.

Alrobaiee, S. (2014). Water pollution – causes and treatments. http://www.watersexpert.se/.

Ostad-Ali-Askari, K., Shayannejad, M., & Ghorbanizadeh-Kharazi, H. (2017). Artificial neural network for modeling nitrate pollution of groundwater in marginal area of Zayandeh-rood River, Isfahan, Iran. *KSCE Journal of Civil Engineering, 21*(1), 134-140.

Ayachi, R., Boukhris, I., Mellouli, S., Amor, N., Elouedi, Z., (2015). *Proactive and reactive e-government services recommendation*. © Springer-Verlag Berlin Heidelberg.

Boehm, A. (2019). Risk-based water quality thresholds for coli phage in surface waters: Effect of temperature and contamination aging. *Environmental Science: Processes & Impacts, 4*(8), 134-142.

Dave, T., Tschofenig, H., and Barnes, M. (2015). *Architectural Considerations in Smart Object Networking* IETF 92 Technical Plenary - IAB RFC 7452. 6 Sept. Web. https://www.ietf.org/proceedings/92/slides/slides-92-iab-techplenary-2.pdf .

Corwin, D.L., & Yemoto, K. (2017). *Salinity: Electrical Conductivity and Total Dissolved Solids*. © Soil Science Society of America 5585 Guilford Rd., Madison, WI 53711 USA.

Enderlein, S., Enderlein, E., & Williams, W. (1990). *Water Quality Requirements.* World Health Organization (WHO), https://www.who.int/water_sanitation_health/ resourcesquality/wpcchap2.pdf .

https://www.biblestudy.org/maps/euphrates-river-valley-map.html.

Ibrahim, T. (2014). *A Road Map to a Successful Application of E-Government in Iraq*. Çankaya University. http://earsiv.cankaya.edu.tr:8080/xmlui/bitstream/handle/123456789/318/%C4%B0brahim%2c%20Thaer.pdf?sequence=1&isAllowed=y.

Ibrahim, T., Mishra, A., Bostan, A. (2019). Role of E-government in Reducing Disasters. *TEM Journal, 8*(4), 1150-1158, ISSN 2217-8309, DOI: 10.18421/TEM84-07.

Internet society. (2015). The Internet of Things: An over view. www.internetsociety.org.

Jing, W., Tingtng, L. (2015). Application of wireless sensor network in Yangtze River Basin water environment monitoring, in Proceedings of the 27th Chinese Control and Decision Conference (CCDC '15), 5981-5985, IEEE, Qingdaob, China, © IEEE.

Kale, V. S. (2016). Consequence of temperature, pH, turbidity and dissolved oxygen water quality parameters. *International Advanced Research Journal in Science, Engineering and Technology*, *3*(8), 186-190.

Keskin, T., Düenci, M., and Kaçaro, F. (2015). Prediction of water pollution sources using artificial neural networks in the study areas of Sivas. Karabük and Bart n (Turkey). *Environmental Earth Sciences, 73*(9), 5333-5347.

LAILIA, N. L., Arafah, F., Jaelani, A., & PAMUNGKAS, A. D. (2015). Development of water quality parameter retrieval algorithms for estimating total suspended solids and chlorophyll-A concentration using Landsat-8 imagery at Poteran island water. *Remote Sensing and Spatial Information Sciences, 2*(2), 55-62.

Leonidas G., and Christopher G. (2016). *Understanding electronic government research and smart city: A framework and empirical evidence*. 99-112 © IOS Press and the authors.

Lopes, N., Pinto, F., Furtado, P., Silva J. (2014). *IoT architecture proposal for disabled people*. In: IEEE 10th international conference on wireless and mobile computing, networking and communications (WiMob), 152-158. DOI: 10.1109/WiMOB. 2014.6962164.

Maojing, N. (2016). *River Water Quality Monitoring and Simulation based on WebGIS – Anhui Yinghe River as an Example*. Sixth International Conference on Instrumentation & Measurement, Computer, Communication and Control, Geoscience, 716-720. DOI: 10.1109/IMCCC.2016.119, © IEEE.

McCaffrey, S. (2010). Water Quality Parameters and Indicators. Waterwatch Coordinator, Namoi Catchment Management Authority, https://sswm.info/sites/default/files/reference_attachments/MCCAFFREY%20ny%20Water%20Quality%20Parameters%20&%20Indicators.pdf.

Sarrayrih, M.A., & Sriram, B. (2015). Major challenges in developing a successful e-government: A review on the Sultanate of Oman. *Journal of King Saud University-Computer and Information Sciences*, *27*(2), 230-235.

Moon, M.J. (2002). The Evolution of E-Government among Municipalities: Rhetoric or Reality? *Public Administration Review, 62*, 424-433.

Mustofa, K. (2013). *Translating the Idea of the E-Government One-Stop-Shop in Indonesia*. © IFIP International Federation for Information Processing.

Nghe, T., Hai, T., Ngon, C. (2020). Deep Learning Approach for Forecasting Water Quality in IoT Systems. *International Journal of Advanced Computer Science and Applications, 11*(8).

Nordfors, L., Ericson, B., Lindell, H., & Lapidus, J. (2009). *eGovernment of tomorrow: Future scenarios for 2020*. Vinnova – Swedish Governmental Agency for Innovation Systems.

Northeast Georgia Regional Development Center. (1998). Watershed Protection Plan Development Guidebook.
https://epd.georgia.gov/sites/epd.georgia.gov/files/related_files/site_page/devwtrplan_b.pdf.
Rajput, A., Nair, K. (2013). Significance of Digital Literacy in E-Governance. *The SIJ Transactions on Industrial Financial & Business Management, 1*(4), 136-141.
Ramos, P. M., Pereira, J. D., Ramos, H. M. G., & Ribeiro, A. L. (2008). A four-terminal water-quality-monitoring conductivity sensor. *IEEE Transactions on Instrumentation and Measurement*, *57*(3), 577-583.
Saleh, H. (2013). Design of disaster early warning systems using artificial intelligence. Higher Commission for Scientific Research - Damascus - Syria, http://www.arsco.org/detailed/a8fbcc55-1c65-48bd-be39-67872f50decf .
Shalini, E., Surya, P., Thirumurugan, R., & Subbulakshmi, S. (2016). Cooperative flood detection using SMS through IoT. Int. J. Adv. Res. Elect., *Electron. Instrum. Eng, 5*(3), 3410-3414.
Signs, V. (2010). *The Five Basic Water Quality Parameters*, The Clean Water Team Guidance Compendium for Watershed Monitoring and Assessment State Water Resources Control Board 310.doc, http://home.iitk.ac.in/~anubha/Water2.pdf
The Food and Agriculture Organization (FAO). (2008). Euphrates –Tigris River Basin, Irrigation in the Middle East region in figures – AQUASTAT Survey, http://www.fao.org/nr/water/aquastat/basins/euphrates-tigris/Euphrates.tigris-CP_eng.pdf
Ullo, S., Sinha, G. (2020). Advances in Smart Environment Monitoring Systems Using IoT and Sensors. MDPI journal. *Sensors 2020, 20*, 3113 DOI: 10.3390/s20113113.
World Health Organization (WHO). (1996). Total dissolved solids in Drinking-water, Guidelines for drinking-water quality, 2nd ed. Vol. 2. Health criteria and other supporting information. World Health Organization, Geneva, https://www.who.int/ water_sanitation_health/dwq/chemicals/tds.pdf .

Abstract

Water could be some-times a source of danger on people's lives and property. Although it is one of the most important elements of life on this planet. This article define the threat of water pollution in Tigris River in Iraq. by collecting a data that generated by sensors that installed in a water pollution sensing project in Baghdad city, also this article aimed to detect and analyze the behavior of water environment. It is an effort to predict the threat of pollution by using advanced scientific methods like the technology of Internet of Things (IoT) and Machine learning in order to avoid the threat and/or minimize the possible damages. This can be used as a proactive service provided by E-governments towards their own citizens.

Keywords:
Internet of Things, E-government, Water Pollution prediction, Tigris River,
Artificial Neural Network

MIDDLE POMERANIAN SCIENTIFIC SOCIETY OF THE ENVIRONMENT PROTECTION

Rocznik Ochrona Środowiska

Volume 22. Year 2020 ISSN 1506-218X 130-143

The Level of Risk and Decision-making in Managing Industrial Activity with the Elimination of Negative Environmental Impacts

Oľga Végsöová, Martin Straka[*]*, Kamil Kyšeľa*

Technical University of Kosice, Slovakia

[*]*corresponding author's e-mail: e-mail: martin.straka@tuke.sk*

1. Introduction

Surface extraction has a long tradition in the Central European region. Since time immemorial, the surface method of extracting raw materials has been one of the irreplaceable activities of our ancestors, and this method, considering modern technologies, has an important economic dimension as well as social and societal dimension. Ancic et al. (2017) point out how the extraction of minerals leaves indelible marks on the cultural and economic development of the mining region.

In recent years, high environmental demands have been placed on all methods of obtaining raw materials. In the case of surface extraction of raw materials, these requirements are particularly strict. Rotz et al. (2018) note the need to increase the efficiency of already approved quarries in relation to the increasing requirements for the authorization of new areas for extraction. At present, the environmental requirements for the operation of a quarry have been noticeably increasing. Ogrodnik et al. (2019) consider the main problem in extractive industries to be addressing the negative impact of extraction on the environment. For this reason, quarry operators are forced to renew material and technical equipment used for the extraction and subsequent transport of raw materials. Patyk et al. (2019) state that a rational choice of components used in extraction must meet economic, environmental and safety requirements. Regular modernization of quarry facilities contributes to increasing ecological standards protecting the environment and also the people working in the quarry or living in its immediate vicinity. Rodovalho et al. (2020) take the view that, in connection with the extraction of minerals, the handing of waste generated during the extraction process and its subsequent disposal should not be neglected either. It is undeniable that

irresponsible management of mining waste can have adverse consequences for nature and for the health of the population.

Kong et al. (2017) argue that it is necessary to find a balance between economic development and environmental protection. It is essential to try to minimize the environmental impact on the area in all activities related to the extraction of mineral resources. Randelovic et al. (2014) are of the view that in minimizing the environmental burden on the area extracted from, it is necessary to individually examine the soil characteristics and appropriately choose the form of environmental reclamation used. Urosovic etal. (2018) considers mining to be an important source of pollution in adjacent areas. Babi et al. (2016) are of the opinion that the role of the extractive industries in sustainable development is to balance economic, environmental and social burdens with the benefits of extraction.

Since the end of the 19th century, increasing efforts by companies have been observed to protect employees at work. National legislation seeks to minimize adverse events in the work process. With economic development, new challenges arise in the field of safety at work. According to Kahraman, et al. (2019) globalization brings many threats to working life. These threats are generally linked to the level of economic development of countries. In the European Union, the working conditions of employees are extremely strict concerning safety. Zielinska et al. (2019) consider health and safety in the work environment to be basic prerequisites for the quality of work. Unfortunately, despite high standards of protection for employees at work, undesirable situations still commonly occur which endanger or harm the lives or health of employees. Santos et al. (2020) claim that, despite improving working conditions in the world, each ye hundreds of thousands of people die from occupational injuries and around 2 million people die from occupational illnesses, which offers considerable room for improvement. In the event of harm to health caused to an employee during the performance of work tasks, or in direct connection with them, regardless of their will by a short-acting, sudden and violent action of external influences, we call such an event an accident at work. Pereira et al. (2020) considers accidents at work to be a complex phenomenon and one of the main public health problems.

The existence of an injury at work has a negative economic and social impact on the employee as well as the employer. The employee is excluded from the normal work routine due to the harm to their health and a significant impact on their social ties is also possible. Jonczy et al. (2019) highlight the interesting fact that workers in the extraction sector are exposed to levels of danger that are difficult to reduce or easily eliminate, and so have a low occupational safety culture in comparison with professions where the level of danger is lower or easy to eliminate.

After an accident at work, the employer loses the employee's labour for a certain period of time, which is associated with economic losses for the company and at the same time the employer's attractiveness in the eyes of potential new employees decreases. Singh et al. (2020) and Tilabi et al. (2019) argue that workplace safety management is an urgent requirement for organizations and companies, especially in a highly competitive world, where the success of companies depends on the overall productivity of organizations. Despite the clear motivation of both sides of the working relationship, surface extraction of minerals is unfortunately an activity that is associated with the relatively frequent occurrence of accidents at work. The role of the employer is to create a working environment that will minimize the possibility of accidents at work. Lopez-Garcia et al. (2019) consider the organization of working conditions to be an important task.

Wiganowska et al. (2018) and Trebuna et al. (2019) are of the opinion that the creation of a suitable working environment affects the health and safety of workers at work. Amponsah-Tawiah, et al. (2017) state that the employer's management should invest its resources in protecting the life and health of its employees. Zinoviev et al. (2014) argue that the insufficient allocation of the employer’s financial resources for protection and health at work results in the threat to the life and health of employees multiplying.

There is no doubt that the right choice of extraction method has an exceptional impact on the incidence of accidents at work. Ozturk et al. (2019) argues that mining accidents are one of the critical safety issues worldwide.

Kazanin et al. (2016) and Ižaríková (2019) highlight the need to obtain and evaluate information on the stress-strain state of the rock mass with reference to the importance of this information in terms of safety.

Work in a quarry is based on the deposit exploitation plan. In this plan, it is necessary to assess the dangers and threats which cannot be removed and to propose and suggest measures to eliminate these dangers and threats. The assessment of workplace safety is currently an integral part of the preparatory work before the start of extraction. Szeszenia-Dabrowska et al. (2013) are of the opinion that careful monitoring of working conditions and implementation of preventive health programs should be carried out in areas and divisions of the national economy where a high risk of occupational diseases has been identified.

Measurable and non-measurable factors must be taken into account when assessing the degree of risk. With regard to eliminating or minimizing the degree of risk, it is more difficult to remove non-measurable factors, which largely lie in the human factor in the actual performance of work. Chen et al. (2019) are of the opinion that physiological fatigue, mental fatigue or mental illness are frequent determinants of dangerous situations in the workplace. According to Dieterich et al. (2020) it is necessary to know the exact circumstances of each accident in order to identify the risks that must be minimized for prevention. This view is

also held by Lombardi et al. (2019), according to whom the analysis of accidents, as well as their main causes and determinants, can definitely contribute to the development of more effective preventive interventions.

The aim of the presented paper is to offer a comprehensive and systematic procedure for risk assessment, as well as to apply it in selected activities at the Kecerovský Lipovec quarry. This procedure can assist in the decision-making activities of quarry management, especially with regard to the environmental and safety requirements of the operation.

2. Methodology for the approach for determining risk values for a quarry operation

Measures to ensure safety and health at work are an important part of every quarry operation, and are generally based on the basic safety regulations in force in the Slovak Republic.

In order to carry out an analysis of the examined state of extraction operations, it is necessary to understand basic concepts such as danger, threat and risk. We can imagine danger as an essential property of a material, machine, work activity, etc., which can cause harm to health or damage to machinery. Technology and working activities are characterized by the ability to create an unexpected negative consequence of harm to a person or property. A threat can be defined as an active property of an object, machinery, technology and work activities that can cause a negative phenomenon, or the possibility of activating a threat in a specific space and time. We understand risk as expressing the probability of the occurrence of a negative phenomenon and the consequence of this phenomenon. The risk (R) is thus a function of the probability (P) and consequence (D) of the negative event.

Mathematical expression of a non-linear function of risk:

$$R = f\,(P \times D) \tag{1}$$

Due to the efforts to take into account the risk of other factors when quantifying risk, a broader description of risk is applied:

$$R = P \times D \times E_x \times O \tag{2}$$

where:
E_x – exposure, exposure to threats,
O – application of protective measures.

This means that the value of risk as a function of probability and consequence is multiplied by a coefficient expressing human exposure in the danger area and a coefficient expressing the impact of protective measures. However, the

risk is affected by many more factors than those given in the last definition (E_x, O). These factors can be divided into measurable and non-measurable (see Table 1). The factors listed in Table 1 affecting probability must be taken into account when determining probability and consequence. These factors are therefore the parameters of probability and consequence. It follows from these considerations that it is important for normal work practice, especially in small and medium-sized enterprises, to be able to identify all the relevant factors that affect risk and to be able to assess their impact on the final effect. Therefore, it is appropriate to use methods that give instructions on how to assess the effect of multiple risk factors.

Table 1. Factors influencing the probability of an accident

Factors influencing the probability of an accident	
Measurable	Non-measurable
duration of danger, time of exposure	human factor, attention, classification, stress, etc.
system parameters (machine speed, etc.)	level of maintenance activities
suddenness of event	quality of inspection and testing activities
	reliability and compliance with security measures
	diversity of threat existence

There is an increasing emphasis on safety in quarry operations, so risk assessment is an integral part of any such operation.

In practice, there are cases where a dangerous situation is not addressed by a risk prevention measure. In this case, it is up to the experts and the quarry owners to estimate the degree of risk.

An obvious legal obligation of the employer is to provide a workplace, machinery, working conditions and work aids that do not endanger safety and health at work, which must be an integral and equal part of the performance of work and production tasks.

The analysis is followed by a risk assessment. It is based on an assessment - an estimate of the probability of an accident and an assessment - an estimate of the consequences of this accident or adverse event. Factors influencing the probability of an accident are described in Table 1.

It is also worth noting that when estimating the probability of an accident, we start from different levels of input data, which are defined in more detail in Fig. 1.

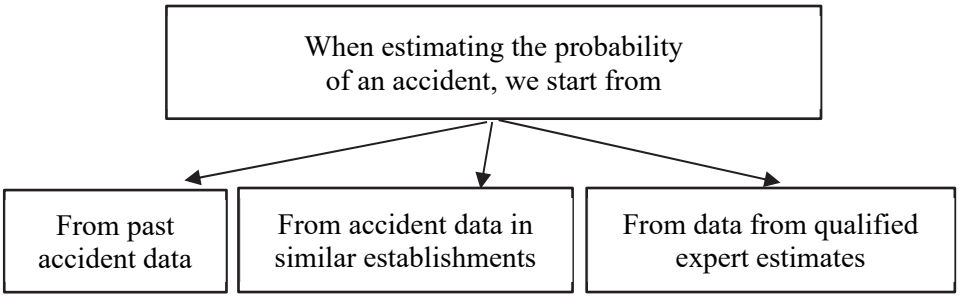

Fig. 1. Relationship of data with the probability of an accident. Source: own elaboration

Determining the influence of the severity of individual factors on the frequency of a particular negative phenomenon is shown in Table 2, where the main aspects are seen as probability, the frequency of occurrence and the duration of the effect of the threat.

Table 2. Determining the influence of the severity of individual factors on the frequency of a particular negative phenomenon

Probability	Class	Frequency of phenomenon	Temporal effect of the threat
Very high	A	Very often	Nonstop
High	B	Several times	Temporary threat
Moderate	C	Sometimes	Rare
Low	D	Rarely	Very rare
Very low	E	Almost none	Almost impossible

The consequences of the negative manifestation of the phenomenon are shown in Table 3. It should be borne in mind that different risk factors may take different levels. It follows from Table 3, that with the decreasing severity of individual factors, the consequences of negative phenomena in the quarry also decrease.

Table 3. Determining the influence of the severity of individual factors on the consequence of a negative phenomenon

Consequence type	Category	Description of the consequence
Catastrophic	I.	death due to an accident at work or complete destruction of the system, irreparable damage
Critical	II.	serious accident at work, occupational disease or extensive damage to the system, loss of production, large financial losses.
Little significant	III.	registered occupational injury, suspected occupational disease or minor damage to the system, minor financial loss
Negligible	IV.	registered occupational injury, negligible system failure, no financial loss

After determining the effect of probability and the consequence of an adverse event, we use Table 4. The highest risk is value 1 and the lowest is value 20.

Table 4. Determining the influence of the severity of individual factors on the consequence of a negative phenomenon

Result Probability	Catastrophic I.	Critical II.	Low significance III.	Negligible IV.
A – very high	1	3	7	13
B – High	2	5	9	16
C – Medium	4	6	11	18
D – Low	8	10	14	19
E – very low	12	15	17	20

Numerical values for risk resulting from Table 5 must then be divided into four groups as shown in Table 5.

Table 5. We classify numerical risk values into groups

Point range	Risk scale	Safety criteria
1-5	unacceptable	the system is unacceptable – immediate application of protective measures, immediate shutdown of the system
6-9	adverse	the system is dangerous – application of protective measures
10-17	moderate	the system is safe, conditional on training of operators, inspections, instructions, etc.
18-20	acceptable	the system is safe

For the first two levels, the system cannot be considered safe. Appropriate measures must be taken to remedy the problem. The third level, moderate, enables the assessment of the system to be completed however with certain conditions, e.g. employees must be trained. The fourth level is acceptable and therefore the situation in the workplace can be considered to be safe.

3. Application of methodology – Case Study in the Andesite Quarry in Eastern Slovakia

The andesite quarry we analysed is located in the eastern part of Slovakia, near the town of Košice at the western foot of the hills known as the Slanské vrchy. This quarry is one of the most important deposits in Slovakia. It is used for quarry stone and crushed stone. The extracted raw material is mostly used for the construction of roads. Dark-grey andesites with feldspar outgrowths appear in the wall of the quarry. The properties of the mined raw material are given in Table 6.

Table 6. Properties of the raw material mined in the quarry

Property	Dimension	Value
absorbability	%	1.2
porosity	%	1.8
abrasion	%	21.4
weight loss after ventilation	%	0.1
weight loss after freezing	%	0.2

During the exploration of the deposit, the extraction is guided by surface extraction by a wall quarry through an external notch in 3 levels of the quarry, in a combined manner of face fronts. The method of rock separation is subordinated to the main production in the quarry, namely gross stone production. The management of extraction works is determined by the current state of digging in the quarry. Methods of mechanical rock separation are used in extraction.

Based on the method mentioned in the previous chapter, a risk assessment was performed for the core work activities in the extraction operation at the Kecerovský Lipovec quarry, which are level preparation and extraction. In both cases, the points-based method was used to assess the risk.

During the process of preparatory work or when opening a new level, it is necessary to take into account the threats that most often occur during the process in question. These threats include, in particular, injuries to the upper and lower limbs, fall of the extraction machinery, damage to the extraction machinery, etc. Table 7 shows the assessment of the probability, consequence and the result of the threat.

Table 7. Risk assessment for preparatory work, overburden work to open a new level

Threat identification	Probability	Result	Result
Injuries to the leg and other parts of the body when descending and exiting the extraction machinery	D	III.	14
Fall from the machinery during maintenance work and cleaning work	C	III.	11
Injury caused by extraction machinery (crash, push, pass)	D	II.	10
Fall of the extraction machinery to depth, overturning of the extraction machinery	D	II.	10
Damage to the extraction machinery by other extraction machinery – an accident	D	III.	14
Fall while working with hand tools	D	III.	14
Injury to employees caused by a fall or landslide	D	III.	14

Table 7 therefore leads to a risk assessment during the preparatory work, or overburden work. According to the established procedure, the level of risk was calculated, where the sum of points for the overburden is 83, the number of the parameters for the overburden is 7, the arithmetic mean is therefore 12. From the

given data it is clear under Table 6, that the assessed extraction work activity is moderate on the risk scale – moderate. In this case, however, the importance of the measures must not be forgotten, especially in the form of quality expert training, inspections, instructions, etc.

Table 8 represents the results according to the set methodology, based on which number of points for overburden is 131, the number of parameters for overburden is 10, the arithmetic mean is 13. From this data it is clear that overburden belongs in the moderate risk group. The Kecerovský Lipovec quarry can be considered a safe workplace, but we must always keep the relevant safety criteria for individual work activities in mind.

Table 8. Risk assessment for preparatory work and overburden work to open a new level

Identification of threat	Probability	Result	Result
Injuries to the leg and other parts of the body when descending and exiting the extraction machinery	D	III.	14
Fall from the machinery during cleaning and maintenance	D	III.	14
Collision injury, pressed by machinery	D	II.	10
Overturning of the machinery	D	III.	14
Damage to the machinery by other extraction machinery – accident	D	III.	14
Employees falling during the performance of work	D	III.	14
Injury to employees caused by a fall or landslide	D	III.	14
Injury carrying load	D	III.	14
Injury to the leg or other parts of the body while descending from and exiting the machinery	D	III.	14
Fall from the machinery during maintenance and cleaning work	C	III.	11
Injury caused by the extraction machinery-impact, pressing, running over	D	II.	10
The fall of the extraction machinery in depth, the overturning of the extraction machinery	D	II.	10
Damage to the machinery by other extraction machinery – an accident	D	III.	14
Employee falling in the performance of work	D	III.	14
Injury to employees caused by a fall or landslide	D	III.	14

Given the cases of both risks, which are at an acceptable level according to the methodology used, it is necessary to inform employees about the measures taken and the residual risks. It is important to know whether the safety measures at the workplace are sufficient and it is necessary to monitor whether there are ongoing threats, especially when introducing new machines, using new substances, etc. In the event that a new risk arises, every effort must be made for its mitigation. Each official information provided for employees must be properly documented so that there is no doubt that employees are not aware of the possible risks. This makes it possible to minimize any legal claims in the event of accidents or incidents.

4. Conclusion

We analysed an andesite quarry in Eastern Slovakia, which is one of Slovakia's most important andesite deposits and it is able to ensure the supply of the entire immediate vicinity with sufficient excavated rock. In terms of economic supply, mineral extraction is a promising opportunity for the development of the whole region. As early as the quarry's design phase, high requirements were placed on a low ecological footprint of the structure, but the main goal of the design activity was to define extraction processes so that the work activities of employees in the quarry would fulfil high safety criteria. However, despite the perfect and detailed design, it cannot be expected that nothing undesirable will occur during extraction as a result of subjective and objective influences. With this in mind, the task of this paper was to evaluate the degree of risk of individual activities associated with the operation of the quarry and on the basis of that data to adapt the extraction of andesite in the Kecerovský Lipovec quarry to high environmental and safety requirements.

It is undeniable that the degree of risk in quarry operation depends on the specific phase of quarry use. For this reason, it is desirable to consistently distinguish between risk in preparatory work – overburden work and risk in work performed as part of extraction. The basic monitored criteria for assessing the degree of risk was the result of the threat, which resulted from the identification of the threat, probability and consequence. The identification of the threat included a variety of adverse events that may adversely affect the physical safety of workers and the operability of the extraction facilities. As for the probability of the occurrence of an adverse circumstance, it is based on the frequency of the threat and the length of its duration. The consequences of the adverse event can range from negligible to catastrophic. From the analysis and evaluation, it is clear that the level of risk in both monitored phases of extraction activity in the quarry is in the moderate risk group.

The main benefit of the paper is a comprehensive and systematic view of the risk assessment of individual activities in the Kecerovský Lipovec quarry. The paper offers a description of threats, with the main emphasis on the resulting level of risk based on the determination of the probability and the consequence of the event. It is clear from the research that the extraction activity in the Kecerovský Lipovec quarry is at a minimum level with regard to the burden on the environment and workers and does not represent such a threat to its surroundings that could be assessed as undesirable. The facts presented in the research part can serve as an important basis for decision-making activities associated with the operation of the quarry so that solutions are selected are those that minimize the potential negative effects on the environment. However, it is necessary to ask the question whether the extraction activity in the Kecerovský Lipovec quarry, in addition to the environmental and safety point of view, also meets the economic requirements for the rational use of the environment and resources. It is also necessary to take into account the lack of staff for individual extraction jobs in the region resulting from the significant outflow of this type of labour out of the region.

The submitted paper is a part of the projects "Projects of applied research as a means for development of new models of education in the study program of industrial logistics" KEGA 016TUKE-4/2020 and the project "Research and development of new smart solutions based on the principles of Industry 4.0, logistics, 3D modelling and simulation for streamlining production in the mining and building industry" VEGA 1/0317/19.

References

Ancic, M.P., Gasparovic, S. (2017). Quarries on the island Veliki Brijun the beginnings of their rehabilitation and adaptive reuse in Croatia. *Prostor, 25*(1), 75-85.

Amponsah-Tawiah, K., Mensah, J. (2016). Occupational health and safety and organizational commitment: Evidence from the Ghanaian Mining industry. *Saffety and Health at Work, 7*(3), 225-230.

Babi, K., Asselin, H., Benzaazoua, M. (2016). Stakeholders' perceptions of sustainable mining in Marocco: A case study of the abandoned Kettara mine. The *Extractive Industrries and Society, 3*(1), 185-192.

Dieterich, C., Herrmann, C., Parzeller, M. (2020). Death at work-An analysis of fatal work accidents based on autopsies performed at the institute of legal medicine in Frankfurt am Main from 2005 to 2016. *Rechtsmedizin, 30*(3), 144-152.

Chen, Z.B., Oiao, G.Z., Zeng, J.C. (2019). Study on the relationship between worker states and unsafe behaviours in coal mine assidents basted on a Bayesian networks model. *Sustainability, 11*(18), Article Number: 5021.

Ižaríková, G. (2019). Supplier planning with analytical hierarchy process. *Acta Tecnología*, *5*(4), 103-107.

Kaharaman, E., Akay, O., Kilic, A.M. (2019). Investigation into the relationship betwen fatal work accidents, national income, and employment rate in developed and developing countries. *Journal of Occupational Health*, *61*(3), 213-218.

Kazanin, O.I., Rudakov, M.L. (2016). Banchmarking initiatives in the Fied of occupational safety and health in the context of development of the coal industry of Rusia. *Research Journal of Pharmaceutical Biological and Chemical Sciences*, *7*(2), 2092-2099.

Kong, R., Xue, F.F., Wang, J., Zhai, H.Y. (2019). Research on mineral resources and environment of salt lakes in Qinghai province based on system dynamics theory. *Resources Policy, 52,* 19-28.

Lombardi, M., Fargnoli, M., Parise, G. (2019). Risk profiling from the European statistics on accidents at work (ESAW) accidents' databases: A case study in construction sites. *International Journal of Environmental Research and Public Health, 16*(23), Article Number 4748.

Lopez-Garcia, J.R., Garcia-Herrero, S., Gutierrez, J.M., Mariscal, M.A. (2019). Psychosocial and ergonoimc conditions at work: Influence on the probability of a workplace accident. *Biomed Research International, 8*, 473-481.

Morcinek-Slota, A. (2019). Impact of occupational safety culture on the occurrence of accidents in a selected coal mine. *Mining of Sustainable Development, 216*, Article Number: 012035.

Ogrodnik, R. (2019). Investment outlays on environmental protection in Polish coal mining. *Energy and Fuels, 10*8, Article Number: UNSP: 01008.

Ozturk, I., Mevsim, R., Kinik, A. (2019). *Ermenek mine accident in Turkey: The root Causes of a disaster*. Proceedings of the 20th congress of the international ergonomics association (IEA 2018). In book: Proceedings of the 20th Congress of the International Ergonomics Association (IEA 2018).

Patyk, M., Bodziony, P., Kasztelewicz, Z. (2019). Analysis of quarrying equipment operating cost structure. *Inzynieria Mineralna-Journal of the Polish Mineral Engineering Society*, *2*, 311-318.

Pereira, K.T., Silva, A.C.R.D., Silva, L.F. (2020). Prevalence study on self-declared work accidents in areas covered by family health strategies: a coross- soctional study. *Sao Paulo Medical Journal*, *138*(1), 79-85.

Randelovic, D., Cvetkovic, V., Mihailovic, N., Jovanovic, S. (2014). Relation between edaphic factors and vegetation development on Copper mine wastes: A case study from Bor (Serbia, SE Europe). *Environmental Management*, *53*(4), 800-812.

Rodovalho, E., Quaglio, O., Felsch, W.S., Pascual, R., de Tomi, G., Tenorio, J.A.S. (2020). Reducing GHG emissions through efficient tire consumption in open pit mines. *Journal of Cleaner Production*, *255*, Article Number:120185.

Rotz, M., Trynoski, R. (2018). 3D Geologic Modelling and mine planning to improve quarry and plant efficiency at cement operations. *2018 IEEE-IAS/PCA Cement Industry Conference (ISA/PCA)*.

Santos, A.J.R., Santos, S.P., Amado, C.A.F., Rebelo, E.L., Mendes, J.C. (2020). Labor inspectorates' efficiency and effectiveness assessment as a learning path to improve work-related accident prevention. *Annals of Operations Research, 288*(2), 609-651.

Singh, A., Misra, S.C., (2020). A dominance based rough set analysis for investigation employee perception of safety at workplace and safety compliance. *Safety Science, 127*, Article Number: UNSP 104702.

Szeszenia-Dobrowska, N., Wilczynska, U. (2013). Occupational diseases among workers employed in various branches of the national economy. *Medycyna Pracy, 64*(2), 161-174.

Tilabi, S., Tasmin, R., Takala, J., Palaniappan, R., Abd Hamid, N. A., Ngadiman, Y. (2019). Technology development process and managing uncertainties with sustainable competitive advantage approach. *Acta logistica*, *6*(4), 131-140.

Trebuna, P., Pekarcikova, M., Edl, M. (2019). Digital value stream mapping using the tecnomatix plant simulation software. *International Journal of Simulation Modelling*, *18*(1), 19-32.

Urosevic, S., Vukovic, M., Pejcic, B., Strbac, N. (2018). Mining-metallurgical sources of pollution in eastern Serbia and environmental consciousness. *Revista Internacional de Contaminacion Ambiental, 34*(1), 103-115.

Wyganowska, M., Tobor-Osadnik, K. (2018). Working environment and observance of occupational health and safety regulations – case study. *4th Polish mining congress-session: Human and Environment Facing the Challenges of Mining, 174*, Article Number: 012016.

Zielinska, A., Bajdur, W. (2019). Accident rates in Poland's foodstuff industry from the perspective of occupational safety management in the European Union. *Global Journal of Environmental Science and Management-GJES,* 5, 72-77.

Zinoviev, V.P., Kuznetsov, M.S. (2014). Labour conditions, traumatism, professional diseases of Siberian miners in the late 19th early 20th centuries. *Tomsk State University Journal, 379*, 127-135.

Abstract

This paper focuses on the assessment of the degree of risk in all phases of extraction activities in a selected quarry in the Slovak Republic. The research part of the paper assesses the degree of risk resulting from the assessment of the threat, the probability of the threat and the consequence of an adverse event in extraction activities. The paper offers an important basis for decision-making in quarry management in order to eliminate the negative consequences of andesite mining on the environment, equipment and people. The extraction activity in the Kecerovský Lipovec quarry is assessed by this paper as low risk for two phases of extraction, specifically the preparation phase, and the extraction itself. The paper also highlights the importance of taking measures. Regarding the safety criteria in the Kecerovský Lipovec quarry, it is possible, based on the results of the analysis and evaluation, to consider the quarry to be safe. However, a condition for this is the necessary expert training of workers in all activities performed while working in the quarry. Here, the need for personnel to strictly adhere to the set standards for extraction activities is of prime importance. This finding confirms the above that the aim of diagnosing and naming the potential for adverse events in the extraction process must be to minimize risks, as their absolute exclusion is not possible due to the human factor and unforeseeable circumstances.

Keywords:
risk, danger, threat, risk analysis, risk assessment

MIDDLE POMERANIAN SCIENTIFIC SOCIETY OF THE ENVIRONMENT PROTECTION

Rocznik Ochrona Środowiska

Volume 22. Year 2020 ISSN 1506-218X 144-155

Energy Consumption Determination of the Heat Storage Device Based on the Phase Change Material Depending on the Temperature Ranges

Vladyslav Bondarenko[1], Abdessamad Faik[2,3], Yaroslav Grosu[2,4], Victor Stoudenets[1]*

[1]National Technical University of Ukraine Igor Sikorsky Kyiv Polytechnic Institute, Kyiv, Ukraine

[2]Centre for Cooperative Research on Alternative Energies (CIC energiGUNE), Basque Research and Technology Alliance (BRTA), Vitoria-Gasteiz, Spain

[3]Materials Science, Energy and Nano-engineering, Mohammed VI Polytechnic University, Ben Guerir, Morocco

[4]University of Silesia, Katowice, Poland

[*]corresponding author's e-mail: v.stoudenets@kpi.ua

1. Introduction

The work deals with the peculiarities of the thermal energy storage in the concentrating solar unit based on Stirling engine, which is an ecological engineering system that includes the elements of material engineering. Thermal energy storage is one of the key functions in the concentration solar systems operation (Liu et al. 2016, Zhang et al. 2016), in particular, solar dish Stirling units (Andraka et al. 2015).

The purpose of the work is to study the operation of the heat storage device (HSD) based on the phase change material (PCM), Mg-51%Zn eutectic metal alloy (Blanco-Rodríguez et al. 2014a,b), and to determine its basic energy characteristics.

The battery consists of two concentric steel cylinders with the bottom space filled with the alloy. The design of the heat storage device is determined by its purpose. It is used for the continuous operation of the solar dish Stirling UDS-1 (Stoudenets el al. 2019, Stoudenets & Dudarchuk 2019).

The previous work (Bondarenko 2018a) described the process of creating the heat storage from the alloy Mg-51%Zn with the next parameters:
PCM phase transition specific heat – 155 kJ/kg; PCM specific heat – 0,73 kJ/(kg K); PCM mass – 143 g; HSD net weight – 197 g.

In the course of the experimental studies, the heat storage device was heated to a predetermined temperature (higher than the melting temperature of the alloy) and cooled independently. The melting temperature is 337°C. During the cooling the heat storage device temperature was measured at four points. The work (Bondarenko 2018b) describes the conduct of experimental studies measuring the basic characteristics of the solar unit and the obtained experimental data are presented.

2. Investigation of the heat storage when cooled on the outdoor air

Using thermograms obtained by the heat storage cooled independently on the air, the thermogram of the heat recovery process averaged over the heat storage was obtained (Fig. 1). In this case, we consider that thermocouple sensors mounted on the heat storage surface on the insulation side indicate the temperature of the storage substance, considering that the steel wall of the heat storage shell has a thickness of 0.5 mm and a thermal conductivity of 26.1 W/m·K. The average temperature of the accumulating substance is defined as the arithmetic mean between the statements of the four temperature sensors.

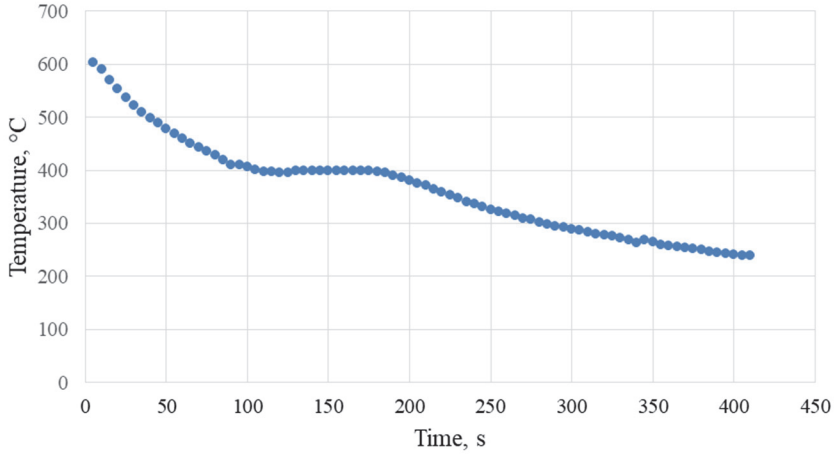

Fig. 1. Averaged thermogram of the heat transfer process by the heat storage when cooled on the outdoor air

Based on the experimental data, the heat flow from the heat storage to the environment was calculated, except for the heat of the phase change. This calculation is somewhat different from the approach used for phase transitions in liquid media, e.g. (Pavlenko & Koshlak 2019). In this case, only the explicit heat is taken into account in the value of the heat flux, since with the phase change the body temperature does not change. The heat flow diagram from the heat storage with the exception of the heat of the phase change is shown in Fig. 2.

Since the heat released by the heat storage into the environment is equal to the change in the internal energy of the heat storage, the heat flux, except for the heat of the phase change, is calculated by the formula (1):

$$Q = \frac{\left(m_1 c_1 + m_2 c_2\right)\left(t_2 - t_1\right)}{\tau}, \tag{1}$$

where:

m_1 – mass of the storage substance, kg; c_1 – specific heat capacity of the storage substance, kJ/(kgK); m_2 – mass of the heat storage shell, kg; c_2 – specific heat capacity of the heat storage shell, kJ/(kgK); Δt – temperature change of the storage substance, °C; τ – time period, sec.

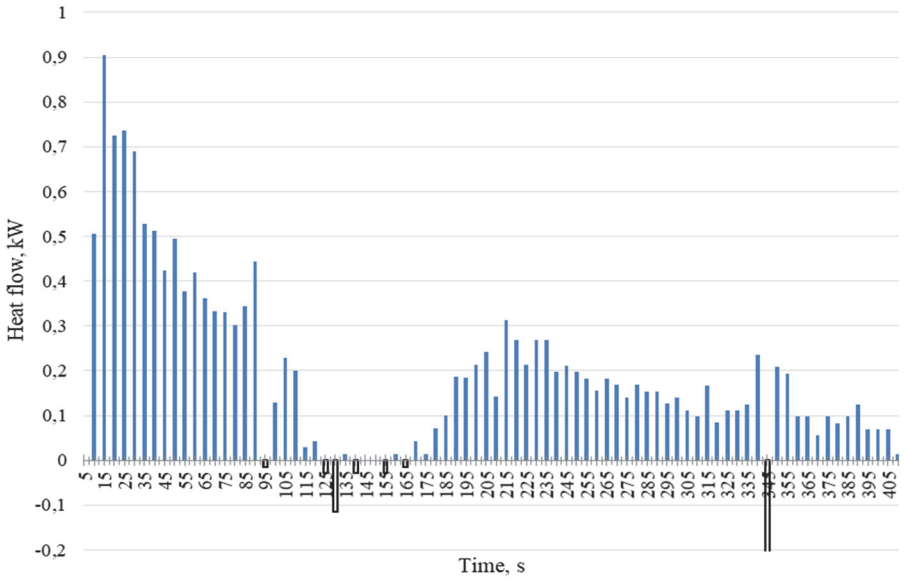

Fig. 2. Heat flow except heat of phase change from heat storage when cooling outdoors

The cooling process can be divided into three phases:

- cooling of the metal in the liquid phase,
- phase change,
- cooling of the metal in the solid phase.

Thus, Figure 2 describes the heat flow during the first and third phases. To determine the heat flux component of heat storage corresponding to the secreted heat release (phase 2), it is necessary to take into account the heat of the phase change of the substance and divide it evenly over the time during which the phase change occurs, since during this period the temperature of the heat storage does not change significantly and the amount of heat flux is permanent. But since the phase change process in the heat storage volume is uneven (the metal at the top of the heat storage reaches the phase change temperature earlier than the lower part), it is difficult to determine the time limits of the phase change. To correctly divide a thermogram into 3 zones, it is necessary to describe the temperature curves in each zone with a mathematical expression that reflects the nature of the temperature change. When the body is independently cooled, the temperature changes exponentially, and during the phase change the temperature is constant, so the schedule of the heat storage temperature changing will consist of two exponents and one horizontal section. The first interval is attributed to the period from 5 to 90 seconds, and to the third interval – from 185 to 410 seconds.

Since the process of the heat storage which cooled independently in the air is exponential, the schedule of temperature change should be described by the function (2).

$$t(\tau) = t_0 + ae^{-b\tau} . \tag{2}$$

As a result of the approximation of the experimental data in the first and third sections, a diagram of temperature change over time is presented in Fig. 3, and the corresponding heat flow diagram is shown in Fig. 4.

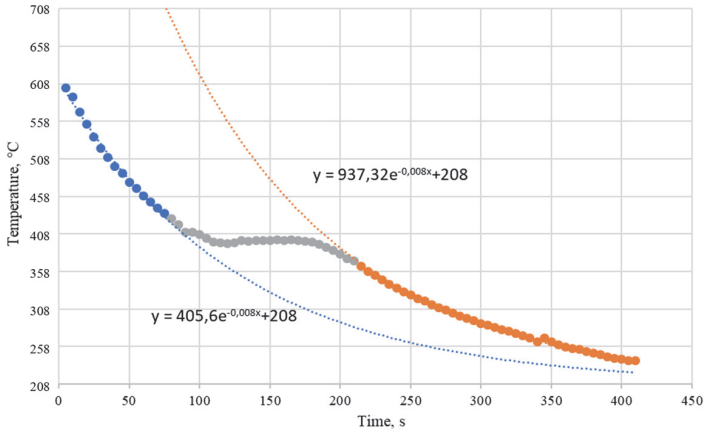

Fig. 3. Averaged thermogram of the heat transfer process by the heat storage after extrapolation of sections

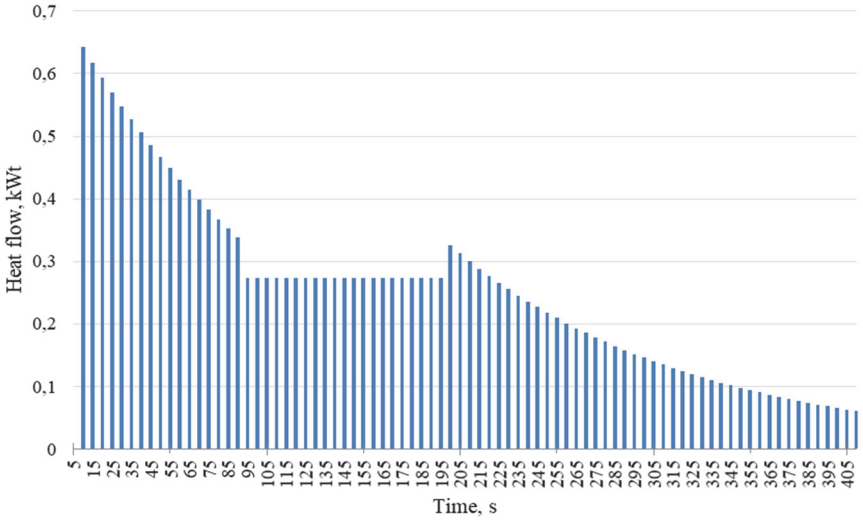

Fig. 4. The heat flow diagram is obtained from the result of mathematical analysis of experimental data

Thus, the amount of heat stored by the heat storage due to the heating of the liquid metal is 46.3 kJ, during the phase change is 22.2 kJ and during the cooling of the solid phase of the metal is 36.6 kJ. The amount of stored heat per unit mass of the HSD is 0.31 kJ/g.

3. Modeling the process of the heat storage cooling on the air using SolidWorks software

Numerical modeling is used to solve various problems of conversion and storage of thermal energy. Modeling of processes in heat exchangers and heat accumulators is often carried out using the universal ANSYS software package. Examples can be given of using ANSYS for internal and external problems in heat exchangers (Deshko et al. 2016, Orlowska et al. 2019) and for thermal storage (Xu et al. 2015, Gorobets et al. 2018). In our study, we used Solidworks software product as more adapted to the specific problem being solved.

Using the data obtained from the experiment, a heat storage model was developed. The outer walls of the heat storage are adiabatic. The inner walls are the real walls that take part in both convective and radiation heat transfer. Heat storage wall material is AISI 304 stainless steel. Heat storage temperature depends on time and consistents with the results of the experiment.

Fig. 5 shows the dependence of the heat storage temperature on time.

The appearance of the model and calculation area is shown in Fig. 6.

The simulation resulted in the following data:

- heat fluxes (convective and radiation component),
- heat transfer coefficients from the heat storage,
- air temperature distribution heated by the heat storage.

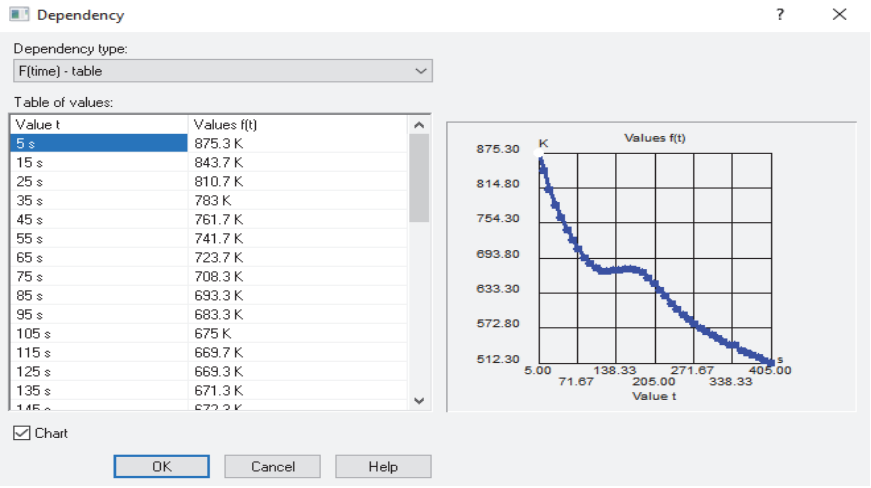

Fig. 5. Dependence of the heat storage temperature on time (experimental data)

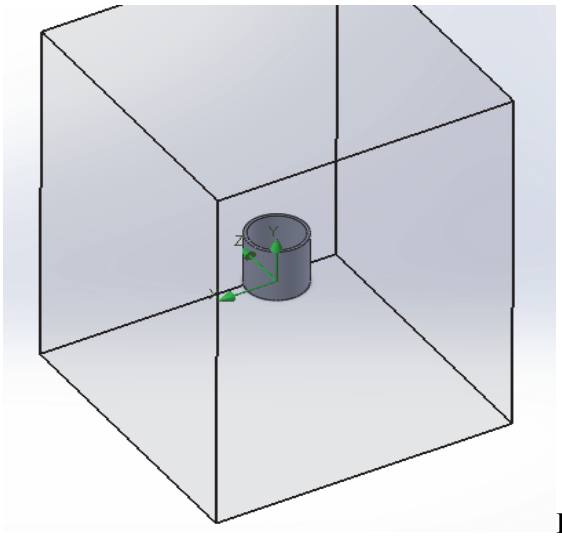

Fig. 6. Appearance of the model

The distribution of temperature fields at time 5, 135 and 405 seconds is shown in Fig. 7-9.

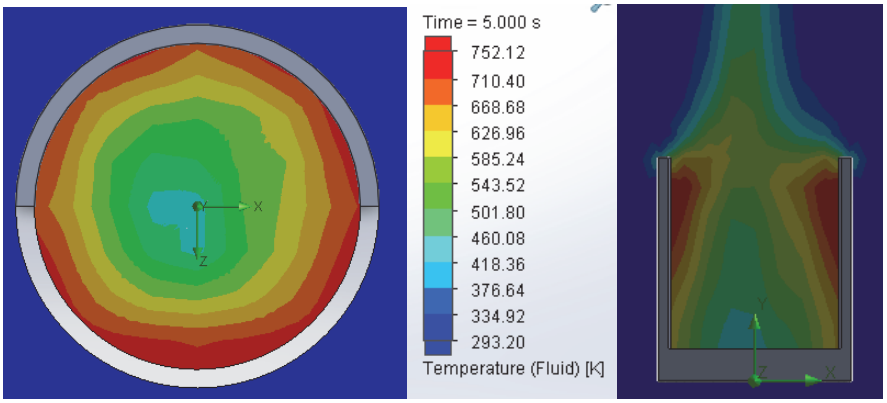

Fig. 7. The distribution of air temperature fields at a time of 5 seconds

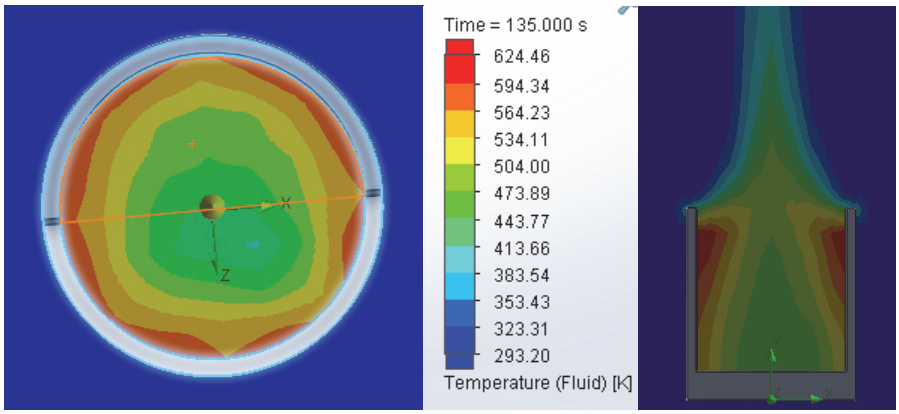

Fig. 8. The distribution of air temperature at a time of 135 seconds

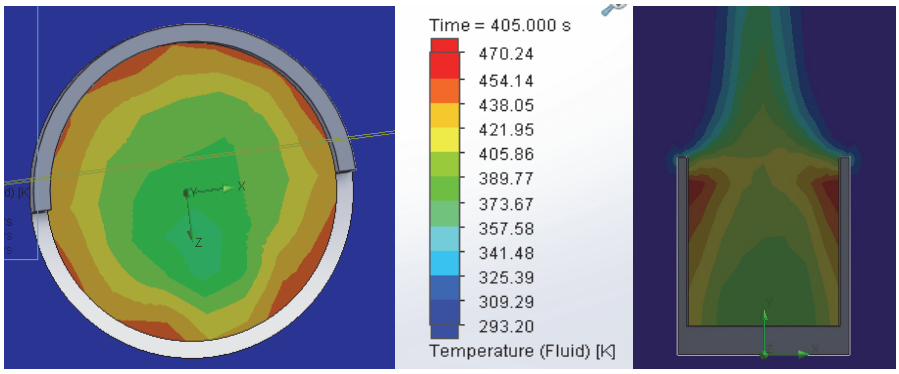

Fig. 9. The distribution of air temperature fields at a time of 405 seconds

Fig. 10-12 show diagrams of heat loss of the heat storage over time.

The simulated heat flux values shown in Fig. 12 are correlated with the values obtained after processing the experimental data and are presented in Fig. 2.

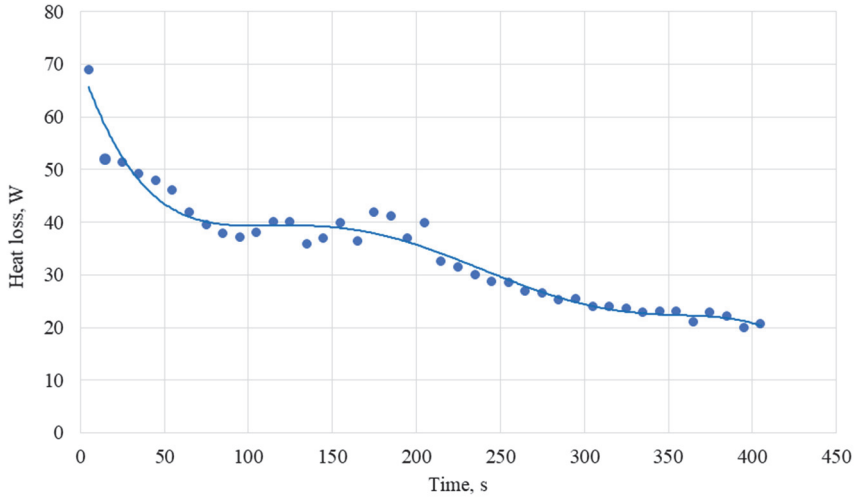

Fig. 10. Dependence of convective heat loss of the heat storage on time

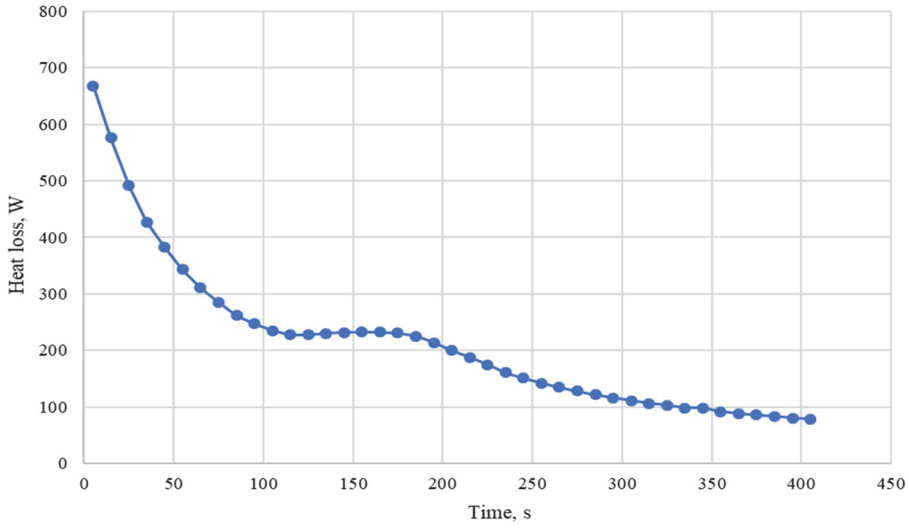

Fig. 11. Dependence of radiation heat loss of the heat storage on time

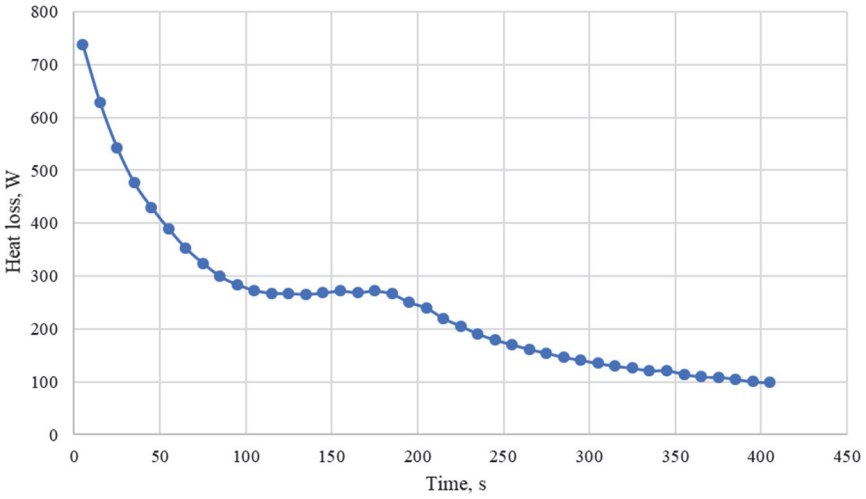

Fig. 12. Dependence of total heat loss of the heat storage on time

On the basis of the obtained results, the heat capacity of the heat storage in different temperature ranges of its use was calculated (Fig. 13). The phase change is included in each range. The difference between the initial and final temperatures of each range is 200°C.

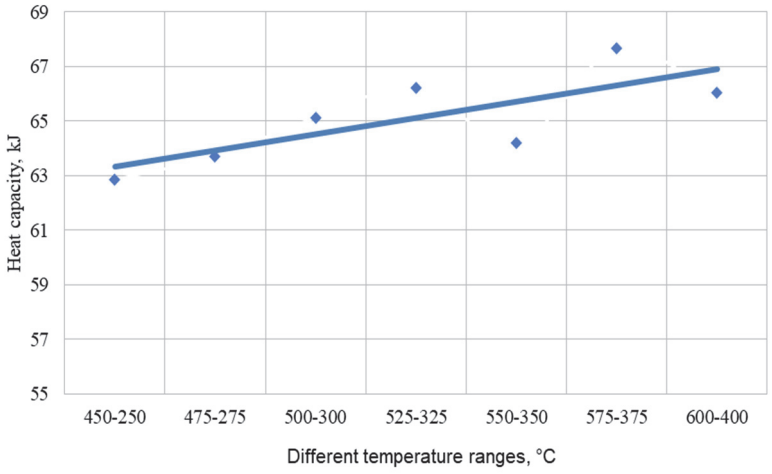

Fig. 13. Dependence of heat storage heat capacity on temperature ranges

4. Conclusions

As a result of the studies, the following HSD basic energy characteristics were obtained.

1. The total amount of heat given off by the HSD according to the simulation results is 102.2 kJ. When approximating the experimental data, the corresponding value is 105.1 kJ. Thus, the difference between the calculation results and the simulation is less than 3%.
2. The amount of heat stored by the heat storage due to the heating of the liquid metal is 46.3 kJ, during the phase change – 22.2 kJ and during the cooling of the solid phase of the metal – 36.6 kJ.
3. The amount of stored heat per unit mass of the HSD is 0.31 kJ/g.
4. The dependence of heat capacity on the interval of operating temperatures of the heat storage is determined. At higher initial and final temperatures (at regular working intervals) the heat capacity is higher.

References

Andraka, C.E., Kruizenga, A.M., Hernandez-Sanchez, B.A., & Coker, E.N. (2015). Metallic phase change material thermal storage for dish Stirling. International Conference on Concentrating Solar Power and Chemical Energy Systems, SolarPACES 2014, No.SAND2014-15888C. *Energy Procedia, 69,* 726-736.

Blanco-Rodríguez, P., Rodríguez-Aseguinolaza, J., Risueño, E., Faik, A., Tello, M., Doppiu, S. (2014). Corrigendum to "Thermophysical characterization of Mg-51%Zn eutectic metal alloy: A phase change material for thermal energy storage in direct steam generation applications". *Energy*, *75*, 630.

Blanco-Rodríguez, P., Rodríguez-Aseguinolaza, J., Risueño, E., Tello, M., (2014). Thermophysical characterization of Mg-51%Zn eutectic metal alloy: A phase change material for thermal energy storage in direct steam generation applications. *Energy*, *72*, 414-420.

Bondarenko, V.V. (2018). Doslidzhennia teplovoho akumuliatora dlia soniachnoi enerhoustanovky na bazi dvyhuna Stirlinha (Research of thermal accumulator for solar power unit based on Stirling engine). *Proceedings of the scientific and technical conference "Enerhetyka. Ekolohiia. Liudyna (Energy. Ecology. Human) 2018*". Institute of Energy Saving and Energy Management of NTUU "KPI". 165.

Bondarenko, V.V. (2018). Vyhotovlennia teplovoho akumuliatora dlia soniachnoi enerhoustanovky na bazi dvyhuna Stirlinha (Manufacturing of thermal battery for solar power unit based on Stirling engine). *Proceedings of the 16th International Scientific and Practical Conference of Postgraduate, Undergraduate, and Students "Suchasni problemy naukovoho zabezpechennia enerhetyky (Modern Problems of Scientific Energy Supply)" April 24-27, 2018. Kyiv*. 233.

Deshko, V.I., Karvatskii, A.Y., & Sukhodub, I.O. (2016). Heat and mass transfer in cross-flow air-to-air membrane heat exchanger in heating mode. *Applied Thermal Engineering*, *100*, 133-145.

Gorobets, V., Antypov, I., Trokhaniak, V., Bohdan, Y. (2018). Experimental and numerical studies of heat and mass transfer in low-temperature heat accumulator with phase transformations of accumulating material. *MATEC Web of Conferences, 240*, 01009.

Liu, M., Tay, N.S., Bell, S., Belusko, M., Jacob, R., Will, G., ... & Bruno, F. (2016). Review on concentrating solar power plants and new developments in high temperature thermal energy storage technologies. *Renewable and Sustainable Energy Reviews*, 53, 1411-1432.

Orlowska, M., Szkarowski, A., Mamedov, Sh. (2019). Numerical Analysis of the Influence of the Angle of Inclination of the Screen on the Intensity of Heat Exchange from a Flat Heat Exchanger in a Partially Limited Space. *Rocznik Ochrona Środowiska, 21*(1), 728-737.

Pavlenko, A., Koshlak, H. (2019). Heat and Mass Transfer During Phase Transitions in Liquid Mixtures. *Rocznik Ochrona Środowiska, 21*(1), 234-249.

Stoudenets, V.P., Dudarchuk, D.V. (2019). The 1 kW Stirling Engine for Solar Power System with Parabolic Concentrator and Electric Generator. *Journal of New Technologies in Environmental Science.* 153-165.

Stoudenets, V.P., Tsyrin, N.N., Ievtushenko, O.V. (2019). *Solar Power Systems Based on Stirling Cycle Machines and Thermomolecular Technology.* Management of Technological Processes in Energy Technologies / General editorship of A.M. Pavlenko // Politechnica Świetokrzyska Kielce University of Technology. 146-182.

Xu, B., Li, P., & Chan, C. (2015). Application of phase change materials for thermal energy storage in concentrated solar thermal power plants: a review to recent developments. *Applied Energy*, *160*, 286-307.

Zhang, H., Baeyens, J., Caceres, G., Degreve, J., & Lv, Y. (2016). Thermal energy storage: Recent developments and practical aspects. *Progress in Energy and Combustion Science*, *53*, 1-40.

Abstract

The work concerns determining the energy performance of the heat storage device based on the phase change material for the solar dish Stirling unit. Experimental studies were performed with the heat storage material, made of the eutectic metal alloy Mg-51%Zn. The energy characteristics are determined by mathematical analysis of the experimental data and simulation of the process of cooling the heat storage.

Keywords:
heat storage, phase change material, solar dish Stirling

MIDDLE POMERANIAN SCIENTIFIC SOCIETY OF THE ENVIRONMENT PROTECTION

Rocznik Ochrona Środowiska

Volume 22. Year 2020 ISSN 1506-218X 156-170

Proposal of a Logistics Solution for an Emergency at a Nuclear Facility

Oľga Végsöová, Martin Straka, Kamil Kyšeľa*

Technical University of Kosice, Slovakia

**corresponding author's e-mail: e-mail: martin.straka@tuke.sk*

1. Introduction

At present, when solutions are being sought to mitigate the effects of global warming and climate change, nuclear energy is one of the interesting alternative energy sources in the ecological energy sector, of course assuming it is used in a safe form.

Proponents consider nuclear energy to be one of the possible solutions to the looming energy crisis, while its opponents fight against the use of nuclear energy, because of: fear of radiation, the risks associated with the operation itself or problems with nuclear waste.

As already indicated, a nuclear power plant and its operations have only a minimal negative impact on the environment. Nuclear power plants do not emit any greenhouse gases, so they contribute to reducing emissions. Zhang et al. (2020) points out that the aim of using nuclear and renewable energy is to reduce greenhouse gases and improve the quality of the environment. Soder (2009) argues that at a time of climate change, dwindling oil supplies and high consumer prices, nuclear energy is an essential part of the future energy spectrum. Chen et. al. (2019) stated that nuclear energy has become a common source of energy for communities around the world. Despite the relatively small number of global incidents, there is still potential for a nuclear disaster. The construction of a nuclear power plant has a great economic benefit in terms of the development of a region, having a positive impact on employment and therefore on the living standards of the population living in the vicinity. Fuentes-Saguar et al. (2017), point out in their work that a possible decommissioning of a nuclear power plant would have a demonstrably adverse effect on employment and created added value in the region.

Over time, however, the impact on the environment and ecology has become the most important criteria. According to Deng et.al. (2018) The development of nuclear energy is a key measure for implementing energy saving and emission reduction strategies worldwide.

One of the chief elements acting on humans is radon, which is found in building materials, Ali et al. al. (2019) point to the direct effect of radon on human health and the possibility of cancer when it enters the lungs. Humans are also commonly exposed to radiation from TVs, watches and, last but not least, X-rays used in medicine. Pogue et. al. (2018) consider the possible carcinogenic effects to be one of the disadvantages of X-rays. Furukawa et. al. (2020), in their work, unequivocally confirmed the negative impact of radiation on human DNA as well as the mechanisms of its natural regeneration.

Nuclear power plants are a critical part of infrastructure from the perspective of safety. The failure of a nuclear power plant causes not only economic losses, but it is a particular threat to the safety of the whole country and significantly affects the surrounding environment. Connor et. al. (2020) argue that immediately after a large-scale release of radioactive material into the environment, it is necessary to quickly determine the spatial distribution of radioactivity. Mlakar et. al. (2019) point out that nuclear power plants should constantly invest resources in improving safety and risk management. Persons in the immediate vicinity of a nuclear power plant are exposed to the greatest risks. Therefore, it is important to properly create and model situations describing evacuation from the power plant. Liu et. al. (2012) argue that that emergency evacuation is one of the most important nuclear accident risk management measures. Evacuation management systems contain various complexities that present many challenges for decision makers. Lee et. al. (2019) state that the occurrence of an emergency or crisis situation usually requires an immediate solution for the protection of the population.

Failure management includes pre-planned, dedicated activities that ought to make optimal use of the plant's existing equipment in a normal as well as unusual manner if the design limits are exceeded. The main objective in the event of a nuclear power plant failure is to protect human lives. Shimada et. al. (2018) point out that the decision to evacuate is crucial, especially for vulnerable populations. The primary problem that must be solved in the event of an exceptionally undesirable circumstance in a nuclear power plant is the evacuation of people located in the power plant building itself. In order to actively react to these emergencies, it is necessary to develop an emergency rescue plan before an adverse event occurs. Zong et. al. (2019) hold the opinion that emergency evacuation research has become an important and urgent issue. The evacuation process places high organizational demands on cooperation among the rescue and security forces. Řehák and

Folwarczny (2012) and Folwarczny and Pokorný (2006) argue that the rescue process requires the cooperation of different actors in a complex environment, so effective communication is needed to streamline emergency operations. Effective communication is a prerequisite for timely and therefore successful intervention. The aim must be predetermined communication with a predetermined range of communication topics, having a positive effect on the accuracy and speed of obtaining information from the communication partner. Gallego et. al. (2017) argue that the aim of communication is to provide accurate and clear messages that can serve to reassure the public. Gershon et. al. (2012) state that time is the most valuable resource in an emergency. Shorter rescue times could save more lives and reduce overall damage. Xie et al. (2020) are of the opinion that accident detection and rescue response times should be shortened in order to enable victims to receive the necessary emergency care as soon as possible.

Phark (2018) points out that evacuation performed by recommendation and leading through natural authority and social contact is most effective. Yang et. al. (2015) point out that the efficiency of evacuation increases with an increasing number of escorts until the number reaches the optimal level. Murakami et.al. (2015), Koščo et al. (2019), Trebuna et al. (2019) and Dyntar et al. (2020) state that it is necessary to adapt the evacuation plan to the specific conditions in order to increase the success of the evacuation.

Based on the studied literature, the article deals mainly with the time aspect of the evacuation of persons located in the nuclear power plant. In this paper, we model the evacuation from one building in the power plant complex, which has a nuclear shelter.

2. Theoretical basis, safety assessment at a nuclear facility

The importance of safety is significant in the production of electricity in a nuclear power plant. It is therefore necessary to address the situation of an emergency caused by the failure of a nuclear installation, and it is important to inform the public in a timely and thorough manner. Table 1 from Bromová et al. (2013) offers us an overview of the severity of individual areas affected by an emergency.

The information flow and the procedure for dealing with emergencies differ based on certain degrees of severity of these events. The internal emergency plan states the classification and assessment of incidents based on their severity that have an actual or potential impact on the level of nuclear safety. According to Table 2, which is part of the internal emergency plan of Slovenské elektrárne (2011) we classify extraordinary events according to their severity into three degrees.

Table 1. Description of the impact of degrees of severity on the individual areas affected by the emergency.
Source: own elaboration

Stage	Relevant name	Impact on			Source	Measures
		People and the environment	Radiation barriers	Depth protection		
1	Anomaly	little impact	negligible impact	deviation from the approved operating mode	stolen or lost source with low radioactivity	
2	Accident	excess irradiation of the employees of the given operation (above the permitted values)	spread of contaminati on - significant	serious breach of security measures without real consequences	finding an abandoned high-level radioactive source, equipment or transport container with intact safety precautions; insufficient packaging of a sealed highly radioactive source	
3	Serious accident	greater impact on the health of employees (acute effects of irradiation); little impact on the population living in the vicinity of the SW	spread of contaminati on - large	safety barriers gone	a lost or stolen highly radioactive sealed source; a highly radioactive sealed source that has been delivered to a different location than the intended delivery location	

Table 1. cont.

Stage	Relevant name	Impact on			Source	Measures
		People and the environment	Radiation barriers	Depth protection		
4	Accident with effects in a nuclear facility	irradiation of the population within the permitted limits; lethal irradiation of employees	there is significant damage to the reactor core			
5	Accident with effects on the environment	leakage of radioactive material – limited	serious damage to the reactor core occurs			likely deployment of some of the planned measures (considering gravity of the situation)
6	Serious accident	leakage of radioactive material – serious				likely deployment of planned countermeasures
7	Large accident	extensive impact on public health and the environment				deployment of the planned measures and, depending on the gravity of the situation, the deployment of extended measures

Table 2. Characteristics of degrees of classified events based on severity.
Source: Slovenské elektrárne (2011)

1st degree	Alert	A condition in which the performance of safety functions is endangered or impaired.
		Safety barriers are compromised or inoperable.
		There is a possible threat of leakage, or the leakage of radioactive substances has occurred in the facilities of the nuclear facility.
2nd degree	Emergency on the site of a nuclear facility	A situation in which there is a possibility of leakage or the result of the situation is the leakage of radioactive substances outside the structures of the nuclear facility and into adjacent territory.
3rd degree	Emergency around a nuclear facility	A situation in which there is a possibility of a serious leakage of radioactive substances or the result of this situation is a serious leakage of radioactive substances into the area around a nuclear installation.

Since the intended evacuation takes place in groups for calculation, formulas will be used which focus on calculating the evacuation of the stream of evacuees. Therefore, first of all, it is necessary to calculate the density of the stream, where we use formula proposed by Folwarczny and Pokorný (2006), defined as:

$$D_p = \frac{E \,.\, f}{b \,.\, l} \tag{1}$$

where:
D_p – density of stream [-],
E – number of persons [persons],
f – area per person [$m^2 \cdot person^{-1}$],
b – current width [m],
l – current length [m].

Since we assume that people will move only on horizontal paths without obstacles, we will use the formula for the calculation:

$$v = 112 \,.\, D_p^4 - 380 \,.\, D_p^3 + 434 \,.\, D_p^2 - 217 \,.\, D_p + 57 [\mathrm{m.min^{-1}}] \tag{2}$$

where:
v – speed of movement of persons [$m \cdot min^{-1}$],
D_p – current density [-].

3. Case study, proposal of an evacuation plan for the Mochovce Nuclear Power Plant

Evacuation, as one of the basic ways of protecting the population, ensures the safe movement of persons from the endangered building at the Mochovce Nuclear Power Plant (Mochovce NPP) to the open area and the possible transfer of persons by means of transport to the designated evacuation points. The analysis evaluated the possibilities for the potential arrival times of the external rescue services with which Mochovce NPP has a contractual agreement.

The proposed evacuation is intended for a building with a capacity of 400 people and at the same time this building has a shelter in case of an emergency.

The case study offers two proposals. Both proposals involve evacuation in groups; group A consists of 20 people and group B consists of 50 people.

The calculations are adapted to the assumption that only one pair of firefighters will escort the groups. The building from which the evacuation takes place is defined as follows. The entrance of the building is oriented to the west, directly feeding onto the road along which the evacuation will take place. Assuming that the building is single-storey, we are working with an area of 700 m^2. Due to this area, a capacity of 400 people was chosen. If each person has an area of 1 m^2 available, the rest is calculated as non-efficient area (walls etc.). The length of the road leading from the evacuation building to the assembly point is 70 metres. The width of the road is 7.5 metres (3 metres per lane). The assembly in the form of the parking lot has dimensions of 50x100 metres. We work with an area of 5000 m^2. It follows that evacuees can gather at this location. Given that both men and women can move in this building, and we know that the structures of the bodies of the sexes are different. The calculations be based on the physiological structure of the figure of the man as the largest possible alternative. The width of a person is measured at shoulder height and for a man this average value is 510 mm. For the front-back dimension, this value is approximately 280 mm. Fig. 1 shows the structure described.

The following variants were considered for the evacuation plan of Mochovce NPP, labelled A and B.

Group A will consist of 20 people. Evacuees will be moved in a formation consisting of two lines and the number of persons in a row will be 10. For this reason, the approximate width of the stream of persons will be 1020 mm and the approximate length of the lines will be 3000 mm. The area per person is a table value for an adult in moderate clothing, $f = 0.113$ m^2 per person.

The results of variant A show the total time of evacuation from the given building to the assembly point in groups of 20 people and accompanied by only one group of accompanying firefighters; the time taken is expected to be 122 minutes.

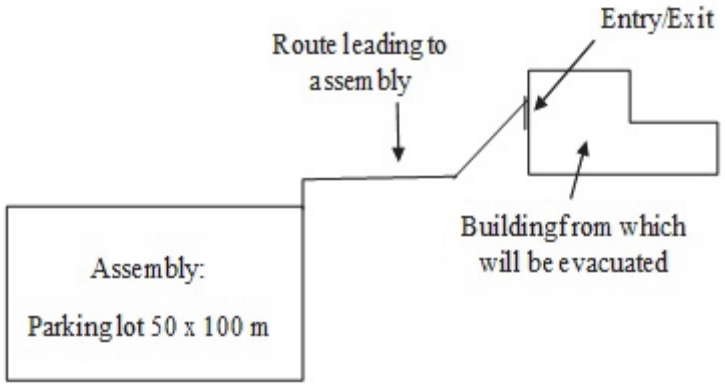

Fig. 1. Drawing of the structures that we need for evacuation. Source: own elaboration

Group B will consist of 50 people. Evacuees will be moved in a formation of 3 lines, in each of which there will be 16 persons, with the exception of 1 row that will consist of 17 persons. However, we ignore the data on this last person in the calculation; due to the number of people in this large group, it is not necessary to take this data into account. The width of the stream will be 1530 mm and the length of a row will be approximately 4800 mm. The area per person is a tabular value for an adult in moderate clothing, $f = 0.113$ m^2 per person.

The design of Option B results in a total expected evacuation time of 52 minutes from the given building to the assembly point in groups of 50 people and accompanied by only one group of accompanying firefighters.

In the event of an emergency, Mochovce NPP has the opportunity to call on the help of external organizations. Due to the fact that the organizations are not in close proximity to the facility, it is necessary to calculate the approximate time of arrival after which the organizations could start the activities necessary to deal with the emergency situation.

When looking for the route, there are two suitable routes in the direction from the premises of VUJE a.s., Trnava to the premises of Mochovce NPP, which are marked on the map in Fig. 2. As seen on the map, they vary in length. Travel time is calculated for both routes, due to the fact that the routes differ in length and particularly differ in terms of the roads the routes follow. Route A leads along first-class roads as we can see on the map, therefore the maximum speed is 50 km · h^{-1}. Route B, which is longer, runs on expressways and on the roads of the European road network, where the maximum permitted speed is 130 km · h^{-1}. It also includes first class routes, on which the maximum permitted speed is 50 km · h^{-1}. Therefore, in the case of B, the average speed is 90 km · h^{-1}.

The map in Fig. 3 shows two routes from the premises of the fire station in Levice to the premises of Mochovce NPP. Both of the routes follow first class roads, where the max. allowed speed 50 km · h^{-1}. With regard to regulations, the speed for the calculations is set at 45 km · h^{-1}.

From the Fire and Rescue Brigade's station based in Malacky, there are three potential roads leading to the Mochovce NPP site, as shown in Fig. 4. The shortest, route A, leads mostly along roads that are part of the European road network in combination with first class roads. Assuming that the vehicles used in the intervention will be fire engines or larger, the average speed will be 83 km · h^{-1} because on expressways and motorways, vehicles weighing more than 3500 kg have a maximum permitted speed of 100 km · h^{-1}. Routes B and C are also combinations of European network routes and first-class roads, but the average speeds are different in the calculations due to the varying lengths of the different types of roads used.

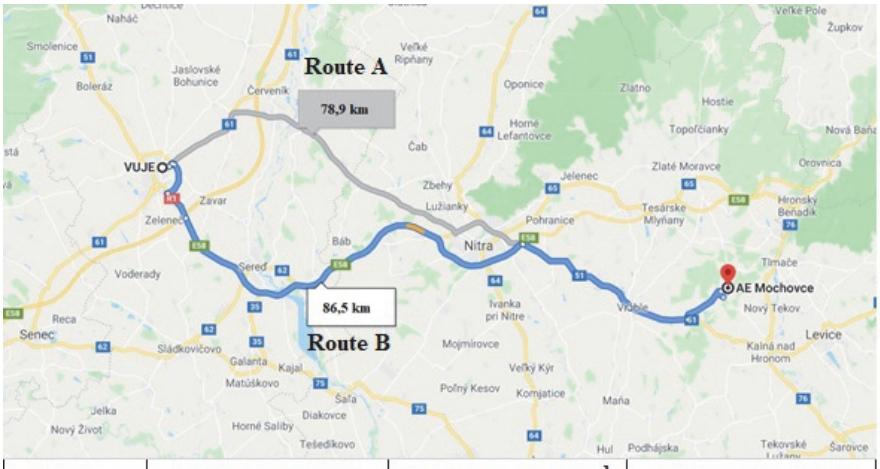

Route	Route lenght [km]	Driving speed [km.h^{-1}]	Driving time [min]
A	78,9	50	95
B	86,5	90	58

Fig. 2. Lengths routes VUJE as, Trnava - Mochovce NPP. Source: own elaboration

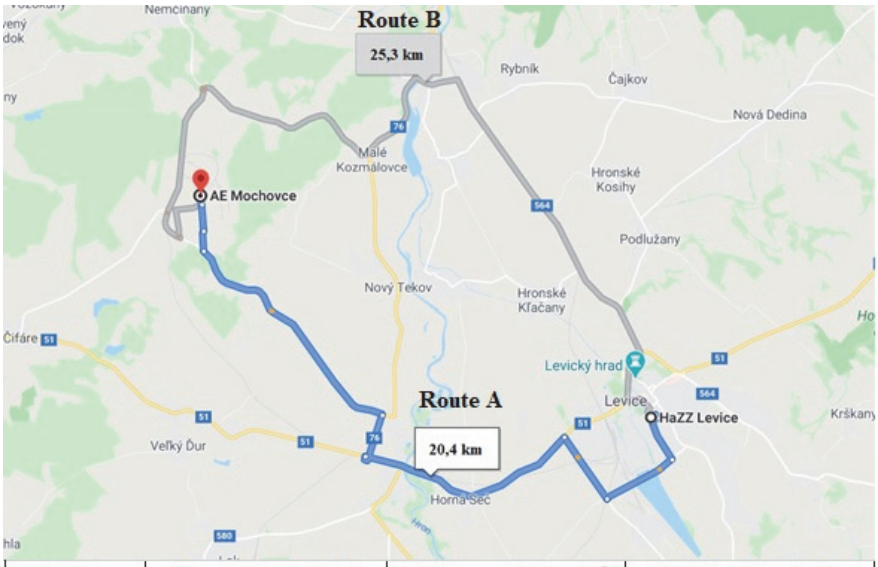

Route	Route lenght [km]	Driving speed [km.h^{-1}]	Driving time [min]
A	20,4	45	29
B	25,3	45	35

Fig. 3. Route lengths Fire and Rescue Corps Levice - Mochovce NPP. Source: own elaboration

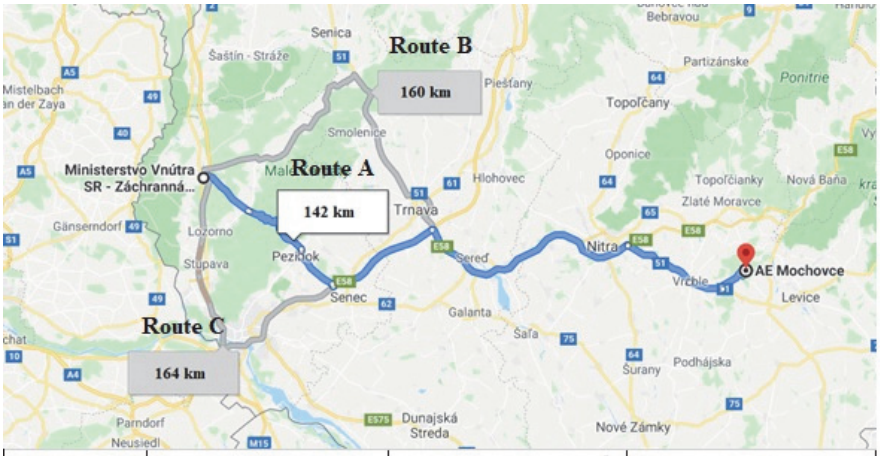

Route	Route lenght [km]	Driving speed [km.h^{-1}]	Driving time [min]
A	142	83	190
B	160	70	138
C	164	87	114

Fig. 4. Route lengths Fire and Rescue Brigade to Mochovce NPP. Source: own elaboration

4. Conclusion

A nuclear power plant is a complex and extensive facility in which special emphasis is placed on safety and evacuation procedures. Even during the design stage of the nuclear power plant, care must be taken to ensure that the location of the buildings and the nuclear shelter is such that the transfer to the evacuation assembly point is as efficient as possible.

An important role for government authorities is to anticipate the deployment of rescue services, so as to ensure, as far as possible, their quick arrival at the site of an emergency at a nuclear power plant. The proper location of all rescue services is essential for the safety of the whole area. The construction of such a system will significantly increase the protection of employees of the Mochovce NPP, as well as the population living in the area around of the structure in question.

The main motivation for the submitted contribution is therefore the aforementioned rescue of nuclear power plant employees and the surrounding population, but also the provision of the maximum possible level of safety for all the units involved.

The proposal points out how the number and formation of the evacuated group affects the time of the evacuation. It is logical that the more people we put in the group, the faster the evacuation will take place. However, the number of people in the group is determined by the surrounding environment and, last but not least, by employees' regular practices. Due to the size of the group, there are other aspects that need to be monitored, such as the increasing demands on supervision by escorts in a larger group. This supervision is necessary in view of the strain on the situation associated with the emergency. As we can see from the results, the fewer people in the group, the longer the evacuation time will be. It is therefore necessary to model a group size the composition of which will not place excess demand on the necessary supervision of the group and at the same time the number of individuals in the group will be maximized.

The evacuation time is not only affected by the number of individuals in the group but also by the number of trips that firefighters have to take during the evacuation.

A clear comparison of the evacuation design of variants A and B is shown in Fig. 5.

As regards calling external rescue services, the most effective help that arrives at the destination first in our case is the Levice Fire and Rescue Brigade, which must travel along a route of 20.4 km, taking 29 minutes.

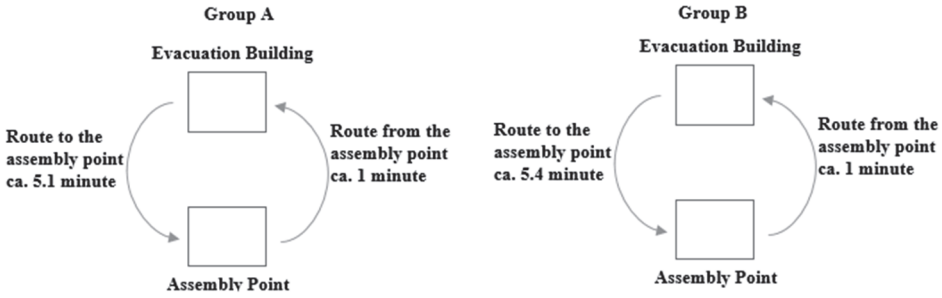

Description	Group A	Group B
D_p	0.74 [-]	0.77 [-]
v	13.7 m. min^{-1}	13.1 m. min^{-1}
X	5.1 min	5.4 min
Number of groups	20	8
Cycle there	102 minutes	44 minutes
Cycle back	20 minutes	8 minutes
Total cycle of evacuation	122 minutes	52 minutes

Fig. 5. Comparison of proposals A and B for evacuation in Mochovce NPP.
Source: own elaboration

In the case study, we start from the assumption that all examined external basic components are ready in terms of material and personnel for an emergency situation at Mochovce NPP.

The optimal way to perform this process as safely as possible in the shortest possible time could be to set up more groups of accompanying firefighters to accompany groups with fewer evacuees. However, we would then need a large number of staff members, which sometimes cannot be provided if we realize that the numbers of rescue services are limited and dependent on the travel times of external rescue services, which are also part of the work and depend on their location in the region.

The present proposal also points out how the evacuation of people from the power plant is to take place. The calculations confirmed the strengths as well as weaknesses of the evacuation removal process from the power plant area.

This knowledge and the suggestions for evacuation can be applied and adapted to similar structures and situations. At the same time, it is possible to assume that the travel times of external organizations will be an informational benefit in the creation of evacuation and rescue plans for the nuclear power plant and can also serve as a basis for providing technical assistance to units involved in dealing with emergencies at Mochovce NPP.

The submitted paper is a part of the projects "Projects of applied research as a means for development of new models of education in the study program of industrial logistics" KEGA 016TUKE-4/2020 and the project "Research and development of new smart solutions based on the principles of Industry 4.0, logistics, 3D modelling and simulation for streamlining production in the mining and building industry" VEGA 1/0317/19.

References

Ali, F.S.A, Mandi, K.H., Jawad, E.A. (2019). Humidity effect on diffusion and length coefficient of radon in soil and building materials. *Energy Procedia, 157*, 384-392.

Bromová, E., Vargončík D., Sovadina, M. (2013). *Jadrová energia a energetika* [in Slovak]. Simopt, s.r.o., Slovak Republic, 1-72, ISBN: 978-80-87851-06-7.

Chen, X., Frazier, C., Manandhar, R., Han, Z.G., Jia, P. (2019). Inequalities of Nuclear Risk Communication Within and Beyond the Evacuation Planning Zone. *Applied Spatial Analysis and Policy, 12*(3), 587-604.

Connor, D.T., Wood,K., Martin, P.G., Goren, S.,Megson-Smith, D.,Verbelen, Y., Chyzhevskyi, I., Kirieiev, S., Smith, N.T., Richardson, T., Scott, T.B. (2020). Radiological Mapping of Post-Disaster Nuclear Environments Using Fixed-Wing Unmanned Aerial Systems: A Study ‚From Chornobyl. *Frontiers in Robotics and AI, 6*(149). Article Number: 149.

Dyntar, J., Strachotová, D., Botek, M. (2020). Adjusting direct distance to road for V4 countries. *Acta logistica, 7*(2), 85-93.

Folwarczny, L., Pokorný, J. (2006). *Evakuace osob* [in Czech]. Ostrava: Sdružení požárního a bezpečnostního inženýrství, 1-120, ISBN 978-80-8663-492-0.

Fuentes-Saguar, P.D., Vega-Cervera, J.A., Cardenete, M.A. (2017). Socio-economic impact of a nuclear power plant: Almaraz (Spain). *Applied economics, 49*(47), 4782-4792.

Furukawa, S., Nagamatsu, A., Nenoi, M., Fujimori, A., Kakinuma, S., Katsube, T., Wang, B., Tsuruoka, C., Shirai, T., Nakamura, A.J., Sakaue-Sawano, A., Miyawaki, A., Harada, H., Kobayashi, M., Kobayashi, J., Kunieda, T., Funayama, T., Suzuki, M., Miyamoto, T., Hidema, J., Yoshida, Y., Takahashi, A. (2020). Space Radiation Biology for "Living in Space". *Biomed Research International,* Article Number: 4703286.

Gallego, E., Cantone, M.C., Oughton, D.H., Perko, T., Prezelj, I., Tomkiv, Y. (2017). Mass media communication of emergency issues and countermeasures in a nuclear accident: fukushima reporting in european newspapers. *Radiation protection dosimetry, 173*(1-3), 163-169.

Gershon, R.R.M., Magda, L.A., Riley, H.E.M., Sherman, M.F. (2012) The World Trade Center evacuation study: Factors associated with initiation and length of time for evacuation. *Fire and materials, 36*(5-6), 481-500.

Koščo, J., Tauš, P., Šimon, P. (2019). Negative impacts of photovoltaic electric station operation for distribution of electrical energy in Sobrance. *Acta Tecnología, 5*(2), 23-27.

Lee, J.H., Yilmaz, A., Denning, R., Aldemir, T. (2019). Use of Dynamic Event Trees and Deep Learning for Real-Time Emergency Planning in Power Plant Operation. *Nuclear Technology, 205*(8), 1035-1042.

Liu, J.F., Yuan, W.F. (2012). Emergency Evacuation from a Multi-room Compartment. *Progress in Structure, PTS, 1-4, 166-169*.

Mlakar, P., Boznar, M.Z., Grasic, B., Breznik, B. (2019). Integrated system for population dose calculation and decision making on protection measures in case of an accident with air emissions in a nuclear power plant. *Science of the Total Environment, 666*, 786-800.

Murakami, M., Ono, K., Tsubokura, M., Nomura, S., Oikawa, T., Oka, T., Kami, M., Oki, T. (2015). Was the Risk from Nursing-Home Evacuation after the Fukushima Accident Higher than the Radiation Risk? *Plos One, 10*(9), Article Number: e0137906.

Phark, C., Kim, W., Yoon, Y.S., Shin, G., Jung, S. (2018). Prediction of issuance of emergency evacuation orders for chemical accidents using machine learning algorithm. *Journal of Loss Prevention in the Process Industries, 56*, 162-169.

Pogue, BW., Wilson, B.C. (2018). Optical and x-ray technology synergies enabling diagnostic and therapeutic applications in medicine. *Journal of Biomedical Optics, 23*(12), Article Number: 121610.

Řehák, D., Folwarczny, L. (2012). *Východiska technického a organizačního zebezpečení ochrany obyvatelstva* [in Czech]. Ostrava: Sdružení žárního a bezpečnostního inženýrství, *ISBN 978-80-7385-117-0.89.*

Shimada, Y., Nomura, S., Ozaki, A., Higuchi, A., Hori, A., Sonoda, Y., Yamamoto, K., Yoshida, I., Tsubokura, M. (2018). Balancing the risk of the evacuation and sheltering-in-place options: a survival study following Japan's 2011 Fukushima nuclear incident. *BMJ Open, 8*(7), Article Number: e021482.

Slovenské elektrárne (2011). *Vnútorný havarijný plán 0-PLN/0001* [in Slovak]. Interný dokument Slovenské elektrárne, a.s..

Trebuna, P., Pekarcikova, M., Edl, M. (2019). Digital Value Stream Mapping using the Tecnomatix plant simulation software. *International Journal of Simulation Modelling, 18*(1), 19-32.

Xie, R.H., Pan, Y., Zhou, T.J., Ye, W. (2020). Smart safety design for fire stairways in underground space based on the ascending evacuation speed and BMI. *Safety Science, 125*, Article Number: UNSP 104619.

Yang, X., Yang, X., Wang, Q., Kang, Y., Pan, F. (2020). Guide optimization in pedestrian emergency evacuation. *Applied Mathematics and Computation, 365,* Article Number: 124711.

Zhang, J., Leng, R.X., Chen, M.Y., Tian,X., Zhang, N. (2020). The future role of nuclear power in the coal dominated power system: The case of Shandong. *Journal of Cleaner Production, 256*, Article Number: 120744.

Zong, X.L., Wang, C.Z., Du, J.Y., Jiang, Y.L. (2019). Tree hierarchical directed evacuation network model based on artificial fish swarm algorithm. *International Journal of Modern Physics C, 30*(11), Article Number: 1950097.

Abstract

This paper examines the evacuation of people in the event of an emergency caused at a nuclear facility. The study describes the emergency preparedness of the Mochovce Nuclear Power Plant. The paper describes the proposal of the logistics solution and the implementation of protective and emergency preparation, which is determined by the internal emergency plan, based on the information flow in the event of an emergency and the activities of individual emergency response units. The above results indicate that the fewer people there are in one evacuated group, the longer the evacuation time will be. However, the reason is not the length of time to get to the assembly point itself, but the number of groups that must be created and therefore the higher number of trips that firefighters have to take. The optimal way to carry out this process safely, in the shortest possible time, could be to set up more groups of escorting firefighters, who would accompany groups with smaller numbers of evacuees. Strict preparation and adherence to preprepared instructions, based on logistical principles in the event of an emergency at a nuclear facility, minimizes loss of life and harm to the health of persons, and also damage to property or the environment.

Keywords:
environmental protection, nuclear power plant, emergency, logistics, evacuation

MIDDLE POMERANIAN SCIENTIFIC SOCIETY OF THE ENVIRONMENT PROTECTION

Rocznik Ochrona Środowiska

Volume 22. Year 2020 ISSN 1506-218X 171-180

Resource Saving and Eco-Friendly Technology for Disposal of Used Railroad Engine Oils

Yuliia Zelenko[1], Maryna Bezovska[1],
Valeriy Kuznetsov[2], Antonina Muntian[1]*
[1]Dnipro National University of Railway Transport named after Academician V. Lazaryan, Ukraine
[2]Railway Institute, Warsaw, Poland
[*]corresponding author's e-mail: vkuznetsov@ikolej.pl

1. Introduction

Waste generation is a significant problem for many sectors of the national economy of Ukraine, in particular for rail transport. The wastes featuring significant amounts are the oil-contaminated ones, among which it is necessary to single out the used engine oils of the engines of traction rolling stock of diesel-electric locomotives and diesel trains.

The waste oils after being discarded today are most often used without regeneration as heating and boiler fuel directly at railway enterprises or transferred for further use or regeneration to other enterprises. For example, waste oils can be used to lubricate forms at ferroconcrete products and construction plants as well as for other purposes instead of the corresponding fresh petroleum products (Chervinskiy et al. 2015, 2016, Pyza et al. 2018, Jacyna et al. 2018, Liu et al. 2019, Ashtiani et al. 2019).

For purification (regeneration) of used oils, most often there are used the simplest physical methods, such as settling, filtration and centrifugation. For settling one uses steel vertical and horizontal oil tanks. Such tanks are manufactured at factories and get on site in the finished form. These tanks are designed for an internal pressure of 0.07 MPa, with a tapered or flat bottom; they are installed above the ground on supports or underground at a depth of not more than 1.2 m from the ground level. In addition to the tanks the railways use different types of containers.

Clarification of oils here takes a sufficiently long period (from a few to six months); the obtained product, after being checked for its compliance with

the quality standards, can be reused for the same needs as a fresh one, but its useful life is much less because of the rapid loss by oil of its main operational parameters. Yet this method is the most widespread in the railway enterprises because it does not require large investments, specially trained personnel and high running costs.

Filters and centrifuges are used for fine clarification of used engine diesel oils. The main drawback of filters is their impossibility of removing water from oil. This problem can be solved with the help of separators.

However, all of the above methods only give a slight effect, clarifying the oil, but not removing the main aging products from it.

To obtain a better effect, a combination of different methods with the use of special additives must be applied to make the product complying with DSTU standards by all parameters. Only in this case can we talk about obtaining a completely restored product.

Thus, the simplest methods used today for the recovery of waste oils on the railways do not give a full effect; therefore, it is more rational to use the latest developments that will quickly pay off and give a significant ecological and economic effect.

2. Materials and methods

We have developed and proposed a scheme for the recovery of waste oils of the brand M-14B_2. It is more environmentally friendly unlike the most common and still used scheme of cleaning with sulphuric acid. As the sulfuric acid substituent – alkylbenzene sulfonic acid (ABSA) is a substance of hazard class 3 and sulfuric acid belongs to hazard class 2. In addition, the purified product yield in this scheme is more than 90% while the product yield in case of the sulfate acid purification is about 60%.

The general scheme includes heating the waste oil, mixing it with ABSA and SAS Neonol, centrifuging and doping to bring all of the operational parameters of the oil to the standards specified in the technical specifications and standards. The schematic representation of the regeneration process is shown in Figure 1 (Zelenko & Bezovska 2013, Zelenko et al. 2013). It is worth noting that it was the new combination of reagents that gave a positive result in the course of laboratory studies that made the further development of the scheme possible.

It is proposed to pump the waste oils from the diesel locomotive to the special balance tank and after settling to the first-stage mixer. Next, the oil is heated to the desired temperature in the mixer, then from the special containers there is added the required amount of reagents: ABSA and subsequently neonol. After mixing, the mass is fed through pipeline to the centrifuge and then to the

second-stage mixer. Besides, a dosing pump supplies an additive to the same mixer, and the mixing process is in progress.

Subsequently, the finished oil is pumped to a special storage tank or directly into an oil tank car for light petroleum products. If necessary, it is possible to transport the prepared oil to other users by rail or tank-vehicles. Also, the scheme provides for a sludge collecting container for discharging by-products from the first-stage mixer and centrifuge; these products are subsequently processed in a mixture with the process sludge of the enterprise.

As a tank for storing finished products, we propose to use the horizontal tank-cisterns, which are most often used as ready-storage tanks.

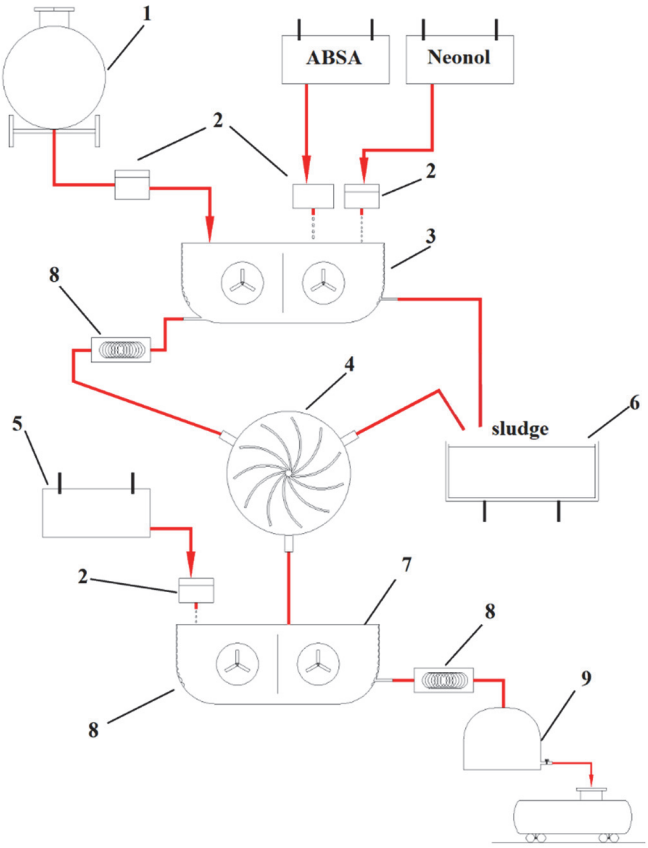

Fig. 1. Scheme for treatment of discarded waste oil; 1 – balance tank, 2 – dosing pumps, 3 – first-stage mixer with heating, 4 – centrifuge, 5 – additive storage tank, 6 – sludge collector, 7 – second-stage mixer, 8 – pumps, 9 – storage tank for restored oil

The main parameters monitored by us at all stages of the research were as follows:

- contamination, (τ cm^{-1}) – determines the degree of oil contamination by various impurities and is an indicator by which diesel oils are most often discarded at railway enterprises,
- pH – determines corrosive aggressiveness of oils,
- open flash point, °C – characterizes the presence of lightly boiling fractions in oils, in particular a significant deviation of this indicator from the norm indicates that the oil is diluted by fuel,
- viscosity at 100°C, mm^2/s – the most important indicator that determines starting and operation characteristics of machines,
- base number, mg KOH/g – an indicator that reflects the ability of oils to neutralize corrosive and aggressive products that are usually formed during its operation,
- water content, % – the appearance of this component contributes to the formation of low-temperature deposits, which impair the functioning of the diesel locomotive system, in particular filtration and subsequent feeding to the surfaces of friction.

3. Results and discussion

Below there are Figures 2-6, which show the main parameters of used and recovered oils compared with the discarding indicators and TU standards (except for water that was absent at all stages of the research). All data were obtained during experimental research at the university laboratory. Also the results were further confirmed at the depot's chemical engineering laboratory, where the rejected oil was received for testing.

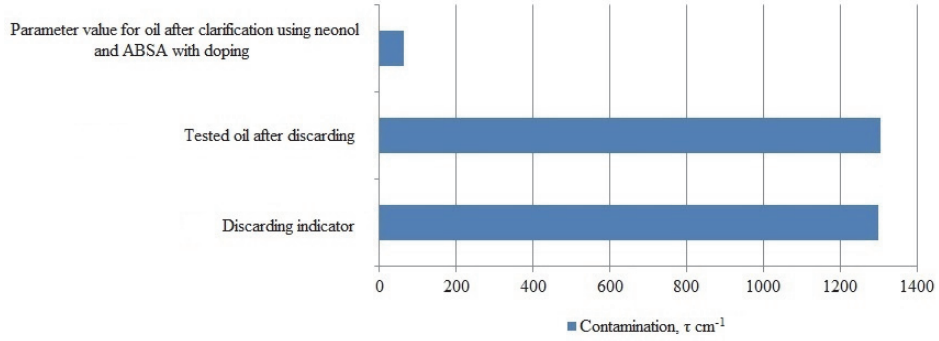

Fig. 2. Contamination

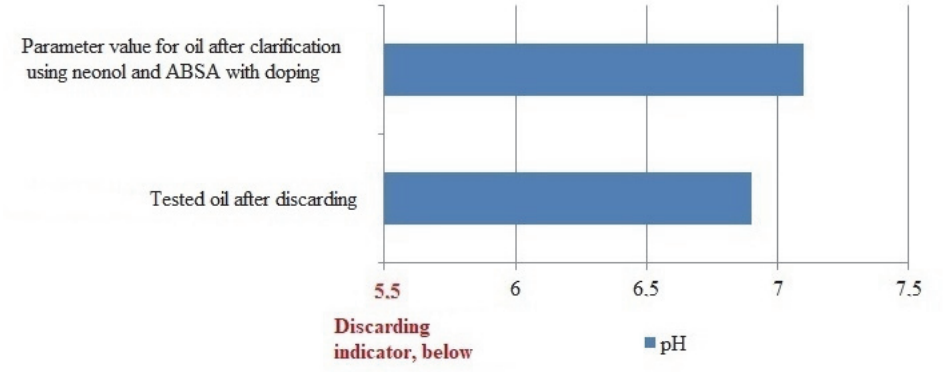

Fig. 3. pH

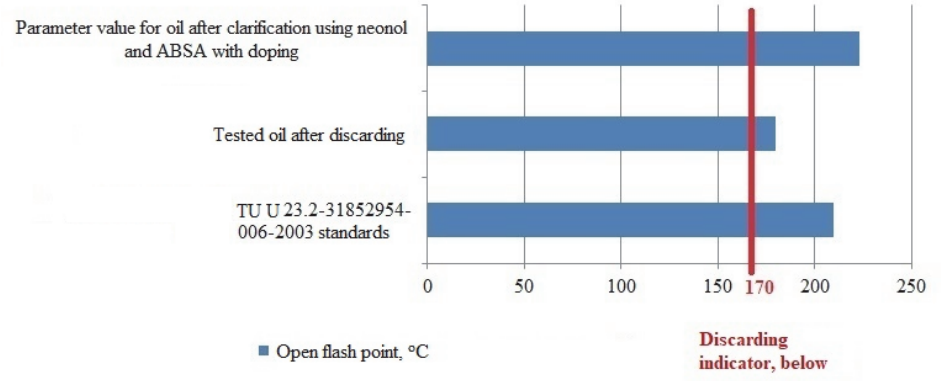

Fig. 4. Open flash point

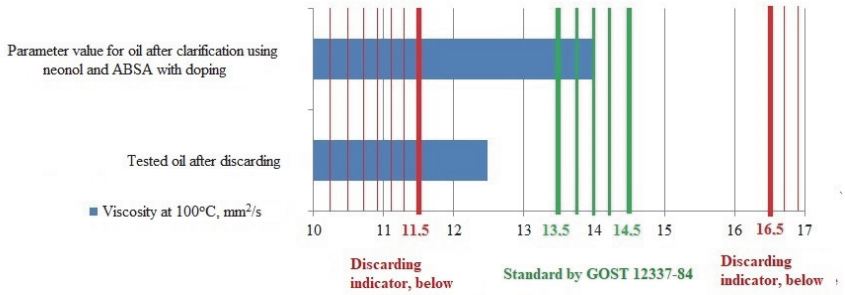

Fig. 5. Viscosity

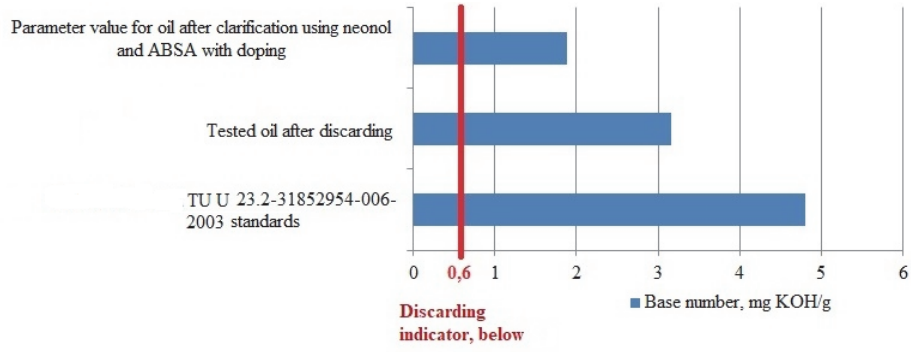

Fig. 6. Base number

We propose two options of implementation of the technological scheme: the first – to obtain small amounts of oil, which will accumulate in a special storage tank in the territory of line units of the railways for their internal needs; the second – for obtaining significant amounts of recovered oil at large oil regeneration stations serving a great number of enterprises. The calculation will be made on the basis of a greater amount of neonol to obtain universal-sized equipment, i.e. 2.7% by weight.

It should be noted that this scheme can also include the processing of oil-containing sludge, which will be processed together with sludge formed after oil purification. In particular, we recommend that these wastes be separated by means of surface-active substances into three fractions – water, hydrocarbons and solid residues; herewith the first two components can be used in production. Thus, the introduction of such a process scheme will solve the problem of utilization of main railway oil waste and the following environmental problems of Railways:

Implementation of this scheme solves the following environmental problems of railways:

- minimization of the amount of used oils – the main waste by volume from the locomotive facilities,
- there is a return of valuable raw materials (oils) to the technological process in the form of recovered engine oil and washing liquid for diesel locomotive systems,
- the amount of oil sludge will be significantly reduced,
- recovered oils and washing liquids do not have the degree of toxicity as that of the used oils, and therefore do not pose a threat to the environment.

When developing the general scheme for restoring the operational quality of the used engine oils, we proceeded from the results of the performed laboratory

tests on different purification methods and an optimized variant of the chosen technology, namely, the temperature conditions, the number of reagents and the time of their contact with the oil.

Comparing the main operating parameters of the recovered M-14B_2 oil after using the scheme with neonol and ABSA and the methods proposed by different manufacturers, we can see that the parameters of oil recovered under the proposed scheme are not worse, and in some cases even exceed the parameters of existing plants. In particular, the kinematic viscosity of the oils after clarification in existing plants is up to 13 mm^2/s at 100°C (based on the published data of the oil-purifying equipment developers), while after using our technology it is 14 mm^2/s.

Considerable attention was also paid to the ecologo-toxicological side of this issue. After all, used petroleum products are toxic waste, which have a low biodegradation degree (10-30%). The toxicity of petroleum products is determined by the combination of hydrocarbons that are part of their composition. In particular, arenes are the strongest carcinogens in the composition of petroleum products, and olefins, sulphur compounds, nitrogen and oxygen also have a significant toxic effect. The used petroleum products have particularly negative effects on human central nervous and cardiovascular system, endocrine system, reduce haematological parameters, cause damage to the liver and thyroid gland (Davydova & Tagasov 2002, Evdokimov 2010, Fuks et al. 2004, Markisova et al. 2013, Miao Yu 2012, Ryabtsev 2010, Stan et al. 2018).

Excessive damage is caused by petroleum products on the environment and especially on water resources. Thus, according to experts, one litre of waste oil can pollute about seven million litres of groundwater.

It should be noted that the main compounds that form the negative toxicological profile of oily waste (including waste oils) are benz(α)pyrene, furans, dioxins, polychlorinated biphenyls, and others. The main recommendation of the international community for the composition of oils from this point of view is the absence of heavy metals and chlorinated compounds in them. That is why we checked the fresh, used and recovered M-14B_2 oils according to the proposed scheme for the content of benz(α)pyrene, heavy metals (lead, nickel, cuprum, cobalt, chromium, zinc) and chloride ions.

4. Conclusion

Based on the results obtained, we propose to apply the developed scheme of cleaning the M-14B_2 oil. At the laboratory the following advantages of the scheme were confirmed: the purification efficiency – more than 95% and the maximum yield of the purified oil – 90%. After the recovery process, such oil can be recommended for reuse directly at the establishment where it was formed.

After comparing the environmental indicators of fresh, discarded and recovered oils M-14B_2 we found that chloride ions are absent at all stages; also, when working with the oils of both brands there appears a benz(α)pyrene, which completely disappears from the oils after processing them according to the proposed schemes; a significant reduction in the amount of toxic elements (lead by 82.61%, nickel by 84.62%, copper by 85.29%, zinc by 87.50%) after the treatment of oils according to the proposed schemes confirms the safety of recovered oils and the ecological compatibility of the schemes (Zelenko & Bezovska 2019, Zelenko et al. 2014, 2016).

It should be noted that the presence of heavy metals in waste oils says not only about their environmental hazard, but also indicates the unsatisfactory operation of diesels, because according to the recommendations of the Organisation for Cooperation between Railways (Recommendations) after exceeding certain concentrations of metals in oils, it can be concluded that diesel is in an emergency condition and needs repairing.

After conducting technical and economic assessment of the process scheme components, calculations of fees for waste placement, ecological and economic efficiency of the proposed environmental measures, we determined the magnitude of the conditional environmental effect, which was more than 70 thousand UAH with an accumulation of about 30 tons of waste oil per year (the case of one railroad linear unit). According to our calculations, on condition of annual savings of 300 thousand UAH on average for the purchase of new oil, this scheme will have a positive effect already in 4 years and 11 months after the introduction.

Thus, the implementation of the proposed scheme will return valuable raw materials (oil) to the process cycle, will create almost non-waste production of recovered oils, as well as promote the creation of a non-waste production-territorial complex on the basis of the linear unit of the railway, which will give an opportunity to obtain significant economic effect.

References

Ashtiani, I.H., Rakheja, S., Ahmed, W. (2019). Investigation of coupled dynamics of a railway tank car and liquid cargo subject to a switch-passing maneuver. Proceedings of the Institution of Mechanical Engineers, Part F. *Journal of Rail and Rapid Transit, 233*(10), 1023-1037.

Chervinskiy, T. I., Hrynyshyn, O. B., Korchak B. O. (2015). Regeneration of waste motor oils in the presence of carbamide. Bulletin of the National University "Lviv Polytechnic". *Chemistry, technology of substances and their application, 812*, 158-162. Access mode: http://nbuv.gov.ua/UJRN/VNULPX_2015_812_29 (in Ukrainian).

Chervinskiy, T.I., Hrynyshyn, O.B., Korchak, B.O. (2016). Regeneration of waste petroleum oils by thermal-oxidative method. *Oil & Gas Industry of Ukraine, 2*, 32-34. (in Ukrainian).

Davydova, S. L., & Tagasov, V. I. (2002). *Heavy metals as supertoxicants of the XXI century*: [tutorial]. M.: RUDN Publ. H., 140 (in Russian).

Evdokimov, A. Yu., Fuks, I.G., Shabalina, T.N., Bagdasarov, L.N. (2000). *Lubricants and problems of ecology*. M.: GUP Publishing house "Oil and Gas" of the Gubkin Russian State University of Oil and Gas, 424 (in Russian).

Fuks, I.G., Spirkin, V.G., Shabalina, T.N. (2004). *Fundamentals of chemmotology. Chemmotology in the oil and gas business*: [tutorial]. M.: FGUP Publishing house "Oil and Gas" of the Gubkin Russian State University of Oil and Gas, 280 (in Russian).

Jacyna, M., Wasiak, M., Lewczuk, K., Chamier-Gliszczyński, N., Dąbrowski, T. (2018). Decision Problems in Developing Proecological Transport System. *Rocznik Ochrona Środowiska*, *20*(2), 1007-1025.

Liu, X.-J., Wang, F., Zhai, L.-L., Xu, Y.-P., Xie, L.-F., Duan, P.-G., (2019). Hydrotreating a waste engine oil and scrap tire oil blend for production of liquid fuel. *Fuel, 249*, 418-426.

Markisova, N.F., Grebenyuk, A.N., Basharin, V.A. (2013). *Toxicology of petroleum products*: [methodical manual]. St. Petersburg: Nevsky dialect, 128 (in Russian).

Miao, Yu, Hongzhi, Ma, Qunhui, Wang, (2012). Research and recycling advancement of used oil in China and all over the World. *Procedia Environmental Sciences, 16*, 239-243.

Pyza, D., Jacyna-Gołda, I., Gołda, P., Gołębiowski, P. (2018). Alternative Fuels and Their Impact on Reducing Pollution of the Natural Environment. *Rocznik Ochrona Środowiska*, *20*(1), 819-836.

Recommendations for implementation of diagnostic control system of diesel-electric locomotives and diesel trains according to the oil analysis results: P 647/1 [Electronic resource]. - [Valid from 2009-2-3-10]. - [2nd ed.]. - Warsaw: 2009. - 32 p. - Access mode: http://osjd.org/isvp/public/osjd?STRUCTURE_ID=5070&layer_id=4581&refererLayerId=4621&id=91&print=0

Stan, C., Andreescu, C., Toma, M. (2018). Some aspects of the regeneration of the used motor oil. *Procedia Manufacturing*, *22*, 709-713.

Zelenko, Y., Bezovska, M. (2019). *Development of an environmentally friendly scheme for the recovery of used engine oils*. New stages of development of modern science in Ukraine and EU countries. Monograph. 3rd ed. Riga, Latvia: “Baltija Publishing”. 143-164.

Zelenko, Y., Bezovska, M., Leshchynska, A., Shnaiderman, A. (2019). *Disposal of technological sludge of railway infrastructure enterprises.* MATEC Web-Conferences 294, 02006.

Zelenko, Yu. V., Bezovska, M.S., Leshchinska, A.L. (2013). Development of innovative resource-saving technologies of utilization of the oil containing wastes. *Journal "Technology Audit and Production Reserves"*, *1/2*(9), 17-21. (in Ukrainian).

Zelenko, Yu. V., Tarasova, L. D., Bezovska, M. S. (2016). *Increase of the level of ecological safety while handling the used motor oils of railway infrastructure*: [monograph]. Dnipro: Lithograph Publ. H., 150 (in Ukrainian).

Zelenko, Yu., Myamlin, S., Sandovskiy, M. (2014). *Scientific foundation of management of the environmental safety of oil product turnover in railway transport*. D.: Lithograph Publishing House, 332.

Abstract

The article deals with the problems of handling used motor oils on the railways of Ukraine. At the moment, this waste is transferred to other enterprises for disposal. But, based on international experience, it is advisable to be regenerated directly at the enterprise where it is formed. The purpose of this work is to develop a modern scheme for oil waste disposal. In this regard, various indicators were investigated, reflecting both the operational suitability of oils and their toxicological parameters. As a result, we proposed a scheme and selected special equipment for handling the used engine oils, which allows to reduce the technogenic load associated with their accumulation, handling and minimization, contributes to the return of oil to the technological process. The calculated value of the conditional environmental effect and the approximate payback period allowed us to draw conclusions about the undoubted environmental and economic effect of implementing the proposed scheme.

Keywords:
waste, engine oils, railway enterprises, restoration, treatment scheme

MIDDLE POMERANIAN SCIENTIFIC SOCIETY OF THE ENVIRONMENT PROTECTION

Rocznik Ochrona Środowiska

Volume 22. Year 2020 ISSN 1506-218X 181-195

Environment and Risks of Iron Production

Petr Besta[1], Roman Kozel[1], Kamila Janovská[1], Šárka Vilamová[1], Drahomír Foltan[1], Marian Piecha[2]*

[1]VŠB - Technical University of Ostrava, Czech Republic
[2]LLM, Ministry of Industry and Trade Czech Republic, Praha, Czech Republic
[*]corresponding author's e-mail: petr.besta@vsb.cz

1. Introduction

The blast furnace plant includes not only the operation of its own blast furnaces but also many preparatory and auxiliary operations with relative autonomy (Fig. 1). The operation of the blast furnace is then continuous. The feedstocks must also be prepared and replenished continuously, and iron will be tapped at regular intervals (Kret 2013).

Blast furnace operation is an important source of pollutants that affect the working environment, but also the surroundings of the company. Most relevant studies focus on the secondary consequences that deal with the production of specific pollutants. However, higher fuel consumption, higher energy performance, repeated entry of raw materials into the process (sintering) can be affected by differences in the reducibility of individual ore raw materials. Significant differences in the degree of reduction of ore raw materials can fundamentally affect the technological process of iron production. The research goal of the article can be classified into two levels. The first one concerns the analysis of current scientific work and the definition of the main sources of pollutants in the blast furnace process. The experimental part was focused on the production of pollutants in the agglomeration process and evaluation of the degree of reducibility for three types of ore raw materials. The research was carried out in the environment of the selected metallurgical company in the Czech Republic. The evaluation of the reducibility of the monitored ore raw materials was focused on finding possible deviations in the degree of ore reduction. Significant variations in this technological parameter can contribute to the production of pollutants in the production of iron and inefficiencies in the production process.

In addition to controlling the technological process of the blast furnace itself, other operations connected with material preparation, transport, blast furnace product processing and other related activities are essential. A separate part of the production plant deals with the processing and preparation of the metal-bearing component (mainly ore). Sintering or palletizing processes are used for their treatment.

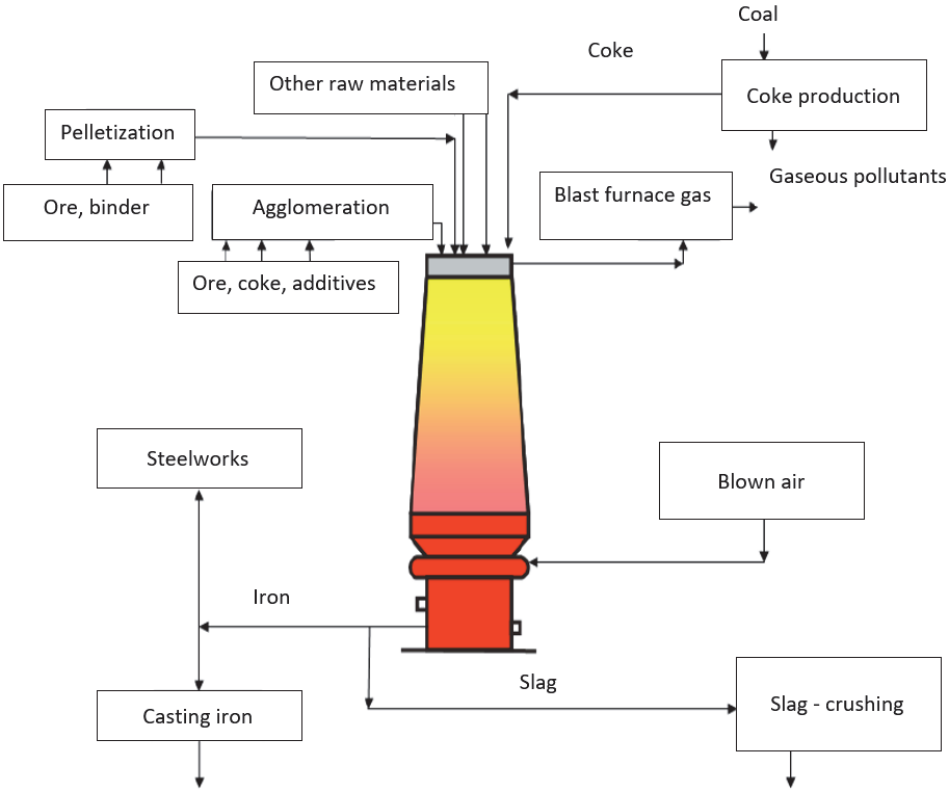

Fig. 1. General diagram of the blast furnace plant (Kret 2013, Besta & Lampa 2019)

Agglomeration or sintering of iron ores is the heating of the powder agglomeration mixture (ore, fuel, additives) to such a temperature that the surface of the individual grains of the charge is melted and the resulting melt forms liquid bridges between the grains which ensure that solid porous material is formed after solidification). The feedstock thus prepared is then used in the blast furnace process (Brož 1998). Agglomeration processes can be divided into cold and warm sections according to their character. The cold section serves to feed raw materials and to adjust grain size and to average the chemical composition of the

material (tippers, crushers, screens, homogenization heaps). The task of the warm section is to produce the agglomerate of the required quality from the supplied ores, concentrates, fuel and additives (daily reservoirs, mixture preparation and batching, pre-pelletizing equipment, sintering belts, sinter coolers).

Blast furnace coke is used as fuel in the blast furnace process. Coke is a solid, porous, degassed residue from coal carbonization leading to temperatures of 950 to 1050°C (Kret 2013). Coke production can, therefore, be another related manufacturing operation. Slag-forming additives are the alkaline additives (limestone, dolomitic limestone and dolomite), which form slag during the transition to the liquid phase in order to permanently bind the acidic tailings of the ores and other undesirable additives (Smallman 2013). If the metallurgical plant uses fuel supplies and slag-forming additives, it is usually necessary to adjust their granulometric homogeneity (Najafabadi et al. 2018).

The profile of the blast furnace and its dimensions are adapted to the production technology. The lower cylindrical portion of the profile is called the hearth. Here, pig iron and slag accumulate and are periodically discharged through tap holes (Kret 2013). The upper part of the hearth is interrupted by the blast tuyeres for blowing hot air and additional fuels (Besta & Lampa 2019). The hearth is followed by a saddle in the shape of a truncated cone with the upper wider base (Geerdes at al. 2010). This shape of the saddle provides the necessary deflection of the hot gas streams from the oxidation compartments from the furnace lining, which would otherwise be prematurely destroyed. The gradual transition of the saddle into the shaft is secured by the belly. The most capacious part of the blast furnace is the shaft in the shape of a truncated cone or two truncated cones. Preheating of raw materials, decomposition of carbonates, and indirect reduction take place in the shaft. The upper part of the furnace is called the furnace top and serves to charge the furnace with a charge and to conducting the charge gas away from the furnace. Output products and wastes (agglomeration dust, blast furnace discharge, blast furnace sludge, slag) are also subject to processing. Waste treatment is given by the possibilities of their further use in other industrial areas (Fahimnia et al. 2015), but also by their possible re-use in the production of iron or other metallurgical processes. The production and processing of waste are also demanding due to the quantity. Only in the case of slag, it is 200-400 kg (Wu et al. 2018) per tonne of pig iron produced.

The metal-bearing burden portion of the batch is usually formed by iron or manganese ore, but also metal-bearing waste from industrial production. The metal-bearing constituents can be contained in the blast-furnace burden in the form of natural or sorted ore, but more often as blast furnace ore treatment products, i.e. agglomerates or pellets. From the chemical point of view, we distinguish four groups of iron ores (Brož 1998):

- Anhydrous oxides – ferric oxide Fe_2O_3 – hematite or bloodstone with the iron content of 70% in pure state, in nature up to 60%, ferrous-ferric oxide Fe_3O_4 – magnetite or lodestone with the iron content of 72.4%, pure, in nature 68%.
- Hydrated iron oxides $Fe_2O_3 \cdot nH_2O$ – limonites or brown hematites, hydro hematite $Fe_2O_3 \cdot nH_2O$, where $n < 1$, contains in the pure state 62-69% of Fe, götit $Fe_2O_3 \cdot H_2O$, where $n = 1$, i.e. $FeO \cdot OH$ contains in the pure state 62.9% of Fe, hydrogötite or limonite $Fe_2O_3 \cdot nH_2O$, where $1 < n < 1.5$, contains in the pure state 59.8 to 63% of Fe.
- Carbonates, iron spar or siderite $FeCO_3$, contains up to 50% of Fe in the pure state.

In many deposits, ore minerals occur in a combined composition. We can talk about belt deposits. In that case, the individual layers can contain different types of ores (Clout et al. 2015). Besides the content of the metal itself, the content of pollutants and other negative substances is a key factor. All of these aspects can influence not only the iron oxide reduction process, but the production technology as a whole.

The iron ore burden brings the required amount of iron to the blast furnace in the form of its oxides or other compounds that replace these oxides. The main components of the iron ore burden are agglomerate, pellets and lumpy ore. The main reducers of iron oxides in the blast furnace are carbon monoxide, carbon and hydrogen (Shamsuddin 2016). The carbon reduction is referred to as direct, while the reduction with hydrogen and carbon monoxide as indirect. The reduction with carbon monoxide is predominant, accounting for a total volume within the range of 50-70%. The hydrogen reduction has the smallest effect, which can be 5-15% (Hosford 2011) depending on the type of fuel used. The importance of the hydrogen reduction increases significantly with the higher use of hydrocarbon fuels.

The iron reduction from its oxides proceeds gradually from the higher oxides to the lower ones in two planes (Brož 1998):

- $Fe_2O_3 \rightarrow Fe_3O_4 \rightarrow Fe_{1-y}O \rightarrow Fe$ (oxidation reduction order at temperatures above 570°C).
- $Fe_2O_3 \rightarrow Fe_3O_4 \rightarrow Fe$ (at temperatures below 570°C).

The highest percentage of the iron oxide reduction is with carbon monoxide. This reduction occurs throughout the height of the blast furnace. The direct reduction with carbon is less frequent due to imperfect contact between the two solid phases. The area of contact of the solid materials is inadequate and does not allow a higher proportion of the direct reduction with coke carbon (Kret 2013).

The reduction of iron oxides with carbon monoxide takes place at a temperature above 570°C according to the following structure (1), (2), (3):

$$3Fe_2O_{3(s)} + CO_{(g)} = 2Fe_3O_{4(s)} + CO_{2(g)} \quad (1)$$

$$FeO_{(s)} + CO_{(g)} = Fe_{(s)} + CO_{2(g)} \quad (2)$$

$$Fe_3O_{4(s)} + CO_{(g)} = 3FeO_{(s)} + CO_{2(g)} \quad (3)$$

The reduction of iron oxides with carbon monoxide takes place at a temperature below 570°C as follows (4), (5):

$$3Fe_2O_{3(s)} + CO_{(g)} = 2Fe_3O_{4(s)} + CO_{2(g)} \quad (4)$$

$$Fe_3O_{4(s)} + 4CO_{(g)} = 3Fe_{(s)} + 4CO_{2(g)} \quad (5)$$

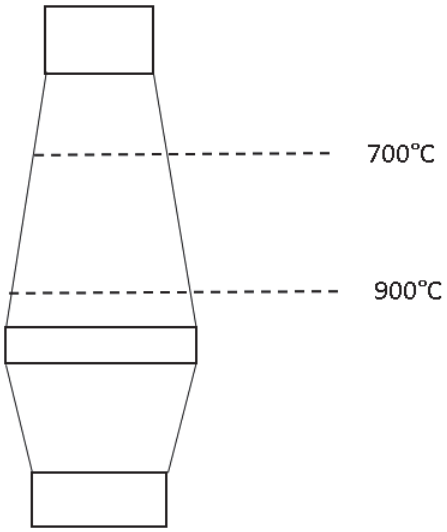

Fig. 2. Blast furnace monitored area defined by the given temperatures

The reduction of iron oxides takes place over the entire height of the blast furnace. The carbon monoxide reduction at the gas-solid interface has special significance. This gas is produced by exothermic reactions in the lower parts of the blast furnace (Bechara et al. 2018). It then rises to the higher parts of the furnace, which results in a large portion of iron oxide reduction. A significant part of the reduction processes takes place in the largest part of the blast furnace (shaft). The key area is the temperature range of 700-900°C (Fig. 2), which is located in the largest part of the blast furnace in terms of volume.

2. Methods

The research goal of the article has an analytical and experimental level. Knowledge about the harmfulness of individual parts of the blast furnace process was evaluated analytically. Part of the blast furnace plant, which is one of the largest producers of pollutants, is the sintering of iron ore. Within this section, the share of individual dust parts was determined on the basis of records of long-term measurements in the monitored company, and on the basis of chemical analysis, the concentration of selected key elements in agglomeration dust. The degree of reduction of iron ore from deposits in Russia (Kursk), South Africa (Sishen), Ukraine (Krivoy Rog) was then evaluated in the laboratory. The degree of reduction was determined for the samples in laboratory conditions using homologous equipment. The reduction processes were evaluated for three specific temperatures, in relation to the individual parts of the blast furnace and to the ore sintering process. The evaluation of the degree of reducibility of iron ores was carried out with regard to their consequences in the blast furnace and agglomeration process, which adversely affect the ecological impacts of iron production.

3. Negative impacts of individual parts of the production plant on the environment

Iron production can have a very negative impact on the environment and can be considered a major polluter. Emissions from iron production can be divided according to the state into solid and gaseous. In the case of solid emissions, it is an airborne material (dust). The gaseous pollutants that pollute the environment are mainly SO_2, CO, NO_x (Ubando et al. 2019). These gases are produced not only in the blast furnace process itself but also as products of other operations (e.g. ore sintering). In addition to these pollutants, increased attention is currently being paid to heavy metal contamination of the environment (As, Hg, Pg, Zn, Cr or Cd). The risk of contamination with these elements is mainly due to the possible contamination of soil material.

In terms of the structure of the blast furnace plant, the following are the key components that produce the most significant amount of pollutants:

- blast furnace,
- agglomeration,
- foundry processes,
- slag processing.

The negative aspect related to environmental pollution is the frequent use of waste materials in the blast furnace process (Wu et al. 2018). Metallurgical companies are constantly trying to reduce production costs, especially in the area

of expenditure on raw materials (Piecyk et al. 2015). Therefore, blast furnace wastes which contain a certain amount of iron or manganese, as well as the necessary basic components such as MgO and CaO, are reused. However, the waste materials also contain many of the pollutants mentioned above, which in this way repeatedly enter the production process. The main wastes of blast-furnace production that are reused are mainly: slag, iron scales, blast furnace slopping, agglomeration dedusting.

4. Negative consequences of the agglomeration process

Sintering processes involve sintering of ores, alkaline additives and fuel in the form of coke. The produced material has a porous character and is subsequently fed into the blast furnace (Besta et al. 2017, Haverland et al. 2018). The sintering mixture is ignited by means of blast furnace gas at a temperature of 1 300°C. Gradually, the individual grains of the agglomeration mixture are melted, and the whole layer is gradually burnt (Vilamova et al. 2016). This is due to the vacuum suction of air, which supports the shift within the combustion front. After the entire agglomeration mixture is completely burned, a solid porous material, called agglomerate, is formed. The quality requirements for the size of the agglomerate produced are above 5-6 mm.

Emissions arising from agglomeration processes can be divided in terms of their place of origin. The first area concerns the preparation of the sinter mixture, furthermore the emission of sintering itself, and the third important place is in the cooling and treatment of the sinter. The preparation of the agglomeration mixture includes mainly transport, storage, treatment and preparation of ore materials before sintering. According to the research carried out, the dominant negative effect is primarily dustiness, which arises during mechanical processes. Dust emission reduction is achieved by hermetization and extracting of dust from transport routes and transfer points. Dust and dust particles from this production segment mainly affect the working environment and hygiene conditions. The environmental impact is limited.

The main proportion of emissions from sintering processes, as analysed in the research conducted, are waste gases, which are generated during sintering. These waste gases pass through electrostatic precipitators, and waste dust is formed, which can be returned to the production process. The average amount of waste gases is in the interval 2 500-4 500 m^3 per tonne of sinter mixture produced. The amount of dust particles in these waste gases range from 0.5-3.5 g/m^3. The composition of the sintering waste dust according to the particle size is shown in Table 1.

The largest proportion is within the smallest dimension of dust particles, i.e. in the interval 0-0.1 mm. This places high demands on the capture of these

microscopic dust particles. In terms of their impact on the human organism, they can be considered the most dangerous because of their size. Due to their size, these small particles can pass through the respiratory system into the body. The use of electrostatic separator is necessary for their capture in the production process. These then allow the concentration of dust particles to be reduced to 40-60 mg/m^3. When using mechanical separators, their efficiency is 20-30% lower. A significant problem with mechanical separators is the fact that it is much less challenging to capture small fractions below 0.1 mm.

Table 1. Share of individual dust particle sizes

Size (mm)	Proportion within the total quantity (%)
0-0.1	86.8
0.1-0.25	5.8
0.25-0.5	2.9
0.5-0.75	2.6
above 0.75	1.9

Table 2. Contents of some elements in sintering waste dust

Element	Content (%)
Fe	52.8
Mg	2.1
Ca	2.8
S	0.35
Zn	0.020
Pb	0.34
Cd	0.008
As	0.002

The captured waste (Table 2) is rich in iron content and is therefore often reused in the production. An advantage is also the content of alkaline substances and their compounds based on magnesium and calcium. The negative aspect is the content of pollutants that are returned to the process.

5. Reducibility of iron oxides for the types of ores used

Another critical parameter is the quality of the raw materials, especially the ores used. The key is the content of pollutants such as sulphur, phosphorus or silicon compounds. At the same time, the degree of iron oxide reduction, which contributes to the efficiency of the technological process, is essential. An

adequate technological process enables the efficient use of resources, reducing fuel consumption and ultimately, the overall environmental burden.

Ore minerals may contain different types of ores, different amounts of the metal in question, but also a variety of harmful elements. Everything can fundamentally influence the technological parameters of the blast furnace process. The chemical composition of the selected three types of ore minerals is shown in Table 3.

Table 3. Chemical composition of selected types of ore

	Ore minerals – kind		
Content of elements	Russia – Kursk –Magnetite	Republic of South Africa – Sishen – Hematite	Ukraine – Krivoy Rog – Magnetite
Content of Fe (%)	61	69	60
Content of P (%)	0.069	0.039	0.025
Content of S (%)	0.019	0.005	0.016
SiO_2 (%)	5.2	1.3	4.1
Al_2O_3 (%)	3.8	0.85	5.0
$SiO_2 + Al_2O_3$ (%)	9.0	2.15	9.1

In the case of different types of ores (hematite, magnetite), there will be a different ratio of the reduction of oxides in relation to the given boundary temperature. At the same time, the ore mineral from South Africa contains a significantly larger proportion of the metal-bearing part. Ore minerals within individual deposits are often formed by more kinds of oxides. A very important aspect is the content of harmful substances, but also the character of ore minerals in terms of alkalinity. This can be measured as the proportion of basic and acidic components. We consider ore minerals containing a larger proportion of SiO_2 and Al_2O_3 to be acidic. This is especially the case with ore from deposits in Russia, Ukraine, but also in some Baltic states. Ore minerals from Australia, Brazil, but also South Africa have a basic character (higher share of CaO, MgO). Table 3 shows that ore minerals from Russia and Ukraine contain several times higher levels of SiO_2 and Al_2O_3 than ore from South Africa.

The types of ores under review were analysed by a laboratory with respect to their degree of reducibility. Ore raw materials were heated in the furnace to the temperature of 700-900°C. This temperature range is significant in terms of location in the blast furnace. For most of the blast furnaces, the largest part of the blast furnace in the shaft is used to heat the charge to this temperature.

Dimensionally, this part of the furnace is the largest in terms of the blast furnace structure, and a significant amount of carbon monoxide reductions occur here.

The heating rate was 90°C per minute. The reduction processes were evaluated for the time of 20, 60, 80, 100 minutes. After this time, the corresponding ore samples were removed from the furnace and cooled to the ambient temperature. Subsequently, the weight loss of the ores was determined. This was done as a proportion of weight loss to the total weight of removable oxygen in the form of iron oxides. Table 4 shows the results of the laboratory measurements.

Table 4. Determined values of the degree of reduction of the selected ore raw materials

Time (min.)	Temperature (°C)	Ore minerals – kind		
		Russia – Kursk – Magnetite	South African Republic – Sishen – Hematite	Ukraine – Krivoy Rog – Magnetite
		Degree of reduction (%)		
20	700	19.2	20.9	18.9
40	700	27.6	29.8	28.6
60	700	34.3	36.7	34.5
80	700	36.1	42.8	37.6
100	700	42.1	54.3	44.1
20	800	26.5	28.1	25.3
40	800	34.3	36.2	32.6
60	800	41.6	42.3	40.8
80	800	47.1	53.2	46.5
100	800	54.8	62.9	56.8
20	900	35.4	38.7	35.9
40	900	47.5	50.1	47.1
60	900	56.1	59.7	58.2
80	900	61.9	68.5	60.6
100	900	66.8	74.3	68.1

The degree of reduction (%) was determined for all three ore raw materials from Russia, South Africa and Ukraine. Graphically, the results are shown in Fig. 3 (for 700°C). The degree of reduction is shown separately for each boundary temperature (700, 800, 900°C).

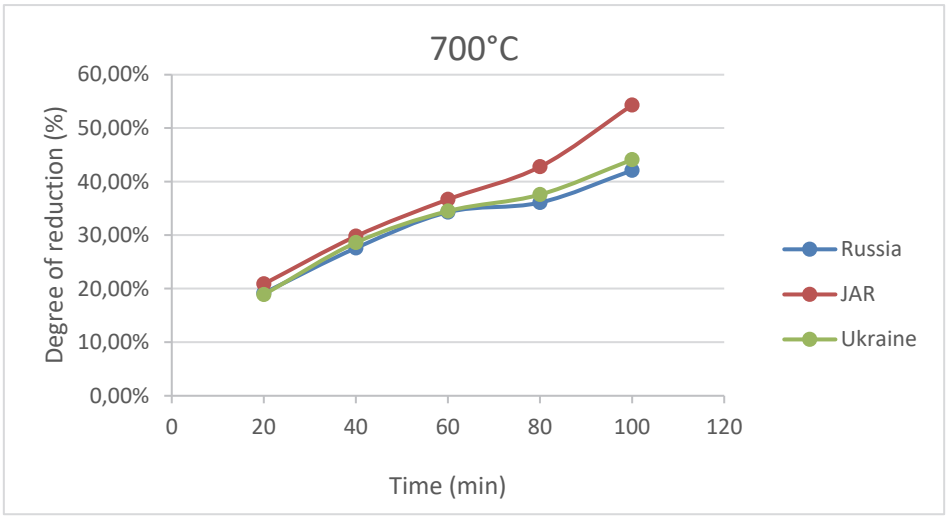

Fig. 3. Development of reducibility for the temperature of 700°C

In the laboratory research, the reducibility was analysed for three types of ore raw materials. Hematite and magnetite ore raw materials from different sites were compared. The degree of reducibility was determined separately for temperatures of 700, 800 and 900°C and for the times of 20, 40, 60, 80 and 100 minutes. The furnace heated ore samples were divided into several working vessels according to the classification mentioned above. They were heated to the corresponding temperatures for specified time intervals. Subsequently, they were gradually withdrawn from the furnace and evaluated for weight change after cooling to the ambient temperature. The reducing abilities of different ores were compared. The progression and intensity of the reducing abilities shown in Figure 3 show high similarity. There are a few key facts to identify. Hematite (South Africa) showed a higher degree of reducibility for all temperatures studied. At the same time, Hematite tended to form messy and easily reducible FeO compounds. This could affect the higher degree of reduction in this ore raw material. A significantly higher degree of reduction was then found for the heating times of 80 and 100 minutes. For Hematite, a higher degree of reduction at these times can be clearly identified for all the temperatures monitored. In the case of Magnetite from both sites under review, the reduction degrees for the indicated heating times were very similar. Therefore, a simple arithmetic mean for the indicated heating times was set for both Magnetite-based ore raw materials (Russia, Ukraine). The value thus obtained was compared with the ore raw material from South Africa. This comparison, which compares Magnetite and Hematite, is shown in Table 5. In the case of the heating times of 20, 40, 60 minutes, the reduction degree of

Hematite is higher in the range of 2.6-8.9%. Significantly higher differences was found in the case of the times of 80 and 100 minutes. Here the degree of Hematite reduction is higher than that of Magnetite in the interval of 9.2-20.6%. This may also be due to the fact that, for longer heating times, a larger proportion of fine-grained portions was formed in the case of Magnetite. For these fine-grained portions, it is more difficult to accurately determine the degree of reduction. The formation of a fine-grained fraction results from cracking, which is caused by higher local stresses due to rapid changes in the volume of the material.

Table 5. Comparison of reducibility for Magnetite and Hematite

Time (min.)	Temperature (°C)	Degree of reduction		Difference (%)
		Magnetite – average (%)	Hematite (%)	
20	700	19.05	20.9	8.9
40	700	28.1	29.8	5.7
60	700	34.4	36.7	6.3
80	700	36.85	42.8	13.9
100	700	43.1	54.3	20.6
20	800	25.9	28.1	7.8
40	800	33.45	36.2	7.6
60	800	41.2	42.3	2.6
80	800	46.8	53.2	12.0
100	800	55.8	62.9	11.3
20	900	35.65	38.7	7.9
40	900	47.3	50.1	5.6
60	900	57.15	59.7	4.3
80	900	61.25	68.5	10.6
100	900	67.45	74.3	9.2

Heating Hematite and Magnetite-based ore raw materials had essentially a similar effect on the reduction character. The highest degree of reduction was found in ore raw material from South Africa (Hematite). In the monitored range of heating times, there were the highest differences in the heating times of 80 and 100 minutes. These facts can be used not only in the blast furnace process of iron production but especially in the process of preparation of ore raw materials in the sintering process. In optimizing the sintering belt performance, it is necessary to

effectively control the sintering time relative to the type of ore raw material used in addition to other relevant parameters. Other consequences of the reduction of ore raw materials are then due to technical aspects of the blast furnace operation. Inefficiency in ore sintering means: higher CO production, higher SO_2 production, higher energy consumption. Ineffectiveness in ore sintering therefore negatively affects the environment.

From the point of view of the defined research goal, the detected deviations in the reducibility of the monitored iron ores can be considered less significant. According to the performed laboratory measurements, the ores showed a very comparable degree of reduction. The measured and evaluated deviations would not mean a disturbance of the technological conditions of the blast furnace operation and would not represent an increase of the ecological burden for the environment. Within the research goal, not only ore raw materials from different deposits but also raw materials with different chemical composition were evaluated. In the case of Hematite, a higher degree of reduction was found compared to ore raw materials based on Magnetite. Given the research goal, this difference can be assessed as moderately significant. With a fundamentally significant difference in the composition of the blast furnace charge, this difference can affect the operation of the blast furnace and have environmental consequences. If the monitored ore raw materials are adequately homogenized, the differences found will not have a major impact. If the rules for the treatment of ore raw materials are observed, their processing will not significantly affect the production technology or increase the ecological burden.

6. Conclusions

From the point of view of individual parts of the blast furnace plant and their impact on the environment, the agglomeration processes during ore sintering can be considered particularly harmful. The problem is the production of gaseous and solid pollutants. In the case of dust particles, the largest proportion is fine-grained material, which is the most negative in terms of human health. Installation and use of electrostatic precipitators are necessary to reduce emissions. These make it possible to filter emissions according to environmental requirements. However, in the case of using these separators, it is important to maintain the constant composition of the sinter batch and to use quality fuel and its adequate quality.

From the point of view of the analytical goal of the article, sintering can, therefore, be considered as an important source of pollutants in the blast furnace plant. The main problem is mainly in the production of fine-grained dust parts. As the research has shown, this is by far the largest part.

The experimental goal of the article focused on the evaluation of the degree of reducibility did not confirm large differences for individual ore raw materials. No major differences were identified in terms of different chemical

composition (Magnetite, Hematite). The processing of different ore raw materials in different proportions will not mean problems in the technology of iron production and will not be secondarily a source of higher environmental burden. Nevertheless, in the case of using a larger number of ores, quality homogenization can be recommended to the maximum. Overall, from the point of view of the degree of reducibility, the monitored ore raw materials can be evaluated very comparably. The utilization of all monitored ore materials should not mean a deterioration of the technological parameters of the blast furnace process, and therefore, no higher environmental burden. In the case of ore materials, however, it is necessary to monitor their quality continuously, especially in relation to the content of pollutants. Any harmful substances that will enter the blast furnace process will then be allocated in the metal, production waste, or in the form of emissions. In the case of processing of ore materials of different quality, more attention should be paid to the tailings selection and material homogenization. Overall, current iron producers must take into account not only technological, cost, but also environmental requirements.

The article was created thanks to the project No. CZ.02.1.01/0.0/0.0/17_049/0008399 from the EU and CR financial funds provided by the Operational Programme Research, Development and Education, Call 02_17_049 Long-Term Intersectoral Cooperation for ITI, Managing Authority: Czech Republic – Ministry of Education, Youth and Sports.

The work was supported by the specific university research of the Ministry of Education, Youth and Sports of the Czech Republic No. SP2020/61.

The article was supported by a specific university research by Ministry of Education, Youth and Sports of the Czech Republic No. SP2018/22 Risk Management Study of Industrial Enterprises in the Czech Republic.

References

Bechara, R., Hamadeh, H., Mirgaux, O., Patisson, F. (2018). Optimization of the iron ore direct reduction process through multiscale process modeling. *Materials*, *11*(7), 1094-1106.

Besta, P., Lampa, M. (2019). Iron production logistic aspects. *Acta logistica*, *6*(4), 179-186.

Besta, P., Wicher, P. (2017). The optimization of the production of sinter as the feedstock of the blast furnace process. *Metalurgija*, *56*(1), 131-134.

Brož, L. (1998). *Hutnictví železa.* SNTL, 1998. (Original in Czech).

Clout, J.M., Manuel, J.R. (2015). Iron ore-Mineralogical, chemical, and physical characteristics of iron ore. Elsevier, 2015.

Fahimnia, B., Bell, G.H., Hensher, D.A., Sarkis, J. (2015). *Green Logistics and Transportation: A Sustainable Supply Chain Perspective*. Springer.

Geerdes, M., Chaigneau, R., Kurunov, I. (2010). *Modern Blast Furnace Ironmaking*. IOS Press.
Haverland, J., Besta, P. (2018). Determination of importance of ore raw materials evaluation criteria. *Acta logistica, 5(2),* 39-43.
Hosford, W.F. (2011). *Physical metallurgy*. CRC Press.
Kret, J. (2013). *Teorie procesů při výrobě železa a oceli*, VŠB – Technical University of Ostrava. (Original in Czech).
Najafabadi, A., Masoumi, A., Allaei, S. (2018). Analysis of abrasive damage of iron ore pellets. *Powder technology*, *33*(1), 20-27.
Piecyk, M., Browne, M., Whiteing, A. McKinnon, A. (2015). *Green Logistics: Improving the Environmental Sustainability of Logistics*. Kogan Page Publishers.
Shamsuddin, M. (2016). *Physical Chemistry of Metallurgical Processes.* John Wiley & Sons.
Smallman, R.E. (2013). *Modern physical metallurgy.* Butterworth-Heinemann.
Ubando, A.T., Chen, W.H., Tan, R.R., Naqvi, S.R. (2019). Optimal integration of a biomass-based polygeneration system in an iron production plant for negative carbon emissions. *International journal of energy research*. October 2019, special issue.
Vilamova, S., Besta, P., Kozel, R., Janovska, K., Piecha, M., Levit, A., Straka, M., Sanda, M. (2016). Quality quantification model of basic raw materials. *Metalurgija*, *55*(3), 375-378.
Wu, S., Que, Z., Zhai, X., Li., K. (2018). Effect of characteristics of fine iron ores on the granulation behavior of concentrate in sintering granulation process. *Metallurgical research & technology*, *65*(2), 202-208.

Abstract

Iron production is one of the production processes that create a large number of negative externalities towards their surroundings. Iron production is based on the use of a wide range of production operations, which include not only the blast furnace process but also the treatment and processing of ores, sintering, pelletizing and processing of metallurgical waste and its possible storage. All parts of the blast furnace process can have a negative impact on the environment. Within the individual parts of the blast furnace plant, a number of pollutants are produced which negatively affect the environment. They can have both solid and gaseous states. In the case of solid emissions, it is airborne dust, and the gaseous form represents pollutants in the form of sulphur, nitrogen or carbon oxides. From the point of view of the blast furnace plant structure itself, blast furnace, agglomeration processes, palletization processes or the processing of waste from production can be classified as emission points. The article deals with the classification of basic impacts of blast furnace production on the environment. It analyses in detail the negative externalities in ore sintering. It also deals with the analysis of research, which was focused on the degree of reduction of iron oxides ore. The efficiency of the reduction process is crucial in terms of resource use, but also the overall amount of negative externalities. The research was carried out in the environment of a selected iron producer in the Czech Republic.

Keywords:
environment, iron, ore sintering, blast furnace, cost

MIDDLE POMERANIAN SCIENTIFIC SOCIETY OF THE ENVIRONMENT PROTECTION

Rocznik Ochrona Środowiska

Volume 22. Year 2020 ISSN 1506-218X 196-202

Hydrocarbon Synthesis During Methane Pyrolysis

Anatoliy Pavlenko[1], Engvall Klas[2]*

[1]Kielce University of Technology, Poland

[2]KTH Royal Institute of Technology, Sweden

[*]corresponding author's e-mail: apavlenko@tu.kielce.pl

1. Statement of the problem

In the process of thermal-oxidative pyrolysis at a temperature of 1300-1600°C, gases, containing CO and H_2, can be produced; therefore, their conversion is reduced to catalytic hydration by Fischer-Tropsch reaction.

The Fischer-Tropsch process has become attractive due to the price rise and resulting shortage of hydrocarbons. The main disadvantage of this process is its low selectivity. Therefore, the efforts of scientists, working in this field, are focused on increasing the process selectivity to produce raw materials for the oil refining industry, as well as on development of modified catalysts that will allow to produce narrow fractions of hydrocarbons.

The catalytic conversion of pyrolysis gases (methane) may involve solutions to a number of scientific problems, including the following:

- production of organic intermediate products (ethylene, propylene),
- development of waste-free technological processes,
- production of raw materials for organic synthesis.

2. Identification of previously unsettled parts of the general problem

Paper (Gudiyella et al. 2018, Duy Khoe Dinh et al. 2019, Qi Zhang et al. 2016) presents information on the conversion of products of natural gas thermal-oxidative pyrolysis into a mixture of hydrocarbons based on Co – 6.2% wt., MgO – 7.1% wt., ZrO_2 catalyst. Since by using this catalyst, during conversion from synthesis gas to pyrolysis gas, containing 4% acetylene, a significant increase in the percentage of liquid hydrocarbon yield (up to 35%), was achieved; we think it would be relevant to study the conversion of pyrolysis gases based on other catalysts that could be applied in practice.

3. Statement of assignment and methods of its solving

The method for producing the catalyst is described in (Pavlenko & Koshlak 2015, Pavlenko & Koshlak 2017, Koshlak 2019, Pavlenko & Koshlak 2019, Dąbek et al. 2018, Dąbek et al. 2016). The experiments on pyrolysis gas conversion of into a mixture of hydrocarbons made it possible to determine the effect of their yield increase during conversion from synthesis gas ($CO:H_2$ = 1:2) to methane pyrolysis gases based on other catalysts as well. Co-catalysts (64.5 CoO-3.2 CuO-32.3 Ca $Ca(AlO_2)_2$, when used with pyrolysis gases with an acetylene content (6%), can increase the yield of liquid hydrocarbons by nearly 3 times and the yield of gaseous hydrocarbons - by more than 3 times (Table 1).

The data analysis, shown in Table 1, demonstrates that under experimental conditions at a temperature of 473 K, pressure of 0.1 MPa, and space velocity of 100 h^{-1}, for pyrolysis gases, the content of alcohols C_1-C_4 is 19 times higher than when using synthesis gas and is up to 15% wt.

Note, that with a decrease in the feed rate of pyrolysis gases (increase in contact time) from 100 h^{-1} to 60 h^{-1} hydrocarbons distribute in a different way. The yield of liquid fractions C_5-C_{18} increases.

Table 1. Effect of mixture composition on yield and distribution of hydrocarbon synthesis products

Mixture	Product yield, g/nm^3					C_1-C_4, % mass
	A_1	A_2	A_Σ	A_3	A_4	
Synthesis gas $CO:H_2$ = 1:2 (volume)	10.2	42.9	53.1	13	58.2	0.8
Pyrolysis gases C_2H_2 = 6,4% (volume)	26.9	138.8	165.7	25.5	46.1	14.5
[1]Pyrolysis gases C_2H_2 = 6,7% (volume)	44	123	167	86	77	7.1
[2]Pyrolysis gases C_2H_2 = 6,7% (volume)	11	92.5	103.5	16.3	38.8	6.2

[1] – volumetric speed 70 hour^{-1},
[2] – volumetric speed 70 hour^{-1}, catalyst after regeneration,
A_1 – liquid hydrocarbon yield C_5-C_{18},
A_2 – liquid gas yield C_1-C_4,

A_{Σ} – total hydrocarbon yield,
A_3 – CO_2,
A_4 – H_2O.

In our experiments, after 50 hours of operation on $CO+H_2+C_2H_2$ mixtures, the catalyst activity decreased by 7%. To restore its initial activity, the catalyst was regenerated with hydrogen at 673K (Table 2). When hydrogen is fed, the molecular layer of C-atoms is hydrated and taken off the catalyst surface in the form of methane.

Table 2. Effect of catalyst regeneration time on the composition of products (T = 673K)

Regeneration time, minutes	content of components, % volume			
	O_2	N_2	CH_4	CO_2
100	0.13	0.63	1.35	0.13
150	0.12	0.59	1.1	0.1
190	0.11	0.54	0.88	0.07
250	0.14	0.68	0.58	0.07
290	0.12	0.59	0.58	0.07

4. Study results and their discussion

The hydrocarbon synthesis process based on pyrolysis gas is characteristic of preferential yield of ethylene compared to propylene. Quantitative and qualitative distribution of olefin hydrocarbons is shown in Fig. 1.

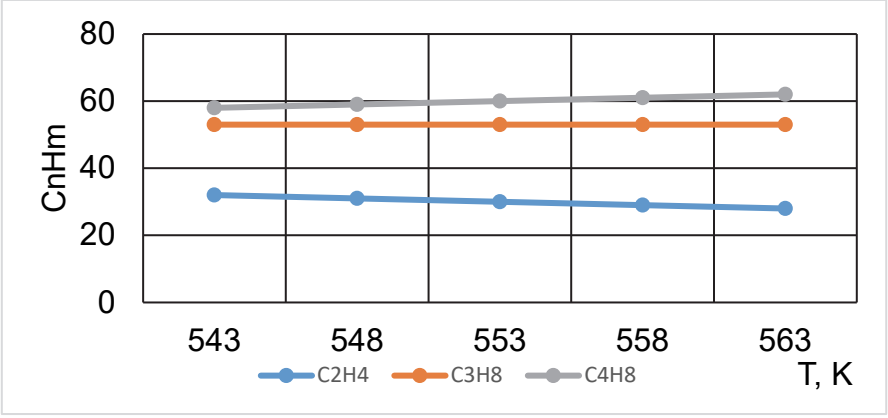

Fig. 1. Dependence of hydrocarbon yield on temperature

Based on the presented data, it follows that the main component of olefin hydrocarbons is ethylene; its proportion, with gas-synthesis temperature increase, decreases due to increase of propylene and butylene content.

Increase in the space velocity of pyrolysis gases up to 700 h^{-1} (Fig. 2) causes an increase in the amount of olefin hydrocarbons by 20%, the catalyst efficiency increases by 3 times.

Figure 2 shows the dependence of individual hydrocarbon yield on the space velocity; its analysis shows that ethylene and butylene are main hydrocarbons, methane and ethane are saturated hydrocarbons. Values within 700-740 h^{-1} ranges are considered as the optimal space velocity. Propane and butane were not among the synthesis products.

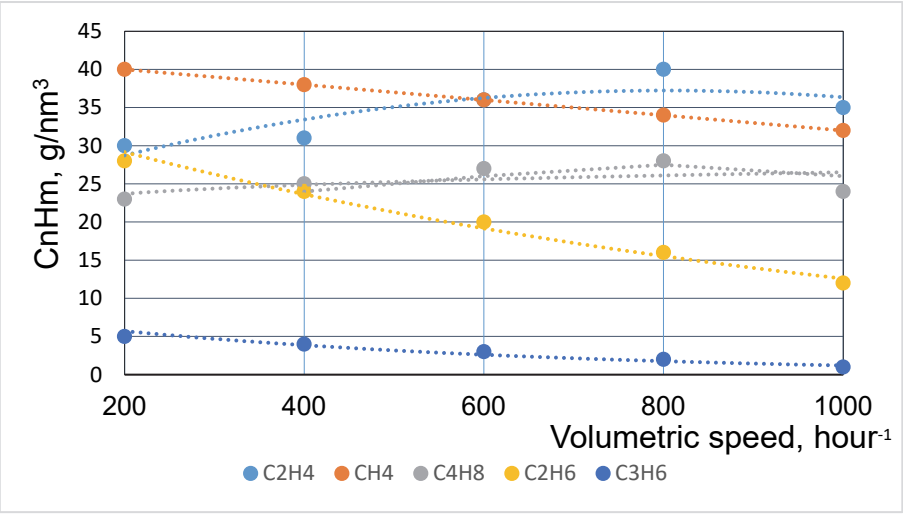

Fig. 2. Dependence of hydrocarbon yield on space velocity

The data, obtained during hydrocarbon synthesis from acetylene-containing methylene gas pyrolysis, made it possible to assert, that with acetylene in the amount of 4-5%, CO conversion decreases by 8%, compared to results of the process based on "pure" synthesis gas. At the same time, despite a decrease in CO conversion, the transition from synthesis gas to pyrolysis gas increases hydrocarbon yield, thus, making the process more selective.

A similar effect of CO conversion decrease upon introduction of unsaturated hydrocarbon additives into synthesis gas is demonstrated in paper (Hee-seok et al. 2016, Qi Zhang et al. 2016). The authors of this paper attributed this effect to competitive CO replacement by ethylene and acetylene from active catalyst surface sites. However, we assume, that increase in the total hydrocarbon

yield, is related to the fact that a part of hydrocarbons is formed by means of adsorbed ethylene or acetylene.

Thus, the obtained data indicate a rather complex process of acetylene and synthesis gas interaction. Acetylene affects the degree and direction of synthesis gas conversions, interacting and participating in unsaturated hydrocarbon formation. The data analysis on methane pyrolysis gases conversion based on modified co-catalysts showed, that use of methane pyrolysis gases with 4-7% acetylene content as a basic raw material makes it possible to intensify the hydrocarbon synthesis process.

5. Conclusions

Basic laws of hydrocarbon synthesis from the pyrolysis methane gas based on modified co-catalysts were studied. The liquid hydrocarbon yield was increased by nearly 3 times, for gaseous hydrocarbon – up to 5 times when using pyrolysis gases based on modified catalyst (65% CoO-3% CuO, 32.5% Ca $(AlO_2)_2$).

It was demonstrated that the 10Co-0.4Pd/SiO_2 catalyst is selective relative to olefin hydrocarbons. In comparative conditions, at the same synthesis temperatures and catalyst load, the yield of low-molecular $C_{20}C_5$ olefin hydrocarbons for pyrolysis gases increases up to 3 times.

The project is supported by the program of the Minister of Science and Higher Education under the name: "Regional Initiative of Excellence" in 2019-2022 project number 025 / RID / 2018/19 financing amount PLN 12,000,000.

References

Dąbek, L., Kapjor, A., Orman, Ł. (2016). Ethyl alcohol boiling heat transfer on multilayer meshed surfaces. *Proc. of 20th Int. Scientific Conference on The Application of Experimental and Numerical Methods in Fluid Mechanics and Energy 2016, Terchova, Slovakia, AIP Conference Proceedings, 1745*, 020005. DOI: 10.1063/1.4953699

Dąbek, L., Kapjor, A., Orman, Ł. (2018). Boiling heat transfer augmentation on surfaces covered with phosphor bronze meshes. *Proc. of 21st Int. Scientific Conference on The Application of Experimental and Numerical Methods in Fluid Mechanics and Energy 2018, Rajecke Teplice, Slovakia, MATEC Web of Conferences, 168*, 07001. DOI: 10.1051/matecconf/201816807001

Duy, Khoe, Dinh, Dae, Hoon, Lee, Young-Hoon, Song, Sungkwon, Jo, Kwan-Tae, Kim, Muzammil, Iqbal, Hongjae, K. (2019). Efficient methane-to-acetylene conversion using low-current arcs. *RSC Advances 9*(56), 32403-32413. DOI: 10.1039/C9RA05964D.

Gudiyella, S., Buras, Z.J., Chu, T-C., Lengyel, I., Pannala, S., Green, W.H. (2018). Modeling Study of High Temperature Pyrolysis of Natural Gas. *Industrial & Engineering Chemistry Research*, *57*(22), 7404-7420. DOI: 10.1021/acs.iecr. 8b00758.

Hee-seok, Kang, Dae, hoon, Lee, Kwan-tae, Kim, Sungkwon, Jo, Sunghyun, Pyun, Young-hoon, Song, Sangseok, Yu. (2016). Methane to acetylene conversion by employing cost-effective low-temperature arc. *Fuel Processing Technology*, *148*, 209-216. DOI: 10.1016/j.fuproc.2016.02.028.

Koshlak, H., Pavlenko, A. (2019) Method of formation of thermophysical properties of porous materials [Metoda formowania właściwości termofizycznych materiałów porowatych] *Rocznik Ochrona Środowiska, 21*(2), 1253-1262.

Pavlenko, A., Koshlak, H. (2015). Production of porous material with projected thermophysical characteristics. *Metallurgical and Mining Industry, 1*, 123-127.

Pavlenko, A., Koshlak, H. (2017). Design of the thermal insulation porous materials based on technogenic mineral fillers *Eastern-European Journal of Enterprise Technologies,* 5(89), 58-64. DOI: 10.15587/1729-4061.2017.111996

Pavlenko, A., Koshlak, H. (2019). Heat and mass transfer during phase transitions in liquid mixtures [Przenoszenie ciepła i masy podczas przemian fazowych w mieszaninach ciekłych], *Rocznik Ochrona Środowiska, 21*(1), 234-249.

Qi, Zhang, Jinfu Wang, Tiefeng, Wang, (2016). Enhancing the Acetylene Yield from Methane by Decoupling Oxidation and Pyrolysis Reactions: A Comparison with the Partial Oxidation Process. *Industrial & Engineering Chemistry Research*, *55*(30), 8383-8394. DOI: 10.1021/acs.iecr.6b00817.

Abstract

The catalyzed conversion of acetylene to higher hydrocarbons has been studied by many researchers. The importance of these processes is determined by the fact that a successful conversion of this type will create technologies for obtaining cheap alternative synthetic fuel. Acetylene can be obtained in large quantities from coal and methane, which opens up the possibility of obtaining the specified synthetic fuel. However, the lack of an effective catalyst for continuous conversion has not allowed the development of this alternative fuel route.

Features of hydrocarbon synthesis during methane pyrolysis, based on modified catalysts, are presented in the paper. It is demonstrated that production of hydrocarbons from pyrolysis gas using modified catalysts can be intensified.

Keywords:
methane pyrolysis, modified catalysts, hydrocarbons

Synteza węglowodorów podczas pirolizy metanu

Streszczenie

Katalityczna konwersja acetylenu do wyższych węglowodorów była przedmiotem badań wielu badaczy. Znaczenie tych procesów determinuje fakt, że udana konwersja tego typu pozwoli nam opracować nowe technologie pozyskiwania taniego alternatywnego paliwa syntetycznego. Acetylen można uzyskać w dużych ilościach z węgla i metanu, co otwiera możliwość uzyskania określonego paliwa syntetycznego. Jednak brak skutecznego katalizatora do ciągłej konwersji nie pozwolił na opracowanie tej alternatywnej drogi paliwowej.

W artykule przedstawiono cechy syntezy węglowodorów podczas pirolizy metanu na modyfikowanych katalizatorach. Wykazano, że można zwiększyć produkcję węglowodorów z gazu pirolitycznego na modyfikowanych Co-katalizatorach.

Słowa kluczowe:
piroliza metanu, modyfikowane katalizatory, węglowodory

MIDDLE POMERANIAN SCIENTIFIC SOCIETY OF THE ENVIRONMENT PROTECTION

Rocznik Ochrona Środowiska

Volume 22. Year 2020 ISSN 1506-218X 203-213

Ecological Peculiarities and Problems of Glued Timber Structures Reinforcement

Aleksander Chernykh[*]*, Stefania Mironova, Shirali Mamedov*

Saint Petersburg State University of Architecture and Civil Engineering, Russia

[*]*corresponding author's e-mail: ag1825831@mail.ru*

1. Introduction

The environmental benefits of timber, as a structural material, are undeniable (Pavlenko & Shkarovskiy 2018). Glued timber structures (GTSs) are superior to products from lumber in some strength and stiffness characteristics, but they also have a number of disadvantages. Therefore, the correct calculation of the elements of building structures from GTSs is so important.

A lot of works are devoted to the problems of wooden structures reinforcement. In most cases, they give recommendations for extending the service life of traditional solid wood, modern GTSs only begin. This is due to many reasons: tested with practice (Kiryutina 2016). The problems of localization of defects of modern:

- the brevity of their "biography",
- insufficiency of studying the stress-strain state (SSS), not only the nodes of conjugation of elements, but also the elements themselves,
- the lack of generally accepted approaches to assessing their strength, and the most important is the presence of different opinions on the parameters of structures made of materials with an increased degree of anisotropy in comparison with solid timber (Serov 2015, Glukhikh & Chernykh 2013).

2. Analysis of the existing situation

A thorough study of the nature of the occurrence of defects and signs of timber destruction in modern GTSs (Serov & Mironova 2013) makes it possible to more accurately assess the causes of their limit state. As a result of such studies, it was found that there exists such a geometrical location of inclined areas in which the ratio of the normal stresses to the strength characteristics of the material

is greatest (Serov 2000, Serov et al. 1999). Therefore, the concept of homogeneity of SSS as applied to glued wood can be interpreted more widely than generally accepted. When assessing the strength of the GTSs, considering them along the cross sections is not enough. Should be taken into account the gradient of stresses along inclined areas located not in one cross section, but in their totality (1):

$$\omega_1 = \omega_{max} = \frac{\sigma_1}{R_\alpha} \tag{1}$$

where:
ω_1 – relative value of the stresses of the corresponding area,
σ_1 – limit strength of wood in the direction of the main stresses,
R_α – calculated resistance of timber at an angle α to the timber fibers.

In the transition from one elementary stress area to another, a gradient of the orientation angle also arises in the dangerous region. The presence of such an area, the size of which is comparable with the cross sections of the GTSs elements, leads to the achievement of the ultimate limite state of the structure, despite the small value of stresses arising in the directions of the axes of symmetry of the material. The destruction in glued timber in this case occurs at areas of minimum relative strength. An example is the nature of the fracture of specimens subjected to uniaxial tension, i.e. the absence of a gap perpendicular to maximum stresses (Serov 2015).

The assertion that all defects of solid timber structures are eliminated in the GTSs is incorrect. On the contrary, new specific "paradoxes" and problems arose. Even in the bent glued frames of Getzer's company splintering cracks and breaks appeared on beveled edges. Studies have shown that even with a smooth cutting of the glued blocks to form the tapering of GTS elements, additional tangential and normal stresses could arise in them stretching the timber across the fibers. Cracks also appeared in bent-glued beams, the occurrence of which can be explained by calculations according to the formulas of "bent beam" (Serov et al. 1999). Stresses stretching the timber across the fibers are small in the absolute value, but they are large in comparison with the corresponding resistance of glued wood, the degree of anisotropy of which is much higher than that of the solid one.

The resistance increased along the fibers due to the removal of large defects and gluing of the boards along the length of the toothed spike, dispersing the remaining small knots in the glued bag, increasing the homogeneity of the material, and so on. Across the fibers, on the contrary, the characteristics decreased as a consequence of gluing layers with unavoidable cut fibers through the plastic. This happens when sawing always saves logs, cutting a thin layer, as well as knots, which are then glued to adjacent layers almost across the fibers (Byzov & Melekhov 2016).

3. Defects in the GTSs caused by design errors

In modern GTSs with undercutting and benches already at the design stage there is the inevitability of cleavage cracks, i.e. in fact, strengthening of such structures is required even before external loads are applied. A vivid example is a bent glued frame with a ledge in the crossbar. Cracks arising in the places of such ledges can reach the support node in the column (Fig. 1). In other words, an attempt to improve these designs from a technological point of view transferred these glued laminated bent frames (GLBFs) from some of the most reliable and long-span frames to unreliable ones.

In addition to such frames, in structures of powerful glutinous blocks, sometimes knots are laid which were designed more than half a century ago for TSs, but which did not receive application, and are also not suitable for GTSs.

In some GTSs developed in the last decade and approved as model ones, the inevitability of the occurrence of cracks was a priori laid. References in publications on the poor quality of adhesives, on technological flaws did not reveal the essence of misses. Examples include MDA-type arches, glued frames of the GLBF type (Fig. 3).

In the squeezed-bending elements of TSs with small spans, the transmission of longitudinal forces (N) with the eccentricity (e) at the nodes was justified, since the support SSS did not go to the beyond. With the increase in spans and cross sections of GTS elements, similar methods of reducing bending moments in the middle of their length proved to be irrational. For example, in the MD with a span of more than 12 m cracks have already appeared from normal working loads. The pre-node sections of the glued blocks represented samples for gluing of enormous dimensions.

Analysis of the SSS even of standard samples leads to the conclusion that they had been cracked along main successively placed stretched areas in the form of shearing with cleavage. If we also take into account transverse forces in the MDA, from which normal stresses arise stretching the timber across the fibers (Serov 2015), then the appearance of cracks outside the stamp is inevitable (see Figure 4). Equally illiterate from the engineering point of view is the solution of the cornice unit in the glued timber frames (GTFs)). In 1970, the head of the German firm, Erwin Dimter, showed the Muscovites a colorful movie about the production of frames made from rectilinear elusive elements by gluing blocks onto a toothed spike, cut through the entire section of the diagonal direction. The simplest technology attracted not only officials, but also some specialists. First, the GTFs were used in experimental construction, and after 2 years they became standard. But the SSS of broken rods turned out to be prohibitive, especially in the stretched zone. Formally, the distributive α in the diagonal section of the broken rod can be represented in the form of a curved rod of GTS with a curvature radius tending to

zero. Most often, such nodes are calculated according to the Henri Navier formula with the coefficients (Serov et al. 2011), which does not correspond to the actual SSS. And yet, despite the aspiration to zero α in the outgoing corner of the stretched edge of the diagonal section, the cracks originate in the stretched zone and sometimes reach the support (Fig. 5a and 5b).

Fig. 1. Fragments with cracks passing in the GLBF from the ledge in the crossbar to the support

Fig. 2. The nature of the defects of GLBFs with a ledge in the crossbar during operation

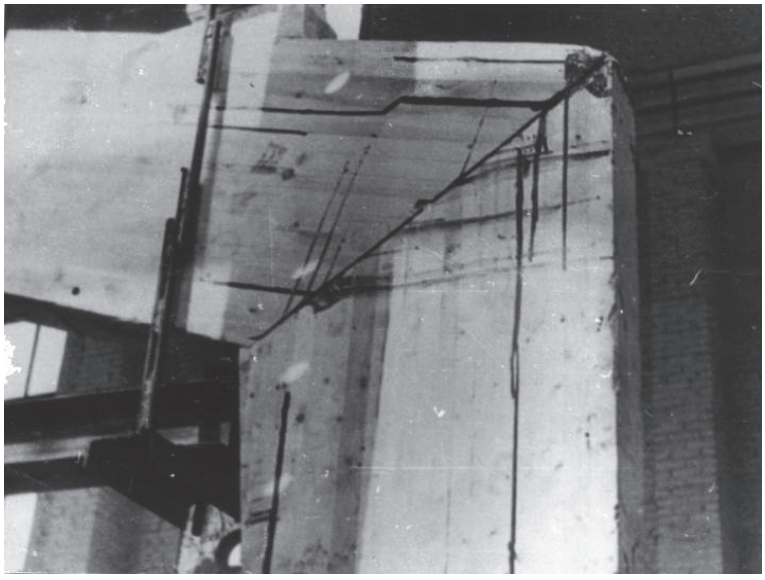

Fig. 3. The nature of glued timber frames destruction in the stretched zone of the cornice unit with short posts

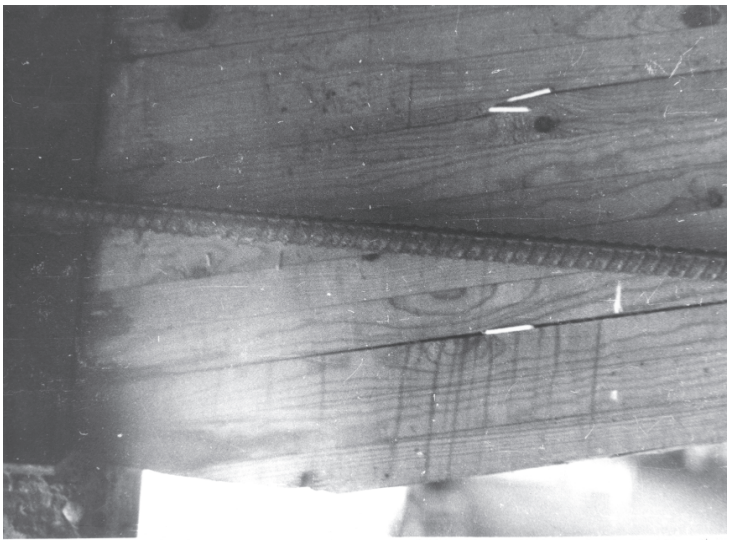

Fig. 4. Cracks in the pre-support zones of glued MDA blocks (marked with matches) when the sloping section leaves the support platform

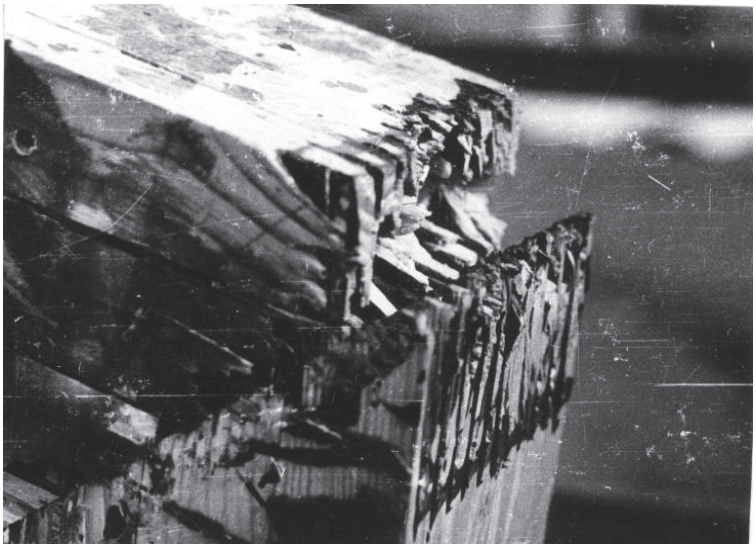

Fig. 5a. The nature of glued laminated timber frames or (GLTFs) destruction in the stretched zone of the cornice unit

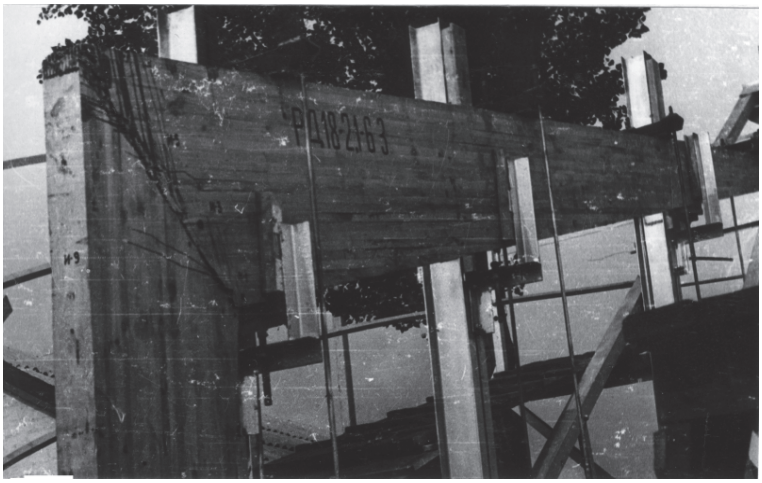

Fig. 5b. The nature of glued laminated timber frames or (GLTFs) destruction in the stretched zone of the cornice unit

4. Features of reinforcing GTSs

The main feature of reinforcement of the large-span GTSs is their two-stage operation. First, it is necessary to "heal" the resulting cracks, and then eliminate the possibility of their formation in the above-mentioned hazardous areas during subsequent operation (Arkaev et al. 2012).

At the first stage, even an "increase" in crack opening is desirable. For this purpose a GTS is fully unloaded, up to the "exclusion" of support reactions and the SSS zone with a crack. After that – on the contrary, the beam is supported from below and reinforcement of the structure is done.

At full unloading the sloping holes are drilled in steps of 300 mm along the cracks, through which the glue is injected by injectors. To reduce glue losses, the cracks are glued from both sides with a transparent tape. The injection is carried out until the glue is squeezed out of the cracks. Only after that, the GTS is supported or pressed. Extract under stress is carried out prior to polymerization of the glue (up to collapsible strength). At the end of this exposure, the actual GTS reinforcement is performed either by glued or screwed rods in the direction of the trajectory of the principal tensile stresses (realization of the string principle).

We can use the beams of Grand Menshikov Palace in Oranienbaum, Solombala Factory and the Arch of Sports Palace in Arkhangelsk, as well as the arches of the Dobrynya Shopping Center in Petrozavodsk as examples of TS and

GTS reinforcement with the implementation of the string principle (Serov & Naychuk 2010).

In 1977, when analyzing the results of the semi-arch test for the future Sports Palace in Arkhangelsk for the Olympics-80, we found the root cause of the emergence of a main crack that spread from the end of the semi-arch at the mobile support at 13.6 m with a half-32.76 m. It turned out that under short-term control load the marginal normal stresses exceeded the calculated resistance by 2.25 times, the tangential stresses by 2.01 times, and the main tensile stresses in the support zone by approximately 3.5 times. To solve the problem, we proposed the reinforcement of the arched zones of arches in the direction of dangerous principal tensile stresses by gluing three steel bars of the periodic profile Ø = 20 mm into pre-drilled holes in the prong zones with a pitch of 500 mm. As a result, hardening of the arched zones of the arches in the manufacturing process, localization of local dangerous tearing stresses, approaching the curve of the strong resistance of glued wood to the tension at an angle to the fibers faster than others took place (Naychuk 2016). This eliminated the risk of cracks in the arches under working loads and impacts. The structures have been successfully used from 1980 to the present. When they were inspected in 1983 and 1988, only two arches revealed surface cracks in the area of installation of the air heaters.

In 1977 at the Department of the LISI House of Culture, we together with V.D. Popov tested two series of glued laminated beams with pre-support zone reinforcement in various ways and without (Popov & Serov 1978). In the foreign press, works about such kind of reinforcement appeared two or three years later (Serov 2015). It was considered that the most effective and technologically accessible method of plywood strips reinforcement on glue, however, a method for pasting rods into drilled holes. At the same time, the co-work of differently modular materials, which react to changes in the temperature and humidity of the medium in a different way, but with a rigid interface between them, casts doubt on the relation to this method of strengthening as commonly accepted.

From our point of view, there are two approaches for GTS reinforcement improvement:

1) its non-metallic manufacturing from timber or other materials close in properties to timber,
2) providing not rigid – adhesive interrelation of the reinforcement element with wood, but mechanical damping – "tracking", for the indicated deformations of the intensified zones of GTSs and kept long under operating temperature and humidity conditions.

Among the disadvantages of reinforcement by gluing the rods is also the requirement to perform it under factory conditions (the arches of the Sport Palace

were reinforced directly at the factory – when gluing the semi-arches). With variable temperature and humidity conditions, it is more reliable to carry out the screwing of a new generation of screws rather than gluing.

5. Conclusions

Reinforcement of glued laminated beams and other structures with cracks is recommended not only in cases where it is necessary to increase the resistance of beams to the main tensile stresses in areas located in the bearing zones, but also at the points of inflection of the glued bent beams, where glue is usually "forced" to work for tension across the fibers (Figure 3).

Unfortunately, we have to state that so far, many specialists continue to consider the need for reinforcement in the presence of the GTS pre-support zones, the overstretching shear stresses and the danger of structural failure from shear.

Long research of our scientific school SPbGASU persuades us that this is only a "visual deception". Timber even in uniaxially loaded laboratory samples, and even more so in the GWSs, is destructed by normal stresses acting at an angle to the fibers.

Therefore, in each specific case, it is necessary to value the SSS taking into account all its components and the load-bearing capacity for a particular criterion of destruction (Serov 1999).

References

Arkaev, M.A., Zhadanov, V.I., Stolpovsky, G.A., Ukrainchenko, D.A., Lisov, S.V. (2012). *Reinforcement of wooden structures of operated buildings and structures.* Orenburg: IPK “University”.

Byzov, V., Melekhov, V. (2016). Structural sawn timber: resource enhancement. *Magasine of Civil Engineering, 5,* 67-76.

Glukhikh, V., Chernykh, A. (2013). *Anisotropy of wood. The technological aspect.* St. Petersburg: SPbGASU.

Kiryutina, S. (2016). The operational level of quality of wooden buildings. Wall settlement issues. *Bulletin of civil engineers. SPb: SPbGASU, 2*(55)*,* 33-38.

Naychuk, A. (2010). On the issue of assessing the bearing capacity of steel screw rods screwed at an angle to the wood fibers. *Industrial and civil engineering. Moscow,* 21-23.

Pavlenko, A., Szkarowski, A. (2018). Thermal insulation materials with high-porous structure based on the soluble glass and technogenic mineral fillers. *Rocznik Ochrona Środowiska, 20(1),* 725-740.

Popov, V., Serov, E. (1978). Hardening of support zones of adhesive beams. *Glued wood and plastic structures. Leningrad: LISI,* 15-21.

Serov, E. (2015). *The development of glued wooden structures. Problems and views.* St. Petersburg: SPbGASU.

Serov, E., Mironova, S. (2013). *Strengthening bent and compressed-curved elements of wooden structures*. St. Petersburg: SPbGASU.
Serov, E.N. (2000). Problems of views and ways to improve the design standards of glued wooden structures*. Izv. Universities. Forest magazine. Arkhangelsk. 5-6.* 139-144.
Serov, E., Meleshko, L., Orlovich, R. (1999). *Strength of wooden structures in a difficult stress state.* Wood and wood materials in building structures: Mater. Int. scientific conf. Szczecin, Poland, 83-89.
Serov, E.N., Sannikov Yu.D., Serov A.E. (2011). *Design of wooden structures*. Moscow: DIA.
Serov, E., Naychuk, A. (2010). Stan naprężeń złącz elementów drewnianych za pomocą wkrętów stalowych. *Przegląd Budowlany, Warsawa, 12,* 51-53.

Abstract

Long evolution of solid timber structures has developed sufficiently reliable engineering solutions and methods of timber structures reinforcement. The experience of mass production and application of new glued timber structures has shown that the simple transfer of traditional methods of calculation and design to modern structures is not always correct. The design and reinforcement of modern are still being developed. Graphical representation of the fields of operating normal stresses and wood resistance fields show that even with simple uniaxial stretching along the fibers the limiting state initially arises not at the direction of the principal axes of symmetry but at an angle to the fibers. The current trends in management, diagnostics, design and reconstruction of buildings show that almost all problems of preserving wooden and other structures in ordinary reconstructed objects, as well as in architectural, historical and cultural monuments are based on the competence level of the personnel not only in the restoration industry, but in construction industry too.

Keywords:
bearing capacity of timber structures, glued timber structure reinforcement,
stress gradient, stress – strain state (SSS)

Właściwości ekologiczne i problemy wzmocnienia konstrukcji z drewna klejonego

Streszczenie

Długotrwała ewolucja konstrukcji z litego drewna rozwinęła znacząco niezawodne rozwiązania inżynieryjne i metody wzmacniania konstrukcji drewnianych. Doświadczenie w masowej produkcji i stosowania konstrukcji z drewna klejonego wykazało, że proste przeniesienie tradycyjnych metod obliczania i projektowania na nowoczesne konstrukcje nie zawsze jest poprawne. Projektowanie i wzmocnienie nowoczesnych konstrukcji są wciąż rozwijane. Graficzne przedstawienie obszarów występowania normalnych naprężeń i obszarów oporu drewna pokazuje, że nawet przy prostym jednoosiowym rozciągnięciu wzdłuż włókien stan graniczny pojawia się początkowo nie w kierunku głównych osi symetrii, ale pod kątem w stosunku do włókien. Obecne trendy w

zarządzaniu, diagnostyce, projektowaniu i rekonstrukcji obiektów budowlanych pokazują, że prawie wszystkie problemy związane z konserwacją konstrukcji drewnianych i innych rekonstruowanych w zwykłych obiektach, a także w zabytkach architektonicznych, historycznych i kulturowych opierają się na poziomie kompetencji personelu nie tylko w branży restauratorskiej, ale także w budownictwie.

Słowa kluczowe:
wytrzymałość konstrukcji z drewna klejonego, wzmocnienie konstrukcji z drewna, gradient naprężeń, stan tensorowo-odkształceniowy

MIDDLE POMERANIAN SCIENTIFIC SOCIETY OF THE ENVIRONMENT PROTECTION

Rocznik Ochrona Środowiska

Volume 22. Year 2020 ISSN 1506-218X 214-225

Water Quality Management at the Tailings Storage Facility of the Gaisky Mining and Processing Plant

Dmitry A. Babenko[*]*, Mariya A. Pashkevich, Alexey V. Alekseenko*

Saint Petersburg Mining University, Russia

[*]*corresponding author's e-mail: dima_babenko93@mail.ru*

1. Introduction

Industrial enterprises of the commodity sector are the growth points that contribute to the economic and technological development (Litvinenko 2020). However, the environmental issues require detailed study (Bonotto et al. 2019, Safiullin et al. 2019, Végsöová et al. 2019) as the areas affected can become hotspots of engineering concern (Koptev et al. 2017, Nikolaevna et al. 2020). Extractive and processing industries produce mineral waste, stored in the dumps and tailings. Their long-term operation can result in the pollution of environmental components and cause additional spending on the elimination of the negative impact (Bazhin et al. 2016, Kruk et al. 2018, Nedosekin et al. 2019, Semyachkov et al. 2012).

The studied metallurgical enterprise performs underground mining of copper ore and its flotation concentration. Flotation is based on the differences in physicochemical properties of mineral surfaces (Abramov 1984, Krasotkina et al. 2017). The studied tailings of *the Gaisky Mining and Processing Plant* (Gaisky GOK) include a tailings pond, a pond of clarified water, and a pond of acid mine waters. Depleted pits of the Gai deposit are considered too, as one of the quarries is being reclaimed by filling with beneficiation waste (Aleksandrova et al. 2019). Enrichment tailings are mixed with acid mine waters in the main building of the factory and then pumped to the abandoned quarry and partly to the tailings storage. The tailings storage of the Gaisky GOK is a hydraulic-fill hill-type dam, put into operation in 1966 (Recommendations 1986). Its total area is approximately 190 hectares, the maximum storage capability is 52.5 million m^3.

The chief research objectives are assessment and reduction of the adverse impact of enrichment waste on natural waters as well as prevention of the loss of

potential raw materials of technogenic deposits with the infiltration through dams and bases of waste storage.

2. Materials and methods

The waste of copper ore enrichment at the Gaisky GOK consists of ca. 315 mm-sized particles of waste rock in a mixture with water, which are being transported through the slurry pipeline and stored in the quarry No. 2, with a capacity of ca. 70 million m^3, and partially in the tailings storage. The composition of the liquid phase of the enrichment waste is presented in Table 1. The mineral composition of the tails is represented by pyrite, chalcopyrite, sphalerite, quartz, feldspar, chlorite, and sericite. Chemical composition: Fe_2S, $CuFeS_2$, ZnS, SiO_2, aluminosilicate mixtures, and hydrochloric acid salts.

Table 1. Alkalinity level and composition of the liquid phase of tailings, mg/dm^3

Parameter	Value	Parameter	Value
Solids	5096-5230	Sodium	450-650
Suspended matter	up to 300	Potassium	45-68
Petroleum products	0.25-4.15	Magnesium	2-848
Chlorides	468.9-587.6	Iron	0.01
Sulphates	1777.2-2559.0	Copper	0.04-4.65
Hydrocarbonates	14.48	Zinc	11.8
pH up to 11.95			

In accordance with the Goldschmidt geochemical classification of elements, tailings contain mainly chalcophile elements that are being washed out of the tailings and quarry can lead to pollution of natural waters (Brysiewicz et al. 2019, Bushuev et al. 2018, Zubala 2019). In order to confirm or refute this, samples of groundwater and surface water in the area of the tailings pond, recycled water at the concentrator, and from the sedimentation pond and the acid mine pond were taken and analyzed. The sampling points are shown on the schematic map (Fig. 1).

Surface water was taken from the bordering Yalangas watercourse, 1 km North-West of the tailing dump. In total, two samples were taken: 500 m upstream from the tailing dump (sample A) and 500 m downstream (sample B). Samples were also taken from 3 observation wells. Sampling conditions were chosen in accordance with the GOST 31861-2012. The samples were analyzed in the laboratory of the Saint Petersburg Mining University. The cationic composition was determined using the Shimadzu ICPE-9000 analyzer; anions were found with the DR-5000 spectrophotometer.

Fig. 1. Schematic map of the study area

3. Results and discussion

The presented graphs (Fig. 2a and 2b) show that the concentrations of Fe, Mg, Mn, and Na exceed the MPC according to the GN 2.1.5.1315-03 in the samples taken downstream of the tailing dump. The specific combinatorial pollution index was calculated for the Yalangas river as well. The value of 5.84 characterizes the water quality as "low" (class 4A) in accordance with the RD 52.24.643-2002.

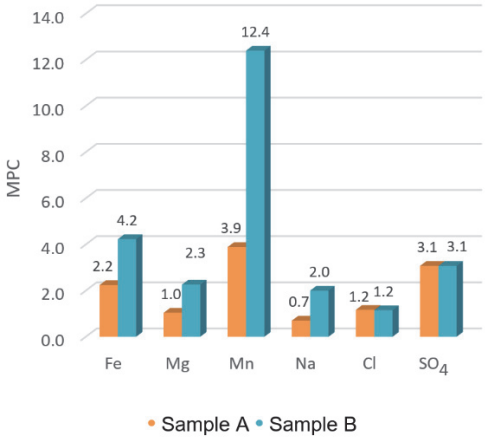

Fig. 2a. Surface water composition

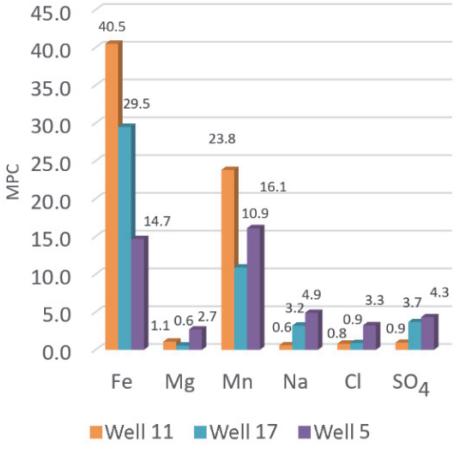

Fig. 2b. Groundwater composition

Based on the data presented, it was concluded that the operation of the tailing dump harmed surface and groundwater in its vicinity (Bolshunova et al. 2017, Gałuszka et al. 2018, Sliti et al. 2019, Yusupov & Karpenko 2016). The research conducted by A.G. Talalay, A.B. Makarov, and B.B. Zobnin, allow considering the tailings of copper ores as technogenic deposits (Makarov 2000).

Processing wastes were sampled; particle-size distribution and chemical composition were determined. Following the storage scheme at the enterprise, it was decided to take samples at the tailings dump site, as they have the average composition. First of all, particle-size distribution was analyzed by the sieve method, the results of which identified 4 grades (Fig. 3.)

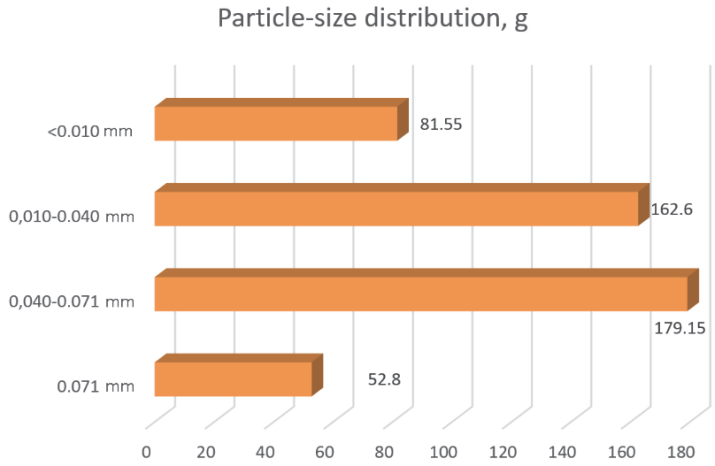

Fig. 3. Particle-size distribution of the studied tailings samples

The graph shows that the predominant size grade is 0.071-0.040 mm, its weight in the sample of 500 g is 179.15 g (35.83%), followed by a class of 0.040-0.010 mm – 162.6 g (32.52%), < 0.010 mm – 81.55 g (16.31%) and > 0.071 mm (10.56 %).

The X-ray fluorescence analysis was carried out for each size grade, in order to determine the component composition of the tails. The results are presented in Table 2.

The gross content of the components (Table 3) was consequently determined using an emission spectrometer with inductively coupled plasma Shimadzu ICPE-9000.

Table 2. Chemical composition of the tailings by size grades, %

Particle-size grade, mm							
>0.071		0.071-0.040		0.040-0.010		<0.010	
Component	%	Component	%	Component	%	Component	%
SiO_2	52.8516	SO_3	31.8341	SO_3	42.2181	Fe_2O_3	29.2247
SO_3	16.9446	Fe_2O_3	30.9487	Fe_2O_3	37.5378	SO_3	28.8020
Fe_2O_3	15.0397	SiO_2	28.4495	SiO_2	14.6119	SiO_2	27.4349
Al_2O_3	8.1800	Al_2O_3	4.4016	Al_2O_3	2.7871	Al_2O_3	8.4635
MgO	2.2164	MgO	1.2698	MgO	0.9711	MgO	2.5597
CaO	1.6646	Na_2O	0.9910	Na_2O	0.7139	Na_2O	1.3656
Na_2O	1.5894	CaO	0.9005	ZnO	0.2994	K_2O	0.6664
K_2O	0.6667	ZnO	0.2948	CaO	0.2564	CaO	0.3963
TiO_2	0.4314	K_2O	0.2627	CuO	0.1996	ZnO	0.3454
ZnO	0.1370	TiO_2	0.2460	TiO_2	0.1655	TiO_2	0.3317
CuO	0.0871	CuO	0.2288	K_2O	0.1351	CuO	0.2081
P_2O_5	0.0810	P_2O_5	0.0479	P_2O_5	0.0538	P_2O_5	0.1008
MnO	0.0656	PbO	0.0403	BaO	0.0282	MnO	0.0460
BaO	0.0340	MnO	0.0327	As_2O_3	0.0224	BaO	0.0338
As_2O_3	0.0109	BaO	0.0305			As_2O_3	0.0210
		As_2O_3	0.0212				

Table 3. Bulk concentrations of major polluting elements

Particle-size grade, mm	Component						
	Cu	Fe	S	Zn	Pb	Au	Ag
	kg/t					g/t	
<0.010	5.3565	284.9950	255.9624	3.3500	0.4315	n. d.	3.95
0.040-0.010	5.4065	437.9950	462.9624	3.0300	0.1925	0.0766	2.84
0.040-0.071	4.9565	356.9950	377.9624	2.3400	0.1385	0.0541	1.88
>0.071	1.9665	179.9950	174.9624	2.0800	0.0990	0.0313	1.04

As a result of moisture infiltration into the aquifer, such valuable components as copper, zinc, silver, and gold, and such dangerous as sulfur can migrate (Bonotto & Garcia-Tenorio 2019, Kasimov et al. 2016, Yusupov et al. 2017, Zhang et al. 2018). It should be taken into account that tailing dumps are the facilities designed for storing industrial waste, while quarries are not specially prepared for that (Kremcheev et al. 2018, Nagornov et al. 2019). This is a relatively new trend. The sides of the quarry are composed of different-sized rocks, which is a factor of increased filtration. It is necessary to conduct observations of groundwater and surface water in the quarry area, taking into account the peculiarities of the existing natural and man-made geosystem (Pochechun et al. 2014). As a result of this work, it was concluded that the waterproofing insulation of the

tailings is feasible for two reasons (Bortnikov et al. 2014, Coulombe et al. 2012, Krzaklewski & Pietrzykowski 2002, Wang et al. 2017, Zhao et al. 2011):

- reduction of negative load on groundwater and surface water,
- preservation of useful components for future use of enrichment waste as a technogenic deposit.

In this regard, in order to preserve the technogenic deposit of the Gaisky Mining and Processing Plant (Gaisky GOK) and reduce the environmental load on underground and surface water, a waterproofing technology was developed. As of today, various waterproofing techniques are used, the choice of which depends on the set of waste parameters and materials used (Dos Santos & Gardoni 2014, Lee & Shang 2013, Weishi et al. 2018, Zhu et al. 2015). Analysis of methods of waterproofing allows us to identify the main of them, applied to increase the groundwater protection efficiency:

- based on natural materials (clay, loam),
- based on polymeric materials (geomembranes, geomats),
- based on waste oil products.

Application of natural clays as a waterproof layer is extremely time-consuming: the volume of the applied material should be from 0.35 to 1.0 m^3/m^2; pre-treatment is required before application. Clays of the protective layer are exposed to infiltrating aggressive waste. As a result of the impact the structure of a protective layer changes with the further dissolution of argillaceous minerals both in an acid and alkaline environment. The initial clay strength is reduced, and the risk of waste infiltration into the groundwater increases.

Waterproofing of constructions using geomembranes is a very laborious method, as well as expensive: the price per square meter of a geomembrane can reach ca. 12 USD in Russia. Moreover, the stitching of finished sheets creates seams that pose a threat to the coating integrity, which is absolutely unacceptable. Toxicity and destruction under the influence of aggressive media are the disadvantages of insulation with waste oil products.

Following the review results, granules of secondary polyethylene of low and high pressure and polypropylene were chosen as the materials for the study.

Low-density polyethylene (LDPE) is a waxy material of unexpressed color, obtained industrially by the polymerization of gaseous polyethylene. LDPE is a thermoplastic polymer with a density of 910-930 kg/m^3. The literature review shows that this polymer has relatively high reliability at the break, resistance to multiple bending, impact, and low temperatures.

High-density polyethylene (HDPE) is a less waxy polymer than LDPE, resistant to fats and oils, but subjected to impact and bending. The values of

resistance to compression and stretching of LDPE and HDPE are comparable. The density of HDPE is 940-960 kg/m^3.

Polypropylene (PP) is a linear polymer obtained during the propylene polymerization in the presence of catalysts. The density of polypropylene is 900-920 kg/m^3. It is highly resistant to the impact but can be destroyed by multiple bending and under low temperatures.

Secondary polyethylene and polypropylene pellets are products of recycling of used polymers. The physical and mechanical properties of these polymeric materials and their products determine their behavior as a result of external loads. The determination of these properties on a trial basis allows identification of the dependence of stresses on deformation (tensile diagram). The dependence analysis allows finding the main parameters of elasticity, strength, and plasticity (modulus of elasticity, fracture resistance, and ultimate strength). Physical and mechanical properties of polymers have a number of features as compared to non-plastic materials (Lyamkin 2000):

- ability to develop large reversible deformations (hundreds or even thousands of percent),
- relaxation patterns, i.e. the ratio of strain and stress for the impact duration,
- dependence of physical and mechanical properties on the conditions of its manufacture, processing, and preliminary changes (due to the different types of supramolecular structure with a long period of rearrangement).

To determine the dependence of the physical and mechanical properties of the materials on the manufacturing temperature, a step equal to 10°C and an interval from 160 to 230°C were chosen. The total number of plates for finding strength under tensile loads of polymers was 63. Figures 4a, 4b, and 4c reflect the dependence of changing polymer strength on the temperature. The results of this experiment allow us to draw the following conclusions:

- the strength of samples processed at different temperatures does not change linearly,
- the value of the tensile strength of polymers at temperatures commensurate with the melting point is not the greatest. This is due to incomplete homogenization of the material, the presence of excessive moisture and volatile impurities,
- the temperature range of 185-195°C for polymeric material processing is the optimal,
- the decrease in the strength of the test samples at temperatures above 200°C is determined in connection with thermal and thermo-oxidative destructive processes.

The developed waterproofing technology suggests applying the polymer granules processed by melting to the prepared surface. The surface is anticipatorily prepared by cleaning from large rock debris, roots, etc. The prepared layer is consequently leveled with a layer of clay, 20-40 centimeters-thick. Then sand of medium particle-size with a thickness of 15-20 centimeters is applied, this minimizes the load on the clay horizon during the laying of the polymer material.

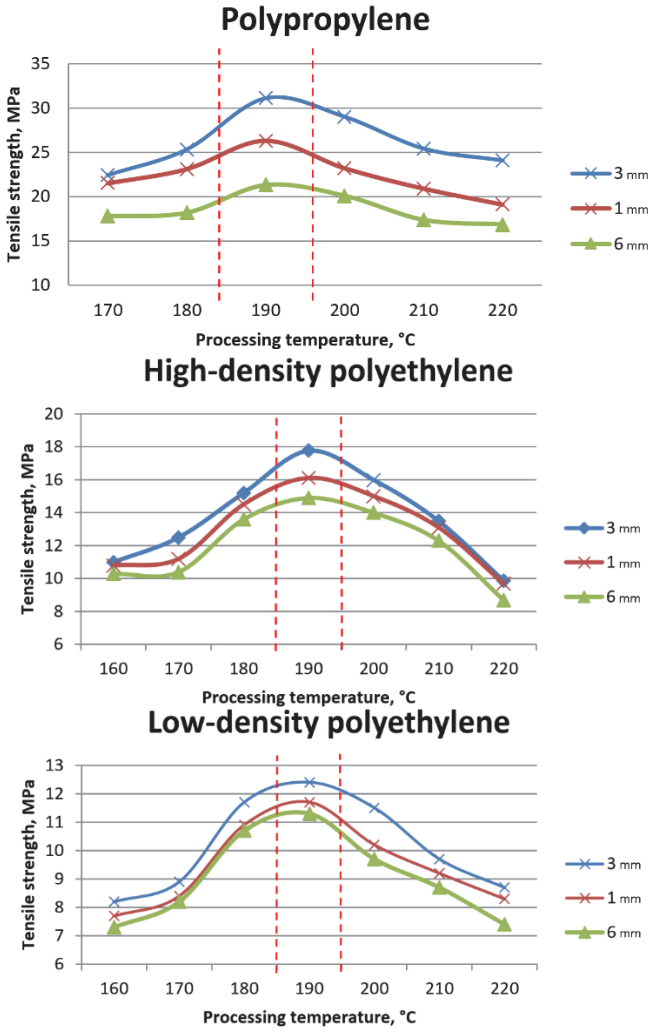

Fig. 4 (a, b, c). Dependence of strength properties of polymer samples on the ambient temperature

The mixture of polymers is extruded onto the prepared layer at a temperature of 185-195°C, after cooling the surface, a drainage layer of coarse-grained material (sand) with a thickness of 10-15 centimeters is applied. The drainage layer of the collecting and irrigation systems is developed afterward. The mixture is prepared at the place of its application, loaded into the hopper of the extrusion machine, where it is subjected to electro-thermal heating to a melting point of 185-195°C. After that, the molten mixture is applied to the prepared surface in strips of 2.0-2.5 m, with a mutual overlap of 0.15-0.20 m by means of screw feeding to the extruder. Overlapping of the stacked polymer mixture strips will improve the integrity of the entire coating, as well as eliminate the need for the coating stitching, as in the case of geomembranes.

The main operation issue of such a screen is the impact of static and dynamic loads and aggressive environment (acidic or alkaline), which leads to fairly rapid, within few years, deterioration of the strength properties of polymer screens, and their consequent destruction. The blending of additives into the polymer, as well as the application of a coarse sand layer, are the relevant solutions since the layer distributes the load from the tailings body and does not violate the integrity of the polymer material properties.

4. Conclusions

The conducted research has confirmed that the long-term operation of the tailings leads to contamination of groundwater and surface water. The study of enrichment waste samples showed that the concentration of useful elements allows considering the tailings as a technogenic deposit. The physical and mechanical properties of secondary polymers under tensile loads were determined. The tested protective approach suggests applying the polymer granules processed by melting to the prepared surface. The developed waterproofing technology reduces the negative impact on natural waters, as well as preserves raw materials for potential further secondary extraction.

The analyses were performed using the equipment of the Common Use Centre of the Saint Petersburg Mining University. Author Contributions: Babenko D.A. – resources, methodology, investigation, writing – original draft preparation; Pashkevich M.A. – supervision, project administration, writing – review and editing; Alekseenko A.V. – translation, data curation, conceptualization, validation, formal analysis, visualization, software.

References

Abramov, A.A. (1984). *Flotation enrichment methods*. Textbook for universities. Moscow, 383.

Aleksandrova, T.N., Talovina, I.V., Duryagina, A.M. (2019). Gold–sulphide deposits of the Russian Arctic zone: Mineralogical features and prospects of ore benefication. *Chemie der Erde.* DOI: 10.1016/j.chemer.2019.04.006.

Bazhin, V.Y., Beloglazov, I.I., Feshchenko, R.Y. (2016). Deep conversion and metal content of Russian coals. *Eurasian Mining*, *2*, 28-32.

Bolshunova, T.S., Rikhvanov, L.P., Mezhibor, A.M., Baranovskaya, N.V., Yusupov, D.V. (2017). Biogeochemical features of epiphytyc lichens from the area of the tailing of a gold-polymetallic deposit (Kemerovo region, Russia) comparative to a reference area. *International Multidisciplinary Scientific GeoConference Surveying Geology and Mining Ecology Management, SGEM, 17*(51), 165-172.

Bonotto, D.M., Garcia-Tenorio, R. (2019). Investigating the migration of pollutants at Barreiro area, Minas Gerais State, Brazil, by the 210 Pb chronological method. *Journal of Geochemical Exploration, 196,* 219-234.

Bortnikov, A.V., Kutolin, V.A., Samukov, A.D., Shuloyakov, A.D., Shirokikh, V.A. (2014). A study of possibilities for granitic rocks processing dispersed waste material utilization in mineral cotton production. *Obogashchenie Rud, 6,* 33-37.

Brysiewicz, A., Bonisławska, M., Czerniejewski, P., Kierasiński, B. (2019). Quality Analysis of Waters from Selected Small Watercourses within the River Basins of Odra River and Wisła River. *Rocznik Ochrona Środowiska, 21,* 1202-1216.

Bushuev, Y.Y., Leontev, V.I., Machevariani, M.M. (2018). Geochemical features of Au-Te epithermal ores of the Samolazovskoye deposit (Central Aldan ore District, Yakutia). *Key Engineering Materials, 769 KEM,* 207-212.

Coulombe, V., Bussière, B., Côté, J., Garneau, P. (2012). Performance of insulation covers to control acid mine drainage in cold environment. *Proceedings of the International Conference on Cold Regions Engineering,* 789-799.

Dos Santos, L.S., Gardoni, M.D.G.A. (2014). Study of the durability of geomembranes for waterproofing of reservoirs of gold tailings dams in Brazil. *10th International Conference on Geosynthetics, ICG*.

Gałuszka, A., Migaszewski, Z.M., Dołęgowska, S., Michalik, A. (2018). Geochemical anomalies of trace elements in unremediated soils of Mt. Karczówka, a historic lead mining area in the city of Kielce, Poland. *Science of the Total Environment, 639,* 397-405.

Kasimov, N.S., Kosheleva, N.E., Timofeev, I.V. (2016). Ecological and Geochemical Assessment of Woody Vegetation in Tungsten-Molybdenum Mining Area (Buryat Republic, Russia). *IOP Conference Series: Earth and Environmental Science 41(1),* 012026.

Koptev, V.Y., Kopteva A.V. (2017). Improving paraffin deposits detection methodology for better ecological safety during hydrocarbon transportation. *International Journal of Applied Engineering Research*, *12*(5), 618-621.

Krasotkina, A.O., Machevariani, M.M., Korolev, N.M., Makeyev, A.B., Skublov, S.G. (2017). Typomorphic features of niobium rutile from the polymineral occurrence Ichetju (the Middle Timan). *Zapiski Rossiiskogo Mineralogicheskogo Obshchestva, 146*(2), 88-100.

Kremcheev, E.A., Gromyka, D.S., Nagornov, D.O. (2018). Techniques to determine spontaneous ignition of brown coal. *Journal of Physics: Conference Series, 1118*(1), 012021.

Kruk, M.N., Guryleva, N.S., Cherepovitsyn, A.E., Nikulina, A.Yu. (2018). Opportunities for improving the corporate social responsibility programs for metallurgical companies in the Arctic. *Non-ferrous Metals*, *44*(1), 3-6.

Krzaklewski, W., Pietrzykowski, M. (2002). Selected physico-chemical properties of zinc and lead ore tailings and their biological stabilisation. *Water, Air, and Soil Pollution, 141*(1-4), 125-142.

Lee, J.K., Shang, J.Q. (2013). Thermal properties of mine tailings and tire crumbs mixtures. *Construction and Building Materials, 48,* 636-646.

Litvinenko, V.S. (2020). Digital Economy as a Factor in the Technological Development of the Mineral Sector. *Natural Resources Research*, *29*(3), 1521-1541.

Lyamkin, D.I. (2000). *Mechanical properties of polymers*: Textbook. Moscow, 64.

Makarov, A.B. (2000). Technogenic deposits of mineral raw materials. *Soros Educational Journal, 6*(8).

Nagornov, D.O., Kremcheev, E.A., Kremcheeva, D.A. (2019). Research of the condition of regional parts of massif at longwall mining of prone to spontaneous ignition coal seams. *International Journal of Civil Engineering and Technology, 10*(1), 876-883.

Nedosekin, A.O., Rejshahrit, E.I., Kozlovskiy, A.N. (2019). Strategic approach to assessing economic sustainability objects of mineral resources sector of Russia. *Journal of Mining Institute*, *237*, 354-360.

Nikolaevna, P.A., Sergeevich, S.A. (2020). Peculiarities of assessing the reservoir properties of clayish reservoirs depending on the water of reservoir pressure maintenance system properties. *Journal of Applied Engineering Science*, *18*(1), 10-14.

Pochechun, V.A., Melchakov, Yu.L. Babenko, D.A. (2014). The use of a systematic approach in the study of natural and man-made geosystems. *Bulletin of Tambov University. Series: Natural and Technical Sciences, 19*(5), 1551-1554.

Recommendations for the design and construction of sludge collectors and tailings of metallurgical industry (1986) VODGEO Institute. Moscow, 128 p.

Safiullin, R.N., Afanasyev, A.S., Reznichenko, V.V. (2019). The concept of development of monitoring systems and management of intelligent technical complexes. *Journal of Mining Institute*, *237*, 322-330.

Semyachkov, A.I., Drebenstedt, C, Vorobiev, A.E. (2012). *Geoecology*. Textbook for higher mining and geological educational institutions. Yekaterinburg, 289.

Sliti, N., Abdelkrim, C., Ayed, L. (2019). Assessment of tailings stability and soil contamination of Kef Ettout (NW Tunisia) abandoned mine. *Arabian Journal of Geosciences, 12*(3), 73.

Végsöová, O., Straka, M., Rosová, A. (2019). Protecting and securing an environment affected by industrial activity for future utilization. *Rocznik Ochrona Srodowiska*, *21*(1), 98-111.

Wang, W., Zhao, Y., Liu, H., Song, S. (2017). Fabrication and mechanism of cement-based waterproof material using silicate tailings from reverse flotation. *Powder Technology, 315,* 422-429.

Weishi, L., Guoyuan, L., Ya, X., Qifei, H. (2018). The properties and formation mechanisms of eco-friendly brick building materials fabricated from low-silicon iron ore tailings. *Journal of Cleaner Production, 204,* 685-692.

Yusupov, D.V., Bolshunova, T.S., Mezhibor, A.M., Rikhvanov, L.P., Baranovskaya, N.V. (2017). The use of Betula Pendula R. Leaves for the assessment of environmental pollution by metals around tailings from a gold deposit (Western Siberia, Russia). *International Multidisciplinary Scientific GeoConference Surveying Geology and Mining Ecology Management, SGEM, 17*(41), 665-672.

Yusupov, D.V., Karpenko, Yu.A. (2016). REE, Uranium (U) and Thorium (Th) contents in Betula pendula leaf growing around Komsomolsk gold concentration plant tailing (Kemerovo region, Western Siberia, Russia). *IOP Conference Series: Earth and Environmental Science, 43*(1), 012053.

Zhang, Z., Sui, W., Wang, K., Tang, G., Li, X. (2018). Changes in particle size composition under seepage conditions of reclaimed soil in Xinjiang, China. *Processes, 6*(10), 201.

Zhao, F.-Q., Li, H., Liu, S.-J., Chen, J.-B. (2011). Preparation and properties of an environment friendly polymer-modified waterproof mortar. *Construction and Building Materials, 25*(5), 2635-2638.

Zhu, P., Zheng, M., Zhao, S., Wu, J., Xu, H. (2015). Synthesis and thermal insulation performance of silica aerogel from recycled coal gangue by means of ambient pressure drying. *Journal Wuhan University of Technology, Materials Science Edition, 30*(5), 908-913.

Zubala, T. (2019). Time and Space Variability of Water Quality in the Inner-city River in Lublin from the Aspect of Existing Natural and Land Use Conditions. *Rocznik Ochrona Środowiska, 21,* 712-727.

Abstract

The paper justifies the waterproofing technology for waste storage conservation. The paper presents the results of full-scale monitoring of the quality of surface and groundwater affected by the tailings of the Gaisky Mining and Processing Plant. The determined chemical composition of enrichment waste is described. The existing methods of waste storage waterproofing are reviewed. The studied residuals of copper ore enrichment can be insulated with a mixture of processed secondary polyethylene and polypropylene pellets. The physical and mechanical properties of recycled polymers are investigated. The proposed technology of covering with a waterproofing coating can be applied to preserve technogenic deposits aiming at their future secondary extraction, as well as to ensure the environmental safety of newly designed facilities. The implementation of this technique will improve the regional environmental situation and reduce the migration of potentially hazardous substances as a result of seepage, thus reducing the pollution of natural waters.

Keywords:
ore dressing waste, tailings storage, adverse impact, secondary polymers, waterproofing

MIDDLE POMERANIAN SCIENTIFIC SOCIETY OF THE ENVIRONMENT PROTECTION

Rocznik Ochrona Środowiska

Volume 22. Year 2020 ISSN 1506-218X 226-241

Noise Charge in Rail Transport – EU Regulations Versus Operation of Logistics Systems

Paweł Zając[1], David Staš[2], Radim Lenort[2]*

[1]Wroclaw University of Science and Technology, Poland

[2]ŠKODA AUTO University, Czech Republic

[*]corresponding author's e-mail: pawel.zajac@pwr.edu.pl

1. Introduction

The different kinds of transport systems, including air, rail and road transport types must reduce the unpleasant and harmful side effects of its operation – noise. Noise impacts can be analysed not only in the surroundings of the transport system, but also, for instance, in terms of impact of noise on the operator (other people, operator) in the cabin of the vehicle, in the compartment where the passengers travel. This paper focuses on the problem of noise in the close vicinity of the transport system; by this we mean people who are often not connected with it, residents of areas close to the operation of transport systems. Many works have been published on this subject, e.g. (Janas 2018, Zagubień 2016, Janas 2019, Jacyna at el. 2018, Szyszlak-Bargłowicz at el. 2013, Profaska, 2012, Chudzikiewicz et al. 2018, Chamier-Gliszczyński 2011a,b). In the next step, the substantive scope of the paper was narrowed down to rail freight transport – the so-called cargo. The issue is entirely new to all, as the EU has introduced a noise-related charge for a freight train running on a specific rail route. The charges are related to people's comfort of living; exceeding the permissible noise level will result in charges and, in special cases, prohibiting overly noisy freight trains from running on certain sections of track, over a certain period of time etc. The noise generated is not always the result of over-exploitation of rolling stock and can cause accelerated degradation of the infrastructure in the close vicinity of the transport system. The implementation of new infrastructure projects will necessitate new solutions for the protection of people and the environment from noise. These are solutions that minimize the acoustic impact of railway lines other than standard noise barriers (e.g. dampers/rail inserts/structural solutions for wagons and loco-

motives). Ensuring adequate acoustic comfort for rail traffic is now standard practice in the EU. In Poland, PLK S. A., while carrying out works related to upgrade/revitalisation of railway lines, applies special noise protection devices – acoustic screens, which are designed to reflect or absorb acoustic waves in order to maintain the normative noise level for the protected area.

By analogy, hybrid solutions are applied, e.g. vehicles with two power units (internal combustion engine and electric motor), thus making efficient use of available energy possible (Maharjan at el. 2020). This analogy is a hybrid solution where noise protection is in the form of acoustic screens and photovoltaic panels are used that generate electricity, while maintaining the required level of noise protection. In terms of new research, the following are important: optimisation of the use of generated energy (Woźniak et al. 2015), protection of elements of railway infrastructure systems against theft and devastation (thieves and hooligans), constant supervision – monitoring of equipment operation.

This new knowledge will enable the introduction of various sound protection measures appropriate to the severity of the sound source. The developed recommendations will determine their effectiveness and scope of application taking into account the mutual geometric position of the system: sound source – minimizing device – protected area.

All existing solutions meet the provisions of Art. 174 (Journal of Laws of 2013) and the maintenance of the limit values specified in (Journal of Laws 2014) in the areas under acoustic protection, adjacent to railway lines.

2. Analysis of the current situation

Freight trains made up of wagons and locomotives can have different environmental impacts. The noise depends on the type of material transported, speed and the loading of the wagon. In addition, wagons may be leaking and lubricants may leak into the environment.

When analysing the rolling stock, it is possible to carry out the primary division of wagons according to the purpose of the wagon and distinguish between: wagons for transporting cargo and wagons for transporting people.

The second criterion of division may be gross weight of the wagon. A distinction can be made between wagons with one axle, two axles or three axles in the wheelset.

For single-axle wagons, there is no bogie in the suspension, but only an axle-box system with a solebar with a single degree of freedom, enabling vertical movements of the body. The springing element is made up of leaf springs, which are characterized by high internal friction, which is used as a frictional damper damping the body vibrations. These types of wagons have a gross weight limit of about 30 Mg (15 Mg per axle). The lateral and longitudinal movement of the

wagon suspension occurs within the existing mechanical play, which limits the maximum speed of the wagon. With the increase of the total weight of the wagon and in order to meet the requirements of increasing the driving speed in the wagons' wheelsets, bogie systems have appeared with two or three running axles, with one or two degrees of springing.

The simplest bogie is the 1XT model with two axles and one degree of springing. The suspension uses leaf springs (two per axle). No additional vibration damping elements were used, but only the internal friction of the spring itself was used for vibration damping. This type of solution has a speed limit of about 100 km/h.

An example of a two-axle single-springing bogie that uses helical springs as a springing element is the 2XT family. 14 sets of spring columns were used in the bogie's suspension (one spring column consists of two springs of different diameters arranged coaxially), with seven springs on each side and a wedge friction damper as a damper. The maximum load capacity of the bogie is 17.5 Mg, and the total rail pressure is 20 Mg.

Three-axle 7TNa bogies, similar in design to 1XT bogies, were used for heavy freight wagons. The suspension uses leaf springs. There were no additional separate damping systems.

Due to the required driving comfort and the ever-increasing need to raise the driving speed of passenger trains, double-axle bogies with double springing are most often used in passenger cars. The most popular family of double-axle bogies for passenger wagons is 25A. In wagons, depending on the maximum permitted speed, the 25AN variety (speed up to 160 km/h) and 25ANa (speed up to 200 km/h) is used. Due to the required driving comfort, a sophisticated springing system is used in the suspension. It comprises the following: springing elements in first degree suspension (between the wheel axle and the bogie), and springing elements in second degree suspension (between the bogie and the wagon body). In some solutions, an elastomeric spring is additionally used between the solebar and the axle-box.

The springing elements are usually sets of springs (two springs each arranged coaxially in different lengths and with different stiffness with countertorsional coils, which prevents the deflection of one spring from blocking if the other breaks). They are made of 50S2 (55S2) spring steel bars with circular cross-section. They usually have linear stiffness characteristics and minimal hysteresis. A relatively new solution is the use of flexicoil springs. It is made of variable diameter wire, which ensures its progressive stiffness characteristics. In addition, these types of springs have a large outer diameter, which means that they can carry a large amount of lateral loads.

In order to improve the riding comfort and increase the maximum speed (above 200 km/h), air springs are used in the latest wagons. They are characterized by low weight, small size, high durability. Like steel springs, air springs have little hysteresis and require additional vibration damping systems.

Damping is provided by vibration dampers that dissipate the energy of vibrations from both the wagon body and the bogie.

The simplest vibration damper used in the suspension of wagons that use springing elements in the form of helical springs are friction dampers. Here, vibration damping consists in creating a resistance force for the relative movement of two surfaces between which friction occurs. The most commonly used frictional dampers in the railway industry are: cylindrical damper, scissor damper. The structural diagrams are shown in Figures 1 and 2.

The damping characteristics of friction dampers are shown in Figures 3 and 4.

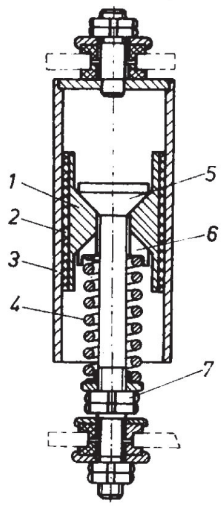

Fig. 1. Cylindrical friction damper diagram: (1 – runner, 2 – pad, 3 – bush, 4 – spring, 5 – head, 6 – wedge pad, 7 – spring tension adjustment nuts)

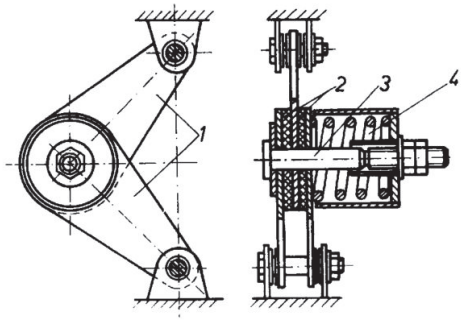

Fig. 2. Scissor friction damper diagram: (1 – arms, 2 – friction discs, 3 – screw, 4 – spring)

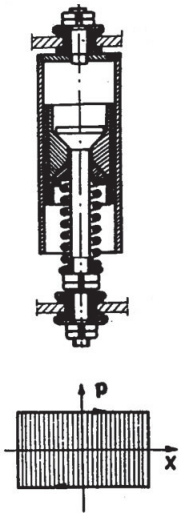

Fig. 3. Damping characteristics of friction damper with constant friction force

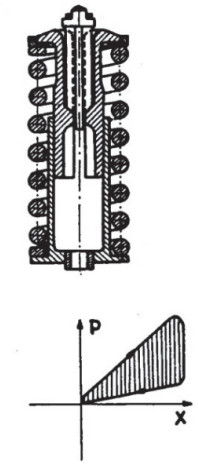

Fig. 4. Damping characteristics of friction damper with progressive friction force

More modern SA hydraulic vibration dampers. These are divided into: single-acting dampers, double-acting dampers (Kosobudzki at el. 2018).

Due to the damping characteristics, the following can be distinguished: linear dampers – the damping increases linearly with the relative speed of the piston and cylinder, non-linear dampers – the damping increases non-linearly with the relative speed of the piston and cylinder.

The engineering diagram of the double-acting hydraulic damper and its damping characteristics are shown in Figures 5 and 6.

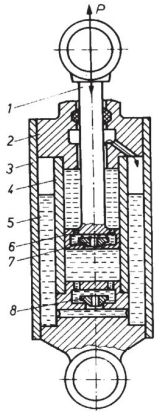

Fig. 5. Engineering diagram of double-acting hydraulic damper: 1 – piston rod, 2 – guide sleeve with seal, 3 – outer cylinder, 4 – inner cylinder, 5 – chamber, 6 – piston, 7 – decompression valve, 8 – compression valve)

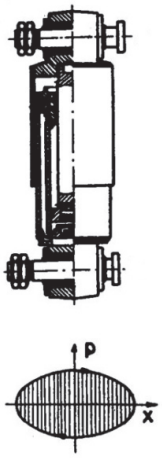

Fig. 6. Linear damping characteristics of hydraulic damper

Hydraulic dampers are used for damping of vertical vibrations (so-called galloping) in the first degree of springing and for damping of vertical, transverse (so-called swaying) and lateral vibrations in the second degree of springing.

Due to their dynamic properties, bogies are classified as supercritical or subcritical. This means that supercritical bogies move at speeds that generate vibrations of frequency exceeding the bogie's own vibrations. An example of this is the 1XT family of bogies. Subcritical bogies move at speeds where the vibrations do not exceed the bogie's own vibrations. An example of this is the 25TN bogie family. It shows an increase in the tendency of swaying (high value of WZ running smoothness index) on tracks with a small width (about 1432 mm) and small rail inclination (1:40).

The solution to improve the WZ index is to replace dry friction sliding elements in the lateral direction in second degree of springing with flexible elastomeric pads. Additionally, to reduce the dynamic loads accompanying the swaying, torsion bars are used in passenger cars, cooperating with horizontal hydraulic dampers mounted between the bogie frame and the car body. The advantages of using dampers for damping the horizontal rotation of the bogie are particularly evident at high speeds (above 160 km/h). The desired shape of the swaying damper hysteresis is rectangular, which corresponds to the characteristics of a friction damper. For swaying dampers, their maximum damping occurs already at very low speeds, in the range of 2-3 mm/s and remains constant also at higher speeds. Another place where lateral loads are damped is the use of spherical layered elastomeric pads applied on spring columns, which not only increase the possibility of relative lateral displacement of the wagon body and bogie frame (longer damping distance), but these pads also act as rubber-metal dampers with high hysteresis and do not affect vertical vibrations in practice. In addition, they isolate vibrations generated by the bogie's wheelset, limiting their transmission to the wagon body (Cunha at el. 2020).

An advantageous effect, due to the progressive increase in stiffness versus deflection and the large hysteresis loop, is brought about by rubber, which is increasingly used as a material for manufacturing damping elements. The damping characteristics of springing elements made of different materials are shown in Figure 7.

Rubber is used to make springing elements in the first degree of springing, e.g. a Chevron spring. They ensure that the bogie's axles are guided in a zero-clearance manner, which significantly reduces impact loads and vibrations transmitted to the wagon body. Modern elastomeric materials are introduced successfully in the automotive industry. It turns out that they have similar properties to rubber elements, but their durability is much greater. In addition, they allow a wide range of changes in their elastic and damping properties through adjustments to the chemical composition.

In order to select the mechanical properties and design the elastic-damping element properly, the entire system in which the element will operate must always be considered. This is why analyses related to the intended operation of the entire assembly are vital. The necessary input data includes information on load spectra, operating temperatures, static loads and dynamic characteristics of the entire system.

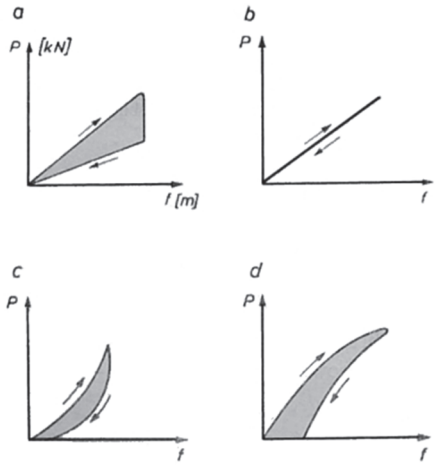

Fig. 7. Damping characteristics: a – leaf spring, b – steel helical spring, c – rubber spring, d – pneumatic spring.

In order to analyse the work of the proposed elastic-damping element in terms of vibration transmission, it is planned to model the dynamic system with the finite element method and multi-body systems as accurately as possible. With the collected information on load profiles it will be possible to determine the routes of vibration transfer through the system and to identify the most important elements affecting this transfer. This will allow to select and focus on developing possible changes in the system that will have the greatest effect.

Elastomeric elements are objects with strongly non-linear characteristics in which it is difficult to separate the purely damping part from the purely elastic part. For this reason, special methods based on the identification of non-linear models should be used for analysis, which may include energy and power balancing methods developed in our department. With appropriate mathematical models and laboratory equipment, it will be possible to design, analyse and optimise, in terms of effectiveness of vibration damping and durability, the proposed solutions for reducing the dynamic effects on the passengers (cargo) transported and the railway infrastructure affected by vibrations caused by train movements.

Cargo in older wagons in particular hit the walls and displace during transport, as shown in the figure below.

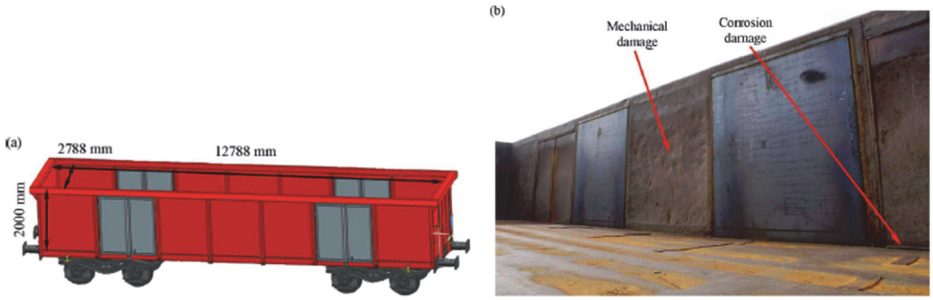

Fig. 8. The EAOS 1415 A3 coal car: a) virtual model, b) damage elements of the box

3. Noise level measurement principles according to [standard]

The noise of freight trains can be measured outside the railway line, as well as inside, for example in passenger cars or at the engineer's position. A draft amendment to the TSI ((EU) No 1304, 2014) was adopted by the EU Member States via the Committee on Railway Interoperability and Safety in 2019. A deadline was set for the mandatory fitting of freight wagons with composite brake blocks.

Work on the revision of the Technical Specification for Interoperability with regard to noise started in early 2016. From the beginning, they have been of great interest due to the potentially high costs of adaptation to new requirements.

The adopted draft assumes selection of special sections of railway lines (so called silent sections), on which freight trains with cast-iron brake blocks will be prohibited. These will be sections with a minimum length of 20 km, on which an average of more than 12 freight trains travelled overnight during the period 2015-2017. The list of silent sections will be published by the European Union Railway Agency 9 months after the specification enters into force. It is to be expected that the main freight lines both in Poland and abroad will be silent sections. In the course of the work, Poland negotiated the so-called special case to allow the continued operation of tyred wheelsets, which constitute a significant part of the Polish freight wagon fleet. These trains will be permitted for domestic service regardless of the status of the line until the end of 2036. They will also be able to enter the Czech Republic and Slovakia without restrictions until the end of 2026. Similar regulations will also apply to other types of wagons, which would be very costly to adapt to new requirements. This will allow railway undertakings operating in Poland to avoid significant costs associated with adaptation to new requirements.

Freight wagons not covered by the exemptions and running on silent sections will have to be fitted with composite brake blocks by 7 December 2024. The process of replacing the blocks can be supported by CEF funding ranging

from €250 per wagon in service up to 100 km/h to €600 per wagon in service up to 120 km/h.

Noise level in rail traffic is calculated in octave bands. For rail traffic noise, the A-weighted average sound pressure level is calculated, based on the results obtained for the octave bands, for the daytime, evening and night time as defined in Article 5 of Directive 2002/49/EC, by aggregating data from all frequencies.

$$L_{Aeq,T} = 10 \times \log \sum_{i=1} 10^{\left(L_{Aeq,T,i}+A_i\right)/10}$$

A_i stands for the correction curve A as defined in (PN-EN 61672-2, 2014), is the frequency band index, while T is the time corresponding to day, evening or night time.

The Directive has systematised the classification and descriptors of railway vehicles. In addition, it has been applied to the existing track infrastructure, which is extremely diverse due to the presence of several important elements that determine their acoustic properties and characterise them. Some elements have a large impact on the acoustic properties, while others have a small impact. As a rule, the most important elements affecting noise emissions in rail traffic are: rail head roughness, rail pad stiffness, sleeper, rail interfaces and track curvature radius. Alternatively, the general characteristics of the track can be defined, in which case the rail head roughness and the rate of decay of track vibrations according to (PN-EN ISO 3095, 2005) are two basic parameters determining the acoustic characteristics of the track, plus the radius of curvature of the track. Noise measurement points for calculating equivalent noise sources are shown in the Fig. 9.

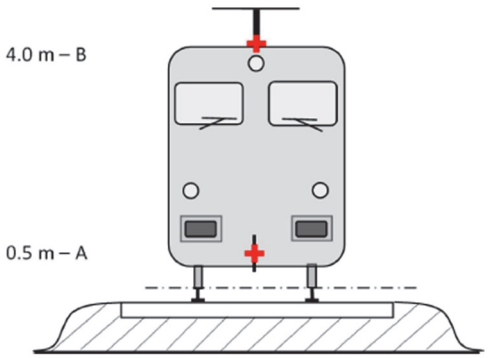

Fig. 9. Location of equivalent noise sources

The physical sources of noise are divided into different categories, depending on the mechanism of noise emission; these are: 1) rolling noise (taking into account not only the vibrations of the sleeper and track as well as vibrations of wheel, but also, if any, the noise emitted by the superstructure of freight rail vehicles); 2) traction noise; 3) aerodynamic noise; 4) impact noise (from switches, crossings and nodes); 5) noise of squeaks; 6) noise caused by the acoustic impact of associated infrastructure facilities, such as bridges and viaducts.

1) Wheel and rail head roughness noise emitted from the three sound propagation routes to the surface of the radiated sound beam (tracks, wheels and superstructure) means rolling noise. It is assumed that the noise source is located at a height of h = 0.5 m (area of the radiated A-beam) reflecting the acoustic impact of track surfaces, including in particular plate tracks (their part responsible for sound propagation) and reflecting the noise impact of the wheels and vehicle superstructure (for freight trains).
2) The heights of the equivalent sources of noise emitted by the train vary from 0.5 m (source A) to 4.0 m (source B) depending on the physical location of the given element. Sound sources such as transmissions and electric motors are often located at the axle height, i.e. 0.5 m (source A). Shutter guards and diffusers can be located at different heights; the exhaust systems of engines of diesel-powered vehicles are often located at roof height, i.e. 4.0 m (source B). Other traction noise sources, such as fans or diesel engine units, may be located at a height of 0.5 m (source A) or 4.0 m (source B). If the exact height of the source location is within the range of model heights, the acoustic energy dissipates in proportion to the nearest heights of the adjacent source. For this reason, the method assumes two source heights, namely 0.5 m (source A) and 4.0 m (source B), while the equivalent sound power associated with each of these sources is divided between the two sources depending on the specific configuration of the source located on a given type of unit.
3) The aerodynamic noise acoustic impact is related to a source located at a height of 0.5 m (modelling of shields and screens, source A) and a source located at a height of 4.0 m (modelling of all components located above the vehicle roof and the trolley, source B). The choice of a source position height of 4.0 m that takes into account the acoustic impact of the current collector is considered to be a simple model, and the adoption of this height requires an in-depth analysis if the main purpose of the model is to determine the correct height of the sound barrier. (UE 2015/996, 2015)
4) The impact noise is related to a sound source located at a height of 0.5 m (source A).
5) The noise from squeaks is related to a sound source located at a height of 0.5 m (source A).
6) The noise emitted by bridges is related to a sound source located at a height of 0.5 m.

4. Transport and logistics system versus the new (EU 2015/996, 2015)

The EU's intention is to create legal and technical solutions that allow for the introduction of charges to carriers for the operation of wagons that fail to meet the standards to a different extent, including with respect to noise. If the carrier refuses to pay the "noise charge" and does not use "silent" rolling stock, his wagons will run on different, usually longer routes compared to silent trains.

Changes in the transport and storage infrastructure may be manifested by an increase in the reloading of goods at intermodal terminals or, in general, at logistics centres.

Until recently, the operation of intermodal terminals was associated with the risk of noise generated during container transhipment. It is relatively easy to protect workers from the negative effects of noise with hearing protectors or anti-vibration gloves. However, the reloading work takes place in the open air and many terminals are located close to residential areas, so it is important to reduce the noise generated during the work.

One of the solutions is to introduce modern silent motors in terminal equipment. The reduction of noise generated during the placement of the spreader on the container, on the other hand, comes from a system for controlling the spreader movement speed.

Reachstackers and cranes (Zajac 2015, 2016) use an optical system mounted under the spreader used to monitor the distance between the spreader and the container. As the spreader hits the container, the spreader lowering speed is reduced (https://intermodalnews.pl).

In the process of transshipment of single cargo, such as containers, the transshipment cannot be carried out by means of tipplers (which is acceptable for granular materials), as is the case with wagons, and transshipment equipment with a spreader or bucket is used instead which is basically "dropped" from a certain height to the level of the container on the railway wagon, hitting its surface.

The capacity of one transshipment machine is currently around 1,800,000 kg per hour; there are usually several of those working on a single transshipment operation. The machines move on rails when unloading containers. Each machine can reach a height of up to 70 m, with a maximum reach of 50 m and a weight of 610,000 kg – 170 of which is the counterweight. The weight of the spreader that is dropped is around 15000 kg (Kwasniowski & Zajac 2016).

The machines are controlled by operators who sit in the cabins at a fairly large height, even about 30 meters above terminal level, using joysticks, aided by image from the CCTV cameras installed on the machine. There are two images: one is the image from the camera mounted on the crane, and the other shows data useful for work. Among other things, the distance between the spreader and the

container is indicated – i.e. the place of unloading. The meters remaining to the container are calculated by the operator, however.

Combining these two opposite trends in the context of noise reduction at transshipment terminals, i.e.: noise reduction by reducing the transshipment speed versus increasing the transshipment speed in the context of increasing the efficiency of transport systems (Zajac & Kwasniowski 2017, Woźniak et al. 2015).

5. Conclusions

1. It is reasonable and understandable to set a permissible noise level for freight trains in the EU – such regulations have already been introduced for air pressure control systems in car wheels, for example. At present, the noise level has been set for freight trains. In addition, there is discussion among EU experts on the introduction of a minimum value for the air resistance coefficient – to charge for vehicles that have a c_x value that is too high, which translates into its energy consumption.
2. The setting of an acceptable noise level for means of transport protects against the negative effects of noise on the human body. The formulation of guidelines for the determination of permissible noise levels is justifiable – not only in the human context but also in the environmental context.
3. A charge for exceeding the permissible noise level in rail transport may result in a transfer of the cargo stream to other modes of transport but it is likely to generate additional transshipments at terminals from "noisy" to "quiet" wagons, in logistic centres, which may reduce noise on the railway line but increase the noise caused by transshipments at unauthorised times, resulting in exceeding the permissible noise levels in the silence zones neighbouring with logistic centres. This increase in noise is expected to be significant.

References

Chamier-Gliszczyński, N. (2011a). Sustainable operation of a transport system in cities. Advanced Design And Manufacture IV, Book Series: *Key Engineering Materials, 486*, 175-178.

Chamier-Gliszczyński, N. (2011b). Environmental Aspects of Maintenance of Transport Means. End-of Life Stage of Transport Meeans. *Maintenance And Reliability, 2*, 59-71.

Chudzikiewicz, A., Bogacz, R., Kostrzewski, M., Konowrocki, R. (2018). Condition monitoring of railway track systems by using acceleration signals on wheelset axle-boxes. *Transport, 33*(2), 555-566. DOI: https://doi.org/10.3846/16484142.2017.1342101

Cunha, A., Caetano, E., Ribeiro, P., Müller, G. The identification of nonlinear damping of the selected components of MDOF complex vibratory systems. *Mater. Plast., 57*(2), 140-151. DOI: https://doi.org/10.37358/MP.20.2.5360

Journal of Laws, 2013, item 1232, the Environmental Protection Act.
Journal of Laws, 2014, item 112, Regulation of the Minister of the Environment of June 14, 2007 on permissible noise levels in the environment.
Gasowski, W., Sobas, M. (2013). Structural methods of noise reduction in running gears of freight wagons. Railway vehicles.
Gu, W., Ma, T., Ahmed, S., Zhang, Y., Peng, J. (2020). A comprehensive review and outlook of bifacial photovoltaic (bPV) technology. *Energy Conversion and Management, 223*, 113283.
Guerrero-Lemus, R., Vega, R., Kim, T., Kimm, A., Shephard, L. E. (2016). Bifacial solar photovoltaics – A technology review. *Renewable and sustainable energy reviews, 60*, 1533-1549.
Jacyna, M., Wasiak, M., Lewczuk, K., Chamier-Gliszczyński, N., Dąbrowski, T. (2018). Decision Problems in Developing Proecological Transport System. *Rocznik Ochrona Środowiska, 20*(2), 1007-1025.
Janas, L. (2018). Badania hałasu w otoczeniu mostów kolejowych blachownicowych o różnych rodzajach konstrukcji. *Rocznik Ochrona Środowiska, 20*(2), 1066-1078.
Janas, L. (2019). Identification and Analysis of Noise Sources in a Plate Girder Railway Bridge with Orthotropic Deck. *Rocznik Ochrona Środowiska, 21*(1), 600-610.
Kosobudzki, M., Jamroziak, K., Bocian, M., Kotowski, P., Zając, P. (2018). *The analysis of structure of the repaired freight wagon*. In: AIP Conference Proceedings, 2029(1), 020030). AIP Publishing LLC.
Kwasniowski, S., Zając, P. (2016). *Method of assessment of energy consumption of forklifts in warehouses with specific operating conditions*. In: 1st Renewable Energy Sources-Research and Business (RESRB-2016), June 22-24 2016, Wrocław, Poland (pp. 303-312). Springer, Cham.
Maharjan, R., Shahbakhti, M., Rezaei, R., Möllmann, R., Huang, Y., & Delebinski, T. (2020). *Optimization of Diesel Engine and After-treatment Systems for a Series Hybrid Forklift Application* (No. 2020-01-0658). SAE Technical Paper.
Nordmann, T., Vontobel, T., Clavadetscher, L. (2012). 15 years of practical experience in development and improvement of bifacial photovoltaic noise barriers along highways and railway lines in Switzerland. *Cell, 14*, 12-3.
PN-EN 61672-2: 2014-03 / A1: 2017-10, Electroacoustics, Sound level meters, Part 2: Type tests, original EN 61672-2: 2013 / A1: 2017 [IDT], IEC 61672-2: 2013 / AMD1: 2017 [IDT]PN-EN ISO 3095:2005, Kolejnictwo – Akustyka – Pomiar hałasu emitowanego przez pojazdy szynowe.
Profaska, M., Korban, Z., Kernert, R. (2012). Przykładowe badania uciążliwości emisji hałasu z ciągu komunikacyjnego. *Rocznik Ochrona Środowiska, 14*, 800-813.
Szyszlak-Bargłowicz, J., Słowik, T., Zając, G., Piekarski, W. (2013). Inline plantation of virginia mallow (Sida hermaphrodita R.) as biological acoustic screen. *Rocznik Ochrona Środowiska, 15*, 538-550.

UE 2015/996 z dnia 19 maja 2015 r. ustanawiająca wspólne metody oceny hałasu zgodnie z dyrektywą 2002/49/WE Parlamentu Europejskiego i Rady https://intermodal-news.pl/2020/03/06/innowacyjne-rozwiazania-redukuja-halas-na-terminalach/

UE nr 1304/2014 w zakresie stosowania technicznych specyfikacji interoperacyjności podsystemu "Tabor kolejowy – hałas" w odniesieniu do istniejących wagonów towarowych

Woźniak, W., Sąsiadek, M., Stryjski, R., Mielniczuk, J., Wojnarowski, T. (2016). *An algorithmic concept for optimising the number of handling operations in an intermodal terminal node.* Proceeding of the 28th International Business-Information-Management-Association (IBIMA), Seville, Spain, ISBN: 978-0-9860419-8-3, 1-7, 1490-1500.

Woźniak, W., Stryjski, R., Mielniczuk, J., Wojnarowski, T. (2015). *Concept for the Application of Genetic Algorithms in the Management of Transport Offers in Relation to Homogenous Cargo Transport.* 26th IBIMA Conference, Madrit, ISBN: 978-0-9860419-5-2, 2329-2340,

Zagubień, A. (2016). Pozazawodowe narażenie na hałas niskoczęstotliwościowy–analiza na podstawie wybranego środka transportu. *Rocznik Ochrona Środowiska, 18(1)*, 626-641.

Zajac, P. (2015). Evaluation method of energy consumption in logistic warehouse systems. Switzerland: Springer International Publishing. DOI: https://doi.org/10.1007/978-3-319-22044-4

Zajac, P. (2016). The energy consumption in refrigerated warehouses. Springer International Publishing. DOI: https://doi.org/10.1007/978-3-319-40898-9

Zajac, P., Kwasniowski, S. (2017). *Modeling forklift truck movement in the VDI cycle and the possibility of energy recovery*. In 23rd International conference on engineering mechanics, 1094-1097.

Abstract

The paper discusses the way of determining the noise level in railway traffic according to new EU recommendations, the introduction of which will result in new charges to be borne by the carriers who, during the provision of transport and handling services, use wagons of the old generation – i.e. such wagons that generate noise above the permitted level on a given section of railway road, determined on the basis of EU regulations. The analysis of technical condition of wagons used in transport in Poland was conducted. The method of determining the noise level in terms of exceedances and charges was discussed. The issue of an optional increase in the reloading of cargo units at railway terminals to transport cargo in silent wagons on designated silent sections of routes was raised – this may affect the development and operation of logistics centers.

Keywords:
charges, noise, wagon, train, noise measurement, noise standard

Opłata za hałas w transporcie kolejowym – przepisy UE, a działanie systemów logistycznych

Streszczenie

W artykule omówiono sposób określania poziomu hałasu w ruchu kolejowym według nowych rekomendacji UE, których wprowadzenie będzie skutkować nowymi opłatami ponoszonymi przez przewoźników, którzy podczas świadczenia usług transportowo-przeładunkowych korzystają z wagonów starej generacji – tzn. takich wagonów, które generują hałas powyżej dopuszczalnego na danym odcinku drogi kolejowej, ustalonego na podstawie przepisów UE. Przeprowadzano analizę stanu technicznego wagonów stosowanych w przewozach w Polsce. Omówiono sposób określania poziomu hałasu pod kątem określenia przekroczeń i opłat. Poruszono zagadnienie opcjonalnego zwiększenia przeładunków jednostek ładunkowych na terminalach kolejowych aby na wyznaczonych cichych odcinkach tras ładunki transportować cichymi wagonami – co może wpłynąć na rozwój i działanie centrów logistycznych.

Słowa kluczowe:
opłaty, hałas, wagon, pociąg, pomiar hałasu, norma hałasu

MIDDLE POMERANIAN SCIENTIFIC SOCIETY OF THE ENVIRONMENT PROTECTION

Rocznik Ochrona Środowiska

Volume 22. Year 2020 ISSN 1506-218X 242-255

Mining, Production and Development of Small Fractions of Gravel and Sand Aggregates in North-Western Poland

Wiesław Kozioł, Ireneusz Baic[*]

Łukasiewicz Research Network – Institute of Mechanised Construction and Rock Mining, Katowice Branch, Poland

[*]*corresponding author's e-mail: i.baic@imbigs.pl*

1. Introduction

The gradual deterioration in the quality of raw material base of natural aggregates combined with the simultaneous increase in the demand of the construction industry for the best quality coarse fractions with grain sizes of 5-8, 8-11 mm, etc. (Kozioł & Baic 2018a, Kozioł et al. 2018c, Kozioł & Galos 2013) has a major impact on the growing volume of hard to sell and non-transferable (waste) fractions of aggregates produced in Poland. This applies especially to gravel and sand aggregates since in their resources the share of very fine fractions (below 2 mm) is systematically increasing while the demand for such fractions in construction is limited and they are often treated as useless (waste) material (Domski & Głodkowska 2017, Głodkowska & Laskowska-Bury 2015). Problems with selling fine (waste) sands can be observed, among others, in the north-western region of the country. Since it is practically unknown what the volume of mining, production and consumption of these aggregates is, an attempt was made to assess the quantity of extracted and produced sand fractions of aggregates on a national and regional scale (provinces, regional zones).

2. Resources and mining of gravels and sands in Poland

Gravels and sands belong to the most abundant Polish minerals. The national balance of mineral resources includes over 10,000 documented deposits with total balance resources of approx. 19.470 billion Mg. There are 4,000 developed deposits with economic resources of 3.518 billion Mg. There are over 2.627 active mining plants extracting this type of minerals, and their total economic resources are 2.679 billion Mg (Bilans zasobów…ed. Szuflicki et al. 2008-2019). Domestic sands and gravels extraction in 2018 amounted to 197 million Mg and

since 2015 it has been on an upward trend due to the growing demand caused by the good economic situation in infrastructure (roads) and volumetric construction. The statistical self-sufficiency ratio of economic resources of gravel and sand deposits (including losses) is currently about 15 years, so it is not high given the major problems with obtaining concessions for the exploitation of new deposits. Deposits of gravel and sands are relatively shallow throughout the country and are exploited in all provinces and in the Baltic Sea Area. However, natural conditions are such that they are unevenly distributed. It concerns both the number of deposits, the size of resources, their grain and petrographic composition, their quality, the geological and mining conditions as well as the environmental, social, technical and economic determinants of their exploitation. This situation is, among other things, a consequence of the diverse geological conditions in which crumb sedimentary rock deposits are formed. The most general distinction in the country can be made between two main raw material zones of crumb deposits: the vast zone of the Polish Lowlands and the Carpathian and Sudeten zone (Radwanek-Bąk et al. 2018, Ney 2007). In the first one, covering about 80% of the country's area, there are sediments whose origin is related to the activity of glaciers or glacial waters (the so-called glaciofluvial sediments). The second one is dominated by river accumulation sediments: gravel and sand of river terraces and alluvial fans. In addition, there are also concentrations of crumb minerals on the bottom of the Baltic Sea, although some of them are also of glacial origin. Taking into account more detailed genetic conditions and the resulting regional differentiation of geological and raw material parameters of gravel and sand deposits, three basic occurrence zones are most frequently distinguished (Kozioł et al. 2018, Radwanek-Bąk et al. 2018). The **northern zone** includes the northern part of Polish Lowlands with dry and waterlogged sandy gravel and gravelly sand deposits, containing mainly Scandinavian material – crystalline formations and limestones with an admixture of quartz and sandstones. In the text (Kozioł et al. 2018), this zone includes the following provinces: Zachodniopomorskie, Pomorskie, Warmińsko-Mazurskie, Podlaskie and Lubuskie. The **central zone** includes the southern part of the Polish Lowlands, where partially waterlogged and waterlogged sand and gravel deposits occur, with relatively small resources. This zone is the largest in terms of surface area. It consists of 6 province: Wielkopolskie, Kujawsko-Pomorskie, Mazowieckie, Łódzkie, Świętokrzyskie and Lubelskie. The Carpathian and Sudeten area constitutes the **southern zone** with the predominance of sandy gravel deposits, both fully and partially waterlogged, river accumulation (80-90%) and glaciofluvial accumulation. The following provinces belong to the southern zone: Dolnośląskie, Opolskie, Śląskie, Małopolskie and Podkarpackie.

A serious problem for the production of gravel and sand aggregates in Poland is the deteriorating quality of the grain size of the mineral in the gravel and sand deposits, which has an impact on the production volume of the sought-after gravel assortments and the increase in production costs. The Balance of Mineral Resources and Waters in Poland (Bilans zasobów…ed. Szuflicki et al. 2008-2019), distinguishes three basic subgroups of gravel and sand deposits, differentiated according to the sand point (SP) which determines the percentage share in resources of sand with grain size below 2 mm:

- gravels for which SP is lower than 30%,
- sands with gravel (SP between 30-75%),
- sands – SP > 75%.

The analysis of changes in the volume of resources within the period of 12 years (2007-2018) (Bilans zasobów…ed. Szuflicki et al. 2008-2019), Kozioł et al. 2018b, own calculations) shows that despite the exploitation, we are experiencing quite a large increase in resources, because the total balance resources of gravel and sands in Poland have increased by approx. 29.6% and the economic resources – by 85%; however, it is unfavourable that it is mainly the sand resources (SP > 75) that are growing. The economic resources of sand deposits have doubled (by 198%), while the resources of sand and gravel deposits have increased by almost 50% and the resources of gravel deposits have decreased over 50%. The share of sands in industrial resources has been increasing particularly fast from 25.7 to 45.7%.

3. Resources and mining of gravel and sands in north-western Poland

The following provinces were included in the **north-western** zone of gravel and sand aggregate mining: West Pomeranian and Pomeranian as well as the Baltic Sea Area.

3.1. West Pomeranian Province

In West Pomeranian Province, the balance resources of gravel and sands amount to 1.2 billion Mg, which constitutes about 6.2% of the national resources. These deposits are mainly related to glacial and partially river accumulation. In terms of grain composition, the deposits classified as sand with gravel (SP – 30 to 75%) are predominant, although their share is decreasing. Over 10 years, the share of this group of deposits decreased from 83.7 to 55.0%, and the share of sand deposits increased from 16.3 to 45% (Kozioł, Baic, Stankiewicz 2018c). Industrial resources amount to 347 million Mg, which represents approximately 9.0% of national resources. In terms of the volume of national resources, the West

Pomeranian Province is ranked as the 4th in Poland. In 2018, the extraction of gravels and sands in the West Pomeranian Province totalled 17.15 million Mg and – in comparison with 2017 – it decreased by 1.547 million Mg. 78 deposits were exploited, including 3 deposits producing over 1.0 million Mg (Ginawa, Sępólno Wielkie, Witankowo III) and 7 deposits producing between 0.5 and 1.0 million Mg. Half of the active deposits do not exceed the volume of 40 thousand Mg/year, so their extraction classifies as typical mining for small deposits (up to 2 ha and up to 20 thousand m^3) carried out on the basis of simplified county level permits (concessions). The exploited deposits are mostly sandy gravel (SP 50-75%) or gravelly sand (30-75%) types. The share of sand fractions in the extracted mineral has been increasing - over 12 years (2007-2018), the average sand point value increased from 63.2 to 72.8%. The largest companies involved in the extraction and production of gravel and sand aggregates in the West Pomeranian Province are: Lafarge Kruszywa, Beton Sp. z o. o. and Szczecińskie Kopalnie Surowców Mineralnych, whose total share of extraction in the province exceeds 40%. There are also about 10 companies with the output of 0.5 to 1.0 million Mg.

3.2. Pomeranian Province

In the Pomeranian Province, the balance resources of gravel and sands amount to 1.129 billion Mg, which is about 5.8% of the national resources (Bilans zasobów…ed. Szuflicki at al. 2008-2019). These deposits are mainly related to glacial accumulation. In terms of grain composition, sandy gravel and gravelly sand deposits predominate, but their share in the resources has decreased within 12 years from about 80 to 57%, and the share of sand deposits has increased to 43%. Economic resources have increased in recent years to 343 million Mg. In 2018, 167 deposits were exploited, with the total output of 19.18 million Mg, which increased by 4.15 million Mg, i.e. by 21.68%, compared with 2017. More than 60% of the exploited deposits are very small, with the output of less than 40 thousand Mg/year (county level permits). The output from only 2 deposits exceeded 1 million Mg/year, i.e. the Gliśno and Mirowo deposits. Out of 6 deposits, the extraction output ranged from 0.5 to 1.0 million Mg. The largest aggregate producers are Lafargeholcim Sp. z o. o. and Kruszywa Polskie Sp. z o. o.

3.3. Baltic Sea Area

Currently, within the Baltic Sea Area, 3 deposits of sand and gravel (Słupsk Bank, South Baltic Central Bank, Koszalin Bay) are documented with total resources of 136.3 million Mg of balance resources, 89,94 million Mg of industrial resources and 0.83 million tons of extraction in 2018 (Bilans zasobów…ed. Szuflicki et al. 2008-2019). These deposits are located at depths of 15 to 30 m and their average thickness is 0.9 to 1.0 m (maximum - about 5.0 m). They are located at a distance of 3.0 km (north of Koszalin) up to 90 km from the

borders of the area. These are sand and gravel type deposits with a relatively high share of gravel fraction; sand points of the resources range from 53.7% (South Central Shoal) to 64% (Słupsk Shoal) (Kozioł et al. 2011, Kozioł et al. 2017). The South Shoal bed is operated. At the end of 2018, a new, modern dredger by Royal IHC, equipped with an aggregate extraction and processing system, started its operation on this deposit. The vessel – a dredger with the total length of 142 m and a width of 23 m – is equipped with suction heads (mining unit), a set of pumps with a pipeline system, and a processing plant with an aggregate hold. The advantage of the dredger is the possibility to obtain mainly the desired coarse, gravel aggregate fractions by preliminary screening (sieving) of sand fractions. Thanks to this, about 80% of the gravel fractions are obtained from the extracted material, while in the land exploitation the yield of these fractions, depending on the SP, amounts to only 20-30%. The recipients of the produced aggregate are most of the contractors of the Tri-city construction sites, e.g. the tunnel under the Martwa Wisła River, the Pomeranian Metropolitan Railway, the Southern Ring Road of Gdańsk, etc. (Kiewlicz 2019). The production capacity of the dredger is estimated at 2.5 million Mg/year, depending on the customers' demand for aggregate.

4. Change in grain size of gravel and sands on a national scale and in the north-western zone

The parametric quality index (grain size distribution) of documented and exploited gravel and sand resources is defined in geological documentation as the so-called sand point (SP). The assessment of the quantity of fine fractions in the total aggregate and sand resources can be approximated based on the calculation of average sand points in the analysed resources. Assuming the division of documented gravel and sand resources into three basic groups (Bilans zasobów…ed. Szuflicki et al. 2008-2019, Kozioł et al. 2018c), namely sands, sands with gravel and gravel, and determining for each of these groups the average (medium) sand points (SP), i.e. sands – 85%, sands with gravel – 60%, gravel – 25%, the average sand points for the balance, economic and exploited deposits were calculated on the basis of annual balance sheets of minerals. Sample calculations for 2 provinces, 3 zones and the whole country are presented in Table 1 (balance resources), Table 2 (exploited deposits), Figure 1 (balance resources) and Figure 2 (economic resources). The analysis was conducted for the years 2007-2018, which allowed to determine the trend in changes in the content of fine fractions in resources and extracted mineral over a 12-year period.

Table 1. Average sand points in balance resources of gravel and sand aggregate in the years 2007-2018 (Bilans zasobów…ed. Szuflicki et al. 2008-2019, Kozioł et al. 2018c, own calculation)

Description	Average SP in balance resources in years, %											
	2007	2008	2009	2010	2011	2012	2013	2014	2015	2016	2017	2018
Poland	**64.6**	**64.7**	**65.2**	**65.8**	**66.1**	**66.5**	**66.7**	**66.9**	**67.4**	**67.5**	**67.7**	**67.8**
northern zone	62.3	62.6	63.4	63.9	64.3	65.1	65.2	65.5	66.0	66.4	66.7	66.7
central zone	78.4	78.0	78.4	79.0	79.1	79.4	79.5	79.7	79.8	80.0	80.4	80.4
southern zone	58.6	58.8	59.1	59.6	59.9	59.9	60.1	60.2	60.7	60.5	60.3	60.4
Provinces												
Pomeranian	65.1	64.5	65.8	66.5	66.9	67.4	68.3	68.6	69.9	70.7	71.0	71.1
West Pomeranian	64.1	64.4	65.3	66.2	66.0	68.7	68.7	69.9	71.0	71.2	72.0	72.1

Table 1 and Figure 1 show that in 2018 the average sand point in the country in terms of balance resources was 67.8% and it increased by 5% over the period of 12 years. The resources in the southern zone have the lowest SP (60.4%), while in the central region the average SP is the highest and amounts to 80.4%. In the Pomeranian Province, the average SP increased within 12 years from 65.1 to 71.7%, i.e. by 10.9%. An even greater deterioration of aggregate grain size occurred in the West Pomeranian Province, i.e. by 11.2% (SP increased from 64.1 to 72.1%). In the economic resources in Poland in 2018, the average SP was higher in comparison with the balance resources – 70.6%, and – what is characteristic – it increased by as much as 11.5% within the 12-year period; thus, the average annual growth of SP in the economic resources was ca 1% (Fig. 2). In the Pomeranian Province, the average SP of economic resources increased by as much as 11.4% (up to 74,2%), while a slightly smaller increase was recorded in the West Pomeranian Province by 11.1% (up to 70.9%). From the point of view of exploitation, SP values in the exploited deposits are important (Table 1). In 2018, the average SP in exploited deposits reached 69.3% and increased by 3.9% within the 12-year period. The lowest SP was recorded in the southern zone (62.4% – increase by 4.2%) and the highest in the central zone (80.0%). In the Pomeranian Province, the average SP in the exploited deposits remained at the level of 2007 (69,5%); while in the years 2013-2014, it was at a much lower level – 66.0%. In the West Pomeranian Province, SP increased from 63.2 to 72,8%, or 15,2%.

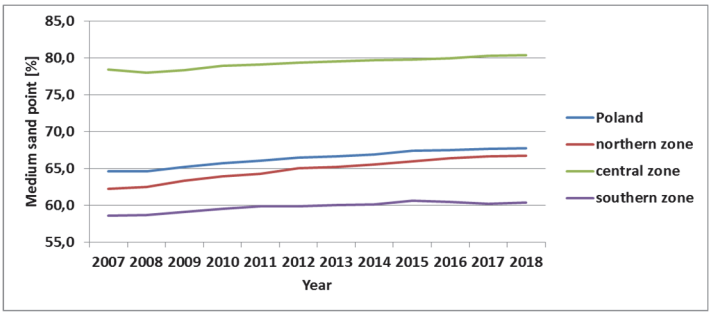

Fig. 1. Trends in the changes in average sand points of for balance resources in the years 2007-2018 (Bilans zasobów…ed. Szuflicki et al. 2008-2019, Kozioł et al. 2018c, own calculation)

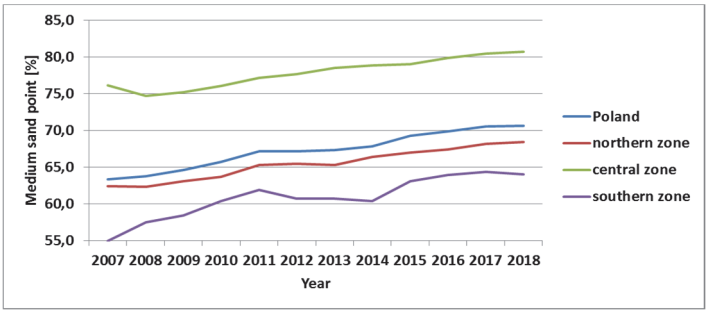

Fig. 2. Trends in the changes in average sand points of economic resources in the years 2007-2018 (Bilans zasobów…ed. Szuflicki et al. 2008-2019, Kozioł et al. 2018c, own calculation)

Table 2. Average sand points in resources extracted of gravel and sand aggregate in the years 2007-2018 (Bilans zasobów…ed. Szuflicki et al. 2008-2019, Kozioł et al. 2018c, own calculation)

Description	Average SP in resources extracted in years, %											
	2007	2008	2009	2010	2011	2012	2013	2014	2015	2016	2017	2018
Poland	**66,7**	**65,9**	**67,4**	**68,2**	**70,1**	**70,2**	**70,0**	**67,5**	**68,8**	**69,9**	**70,1**	**69,3**
northern zone	63,9	63,7	65,2	65,7	66,0	66,1	65,8	64,6	66,0	67,2	67,7	66,9
central zone	75,5	74,5	75,7	76,4	78,6	79,6	79,8	78,4	79,8	79,9	80,3	80,0
southern zone	59,9	59,9	61,5	62,1	64,5	64,5	63,2	61,9	63,2	65,1	63,5	62,4
Provinces												
Pomeranian	70,0	67,2	66,6	68,6	68,2	67,2	66,1	66,0	66,7	70,1	68,5	69,5
West Pomera-nian	63,2	64,3	65,7	65,4	65,5	67,0	67,9	66,4	66,2	67,7	74,0	72,8

5. An analysis of the production of sands extracted from exploited deposits

Having estimated the content of sands (0-2 mm) in the extracted mineral, an attempt was made to assess the amount of recovery (production) of this fraction in the extraction and treatment process. In some of the gravel and sand mining technologies applied, part of the fine fractions is already lost in the mining process. In particular, this applies to exploitation under the water surface, which is predominantly used in Poland (approx. 75% of gravel and sand extraction). Actually, only the use of suction dredgers enables the recovery of the majority of fine sand fractions from the extracted mineral, whereas when mining with single-bucket dredges (of grapple, scoop or scraper type) and multi-bucket dredgers (of ladder or chain type), the sand fractions are often melted directly in the post-extraction pit (Witt 2013). In Poland, depending on the mining technology, the demand (which is variable) and region, the recovery (production) of small fractions ranges from 60 to 80% of this fraction's content in the extracted mineral. In the aforementioned work (Kozioł et al. 2018c), the average recovery rate of 70% was assumed for a sample determination of the production volume of fine sand assortments in 2016 (Table 3). In 2016, when 173.2 million Mg of gravel and sand were mined, it was practically possible to obtain approx. 51.8 million Mg of gravel aggregates and 84.6 million Mg of sand assortments (0-2 mm); thus, the estimated total production of gravel and sand aggregates was probably approx. 136.4 million Mg, i.e. approx. 78.7 % of the annual production of gravel and sand according to *The Balance of Mineral Resources and Waters in Poland* (Bilans zasobów…ed. Szuflicki et al. 2008-2019, The Balance 2008-2018). The remaining part (21.3%) is made up of losses (useless fractions). Table 3 presents the results of calculations of production (recovery) of fine sand assortments (0-2 mm) in particular regional zones and in the Pomeranian and West Pomeranian Provinces.

Table 3. Production (recovery) sands and gravels in the year 2016 (Kozioł et al. 2018c, own calculation)

Description	Mining in 2016, thousand Mg	SP in resources, %	Fraction's share in the mineral, thousand Mg		Recovery of 0-2 mm fraction, million Mg
			0-2 mm	>2 mm	
Poland	173239	69.9	120764	51825	84.6
northern zone	72039	67.2	48410	23629	33.9
central zone	46596	79.9	37230	9366	26.1
southern zone	53954	65.1	35124	18830	24.6
Provinces:					
Pomeranian	17791	70.1	12471	5320	8.7
West Pomeranian	10633	67.7	7199	3434	5.0

In fact, the amount of recovery of small fractions varies, as part of the extracted mineral is used in the form of all-in aggregates (sand and gravel mixture) and sand with the admixture of gravel. The share of these fractions in the production and consumption of aggregates differs depending on the quality and size of resources and the variable demand on the part of the construction industry. A higher share of the consumption of all-in aggregates and sand results mainly from the implementation of road construction engineering works (mainly for road foundation) in some years and provinces. An example of such a period is the years 2011-2012, when approximately 50% of gravel and sand extraction was consumed by road construction in the form of raw sands (Kozioł & Galos 2013); also at present, an increase in demand for these aggregates can be observed.

6. Balance of production and demand for fine assortments of gravel and sand aggregates – an attempt at assessment

Fine assortments of gravel-sand and crushed-stone aggregates are used both in the construction industry as well as outside the construction industry in various branches of economy. Quantitatively, however, the basic demand concerns the construction industry, including primarily the production of concrete and concrete products (prefabricated elements, etc.) (Głodkowska 2018, Naziemiec 2013). The zone division of extraction and production of gravel and sands shows that the positive balance of sand production takes place mainly in the northern region (+19.4 million Mg), while the southern region (+3.2 million Mg) is in balance with the deficit observed in the central region (-3.0 million Mg). Relatively large positive balance of sand production is recorded in two provinces: Pomeranian (+5.3 million Mg) and West Pomeranian (+3.0 million Mg) (see table 4).

Summing up, it can be stated that, for example in 2016, from the production (recovery) balance and forecast consumption of fine sand fractions, almost 20 million Mg of these sands does not find domestic demand and in the majority of cases it is probably transported back to the post-extraction pits. The lack of periodic demand for such sands should be the basis for their classification as a by-product and their storage in separate storage sites.

Between 2017 and 2021 these figures probably are and will be smaller due to the good economic situation in the construction industry, both infrastructural (roads, railways) as well as volumetric, which will result in higher sand consumption, similarly as in the years 2010-2012.

Table 4. Estimation of production and consumption balance of fine gravel and sand aggregate assortments in 2016 (Kozioł et al. 2018c, own calculation)

Description	Extraction in 2016, thousand Mg	Fraction's share in the mineral, thousand Mg		Recovery of 0-2 mm fraction, million Mg	Predicted consumption for concrete	Other consumption	Balance (recovery - consumption)
		0–2 mm	>2 mm		million Mg	million Mg	million Mg
Poland	173239	120764	51825	84.6	29.0	36.0	19.6
northern zone	72039	48410	23629	33.9	6.5	8.0	19.4
central zone	46596	37230	9366	26.1	13.0	16.1	- 3.0
southern zone	53954	35124	18830	24.6	9.5	11.9	3.2
Provinces:							
Pomeranian	17791	12471	5320	8.7	1.5	1.9	5.3
West Pomeranian	10633	7199	3434	5.0	0.9	1.1	3.0

7. Final conclusions

1. The above analysis the databases of gravel and sand deposits shows that with the development of documented resources, the share of resources classified as sands increases. A particularly large increase in sand fractions occurs in the industrial resources in the years 2007-2018, i.e. from 25.7% to 45.7%.
2. A measurable indicator of deterioration in resource quality is the trend of changes in the average sand point (SP) of natural aggregates in (percentage fine fraction content 0-2 mm) in documented resources of deposits. In 2018, the average sand point in the documented balance resources was 67.8% and it increased by 5% over the period of 12 years (2007-2018). The lowest SP was recorded in resources in the southern region (zone) (60.4%), including two provinces: Małopolskie (50.4%) and Opolskie (58.1%). In the central region, the average SP reaches 80,4%, including 84.2% in the Lubelskie Voivodeship and 83.1% in the Świętokrzyskie Voivodeship.
3. In the economic resources in Poland in 2018, the average SP was higher in comparison with the balance resources, namely 70.6%, and – what is characteristic – it increased by as much as 11.5% during the period of 12 years, i.e. the average annual growth of SP in industrial resources is ca 1%. The highest growth was recorded in the southern region (by 16.4%); thus, the region with the best deposits in terms of quality (grain size) experiences the fastest deterioration.
4. The average PP values in exploited deposits are lower similar in the compared to the value in economic resources (national average 69.3%), which means that deposits with a more favourable granulation are exploited.

5. After the sand content in the extracted mineral was estimated, an attempt was made to assess the amount of recovery (production) of this fraction in the extraction and treatment processes. Estimated calculations show that in 2016, when approximately 173.2 million Mg of gravel and sand were mined, it was actually possible to obtain approximately 51.8 million Mg of gravel aggregates and 84.6 million Mg of sand assortments (0-2 mm); thus, the estimated total production of gravel and sand aggregates probably amounted to approx. 136.4 million Mg, i.e. about 78.7% of the annual production of gravel and sand according. The remaining part (21.3%) represents losses (useless fractions).
6. The zone division of extraction and production of gravel and sands shows that the positive balance of sand production occurs mainly in the northern region (+19.4 million Mg), while the southern region (+3.2 million Mg) is in balance with the deficit in the central region (-3.0 million Mg). Relatively large positive balance of sand production is recorded in two provinces: Pomeranian (+5.3 million Mg) and West Pomeranian (+3.0 million Mg).
7. The volume of fine fractions recovery is changeable because part of the extracted sand and gravel mineral is used in the form of all-in aggregates (sand and gravel mixture) and sand with admixture of gravel. The share of these fractions in the production and consumption of aggregates differs depending on the quality and volume of resources and the alternating demand on the part of the construction industry. A higher share in the consumption of all-in aggregates and sand in some years and provinces results chiefly from the implementation of road infrastructure engineering works (mainly for road foundation). An example of such a period are the years 2011-2012, when approximately 50% of gravel and sand extraction in the form of raw sands was consumed by road construction, and there has also been an increase in demand for sands due to the good economic situation in road infrastructure and volumetric construction.
8. Deterioration of the quality of the raw material base and, at the same time, the increase in the building industry demand for thick aggregate fractions (5/8, 8/11, etc.) contribute to an increase in the extraction of gravel and sand aggregates with a simultaneous increase in the production of fine, hardly marketable assortments of aggregates. The lack of periodic demand for such sands should be the basis for their classification as a by-product and their storage in separate storage sites.
9. In the future, the presented research results should contribute to the development of more accurate market forecasts regarding the demand for and production of natural aggregates in Poland and in individual regions, including especially gravel and sand aggregates.

References

Bilanse zasobów kopalin i wód podziemnych w Polsce z lat 2008-2019 (The Balance of Mineral Resources and Waters in Poland ed. Szuflicki et al.). PIG – PIB, Warszawa, 2008-2019.

Głodkowska, W. (2018). Fibrokompozyt drobnokruszywowy – modele opisu właściwości i zastosowanie (Waste Sand Fiber Composite – Models of Description of Properties and Application). *Rocznik Ochrona Środowiska, 20*(3).

Kiewlicz, R. (2019). Jedyna taka firma w Polsce. Wydobywa kruszywo z dna Bałtyku. (The Only Such Company in Poland. Extraction of aggregate from the bottom of the Baltic Sea), https://biznes.trojmiasto.pl/Jedyna-taka-firma-w-Polsce-wydoby-wa-kruszywo-z-dna-Baltyku-n130732.html (access on April 20, 2019)

Kozioł, W., Baic, I. (2018). Kruszywa naturalne w Polsce – aktualny stan i przyszłość (Natural Aggregates in Poland. Current Condition and Future Prospects). *Przegląd Górniczy SIiTG Katowice*, 1-8.

Kozioł, W., Baic, I. (2018). Górnictwo skalne w Polsce szanse i zagrożenia (Rock Mining in Poland. Opportunities and Threats). *Inżynieria Mineralna 2*(42), 65-72.

Kozioł, W., Baic, I. Ciepliński, A. (2018). Kruszywa żwirowo-piaskowe. Tendencje zmian jakości zasobów (Gravel and Sand Aggregates. Trends in Resource Quality). *Kruszywa Mineralne, 2,* 69-84. Wydział Geoinżynierii, Górnictwa i Geologii Politechniki Wrocławskiej. Wrocław.

Kozioł, W., Baic, I., Góralczyk, S., Borcz, A. (2017). Środowiskowe aspekty eksploatacji kruszyw żwirowo-piaskowych spod wody w Polsce (Environmental Aspects of Sand and Gravel Aggregates Exploitation from under the Water in Poland). *Rocznik Ochrona Środowiska, 19,* 731-744.

Kozioł, W., Baic, I. Stankiewicz, J. (2018). Wydobycie i produkcja drobnych frakcji kruszyw naturalnych oraz technologie ich zagospodarowania. (Extraction and Production of Fine Fractions of Natural Aggregates and Technologies of Their Management). *Monografia IMBiGS, Warszawa, 212*.

Kozioł, W., Ciepliński, A., Goleniewska, J., Machniak, Ł. (2011). Eksploatacja kruszyw z obszarów morskich w Polsce i Unii Europejskiej (Aggregates exploitation of sea areas in Poland and UE). Górnictwo i Geoinżynieria, *Kwartalnik AGH, 35*(4/1), 215-232.

Kozioł, W., Galos, K. (2013). Scenariusze zapotrzebowania na kruszywo naturalne w Polsce i w poszczególnych jej regionach (Scenarios of Demand for Natural Aggregate in Poland and Its Regions). *Wyd. Poltegor-Instytut, Kraków-Wrocław, 206*.

Naziemiec, Z. (2013). Odzysk i zastosowanie piasków drobnych (Recovery and Application of Fine Sands). *Surowce i Maszyny Budowlane, BMP Racibórz, 1*, 72-77.

Ney, R. (red.) (2007). *Surowce mineralne Polski. Surowce skalne – Kruszywa mineralne (Mineral Resources of Poland. Raw Rock Materials – Mineral Aggregates)*. Instytut Gospodarki Surowcami Mineralnymi i Energią PAN, Kraków.

Radwanek-Bąk, B., Miśkiewicz, W., Bąk, B. (2018). Piasek piaskowi nie równy (Each Sand Is Different). *Kruszywa: produkcja – transport – zastosowanie, 1*, 32-37.

Witt, A.(red.) Schmidt, T., Pomorski, A. (2013). *Eksploatacja krajowych złóż piasków I żwirów spod lustra wody z uwzględnieniem wprowadzenia nowych rozwiązań*

technologicznych (Underwater Exploitation of Domestic Sands and Gravel Deposits with Introduction of New Technological Solutions). Poltegor – Instytut Wrocław.

Abstract

The gradual deterioration in the quality of raw material base of natural aggregates combined with the simultaneous increase in the demand of the construction industry for the best quality coarse fractions with grain sizes of 5-8 mm, 8-11 mm, etc., has a major impact on the growing volume of hard to sell and non-transferable (waste) fractions of aggregates produced in Poland. This applies especially to gravel and sand aggregates since in their resources the share of very fine fractions (below 2 mm) is systematically increasing, while the demand for such fractions in construction is limited and they are often treated as useless (waste) material. Problems with selling fine (waste) sands can be observed, among others, in the north-western region of the country. Since it is practically unknown what the volume of mining, production and consumption of these aggregates is, an attempt was made to assess the quantity of extracted and produced sand fractions of aggregates on a national and regional scale (provinces, regional zones). What constitutes a measurable indicator of the deterioration in the quality of resources is the tendency towards change in the average sand point (the percentage content of fine fraction of 0-2 mm) in the documented resources. For example in 2018, the average sand point in the balance resources was 67.8% and it increased by 5% over the period of 12 years (2007-2018). In the economic resources in Poland in 2018, the average SP was higher in comparison with the balance resources, namely 70.6%, and – what is characteristic – it increased by as much as 11.5% during the period of 12 years, i.e. the average annual growth of SP in industrial resources is ca. 1%. The highest growth was recorded in the southern region (by 16.4%); thus, the region with the best deposits in terms of quality (grain size) experiences the fastest deterioration. Estimated calculations show that in 2016, it was actually possible to obtain approximately 51.8 million Mg of gravel aggregates and 84.6 million Mg of sand assortments (0-2 mm); thus, the estimated total production of gravel and sand aggregates probably amounted to approx. 136.4 million Mg, i.e. about 78.7% of the annual production of gravel and sand according to PGI. The remaining part (21.3%) represents losses (useless fractions). The zone division of extraction and production of gravel and sands shows that the positive balance of sand production occurs mainly in the northern region (+19.4 million Mg), while the southern region (+3.2 million Mg) is in balance with the deficit in the central region (-3.0 million Mg). Relatively large positive balance of sand production is recorded in two provinces: Pomeranian (+5.3 million Mg) and West Pomeranian (+3.0 million Mg). The lack of periodic demand for such sands should be the basis for their classification as a by-product and their storage in separate storage sites. The analysis and calculations should contribute to the development of more accurate market forecasts of demand for and production of natural aggregates, especially of gravel and sand, both in Poland and in individual regions.

Keywords:
rock raw minerals, gravel and sand aggregates, gravel and sand extraction

Wydobycie, produkcja i zagospodarowanie drobnych frakcji kruszyw żwirowo-piaskowych w Polsce północno-zachodniej

Streszczenie

Stopniowe pogarszanie się jakości bazy surowcowej kruszyw naturalnych i równocześnie wzrost zapotrzebowania budownictwa na najlepsze jakościowo grube frakcje o uziarnieniu 5-8 mm, 8-11 mm, itd., ma duży wpływ na wzrost frakcji trudno zbywalnych i niezbywalnych (odpadowych) produkowanych w kraju kruszyw. Dotyczy to szczególnie kruszyw żwirowo – piaskowych w zasobach których systematycznie wzrasta udział frakcji drobnych (poniżej 2 mm), na które jest ograniczone zapotrzebowanie budownictwa i często traktowane są jako materiał nieużyteczny (odpadowy). Problemy ze zbyciem drobnych (odpadowych) piasków występują miedzy innymi w regionie północno-zachodnim kraju. Ponieważ praktycznie nie wiadomo jakie jest wydobycie, produkcja i zużycie tych kruszyw podjęto próbę oceny w skali kraju i poszczególnych regionów (województw, stref regionalnych) ilości wydobywanych i produkowanych frakcji piaskowych kruszyw. Wymiernym wskaźnikiem pogarszania się jakości zasobów kruszyw jest tendencja zmian średniego punktu piaskowego (procentowa zawartość frakcji drobnej 0-2 mm) w udokumentowanych zasobach. Przykładowo w 2018 r. w zasobach bilansowych średni punkt piaskowy wyniósł 67,8% i w ciągu 12 lat (2007-2018) wzrósł o 5%. W zasobach przemysłowych w kraju w 2018 r. średni PP był wyższy w porównaniu do zasobów bilansowych – 70,6% i co charakterystyczne w ciągu 12 lat wzrósł aż o 11,5%, czyli średnioroczny wzrost PP w zasobach przemysłowych wynosi ok. 1%. Najwyższy wzrost odnotowano w regionie południowym (o 16,4%), czyli w regionie mającym pod względem jakości (uziarnienia) najlepsze złoża, następuje najszybsze ich pogorszenie. Z przeprowadzonych szacunkowych obliczeń wynika, że w 2016 roku praktycznie możliwe było do uzyskania ok. 51,8 mln Mg kruszyw żwirowych i 84,6 mln Mg asortymentów piaskowych (0-2 mm), czyli szacowana łączna produkcja kruszyw żwirowo-piaskowych prawdopodobnie wyniosła ok. 136,4 mln Mg to jest ok.78,7% rocznego wydobycia wg PIG żwirów i piasków. Pozostałą część (21,3%) stanowiły straty (frakcje nie użyteczne). Z podziału strefowego wydobycia i produkcji żwirów i piasków wynika, że dodatnie saldo produkcji piasków ma głownie region północny (+19,4 mln Mg), zaś region południowy (+3,2 mln Mg) bilansuje się z deficytowym regionem środkowym (-3,0 mln Mg). Stosunkowo duże saldo dodatnie produkcji piasków mają województwa pomorskie (+5,3 mln Mg) i zachodniopomorskie (+3,0 mln Mg). Brak okresowego zapotrzebowania na tego typu piaski powinien być podstawą do ich uznania jako produkt uboczny i ich składowania na oddzielnych składowiskach. Analiza i obliczenia powinny się przyczynić do opracowania dokładniejszych prognoz rynkowych zapotrzebowania i produkcji w Polsce i w poszczególnych regionach kruszyw naturalnych w tym szczególnie kruszyw żwirowo-piaskowych.

Słowa kluczowe:
surowce skalne, kruszywa żwirowo-piaskowe, wydobycie żwirów i piasków

MIDDLE POMERANIAN SCIENTIFIC SOCIETY OF THE ENVIRONMENT PROTECTION

Rocznik Ochrona Środowiska

Volume 22. Year 2020 ISSN 1506-218X 256-264

Experimental Research of Temperature Distribution on the Surface of the Front Plate, of a Flat Plate Heat Exchanger

Magdalena Orłowska

Koszalin University of Technology, Poland

corresponding author's e-mail: magdalena.orlowska@tu.koszalin.pl

1. Introduction

Convective research, both experimental and numerical, arouses considerable interest among scientists. It is necessary to carry out tests of heating systems and devices with new constructions in construction: multi-storey buildings, glass walls, ventilation and air-conditioning ducts. During operation, operational problems arise, e.g. horizontal unevenness of the temperature (large office room dimensions, multi-use, new wall constructions, humidity problems, etc. Therefore, new research on these issues is needed. Particularly valuable are works that help support the intensity of natural convection.

In the work (Kalendar et al. 2019, Kalendar et al. 2016) the influence of the complexity of surface shapes on the convective heat exchange process was investigated. The scientific article concerned hexagonal and octagonal isothermal polygons of various shape proportions. Differences in temperature cause differences in fluid density and buoyancy force depends on them, other fluid properties are assumed to be constant. A numerical solution was obtained for the full three-dimensional form of the ruling equations, while these equations were written in a dimensionless form. The influence of Pr and Ra number in the examined range and their influence on Nusselt number were shown. Empirical correlation equations for the average speed in the studied area were obtained.

The study (Han-TawChen et al. 2016) investigated free convection on various models from the obtained experimental data, which was introduced into the three-dimensional computing package. Fluid flows in single-tube vertical plate heat exchangers with fins and tubes were investigated for different fin spacing values and tube diameters. On the basis of the obtained calculations, correlations between the Nusselt number and the Rayleigh number were created.

On the subject of convection, apart from experimental or numerical works, there are also works of an analytical nature. An example of this is the work (Schaub et al. 2019) where the obtained calculation procedure allows to predict heat transfer by unstable natural convection. Earlier studies collected data on laminar, transient and turbulent flow, the Grashoff number for a surface with a constant temperature in a given range, or a constant heat flux in a given range. The physical model assumes a variable proportion of the potential and kinetic energy of fluid molecules for the unstable case.

Earlier research on identifying issues was conducted in an experimental but also numerical way. Experimental research of this work concerns checking the temperature distribution on the front panel of a flat plate heat exchanger. Panels are a very popular type of heaters used in our home. First of all, simple construction, light construction, low thermal inertia, moderate cost, the ability to choose the color, a wide range of sizes determine their choice.

The article is a continuation of the author's research on the convective heat exchange with radiators (Orłowska & Czapp 2012, Orłowska 2019, Orłowska et al. 2019).

2. Research methodology

The theoretical description of the phenomenon boundary layer of heat exchange during free convection with a vertical plate, omitting the pressure drop along the plate, includes equations: continuity, motion and energy. The equations indicate that in free convection, the velocity values depend on the temperature field and do not fall under the uniqueness conditions. If so, the Reynolds number is part of the Grashof number

$$Gr = \frac{\beta g l^3}{v^2} \Delta T \tag{1}$$

where:
β – coefficient of fluid volume expansion,
g – gravitational acceleration,
v – velocity component in the direction of y,
l – linear dimension,
ΔT – temperature difference.

The radiator chosen for experimental research is: Purmo Plan Ventil Compact M, FCVM, dimension: height 90 cm, width 100 cm, thickness 10 cm, type 22, power 2301 W PN-EN 442-2 for parameters 75/65/20°C, middle and bottom connection, maximum working pressure 10 bar, color – white, weight

58.8 kg, Water temperature in the storage tank: 45°C, Installation water flow rate: 180, 280, 380 l/h, System water pressure: Pump gear: third.

The radiator is made of deep-pressed DC01 cold-rolled low-carbon steel sheet in accordance with PN-EN 10130 (https://www.purmo.com/pl/produkty/grzejniki-plytowe/purmo-plan-ventil-compact-m.htm).

The research stand Fig. 1 is located at the Koszalin University of Technology, the Faculty of Civil Engineering, Environmental and Geodetic Studies, in the Department of Building Networks and Installations.

Fig. 1. Testing stand (own photo)

The front panel of the radiator is divided into 12 elements with dimensions of 25x30 cm – Fig. 2. The individual fields in the upper, middle and lower parts of the hob have been given the numbering – Fig. 3. From the side of the wall, the radiator is insulated, only the end surface of the heat exchanger was dealt with by examining heat exchange to the environment.

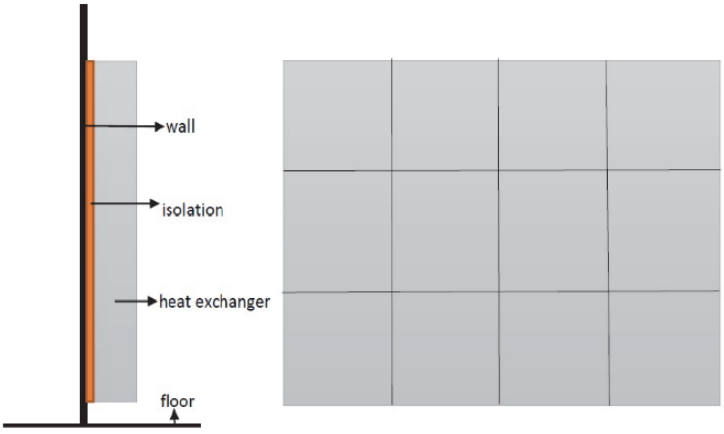

Fig. 2. Heat exchanger – testing stand (side view and front view of heat plate)

1	2	3	4	HIGH PART
5	6	7	8	MIDDLE PART
9	10	11	12	LOW PART

Fig. 3. Division of the plate into measuring elements

In each of the 12 designated fields, the temperature was measured with a FLIR E6 wifi infrared camera. The camera gives the possibility of spot measurement and has the function of multi-spectral imaging. It is possible to apply thermal and digital photos. Thanks to this, the measurement is more precise and the analyzed object is examined more accurately (https://www.conrad.pl/p/kamera-termowizyjna-flir-e6-wifi-20-do-250-c-160-x-120-px-9-hz-1545476). Specifications of camera: „IR resolution 160×120 pixels, Thermal sensitivity/NETD <0.06°C (0.11°F) / <60 mK, Field of view (FOV) 45×34°, Minimum focus distance 0.5 m (1.6 ft.), Image frequency 9 Hz, Detector type: Uncooled microbolometer, Object temperature range -20°C to +250°C (-4°F to +482°F), Accuracy ±2°C (±3.6°F) or ±2% of reading, for ambient temperature 10°C to 35°C (+50°F to 95°F) and object temperature above +0°C (+32°F), Emissivity table of predefined materials/variable from 0.1 to 1.0" (https://www.atel.com.pl/doc/03084_DS.pdf). The emissivity of the tested object, based on the manufacturer's data. Possible reflection of radiation from surrounding objects due to the glossy surface radiator were not included.

3. The results of experimental analyzes

The graphs in the figures 4-7 show the temperature fields of the flat heat exchanger heating plate, which have a huge impact on the process of free convection. Measurements were made in several measurement series. The flow rate of the medium was changed Q = 380 l/h, Q = 280 l/h, Q = 180 l/h. The results of experminatal analyzes were given by Fig. 4-7.

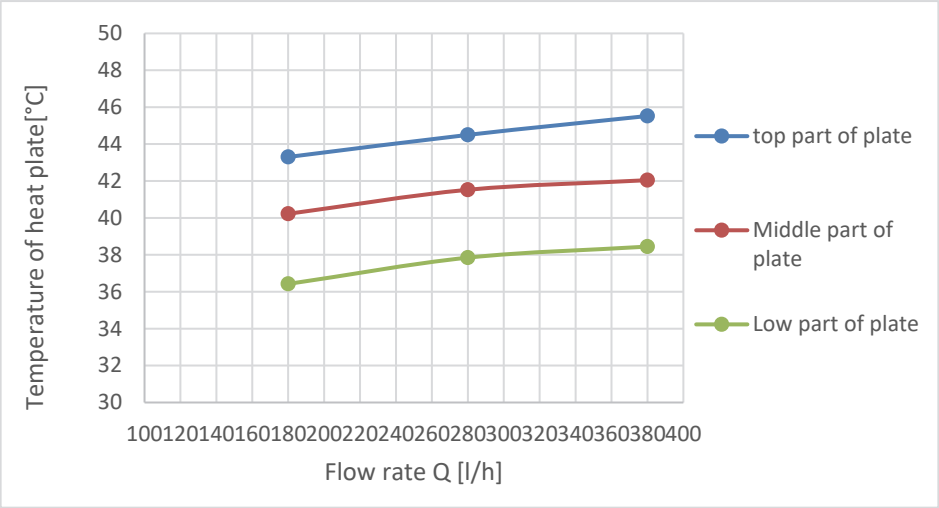

Fig. 4. The fields of temperatures a heating plate temperature T [°C] as a function of flow rate Q [l/h] depending on the height od heat plate (top, middle, bottom)

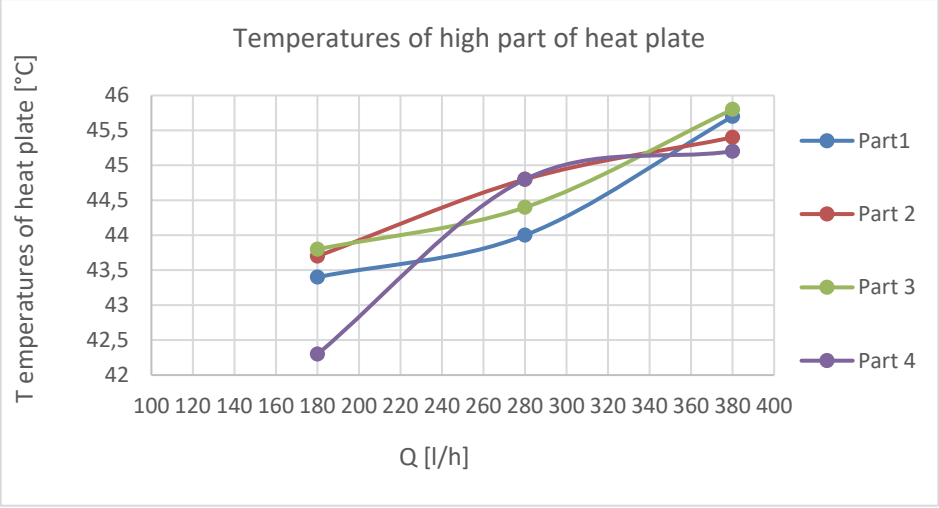

Fig. 5. The fields of temperatures at the high of the heat plate T [°C] in individual elements of the plate (legend) as a function of flow rate Q [l/h]

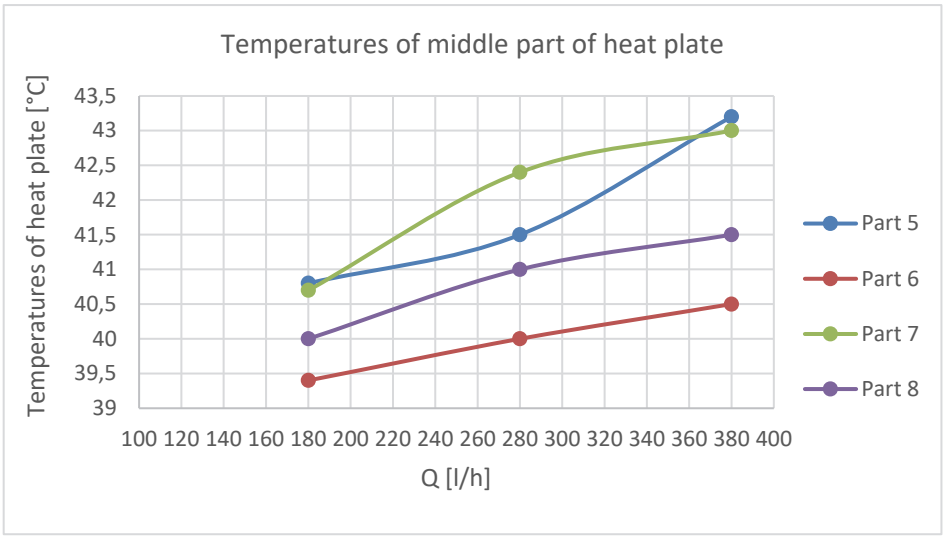

Fig. 6. The fields of temperatures at the middle of the heat plate T [°C] in individual elements of the plate (legend) as a function of flow rate Q [l/h]

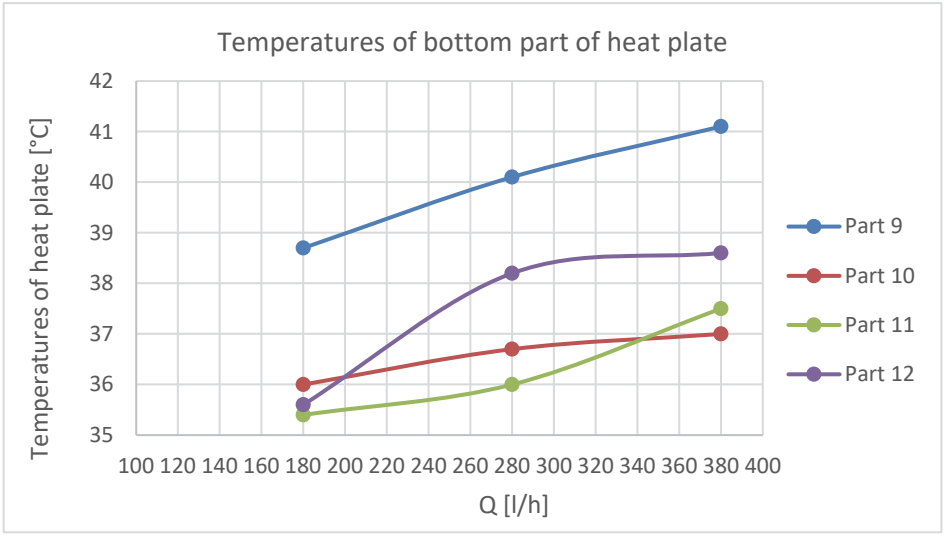

Fig. 7. The fields of temperatures at the bottom of the heat plate T [°C] in individual elements of the plate (legend) as a function of flow rate Q [l/h]

An example view of the heating plate from a thermal imaging camera is given by Fig. 8. The figure shows a pictorial photo of how the temperature fields are shaped. The video camera uses colors to determine the temperature scales. The use of the camera is simple and very convenient.

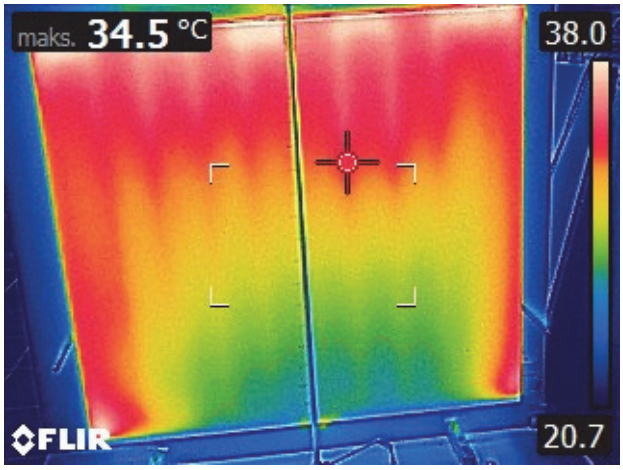

Fig. 8. An example view of the heating plate from a thermal imaging camera

4. Discussion of results, conclusions

The conducted experiment shows that the upper part of the exchanger's hob (fields marked with numbers 1,2,3,4) has the highest temperature, its average is 42°C, slightly lower value of the central part (fields 5,6,7,8) with an average temperature of 41.29°C and the lowest temperature was recorded in the lower part of the plate (fields numbered 9,10,11,12), the average temperature was 39.98°C. The surface, despite the approximate three given average temperature values in each of the tested heights (upper, middle and lower) of the heating plate is not isothermal. Despite the set flow conditions for the three tested different flow rates, the situation is analogous. The way the heater is connected can affect the temperature distribution. In this case, the connection was bottom, middle. The water in the tank is heated by a heater located in the storage heater. During the measurements, the value was observed, but even slight fluctuations certainly affect the result. In addition, the distance between the thermal imaging camera and the hob also plays a role. It was ensured that the measurement was spot-on, it is possible after the correct calibration of the device. The average room temperature, the temperature of other heaters in the room, the air temperature outside the room, additional air vents controlled by the building's air conditioning are also factors that affect the measurements. The work can be related to room heaters which are

very popular heat exchangers in our homes. It turns out that many factors influence the proper operation of the heater in the room. Different temperature of the front surface of the radiator does not always mean there is air in the radiator. Temperature differences on the examined surface indicate the intensity of heat transfer, and thus the efficiency along the path of the water stream in the radiator.

References

Han-TawChen, Yung-ShiangLin, et al. (2016). Numerical and experimental study of natural convection heat transfer characteristics for vertical plate fin and tube heat exchangers with various tube diameters. *International Journal of Heat and Mass Transfer, 100*, 320-331.

Kalendar, A., Kalendar, Ab., et al. (2019). Natural Convective Heat Transfer from Horizontal Isothermal Surface of Polygons of Octagonal and Hexagonal Shapes. *Journal of Thermal Science and Engineering Applications, 11*(5), 1.

Kalendar, Ab., Karar S. et al. (2016). Correlations for Natural Convective Heat Transfer from Isothermal Surface of Octagonal and Hexagonal Shapes of Different Aspect Ratios. *Heat Transfer-Asian Research (Heat Tran Asian Res), 46*(4).

Orłowska, M., Czapp, M. (2012). Analiza numeryczna wydajności cieplnej konwekcyjnego wymiennika ciepła obudowanego poziomymi płytami. *Rocznik Ochrona Środowiska, 14*, 582-586.

Orłowska, M. (2019). Laboratory stand for flow and energetic experimental research vertical heaters with free convection and the possibility of intensification, *Contemporary Issues of Heat and Mass Transfer,* 417-428.

Orłowska, M., Szkarowski, A., Mamedov, Sh. (2019). Numerical analysis of the influence of the angle of inclination of the screen on the intensity of heat exchange from a flat heat exchanger in a partially limited space. *Rocznik Ochrona Środowiska, 21*, 728-737.

Schaub, M., Kriegel, M. et al. (2019). Analytical prediction of heat transfer by unsteady natural convection at vertical flat plates in air. *International Journal of Heat and Mass Transfer, 144.*

PN-EN 10130:2009, Wyroby płaskie walcowane na zimno ze stali niskowęglowych do obróbki plastycznej na zimno – Warunki techniczne dostawy.

https://www.conrad.pl/p/kamera-termowizyjna-flir-e6-wifi-20-do-250-c-160-x-120-px-9-hz-1545476

https://www.purmo.com/pl/produkty/grzejniki-plytowe/purmo-plan-ventil-compact-m.htm

https://www.atel.com.pl/doc/03084_DS.pdf

Abstract

The purpose of the work was to perform experimental tests on a plate heat exchanger. For this purpose, a laboratory test stand located in the hall of the Koszalin University of Technology was used. The experiment concerned checking the isothermal face of a flat panel radiator. Temperature distributions were checked at three board heights and in twelve finite elements. Temperature distribution fields were obtained depending on the flow rates tested.

Keywords:
radiator, temperature, convection, isothermal

Badania eksperymentalne rozkładu temperatury na powierzchni płyty czołowej płaskiego, płytowego wymiennika ciepła

Streszczenie

Celem pracy było wykonanie badań eksperymentalnych na płytowym wymienniku ciepła. W tym celu wykorzystano laboratoryjne stanowisko badawcze zlokalizowane w sali Politechniki Koszalińskiej. Eksperyment dotyczył sprawdzenia izotermicznej powierzchni płaskiego grzejnika płytowego. Rozkłady temperatury sprawdzono na trzech wysokościach płyty i w dwunastu elementach skończonych. W zależności od badanych natężeń przepływu uzyskano pola rozkładu temperatury.

Słowa kluczowe:
grzejnik, temperatura, konwekcja, izotermiczność

MIDDLE POMERANIAN SCIENTIFIC SOCIETY OF THE ENVIRONMENT PROTECTION

Rocznik Ochrona Środowiska

Volume 22. Year 2020 ISSN 1506-218X 265-280

Financial Inclinations of Visitors to the Wielkopolska National Park

Adam Zydroń[*]*, Dariusz Kayzer, Michał Fiedler, Mariusz Korytowski*

The Poznań University of Life Sciences, Poland

[*]*corresponding author's e-mail: adzyd@up.poznan.pl*

1. Introduction

Forest ecosystems serve a multitude of functions, among which an increasingly important role is being played by their social function. For many years forests have been associated with tourism and recreation, as a result of which demand for advanced methods to measure the value of non-productive functions of forests has been growing (Courtney & Hill 2006). The value of the natural environment is difficult to determine. In the case of forested areas valuation may not be limited to the economic value of the forest or other elements of material value. Ground-breaking concepts for the appraisal of the natural environment were presented in the 1940's (Hotelling 1949) and they were based on the willingness to pay for an opportunity to visit a specific location. The contingent valuation method provides a personal estimation of changes in the quality of the environment based on the conventional welfare theory (Scarpa et al. 2000). Using this method monetary values may be (Kahneman & Knetsch 1992, Arrow et al. 1993, Carson 1997). The contingent valuation has been applied not only in nature conservation (Mueller 2014), but also in other areas, e.g. medicine (Willan et al. 2001, O'Brien et al. 2002). This method has been used e.g. to appraise the value of the the Białowieża Forest (Giergiczny 2009). ascribed to the natural environment, because social attitudes may be to a certain extent systematised and thus methods commonly applied in economics may be used.

The contingent valuation method in the appraisal of non-market benefits derived from the environment has been applied on a mass scale within the last few decades (Mitchell & Carson 1989, Kahneman et al. 1992).

The contingent valuation method providing information on Willingness to Pay (WTP) and Willingness to Accept (WTA) was used in this study to determine the sense of nature value for a landscape dominated by forests within the boundaries of a national park in central Poland. The aim of this study was to identify financial inclinations based on the WTP and WTA approach among visitors to the Wielkopolska National Park.

2. Study area

The Wielkopolska National Park was established based on the ordinance of the Council of Ministers of 16 April 1957 with the boundaries comprising an area of 9600 ha, of which approx. 5100 ha are directly administered by the Park. In 1996 a new resolution of the Council of Ministers concerning WNP changed its area to 7584 ha and created the protection zone around the Park, which joint area together with the Park itself is 14 840 ha. The municipal areas of Puszczykowo, Mosina and Stęszew were excluded from the Park. The Wielkopolska National Park is situated approx. 15 km south of the city of Poznań and it has convenient bus and railway connections with the city (the Poznań-Wrocław line), while through Poznań, thanks to numerous fast trains, it is well connected with Warszawa (www.wielkopolskipn.pl accessed 02.02.2020). Localization of WPN near Poznan makes this park similar in character to the Kampinos National Park localized near Warsaw, so both parks serve as if they were city parks. The Park was established to protect the relief formed by the action of the Scandinavian ice-sheet as well as diverse plant communities and many animal species (Fig. 1). (Wyczyńscy 2006). The structure of revenues to the budgets of national parks is dominated by external sources in the form of subsidies from the state budget and funds obtained from various organizations and support funds (EU funds, Forest Fund, NFOŚiGW, WFOŚiGW). Whereas, in WPN in the year 2016, the touristic access generated revenues more than twenty times lower than the costs.

3. Methods

This study was based on a set of data provided by a questionnaire survey conducted in the Wielkopolska National Park, in the communes in its vicinity, as well as on-line. Only questionnaires filled in by individuals who actually visited the Park were used in this study. A total of 1450 questionnaires were collected and they were subsequently used as a source of information to determine the social value of the park (for this reason only the questionnaires, in which the respondents declared they visited the Park, were included in the analyses (1332 questionnaires). The sociological characteristics of the respondents are presented in Table 1.

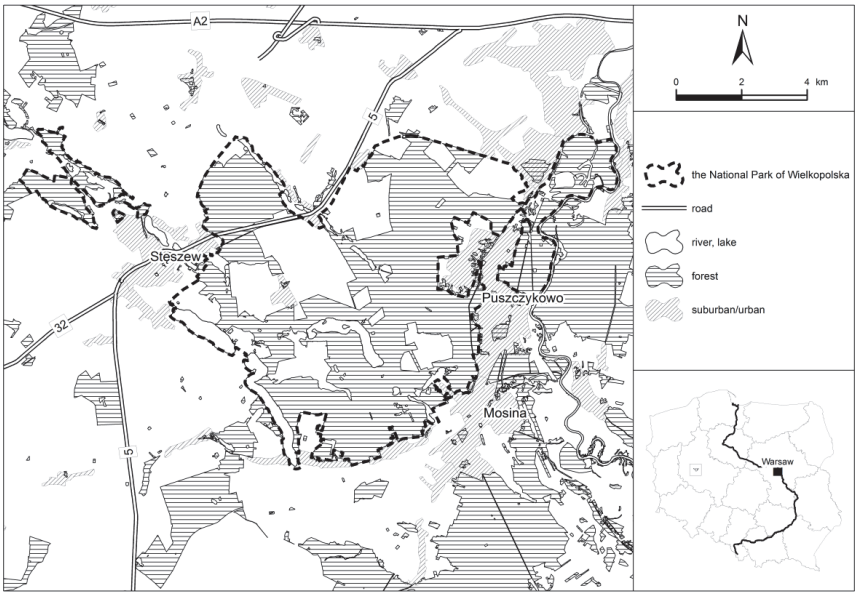

Fig. 1. Location of the study area - the Wielkopolska National Park
Source: the Wielkopolska National Park 2020

Table 1. Sociological characteristics of respondents

Sociological trait	Category of sociological trait	Percentage share in %
Sex	Female	61.0
	Male	39.0
Age	below 18 years	15.1
	18-25 years	37.1
	26-40 years	23.1
	41-60 years	20.1
	over 60 years	4.6
Monthly net income per person	Max. 100 zł	0.6
	From 100 to 200 zł	2.0
	From 200 to 500 zł	9.0
	From 500 to 1000 zł	26.1
	From 1000 to 2 500 zł	43.4
	Over 2 500 zł	18.9

Table 1. cont.

Sociological trait	Category of sociological trait	Percentage share in %
Education	elementary	15.8
	Vocational	5.6
	Secondary	41.8
	higher	36.8
Profession	Student	38.5
	Office worker	16.6
	Manual worker	5.1
	Scientific worker	5.3
	Services and retail	8.0
	Farmer	2.0
	Forester	1.0
	Business owner	6.5
	Schoolchild	8.4
	Professional	4.4
	Unemployed/not in employment	4.4

The questionnaire was preceded by an introduction, which briefly presented the history and characteristics of the park. It contained information concerning the purpose of the questionnaire, i.e. estimation of the social value of the natural environment in the Wielkopolska National Park in terms of benefits related to leisure and recreation. It was stressed in the Introduction that the questionnaire was conducted by employees of the Poznań University of Life Sciences and it is anonymous, while its results would be used only for scientific purposes.

The second part of the questionnaire was composed of 27 closed and open questions, which referred to the preferences and frequency of visits to the park by respondents. The aim of this part of the questionnaire was to determine the propensity of the respondents to transfer a certain amount of money to the visited location, or in the case of a lack of a response or a negative attitude to incurring costs for environmental protection – to identify the cause for such a declaration. The aim of the questions was also to estimate the amount of money which would be accepted by the Park users as compensation for the prohibition to enter the Park or the amount they would donate for the use of the park. The questionnaire was completed with questions concerning socio-economic aspects and referring

to e.g. the age and sex of respondents, place of residence, approximate net income per person, education and professional situation, attitude to paying fees for environmental protection, membership in environmental organisations and evaluation of sincerity of their responses.

The questionnaire survey was conducted in the period from 1 January to 31 December 2012. In order to prevent collection of data only from individuals regularly using the Park services, which would lead to excessive narrowing of the subject of the study, the process of data acquisition was carried out in three ways. The highest number of questionnaires were left in public buildings and in the seat of the WNP to be filled by residents of the communes located in the vicinity or within the Park boundaries. Next following the assumptions of the classical environment valuation model face-to-face interviews were conducted directly in the park. The last method of data collection for analyses was to provide an interactive on-line questionnaire. Such a data acquisition process was performed on the national scale and the primary aim was to verify the value of the Wielkopolska National Park to individuals who had never visited it.

Data collected through the questionnaire survey were collected and entered in the Excel programme by Microsoft Office. Applying the zero-one system the obtained responses were ascribed the following values in the Table 2: 1 – when the respondent provided an answer, 0 – in the case of no answer given, in the case of open questions – the response in the numerical or text form (Fig. 2).

In order to establish the value of the Wielkopolska National Park two approaches were adopted to economic valuation of non-market goods. The contingent valuation method is based on the determination of the value of goods based on the identified values of Willingness to Pay (WTP) and Willingness to Accept (WTA). The WTP value specifies the maximum amount which respondents are able to pay in exchange for the possibility to use a given good or for its existence. In turn, WTA is based on the amount they are willing to accept as a compensation for the inability to use of a good or its elements.

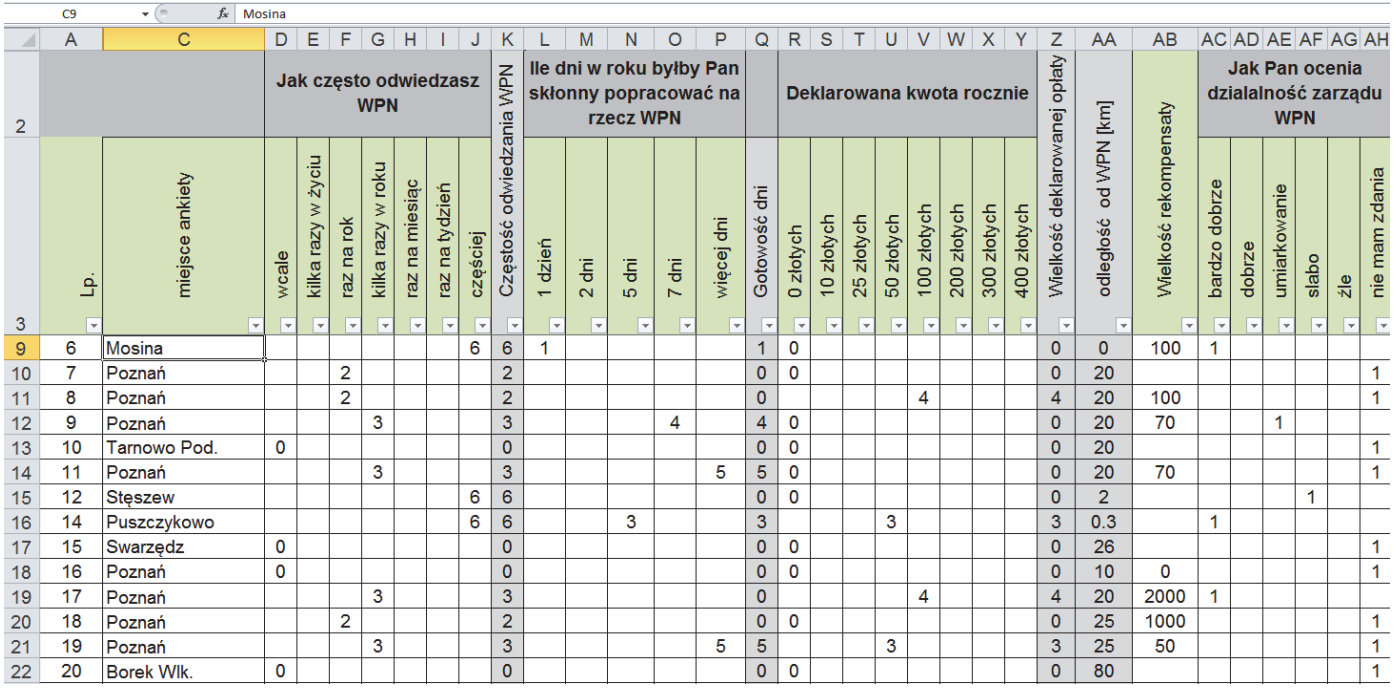

	A	C	D	E	F	G	H	I	J	K	L	M	N	O	P	Q	R	S	T	U	V	W	X	Y	Z	AA	AB	AC	AD	AE	AF	AG	AH
2			Jak często odwiedzasz WPN								Ile dni w roku byłby Pan skłonny popracować na rzecz WPN						Deklarowana kwota rocznie											Jak Pan ocenia działalność zarządu WPN					
3	Lp.	miejsce ankiety	wcale	kilka razy w życiu	raz na rok	kilka razy w roku	raz na miesiąc	raz na tydzień	częściej	Częstość odwiedzania WPN	1 dzień	2 dni	5 dni	7 dni	więcej dni	Gotowość dni	0 złotych	10 złotych	25 złotych	50 złotych	100 złotych	200 złotych	300 złotych	400 złotych	Wielkość deklarowanej opłaty	odległość od WPN [km]	Wielkość rekompensaty	bardzo dobrze	dobrze	umiarkowanie	słabo	źle	nie mam zdania
9	6	Mosina							6	6	1					1	0								0	0	100	1					
10	7	Poznań			2					2						0	0								0	20							1
11	8	Poznań			2					2						0					4				4	20	100						1
12	9	Poznań				3				3				4		4	0								0	20	70			1			
13	10	Tarnowo Pod.	0							0						0	0								0	20							1
14	11	Poznań				3				3					5	5	0								0	20	70						1
15	12	Stęszew							6	6						0	0								0	2					1		
16	14	Puszczykowo							6	6			3			3				3					3	0.3		1					
17	15	Swarzędz	0							0						0	0								0	26							1
18	16	Poznań	0							0						0	0								0	10	0						1
19	17	Poznań				3				3						0					4				4	20	2000	1					
20	18	Poznań			2					2						0	0								0	25	1000						1
21	19	Poznań				3				3					5	5				3					3	25	50						1
22	20	Borek Wlk.	0							0						0	0								0	80							1

Fig. 2. A fragment of the Excel contingency table with questionnaire results; Source: the authors' study

3.1. The logit model approach

The study applied the logit model method, which was used to determine dependencies between inclinations of residents to pay fees for use of the Wielkopolski National Park and selected explanatory variables (Czerwińska-Kayzer 2002, 2013, Cramer 2003).The main concept in this research method was to identify factors, which differentiate the analysed propensity among the population of park visitors to pay fees and accept compensation for prevention of use of park goods. Based on the conducted studies, primarily the standardised interview, the following variables were distinguished:

- the frequency of visits to the Wielkopolska National Park (x_1); 0 – none, 1 – once a year, 2 – several times a year, 3 – once a month, 4 – once a week, 5 – more frequently,
- knowledge concerning the Wielkopolska National Park (x_2); 0 – very limited, 1 – poor, 2 – moderate, 3 – good, 4 – very good,
- willingness to work (number of days) for the Wielkopolska National Park (x_3); 0 – no willingness to work as a volunteer, 1 – 1 day, 2 – 2 days, 3 – 5 days, 4 – 7 days, 5 – more days,
- age of respondent (x_4)
- size of place of residence (x_5); 1 – village, 2 – town up to 20 thousand, 3 – town from 21 thousand to 100 thousand, 4 – city over 100 thousand,
- mean net income per person (x_6); 1 – max. 1000 PLN, 2 – max. 2500 PLN, 3 – over 2500 PLN,
- education (x_7); 1 – elementary, 2 – vocational, 3 – secondary, 4 – higher,
- attitude to financial requirements of environmental protection (x_8); 1 – moderate, 2 – support, 3 – fully support, -1 – against, -2 – strongly against
- membership in environmental organisations (x_9); 1 – I am not a member, 2 – I used to be a member, 3 – I am a passive member of environmental organisations, 4 – I am an active member of environmental organisations
- distance from WNP (x_{10}).

Next the inclinations of residents to pay fees for the possibility to use the services of the Wielkopolska National Park or propensity to obtain a hypothetical compensation in the case of a hypothetical ban on visits to the Park (y) were presented in the form of a logistic regression equation:

$$ln\left(\frac{y}{1-y}\right) = a_0 + a_1x_1 + a_2x_2 + \cdots + a_{10}x_{10}$$

where: $a_0,\ a_1,\ a_2.,\ldots,a_{10}$ are regression coefficients. The measure y takes the 0 value in a situation of a lack of willingness of the respondent to pay fees for the possibility to use the Wielkopolska National Park and a lack of expectation to receive compensation in the case of a hypothetical prevention of use of the Park goods, while the values of 1 in the opposite cases.

3.2. The aim and scope of the study

The most important aim of this study was to determine willingness of individuals actively using the environmental goods to pay fees for the Wielkopolska National Park. Socio-economic factors affecting the WTA vales were identified based on the collected questionnaire material (covering the period from 1 January 2012 to 31 December 2012). The questionnaire survey was conducted in the communes of the Poznań county, the city of Poznań as well as respondents from other regions of Poland. The object scope of this study concerned data collected from questionnaires determining preferences of respondents, their socio-economic characteristics, as well as costs related to the WTA for environment use. The subject scope of this study covered the area of the Wielkopolska National Park.

4. Results

The logit model was applied to establish the potential inclinations of the general public to incur costs and the expectations of compensation in the case of a hypothetical ban on the use of the Wielkopolska National Park goods. Table 2 presents the evaluation of explanatory variables describing inclinations of respondents visiting the Wielkopolska National Park to pay fees for the Park. Analyses of the test results using multiple regression indicated that the willingness to pay fees depends mainly on the attitude of respondents to financial requirements environmental protection, their knowledge concerning the Wielkopolska National Park and membership in environmental organisations. The assessed regression coefficients for the investigated variables are positive, which shows that the propensity to incur costs for the Wielkopolska National Park increases with an increase in the respondents' awareness of nature conservation problems.

Based on the conducted analyses it may be observed that actions enhancing public environmental awareness have a positive effect on the attitude of the general public to incurring costs for the environment. In contrast, failure to provide environmental education results in the lack of interest in nature conservation on the part of respondents, manifested in their lack of declared willingness to allocate funds, as established based on the WTP method.

Table 2. Regression coefficients in the model describing inclinations of respondents visiting the Wielkopolska National Park to pay fees for the Park

Explanatory variable	Regression coefficient	Test statistic	Empirical significance level	Confidence interval
Constant	-0.2493	-0.411	0.681	(-1.440; 0.941)
Frequency of visits to the Wielkopolska National Park (x_1)	-0.0246	-0.320	0.749	(-0.175; 0.126)
Knowledge concerning the Wielkopolska National Park (x_2)	0.2635	2.368	0.018	(0.045; 0.482)
Willingness to work (number of days) for the Wielkopolska National Park (x_3)	0.1009	1.525	0.128	(-0.029; 0.231)
Age (x_4)	-0.1952	-1.604	0.109	(-0.434; 0.044)
Size of place of residence (x_5)	-0.0366	-0.466	0.641	(-0.191; 0.118)
Mean net monthly income per person (x_6)	-0.0292	-0.222	0.824	(-0.288; 0.229)
Education (x_7)	-0.0332	-0.247	0.805	(-0.298; 0.231)
Attitude to financial requirements of environmental protection (x_8)	0.2705	3.375	0.001	(0.113; 0.428)
Membership in environmental organisations (x_9)	0.6532	2.756	0.006	(0.188; 1.119)
Distance from WNP (x_{10})	0.0034	1.342	0.180	(-0.002; 0.008)

Source: the authors' study

Table 3. Regression coefficients in the model describing possibility to receive compensation by visitors to the Wielkopolska National Park in the case respondents are prohibited to use the Park goods

Explanatory variable	Regression coefficient	Test statistic	Empirical significance level	Confidence interval
Constant	-0.0430	-0.080	0.936	(-1.099; 1.013)
Frequency of visits to the Wielkopolska National Park (x_1)	0.0481	0.671	0.502	(-0.093; 0.189)
Knowledge concerning the Wielkopolska National Park (x_2)	0.0965	0.938	0.349	(-0.105; 0.298)
Willingness to work (number of days) for the Wielkopolska National Park (x_3)	0.0062	0.114	0.909	(-0.101; 0.113)
Age (x_4)	-0.4020	-3.406	0.001	(-0.634; -0.170)
Size of place of residence (x_5)	0.2072	2.710	0.007	(0.057; 0.357)
Mean net monthly income per person (x_6)	-0.0019	-0.015	0.988	(-0.250; 0.246)
Education (x_7)	-0.2848	-2.181	0.030	(-0.541; -0.028)
Attitude to financial requirements of environmental protection (x_8)	0.3406	3.924	<0.001	(0.170; 0.511)
Membership in environmental organisations (x_9)	0.1650	1.300	0.194	(-0.084; 0.414)
Distance from WNP (x_{10})	0.0057	2.458	0.014	(0.001; 0.010)

Source: the authors' study

Additionally, education of visitors to the Wielkopolska National Park, their mean net income per person, the size of place of residence or frequency of visits to the Park were found to have no impact on the respondents' willingness to pay fees for the Wielkopolska National Park. This means that the general public, regardless of the status and social origin, declares similar opinions on the need to finance nature conservation.

Analyses of the results of testing the significance of individual explanatory variables (Table 3) showed that receiving a hypothetical compensation in the case of prohibiting respondents from using the goods of the Wielkopolska National Park depends on the age and education of respondents, their opinions on the financial requirements of environmental protection, the size of their town of residence and on the distance of their residence from the Park. A positive effect, i.e. the willingness to receive hypothetical compensation increases with an increase of the level of an individual factor, was related e.g. with opinions on the financial requirements of environmental protection, the size of the place of residence of respondents as well their distance from the Park. It was stated that individuals having a hindered access to protected areas exhibit increased sensitivity to the prohibition of use of the Wielkopolska National Park. Moreover, a negative effect on the declared WTA was recorded for sociological traits related to the age and education of respondents. The willingness to accept compensation for the prohibition to use WPN goods decreases with an increase in age and the level of education of respondents. This shows that older people and more educated individuals appreciate the value of nature and it would be difficult for them to accept a situation of being prevented to visit the park.

5. Discussion

Based on the recorded results it was shown that a vast majority of the general public appreciates the value of the WNP, in which forested areas predominate. A definite majority of respondents declared willingness to incur costs for WNP, either as fees or volunteer work. The results confirm the trend within the society towards increased appreciation of nature value of the environment and non-material values in relation to forests (Paschalis-Jakubowicz 2004, 2005) or protected areas (Matuszewska 2003, Muszyńska-Kurnik 2010, Woś & Owczarek 2009).

Results of the conducted questionnaire survey indicate considerable interest on the part of respondents in the investigated area in terms of its use for tourism and recreation. Thanks to the improving standard of living, tourism and recreation are becoming increasingly common and this form of leisure activity is being selected by a growing part of the Polish population (Kikulski 2008). Causes for the development of tourism and recreation may be related to the changes in the hierarchy of values among the general public, first of all associating a greater

importance with leisure activities, shortening working hours, the need to break from the routine of everyday life, increasing mobility, growing incomes and wealth (Eckert & Cremer 1998, Kikulski 2008). A higher standard of environmental awareness is directly connected with the place of residence, patterns of free time activity and awareness of environmental threats, which is very often local in character (Kaczmarek 2012).

This study shows that environmental education contributes to effective environmental protection as a means leading to changes in human attitudes and behaviour affecting the environment, as also confirmed by other authors (Sikora 2012, Zydroń & Szoszkiewicz 2013, Hłobił 2010, 2012). In this study it was found that the general public, regardless of their status and social origin, declares similar opinions on the need to finance nature conservation. In turn, Gołos in his study (2018) stated significant differences in the willingness to pay (WTP) specific amounts of money depending on the socio-economic variables. Willingness to pay fees increased in the case of respondents with higher education, higher income and in the case of respondents having families. In contrast, it decreased with age (for respondents older than the mean in that survey). Some of the above-mentioned dependencies were confirmed by the results reported by Mandziuk and Pyra (2016), who stated that the lowest WTP amount for the recreation in the Otwock Town Beach (2.34 PLN/day at the mean WTP amount for the sample population at 4 PLN/day) was declared by respondents aged over 51 years. The WTP amount increased with an increase in the monthly net income. Women are willing to pay an almost 2-fold higher WTP amount than men. In turn, studies conducted in 2012 in the Wielkopolska National Park on a sample population of 1002 respondents (all respondents, both visitors and non-visitors to the WNP) indicate that the willingness to incur costs for the environment is not related to the education of respondents or their knowledge on the WNP and frequency of their visits to the Park. Additionally, it was shown that willingness to financially support environmental protection is not significantly related to the level of affluence of the population. Entrepreneurs were the vocational group most frequently willing to incur costs for that purpose, while farmers were least willing to pay (Zydroń & Szoszkiewicz 2013).

6. Conclusions

1. Willingness to pay fees for the WNP increases with the growing awareness of respondents concerning financial requirements of environmental protection, their knowledge on the Wielkopolska National Park and membership in environmental organisations.

2. Inclinations to receive hypothetical compensation for the prohibition to use the park increase with growing awareness of financial requirements related to environmental protection, the size of the place of residence of respondents and their distance from the Park, while they decrease with the respondents' age and the level of education.
3. Based on the conducted analyses it may be stated that environmental education of the general public is necessary to enhance public awareness of the need to finance measures related to conservation of the natural environment.

The publication was co-financed/financed within the framework of Ministry of Science and Higher Education programme as „Regional Initiative Excellence" in years 2019-2022, Project No. 005/RID/2019/20

References

Adamek, A., Ziernicka-Wojtaszek, A. (2018). Ecological Awareness of the Inhabitants of the Upper Silesian Agglomeration. *Rocznik Ochrona Środowiska, 20*, 1640-1655.

Arrow, K, Solow, R., Portney, P., Leamer, E., Radner, R., Schuman, H. (1993). Report of the NOAA panel on contingent valuation. *Federal Register, 10,* 4601-4614.

Bateman, I.J. (2000). *Monetary valuation of environmental preferences: extending the standard economic theory of values*. Centre for Social and Economic Research on the Global Environment (CSERGE), University of East Anglia and University College, London.

Carson, R.T., Flores, N.E., Meade, N.F. (2000). *Contingent Valuation: controversies and evidence. Department of Economics*. University of California, San Diego.

Courtney, P. R., & Hill, G.W. (2006). Demand analysis projections for recreational visits to countryside woodlands in Great Britain. *Forestry, 79*(2), 185-200.

Czerwińska-Kayzer, D. (2007). *Analysis of Private Farm Investments and their Funding in Poland during the Transition Period*. In: Understanding Agricultural Transition, Beckmann V., Hagedorn K. [eds] Shaker Verlag, Aachen, 329-352.

Czerwińska-Kayzer, D. (2013). Inklinacje rolników indywidualnych do realizacji inwestycji rzeczowych w gospodarstwach rolnych [Individual farmers' tendencies to make real investments in farms]. *Zeszyty Naukowe SGGW w Warszawie. Ekonomika i Organizacja Gospodarki Żywnościowej, 104*, 5-13.

Decker, K.A., Watson, P. (2017). Estimating willingness to pay for a threatened species within a threatened ecosystem. *Journal Of Environmental Planning And Management, 60*(8), 1347-1365.

Deluga, W. (2018). Waste Management in Public Awareness. *Rocznik Ochrona Srodowiska, 20,* 1530-1545.

Douglas, C.M., Lorna P., Nick H., Begona A.F. (2002). Valuing the non market benefits of wild goose conservation: a comparison of interviev and group based approaches. *Ecological Economics, 43*, 49-59.

Eckert, A., Cremer, Ch. (1998). *Tourism and the environment*. Rada Europy, Polski Klub Ekologiczny. Kraków.

Georgiou, S. (1996). The contingent valuation method. In: Andersen G., Śleszyński J. [eds.] Economic valuation of the natural environment. *Ekonomia i Środowisko*, Białystok.

Giergiczny, M. (2009). The recreational value of the Białowieża National Forest. *Ekonomia i Środowisko, 2*(36), 116-128.

Gołos, P. (2001). *Valuation of the economic value for the recreational function of forests based on the Gostynin-Włocławek Promotional Forest Complex*. A PhD dissertation. IBL. Warszawa.

Gołos, P. (2018). *Social and economic aspects of non-productive functions of forests and forest management*. A monograph. Instytut badawczy Leśnictwa.

Hłobił, A. (2010). Theory and practice of environmental education for sustainable development in Poland. *Problems of Sustainable Development, 5*(2).

Hłobił, A. (2012). Psychological and pedagogical aspects of active teaching in biology. *Rocznik Ochrona Środowiska, 14,* 960-970.

Hotelling, H. (1949). *Letter*. In: An Economic Study of the Monetary Evaluation of Recreation in the National Parks, Washington, DC: National Park Service.

Kaczmarek, R. (2012). Psychological and pedagogical aspects of ecophilosophy in view of the sustainable development concept. *Rocznik Ochrona Środowiska, 14*, 983-997.

Kahneman, Daniel & Knetsch, J.L. (1992). Valuing public goods: The purchase of moral satisfaction. *Journal of Environmental Economics and Management*, *22*(1), 57-70.

Kikulski, J. (2008b). Tourism and recreation functions of forests in Poland – public concerns and hopes (results of the first stage of research)]. *Sylwan, 6*, 63-677.

Kikulski, J. (2011). Forest management and recreational use of forests]. *Sylwan, 155*, 269-278.

Kikulski, J. 2008a. Preferences for recreation and needs for recreation management of forests in the Iława and Dąbrowa Forest Districts (results of the first stage of research)]. *Sylwan, 5*, 60-71.

Kosmacz, S., Woźniak, A. (1994). Attitudes of residents in protected areas towards the Wielkopolska National Park. *Morena 2*, 93-95.

Mandziuk, A., Pyra, A. (2016). *Valuation of the recreational function of forested areas based on the Otwock Town Beach*. Studia I Materiały CEPL w Rogowie, 18, 49B, 5: 143-152.

Matuszewska, D. (2003). *Tourism functions and conflicts in selected national parks in northern and western Poland*. Bogucki Wydawnictwo Naukowe, Poznań.

Mitchell, R.C. & Carson, R.T. (1989). *Using Surveys to Value Public Goods: The Contingent Valuation Method*. Resources for the Future, Washington DC.

Mueller, J.M. (2014). Estimating willingness to pay for watershed restoration in Flagstaff, Arizona using dichotomous-choice contingent valuation. *Forestry*, 327-333.

Muszyńska-Kurnik, M. (2010). *Atrakcyjność turystyczna Tatrzańskiego Parku Narodowego [Tourism attraction value of the Tatra National Park*]. Materials of the 4th Conference "Nature in the Tatra National Park and the human", 3, 69-73. Zakopane, 14-16.10.2010.

O'Brien, B.J., Gersten, K. Willan, A.R., Faulkner, L.A. (2002). Is there a kink in consumers' threshold value for cost – effectiveness in health care? *Health Economics, 11*, 175-80.

Olmsted, P., Honey-Rosés J., Satterfield T., Chan K.M. (2020). Leveraging support for conservation from ecotourists: can relational values play a role? *Journal of Sustainable Tourism, 28(*3), 497-514.

Paschalis-Jakubowicz P. (2005). *Forests and Polish forestry in the EU – expectations and concerns*. In: The social dimension of forests: CILP, Warszawa.

Paschalis-Jakubowicz, P. (2004). *Use of forests – moral concerns?* In: Pieńkos K. [ed.] Problems of sustainable development of tourism, recreation and sport in forests. AWF, Warszawa: 26-32.

Scarpa, R., Chiltonc, S.M., Hutchinsond, W.G., Buongiornoe, J. (2000). Valuing the recreational benefits from the creation of nature reserves in Irish forests. *Ecol. Econ., 33*(2), 237-250.

Sikora, K. (2012). The effect of environmental and health education on changes in behaviour, attitudes and quality of life of schoolchildren]. *Rocznik Ochrona Środowiska, 14*, 1009-1018.

Todorova, K. (2019). Factors affecting adoption behavior of farmers in Bulgaria - agrienvironment public goods for flood risk management. *Journal of Central European Agriculture, 20*(4), 1248-1258.

Willan, A.B., O'Brien, B.J., Leyva, R.A. (2001). Cost- Effectiveness Analysis When the WTA Is Greate Than the WTP''. *Statistics in Medicine 20*(21), 3251-3259.

Willan, A.R., O'Brien, B.J., Leyva, R.A. (2001). Cost-effectiveness analysis when the WTA is greater than the WTP. *Statistics in Medicine, 20*, 3251-3259.

Woś, B., Owczarek, W. (2009). *Turystyka na obszarach chronionych w percepcji społeczności lokalnej na przykładzie Stobrawskiego Parku Krajobrazowego (Tourism in protected areas as perceived by local inhabitants based on the Stobrawski Landscape Park*).

Wyczyńscy, H.J. (2006). *Wielkopolski Park Narodowy* (The Wielkopolska National Park), An information brochure, Jeziory.

Zydroń, A., Szoszkiewicz, K. (2013). Environmental value and public willingness to pay for that good. *Rocznik Ochrona Środowiska, 15,* 2874-2886.

Abstract

Among all the functions served by forest ecosystems an increasingly important role is played by their social function. These ecosystems have been traditionally associated with tourism and recreation and as a result also interest in the appraisal of non-productive functions of forests has been increasing. The value of the natural environment is not tangible and it may be assessed only based on subjective opinions and attitudes of the general public. A contingent valuation method based on the Willingness to Pay and Willingness to Accept has been applied to determine the nature value of a landscape dominated by forests within the boundaries of a national park in central Poland. The most important aim of this study was to determine the propensity of individuals actively using

the environmental goods to pay fees charged by the Wielkopolska National Park. Dependencies between the inclination of local residents to pay fees for the possibility to use the Wielkopolska National Park and selected variables were determined using the logit model approach. It was observed that the willingness to incur costs for the use of the Wielkopolska National Park grows with an increase in the awareness of the respondents concerning financial requirements related to environmental protection, their knowledge on the Park and membership in environmental organisations. Based on the conducted studies it was found that environmental education provided to the general public is a necessary pre-requisite to making the public aware of the need to finance actions related to preservation of the natural environment and nature conservation.

Keywords:
value of environment, national park, tourism development, nature conservation, forest

Inklinacje finansowe osób odwiedzających Wielkopolski Park Narodowy

Streszczenie

Spośród wielu funkcji jakie pełnią ekosystemy leśne coraz większe znaczenie odgrywa ich funkcja społeczna. Od dawna kojarzone są z turystyką i rekreacją wobec czego rośnie zapotrzebowanie na ocenę wartości pozaprodukcyjnych funkcji lasów. Wartość środowiska przyrodniczego nie jest mierzalna tylko ocenia się ją na podstawie subiektywnych odczuć społeczeństwa. Metoda wyceny warunkowej w formie Willingness to Pay oraz Willingness to Accept została użyta do określenia wartości przyrody krajobrazu zdominowanego przez lasy na obszarze parku narodowego w środkowej Polski. Najważniejszym celem pracy było określenie skłonności osób korzystających czynnie z dóbr środowiska do ponoszenia opłat na rzecz Wielkopolskiego Parku Narodowego. Zależności pomiędzy inklinacją mieszkańców do ponoszenia opłat za możliwość korzystania z Wielkopolskiego Parku Narodowego a wybranymi zmiennymi objaśniającymi określono przy zastosowaniu metody logitowej. Zaobserwowano, że skłonność do ponoszenia opłat na rzecz Wielkopolskiego Parku Narodowego rośnie wraz ze wzrostem świadomości respondenta na temat finansowych wymagań ochrony środowiska, jego wiedzy o Parku oraz przynależności do organizacji ekologicznych. Na podstawie przeprowadzonych badań stwierdzono, że edukacja ekologiczna społeczeństwa jest niezbędnym elementem uświadamiania ludzi o potrzebach finansowania działań związanych z zachowaniem w naturalnym stanie środowiska przyrodniczego.

Słowa kluczowe:
wartość środowiska, park narodowy, rozwój turystyki, ochrona przyrody, las

MIDDLE POMERANIAN SCIENTIFIC SOCIETY OF THE ENVIRONMENT PROTECTION

Rocznik Ochrona Środowiska

Volume 22. Year 2020 ISSN 1506-218X 281-293

Evaluation of Impact of Land Use in Adjacent Areas Causing Damage to Dirt Roads Using GIS Tools – Case Study

Michał Fiedler[*]*, Piotr Stachowski*

Poznań University of Life Sciences, Poland

[*]*corresponding author email: michal.fiedler@up.poznan.pl*

1. Introduction

The existing road network is subjected to considerable pressure and can fail due to lack of bearing capacity, overloading and surface erosion (Ngezahayo et al. 2019). This is particularly evident in the case of dirt roads, which may be seriously damaged as a result of rills and gullies formation (Fig. 1). Analysis of threats of potential damage to unpaved roads needs to include the impact of adjacent areas (Arnáez et al. 2004, Zhang et al. 2019). Relief, land use and maintenance operations performed on roads affect their life cycle. This is not only of economic importance in relation to costs incurred on their repairs and rehabilitation, but also due to traffic restrictions.

Fig. 1. Erosion of investigated road

Roads may absorb surface run-off, thus resulting in a denser hydrographic network (Jones et al. 2000). In that case they accelerate rainwater inflow to watercourses, while at the same time increasing the amount of contaminants washed from the land and road surface. In view of the linear character of roads their role in the modification of surface run-off may be multi-faceted. Roads alter the natural relief, leading to changes in the natural directions of rainwater flow (Benda et al. 2019, Jones et al. 2000). Rural unpaved roads are the most vulnerable to erosion due to the lack of vegetation protection and other protective measures. Thus, during rainstorms, unpaved roads become natural water collection areas and experience the most serious erosion (Yang et al. 2019). This is particularly important in foothill and mountainous areas (Gołąb 2015, Varol et al. 2019).

Topography is an important determinant of surface runoff forming. The extraction of drainage networks from digital elevation models is required for hydrological processes simulations and erosion modelling (Buchanan et al. 2014). A widely used method for extracting drainage networks use calculation of the flow accumulation matrix (O'Callaghan & Mark 1984, Zhou et al. 2019). Effect of soil moisture variability on the runoff can be analysed using topographic wetness index (TWI) (Minet et al. 2010, Raduła et al. 2018).

In order to conduct a comprehensive analysis it is necessary to consider spatial variability of the environment applying GIS techniques and tools (Radecki-Pawlik et al. 2016). Particularly, conducting an effective land planning requires a good understanding of road-induced erosion and sediment production process. River monitoring, sediment determination methods and road erosion models are widely used to estimate the road-induced erosion (Varol et al. 2019). Another indispensable element is availability of high quality data describing analysed areas (Chu et al. 2010, Hancock 2005, Thomas et al. 2016, Vaze et al. 2010). Large areas may be investigated based on LiDAR data (Buchanan et al. 2014, Mohamedou et al. 2019). In turn, satellite images may be used to investigate the land use structure.

2. Methods and description of the study object

The aim of this study was to determine the impact of adjacent areas on the condition of dirt roads and their potential role causing damage to these roads. The investigated area is located in the Komorniki commune, Poznań county (52°19'18" N, 16°48'31" E). Dirt roads a and b are two of the access roads to concrete road c leading to a housing estate (Fig. 2).

In 2014 and 2015, when roads were being constructed in that housing estate, it was the main access road. This led to frequent operations of surface levelling in that two roads. The part of the analysed area located above road a was 15.7 ha in area, at a mean slope of 4.4%. According to Chachaj (1996) northern

part of investigated area is composed of sands and gravels of crevice accumulation. Southern part is built from glacial sands on tills. In the Lithological Map of Poland whole area is described as fluvioglacial gravelly sand (Chachaj & Dobosz 2007).

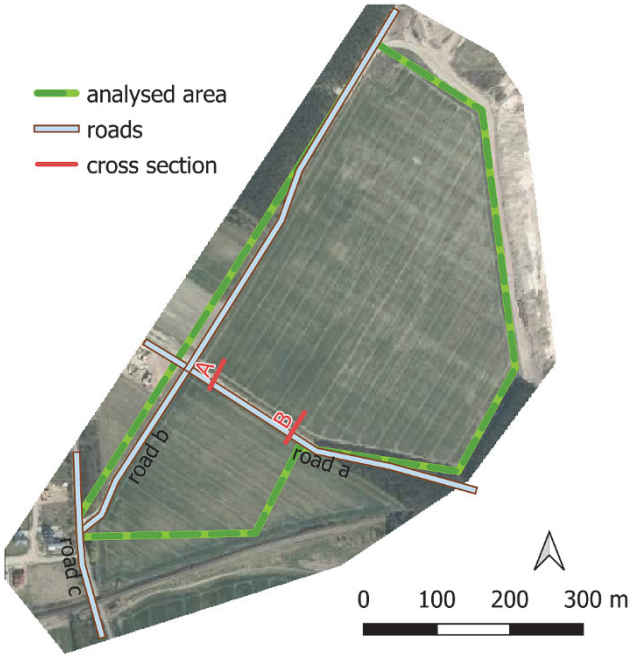

Fig. 2. Analysed area

Spatial analyses were performed using a point cloud generated by LiDAR scanning, provided by the Geodesy and Cartographic Documentation Centre. Raw laser scanning data was processed and the other works related to the generation of the Digital Elevation Model (DEM) and further geomorphological analyses were performed applying such software as SAGA 7.1.1 (Conrad et al. 2015) and QGIS 3.2.

LiDAR data in the form of LAS files contain XYZ coordinates of points and their classes. For the analysed area the mean point density is 6 per 1 m^2, while the mean elevation error is max. 0.2 m. The surface analysis was conducted on points classified in accordance to the LAS format as lying on the ground (classification code 2). Additionally, the points which ordinates were very highly divergent from the mean ordinate of the area (i.e. 21 points with ordinates exceeding 500 m a.s.l. in relation to those within the 80-110 m. a.s.l. range), were manually removed from such a constructed set. The next stage consisted in the construction

of a model of the area in the form of a regular GRID, in which point interpolation was applied based on Cubic Spline Approximation. The grid mesh size was assumed as 0.1 m.

Flow accumulation matrix was calculated using flow tracing algorithm with Rho8 method (Costa-Cabral & Burges 1994). The risk of surface run-off may be evaluated based on the Topographic Wetness Index (TWI), which is a quantitative measure describing the impact of topography on hydrological processes. It indicates areas which tend to accumulate water and may potentially promote surface run-off (Beven et al. 1984, Hjerdt et al. 2004, Hornberger et al. 1985, Quinn et al. 1995). This is determined by the dependence between the size of the area involved in surface run-off and the land slope value. The concept for TWI was developed by (Beven & Kirkby 1979) and the index is calculated from the formula:

$$TWI = \ln \frac{a}{\tan \beta} \tag{1}$$

where:
a – local upslope area draining a certain point per unit contour length,
β – local slope (slope of the cell).

Weather data was collected from the Institute of Meteorology and Water Management National Research Institute for the station in Poznań, located approx. 15 km from the investigated area. The analysed case occurred after heavy rain which took place on 22 and 23 February 2017. The accumulated rainfall over an 16 hour period reached 19.7 mm, and was equal 86% of multiyear mean for February. Mean daily air temperatures for this days were 5.6°C, and were almost 6°C higher than multi-year mean for February. There were also no snow cover.

3. Results and discussion

One of the main factors affecting the condition of dirt roads is related to the inflow of water from adjacent areas (Fig. 3). In order to include the effect of this factor it is required to conduct a detailed analysis of relief for these areas. Existing run-off routes may significantly influence the amount of water and the location, through which water may reach the road. The arrangement of surface run-off routes is affected not only by the relief itself, but also tillage operations causing soil compaction at sites of agricultural machinery working passages and the formation of passage routes (Laflen & Flanagan 2013, Montgomery 2007). This may be revealed applying shading on the digital elevation model (Fig. 4). The arrangement of such furrows following the slope and the related run-off routing may considerably accelerate the formation of surface run-off, as well as

enhance its intensity, causing a marked increase in the surface erosion risk (Bakker et al. 2008, da Rocha Junior et al. 2016, De et al. 2008, Zemke et al. 2019). This is particularly evident in a magnified fragment of the map, in which we can see relief depressions formed by passages of agricultural machines (Fig. 4). Wheel tracks allowed for a preferential flow and created a runoff line in the wheel tracks where the soil was compacted (Morvan et al. 2014, Zumr et al. 2015). Arnáez et al. (2012) found that farming operations carried out with tractors generated wheel tracks approximately 50 cm wide and 5-7 cm deep..

Fig. 3. Roads a and b

It can also be seen that at a small distance from the field end a run-off line, running parallel to the road, is formed due to repeated passages of agricultural machines over the same tracks. In Fig. 4 we can also see irregularities resulting from the location of the object at the overlapping of two LiDAR flights. Incorporation of such formed depressions into the numerical elevation model makes it possible to establish routes of surface run-off and its gradual accumulation (Fig. 5). The darker colour denotes the routing of increasing amounts of water. As can be seen, the above-mentioned passage tracks located in the upper part of the analysed area, above road a, considerably facilitate surface run-off towards that road. At the same time, within the distance of approx. 15 m from the road we may observe an independent surface run-off route, draining water towards the intersection with road b (Fig. 5). This is also evident at the cross-sections of road b (Fig. 6 and 7).

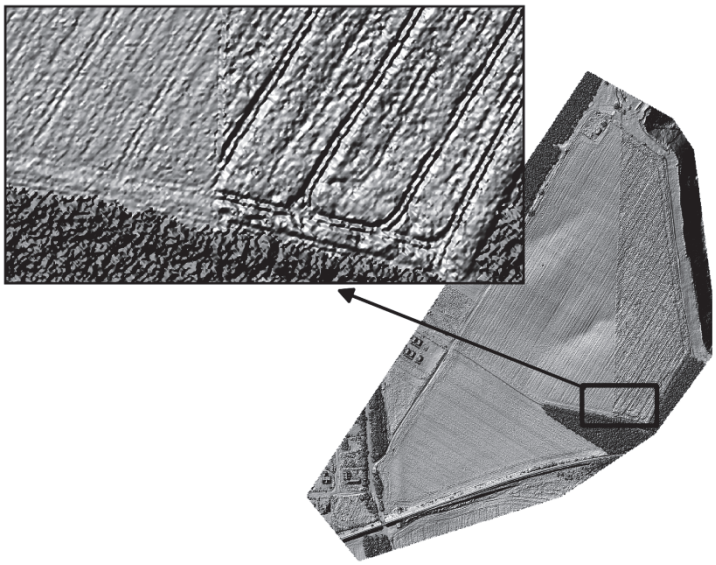

Fig. 4. Shadowing of terrain model

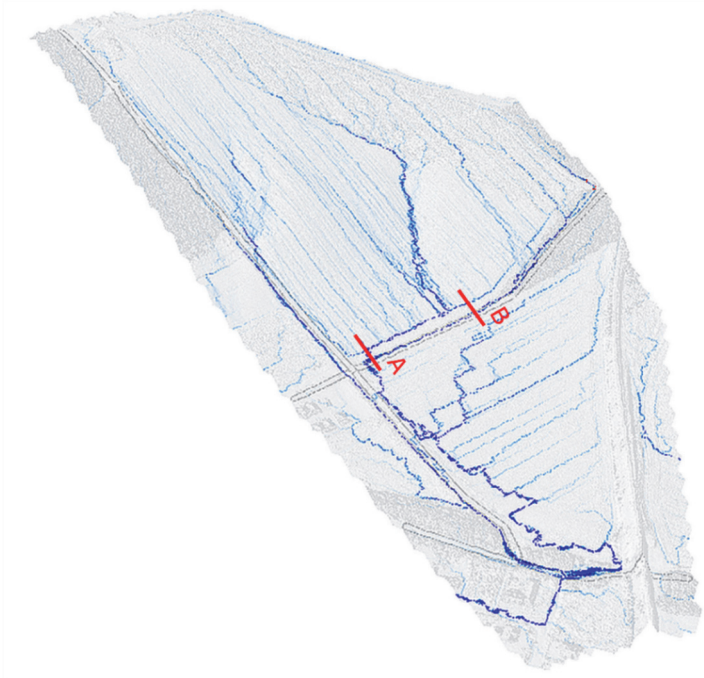

Fig. 5. Flow paths and accumulation of lateral flows (A i B – cross sections)

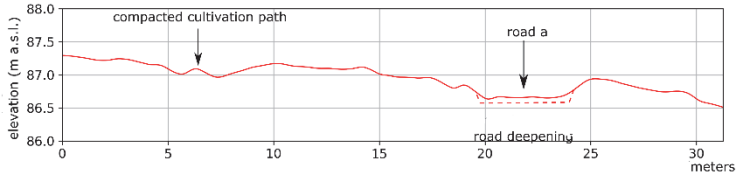

Fig. 6. Cross section A

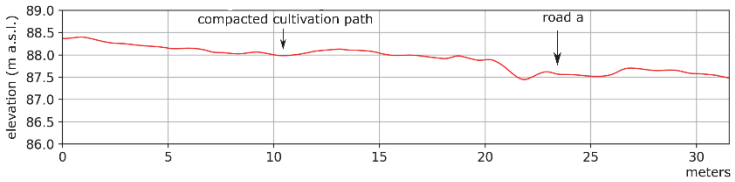

Fig. 7. Cross section B

As can be seen in Fig. 8 run-off from the area located above road a does not flow onto it directly, but reaches it at a certain distance from road b. Initially water is accumulated in a depression of road a (Fig. 9) and next it flows into a field located below. Before year 2015 such an arrangement – apart from a temporary flooding of the hollow – caused no road damage.

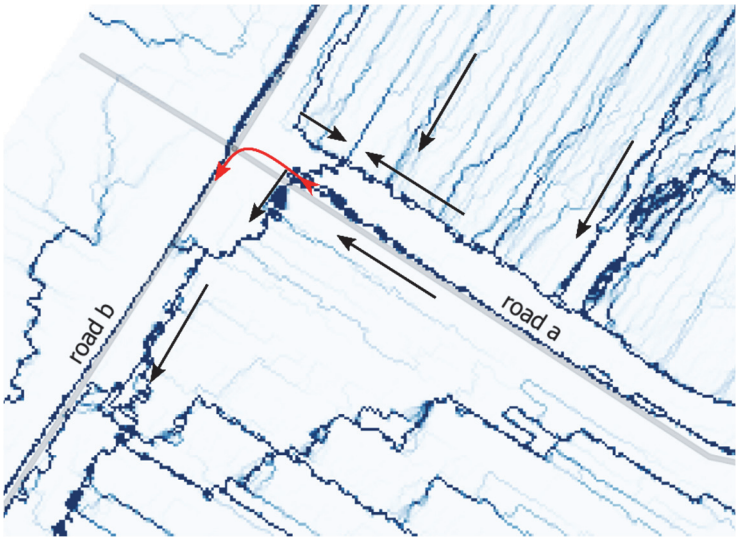

Fig. 8. Directions of water flow (red arrow show water flow after road deepening)

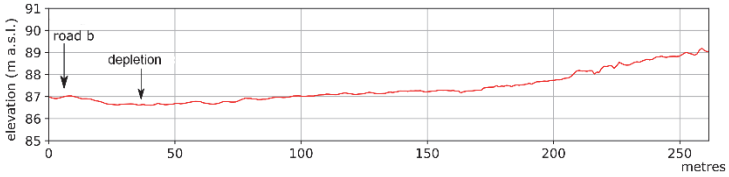

Fig. 9. Profile of road a

Starting from 2015 road a was periodically levelled, which resulted in its deepening by approx. 10 cm (Fig. 6). This led to a change in the direction of water flow, as shown in Fig. 9. A single rainfall, which occurred on 22 and 23 February 2017, caused overflow of the water flowing onto road a in the direction of road b (Fig. 3). The rainfall amounted to slightly below 20 mm within 16 hours. This precipitation washed out road b at a road section of approx. 80 m starting from the intersection of road a, and in the road section of approx. 30 m from the intersection with road C (Fig. 1). The width of the gully ranged from 0.8 to 1.4 m and its depth amounted to as much as 0.55 m. It needs to be stressed here that such considerable damage resulted from the coincidence of several adverse factors, such as a lack of dense vegetation cover, which promoted formation of surface run-off and an increased volume of inflowing water. Another factor was connected with tillage operations following the slope in the land relief what can increase runoff and finally total amount of water flowing to the road (Takken et al. 2001)

The risk of surface run-off may be evaluated based on the Topographic Wetness Index (TWI), which is a quantitative measure describing the impact of topography on hydrological processes. The TWI was chosen because of its well-known high predictive power for small catchments in relatively wet conditions (Minet et al. 2010). The value of TWI reflects the spatial distribution of soil moisture content and the saturation degree of ground surface. High TWI values are ascribed to sites potentially accumulating slope water. The highest values of this index are recorded at a large recharge area and a small slope angle (Radecki-Pawlik et al. 2016). In the study area the highest TWI values are recorded in the area situated above road a (Fig. 10). In turn, low TWI values indicating a lesser water saturation degree may be observed in the area below road a and in a narrow belt of the area between the road and the machinery passage tracks. Such marked differences result mainly from the direction of performed tillage operations. Both areas are characterised by similar soil conditions and land slopes. In turn, in the upper part of the area tillage operations are performed following the land slope, thus promoting surface run-off. In the lower part of the catchment, tillage operations are performed perpendicular to the line of slope, which hinders the formation of run-off (Fig. 10).

It needs to be stressed here that the quality of calculated TWI increases with an increase in the DEM resolution in the modelling process (Buchanan et al. 2014), which at larger areas requires computer equipment of considerable computation capacity (Sørensen et al. 2006).

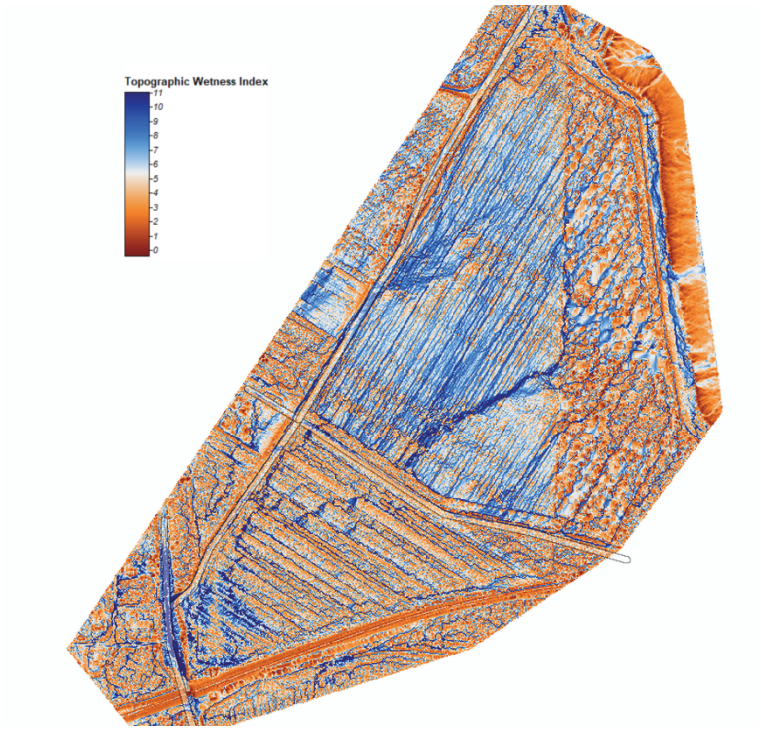

Fig. 10. Spatial distribution of TWI values

4. Conclusions

The study results indicate the necessity to include the impact of relief in areas adjacent to dirt road on their stability and life cycle. When planning road maintenance and rehabilitation operations we need to take into consideration the impact of these operations not only on roads directly subjected to these measures, but also on roads linked to them. The destructive impact of surface run-off is manifested particularly in periods of poorly developed vegetation cover, e.g. in early spring. GIS tools, providing a spatial assessment of the potential distribution of adverse factors, considerably facilitate the analysis of threats related to water inflow onto roads from adjacent areas.

The publication was co-financed within the framework of Ministry of Science and Higher Education programme as „Regional Initiative Excellence" in years 2019-2022, Project No. 005/RID/2018/19.

References

Arnáez, J., Larrea, V., Ortigosa, L. (2004). Surface runoff and soil erosion on unpaved forest roads from rainfall simulation tests in northeastern Spain. *CATENA, 57*, 1-14. DOI: 10.1016/j.catena.2003.09.002

Arnáez, J., Ruiz-Flaño, P., Lasanta, T., Ortigosa, L., Llorente, J.A., Pascual, N., Lana-Renault, N. (2012). Effects of wheel traffic on runoff and soil erosion in slopes cultivated with vineyards. *Cuadernos de Investigación Geográfica, 38*, 115-130. DOI: 10.18172/cig.1278

Bakker, M.M., Govers, G., van Doorn, A., Quetier, F., Chouvardas, D., Rounsevell, M. (2008). The response of soil erosion and sediment export to land-use change in four areas of Europe: The importance of landscape pattern. *Geomorphology, Human and climatic impacts on fluvial and hillslope morphology, 98*, 213-226. DOI: 10.1016/j.geomorph.2006.12.027

Benda, L., James, C., Miller, D., Andras, K., (2019). "Road Erosion and Delivery Index (READI): A Model for Evaluating Unpaved Road Erosion and Stream Sediment Delivery. *J. Am. Water Resour. Assoc., 55*, 459-484. DOI: 10.1111/1752-1688.12729.

Beven, K.J. & Kirkby, M.J. (1979). A physically based, variable contributing area model of basin hydrology / Un modèle à base physique de zone d'appel variable de l'hydrologie du bassin versant. *Hydrol. Sci. Bull., 24*, 43-69. DOI: 10.1080/02626667909491834

Beven, K.J., Kirkby, M.J., Schofield, N., Tagg, A.F. (1984). Testing a physically-based flood forecasting model (TOPMODEL) for three U.K. catchments. *J. Hydrol. 69*, 119-143. DOI: 10.1016/0022-1694(84)90159-8

Buchanan, B.P., Fleming, M., Schneider, R.L., Richards, B.K., Archibald, J., Qiu, Z., Walter, M.T. (2014). Evaluating topographic wetness indices across central New York agricultural landscapes. *Hydrol. Earth Syst. Sci., 18*, 3279-3299. DOI: 10.5194/hess-18-3279-2014

Chachaj, J. (1996). Detailed geological map of Poland in scale 1:50.000. Sheet 507-Mosina. *Polish Geological Institute National Research Institute.*

Chachaj, J. & Dobosz, B. (2007). Lithogenetic Map of Poland. Sheet 507-Mosina. *Ministry of Environment.*

Chu, X., Zhang, J., Chi, Y., Yang, J. (2010). An Improved Method for Watershed Delineation and Computation of Surface Depression Storage. *Watershed Manag., Proceedings 1113-1122*. DOI: 10.1061/41143(394)100

Conrad, O., Bechtel, B., Bock, M., Dietrich, H., Fischer, E., Gerlitz, L., Wehberg, J., Wichmann, V., Böhner, J. (2015). System for Automated Geoscientific Analyses (SAGA) v. 2.1.4. *Geosci. Model Dev. 8*, 1991-2007. DOI: 10.5194/gmd-8-1991-2015.

Costa-Cabral, M.C. & Burges, S.J. (1994). Digital Elevation Model Networks (DEMON): A model of flow over hillslopes for computation of contributing and dispersal areas. *Water Resour. Res., 30*, 1681-1692. DOI: 10.1029/93WR03512

da Rocha Junior, P.R., Bhattarai, R., Alves Fernandes, R.B., Kalita, P.K., Vaz Andrade, F. (2016). Soil surface roughness under tillage practices and its consequences for water and sediment losses. *J. Soil Sci. Plant Nutr., 16*, 1065-1074. DOI: 10.4067/S0718-95162016005000078

De, N.V., Douglas, I., Mcmorrow, J., Lindley, S., Binh, D.K.N.T., Van, T.T., Thanh, L.H., Tho, N. (2008). Erosion and Nutrient Loss on Sloping Land under Intense Cultivation in Southern Vietnam. *Geogr. Res. 46*, 4-16. DOI: 10.1111/j.1745-5871.2007.00487.x

Gołąb, J. (2015). Water runoff from road surface in mountain forests. *Ecol. Quest. 20*, 63. DOI: 10.12775/EQ.2014.017

Hancock, G.R. (2005). The use of digital elevation models in the identification and characterization of catchments over different grid scales. *Hydrol. Process. 19*, 1727-1749. DOI: 10.1002/hyp.5632

Hjerdt, K.N., McDonnell, J.J., Seibert, J., Rodhe, A. (2004). A new topographic index to quantify downslope controls on local drainage: TECHNICAL NOTE. *Water Resour. Res. 40*. DOI: 10.1029/2004WR003130

Hornberger, G.M., Beven, K.J., Cosby, B.J., Sappington, D.E. (1985). Shenandoah Watershed Study: Calibration of a Topography-Based, Variable Contributing Area Hydrological Model to a Small Forested Catchment. *Water Resour. Res. 21*, 1841-1850. DOI: 10.1029/WR021i012p01841

Jones, J.A., Swanson, F.J., Wemple, B.C., Snyder, K.U. (2000). Effects of Roads on Hydrology, Geomorphology, and Disturbance Patches in Stream Networks. *Conserv. Biol. 14*, 7685. DOI: 10.1046/j.1523-1739.2000.99083.x

Laflen, J.M., Flanagan, D.C. (2013). The development of U. S. soil erosion prediction and modeling. *Int. Soil Water Conserv. Res. 1*, 1-11. DOI: 10.1016/S2095-6339(15)30034-4

Minet, J., Laloy, E., Lambot, S., Vanclooster, M. (2010). Effect of GPR-derived within-field soil moisture variability on the runoff response using a distributed hydrologic model. Hydrol. Earth Syst. Sci. Discuss., 7, 8947-8986. DOI: 10.5194/hessd-7-8947-2010

Mohamedou, C., Korhonen, L., Eerikäinen, K., Tokola, T. (2019). Using LiDAR-modified topographic wetness index, terrain attributes with leaf area index to improve a single-tree growth model in south-eastern Finland. *For. Int. J. For. Res. 92*, 253-263. DOI: 10.1093/forestry/cpz010

Montgomery, D.R. (2007). Soil erosion and agricultural sustainability. *Proc. Natl. Acad. Sci., 104*, 13268-13272. DOI: 10.1073/pnas.0611508104

Morvan, X., Naisse, C., Issa, O.M., Desprats, J.F., Combaud, A., Cerdan, O. (2014). Effect of ground-cover type on surface runoff and subsequent soil erosion in Champagne vineyards in France. *Soil Use and Management, 30*, 372-381. DOI: 10.1111/sum.12129

Ngezahayo, E., Ghataora, G.S., Burrow, M.P.N. (2019). Factors Affecting Erosion in Unpaved Roads. *Proceedings of the 4th World Congress on Civil, Structural, and Environmental Engineering (CSEE'19), Paper No. ICGRE 108*. DOI: 10.11159/icgre19.108

O'Callaghan, J.F. & Mark, D.M. (1984). The extraction of drainage networks from digital elevation data. *Comput Vis Graph Image Process., 28*, 323-344 DOI: 10.1016/S0734-189X(84)80011-0

Quinn, P.F., Beven, K.J., Lamb, R. (1995). The in(a/tan/β) index: How to calculate it and how to use it within the topmodel framework. *Hydrol. Process., 9*, 161-182. DOI: 10.1002/hyp.3360090204

Radecki-Pawlik, A., Wojkowski, J., Wałęga, A., Pijanowski, J. (2016). On using the GIS methods for analysing cultural landscapes of land water resources: the Mściwojów water reservoir region. *Acta Sci. Pol. Form. Circumiectus, 14*, 109-133. DOI: 10.15576/ASP.FC/2015.14.4.109

Raduła, M.W., Szymura, T.H., Szymura, M. (2018). Topographic wetness index explains soil moisture better than bioindication with Ellenberg's indicator values. *Ecological Indicators, 85*, 172-179. DOI: 10.1016/j.ecolind.2017.10.011

Sørensen, R., Zinko, U., Seibert, J. (2006). On the calculation of the topographic wetness index: evaluation of different methods based on field observations. *Hydrol. Earth Syst. Sci., 10*, 101-112. DOI: 10.5194/hess-10-101-2006

Takken, I., Govers, G., Jetten, V., Nachtergaele, J., Steegen, A., Poesen, J. (2001). Effects of tillage on runoff and erosion patterns. *Soil and Tillage Research, 61*, 55-60. DOI: 10.1016/S0167-1987(01)00178-7

Thomas, I.A., Jordan, P., Mellander, P.-E., Fenton, O., Shine, O., ÓhUallacháin, D., Creamer, R., McDonald, N.T., Dunlop, P., Murphy, P.N.C. (2016). Improving the identification of hydrologically sensitive areas using LiDAR DEMs for the delineation and mitigation of critical source areas of diffuse pollution. *Sci. Total Environ., 556*, 276-290. DOI: 10.1016/j.scitotenv.2016.02.183

Varol, T., Ertuğrul, M., Özel, H.B., Emir, T., Çetin, M. (2019). The effects of rill erosion on unpaved forest road. *Appl. Ecol. Env. Res., 17*, 825-839. DOI: 10.15666/aeer/1701_825839

Vaze, J., Teng, J., Spencer, G. (2010). Impact of DEM accuracy and resolution on topographic indices. *Environ. Model. Softw., 25*, 1086-1098. DOI: 10.1016/j.envsoft.2010.03.014

Yang, B., Wang, W.L., Guo, M.M., Guo, W.X., Wang, W.X., Kang, H.L., Zhao, M., Chen, Z.X. (2019). Soil erosion of unpaved loess roads subjected to an extreme rainstorm event: a case study of the Jiuyuangou watershed on the Loess Plateau, China. *J. Mt. Sci., 16*, 1396-1407. DOI: 10.1007/s11629-018-5211-z

Zemke, J.J., Enderling, M., Klein, A., Skubski, M. (2019). The Influence of Soil Compaction on Runoff Formation. A Case Study Focusing on Skid Trails at Forested Andosol Sites. *Geosciences, 9*, 204. DOI: 10.3390/geosciences9050204

Zhang, Y., Zhao, Y., Liu, B., Wang, Z., Zhang, S. (2019). Rill and gully erosion on unpaved roads under heavy rainfall in agricultural watersheds on China's Loess Plateau. *Agric. Ecosyst. Environ., 284*, 106580. DOI: 10.1016/j.agee.2019.106580

Zhou, G., Wei, H., Fu, S. (2019). A fast and simple algorithm for calculating flow accumulation matrices from raster digital elevation. *Front. Earth Sci., 13*, 317-326. DOI: 10.1007/s11707-018-0725-9

Zumr, D., Dostál, T., Devátý J. (2015). Identification of prevailing storm runoff generation mechanismsin an intensively cultivated catchment. *J. Hydrol. Hydromech., 63*, 246-254. DOI: 10.1515/johh-2015-0022

Abstract

Surface run-off from areas adjacent to dirt roads may cause considerable damage to these roads. The degree of damage is determined from the amount of flowing water, run-off intensity as well as sites, in which run-off reaches the roads. These parameters result from soil conditions, as well as natural relief and the land form modified by tillage operations. Another parameter influencing the formation and the degree of erosion is connected with maintenance operations regularly repeated in the life cycle of these roads, such as e.g. surface levelling or use of paving materials. The analysis involved GIS tools, which made it possible to consider the impact of spatial variability in the surroundings of such roads on the incidence of adverse factors. The application of LiDAR data made it possible to indicate the formation of surface run-off routes and the resulting threats of damage to dirt roads.

Keywords:
unpaved road, TWI index, DEM, road erosion, surface run-off

Wpływ użytkowania terenów przyległych na erozję dróg gruntowych – analiza przypadku

Streszczenie

Spływy powierzchniowe z terenów przyległych do dróg gruntowych mogą wywoływać znaczne uszkodzenia tych dróg. Stopień uszkodzeń wynika z ilości spływającej wody, intensywności spływu oraz miejsc, w których spływy docierają do dróg. Parametry te wynikają z warunków glebowych oraz naturalnego i wynikającego ze stosowanych zabiegów uprawowych ukształtowania powierzchni terenu. Kolejnym parametrem wpływającym na powstawanie i stopień erozji są cykliczne zabiegi konserwacyjne stosowane w procesie utrzymania tych dróg, jak np. wyrównywanie powierzchni czy stosowanie materiałów utwardzających. W analizie zagadnienia zastosowano narzędzia GIS pozwalające na uwzględnienie wpływu przestrzennej zmienności otoczenia takich dróg na występowanie czynników szkodliwych. Wykorzystanie danych LIDAR pozwoliło na wskazanie ścieżek formowania się spływów powierzchniowych i wynikających z nich zagrożeń uszkodzeniami dróg gruntowych.

Słowa kluczowe:
drogi gruntowe, wskaźnik TWI, NMT, erozja dróg, spływ powierzchniowy

MIDDLE POMERANIAN SCIENTIFIC SOCIETY OF THE ENVIRONMENT PROTECTION

Rocznik Ochrona Środowiska

Volume 22. Year 2020 ISSN 1506-218X 294-307

Analysis of the Possibilities of Rainwater Harvesting Based on the AHP Method

Mateusz Hämmerling, Joanna Kocięcka, Daniel Liberacki*

Poznań University of Life Sciences, Poland

corresponding author's e-mail: joanna.kociecka@up.poznan.pl

1. Introduction

Poland is one of the countries with the largest water deficit in Europe. Poland's water resources per capita are 1580 $m^3 \cdot years^{-1}$ on average. It is almost three times less than the European average (Jokiel et al. 2017). The low water resources combined with the current climate change are a major challenge for polish agriculture, economy, and industry (Ptak et al. 2019, Sojka et al. 2019). Climate change causes modification of the spatial and seasonal distribution of precipitation in Poland (Szwed 2019). As a result, there is a more and more frequent occurrence of short-term, heavy rainfall and prolonged periods of drought. In the face of these changes and the threat of drought, we must think about the possibility of reducing the outflow and increasing water retention. At present, we can see a sharp increase in impermeable surfaces (such as concrete, bricks, asphalt), which is a result of the development of the urban areas. This type of surface causes that water does not reach the soil and plants but is usually discharged directly into the sewerage system. As a result, an increased amount of water flows into the sewage system, which often exceeds its designed capacity. Consequently, urban floods are increasingly frequent (Chudzicki 2018, Tokarczyk-Dorociak et al. 2017). The way to reduce the occurrence of floods in cities is rainwater harvesting (RHW). The two main objectives of rainwater harvesting are 1) to use rainwater for all general purposes and 2) to refill recharge groundwater (Haq 2017). The RHW can be used for purposes such as toilet flushing, cleaning, gardening, and vehicle washing. Accordingly, it is one of the ways to save purified, treated drinking water of high quality (Sendanayake 2016, Słyś et al. 2012). In Poland, the reuse and harvesting of rainwater is a great opportunity to reduce the water deficit problem.

Rainwater harvesting (RHW) is also one of the methods for climate change adaptation. At present, the best solution is to use blue-green infrastructure

(BGI), which mitigates the effects of floods and improves water quality. Furthermore, one of the objectives of BGI is to secure water for regional and agricultural purposes development. This infrastructure also alleviates the heat load. It is particularly effective in cooling densely built-up areas of large cities (Žuvela-Aloiseet et al. 2016). BGI reduces financial costs associated with stormwater in the long-run and creates new recreation places for people. Due to the great value-added, blue and green infrastructure must be taken into account in the spatial planning process, in particular in the formulation of regional (spatial) development strategies (Ghofrani et al. 2017). BGI includes solutions such as rain gardens, rainwater tanks, infiltration trenches and basins, ponds, bioswales, and green roofs. Apart from that infrastructure, rainwater management may also involve using drainage boxes, seepage pits, and underground storage tanks.

The right choice of the proper rainwater system is not obvious. Many factors and conditions must be taken into account during the selection. The choice of the RHW system depends on topography, land use, rainfall as well as the development of demand and economy (Martin et al. 2007). Sometimes, due to the small area of the land, we are unable to implement a new investment. In such cases, we try to adapt to already existing facilities. For example in urban areas, we can use existing ponds as rainwater receivers without compromising their other functions (Stachowski et al. 2017). Another important factor determining the choice of rainwater harvesting solution is the cost of investment. Sakson (2018) has conducted a financial assessment of rainwater collection systems for ten cities in Poland. Its results depended on the location, but in each city, the return on investment was high, especially in the case of detached houses. The cost-effectiveness of the system is extremely important for the individual user. It often happens that the decision to choose a rainwater storage system is made intuitively or is based on one criterion, which is the cost of investment. Such an approach may lead to a number of negative and long-term effects on the catchment water balance (Kordana & Słyś 2017).

This paper presents an analysis of four selected rainwater harvesting systems (RHWS): green roof, drainage boxes, underground storage tank, and infiltration basin. The analysis was conducted using the AHP (Analytic Hierarchy Process) method for two cases: a detached house in the suburbs of a large agglomeration and a block of flats in the city center.

2. Materials and methods

The method of Multi-Criteria Decision Making (MCDM) facilitates the selection of the best solution in various fields of economy, environmental engineering, and business. It is used, among others, for flood risk assessment of areas (Stefanidis et al. 2013), selection of the right location for the construction of solar

farms (Uyan 2013), assessment of the innovativeness of stone mining waste management technology (Kozioł et al. 2011), analysis of the possibility of using the biological early warning system in tap water (Chmist et al. 2019), choosing the best public tender (Marcarelli & Squillante 2019), assessment of the safety of the construction project (Aminbakhsh et al. 2013), and studying the factors responsible for the success of IT services (Chen & Wang 2010). It is also a tool to evaluate and select the most people-friendly design concept based on criteria and decision sub-criteria (Ariff et al. 2008) and to find the best public tender (Marcarelli & Squillante 2019). One of the MCDM is AHP (Analytic Hierarchy Process), which was used in this publication to search for the best variant of rainwater harvesting. The application of this type of method required the analysis have been divided into several steps. In the first step, a hierarchical tree was created.

The hierarchical tree presents the relationship between the factors describing the problem and its potential solutions. It consists of at least three levels. On the first level, the problem under consideration is formulated. On the next levels, there are factors that describe the analyzed problem, while the last level presents solutions. Based on the hierarchical tree, matrices are created in which the individual factors and solutions are compared using the 9-stage Saaty scale. In the scale described in the AHP method, a value of 1 means equal importance of the compared factors or solutions, while the value of 9 means a very strong difference between the pairs being compared. The results of the comparisons are entered into the matrix and the diagonals of the matrix assume values equal to one. In the next step of AHP methods, matrices are being solved and the number of calculations depends on the hierarchical tree level. On the second level, one matrix is solved. On the third level one matrics also solved, but as many times as there are factors on the second level. Then, the results are checked by determining the values of matrixes, CI consequence factor, and IR inconsistencies. The more the intrinsic value of the matrix deviates from the dimension n, the error is greater. If the CI values do not exceed 0.1 and the IR values do not exceed 0.2, then the experts' assessments are consistent (Hämmerling & Spychała 2015). The matrix solutions are local vectors. Based on their values and vectors from the higher level, global vectors are determined, which allowed to determine the best solution to the problem of rainwater harvesting in an urban area.

The problem of rainwater management is currently a very important aspect of the construction of new housing estates as well as existing urban areas. There are several reasons for this. The first reason why is the issue of increasing the intensity of weather phenomena, the second is the possibility of reusing water for irrigation of plants, the third is the changing legal regulations. Preparing the rainwater harvesting system for a given site, the characteristics of different systems were analysed. The most favourable solution was chosen on the basis of

a comparative analysis of various parameters describing the different systems. Multi-Criteria Decision Making is the best for this type of analysis.

The first stage of the AHP method is the decomposition of the problem, i.e. building a hierarchical tree (Fig. 1). At the P1 level, the main goal is stated, which is described in the previous paragraph. On the P2 level, the parameters characterizing the investigated problem and its solutions are determined. During the analysis of different rainwater harvesting systems, several aspects were taken into account, including the costs of construction and exploitation of each solution. The ease of installation and construction of each solution was also taken into consideration. Another factor analysed was the influence of a system on groundwater resource changes. This aspect was both considered in terms of the change in the ordinate of groundwater level in the area and the possibility of absorbing an increased amount of water resulting from intensive rainfall. The study also took into account aspects related to the exploitation of particular elements of a rainwater management system. The convenience of performing particular exploitation and maintenance works and their frequency were analysed. A very important issue discussed in the analysis pertains to the feasibility of the systems in different conditions of land use. The paper analyses the possibilities of building systems in the area of a housing estate of detached houses in the suburbs and blocks of flats located in the city center. When comparing individual systems, the possibility of integration with both designed and the existing environment was also considered. The authors have meant here the integration of a given system into a spatial order and the existing land development. At present, the situation related to legal aspects and increasing costs has a positive impact on the need to use the harvested water again. The analyses took into account the possibility of using the harvested water for e.g. irrigation of the garden or toilet flushing.

In the article, 4 different solutions for harvesting rainwater were analysed using the AHP method. The first of them was a green roof. It is a space located on the roof of the building, covered with plants grown on the vegetation substrate. This solution is becoming increasingly popular due to the possibility of increasing the amount of greenery in intensely built-up areas without allocating additional land for it. Green roofs also create new places for people to relax on the buildings. The second solution analyzed was the drain boxes. They are placed in the soil where they support the infiltration of water coming from the roofs and paved surfaces. Thanks to the underground construction, a large area is not necessary for their installation. The third system is an underground storage tank. The water harvested in it can be reused for irrigation of the garden or flushing the toilets in houses. The last solution analysed by the authors was an infiltration basin. It is one of the elements of the blue-green infrastructure (BGI). Apart from storing rainwater, it allows the excess water to drain into the ground. Infiltration tanks with luxuriant vegetation are also a place where many plant and animal species live. Moreover, this solution creates new recreation places for the residents of the estates.

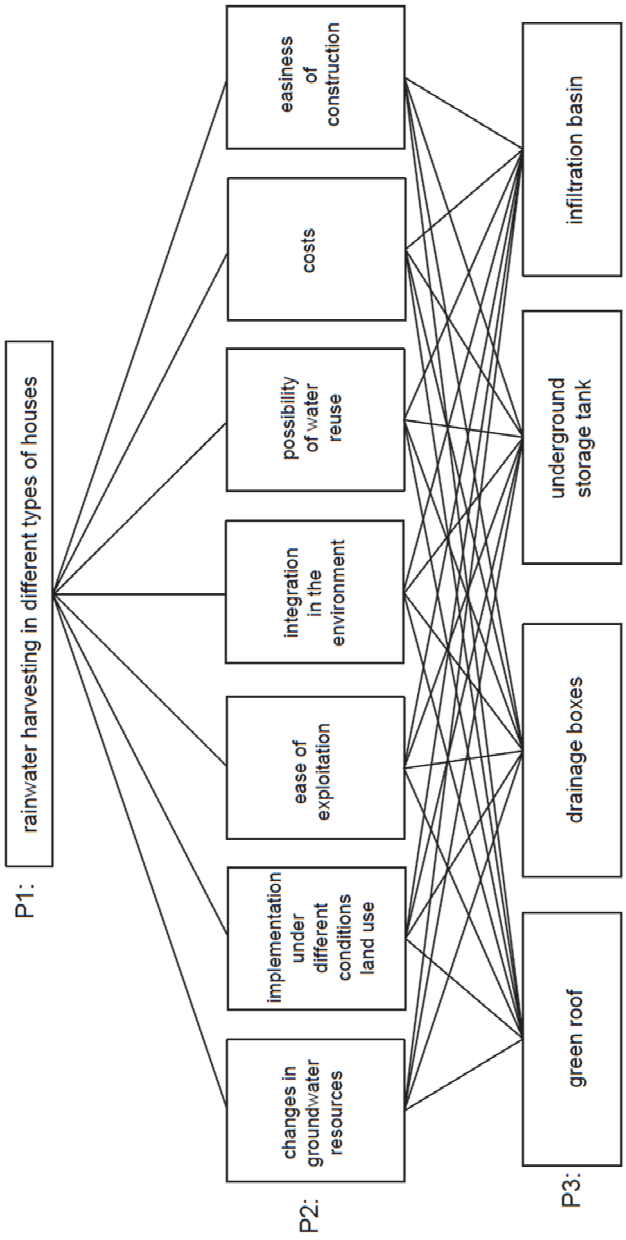

Fig. 1. The hierarchical tree used in the analyses

3. Results and discussion

The calculations using the Multi-Criteria Decision Making (MCDM) methods were performed for two different scenarios (a detached house in the suburbs of a large agglomeration and a block of flats in the city). Fig. 2 shows the global vector values for level 2 of the hierarchical tree. The highest values for both scenarios were obtained by a factor related to the possibility of rainwater reuse (for a detached house 0.35 and a block of flats 0.28). For a detached house, ease of exploitation (0.20) and costs (0.19) were the next most important factors, which had the greatest impact on the choice of rainwater harvesting method. For a block of flats, the second and third most important factors were costs (0.24) and operation and construction ability (0.12). The least important aspect for both scenarios is an adaptation to the environment (0.04 and 0.06). Analysing the results of the second level global vector, it can be concluded that the hierarchy of factors for the two scenarios is similar, and the differences can be explained by the specificity of each scenario. The possibility of reusing rainwater is an extremely important aspect from the point of view of the environment and small water resources as well as from the perspective of the user. For this reason, a slightly higher value of the vector (0.35) has been noted in the case of a detached house, where the reuse of water (for watering the garden or flushing the toilets) allows to significantly reduce the costs of living the household by decreasing the amount of tap water used. In the case of a detached house, the ease of exploitation of the system is also considerable, which has a direct impact on the costs incurred. In the case of a block of flats, ease of exploitation is less important than in the case of a detached house, due to the fact that it is not the responsibility of a single user. The analysis showed that the least significant aspect is the adaptation of the system into the environment. The vector value, in this case, is higher for a block of flats in the city center. This is due to the fact that in a strongly urbanised area, each of the solutions will have a huge impact on the reduction of the negative environmental impact of the buildings (in the suburbs this impact will be smaller). It is worth noting that some of the analysed solutions will contribute not only to the increase of water resources but also to the extension of biologically active areas, which is extremely important in the context of the adaptation of cities to climate change.

At level 3, seven matrixes were calculated. Fig. 3 presents the results of the calculations of local vectors for a detached house. For the factor of groundwater resources change, the infiltration basin (0.45), and drainage boxes (0.43) were most affected. The highest values for the factor associated with the possibility of implementation in various land use conditions were obtained for the underground storage tank (0.36) and drainage boxes (0.34), as these are the solutions that can be applied regardless of the existing land use. On the other hand,

the implementation of the infiltration basin requires a large area, which can be used e.g. to create a resting area, car park, or garage. The easiest to exploit are drainage boxes (0.32) and an underground storage tank (0.32) because, unlike a green roof or an infiltration tanks, they do not require a lot of time and work for their maintenance. In terms of integration into the environment, the best solution is to use the infiltration basin (0.43) and green roofs (0.39). The development of the roof of a detached house increases its market value and makes it more attractive. The green roof also creates additional space for the recreation of purposes. The infiltration reservoir located on the plot can not only serve as a retention function but it can affect the aesthetics of the garden. The biggest possibility of water reuse as grey water is created by an underground storage tank with no outlet (0.56), in which we can accumulate all the precipitation in contrast to other solutions in which water is taken by plants, soaked in the ground or is evaporated and infiltrated. In terms of the cost, the cheapest were the drain boxes (0.38) and the underground storage tank (0.37). Due to constructional requirements, green roofs proved to be a very expensive solution for a detached house. The easiest system to implement is an underground storage tank (0.38) and drain boxes (0.34). A more demanding investment is the system of green roofs due to the construction and the need to perform work at height.

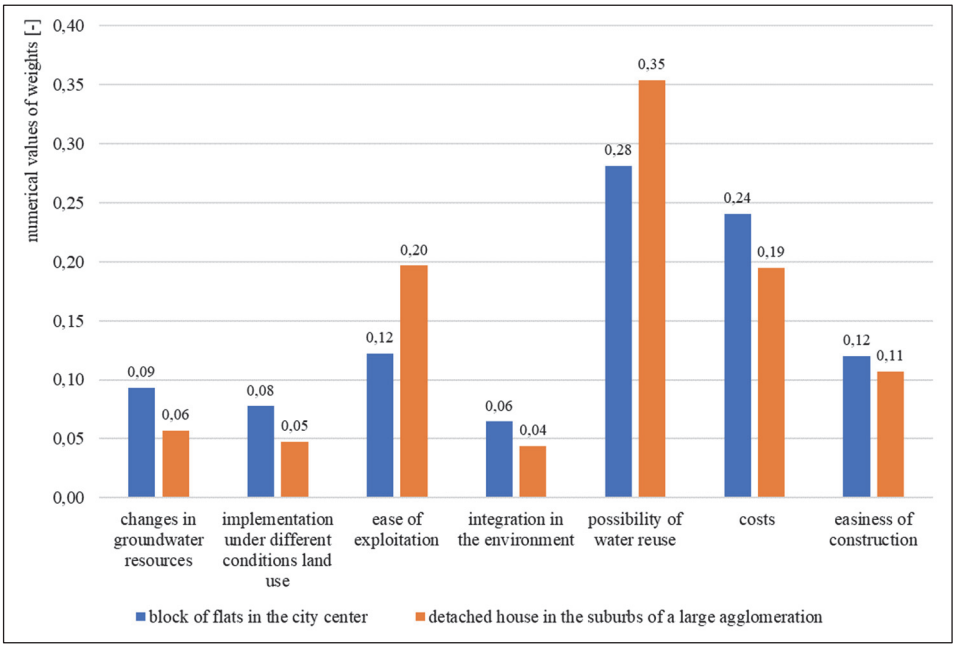

Fig. 2. Results for vectors in level 2

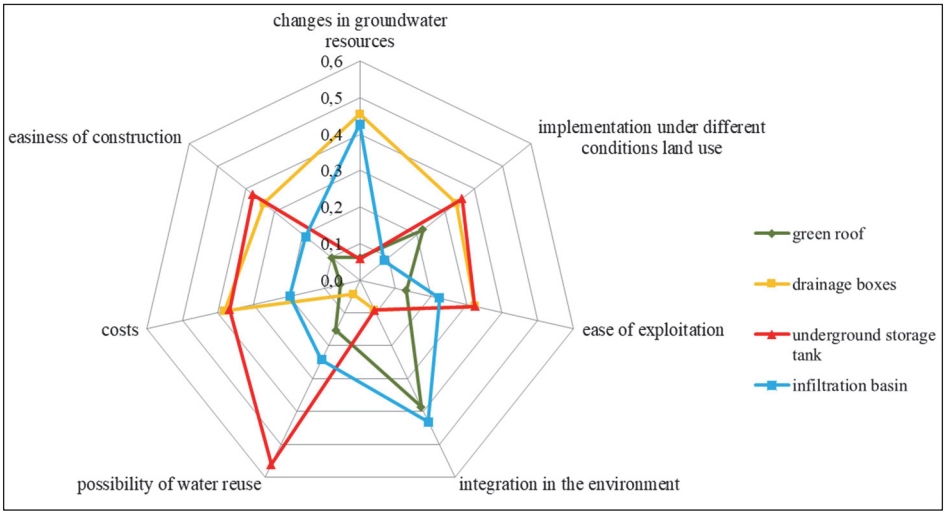

Fig. 3. Results for vectors from level 3 for a detached house located in the suburbs of a large agglomeration

Figure 4 shows the values of local vectors for level 3 in the case of a block of flats located in the city center. In terms of influence on changes in groundwater resources, the most advantageous solutions are the drainage boxes (vector value 0.45) and the infiltration basin (0.43). The result obtained for the underground storage tank is low (0.06) due to the fact that it is an airtight reservoir and the water cannot infiltrate the ground. The vector value for the green roof was also low (0.06). This is determined by the fact that most of the water in the case of this solution will be stored on the roof and will not affect the increase of groundwater resources. When considering the solutions in the context of land use, the best solution will be an underground storage tank (0.35) or drainage boxes (0.31) whose installation do not require a large area. This is extremely important in the case of a block of flats located in the city center. Construction of the infiltration basin (0.08) requires a large area, so this solution cannot always be realized. According to the analysis carried out in view of ease of exploitation for the block of flats, the best system will be an underground storage tank (vector value 0.35). It does not require frequent maintenance or treatments to maintain the functionality of the solution such as green roof (0.12) or infiltration basin (0.22). In the case of both of these systems, users must take into account, among other things, the need for continuous monitoring of the development of vegetation and the use of care treatments. In the case of the system integration with the environment, the greatest benefit for the block of flats will be the installation of a green roof (0.40) or

construction of the infiltration basin (0.40). Both of these solutions will significantly increase the biologically active area and reduce the urban heat island effect. They also perfectly fit into the adaptation plans of cities and the latest trends in increasing the participation of green and blue infrastructure in urban areas. The biggest possibility of reusing water in the case of the block of flats is the underground storage tank (local vector value 0.56). It allows to keep a large amount of water and use it at any time for sanitary purposes of the block inhabitants The drainage boxes are the least favorable solution due to their permeable nature (0.04). The cost analysis showed that the optimal solution will be the drain boxes (0.37). The cost of their installation is much lower than in the case of a green roof (0.05). The construction of the infiltration basin is also associated with high costs (excavation, vegetation) so that the local vector was only 0.20. The ease of construction is also directly related to the cost aspect. The simplest solution will be to install an underground storage tank (0.39) or drainage boxes (0.32), which do not require a lot of work in comparison to the construction of the infiltration tank, which requires a lot of groundwork, which is the reason why the vector reached the lowest value of 0.11. The local vector for green roofs was at the level of 0.18. The ease of construction is related to the type of existing roof in a block of flats. Depending on the case, the adaptation of the structure will require respectively more or less work.

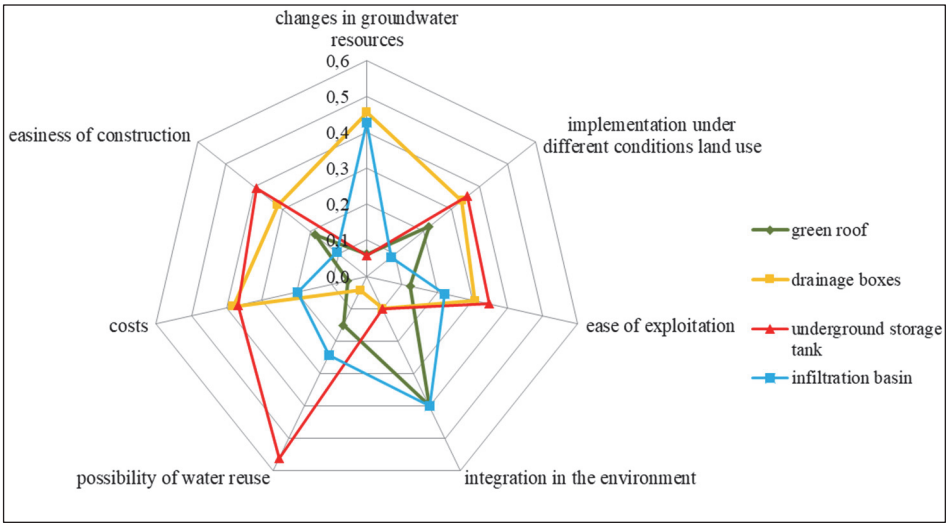

Fig. 4. Results for vectors from level 3 for the block of flats located in the city center

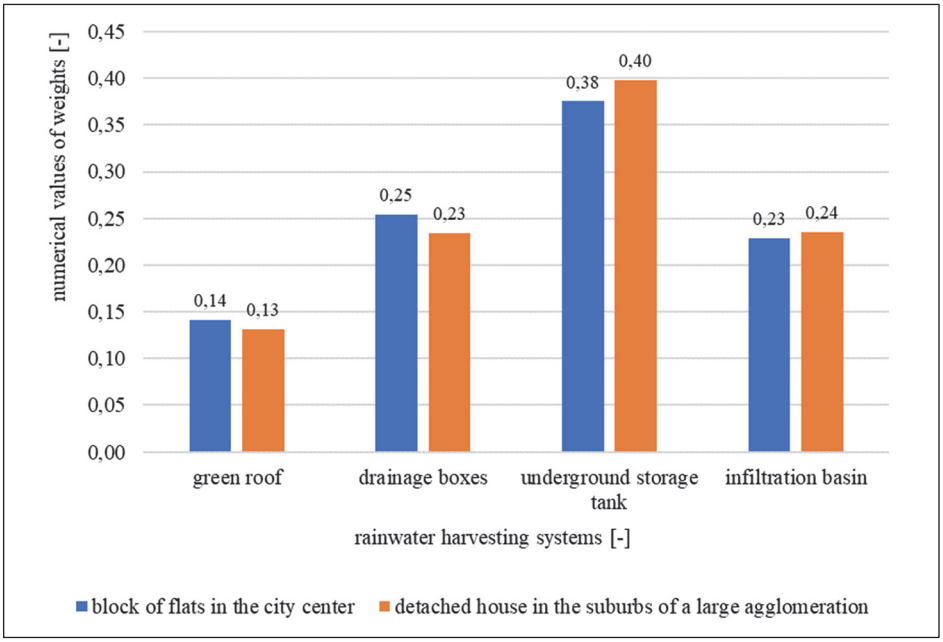

Fig. 5. The results of the global vector solving the problem of rainwater harvesting

Figure 5 shows the results (global vectors) obtained from the solution of all matrices describing the hierarchical tree for the two scenarios. The analysis carried out using the AHP method showed that for a detached house and a block of flats the most beneficial solution for rainwater harvesting is to use an underground storage tank (0.40 and 0.38). For a detached house located in the suburbs of a large agglomeration, the infiltration basin (0.24) was the second in the hierarchy of choice. In the third place were classified drainage boxes (0.23) and on the last place the green roof (0.13). A similar hierarchy of choice of solutions was characterized by the second scenario, for which the second most advantageous option was the use of drainage boxes (0.25), and the third was the construction of the infiltration basin (0.23). According to the analysis conducted using the AHP method, the green roof proved to be the least profitable rainwater harvesting system for the block located in the city center. It should be remembered that the results only represent the factors selected by the experts, which were considered in the AHP analysis. The use of the Multi-Criteria Decision Making (MCDM) method is connected with assigning particular factors and solutions to the weights and it is the experts who decide on the selection of criteria to be considered and their importance in resolution of a given problem.

4. Conclusions

The paper presents an analysis of the possibilities of rainwater harvesting for two different land-use scenarios using the multi-criteria AHP decision making method. In both cases, it can be concluded that the use of an underground storage tank is the best solution. This is mainly due to low construction costs, ease of exploitation and the possibility of reusing the accumulated water. According to the analysis, the systems which, should be used less frequently are the drainage boxes and the infiltration basin. Each of these solutions has its advantages but also disadvantages. Drainage boxes can be installed in different land-use conditions, their operation is not a problem and the cost of construction is not too high. The infiltration basin is characterized by an easy adaptation to the environment but more demanding construction. On the other hand, green roof proved to be the least advantageous solution mainly due to high construction costs and relatively high workload associated with exploitation. The analyses considered two different variants in terms of the land use: a detached house situated in the suburbs of a large agglomeration and a block of flats located in the city center. According to the analysis and the identified factors, in both cases, the best solution was to use an underground storage tank. This system proved to be the most advantageous due to the possibility of water reuse, low construction costs and ease of exploitation.

References

Aminbakhsh, S., Gunduz, M., Sonmez, R. (2013). Safety risk assessment using analytic hierarchy process (AHP) during planning and budgeting of construction projects. *Journal of safety research, 46,* 99-105.

Ariff, H., Sapuan, S., Ismail, N., Yusoff, N. (2008). Use of Analytical Hierarchy Process (AHP) for Selecting The Best Design Concept. *Jurnal Teknologi, 49,* 1-18.

Chen, M., Wang, Shih-Ching. (2010). The critical factors of success for information service industry in developing international market: Using analytic hierarchy process (AHP) approach. *Expert Systems with Applications, 37,* 694-704.

Chmist, J., Szoszkiewicz, K., Hämmerling, M. (2019). Selection of the most effective biological early warning system, based on AHP and Rembrandt Analysis. *Acta Scientiarum Polonorum Formatio Circumiectus, 1,* 95-102.

Chudzicki, J. (2018). Problems Of Rainwater Management: A Case Study Of The City Of Warsaw, Poland. *WIT Transactions on The Built Environment, 184,* 69-79.

Ghofrani, Z., Sposito, V., Faggian, R. (2017). A comprehensive review of blue-green infrastructure concepts. *International Journal of Environment and Sustainability*, 6, 15-36.

Hämmerling, M., Spychała, M. (2015). Wykorzystanie wielokryterialnej metody podejmowania decyzji (AHP) do wyboru przydomowej oczyszczalni ścieków z odprowadzaniem ścieków do gruntu. *Acta Sci. Pol. Formatio Circumiectus, 14*(4), 15-28.

Haq, S.A. (2017) Rainwater-Harvesting Technology. In: Harvesting Rainwater from Buildings. Cham: Springer.

Jokiel, P., Marszelewski, W., Pociask-Karteczka, J. (2017). Hydrologia Polski. Warszawa: PWN.

Kordana, S., Słyś, D. (2017). Analiza kryteriów warunkujących wybór optymalnego rozwiązania systemu zagospodarowania wód opadowych. *Proceedings of ECOpole, 10*(1), 183-191.

Kozioł, W., Piotrowski, Z., Pomykała, R., Machniak, Ł., Baic, I., Witkowska-Kita, B., Lutyński, A., Blaschke, W. (2011). Zastosowanie analitycznego procesu hierarchicznego (AHP) do wielokryterialnej oceny innowacyjności technologii zagospodarowania odpadów z górnictwa kamiennego. *Rocznik Ochrona Środowiska, 13,* 1619-1634.

Marcarelli, G., Squillante, M. (2019). A group-AHP-based approach for selecting the best public tender. Soft Computing, 1-8.

Martin, C., Ruperd, Y., Legret, M. (2007). Urban Stormwater Drainage Management: The Development of a Multicriteria Decision Aid Approach for Best Management Practices. *European Journal of Operational Research, 181*, 338-349.

Ptak, M., Sojka, M., Kałuża, T., Choiński, A., Nowak, B. (2019). Long-term water temperature trends of the Warta River in the years 1960-2009. *Ecohydrology & Hydrobiology 19(3),* 441-451.

Sakson, G. (2018). Cost analysis of a rainwater harvesting system in Poland. *E3S Web Conf. 45:* 00078.

Sendanayake, S. (2016). Rainwater Harvesting for Urban Living, ISBN:978-955-43389-0-6

Słyś, D., Stec, A., Zelenakova, M. (2012). A LCC Analysis of Rainwater Management Variants. *Ecological Chemistry and Engineering, 19*(3), 359-372.

Sojka, M., Kozłowski, M., Stasik, R., Napierała, N., Kęsicka, B., Wróżyński, R., Jaskuła, J., Liberacki, D., Bykowski, J. (2019). Sustainable Water Management in Agriculture-The Impact of Drainage Water Management on Groundwater Table Dynamics and Subsurface Outflow. *Sustainability, 11,* 4201.

Stachowski, P., Oliskiewicz-Krzywicka, A., Pasela, R. (2017). Miejski staw jako odbiornik ścieków opadowych. *Inżynieria Ekologiczna, 18*(1), 1-8.

Stefanidis, S., Stathis, D. (2013). Assessment of flood hazard based on natural and anthropogenic factors using analytic hierarchy process (AHP). *Nat Hazards* 68, 569-585.

Szwed, M. (2019). Variability of precipitation in Poland under climate change. *Theoretical and Applied Climatology, 135,*1003-1015.

Tokarczyk-Dorociak, K., Walter, E., Kobierska, K., Kołodyński, R. (2017). Rainwater Management in the Urban Landscape of Wroclaw in Terms of Adaptation to Climate Changes. *Journal of Ecological Engineering, 18*(6), 171-184.

Uyan, M. (2013). GIS-based solar farms site selection using analytic hierarchy process (AHP) in Karapinar region, Konya/Turkey. *Renewable and Sustainable Energy Reviews, 28,* 11-17.

Žuvela-Aloise, M., Koch, R., Buchholz, S., Früh, B. (2016). Modelling the potential of green and blue infrastructure to reduce urban heat load in the city of Vienna. *Climatic Change, 135,* 425-438.

Abstract

In the face of the current climate change, the increasing incidence of extreme weather events, prolonged periods of drought and water scarcity, attention should be paid to rational water management with particular emphasis on rainwater. Excessive development and sealing of urban catchments result in a faster outflow of water to the sewage system, which prevents it from reaching the soil and plants. This situation intensifies the drought effect and contributes to the occurrence of urban floods. In order to mitigate the negative impact of this process, solutions allowing for rainwater harvesting should be implemented. A wide variety of systems are currently available on the market to harvest and reuse rainwater. In the publication, the authors analysed four solutions: a green roof, drainage boxes, an underground storage tank, and an infiltration basin. The AHP (Analytic Hierarchy Process) method was used to select the best rainwater harvesting system, which is one of the methods of Multi-Criteria Decision Making. The analyses considered two different variants in terms of land use: a detached house located in the suburbs of a large agglomeration and a block of flats placed in the city center. According to the analysis and the assumed factors, in both cases, the best solution was to use an underground storage tank. This system proved to be the most advantageous due to the possibility of reuse of water, low construction costs, and ease of exploitation.

Keywords:
rainwater harvesting, Multi-Criteria Decision Making, AHP, green roof, drainage boxes, underground storage tank, infiltration basin

Analiza możliwości zagospodarowania wody opadowej z wykorzystaniem metody AHP

Streszczenie

W obliczu zachodzących obecnie zmian klimatycznych, występowania coraz częstszych ekstremalnych zjawisk pogodowych, długotrwałych okresów suszy oraz deficytu wody należy nacisk zwrócić uwagę na prowadzenie racjonalnej gospodarki wodnej ze szczególnym uwzględnieniem wód opadowych. Nadmierna zabudowa i uszczelnienie zlewni miejskich powoduje szybszy odpływu wody do kanalizacji, przez co nie trafia ona do gleby i roślin. Sytuacja ta potęguje zjawisko suszy, a także przyczynia się do występowania miejskich powodzi. Aby złagodzić negatywny wpływ tego procesu, należy wdrażać rozwiązania pozwalające na zagospodarowania wód opadowych. Obecnie na rynku dostępnych jest wiele różnorodnych systemów umożliwiających gromadzenie deszczówki oraz jej ponowne wykorzystanie. W publikacji autorzy przeanalizowali cztery rozwiązania: zielony dach, skrzynki rozsączające, podziemny zbiornik bezodpływowy oraz zbiornik infiltracyjny. Do wyboru najlepszego wariantu zagospodarowania wody deszczowej zastosowano metodę AHP (Analytic Hierarchy Process), która jest jedną z metod wielkokryterialnego wspomagania decyzji. W analizach rozważono dwa różne warianty pod względem zagospodarowania terenu: dom jednorodzinny znajdujący

się na przedmieściach dużej aglomeracji oraz blok zlokalizowany w centrum miasta. Według przeprowadzonej analizy oraz założonych czynników, w obu przypadkach najlepszym według rozwiązaniem było zastosowanie podziemnego zbiornika bezodpływowego. System ten okazał się najkorzystniejszy z uwagi na możliwość ponownego wykorzystania wody, niskie koszty budowy oraz łatwość eksploatacji.

Słowa kluczowe:
zagospodarowanie wody opadowej, metoda wielokryterialnego wspomagania decyzji, AHP, zielone dachy, skrzynki rozsączające, podziemny zbiornik bezodpływowy, zbiornik infiltracyjny

MIDDLE POMERANIAN SCIENTIFIC SOCIETY OF THE ENVIRONMENT PROTECTION

Rocznik Ochrona Środowiska

Volume 22. Year 2020 ISSN 1506-218X 308-323

Labels and Certificates for Green Hotels

Mariusz Cembruch-Nowakowski
Pedagogical University of Cracow, Poland
corresponding author's e-mail: mariusz.cembruch-nowakowski@up.krakow.pl

1. Introduction

Tourism is one of the largest industries in the world, creating employment, driving exports and creating prosperity in the destination regions. At the beginning of 2020 the tourism industry has generated 10.4% of global GDP (increase by 3.9% in comparison to 2019) and provided 319 million jobs (Travel & Tourism Economic Impact Report 2019). The World Travel Organization (WTO) predicted that around 1.6 billion tourists will travel in 2020. Unfortunately, Covid-19 pandemic had a devastating impact on the tourism that industry in 2020 and it may affect the industry in the coming years. In May 2020 WTO revised its forecasts, estimating that the number of trips by the end of 2020 could fall of about 60-80% (65% decrease in the number of foreign tourists arriving in the first half of the year) compared to the previous year, which could result in a fall in export earnings at the end of the year of 0.91-1.2 trillion dollars[1].

The hotel industry is one of the leading players in this sector. However, hotels activities, apart from their leading role in the development of tourism and a positive impact on the economy, have also a negative impact, primarily on the environment. That is associated with high consumption of water resources, energy, carbon dioxide emissions and waste generation (e.g. Gossling & Hall 2005, Kasim 2007, Dominiak 2009, Gossling 2015, Cembruch-Nowakowski, 2019). In the face of global climate change, there is a growing need to intensify pro-ecological activities limiting the negative impact of enterprises and service providers, including hotels, on the environment. For many hotels, reduction of natural resources consumption and recycling constitute an important part of their competitive strategy (Potoski & Prakash 2005, Wang 2012). One of the approaches

[1] International Tourist Numbers Down 65% in First Half of 2020, UNWTO. Retrieved from: https://www.unwto.org/taxonomy/term/347/7/11/2020

helping to achieve these involves systematization of pro-ecological activities by introducing at least minimum requirements regarding the need to apply the principles of sustainable development by all participants of the supply chain in tourism. In the hotel industry this could mean the introduction and application of environmental management systems (Gryszel, Jaremen, Rapacz, 2008 p. 368) based on the green hotel concept and the eco-certification. These will provide the opportunity to authenticate the efforts and allow the standardization of hotel facilities in the dimension of pro-ecological activities reflecting both; the care for the environment as well as the Corporate Social Responsibility, that of course has a wider meaning than just protecting the environment.

The quality of the various hotel services are ensured by the system of certificates. However, there are many different standards and it is difficult to compare and integrate various systems of certification. The certification procedures are costly and there are regions of the world where hotels do not have certificates. One can observe, however, that due to the fact that recent decades brought about the general reflection on the need to concentrate on the ecological aspects of hospitality industry functioning, especially the hotel sector, there is a growing interest of hotel owners to increase guests' awareness on the various ecological approaches undertaken by them. Also, the hotel guests are more interested in using the services of green hotels (Cembruch-Nowakowski 2019).

Ecolabels constitute relatively novel dimension of marketing communication, creating an opportunity for entrepreneurs to distinguish themselves from the competitors and increase the brand's value. To make the brand more visible and to communicate the ecological awareness the sets of standards are needed. Certification is an element of building trust and business credibility. However, it should be remembered that certification should be integrated into the corporate social responsibility (CSR) strategy, which in the long run is expected to be beneficial both for the company and for the society. Although there is no consistent system of ecological standards number of labels and certificates promoting pro-ecological and sustainable development of the hospitality sector have been proposed.

This paper reviews the set of highly recognized labels and certificates defining the environmental standards and the wide range of activities oriented on the implementation of good sustainable development practices in tourism, with the emphasis on hotel's activity.

2. Nature of Eco-certification and Eco-labelling

According to Bellson, "to certify is to authenticate or verify in writing or to attest as being true or as meeting certain criteria. A certification mark is statutorily defined as indicator that goods or services in connection with which the mark is used, are certified by proprietor in respect of origin, material, mode of

manufacture of goods, or performance of service, quality, accuracy or other characteristics" (Bellson 2017, p. 40-41) The certificates "…are treated legally as special forms of trademarks. The processes of examination, registration and provisions for redress when infringed are all integrated into the trademark statutes of the world" (Bellson 2017, p. 32).

Eco-certification can therefore be defined as a strict procedure that checks and assesses whether a given product, service or process meets specific environmental standards or requirements. The products, services, processes or providing them legal entities can be granted the certificate after passing the certification procedure ensuring that they meet high standards. Certificates are usually issued by accredited institutions or entities enjoying general trust, fully independent from the entities applying for a certificate. The International Organization for Standardisation (ISO) has defined three general types of voluntary labels. Type I and III are indeed the ecolabells, as they are awarded to the entities which meet the requirements of multi-criteria procedure carried out by authorities assessing and quantifying environmental data of a products using life cycle approach[2]. Eco-labels are usually graphic markings in the form of a logo which indicate that the product, service or entity providing them has met the required environmental criteria and complies with clearly defined safety standards approved by the appropriate certification procedure.

Both eco-certificates and eco-labels can be of international nature such as e.g. ISO 14001, GSTC or Green Globe Certificate or can be recognized only locally, e.g. 'Nature's Best Sweden'. The processes of eco-certification or ecolabelling can involve the procedures accredited by a state institution but they can also be initiated and conducted by non-profit organizations: associations, foundations or other entities. It is worth mentioning that Germany is the precursors of eco-labeling. Already in 1978 the Germany's government initiated the 'Blue Engel' labeling program which aimed to set high standards for the design of environment-friendly products.

Thus the certification can be focused only on products, such as in the case of 'Blue Engel' certification, on services and processes in the enterprise, e.g. management as it is in the case of the Green Key Global label or on the objects or destinations such as the 'Energy Star' program or 'Green Seal', respectively. The objectives of eco-certification or eco-labeling can be diverse. It can include the endemic areas protection or care for natural diversity but also increase the effectiveness of dissemination of the concept of sustainable development, expansion and standardization of pro-ecological activities and the aforementioned corporate social responsibility, increase in the competitiveness of regions and

[2] Retrieved from: https://globalecolabelling.net/what-is-ecolabelling/#types/2019/10/14

entrepreneurs, increase of ecological awareness and improvement or maintaining the general well-being of a given community, including nurturing local culture or promoting ecological programs and ensuring their recognition.

For example, the 'Green Key' eco-labeling program is focused, among others, on hotel activities and has four main goals: environmental and sustainable education of the owner, the staff and the client, environmental and sustainable preservation by the reduction of the impacts of the facility, economical management as a reduction of the consumption induce a reduction of the costs and marketing strategy with the promotion of the label and the facilities awarded[3]. It is thus easy to perceive that the above-mentioned goals adopt complex approach by considering environmental, organizational and social orientation.

3. Benefits of using Eco certification or Ecolabeling

The benefits of introducing and using Eco-Certification and Eco-labels can be identified in several dimensions: environmental, socio-cultural, organizational and also economic. The environmental benefits cannot be underestimated; first of all it should be pointed out that every environment-friendly activity has a positive impact on nature and people. However, the main benefit of using Eco-certification is the contribution to the harmonization of pro-environmental and pro-social activities of various entities, and providing support to the sustainable development in the region. From the social side, it increases the ecological awareness of society (e.g. Poskrobko 2007, Nycz-Wróbel 2012) while contributing to the increase of the well-being of society and the given community by protecting nature and natural resources, as well as, the cultural heritage and traditional values. It also increases the level of social trust in relation to state institutions or entrepreneurs supplying certified products or services.

The main beneficiaries of eco-certification are the owners of these certificates or Eco-labels, i.e. entrepreneurs and service providers. They support the enterprise management system from the substantive side, mainly in the areas covered by certification. Compliance with the principles and requirements established by the certifying authority facilitates the increase in the efficiency and effectiveness of enterprises in various areas of their activities covered by certification, e.g. by reducing the operating costs, strengthening the organizational culture, and increasing the competitive position of the beneficiary. It provides tools to educate employees and can increase their sense of satisfaction, pride from belonging to an organization that adheres to the principles of sustainable development that is environment-friendly. It also creates the opportunity to raise employees' awareness of the importance of introduced environmental requirements and

[3] Retrieved from: https://www.greenkey.global/criteria/2019/10/14

increase their efficiency in the implementation of tasks or consolidate the desired behaviour of employees in the area (subject to certification). It supports strengthening of organizational culture and facilitates employees' acceptance of new operating conditions. It contributes to increasing the image potential of the company, which means that it contributes to strengthening or improving the positive image of the company both in the external environment and among the company's employees. It facilitates the transfer of good practices in respect to the environment and values related to social responsibility to other participants in the supply chain and stakeholders of the company. It leads to an increase in the company's competitiveness in the area of quality and image by promoting positive enterprise activities and social responsibility.

Consumers represent the social side, however, their position is very much associated with the business of the company because they are the main addressees of its basic activities. From the consumer's side therefore Eco-certification facilitates the decision processes regarding the choosing a supplier of environment-friendly products.

The eco-certification or eco-labelling increases the availability of information on the implemented ecological activities or on the benefit of the society of an enterprise / supplier of products and services. It is also important as it increases consumer confidence that the company's declarative space is consistent with the praxeological space in terms of environment-friendly activities.

The economic dimension of benefits is manifested in the use of a more responsible management of natural resources, reduction of social costs associated with avoiding exploitation and environment- unfriendly production (see Berger, 2015), increase the technical level and involvement in the development of new clean innovative technologies/processes.

4. Eco-labelling procedures

The Eco-certification process is generally based on a simple, multi-step algorithm. The starting point involves selection of an accredited certifying authority, which will then carry out an environmental analysis and initial environmental audit of the entity applying for the certificate/label.

The aim of the audit is to determine and evaluate the level of implementation of the requirements of the certifying authority defined as the environmental objectives and tasks that the beneficiary has to meet to obtain the certificate. After the assessing of implementation by the entity the actions aimed at achieving environmental goals and while determining the level of that process the final environmental audit is completed and the certificate is awarded.

According to research results published by the Word Resources Institute the certification processes carried out within various eco-certification programs

lasted from several days to several dozen months, with more than 74% of the 340 certification programs tested, taken between two weeks up to six months[4].

The obtained certificate is granted for defined period of time (usually 2-5 years) but during that time the entity is subjected to cyclic inspections within the so-called internal audits that are aimed to monitor the quality standards of already implemented procedures in accordance with the environmental requirements of the defined certification program (Fig. 1). When the certificate validity period is ending, the entity may undergo again a comprehensive testing procedure called a recertification audit in case it intends to extend the certificate.

An example of such an approach is the 'Green Key' certification process, the 'Green Globe Certificate' or the 'Clean Tourism' certificate awarded by the Partnership for the Environment Foundation.

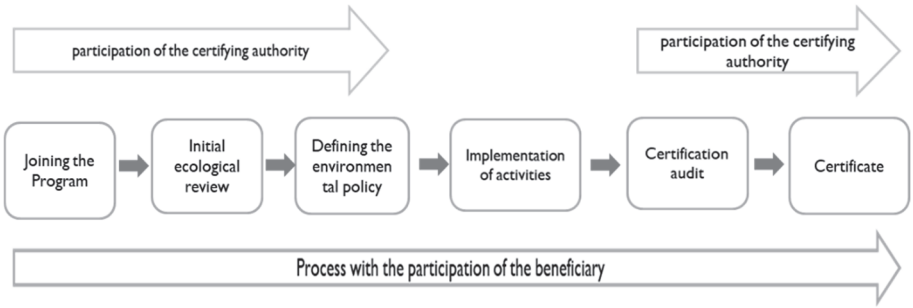

Fig. 1. The example of the certification process. (Own work based on literature)

4.1. Criteria of ecolabeling

The eco-certification systems are based on wide range of criteria allowing to evaluate the compliment of hotel activity to the ecological standards. Usually these criteria are based on already functioning systems designed by prestige international organizations such e.g. Global Sustainable Tourism Council, OECD, EU and consider the environmental standards. The sets of criteria which have to be considered while evaluating environmental aspects of hotel activity are strongly dependent type of the hotel. The parameters which have to be taken into account involve the size of the entity (large hotel chain vs hostel or bed and breakfast) and type of extra services offered, e.g. restaurant, catering, social events. There is, however, the set of criteria which have to be always considered during the certification procedure. They include:

- development and implementation policy including the environmental awareness,

[4] Retrieved from: http://www.ecolabelindex.com/downloads/Global_Ecolabel_Monitor 2010.pdf/2019/11/17

- rational energy management (heat and electricity),
- economical water management, regulated sewage management,
- regulated waste management, waste segregation,
- having an efficient ventilation system and monitoring CO_2 emissions,
- development of green areas around the object,
- care for the preservation of the local natural and cultural heritage,
- environmental education of tourists and employees,
- ethical business conduct.

5. Selected Labels and Certificates suited for green hotels

The aim of the studies presented here was to review the existing programmes used for environmental certification with the emphasis on these addressed to hotel industry, identify the institutions entitled to carry out the certification programmes, their role and importance for the development of the sector.

In order to reach that goal the following research questions were formulated: 1) Which institutions are entitled to perform the certification procedure and to issue the eco-certificates and eco-labels? 2) What kind of criteria the entity has to meet to obtain the given eco-certificate/label, 3) Is the eco label/certificate valid locally, internationally or globally.

The studies were carried out using the internet content. In order to create the list of eco-labels and eco-certificates important for hotel industry the set of 110 eco-labels listed in Global Ecolabel Monitor 2010 published by World Resources Institute and 464 records of eco-certificates listed in Ecolabel Index were considered. After excluding the overlapping records the final list of 468 positions was analysed. To identify the eco-program the set of the following key-words was used: hotel, hotel industry, motel, hostel, hospitality, tourism, tourism business and agrotourism. One has to be aware that the methodology used is oriented towards analysis of the more visible, generally functioning certificates/labels while some of local ones can be neglected. Based on such analysis it was found that from 468 programmes of certifications (excluding the most general ones: ISO 14001 or ISO 26000, ISO 50001)[5], only 44 deal with eco-certification. They are oriented on certification of production and services offered by various sectors of the economy. Some of them are targeted towards widely defined tourism, evaluating various destinations, resorts, marines (e.g. Quality Coast, Vista). Only 18 of eco-labels/eco-certificates (what accounts for less than 4% of all) are directly devoted to the hotel industry. About 28% of them have a global nature, 39%

[5] ISO 14001, ISO 2600 czy ISO 50001 are usually a normative reference and override the eco-certification programs run by third-party certifying organizations. However, they can themselves be used as ecotags directly used for the certification of hotel facilities.

function in several countries while 33% have a local, national character. They were established in a period of time 1989-2007. The oldest one is the global Green Seal certificate while the youngest one is Travelife. All certificates analysed were manager by non-profit organizations functioning as so called third-party. They were based on ISO 14024, ISO 2600, ISO 14020, ISO19019, ISO17021 standards and accreditation of GSTC (Global Sustainable Tourism Council). The range of evaluating and advisory activities carried out by the auditing organization was very similar and usually involved complex analysis of hotel activities concentrating on organization management, human resource management and organizational culture, management of material resources and environmental issues that belong to the corporate social responsibility. The certification process although is quite demanding for the entities under evaluation is very beneficial for them. The certificate awardee can use it for the promotion purposes. It is also introduced to the reference list of the organization responsible for the certification process and co-operating organizations e.g. Tourist advisors. The added value of certification process is that that it usually brings the changes in relations between the management and staff of the hotel as well as between hotel staff and customers.

5.1. Examples of the most popular eco-labels and eco-certificates used in hotel industry

The most popular certificate is the **EcoLabel,** known as EU Flower, developed by the European Union in 1992 year and recognized by the majority of the European travelers[6]. Mandatory criteria which hotel has to fulfill to be allowed to use the EcoLabel include: limited energy consumption, limited water consumption, reduced waste production, use of less hazardous to the environment, renewable resources and substances and promotion of environmental education and communication. and reducing the environmental impacts of the production and processing of food and drinks as the last link in the distribution process.

The international hotel chains are often using the **Green Globe Certificate**[7]. Located in USA, the Green Globe organization operates under the license from Green Globe Ltd UK, the owner of the worldwide brand. The Green Globe Certificate is currently being recognized intercontinentally in 83 countries. It consists of 44 mandatory criteria and over 380 compliance indicators. The indicators vary to some extent by geographical area and include local factors to ensure the harmonization with locally developed standards while maintaining the core criteria. The hotels have to satisfy requirements regarding not only the environmental issues by conservation of resources, reduction of pollution, conservation of

[6] Retrieved from: https://ekonsument.pl/s222_ecolabel_european_flower_html/2019/11/14
[7] Retrieved from: https://www. greenglobe.com/green-globe-certification/2019/11/16

biodiversity, ecosystems and landscapes but also introduce the sustainable management involving implementation of sustainability management system, ensuring legal compliance, effective employee development/training and management, customer satisfaction, accuracy of promotional materials and supporting local entrepreneurs, as well as respecting local communities, promoting local culture and cultural heritage. The Green Globe Certificate is granted for one calendar year and can be renewed based on the on-site assessment by appointed qualified independent auditor. The procedure is quite expensive. Located in Poland, the Intercontinental hotel in Warsaw was awarded the Green Globe Certificate.

Green Key is a voluntary eco-label awarded to around 3200 hotels and other touristic sites in 65 countries worldwide[8]. The program promotes sustainable tourism and aims to contribute to the prevention of climate change by awarding hotels with positive environmental initiatives. It aims on rise of ecological awareness of hotel staff and clients, introduces sustainable methods of operation and technology, reduced usage of resources and energy. The program was initiated in 1994 by nongovernmental organization in Denmark. Currently it operates in 40 countries and continues to grow in numbers and spread across the world. Hotels can be awarded a Green Key label when they adhere to national or international Green Key criteria. 130 criteria of 13 categories consider the environmental management (water, waste, energy, use of chemicals), technical demands, and initiatives for the involvement and awareness of guests, staff and suppliers, corporate social responsibilities, green activities, etc. [9]. The national criteria include the local legislation, infrastructure and culture. The Green Key label can be granted for one year at the time.

Travelife system was initiated in 2007 by British Travel Association (ABTA) and Dutch Association of Tourists Offices (Algemene Nederlandse Vereniging van Reisondernemingen) *(ANVR) supported by Metropolitan University (UK), University of Lund (Sweden) and* European Centre for Ecological and Agricultural Tourism (*ECEAT) – Dutch non-profit organization promoting sustainable development in tourism*[10]*. Travelife methodology is a product of the LIFE project supported by the European Union. The core of that approach is based on the sustainable development concept proposed by the* United Nations Environment Programme (UNEP) and Tour Operators' Initiative (TOI). It promotes sustainability in tourism. Hotel sustainability system is based on 163

[8] Retrieved from: https://www.greenkey.global/our-programme /08/10.2020

[9] Green Key International. Eco-label for hotels and tourism facilities. Retrieved from: https://static1.squarespace.com/static/55371f97e4b0fce8c1ee4c69/t/5e5c c98a9c441026dcb74bc6/1583139230835/Green+Key+Brochure+2020.pdf/09/10/2020.

[10] Retrieved from: http:// http://www.travelifecollection.com/certification/2019/10/09

management, environmental and social criteria in Gold Award (valid from January 2016) and 302 criteria in Gold Award of Excellence.

The criteria formulated for the management are in agreement with ISO 14001, while these concerning the business activity are in agreement with ISO 26000. Also, the OECD guidelines regarding the social responsibility, including human rights, working conditions, environmental protection, biodiversity and honest rules of doing business have to be taken into account while formulating criteria for Travelife certification. Certification program involves three steps. In the first step, in order to acquire the Travelife Status hotel has to undertake the commitment and establish sustainability mission statement, appoint a sustainability coordinator/manager, define job specifications and role profiles. The coordinator is granted a personal Travelife certificate and he/she introduces the good sustainability practices. When the baseline review on the situation in hotel indicates that the hotel operates according to the rules of sustainability development it can be risen to the status of Travelife Partner. Such hotel is entitled to use the logo of Travelife Partner and can take the necessary steps towards the Travelife Certificate. In the third step the online assessment system is carried out. That is followed by the audits performed by third parties - the independent auditor pays on-site visit and assesses the level of compliance with the international criteria of Travelife. When the results of the evaluation are positive the hotel is awarded Travelife Certificate.

Depending on the level of compliance with the standard, the bronze, silver or gold certificate is issued. There are already 17 000 hospitality objects world-wide which have registered to the program since it was initiated, from which 1500 have carried out the necessary audit and 500 were awarded the Travelife label. Travelife is a registered trademark and is owned by ABTA Ltd, London, UK. Travelife system is administrated by non-profit organization located in The Netherlands and supported by British Travel Association (ABTA).

Green Seal Certification is dedicated to businesses and services which meet the Green Seal standards[11]. There are various sets of criteria that have to be met in order to obtain different levels of sustainability (bronze, silver, gold). The process includes annual compliance monitoring and a commitment for continuous improvement.

The certification is dedicated to hotels and lodging properties. The Standard was created 1989 and focuses on waste minimization, management of freshwater resources, energy conservation and management, wastewater management, pollution prevention, environmentally sensitive purchasing. The certification is

[11] Retrieved from: https://greenseal.org/green-seal-standards./2019/11/07

focused on raising the awareness of property owners, their employees, and their guests.

Green Tourism is a non-profit organization established in 1997. Their mission is to encourage and enable decision makers the sustainable choices that reduce their impact on the planet[12]. Certificate covers all aspects of sustainability, from energy and water efficiency, waste management and biodiversity to social and ethical choices.

In addition to certification of international importance, there are also certificates of local range or on the regional level among which the following examples can be mentioned: European Ecotourism Labeling Standard (EETLS), Certification for Sustainable Tourism (CST) for hotels – Costa Rica, Chile Sistema de Distinción en Turismo Sustenatable – Chile, Eco-Certification Malta, Fair Trade Tourism – South Africa, Ecotourism Ireland Certification Programe, Hoteles + Verdes (AHT) – Argentina, Green Star Hotel Certificate – Egypt or the Japan Environmentally Sustainable Accommodations International Standard (ESAIS).

Depending on the type of hospitality properties the managers/owners are interested in various certification programs. While some of them are popular in all hospitality sector, certain are addressed only to the large hotel chains due to the cost of certification and the impact expected. Table 1 presents selected labels and certification programs in relation to the form of hotel business.

Clean Tourism Certificate is a local initiative developed by Polish Environmental Partnership Foundation. The program aim at alignment of activities of Polish hotel owners/manages to the European and global environmental standards. The criteria used in the evaluation process include limitation of the harmful impact on the environment by decreasing and monitoring the level of CO_2 emission, implementation of the organizational and technical improvements in organizational and human management, resource management and relation with stakeholders. The participants of the certification process are getting continuous support. They can also participate in the nationwide initiative aimed at exchange of experiences and promotions. The certificate is awarded by Certification Commission of Polish Environmental Partnership Foundation functioning under supervision of Pure Tourism Certification Chapter.

Table 1 presents classification of eco-certificates based on the type of hotel activity: large hospitality chains, bed and breakfast and independent properties or hostels. AS can be noticed various hospitality sectors apply and comply to the criteria of various accreditation schemes. Such differentiation is justified considering

[12] Retrieved from: https://www.green-tourism.com/about/2019/11/09

the complexity of certification procedures and the costs involved (accreditation fee, additional annual fee based on the turnover of Ecolabeled hotel).

Table 1. Labels and certificates in relation to the form of hospitality business; Source: Own work based on literature

Large hospitality chains	Bed and Breakfasts	Hostels and small accommodations
Audoban International Bio Hotels Earth Check Ecolabel Green Globe Green Key Green Key Global Green Seal Green Tourism Green Tourism Business Scheme Travelife TripAdvisor GreenLeaders	Audoban International Bio Hotels Clean Tourism Earth Check EcoHotels Certified Ecolabel Ecolabel Luxemburg Green Globe Green Key Green Key Global Green Seal Green Tourism Green Tourism Business Scheme Nordic Ecolabel or "Swan" Travelife TripAdvisor GreenLeaders	Bio hotels Clean Tourism EcoHotels Certified Ecolabel Ecolabel Luxemburg Green Key Green Key Global Travelife Green Tourism Green Tourism Business Scheme Nordic Ecolabel or "Swan" TripAdvisor GreenLeaders

Table 1 presents selected certification programs for the hotel industry divided into three criteria for accommodation facilities. The aim of this procedure was to show the comprehensiveness of the eco-certification and eco-labeling approach to the accommodation business, hence the inclusion of the hostel sector and small accommodation facilities, which are an important contribution to the occupancy rate of the accommodation business and thus also to the ecological footprint created by the hospitality industry.

6. Conclusions

Considering the high impact of hospitality sector on environment it is necessary to develop ecological standards of best practices. Many hotel owners try to decrease the negative effects of hotel functioning. At the same time there is a growing number of clients who are interested in choosing the green hotel rather than the standard one. Unfortunately, the access to the information regarding that dimension of hotel activity is not easy. Thus there is a need to develop easily accessible/visible labels for eco-friendly hotels. Several examples of these have been presented in a current paper. One can hope that in the near future the quality standards of the hotels expressed in the number of stars will be accompanied by the eco-label.

Until recently it was expected that in the near future the hotels quality standards expressed in the number of stars will be accompanied by eco-labels. Unfortunately, the prolonged Covid-19 pandemic may significantly slow down these processes. Nevertheless, the certification itself is gaining interest and can be also important during the pandemy. Various actions involving eco and safety procedures are proposed by the international and national tourism organizations that may provide security to the visitors/guests while mitigate the effects of the pandemy on the tourism industry. For example. UNWTO formulated the Global Guidelines to Restart Tourism, with the aim to help the sector to emerge stronger and more sustainable from the COVID-19 crisis. The Polish Tourism Organization developed the project entitled "Rest in Poland – safe (Odpoczywaj w Polsce – bezpiecznie) aimed at increasing tourists' confidence in services offered by accommodation facilities by introducing new certification procedures ensuring a high level safety of offered services in accordance with GIS guidelines[13].

References

Bellson, J. (2017). *Certification and Collective Marks. Law and Practice. Elgar Intellectual Property of Law and Practice*. Cheltenham, Glos: EEP Ltd., UK. DOI: 10.4337/9781785368806

Berger, S. (2015). K.William Kapp's Theory of social costs. History of Political Economy (2015) 47 (suppl_1): 227-252. Retrieved from: https://read.dukeupress.edu/hope/article-abstract/47/suppl_1/227/38842/K-William-Kapp-s-Social-Theory-of-Social-Costs?redirectedFrom=fulltext. Doi:10.1215/00182702-3130523

Bügler, T. (2013). Handbook to achieve the ISO 14001 Certification in the Hotel Industry, Thesis presented to the Department of Bachelor Studies of the University of Applied Sciences HTW Chur , Switzerland.

[13] Turystyka a pandemia – jakie wsparcie otrzymały firmy turystyczne? Retrieved from: https://www.radoczapark.pl/blog/blog/turystyka-a-pandemia-wsparcie-otrzymaly-firmy-turystyczne/7/10/2020.

Cembruch-Nowakowski, M. (2019). Green Hotels – Exception or Norm? *Prace Komisji Geografii Przemysłu Polskiego Towarzystwa Geograficznego [Studies of the Industrial Geography Commission of the Polish Geographical Society], 33*(3). DOI: https://doi.org/10.24917/20801653.333.11

Commission Decision of 2009/578/EC of 9 July 2009.

CSVE (2013): Statistics of wind projects in the EIA process [online]. Czech Association of Wind Energy website [cit. 17.05.2011]. Retrieved from: https://www.csve.cz/clanky/statistikapoctu-projektu-vetrnych-elektraren-v-procesu-eia/347>

Deming, W.E. (1950). *Elementary Principles of the Statistical Control of Quality*. JUSE.

Dominik, P.(2009). Zrównoważony rozwój. Ekologia w hotelarstwie i gastronomii. *Przegląd Gastronomiczny, 4*.

Gössling, S. (2015). New performance indicators for water management in tourism. *Tourism Manage, 46*, 233-244.

Gössling, S., Hall, M.C. (2005). *Tourism and global environmental change: Ecological social, economic and political interrelationships.* Contemporary Geographies of Leisure Tourism and Mobility. http://ecolabelindex.com/downloads/Glo-bal_Ecolabel_Monitor2010.pdf

http://greenseal.org/green-seal-standards.

http://odpowiedzialnybiznes.pl/hasla-encyklopedii/iso-26-000/

http://travelifecollection.com/certification

http://tripadvisor.com/GreenLeaders

https://acca-spa.com.

https://biohotels.info/en/holiday-regions.

https://ekonsument.pl/s222_ecolabel_european_flower_.html

https://globalecolabelling.net/what-is-eco-labelling/#types/

https://greenglobe.com/green-globe-certification.

https://greenkey.global/criteria.

https://greenleafecostandard.net/the-standard.html

https://static1.squarespace.com/static/55371f97e4b0fce8c1ee4c69/t/5e5cc98a9c441026dcb74bc6/1583139230835/Green+Key+Brochure+2020.pdf/ 09/10/2020.

https:ecolabelindex.com/ecolabels/

International Tourist Numbers Down 65% in First Half of 2020, UNWTO. Retrieved from: https://www.unwto.org/taxonomy/term/347 /7/11/2020

Kasim, A. (2007). Towards a Wider Adoption of Environmental Responsibility in the Hotel Sector. *International Journal of Hospitality & Tourism Administration, 8(*2), 25-49, DOI: 10.1300/J149v08n02_02

Luttropp, C., Lagerstedt, J. (2011). Design and The Ten Golden Rules: generic advice for merging environmental aspects into product development. *Journal of Cleaner Production, 14*, 1396-1408. DOI: 10.1016/j.jclepro.2005.11.022.

Nycz-Wróbel, J. (2012). Świadomość ekologiczna społeczeństwa i wynikające z niej zagrożenia środowiska naturalnego (na przykładzie opinii mieszkańców województwa podkarpackiego). Rzeszów. *Zeszyty Naukowe Politechniki Rzeszowskiej. Ekonomia i Nauki Humanistyczne, 286*.

Para, A. (2013). Zasady zrównoważonego rozwoju turystyki – bariery i szanse dla branż. Warszawa: Szkoła Główna Handlowa. *Zeszyty Naukowe. Turystyka i Rekreacja*.

Poskrobko, B. (red.). (2007). Zarządzanie środowiskiem. Warszawa: *PWE*.

Potoski, M.; Prakash, A. (2005). Green Clubs and Voluntary Governance: ISO 14001 and Firms' Regulatory Compliance. *American Journal of Political Science, April, 49(2*), 235-248.

shttps://ec.europa.eu/environment/ecolabel/index_en.htm.

shttps://ecolabelindex.com/ecolabel/green-globe

Turystyka a pandemia – jakie wsparcie otrzymały firmy turystyczne? (2020, October 7). Retrieved from: https://www.radoczapark.pl/blog/blog/turystyka-a-pandemia-wsparcie-otrzymaly-firmy-turystyczne.

Turystyka Odpowiedzialnie, Pierwszy w Polsce branżowy serwis poświęcony turystyce odpowiedzialnej i zrównoważonej. Magazine Basic created by c. bavota, 2015

Wang, R. (2012). The investigation of Green Best Practices for Hotels in Taiwan. *Procedia – Social and Behavioral Sciences, 57*, 140-145.

Abstract

The last decades brought about the environmental awareness of hotel customers and owners resulting in reflection on the need to introduce pro-ecological changes in practices and services offered by the hospitality sector. The idea of "green hotels" is generally accepted. To structure these positive changes and to help customers to select hotels supporting pro-ecological practices one needs to establish clear and easy to understand system communicating the level of particular hotel involvement in that concept. These is evaluated by certification institutions and organizations. Their activities involve certification and labelling and they are also part of practices related to the implementation of sustainable development in tourism. Wide range of criteria considered by certification organizations include these related to environmental protection, alternation of the negative effects of improper management of natural resources, as well as, the so-called corporate social responsibility. Unfortunately, there is no consistent system of ecological standards. The current paper provides an overview of the most important labels and certificates promoting the pro-ecological and sustainable development of the hotel sector. It also analyses selected, leading eco-certification systems in terms of their applicability in various hotel segments.

Keywords:
certificates, ecolabels, green hotels, hospitality sector, pro-ecological practices

Etykiety i certyfikaty w zielonych hotelach

Streszczenie

Ostatnie dziesięciolecia przyniosły wzrost świadomości ekologicznej zarówno właścicieli hoteli jak i gości hotelowych wskazującą na potrzebę wprowadzenia zmian pro-ekologicznych w sposobie funkcjonowania i usługach oferowanych przez hotele. Powszechnie zaakceptowano koncepcję „zielonych hoteli". Istnieje potrzeba usystematyzowania działań podejmowanych przez właścicieli hoteli i ułatwienia gościom hotelowym decyzję dotycząca wyboru hoteli zachowujących standardy pro-ekologiczne. Wciąż brak jest spójnego systemu standardów ekologicznych. Problem ten próbują rozwiązać instytucje i organizacje wydające eko-certyfikaty i eko-etykiety. W swych działaniach stosują one szerokie spektrum kryteriów związanych z ochroną środowiska, ograniczeniem negatywnych efektów niewłaściwego zarządzania a także społecznej odpowiedzialności biznesu. W niniejszej pracy dokonano przeglądu najważniejszych certyfikatów i etykiet promujących praktyki pro-ekologiczne i działania zapewniające zrównoważony rozwój w sektorze hotelarskim. Przeprowadzono także analizę wskazującą na potrzebę doboru typu certyfikacji do danego segmentu hotelarstwa.

Słowa kluczowe:
certyfikaty, eko-etykiety, proekologiczne praktyki, sektor hotelarski, zielone hotele

MIDDLE POMERANIAN SCIENTIFIC SOCIETY OF THE ENVIRONMENT PROTECTION

Rocznik Ochrona Środowiska

Volume 22. Year 2020 ISSN 1506-218X 324-346

The Water Balance in a Dam Reservoir – a Case Study of the Przebędowo Reservoir

Błażej Waligórski[1], Mariusz Korytowski[2], Adam Zydroń[2], Daniel Liberacki[2], Michał Fiedler[2], Rafał Stasik[2]*

[1]State Water Holding Polish Waters; Regional Water Management Authority in Poznań, Poland

[2]Poznań University of Life Sciences, Poznań

[*]corresponding author's e-mail: mariusz.korytowski@up.poznan.pl

1. Introduction

Extreme weather events, particularly droughts, frequently contribute to disturbances in the natural water balance (Characteristics… 2007). As it was reported by Wibig (2012), the present-day climate warming, in Poland manifested in an increase of temperature in the second half of the 20th century by almost 1°C, has led to a growing risk of water deficits. Climate warming results in an increased potential evaporation, which at practically unchanged precipitation totals causes a reduction of the climatic water balance. According to Radzka (2014), in central and eastern Poland in the months of the vegetation season the frequency of negative climatic water balances is 2-fold greater than the incidence of positive balances. The negative values of this index have been recorded most frequently in the spring months, while the positive balances have been most common in September.

For this reason it continues to be of paramount importance to conduct research on water balances both for entire catchments and reservoirs located in such catchments. However, it needs to be stressed here that at the end of the 20th century very few studies concerned water balances of lakes in Poland; as indicated by Choiński (1995) due to problems in preparing water balances for lake waters such case studies were conducted for only several dozen of lakes in Poland.

Depending on the character of a given reservoir the water balance equations may take more or less complex forms. In relation to dammed reservoirs, which location in the river continuum frequently leads to changes in the previous hydrologic conditions, a reliable characterisation of water balance components is often a complicated process. According to Gruszczyński et al. (2009), one of the most

significant changes in the filtration area as a result of damming is related to a unique situation found in the immediate vicinity of the damming structure. This is the site, where hydrogeological conditions have been drastically altered, as it combines the areas with an unchanged drainage base (the region downstream of the damming structure) and areas with a maximum rise of water levels (the region upstream of the damming structure). As it was reported by Traczewska (2012), dammed reservoirs exhibit many characteristics distinguishing them from natural lakes or rivers, and thus they constitute a separate category of surface water bodies.

A reliable determination of individual components of the water balance for a given water body or reservoir not only provides information on its functioning, but also makes it possible to assess its available water capacity. According to Szczykowska and Siemieniuk (2011), water retention in reservoirs, including dammed reservoirs, generally contributes greatly to a marked improvement of the balance of water resources.

In view of the threats related to drought all measures aiming at the determination of the water balances for reservoirs may contribute to the limitation of the adverse effects of droughts.

The aim of this study was to characterise the water balance of a dammed reservoir of Przebędowo in two hydrological years differing in terms of precipitation totals.

2. Material and methods

This study presents the results of investigations conducted in the hydrological years of 2017 and 2018 in the immediate catchment of the Przebędowo reservoir, located in the Wielkopolskie province 25 km north of Poznań in the Murowana Goślina commune (Fig. 1).

According to the physico-geographical regionalisation of Poland (Kondracki 2000) the area of the study with the early post-glacial landscape is located in the Wielkopolska Lake District in the area of the Poznań Warta Gorge (315.52). The total catchment area of the reservoir is approx. 95 km^2, while the direct alimentation area of the lake (catchment direct) covers 1.31 km^2. The areas adjacent to the reservoir are arable lands (cereal crops) composed of fluvial Quaternary (Pleistocene) deposits, while the analysis of layers covered by piezometers showed a predominance of medium sands deposited to a depth of approx. 3 m.

The analysed reservoir was constructed in the valley of the Trojanki river (from 6+915 km to 8+371 km of its course) by the Wielkopolska Land Reclamation and Hydraulic Structure Authority in Poznań and it was commissioned in November 2014. The embankment dam of the reservoir is class IV, it is 334 m in length and 3.30 m in height (Fig. 2).

The reservoir of 1450 m in length and maximum width of 120 m, at the normal pool elevation of 72.50 m a.s.l. has a mean depth of 0.94 m and the pool area of 12.03 ha (Fig. 3, Table 1).

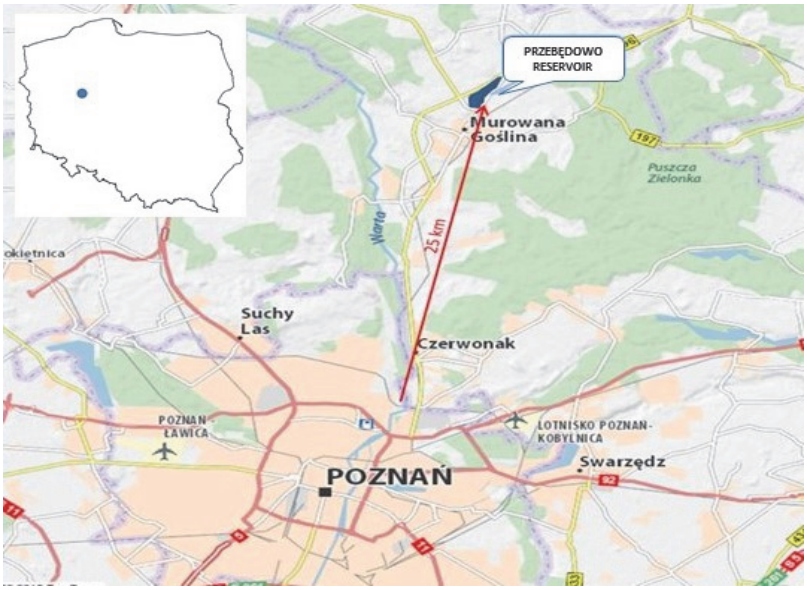

Fig. 1. Location of the Przebędowo reservoir in the Wielkopolska region

Fig. 2. The embankment dam with the spillway-overflow structure (steady level damming) in the Przebędowo reservoir

The shoreline length of the reservoir is 2980 m, shoreline density is 248 m·ha^{-1} and the elongation index is 12. In turn, the flood control capacity derived from the difference between normal and maximum pool level is around 67000 m^3.

Fig. 3. A view of the Przebędowo reservoir (Sojka et al. 2017)

Water levels in the reservoir were measured at the staff gauge installed at the damming structure situated at the reservoir outlet. Additionally, water levels in the reservoir were continuously recorded using a hydrostatic level sensor, which readings were transmitted to a remote telemetry module installed at the spillway tower.

Table 1. Basic morphometric parameters of the Przebędowo reservoir

Item	List	Unit	Value
1	Surface area	ha	12.03
2	Length	m	1450
3	Maximum width	m	120
4	Mean depth	m	0.94
5	Length of shoreline	m	2980
6	Shoreline density	m·ha^{-1}	248
7	Elongation index	–	12
8	Total capacity at normal pool level	m^3	162 350
9	Flood control capacity derived from the difference between normal and maximum pool levels	m^3	67 100

This study was based on measurements of groundwater levels taken at 7 selected wells installed during reservoir construction: P-2 and P-3 in the area adjacent to the reservoir to the west, and wells P-16, P-17, P-18, as well as P-20 and P-21 installed to the east of the reservoir. From May 2016 groundwater levels were measured in additionally installed wells (from 1' to 6') located in the area adjacent to the reservoir at a distance of approx. 10 m from its shore in three representative sections (Fig. 4). Water levels in the years of analysis were measured at 14-day intervals. In turn, weekly water levels in the analysed wells were recreated by calculating mean values from measurements taken every two weeks.

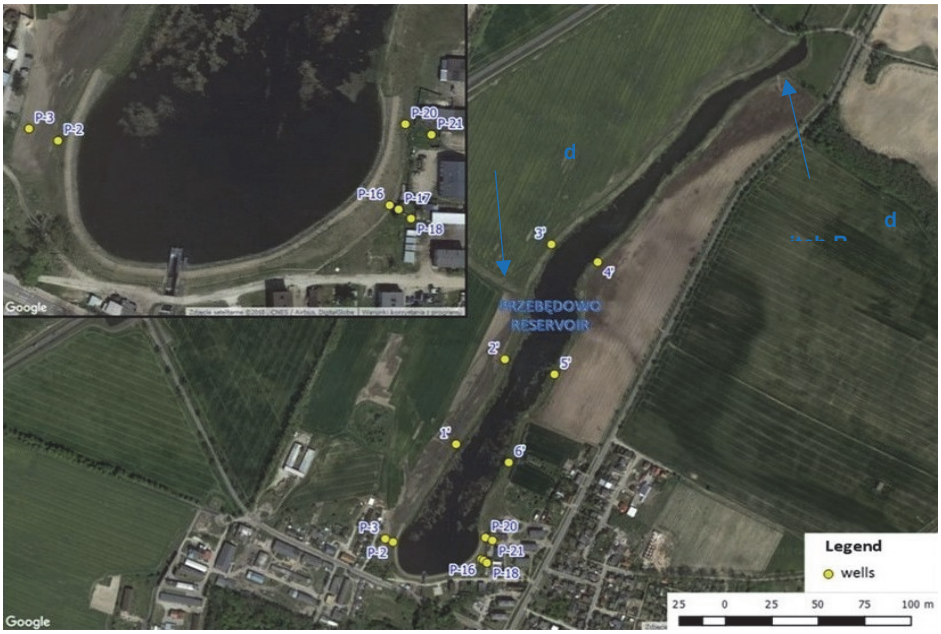

Fig. 4. Location of wells for groundwater level measurements in the area adjacent to the reservoir (source: the authors' study based on Google Earth https://www.google.pl/intl/pl/earth/)

Meteorological conditions in the discussed hydrological years (precipitation and air temperatures), compared to the data from the multiannual period of 2000-2015, were characterised based on the results of measurements recorded at the weather station of the Experimental and Teaching Station of the Forest Arboretum in Zielonka, located approx. 8 km south-east from the reservoir. The weather station is situated in the central part of the Zielonka Forest at 91.00 m a.s.l., at 52˚33″00″

northern latitude and 17˚06′33″ eastern longitude. Measurements have been recorded there continuously since 1986, while readings are recorded three times a day (Grajewski and Pacholczyk 2011).

Moisture conditions for the analysed hydrological years were characterised according to Kędziora (1995, after Kaczorowska 1962) taking into consideration the criteria given in Table 2.

Table 2. Characteristics of moisture conditions in hydrological years

Type of year	% normal precipitation
Extremely dry	below 50
Very dry	50-74
Dry	75-89
Average	90-110
Wet	111-125
Very wet	126-150
Extremely wet	over 150

In view of the considerable, both half-year and yearly, values of water balance components included in the so-called river water exchange (inflow and surface runoff in the Trojanka watercourse) the water balance of the investigated reservoir was expressed in hm^3 and calculated using the following equation:

$$P + Hd + Hp + Hpp + \Delta R_1 = E + \Delta R_2 + Ho + Hopp + Hw \quad (1)$$

where: P – precipitation onto the reservoir surface (hm^3), Hd – inflow to the reservoir from the Trojanka watercourse (hm^3), Hp – surface inflow to the reservoir from adjacent areas (hm^3), Hpp – subsurface inflow to the reservoir from adjacent areas (hm^3), ΔR_1 – increase in retention (hm^3) E – evaporation from the reservoir surface (hm^3), ΔR_2 – loss of retention (hm^3), Ho – outflow from the reservoir with the Trojanka watercourse (hm^3), Hopp – subsurface outflow from the reservoir to adjacent areas (hm^3), Hw – uncontrolled underground outflow (hm^3). At the same time, in view of the relatively small fluctuations in water levels within the reservoir, the water balance of the analysed reservoir was assessed in reference to its surface at normal pool level.

In the calculations for the water balance of the analysed reservoir the precipitation level was adjusted by the correction resulting from the formula proposed by Jaworski, recommended for the conditions prevalent in the Wielkopolska region by Kędziora (1995):

$$Ps = 1.034 \cdot Pz + 0.484 \cdot N + 4.0 \quad (2)$$

where:
Ps – adjusted precipitation (mm),
Pz – precipitation catch (mm),
N – number of days with precipitation in a month.

In turn, precipitation feeding the reservoir was calculated from the dependence:

$$P = Ps \cdot Azb, \tag{3}$$

where:
Ps – adjusted precipitation (mm),
Azb – reservoir surface area (ha).

Values of inflow to the reservoir with the Trojanka watercourse (Hd) and outflows (Ho), as well as surface inflows (Hp) from two drainage ditches (A and B, Fig. 4) feeding the reservoir from the north-west (A) and east (B), were determined based on calculations of flow rates, which in turn were established using water flow velocity measured using a hydrometric current meter (electromagnetic open flow meter FLAT Model 801 by Valeport) with measurements taken once a month. Flows were calculated using characteristic curves plotted based on in-situ measurements.

Values of subsurface inflow to the reservoir from adjacent areas (Hpp) and outflow from the reservoir to adjacent areas (Hopp) were determined using the Darcy formula (Rushton 2003):

$$Q = k \cdot I \cdot O \cdot \Delta h \tag{4}$$

where:
k – hydraulic conductivity ($m \cdot d^{-1}$),
I – hydraulic gradient,
O – length of shoreline (m),
Δh – aquifer thickness (m).

The value of hydraulic conductivity was assumed at $k = 24.704\ m \cdot d^{-1}$, determined as the mean for the values obtained during bore drilling at the installation of piezometers, established using the Hazen method and contained in the documentation from the execution of geotechnical works related to the assembly of piezometers for the small retention reservoir of Przebędowo (2014) and prepared by Geoprogram (W. Andrzejewski, R. Urban) from Bydgoszcz.

The thickness of the aquifer (Δh) participating in the feeding of water to the reservoir from adjacent areas was reversely determined based on the difference between the water level in the reservoir and water levels in the analysed wells (mean value). In turn, the number of days with groundwater being fed by waters stored in the reservoir was determined in the analysed years based on the difference between ordinates of water levels in the reservoir and groundwater levels in the wells included in the analyses.

Monthly evaporation from the reservoir surface was calculated using the formula proposed by Tichomirow (Kędziora 1995):

$$E_1 = d \cdot (15+3 \cdot v) \tag{5}$$

where:
E – monthly evaporation from the water surface (mm),
d – mean monthly humidity deficit (mmHg),
v – mean monthly wind velocity at the anemometer (m/s).

In turn, half-year and yearly values of evaporation were determined from the formula:

$$E=E_1 \cdot Azb \tag{6}$$

where:
E_1 – evaporation from the reservoir surface (mm),
Azb – surface area of the reservoir (m^2).

Increments (ΔR_1) or losses (ΔR_2) of water retention in the reservoir were determined based on changes in water levels recorded at the staff gauge installed at the damming structure. In turn, the value of uncontrolled underground outflow (Hw) was determined as the compliment to the water balance equation.

Data on recorded water levels in the discussed facility were used as kindly provided at the permission of the Director of the former Wielkopolska Land Reclamation and Hydraulic Structure Authority in Poznań (presently the State Water Holding Polish Waters; Regional Water Management Authority in Poznań).

3. Results and discussion

Wielkopolska is a region, in which the vegetation period is one of the longest in Poland, starting the earliest in western Wielkopolska, where it begins around 28 March. In the South Wielkopolska Lowland the vegetation period lasts approx. 228 days, whereas at its northern boundaries it is only 216 days. Mean annual precipitation totals are 500-550 mm, while in the Gniezno Lake District

and in the southern parts of the Kujawy region they are by 50-100 mm lower. The precipitation deficit is observed particularly in the eastern part of the province. Precipitation is highly irregular and differences in precipitation totals in individual years may be as high as 250%. The distribution of precipitation during the year or the vegetation period is also far from uniform. More precipitation in the summer period is recorded in the vicinity of water bodies, reservoirs and river valleys, which are located in the paths of storms. Mean annual temperature for the Wielkopolska region is approx. 8.2°C, in the north it drops to 7.6°C, while in the southern and western edges it reaches 8.5°C. Extreme temperatures in the summer period reach +38°C, while during the harshest winters they drop to almost –30°C (Program… 2016, after Bąk 2003).

The hydrological year of 2017 was very wet, since precipitation total in that year exceeded the multiannual mean by as much as 244 mm, at air temperatures close to the mean (Fig. 5).

The winter half-year in that year was average, with precipitation total of 211 mm, by 18 mm lower than the mean. In turn, the summer half-year was extremely wet, as precipitation total in that half-year was 593 mm and it was higher than the multiannual mean by 263 mm, at air temperature exceeding the mean by 0.2°C.

In turn, the second analysed hydrological year (2018) was a very dry year, in which precipitation total was equivalent to as little as 65% normal precipitation and it was lower than that value by 196 mm, at air temperature higher by 1.1°C compared to the mean. Both the winter and summer half-years of that year were very dry, with precipitation totals lower than the means by 79 mm and 115 mm, at air temperatures higher than the means by 0.4°C and as much as 1.6°C, respectively.

Analyses of mean monthly water levels in the investigated reservoir indicate that in the month preceding the winter half-year of 2017 (November) the mean water level was 317 cm (Fig. 6). Precipitation total of 78 mm, which was observed in November and in December, caused a rise in water levels. Mean monthly water level in the reservoir in December was 328 cm and at the same time it was the highest mean value in the discussed half-year. From January to the end of the analysed half-year a lowering of water levels was recorded in the reservoir.

The lowest mean water level was recorded in April and it amounted to 308 cm, being by as little as 7 cm higher than the level corresponding to the normal pool level. A considerable effect on such a situation was exerted by higher air temperatures in March and April and evaporation from the reservoir surface, which jointly in those months amounted to 113 mm.

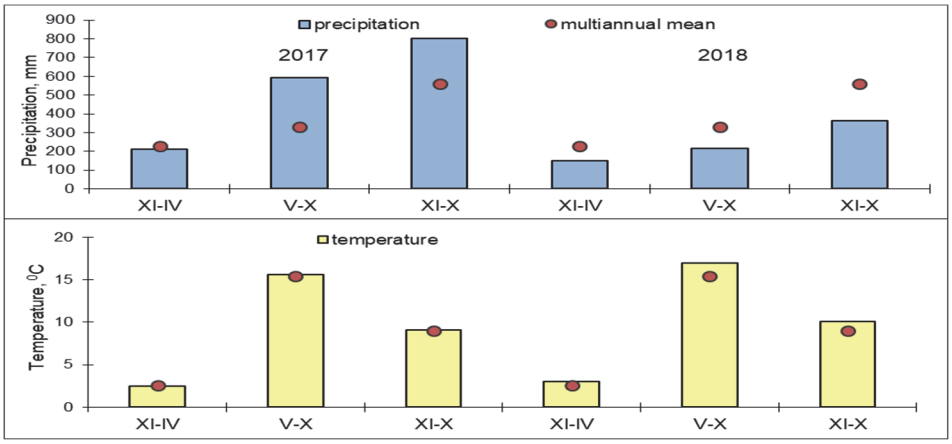

Fig. 5. Half-year and yearly precipitation (P) and average air temperatures (t) in 2017 and 2018 hydrological years, and their deviations from averages of the multiyear period of 2000-2015

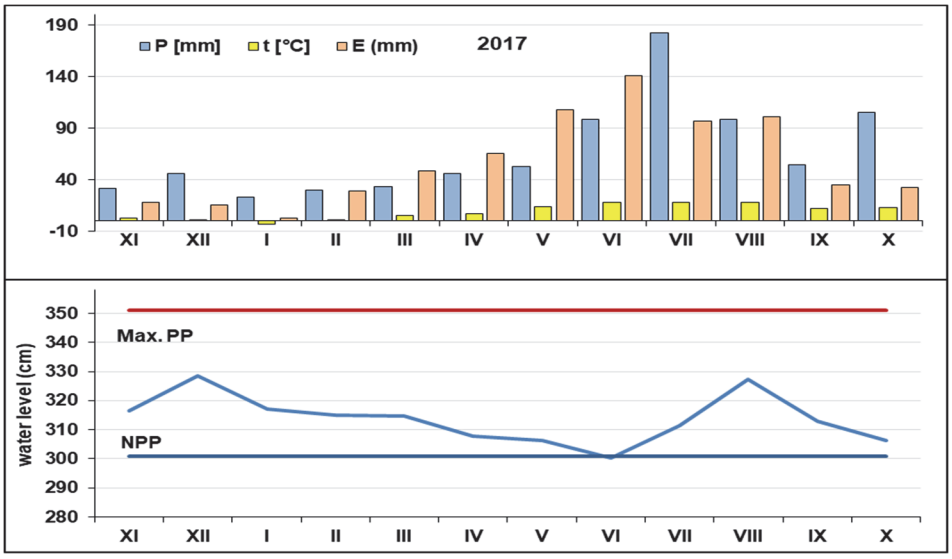

Fig. 6. Mean monthly water levels (cm) in the Przebędowo reservoir and levels corresponding to normal (NPP) and maximum pool levels (Max PP) depending on mean monthly precipitation totals (P) and mean monthly air temperatures (t) as well as monthly evaporation from the reservoir surface (E) in the hydrological year of 2017

In the beginning of the summer half-year (May) of 2017 the mean water level in the analysed reservoir was 306 cm. Higher mean monthly air temperatures observed in May and June (13.8°C and 17.8°C, respectively), as well as high evaporation from the reservoir recorded in those months (jointly 173 mm) contributed to a further lowering of water levels. The mean water level in the reservoir in June was 300 cm and it was the lowest mean level both in the discussed summer half-year and in the entire hydrological year of 2017. In July and August water levels in the reservoir were observed to raise, while their mean values in those months were 311 cm and 327 cm, respectively. A considerable effect on this situation, despite higher air temperatures and evaporation from the reservoir surface, was found for precipitation total of 282 mm, recorded in those months. Results obtained for those months were consistent e.g. with the studies by Błażyca and Rzętała (2013) concerning analyses of changes in water levels in the Pławniowice reservoir, since those authors stressed that maximum water levels were observed in the summer half-year, typically at the turn of July and August following precipitation with high daily totals.

From August to the end of the discussed summer half-year water levels in the reservoir were lowering. The mean water level in September was 313 cm, while in October it was 306 cm. However, it needs to be stressed here that the lowering of the water levels towards the end of the discussed half-year was not directly connected with the course of weather conditions, since precipitation total for September and October was 161 mm, while total evaporation for those months was 67 mm. The values of evaporation calculated for those months were consistent with the results of calculations presented by Górski et al. (2009) in their analysis of the water balance for Lake Czerniakowskie and with the results of direct measurements obtained e.g. for Lake Raduńskie Górne by Wereski et al. (2017). As it was reported by Waligórski et al. (2019), the lowering of water levels in the Przebędowo reservoir was caused by a considerable effect of the anthropogenic factor, related to the opening of bottom gates towards the end of August, in a situation when higher daily precipitation totals and the vegetation debris jamming the damming structure posed a risk of crest overflow spill and flooding of buildings located nearby.

In the winter half-year of the second analysed year of the analyses (2018) the mean water level in the reservoir in November was 305 cm (Fig. 7). In the period from November to February water levels were lowering and during that period they remained below the normal pool level.

Similarly as in the previous analysed year of the study, the marked lowering of water levels in February, when the mean water level was 277 cm and it was lower than normal pool level by 24 cm, was not caused by the weather conditions, but by anthropopressure. In the course of maintenance works performed

in that month due to negligence the bottom gates were left partly open, which resulted in an uncontrolled outflow of water from the reservoir and a lowering of water levels. As it was reported by Mioduszewski and Okruszko (2016), the hydrological functions of this reservoir may be considerably influenced also by its operation. Until the end of the discussed winter half-year the water levels in the reservoir were raising as a result of the bottom gates being completely shut and the progressing reservoir filling. In April the mean water level in the reservoir was 302 cm and it was similar to that corresponding to the normal pool level.

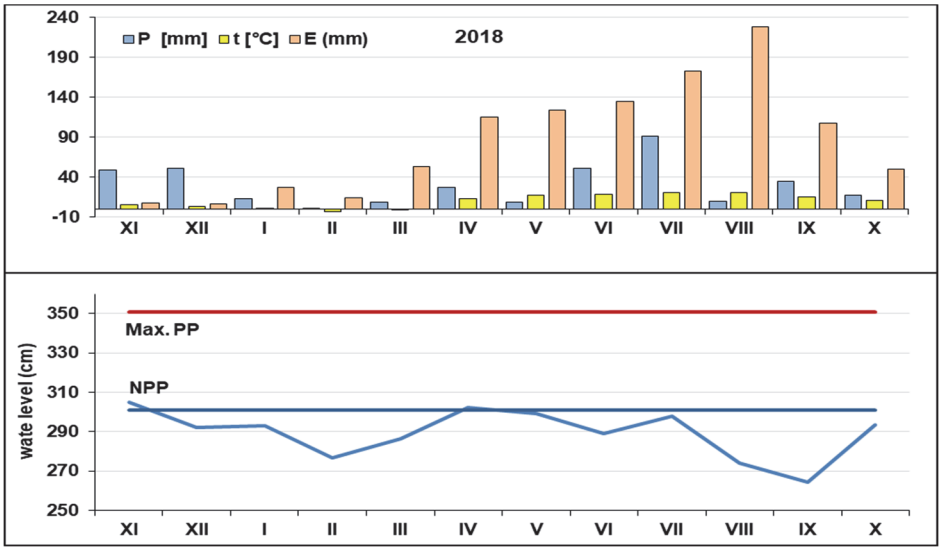

Fig. 7. Mean monthly water levels (cm) in the Przebędowo reservoir and levels corresponding to normal (NPP) and maximum pool levels (Max PP) in view of mean monthly precipitation totals (P) and mean monthly air temperatures (t) and monthly evaporation from the reservoir surface (E) in the hydrological year of 2018

From the beginning of the summer half-year the water levels in the discussed reservoir were falling and in June the mean water level was 289 cm. To a considerable extent this situation was the result of the weather conditions, particularly low precipitation total in May (9 mm) and high evaporation from the reservoir, which total joint value for May and June was as high as 259 mm. A slight increase in water levels in the reservoir was recorded in July due to precipitation total for that month amounting to 92 mm, when the mean water level reached 298 cm.

At the turn of August and September a considerable lowering of water levels was caused to a considerable extent by adverse weather conditions, particularly low precipitation totals in that month, at higher air temperatures and very high evaporation from the reservoir, which jointly amounted to as much as 336 mm. The mean water level in the analysed reservoir in September was 265 cm and it was lowest both in the discussed summer half-year and over the entire hydrological year of 2018.

Towards the end of the discussed half-year water levels were found to increase in the reservoir and in October the mean level was 293 cm. However, throughout the entire analysed summer half-year, which in terms of precipitation was very dry, the mean water levels in the reservoir remained below the level corresponding to the normal pool level (301 cm).

Analysis of the water balance for the Przebędowo reservoir indicates that in the winter half-year of the first year of the study the highest share in terms of increments was recorded for the inflow to the reservoir by the Trojanka watercourse, which in the discussed half-year was 12.9 hm^3 (Table 3).

Table 3. Components of water balances of the Przebędowo reservoir (hm^3) in the winter (XI-IV) and summer (V-X) hydrological half-years of 2017 and 2018

Increments (+) and losses of water (-)	Water balance components	Hydrological half-years			
		2017		2018	
		XI-IV	V-X	XI-IV	V-X
(+)	P	0.03	0.08	0.027	0.032
	Hd	12.9	10.7	5.16	3.59
	Hp	0.165	0.047	0.0025	-
	Hpp	0.0015	0.0002	–	–
	ΔR_1	–	0.011	–	0.004
(-)	E	0.02	0.06	0.03	0.098
	ΔR_2	0.0048	–	0.036	–
	Ho	10.0	9.06	3.75	2.70
	Hopp	0.56	0.55	0.81	0.78
	Hw	2.51	1.16	0.55	0.046

According to Rzętała (2008), when analysing water balances of anthropogenic reservoirs, including dammed reservoirs, in terms of the type of water feeding and artificial control of water circulation, the results of calculations

should be expressed in hm^3 rather than in millimeters, as it is the typical practice in geographical studies.

To a much lesser extent the increments in water resources in that half-year were determined by the inflow to the reservoir from adjacent areas, which was 0.165 hm^3.

In turn, to the lowest extent the increments were determined by precipitation falling on the surface of the reservoir and by the subsurface inflow to the reservoir from adjacent areas, which in the discussed half-year amounted to 0.03 hm^3 and 0.0015 hm^3, respectively. In terms of the water losses the highest share in the water balance equation was found for the outflow from the reservoir with the watercourse, amounting to 10.0 hm^3. Uncontrolled underground outflow determined as the complement in the balance equation was 2.51 hm^3. As reported by Rösler et al. (2007), when characterising the water balance of Lake Sława the greatest methodological problems were caused by water exchange in the underground drainage zone, frequently leading to a situation when the parameters of underground exchange are typically calculated from the water balance difference. The underground outflow is often problematic; as reported by Lange (1993), currently available research results indicate a considerable predominance of feeding by the underground outflow. Some hydrologists even claim that the underground loss of water is rather unlikely due to the strong bottom sealing of lake basins by impermeable sediments. Previously cited Rösler et al. (2007) reported that colmatation, i.e. silting and sealing of lake basic bottoms by sediments, takes place and plays a significant role in blocking the underground outflow. However, according to those authors particularly in flow-through lakes in the outflow zone sediments may be washed away and wide marginal stream valley filled with permeable deposits (sands, gravel) form the so-called underground outflow gateways. Similar observations were reported by Wojtuszewska (2007) and Dąbska and Popielski (2020), in whose opinion operation of dammed reservoirs is frequently connected with hydrogeological problems, the most frequent of which include e.g. excessive filtration to the substrate and within the dam abutment zone. In the latter case this is frequently caused by quick sands or the so-called piping.

In the analysed half-year the losses in the water balance were to a lesser extent determined by subsurface outflow from the reservoir to adjacent areas, amounting to 0.56 hm^3. In turn, the smallest share was recorded for evaporation from the reservoir, which was 0.02 hm^3, and water storage loss in the reservoir, which amounted to 0.0048 hm^3. In the summer half-year of the discussed hydrological year of 2017, similarly as it was in the winter half-year, a major factor in the water balance of the reservoir in terms of increments was related to the inflow

by the watercourse, which amounted to 10.7 hm^3. To a much lesser extent the increments were determined by surface inflow from adjacent areas, which reached 0.047 hm^3. In turn, precipitation falling on the reservoir surface in the discussed half-year amounted to 0.08 hm^3, while the increment in retention was 0.011 hm^3. The lowest share in the water increments in that half-year was observed for subsurface inflow to the reservoir from adjacent areas, being as low as 0.0002 hm^3. In relation to water losses the greatest share in the balance equation in that half-year was recorded for the outflow from the reservoir through the watercourse, which was 9.06 hm^3. Uncontrolled underground outflow and subsurface outflow from the reservoir to adjacent areas amounted to 1.16 hm^3 and 0.55 hm^3, respectively. In turn, water losses related to evaporation from the reservoir amounted to 0.06 hm^3.

In the second analysed hydrological year of 2018, which in terms of precipitation was very dry, both in the winter half-year (XI-IV) and the summer half-year (V-X), the highest share in the water balance of the reservoir in the case of increments was recorded for the Trojanka inflow, amounting to 5.16 hm^3 and 3.59 hm^3, respectively (Table 3). However, it needs to be observed here that these values in relation to inflows from the previous year were much smaller. In the winter half-year of 2018 the difference was 7.74 hm^3, while in the summer half-year it was 7.11 hm^3. To a much lesser degree the increments in the discussed half-years were determined by precipitation falling on the reservoir surface, which in the winter half-year was 0.027 hm^3, while in the summer half-year it reached 0.032 hm^3. The increments to a slight extent were also determined by surface inflow from adjacent areas (in ditches A and B), which was observed only in the winter half-year and amounted to 0.0025 hm^3, as well as the increment of water storage amounting to 0.004 hm^3, reported in the summer half-year. It needs to be stressed here that both in the winter and summer half-years of the discussed hydrological year the reservoir was not fed by groundwaters from adjacent areas (Hpp). In turn, in terms of water losses the highest share in the water balance equation for the analysed reservoir was found for the outflow from the reservoir through the watercourse (Ho), which in the winter half-year amounted to 3.75 hm^3, while in the summer half-year it reached 2.70 hm^3. However, they were much lower values (by approx. 6 hm^3) in comparison to outflows in 2017, being a wet year in terms of precipitation. A significant share in the losses was also found for subsurface outflow from the reservoir to adjacent areas (Hopp), which suggests that in the discussed hydrological year the reservoir played only the feeding function. In the winter half-year the outflow amounted to 0.81 hm^3, while in the summer half-year it was 0.78 hm^3. It may be stated here the analysed Przebędowo reservoir fully served a major function ascribed to retention reservoirs, since as it was reported by Humnicki (2010) and Jaguś et al. (2010) the

main role of such reservoirs is to store water in periods of its excess to be subsequently used during dry spells, e.g. by feeding groundwaters in adjacent areas.

Losses in the water balance equation for the reservoir in the discussed hydrological year were to a lesser extent affected by uncontrolled underground outflow, in the winter half-year amounting to 0.55 hm^3, while in the summer half-year it was 0.046 hm^3. In turn, the least important effect on water losses was observed for evaporation from the reservoir surface, which in the winter half-year amounted to 0.03 hm^3, while in the summer half-year it was 0.098 hm^3, similarly as it was for storage losses, which in the winter half-year amounted to 0.036 hm^3.

Analyses of the percentage share of individual components of the water balance for the Przebędowo dammed reservoir over the entire period of the discussed hydrological years show that in the hydrological year of 2017 increments were determined to the greatest extent by inflow to the reservoir through the Trojanka watercourse (Hd), accounting for 49.3% (Fig. 8).

To a lesser extent the water increments were influenced by the surface inflow from adjacent areas (Hp), which constituted 0.44%, and precipitation (P) falling on the reservoir surface (0.23%). In turn, the lowest shares in the water balance equation were found for the increment in water storage (ΔR_1) and subsurface inflow to the reservoir from adjacent areas (Hpp), which accounted for as little as 0.023% and 0.004%. In terms of losses the greatest share in the water balance for the discussed year was observed for surface outflow from the reservoir (Ho), which accounted for 39.8%, and for uncontrolled underground outflow (Hw) constituting 7.7%. Losses were determined to a lesser extent by subsurface outflows from the reservoir to adjacent areas (Hopp) and evaporation from the reservoir (E), which percentage shares in the water balance were 2.3% and 0.17%, respectively. In turn, the lowest share (0.01%) was found for the water storage losses (ΔR_2). In the second analysed hydrological year of 2018, similarly as in 2017, a crucial share in increments was recorded for the watercourse inflow to the reservoir, which accounted to 49.7%. In turn, the percentage shares of the other water balance components determining the increments, such as precipitation falling on the reservoir surface, surface inflow from adjacent areas and the increment in water storage, were slight. In the case of water losses the greatest role in that year in the water balance was played by the outflow from the reservoir through the watercourse, accounting for 36.6%. A relatively high share was found for the subsurface outflow from the reservoir to adjacent areas (9%) and uncontrolled underground outflow (3.4%). To a lesser extent the losses were determined by evaporation from the reservoir (0.73%) and water storage losses (0.2%).

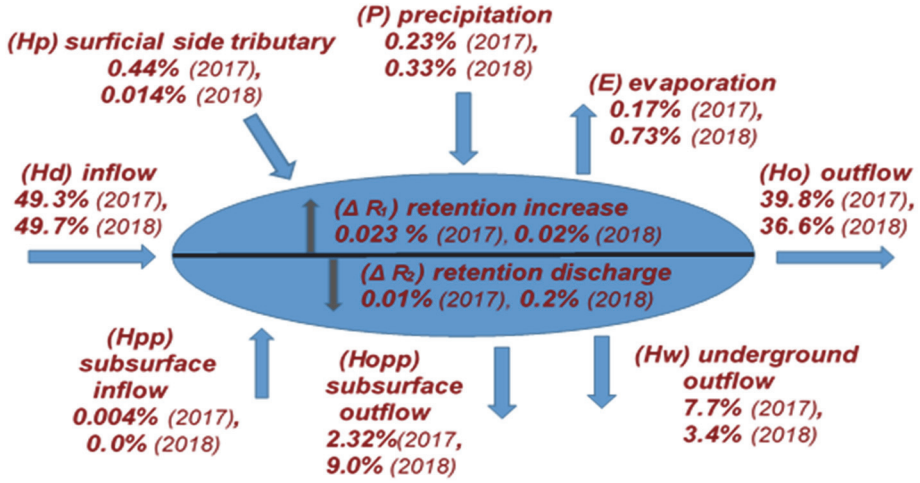

Fig. 8. Graphic representation of water balance components (%) for the Przebędowo reservoir in the hydrological years 2017 and 2018

Results recorded in the discussed years are consistent with e.g. those presented by Rzętała (2000), concerning water balance characteristics of the Dzierżno Duże reservoir, as that author stressed the greatest effect on the water balance exerted by inflow and surface outflow. In turn, precipitation in the case of increments and evaporation from the reservoir in the case of losses played a marginal role in the water balance. Analysis of the water balance components for the Przebędowo reservoir confirmed also the results of a study by Fac-Benedy (2013) concerning hydrological characterisitcs of Lake Drużno, in which the author stressed that the primary elements in the water balance of flow-through lakes are connected with inflow and surface outflow, since the vertical water exchange is less intensive than the horizontal exchange and it does not fundamentally alter the general balance structure. Similar conclusions were also drawn by Kropka and Jagliński (2015) when analysing the water balance for the underground catchment of the Kuźnica Warężyńska reservoir (Kotlina Dąbrowska). Those authors reported the greatest share in the water balance in the case of increments for surface inflow, while in the case of losses surface outflow from the reservoir was definitely dominant.

4. Conclusions

1. Obtained research results showed that in the hydrological year of 2017, which in terms of precipitation was very wet, mean water levels in the reservoir remained between normal and maximum pool levels. The highest mean water level in the winter half-year of that year was recorded in December (328 cm), while in the summer half-year it was in August (327 cm). In turn, for a greater part of the very dry hydrological year of 2018 mean water levels in the reservoir remained below the normal pool level. The lowest mean level was observed in that year in September (265 cm), which to a considerable extent was determined, among other things, by very high evaporation from the reservoir surface (228 mm), which was recorded in August.
2. The conducted analyses confirmed that apart from the weather conditions such as precipitation, air temperatures and evaporation from the reservoir a considerable role for the fluctuations in water levels in the reservoir was played by the anthropogenic factor. It was particularly related with the manner of reservoir operation frequently characteristic to dammed reservoirs and with the artificial control of water circulation.
3. The performed analysis of the water balance for the Przebędowo reservoir showed that in the winter half-years of the analysed hydrological years of 2017 and 2018 the dominant factor in the case of increments was connected with inflow to the reservoir in the Trojanka watercourse, amounting to 12.9 hm^3 and 5.16 hm^3, respectively. To a much lesser extent the increments of water in those half-years were determined by the inflow to the reservoir from adjacent areas and by precipitation. In the case of losses the greatest share in the water balance was observed in the discussed half-years for outflow from the reservoir through the watercourse, which amounted to 10.0 hm^3 and 3.75 hm^3. To a lesser extent losses were determined by the uncontrolled underground outflow and subsurface inflow to the reservoir from adjacent areas. In turn, evaporation from the reservoir surface and water storage losses determined losses only slightly.
4. In the summer half-years the increments in the water balance to the greatest extent were determined by inflows to the reservoir through the watercourse, which amounted to 10.7 hm^3 (2017) and 3.59 hm^3 (2018), while in the case of losses it was outflows from the reservoir amounting to 9.06 hm^3 and 2.7 hm^3. In turn, a lesser role was played in the case of losses by outflow from the reservoir to adjacent areas, which in the discussed half-years was comparable and amounted to a mean 0.66 hm^3.

5. Throughout the entire period of the analysed hydrological years of 2017 and 2018 the greatest share in the water balance for the Przebędowo reservoir was recorded for the components related with the horizontal water exchange. Inflows to the reservoir through the Trojanka watercourse and outflows constituted mean 49% and 38%, respectively. In the dry hydrological year of 2018 a significant share, in comparison to the other components, in the water balance was also found for the subsurface outflows from the reservoir to adjacent areas, accounting for 9%. In contrast, no major share in the water balance was found for the factors related with the vertical water exchange, characteristic of reservoirs having no outlets, such as precipitation and evaporation from the reservoir surface.

The publication was co-financed within the framework of Ministry of Science and Higher Education programme as „Regional Initiative Excellence" in years 2019-2022, Project No. 005/RID/2018/2019.

References

Błażyca, D., Rzętała, M. (2013). *Uwarunkowania wahań stanów wody w zbiorniku Pławniowice [Fluctuations in water levels in the Pławniowice reservoir]*. Acta Geographica Silesiana, 14. Wydział Nauk o Ziemi Uniwersytet Śląski, 27-34.

Charakterystyka Regionu Wodnego Warty [Characteristics of the Warta Water Region]. 2007. Regionalny Zarząd Gospodarki Wodnej w Poznaniu, Pion Zasobów Wodnych, 1-65.

Choiński, A. (1995). *Zarys limnologii fizycznej Polski [An outline of physical limnology of Poland]*. Wyd. Nauk. UAM. Poznań, 298.

Dąbska, A., Popielski, P. (2020). Makrodeformacje filtracyjne gruntów [Filtration macrodeformations of soils]. *Gospodarka wodna, 2*, 15-18.

Fac-Beneda, J. (2013). *Charakterystyka hydrologiczna jeziora Druzno [Hydrological characteristics of Lake Druzno]*. Monografia Przyrodnicza. Regionalna Dyrekcja Ochrony Środowiska w Olsztynie. 15-31.

Górski, D., Banasik, K., Byczkowski, A. Gładecki, J., Hejduk, L. (2009). *Ekspertyza – bilans wodny Jeziorka Czerniakowskiego w Warszawie [Expert opinion – water balance of Lake Czerniakowskie in Warszawa].* Katedra Inżynierii Wodnej i Rekultywacji Środowiska Wydział Inżynierii i Kształtowania Środowiska Szkoła Główna Gospodarstwa Wiejskiego, Warszawa, 55.

Grajewski, S., Pacholczyk, K. 2011. *Charakterystyka warunków meteorologicznych Puszczy Zielonka w latach 1986-2010 [Characteristics of weather conditions in the Zielonka Forest in the years 1986-2010].* Forestry Letters, Agricultural Letters, PTPN, Wydz. Nauk Rolniczych i Leśnych, Prace Kom. Nauk Rolniczych i Komisji Nauk Leśnych, 102, 59-78.

Gruszczyński, T., Leśniak, P., Michalak, J, Nowicki, Z. (2009). *Wyznaczanie zmian zasobów wód podziemnych w rejonach zbiorników małej retencji [Determination of changes in undergorund water resources in the vicinity of small retention reservoirs]*. Państwowy Instytut Geologiczny Warszawa, 109.

Humnicki, W. (2010). *Zmiany warunków hydrogeologicznych wokół zbiorników zaporowych w Pieninach [Changes in hydrogeological conditions around dammed reservoirs in the Pieniny Mts.]* Pieniny – Zapora – Zmiany – Monografie Pienińskie 2: 83-95.

Jaguś, A., Khak, V., Kozyrera, E., Rzętala, M., Rzętała, M, Szczypek, T. (2010). Zmiany w środowisku wywołane spiętrzeniem wód rzeki Angary i jeziora Bajkał [Environmental changes caused by damming of the Angara River and Lake Bajkal]. *Wszechświat, 111*(10-12), 265-271.

Kędziora, A. (1995). *Podstawy Agrometeorologii [Introduction to agrometeorology]*. PWRiL Poznań, 264.

Kondracki, J. (2000). *Geografia regionalna Polski [Regional geography of Poland],* Wydawnictwo Naukowe PWN, Warszawa.

Kropka, J., Jagliński, Ł. (2015). Bilans wodny zlewni podziemnej zbiornika wodnego Kuźnica Warężyńska (Kotlina Dąbrowska) [Water balance of the underground catchment of the Kuźnica Warężyńska reservoir (Kotlina Dąbrowska)]. *Przegląd Górniczy, 12*, 131-139.

Lange, W. (1993). *Metody badań fizyczno-limnologicznych [Methodology of physico-limnological studies]*. Gdańsk, Uniwersytet Gdański, 175.

Mioduszewski, W., Okruszko, T., (2016). *Naturalna mała retencja. Metoda łagodzenia skutków suszy, obniżenie ryzyka powodziowego i ochrona różnorodności biologicznej [Natural small retention. A method to alleviate the effects of drought, to reduce flood risk and to preserve biodiversity].* Podstawy metodyczne. Globalne partnerstwo dla wody.

Program ochrony środowiska dla województwa wielkopolskiego na lata 2016–2020 [Environmental protection program for the Wielkopolskie province for the years 2016-2020]. Poznań, 2016, 170.

Radzka, E. (2014). Klimatyczny bilans wodny okresu wegetacyjnego (według wzoru Iwanowa) w środkowowschodniej Polsce [Climatic water balance for the vegetation period (according to Iwanow) in central-eastern Poland]. *Woda-Środowisko-Obszary Wiejskie, 14*(1), 67-76.

Rösler, A., Bielawny, K., Chmal, M., Chmal, T., Staszkiewicz, S., Szymanowska, K. (2007). *Analiza zmian składowych bilansu wodnego jezior na przykładzie jeziora Sława [1976-2005], [Analysis of water balance components for lakes based on Lake Sława [1976-2005]*, Zadanie DS. H1 6b, 39.

Rushton, K.R. (2003). *Groundwater Hydrology.* The Atrium, Southern Gate, Chichester, 408.

Rzętała, M. (2000). *Bilans wodny oraz dynamika zmian wybranych zanieczyszczeń zbiornika Dzierżno Duże w warunkach silnej antropopresji [Water balance and dynamics of changes in selected pollutants in the Dzierżno Duże reservoir at strong anthropopressure].* Prace Naukowe UŚ w Katowicach, 1913. Wydawnictwo Uniwersytetu Śląskiego, Katowice. 176.

Rzętała, M. (2008). *Funkcjonowanie zbiorników wodnych oraz przebieg procesów limnicznych w warunkach zróżnicowanej antropopresji na przykładzie regionu górnośląskiego [Functioning of water reservoirs and the course of limnic processes at diverse anthropopressure conditions based on the Upper Silesia region].* Wydawnictwo Uniwersytetu Śląskiego, Katowice, 172.

Sojka, M., Korytowski, M., Jaskuła, J, Waligórski, B. (2017). Ocena podatności na degradację zbiornika retencyjnego Przebędowo [Assessment of susceptibility to degradation in the Przebędowo retention reservoir]. *Inżynieria Ekologiczna, 5*, 118-125.

Szczykowska, J., Siemieniuk, A. (2011). Znaczenie zbiorników retencyjnych na terenach rolniczych oraz jakość ich wód. [Meaning retention reservoirs at agricultural land and their water quality]. *Inzynieria Ekologiczna, 26*, 103-111.

Traczewska, T.M. (2012). *Problemy ekologiczne zbiorników retencyjnych w aspekcie ich wielofunkcyjności [Ecological problems of retention reservoirs in view of their multiple functions].* Materiały na Sympozjum Europejskie pt.: „Współczesne problemy ochrony przeciwpowodziowej", 1-8.

Wereski, S., Pawelec, W., Sasim, M. (2017). Biuletyn Państwowej Służby Hydrologiczno-Meteorologicznej, 10(186), Instytut Meteorologii i Gospodarki Wodnej – Państwowy Instytut Badawczy, 34.

Wibig, J. (2012). Warunki wilgotnościowe w Polsce w świetle wskaźnika standaryzowanego klimatycznego bilansu wodnego [Moisture conditions in Poland in view of the standardised climatic water balance index]. *Woda-Środowisko-Obszary Wiejskie, 12.2*(38), 329-340.

Wojtuszewska, K. (2007). Dynamika zmian stanu wód powierzchniowych i podziemnych w rejonie zbiorników wodnych Solina-Myczkowce [Dynamics of changes in the condition of surface and underground waters in the area of Solina-Myczkowce reservoirs]. *Gospodarka surowcami mineralnymi, 23*(3), 119-134.

Abstract

This study presents the results of investigations conducted in the hydrological years of 2017 and 2018 in the immediate catchment of the Przebędowo reservoir, located in the Wielkopolskie province 25 km north of Poznań in the Murowana Goślina commune. The immediate catchment of the reservoir is approx. 95 km^2 in area, while the direct recharge area of the lake (immediate catchment) covers 1.31 km^2. The areas adjacent to the reservoir are arable lands composed of fluvial Quaternary (Pleistocene) deposits, while the analysis of layers covered by piezometers showed a predominance of medium sands deposited to a depth of approx. 3 m. The analysed reservoir was constructed in the valley of the Trojanki river (from 6+915 km to 8+371 km of its course) by the Wielkopolska Land Reclamation and Hydraulic Structure Authority in Poznań and it was commissioned in November 2014. The embankment dam of the reservoir is class IV, it is 334 m in length and 3.30 m in height. The reservoir of 1450 m in length and maximum width of 120 m, at the normal pool elevation of 72.50 m a.s.l. has a mean depth of 0.94 m and the pool area of 12.03 ha. The shoreline length of the reservoir is 2980 m, shoreline density is 248 $m \cdot ha^{-1}$ and the elongation index is 12. In turn, the flood control capacity derived from the difference between normal and maximum pool level is around 67 000 m^3.

The conducted analyses confirmed that apart from the weather conditions such as precipitation, air temperatures and evaporation from the reservoir a considerable role for the fluctuations in water levels in the reservoir was played by the anthropogenic factor. It was particularly related with the manner of reservoir operation frequently characteristic to dammed reservoirs and with the artificial control of water circulation.

Analysis of the water balance for the Przebędowo reservoir showed that in the winter half-years of the analysed hydrological years of 2017 and 2018 the dominant factor in the case of increments was connected with inflow to the reservoir in the Trojanka watercourse, amounting to 12.9 hm^3 and 5.16 hm^3, respectively. To a much lesser extent the increments of water in those half-years were determined by the inflow to the reservoir from adjacent areas and by precipitation. In the case of losses the greatest share in the water balance was observed in the discussed half-years for outflow from the reservoir through the watercourse, which amounted to 10.0 hm^3 and 3.75 hm^3. To a lesser extent losses were determined by the uncontrolled underground outflow and subsurface inflow to the reservoir from adjacent areas. In turn, evaporation from the reservoir surface and water storage losses determined losses only slightly. Whereas in the summer half-years the increments in the water balance to the greatest extent were determined by inflows to the reservoir through the watercourse, which amounted to 10.7 hm^3 (2017) and 3.59 hm^3 (2018), while in the case of losses it was outflows from the reservoir amounting to 9.06 hm^3 and 2.7 hm^3. In turn, a lesser role was played in the case of losses by outflow from the reservoir to adjacent areas, which in the discussed half-years was comparable and amounted to a mean 0.66 hm^3.

Throughout the entire period of the analysed hydrological years of 2017 and 2018 the greatest share in the water balance for the Przebędowo reservoir was recorded for the components related with the horizontal water exchange. Inflows to the reservoir through the Trojanka watercourse and outflows constituted mean 49% and 38%, respectively. In the dry hydrological year of 2018 a significant share, in comparison to the other components, in the water balance was also found for the subsurface outflows from the reservoir to adjacent areas, accounting for 9%. In contrast, no major share in the water balance was found for the factors related with the vertical water exchange, characteristic of reservoirs having no outlets, such as precipitation and evaporation from the reservoir surface.

Keywords:
small-scale water retention, dammed reservoirs, water balances

Bilans wodny zbiornika zaporowego na przykładzie obiektu Przebędowo

Streszczenie

W pracy przedstawiono wyniki badań przeprowadzonych w latach hydrologicznych 2017 i 2018 w zlewni bezpośredniej zbiornika Przebędowo, zlokalizowanego w województwie wielkopolskim, 25 km na północ od Poznania w gminie Murowana Goślina. Powierzchnia zlewni całkowitej zbiornika wynosi około 95 km^2, natomiast obszar bezpośredniej alimentacji jeziora (zlewnia bezpośrednia) zajmuje powierzchnię 1,31 km^2.

Tereny przyległe do zbiornika to grunty orne zbudowane z osadów czwartorzędowych (plejstocen) fluwialnych, a analiza warstw objętych piezometrami wykazała przewagę piasków średnich zalegających do głębokości około 3 m. Analizowany zbiornik został wykonany w dolinie rzeki Trojanki (od km 6+915 do km 8+371 jej biegu), przez Wielkopolski Zarząd Melioracji i Urządzeń Wodnych w Poznaniu i został oddany do eksploatacji w listopadzie 2014 roku. Ziemna zapora czołowa na zbiorniku jest klasy IV, jej długość wynosi 334 m, przy wysokości 3,30 m. Zbiornik o długości 1450 m i szerokości maksymalnej 120 m, przy normalnym poziomie piętrzenia (NPP) wynoszącym 72,50 m n.p.m. ma średnią głębokość 0,94 m i powierzchnię zalewu 12,03 ha. Długość linii brzegowej omawianego zbiornika wynosi 2980 m, jej rozwinięcie kształtuje się na poziomie 248 $m \cdot ha^{-1}$ a wskaźnik wydłużenia wynosi 12. Natomiast rezerwa powodziowa stanowiąca różnicę pomiędzy NPP, a Max. PP osiąga wartość na poziomie około 67000 m^3.

Przeprowadzone badania potwierdziły, że poza czynnikami meteorologicznymi takimi jak opady atmosferyczne, temperatury powietrza oraz parowanie z powierzchni zbiornika duży wpływ na kształtowanie się stanów wody w zbiorniku miał również czynnik antropogeniczny. W szczególności związany z, często charakterystycznym dla zbiorników zaporowych, sposobem eksploatacji zbiornika i sztucznym sterowaniem obiegiem wody.

Analiza bilansu wodnego zbiornika Przebędowo wykazała, że w półroczach zimowych analizowanych lat hydrologicznych 2017 i 2018 czynnikami wiodącymi po stronie przychodów były dopływy do zbiornika ciekiem Trojanka wynoszące odpowiednio 12,9 hm^3 i 5,16 hm^3. W znacznie mniejszym stopniu o przychodach wody w tych półroczach decydowały dopływ do zbiornika z terenów przyległych oraz opad atmosferyczny. Po stronie rozchodów największy udział w równaniu bilansowym miał, w omawianych półroczach odpływ ze zbiornika ciekiem, który wyniósł 10,0 hm^3 i 3,75 hm^3. W mniejszym stopniu o rozchodach decydował niekontrolowany odpływ wgłębny oraz dopływ podpowierzchniowy do zbiornika z terenów przyległych. Parowanie z powierzchni zbiornika oraz ubytki retencji decydowały o rozchodach w sposób nieznaczny. Natomiast w półroczach letnich o przychodach w równaniu bilansowym w największym stopniu również decydowały dopływy do zbiornika ciekiem, które wyniosły 10,7 hm^3 (2017) oraz 3,59 hm^3 (2018), a postronnie ubytków odpływy ze zbiornika kształtujące się na poziomie odpowiednio 9,06 hm^3 oraz 2,7 hm^3. Natomiast w mniejszym stopniu o rozchodach decydował odpływ ze zbiornika do przyległych terenów, który w omawianych półroczach był zbliżony i kształtował się na średnim poziomie 0,66 hm^3.

W skali całych analizowanych lat hydrologicznych największy udział w bilansie wodnym zbiornika Przebędowo miały składowe związane z poziomą wymianą wody. Dopływy do zbiornika ciekiem Trojanka oraz odpływy stanowiły średnio około 49% i 38%. W suchym pod względem opadów roku hydrologicznym 2018 istotny, w porównaniu do pozostałych składowych, udział w bilansie miał również odpływ podpowierzchniowy ze zbiornika do przyległych terenów stanowiąc 9%. Natomiast nie stwierdzono w bilansie wodnym znacznego udziału czynników związanych z wymianą pionową wody, charakterystycznego dla zbiorników bezodpływowych, takich jak opady atmosferyczne oraz parowanie z powierzchni zbiornika.

Słowa kluczowe:
mała retencja, zbiorniki zaporowe, bilans wodny

MIDDLE POMERANIAN SCIENTIFIC SOCIETY OF THE ENVIRONMENT PROTECTION

Rocznik Ochrona Środowiska

Volume 22. Year 2020 ISSN 1506-218X 347-358

Mathematical Model of the Drying Process of Wet Materials

Anatoliy Pavlenko[*]*, Jerzy Zbigniew Piotrowski*
Kielce University of Technology, Poland
[*]*corresponding author's e-mail: apavlenko@tu.kielce.pl*

1. Statement of the problem

Heat treatment of wet materials is a technological process, accompanied by structural and mechanical changes of the dried substance. The research results in drying theory provide scientific basis to study this process intensification and selection of a rational method and optimal mode of heat treatment. The main technological task of heat treatment of materials is to develop combined methods of thermal action on the material with consideration of the main stages of its physico-chemical transformation. It is quite difficult to develop technology and appropriate methods for analytical description of heat treatment processes, involving successive physico-chemical transformations. Thermal swelling of the plastic raw mixture in production technologies of heat-insulating materials can serve as an example of this process. In this case, dehydration, gas formation, frame crystallization and drying processes are implemented. Therefore, the heat treatment method shall provide not only sufficient intensity, but also the best technological material properties.

Selection of rational technology of heat treatment of the material requires knowledge of its temperature field, as the dried product quality largely depends on the magnitude of temperature differences and duration of temperature exposure.

2. Identification of previously unsettled parts of the general problem

Detection of temperature fields and moisture content, when heated, is related to solution of a complex system of non-linear differential equations of heat and mass transfer with moving boundaries (Pavlenko 2018, Pavlenko 2020). However, the limited information on true values of moisture and heat transfer coefficients results only in a qualitative assessment of the processes, thus, complicating use of such solutions in engineering practice.

It is known (Nait-Ali et al. 2017, Dong et al. 2015, Maroulis et al. 2002), that experimentally determined heat transfer coefficients of wet bodies, when heated (thermal conductivity coefficient λ and temperature conductivity coefficient) are represented by effective values with consideration of heat and moisture transfer processes. Then, considering drying only as a thermal process, but with effective heat transfer coefficients with mass transfer, it is possible to obtain analytical dependences, convenient for engineering calculations, determining the temperature field and drying kinetics of wet materials.

3. Problem statement and methods of solution

Let us analyse the symmetrical heating process of wet raw material mixture, 2R thick, with initial moisture content $\overline{U_0}$. Heat transfer from hot heat transfer agent to the material surface occurs according to the law of convective heat exchange at constant values of heat exchange coefficient α and heating medium temperature t_c.

Fig. 1 shows the experimental drying curve and temperature diagram of wet material (2R = 0.16 m) during heating process in an oven at constant temperature of heating air t_c = 100°C (wet-bulb temperature t_m = 42°C). According to the scheme of sequential moisture removal from the material, developed by authors (Nuijten & Knut 2017, Tarnawski et al. 2002), in presented thermogram (Fig. 1) singular points (1-6) are marked, corresponding to a certain type of moisture binding with the body.

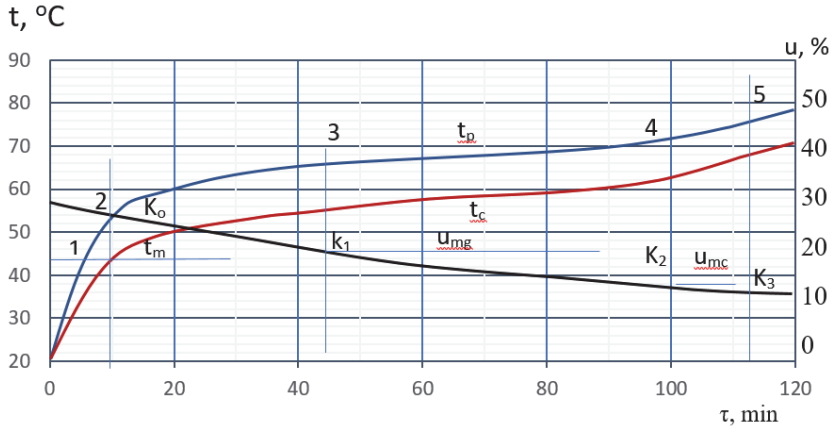

Fig. 1. Surface temperature $t_p(\tau)$, centre temperature $t_c(\tau)$ and moisture content $\overline{U}(\tau)$, constant temperature of heating medium t_c = 100°C

Accordingly, the heating process can be conditionally divided into 6 stages:

- the first stage (0-1) runs at constant moisture content and ends when wet-bulb temperature of material surface is achieved ($t_p = t_m$),
- in the second stage (1-2) capillary moisture, contained in macropores, with negligible binding energy, is removed; at the stage end, temperature in the centre becomes equal to wet-bulb temperature ($t_c = t_m$), drying rate increases to the maximum,
- in the third stage (2-3) macropore moisture is removed from the material; medium-volume moisture content decreases to the maximum hygroscopic value $\bar{u}_{m.g}$ at the stage end, which corresponds to the first critical point k_1 on the drying curve; drying rate remains practicably unchanged,
- in the fourth stage (3-4), micropore capillary moisture is removed; medium-volume moisture content of the material decreases to the maximum adsorption $\overline{U}_{m.c}$, which corresponds to the second critical point k_2 on the drying curve,
- in the fifth (4-5) and sixth (5-6) stages, the polymolecular and monomolecular adsorption moisture is removed; medium-volume moisture content of the material varies from $\overline{U}_{m.c}$ to equilibrium $\overline{U}_{\text{p}}$.

To determine material temperature field in the first stage, with no moisture evaporation present, known solutions are used (Cherki et al. 2014), determining initial conditions for the next stage. The heating process in the second, third and subsequent stages occurs with deepening of evaporation surface of corresponding moisture type from outer surface into the material. Moisture evaporation inside material results in increased pressure of the vapour-air mixture, moving from front of evaporation to the outer body surface of the body and is removed into the environment. Each stage ends, when the surface boundary of phase transformation reaches the plate centre.

With mathematical statement of heat treatment problem, two zones are analysed at the second stage (Fig. 2): central zone 1, where moisture content is taken as constant and equal to initial ($U_1 = \overline{U}_0$), evaporation zone 2, where moisture content also remains unchanged and is equal to medium-volume moisture content of the material at the stage end ($U_2 = \overline{U}_{\text{ко}}$).

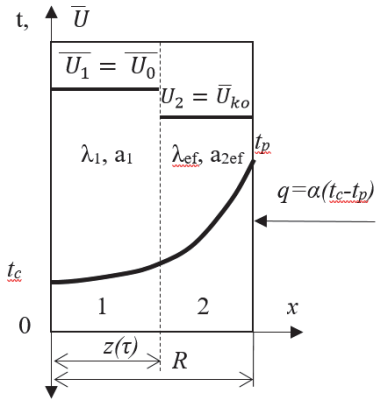

Fig. 2. For mathematical formulation of the problem

We consider that in zone 1 only moisture moves, that is, phase transformation criterion is $\varepsilon_1 = 0$, in evaporation zone 2 moisture moves as vapour ($\varepsilon_2 = 1$). The evaporation surface has a constant temperature equal to wet-bulb temperature t_m. The heat transfer coefficients in each zones are consider as constant.

The following expressions can be used to determine the values of effective thermal conductivity $\lambda_{e\phi}$ and "net" thermal conductivity λ:

$$\lambda_{ef} = \frac{qR}{k_2 \Delta t_k};\ \lambda_{ef} = \frac{(q-q_v)R}{k_2 \Delta t_k}, \tag{1}$$

where q, q_v, Δt_k is a surface heat flow, a heat flow with evaporating moisture and temperature difference over the plate thickness at the end of this heating stage; k_2 is averaging factor of heat flows along the plate thickness, it depends on *Vi* criterion.

These assumptions allow to reduce the problem of heat and mass transfer (Dedic et al. 2003) to the problem of thermal conductivity with a moving boundary of phase transformation, its mathematical formulation includes differential equations of thermal conductivity for two zones:

$$\frac{\partial V_1}{\partial Fo} = \frac{\partial^2 V_1}{\partial x^2}, 0 \le x \le z(Fo) \tag{2}$$

$$\frac{\partial V_2}{\partial Fo} = f_a \frac{\partial^2 V_1}{\partial x^2}, z(Fo) \le x \le 1 \tag{3}$$

with boundary conditions

$$f_\lambda \left(\frac{\partial V_2}{\partial x}\right)_{x=1} = Bi\big(1 - V_2(1, Fo)\big) \tag{4}$$

$$V_1(z, Fo) = V_2(z, Fo) = V_M; \tag{5}$$

$$f_\lambda \left(\frac{\partial V_2}{\partial x}\right)_{x=z(Fo)} - \left(\frac{\partial V_1}{\partial x}\right)_{x=z(Fo)} = \frac{d}{dFo} Ko(Fo) = \Delta Ko \frac{d}{dFo} z(Fo) \quad (6)$$

$$\left(\frac{\partial V_1}{\partial x}\right)_{x=0} = 0 \quad (7)$$

and initial conditions

$$V_1(x,0) = V_0 + \Delta V_0 x^2; V_2(x,0) = V_M; z(0) = 1; Ko(0) = Ko_n \quad (8)$$

Where $V = \frac{t(\chi,\tau)}{t_c}$ - relative temperature; $x = \frac{\chi}{R}$ - relative coordinate; $Fo = \frac{a_1 \tau}{R^2}$ – Fourier number; $Bi = \frac{a \ R}{\lambda_1}$ – Biot number; $Ko(Fo) = \frac{\bar{U}(Fo)r}{C_1 t_c}$ – Kosovich number; $Ki(Fo) = \frac{q(Fo)R}{\lambda_1 t_c}$ – Kirpichev criterion; $z(Fo) = \frac{z}{R}$ - relative coordinate of zone division; $\Delta Ko = \frac{r(\bar{U}_0 - \bar{U}_{k0})}{C_1 t_c}$; $V_M = \frac{t_M}{t_c}$; $V_0 = \frac{t_0}{t_c}$; $\Delta V \ = \frac{\Delta t_0}{t_c}$; $f_\lambda = \frac{\lambda_{2ef}}{\lambda_1}$; $f_a = \frac{a_{2ef}}{a_1}$; $a = \frac{\lambda}{c\rho_0}$; $t(\chi,\tau)$ – temperature function; χ – coordinate; τ – time; λ_{ef}, a_{ef} – effective thermal conductivity and temperature conductivity coefficients; r – vaporization heat; C_1 – specific heat of wet material, attributed to absolutely dry body mass; ρ_o – absolutely dry body density; $\bar{U}(\tau)$ – medium-volume moisture content function; $\bar{U}_{k0}$ – medium-volume moisture content at the end of the second heating stage; t_c – heating medium temperature; t_0 i Δt_0 – temperature of the centre and the temperature difference along plate thickness at the second stage beginning; index "1" refers to the central zone, index "2" – refers to evaporation zone.

The formulated problem (2)-(8) differs from classical Stefan problem in that the boundary condition on the outer plate surface is a time function, and the initial temperature distribution is expressed by a square parabola equation.

To solve the system of non-linear differential equations (2)-(8), the reduction and parametric perturbation (RPP) method is used (Lee et al. 2006), according to this procedure, general solutions of equations (2) i (3) look as follows:

$$V_1(x,Fo) = \sum_{n=0}^{\infty} \frac{x^{2n}}{(2n)!} \cdot \frac{d^n}{dFo^n} \Psi(Fo) \quad (9)$$

$$V_2(x,Fo) = \sum_{n=0}^{\infty} \frac{(1-x)^{2n}}{(2n)! f_a^n} \cdot \frac{d^n}{dFo^n} \varphi(Fo) + \sum_{n=0}^{\infty} \frac{(1-x)^{2n}}{(2n+1)! f_a^n} \cdot \frac{d^n}{dFo^n} \delta(Fo) \quad (10)$$

where: $\Psi(Fo)$ and $\varphi(Fo)$ – temperature functions of the axis and plate outer surface; $\delta(Fo)$ – function of temperature gradient on the plate outer surface.

Solutions (9) and (10) meet the problem initial conditions, when: $\Psi(0)=V_0$;

$$\frac{d}{dFo}\Psi(0)=2\Delta V_0;\ \frac{d^n}{dFo^n}\Psi(0)_{n\geq 2}=0;\varphi(0)=V_M;\frac{d^n}{dFo^n}\varphi(0)_{n\geq 1}=0;$$
$$\frac{d^n}{dFo^n}\delta(0)=0. \tag{11}$$

Complying with solutions (9) and (10), boundary conditions of the problem, we obtain a system of non-linear standard differential equations, to which we introduce a conditional (small) parameter ξ:

$$-f_\lambda\delta(\mathrm{Fo})=\mathrm{Bi}[1-\varphi(\mathrm{Fo})]-\sum_{n=1}^{\infty}\frac{1}{(2n-1)!}\cdot\frac{d^n}{dFo^n}\psi(\mathrm{Fo}); \tag{12}$$

$$\sum_{n=0}^{\infty}\frac{(1-\xi Z)}{(2n)\ !f_a^n}\cdot\frac{d^n}{dFo^n}\phi(Fo)+\sum_{n=0}^{\infty}\frac{(1-\xi Z)^{2n+1}}{(2n)\ !f_a^n}\cdot\frac{d^n}{dFo^n}\delta(Fo)=V_м; \tag{13}$$

$$\sum_{n=0}^{\infty}\frac{(1-\xi h)^{2n}}{(2n)!}\cdot\frac{d^n}{dFo^n}\psi(\mathrm{Fo})=V_м; \tag{14}$$

$$-f_\lambda\left\{\sum_{n=1}^{\infty}\frac{(\xi h)^{2n-1}}{(2n)!f_a^n}\cdot\frac{d^n}{dFo^n}\psi(Fo)+\sum_{n=0}^{\infty}\frac{(\xi h)^{2n}}{(2n)!f_a^n}\cdot\frac{d^n}{dFo^n}\delta(Fo)\right\}= \tag{15}$$
$$=\frac{d}{dFo}Ko(Fo)=N(Fo)=\Delta Ko\frac{d}{dFo}Z(Fo),$$

where: h(Fo)=1-z(Fo) – evaporation zone thickness function.

Required functions Ψ(Fo), φ(Fo), δ(Fo), Ko(Fo), N(Fo) and z(Fo) are given in the form of the following expansions in a series by degrees of a small parameter ξ:

$$\left.\begin{aligned}
&\phi(Fo)=\phi_o(Fo)+\xi\phi_1(Fo)+\xi^2\phi_2(Fo)+...;\\
&\psi(Fo)=\psi_o(Fo)+\xi\psi_1(Fo)+\xi^2\psi_2(Fo)+...;\\
&\delta(Fo)=\delta_o(Fo)+\xi\delta_1(Fo)+\xi^2\delta_2(Fo)+...;\\
&Ko(Fo)=Ko_o(Fo)+\xi Ko_1(Fo)+\xi Ko_2(Fo)+...\\
&N(Fo)=N_o(Fo)+\xi N_1(Fo)+\xi^2N_2(Fo)+...;\\
&Z(Fo)=Z_o(Fo)+\xi Z_1(Fo)+\xi^2Z_2(Fo)+...;\\
&h(Fo)=h_o(Fo)+\xi h_1(Fo)+\xi^2h_2(Fo)+...;
\end{aligned}\right\}. \tag{16}$$

By inserting series (16) in system of equations (12)-(15) and comparing coefficients at the same degrees of parameter ξ, we calculate a sequence of linear differential equations that determine the required functions.

Zero approximation (generating system of equations, determining temperature functions $\Psi_0(Fo)$, $\varphi_0(Fo)$, $\delta_0(Fo)$ and medium-volume moisture content function $Ko_0(Fo)$, moisture removal rate $N_0(Fo)$, phase transformation boundary $z_0(Fo)$ in the absence of perturbations).

$$-f_\lambda \delta_o(Fo) = Bi\left[1-\phi_o(Fo)\right] - \sum_{n=1}^{\infty} \frac{1}{(2n-1)\,!} \cdot \frac{d^n}{dFo^n} \psi_o(Fo); \tag{17}$$

$$\sum_{n=0}^{\infty} \frac{1}{(2n)\,!\, f_a^n} \cdot \frac{d^n}{dFo^n} \phi_o(Fo) + \sum_{n=0}^{\infty} \frac{1}{(2n+1)\,!\, f_a^n} \cdot \frac{d^n}{dFo^n} \delta_o(Fo) = V_м; \tag{18}$$

$$\sum_{n=0}^{\infty} \frac{1}{(2n)\,!} \cdot \frac{d^n}{dFo^n} \psi_o(Fo) = V_м; \tag{19}$$

$$f_\lambda \delta_o(Fo) = \frac{d}{dFo} Ko_o(Fo) = N_o(Fo) = \Delta Ko \frac{d}{dFo} Z_o(Fo). \tag{20}$$

The first approximation (a system of equations, determining the first complement to functions found in the zero approximation)

$$f_\lambda \delta_1(Fo) = Bi\phi_1(Fo) + \sum_{n=1}^{\infty} \frac{1}{(2n-1)\,!} \cdot \frac{d^n}{dFo^n} \phi_1(Fo); \tag{21}$$

$$\sum_{n=0}^{\infty} \frac{1}{(2n)\,!\, f_a^n} \cdot \frac{d^n}{dFo^n} \phi_1(Fo) + \sum_{n=0}^{\infty} \frac{1}{(2n+1)\,!\, f_a^n} \cdot \frac{d^n}{dFo^n} \delta_1(Fo) -$$

$$-Z_o(Fo) \cdot \left\{ \sum_{n=1}^{\infty} \frac{1}{(2n-1)\,!\, f_a^n} \cdot \frac{d^n}{dFo^n} \phi_0(Fo) + \sum_{n=0}^{\infty} \frac{1}{(2n)\,!\, f_a^n} \cdot \frac{d^n}{dFo^n} \delta_0(Fo) \right\} = 0; \tag{22}$$

$$\sum_{n=0}^{\infty} \frac{1}{(2n)\,!} \cdot \frac{d^n}{dFo^n} \phi_1(Fo) - h_o(Fo) \cdot \sum_{n=1}^{\infty} \frac{1}{(2n-1)\,!} \cdot \frac{d^n}{dFo^n} \psi_0(Fo) = 0; \tag{23}$$

$$\frac{f_\lambda}{f_a} h_o(Fo) \frac{d}{dFo} \phi_o(Fo) + f_\lambda \delta_1(Fo) = \frac{d}{dFo} Ko(Fo) = N_1(Fo) = \Delta Ko \frac{d}{dFo} Z_1(Fo). \tag{24}$$

Similarly, the following complements to the main solution are formed.

For practical research of wet material heating processes, the first approximation provides sufficient accuracy.

Therefore, application of RPP method allows transforming the initial non-linear problem of thermal conductivity into a sequence of ordinary linear differential equations.

To solve obtained equations, Laplace's method of integral transformations is used. The calculated analytical dependences, determining temperature

field and drying kinetics of the wet plate are explicit functions, quite simply used in calculations.

Expressions for surface and plate axis temperature functions have the following form:

$$V_2(1,Fo) = V_м + \int_o^{Fo} \Phi_1(Fo - fo)\theta(fo)\,dfo + \phi_1(Fo); \tag{25}$$

$$V_1(0,Fo) = V_o + 2\Delta V_o \cdot G_1(Fo) + \psi_1(Fo), \tag{26}$$

where: $\varphi_1(Fo)$ and $\Psi(Fo)$ – complements to corresponding zero approximation functions.

$$\varphi_1(Fo) = \int_0^{Fo} \Phi_3(Fo - fo)M_1(fo)\,dfo; \tag{27}$$

$$\psi_1(Fo) = \int_0^{Fo} G_2(Fo - fo)M_2(fo)\,dfo \quad . \tag{28}$$

Function of evaporation surface coordinate

$$Z(Fo) = 1 - \frac{Bi}{\Delta Ko}\int_0^{Fo} \Phi_2(Fo - fo)\theta(fo)\,dfo + Z_1(Fo), \tag{29}$$

where:
$$Z_1(Fo) = \frac{1}{\Delta Ko} Ko_1(Fo) \quad . \tag{30}$$

Function of medium-volume moisture content of the material

$$Ko(Fo) = Ko_н - Bi\int_o^{Fo} \Phi_2(Fo - fo)\theta(fo)\,dfo + Ko_1(Fo), \tag{31}$$

where:

$$Ko_1(Fo) = \int_o^{Fo} N_1(fo)\,dfo. \tag{32}$$

Function of moisture removal rate from material:

$$N(Fo) = Bi\int_0^{Fo} \Phi_3(Fo - fo)\theta(fo)\,dfo + N_1(Fo), \tag{33}$$

where:

$$N_1(Fo) = \frac{f_\lambda}{f_a} \cdot \frac{d}{dfo}\phi_o(Fo)\left[1 - Z_o(Fo)\right] + Bi \cdot \phi_1(Fo). \tag{34}$$

The following functions are used in computed expressions:

$$\Phi_1(Fo) = f_a \sum_{n=1}^{\infty} A_n \mu_n^2 \exp\left(-f_a \mu_n^2 Fo\right); \tag{35}$$

$$\Phi_2(Fo) = \frac{1}{1+Bi_1} + \sum_{n=1}^{\infty} A_n \cdot \exp\left(-f_a \mu_n^2 Fo\right); \tag{36}$$

$$\Phi_3(Fo) = -f_a \sum_{n=1}^{\infty} \frac{A_n \mu_n^2}{\mathrm{Cos}\,\mu_n} \exp\left(-f_a \mu_n^2 Fo\right); \tag{37}$$

where:

$$A_n = \frac{2Bi_1}{\mu_n^2 + Bi_1 + Bi_1^2};\ \mathrm{Bi}_1 = \frac{\mathrm{Bi}}{\mathrm{f}_\lambda};$$

μ_n– equation roots: tgμ=- μ/Bi$_1$;

$$G_1(Fo) = \frac{1}{2} - \sum_{k=1}^{\infty} (-1)^{k+1} \frac{2}{\mu_n^3} \exp\left(-\mu_k^2 Fo\right); \tag{38}$$

where:

μ_k =0.5(2k-1)π;

$$G_2(Fo) = 1 - \sum_{n=1}^{\infty} \frac{2}{\mu_k^2} \exp\left(-\mu_k^2 Fo\right); \tag{39}$$

$$\theta(Fo) = 1 - V_м - \frac{2\Delta V_o}{Bi}\left[1 - G_2(Fo)\right]; \tag{40}$$

$$M_1(Fo) = -Z_o(Fo) \cdot Bi_1 \int_o^{Fo} \Phi_3(F0 - fo)\theta(fo)\,dfo; \tag{41}$$

$$M_2(Fo) = 2\Delta V_o\left[1 - Z_o(Fo)\right]\left[1 - G_2(Fo)\right]. \tag{42}$$

To determine the temperature field and drying kinetics in the third and subsequent stages of heating, the same analytical dependences are used, but with new initial conditions, obtained at previous stages.

4. Results and discussion

Calculation results of the heating process of a wet raw material block, *2R* thick = 0.016 m at constant temperature of the heating medium (air) are shown in Fig. 3.

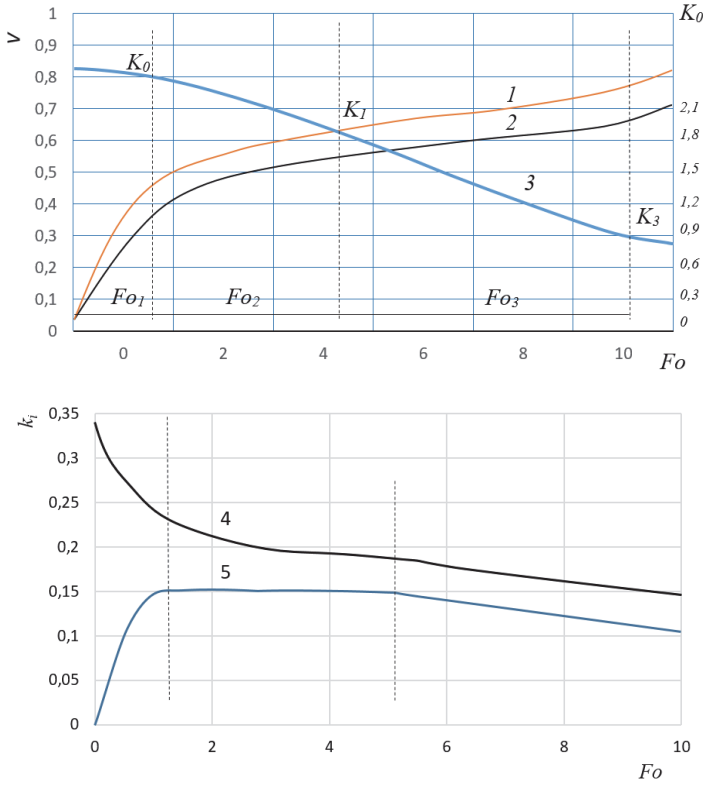

Fig. 3. Temperature and thermal diagrams: 1, 2 – relative temperature of a block surface and centre; 3 – dimensionless function of moisture content *Ko(Fo)*; 4 – surface heat flow *Ki(Fo)*; 5 – dimensionless rate of moisture removal from the material *N(Fo)*

Calculations were performed for the following conditions:

$\overline{U}_0 = 0.37$ kg/kg; t_c=100°C; t_M=42°C; α=15,7 W/(m^{2}K); ρ_o =530 kg/m^3;

λ_1=0.2W/(mK); λ_{ef}=0.25W/(mK); $a_1=0.1\cdot10^{-6}$ m^2/s; $a_{ef}=0.12\cdot10^{-6}$ m^2/s.

Calculated data agree quite well with those found by experiment (Fig. 1), obtained by heating the samples in the oven under the same conditions.

5. Conclusions

Based on the studies of temperature field and moisture evaporation kinetics, the entire heating process can be divided into six stages according to the scheme of sequential removal of moisture from the material. The heating process in each stage runs with deepening of evaporation surface of corresponding moisture type from outer surface into the material. Each stage of symmetrical heating ends, when the surface boundary of phase transformation reaches the plate centre. Experimental data show that temperature distribution over material thickness at the end of each stage is parabolic. Therefore, using the formulas for regular heating mode, it is possible to determine effective heat transfer coefficients, considering heat and moisture transfer.

References

Cherki, A.B., Remy, B., Khabbazi, A., Jannot, Y., Baillis, D. (2014). Experimental thermal properties characterization of insulating cork-gypsum composite. *Construction and Building Materials, 54*, 202-209.

Dedic, A. Dj., Mujumdar, A.S., Voronjec, D.K. (2003). A three dimensional model for heat and mass transfer in convective wood drying. *Drying Technology, 21*(1), 1-15.

Dong, Yi, McCartney, John S., Lu, Ning. (2015). Critical Review of Thermal Conductivity Models for Unsaturated Soils. *Geotechnical and Geological Engineering, 33*, 207-221.

Lee, D.J., Lai, J.Y. Mujumdar, Arun, S. (2006). Moisture Distribution and Dewatering Efficiency for Wet Materials. *Drying Technology, 24*(10), 1201-1208.

Maroulis, Z.B., Krokida, M.K., Rahman, M.S. (2002). A structural generic model to predict the effective thermal conductivity of fruits and vegetables during drying. *Journal of Food Engineering, 52*(1), 47-52.

Nait-Ali, B., Oummadi, S., Portuguez, E., Alzina, A., Smith, D.S. (2017). Thermal conductivity of ceramic green bodies during drying. *Journal of the European Ceramic Society*, *37*(4), 1839-1846.

Nuijten, Anne D.W., Knut, V. (2017). Modelling the thermal conductivity of a melting snow layer on a heated pavement. *Cold Regions Science and Technology, 140*, 20-29.

Pavlenko, A. (2018). Dispersed phase breakup in boiling of emulsion. *Heat Transfer Research, 49*(7), 633-641. DOI: 10.1615/HeatTransRes. 2018020630.

Pavlenko, A. (2020) Energy conversion in heat and mass transfer processes in boiling emulsions. *Thermal Science and Engineering Progress, 15*(1), 100439. DOI: https://doi.org/10.1016/j.tsep.2019.100439. [Accessed 23 April 2020]

Tarnawski, V.R., Leong, W.H., Gori, F., Buchan, G.D., Sundberg, J. (2002). Inter-particle contact heat transfer in soil systems at moderate temperatures. *Int. J. Energy Res., 26*, 1345-1358.

Abstract

The problem of heat treatment of wet materials contains the question of the heat and mass inside the body transfer (an internal problem) and in the boundary layer at the interface between phases (an external problem). The amount of removable moisture depends on the degree of each of these processes development. When heated, the moisture content on the surface decreases, creating a concentration difference across the body. Therefore, a flow of moisture occurs in the body from deep layers to the surface, towards which the flow of heat is directed. Thus, when wet materials are heated, complex processes of moisture and heat exchange occur, mutually affecting the enthalpy and moisture content of both the heated material and the environment.

The features of mathematical model construction of heating and drying of wet materials process are considered in the article. The drying process is defined as a thermal process with effective heat transfer coefficients with consideration of mass transfer. It makes it possible to obtain analytical dependencies that are convenient for engineering calculations, with which you can determine the temperature field and evaluate the kinetics of wet materials drying.

Keywords:
thermal insulation materials, mathematical modelling, heat treatment,
thermal conductivity, thermal processes

Model matematyczny procesu suszenia materiałów wilgotnych

Streszczenie

Problem obróbki cieplnej wilgotnych materiałów obejmuje zagadnienia transferu ciepła i masy wewnątrz komponentu (problem wewnętrzny) i w warstwie granicznej z przemianą fazową (problem zewnętrzny). Ilość usuwanej wilgoci zależy od stopnia rozwoju każdego z tych procesów. Po podgrzaniu zawartość wilgoci na powierzchni zmniejsza się, tworząc różnicę koncentracji w całym materiale. Dlatego w materiale występuje przepływ wilgoci z głębokich warstw na powierzchnię, na którą skierowany jest przepływ ciepła. Oznacza to, że gdy ogrzewane są wilgotne materiały, zachodzą złożone procesy wymiany wilgoci i ciepła, wpływając wzajemnie na entalpię i zawartość wilgoci zarówno ogrzewanego materiału, jak i środowiska.

W artykule omówiono cechy budowy modelu matematycznego procesu ogrzewania i suszenia materiałów zawilgoconych. Proces suszenia definiuje się jako proces termiczny o efektywnych współczynnikach przenikania ciepła z uwzględnieniem transferu masy. Umożliwia uzyskanie zależności analitycznych dogodnych do obliczeń inżynierskich, za pomocą których można określić pole temperatury i ocenić kinetykę suszenia wilgotnych materiałów.

Słowa kluczowe:
materiały termoizolacyjne, modelowanie matematyczne, obróbka cieplna,
przewodnictwo cieplne, procesy termiczne.

MIDDLE POMERANIAN SCIENTIFIC SOCIETY OF THE ENVIRONMENT PROTECTION

Rocznik Ochrona Środowiska

Volume 22. Year 2020 ISSN 1506-218X 359-375

The Problem of Reducing Consumption of Stretch Film Used to Secure Palletized Loads

Sławomir Tkaczyk

Warsaw University of Technology, Poland

corresponding author's e-mail: slawomir.tkaczyk@pw.edu.pl

1. Introduction

Damage to cargo during transport occurs as a result of improper securing of the cargo. In some situations, inadequate securing of cargo causes not only material losses, caused by partial or complete damage to the cargo, but may threaten the safety of participants in the distribution of cargo in the distribution chain as bystanders as well. Irrespective of this, these damages can also affect the unplanned extension of deliveries or even prevent further deliveries. As consequence, there are unplanned additional costs charged to the sender preparing the cargo for shipment. Up-mentioned dangers and difficulties as well as additional costs caused by human errors in packing (Bujak & Zajac 2013) and securing cargo can be remedied and certainly significantly reduced.

The way to achieve this goal is to make manufacturers, distributors and carriers aware of the need for proper packaging and securing the cargo ensuring the safety of all participants in the distribution chain. The aim of the article is to present the problem of rational use of stretch film as the most frequently used method of securing loads. The development of methods and procedures for securing palletized loads with stretch film will allow significant reduction of film used while ensuring proper load security. As the result, there will be a major impact on our safety and the surrounding environment.

2. Packaging and security of the cargo

In the literature, we can find various definitions of packaging. A packaging can be understood as a separable coating of the packed goods, protecting and securing the goods against the influence of mechanical energy during the transport process and influence of environment. According to another definition, packaging can be a product intended to protect other products against damage, as

well as to protect the environment against the harmful effects of the packed goods (Salomon 2017).

The package consists of:

- packaging agent – product made of packaging material, intended to cover the packaged goods or maintain them in their entirety,
- auxiliary packaging agents – used for packaging, sealing and preparation for shipment of packaged goods.

Possible features of the product:

- sensibility to weather conditions,
- susceptibility to accumulation,
- susceptibility to explosion, flammability and self-heating,
- harmful to human health,
- possibility of damage or destruction of other products coming into contact with given type of product or located nearby.

The more of up-mentioned features has a product at the same time, the more difficult it is to choose the right packaging.

From the point of view of logistics (Zajac 2015), the most important is to protect the goods from damage or spoilage (during transport and/or storage). The unit packages (1st grade), then collective packages (2nd grade) and transport packaging (3rd grade) created in the process of goods distribution must meet the requirements of standardisation and dimensional coordination (Szpotański 2010, Świeboda & Zając 2016).

Unit packages are mainly required to protect the product against changes in the required properties. On the other hand, the collective and transport packaging should protect against mechanical damage (e.g. vibrations, impacts, static pressure) and climatic (e.g. rain, temperature, humidity, pressure) during transport and handling.

Second line packaging includes packaging materials and components that are responsible for the grouping of packaged units and participate in the creation of a complete shipping unit. This will include collective cartons, bundle films or so-called seams, adhesives, clips and basic carriers of information (labels, pendants, badges). Third line packages include: all types of cargo pallets (Świeboda and Zając 2017), slip sheets (boards replacing cargo pallets), all loading pads and spacers, mats, protective corners, strapping tapes, information labels, stretch films, heat-shrinkable hoods and others being an integral part of pallet cargo.

In the era of increasingly widespread use of multi-level distribution chains and a logistic point of view, packaging should ensure (IRU 2015, Salomon 2017, Szpotański 2010, Woźniak et el. 2016):

- strength of the structure giving/guaranteeing proper protection of packaged products during transport, storage and reloading,
- proper fastening of the contents inside the packaging, taking into account the possibility proper distribution of the weight of the product on the structural elements of the bottom and sufficient protection against shocks,
- protection against weather conditions during transport appropriate for the product and the climate,
- customized packaging based on the expected methods of storage,
- maximum limitation of the size and weight of the package,
- reasonable and economical use of materials,
- technologically convenient structure ensuring ease of packaging and fastening of products,
- possibly low manufacturing costs (material and labour costs),
- the possibility of reuse or recycling of packaging materials,
- the aesthetic appearance of the packaging and the surfaces allowing required marking.

From an economic point of view, packaging should fulfil required functions at optimal (lowest) cost. The requirements for packaging relate to the cost of packaging and the efficiency of packaging. Naturally, the commodity lose analysis is also being taken into account. The costs of packaging of the products are significant and they are valued at an average of 15% of their total value. As per estimation, proper packaging of products can reduce transport and storage costs by around 6%. Moreover, it can reduce the amount of freight losses caused by quantity loss and deterioration of packaged products by around 8%. It is worth to remember, that the results of insufficient packaging of goods are generally much worse than the effects of possible excessive and too expensive packaging (Rucińska & Kędzior-Laskowska 2015).

The value of packaging materials is approx. 50% of all packaging costs. Additionally, we should take into account losses during transport or storage as the result of the use of unsuitable or under-quality material (cost saving procedures by using cheaper, low quality packaging materials).

Logistics market operators as well as manufacturers of various goods are looking for ways to reduce costs, creating the conflicts between both parties. Manufacturers will try to reduce the cost of collective packaging as much as possible (collective packages do not influence customers' purchasing decisions), while for transport operations, properly packed cargo will determine the safety and quality of the transported cargo. As safe cargos we can call all packages delivered without damage to the contents of the package and without final changes affecting the dimensions of an individual package. In practice, it is very difficult

to be achieved. Damage to the cargo can be affected by following factors: package design features (size, weight, shape) and distribution conditions (distance, transport conditions, reloading). Therefore damages and loses can be stopped by proper packaging and cargo securing during transport.

Preparation of the cargo for transportation – properly selected packaging (shape, resistance to pressure, etc.), and most important – the proper way of forming and securing of the single package is a very important issue for the producer/sender (as the first link in the distribution chain). It has a huge impact on minimizing damage to the cargo during the transport (Deja et al. 2017, Tkaczyk 2016).

When analysing the rationality of the use of packaging, we should not only take under consideration costs of materials but also the cost of packaging (labour), transport, storage, shipping and losses as results of damage of products in packages. The optimal option is to consider a product packaging system where the sum of packaging costs and losses is the lowest while maintaining its functionality. Therefore, economically optimal packaging is considered to achieve a minimum total cost (packaging and losses) (Szpotański 2010).

In order to prevent damage in the supply chain, loads are usually secured with stretch film.

3. Stretch film

Synthetic materials (plastics) consist mainly of synthetic organic polymers, i.e. polyethylene (PE), polypropylene (PP), polyvinyl chloride (PVC), polyethylene terephthalate (PET) or polystyrene (PS). Polyethylene (PE) can be divided in to two types, i.e. low (LDPE) and high density (HDPE) (Fig. 1).

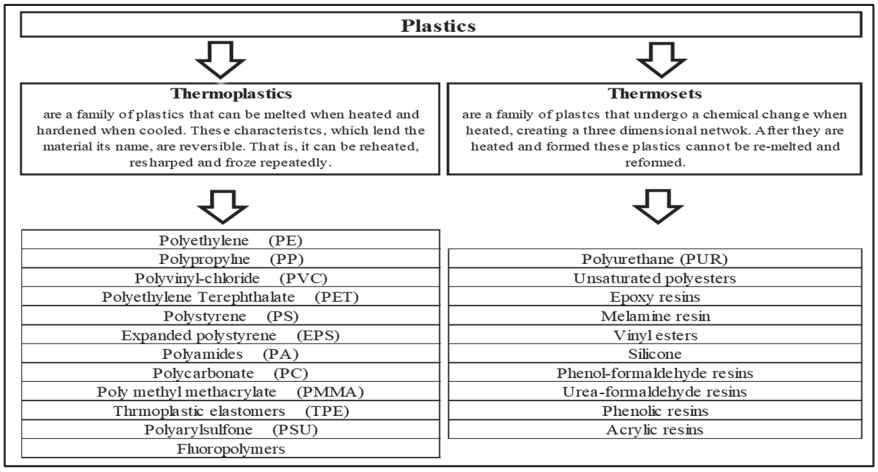

Fig. 1. The division of synthetic materials (PlasticsEurope 2019)

Plastics demand in Europe in 2019 was on the level of 51.2 million tonnes (in 2018 was on the level of 61.8 million tonnes and in 2017 was on the level of 64.4 million tonnes) with a turnover over 360 billion euros (Fig. 2).

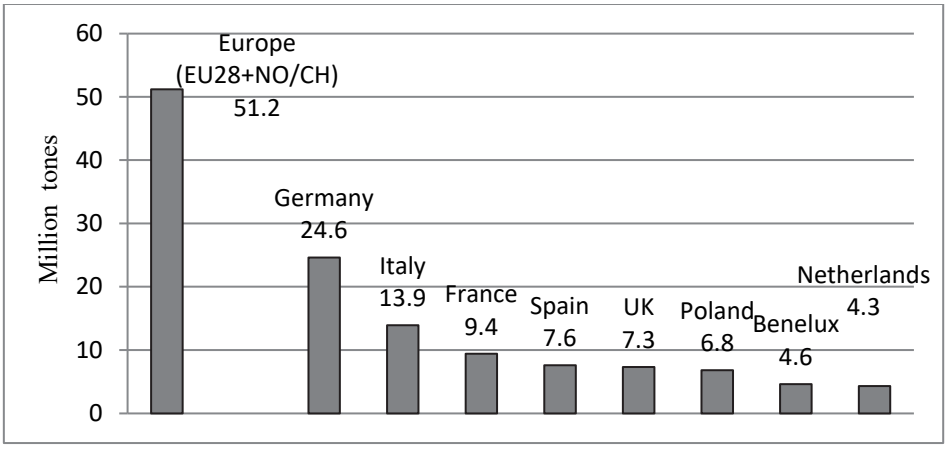

Fig. 2. Synthetic materials demand by country and application segment (PlasticsEurope 2019)

Plastics industry provides employment for more than 1.6 million people in nearly 60000 of companies. The main segments using synthetic materials are: packaging industry 39.9%, construction industry 19.8%, automotive industry 9.9%, electrical and electronic equipment 6.2%, household appliances, sport and leisure 4.1%, agriculture 3.4% and others 16.7% (equipment and mechanical devices, furniture, medical equipment) (Fig. 3). Data collected by Plastics Europe, Association of Plastics Manufacturers in Europe (PlasticsEurope 2019) and EPRO (European Association of Plastics Recycling and Recovery Organisations) (https://ami.international, Lenort et al. 2019).

In the packaging industry, one of the most popular materials is stretch film, produced by linear processing of low-density polyethylene LLDPE (Fig. 4-5). There are two methods of stretch film production: the "blown" extrusion method and the "cast" slot method. LLDPE is divided into butane (C4); hexane (C6); octane (C8) depending on the length of the carbon chains. Depending on which material we use for further processing, we will obtain a film with different properties.

Fig. 3. Plastics demand by segment 2019 (PlasticsEurope 2019)

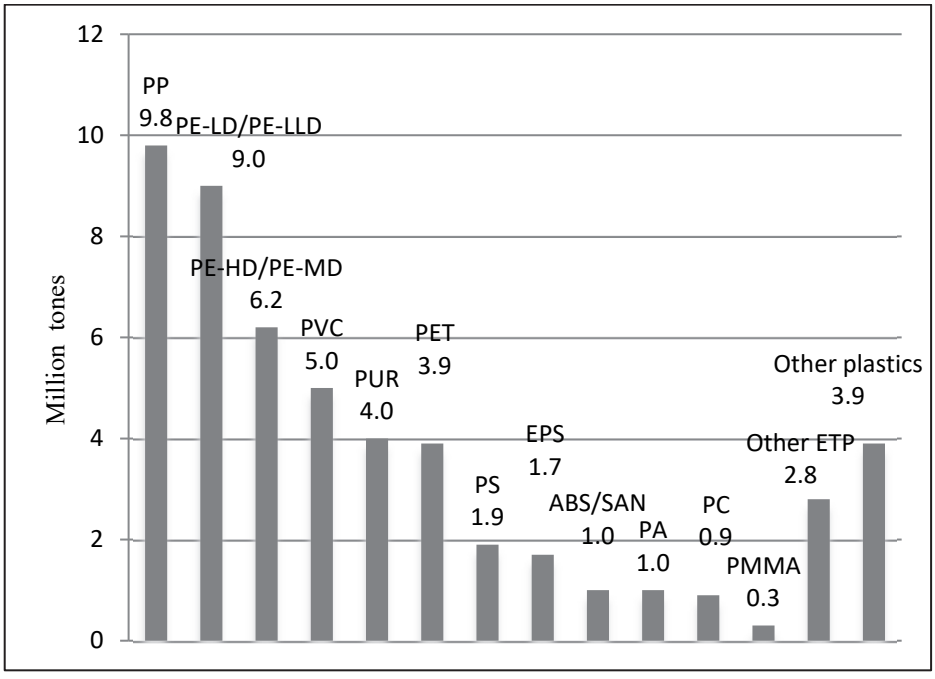

Fig. 4. Plastics demand by resin types 2018 (PlasticsEurope 2019)

Fig. 5. Plastics demand by segments and polymer types in 2018. Total 51.2 M (PlasticsEurope 2019)

Stretch film is the name of a multilayer stretch polyethylene film. The basic raw material for stretch film production is linear low density of polyethylene (LLDPE). It is the most popular and the cheapest form of cargo packaging. It does not require the use of expensive equipment to protect the goods, as in the case of heat-shrink films. In addition to stabilizing function for cargo on pallets, stretch film protects the cargo from the weather conditions. The use of coloured stretch films makes possible to hide the contents of the cargo or to identify a customer or a group of products in logistics centres (http://www.nowafolia.pl, https://opakowania.com.pl, https://tworzywa.org, https://pzpts.pl).

Types of standard stretch films:

- manual – designed for manual wrapping of the load; standard is a 500 mm wide film with a thickness of 17-30 microns. Most popular thickness for manual wrapping stretch film: 23 microns; standard stretch of film: 150-180% (one meter of film can be stretched from 150 cm up to 180 cm during unwinding from the roll until final break), different colours,
- machine – designed for wrapping non-deformable goods using automatic and semi-automatic wrappers (the machine wrapping process saves material and speeds up packing); standard 500 mm wide, 12-30 microns thick, different

colours; it is available in three standards of stretch: standard (150% up to180% stretch), power (200% up to 250% stretch) and superpower (250% up to even 300% stretch).

There are different film classification possibilities:

- standard stretch,
- pre-stretch: pre-stretched film in the production process to a value of about 200%; it is available in both manual and machine versions due to a different production technology (it is created by mechanic stretching the stretch film between 2 rollers - unwinding and winding. Due to the fact, that the secondary roll (winding) is larger and rotates faster than the main roll (unwinding) the stretch film is pulled between them and stretched to the required parameters) the standard width of the pre-stretch is usually 430 mm and it is thinner than the other stretch films (8 up to 12 microns) (http://www.nowafolia.pl, https://opakowania. com.pl, https://tworzywa.org, https://pzpts.pl).

When selecting the stretch film (proper selection of thickness and quality standard of the film for the load to be secured) the specificity of the product, its shape and weight, transport conditions and specification of the wrapping machine should be taken into account.

An important aspect of the widespread and excessive use of plastics is a serious environmental problem. As research shows, we can find them in any environment - in rainwater, in human bodies (6000 plastic particles), which was confirmed by research conducted in Germany – the presence of plastic was found in the organisms of 97% of the examined children (micro-particles with a diameter of 5 μm and nanoparticles with a diameter of <100 nm enter the body through various routes: dermal, digestive and respiratory), in sewage sludge (4196-15385 kg/dry weight), in rivers, e.g. in the Danube (approx. 900 particles/m^3), in ocean waters (from 8 to 9200 particles/m^3) where plastic waste formed a huge island of trash in the Pacific Ocean with the area 5 times larger than area of Poland. Estimated weight of drifting waste can be even 3 million tonnes (Bukowska & Kik 2019, Stachurek 2012).

Extremely important in the protection of the environment and living organisms is the handling of used plastic. It can be collected in landfills, where it can last from 100 up to 1000 years or it can be recycled (Directive of the European Parliament and UE Council from2 7 March 2019 about the reduction of the environmental impact of certain plastic products, 2019. Until 2015, there was only one waste incineration plant in Poland, located in Warsaw. Currently, we also have incineration plants in Białystok, Bydgoszcz, Konin, Kraków, Poznań and Rzeszów (Mroziński 2009).

4. Solutions for limiting the use of the film

With the ever-increasing demand for stretch film, both manufacturers and operators involved in supply chain (Chamier-Gliszczyński & Staniuk 2018) freight transport are paying increasing attention to optimising of freight packaging costs. To reduce stretch film consumption companies implement more or less advanced solutions (Fig. 6-9).

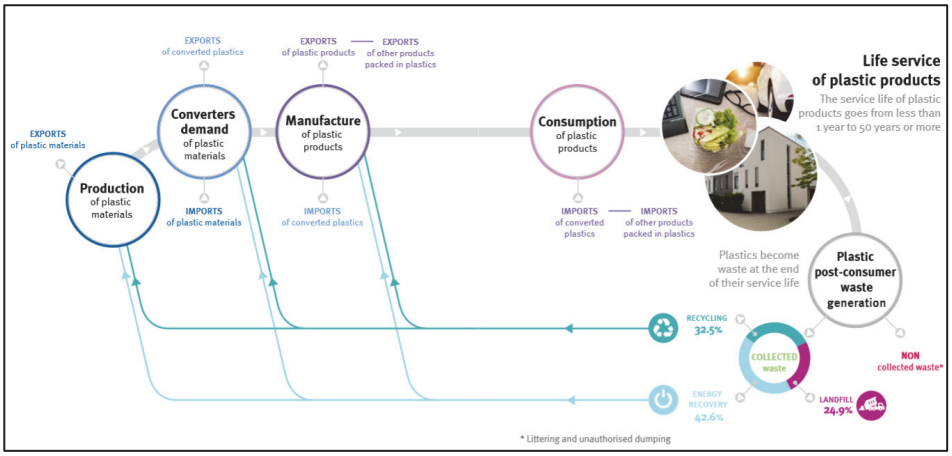

Fig. 6. The life cycle of plastic products (PlasticsEurope 2019)

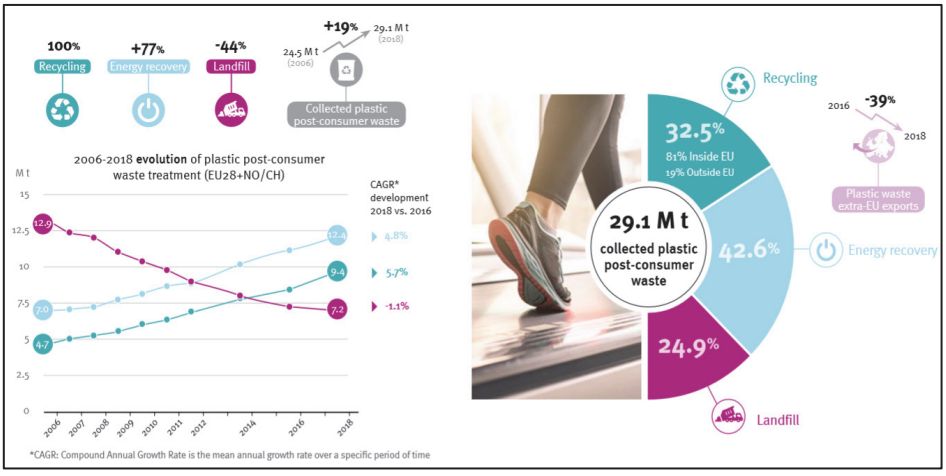

Fig. 7. Plastic postconsumer waste treatment in 2018 (PlasticsEurope 2019)

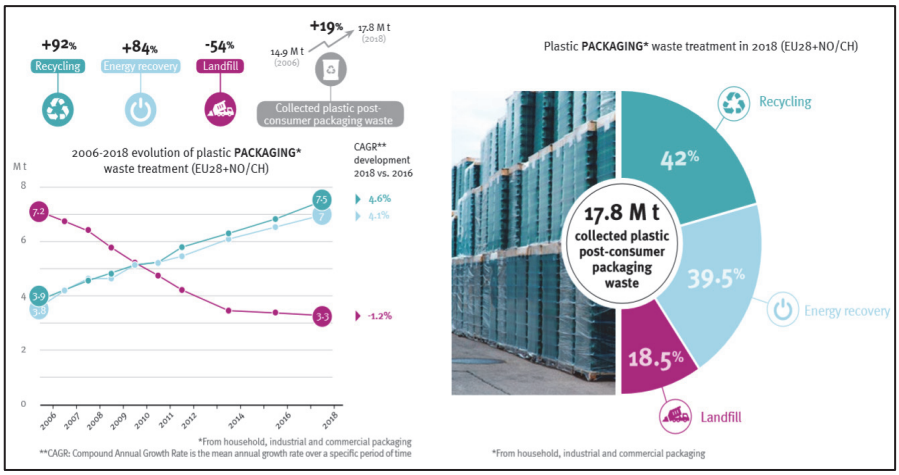

Fig. 8. Recycling is the first option for plastic packaging waste (PlasticsEurope 2019)

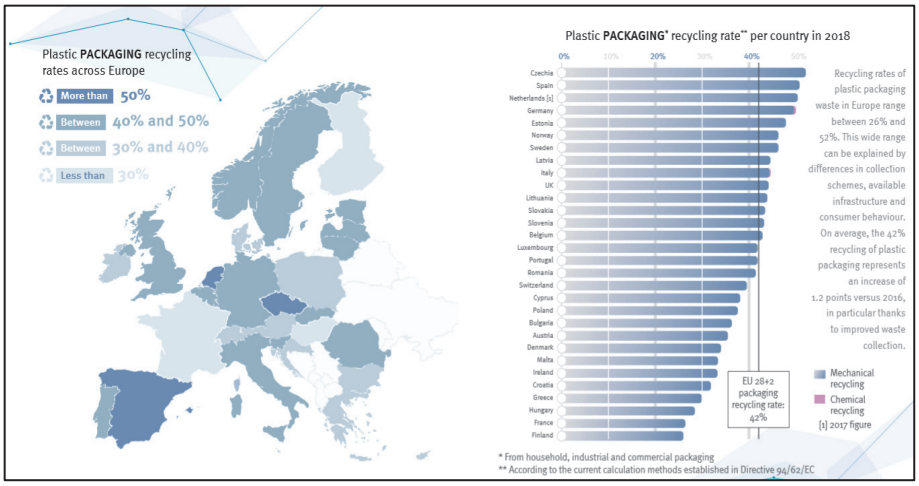

Fig. 9. Plastic packaging recycling (PlasticsEurope 2019)

One of the simplest solutions to reduce the consumption of stretch film is to use stretch film with higher parameters. It is commonly believed that the thicker the film, the more durable it is. However, film manufacturers are increasingly paying attention to the efficient and ecological aspect of film production. Stretch with a higher quality standard (Power or Superpower) can enable more efficient use of one meter of stretch to secure the goods. On the other hand, thin films allow a better use of a kilogram of stretch to wrap the load, within less waste. Currently, increasingly grows the use of pre-stretch film. Experts mention

greater comfort of use, higher efficiency (pre-stretch means up to 65% less consumption per kg of film, half as much waste and 3 times more stretch!) and thus lower cargo-securing costs.

Pre-stretch films are used in following cases (http://www.nowafolia.pl, https://opakowania.com.pl, https://tworzywa.org, https://pzpts.pl):

- packaging light and/or delicate products on a pallet e. g. plastic packaging (bottles, containers, dishes, pans), where thick stretch films are not needed,
- pallet wrapping on straight wrappers without a pre-stretch system (with a mechanical brake); as they have low stretch, significant savings can be made on wrappers without a stretch system, replacing the thick stretch films currently in use.

Another way to reduce film wear is to use film with Nano-layers. It is an extremely ecological, but also economic product. By using Nano- layers, the same gripping forces have been achieved as in a traditional film, but with much less material used. The producer of this film claims: "the improvement of film parameters, leading to a reduction in the number of film used to wrap individual pallets will be an important developmental direction for the coming years".

Another way to reduce the consumption of stretch film is to introduce changes in the management and control of stretch film consumption. One of methods, implemented on the Polish market, is the application of ASM (Auto-Stretch Manager) film consumption management, which consists in the use of a device allowing for the control of stretch film consumption. Its operation is simple - after scanning the employee's ID, the feeder retrieves used film rolls and issues new rolls. The device weighs the used rolls and records how many kilograms of film have been used. The device connected to the storage system enables the collected data to be compared with the number of packed pallets, cartons and global film consumption (in cubic meters). On the basis of the obtained unit indicators of film consumption, it is possible to determine the quantity and level of film consumption in the warehouse check for what purpose it was used and control its quality. By using ASM the operator can reduce film consumption by approx. 10% (https://www.eurologistics.pl/eurologistics/newsy/autorskie rozwiazania logistyczne).

Another approach to the problem of reducing film consumption can be observed in one of the Polish film producers. In his opinion, "among the challenges that producers face, especially important can be re-modelling of the business to function in accordance with the requirements (philosophy) of the Closed Circuit Economy. An effective system of selective waste collection (Chamier-Gliszczyński 2010, Chamier-Gliszczyński 2011, Chamier-Gliszczynski & Krzyzynski 2004) will undoubtedly increase the level of recyclates used in plastic products, which will have a significant and positive impact on the environment

and allow full use of the fantastic possibilities of plastics for reprocessing. However, a huge task will be reminding this to consumers. Products as stretch film, that are produced from one component, are fortunately an excellent raw material for reprocessing" (Ergis 2020).

All the above mentioned ways of reducing the use of stretch film increase the efficiency of using one meter of film to secure the load. Currently, it is necessary to implement methods and procedures to rationalize (optimize) the consumption of stretch film protecting the transported palletized cargo. Testing methods for the behaviour of cargo and its components in transport processes have been developed on the basis of experience and laboratory tests of packaging, cargo transport and storage procedures conducted by organisations established for this purpose and research units operating in large transport companies, such as ASTM International (American Society for Testing and Materials), ISTA ((International Safe Transit Association) or EUMOS (Europe Move It Safe).

On the basis of gained experience, EU developed the Directive 2014/47/EU to guarantee the safety of cargo transportation on EU roads by ensuring proper securing of cargo on the vehicle. To guarantee quality standards, EUMOS developed the EUMOS 40509 method (included in Directive 2014/47/EU), which aims to guarantee the safety and rigidity of the cargo (EUMOS 40509, 2012). Currently (as of June 2020), EUMOS 40509 standard is in force since 2012. Recently it is being updated and will be published in the third quarter of 2020.

EUMOS 40509 is a dynamic test system that can be used to assess the stiffness and safety of accelerated or decelerated cargo, similar to road transport (EN 12195-1, 2011), (EN 12642, 2006), (Regulation of the Minister of Infrastructure of 25 January 2018 on the method of cargo transportation, 2018), (Regulation of the Minister of Infrastructure of 24 December 2019 amending the Regulation on technical conditions of vehicles and the scope of their necessary equipment, 2019). The method is addressed (inter alia) to manufacturers of goods transported on pallets, where they bear full responsibility for the compliance of the transported product with the above-mentioned legal act. The direct advantages of using this method can be demonstrated within following:

- assessment of the stiffness and safety of cargo subjected to horizontal accelerations and decelerations,
- compliance with the European Directive 2014/47/EU,
- reduction of the cost of packaging ensuring the safety of the transported cargo and safety in warehousing (Kostrzewski 2013),
- increase of road transport safety.

To comply with EUMOS 40509, there must be performed a stability test (Fig. 10). On the horizontal stabilizer can be performed personalized tests. By simulating the conditions of individual loads transport, by way of experiments, is possible to select a film suitable for each customer with exact parameters such as thickness, holding force, stretch, puncture resistance (Tkaczyk 2016, Kostrzewski 2020, Kielec et al. 2018). At the same time, it guarantees the appropriate level of cargo stiffness (determined on the basis of cargo deformation, where the maximum value of deformation is determined by the EUMOS standard).

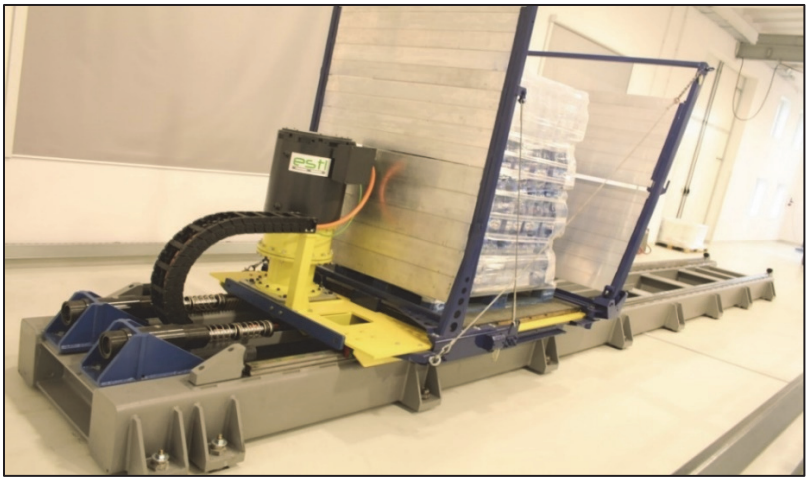

Fig. 10. Stability tester for tests conducting according to EUMOS 40509 (Ergis 2020)

It is important to understand that good stability of the pallet requires an appropriate wrapping specification. The use of higher quality stretch film has the effect of reducing its use while maintaining and improving the rigidity of the palletised load. There is currently only one independent institute, ESTL, which specialises in cargo packaging and securing tests and can offer certification in Western Europe. In Spain, ITENE can also issue certificates.

5. Conclusions

The material losses as results from damage to goods during transport are enormous. It is estimated that on the American market it is U$ 2.6 trillion. It is difficult to obtain data on this subject on the Polish market (CDS 2020, https://its.waw.pl). However, there are even greater losses than just material ones. Many people lose their lives or are injured due to poorly secured goods for car transport. Statistics for 2014 show that 1200 people in Europe have died in accidents as a result of this problem.

Therefore, it will be essential, to take action for significant improvement of methods and procedures of securing the cargo transported. The development of a research method enabling the analysis and assessment of possible behaviours of cargoes transported in the supply chains, used to secure the cargo of stretch film and packaging methods used in the shaping of the juniper, will significantly improve the safety of all the cargo types participating in the execution of the transport. It will reduce the use of the stretch film while reducing the safety risk, damage or destruction of the load and difficulties occurring in logistic processes. Moreover, it will reduce the costs of operations for all.

The development of a research method and the implementation of new procedures rationalizing (optimizing) the use of stretch film will help to protect better the planet's environment and its resources. The problem of proper cargo securing becomes even more important when we become aware of other threats. Cargo load, when properly secured with stretch film, protects environment from pollution. It means, that stretch film is no longer understood as environmental pollution (rubbish) and becomes a tool to ensure safety and reduce the effects of the transported products on the environment. Minimizing level of damage and number of damaged loads is another important subject, which we often do not pay attention to. It causes a secondary reduction in the use of the natural resources of the environment, necessary for the re-production of damaged or destroyed products.

The direct and indirect costs of damaged and destroyed products, the costs of used natural resources for the re-manufacturing of goods many times exceed the costs of production and disposal of stretch film used for securing cargo. Nevertheless, it is necessary to strive to reduce the use of stretch film by using appropriate methods and procedures for securing loads with stretch film. Taking into account economic and ecological criteria, we have to ensure high quality of stretch film and its optimal use, as it plays a key and irreplaceable role in the distribution chains of products transported in bulk in the global economy.

References

Bujak, A., Zajac, P. (2013). *Monitoring of cargo in logistic systems of transport and storage*. In International Conference on Transport Systems Telematics, Springer Berlin, Heidelberg, 361-369.

Bukowska, B., Kik, K. (2019). *Plastic in the environment. What do we know about its harmfulness*. Łódź: Foundation for Enterprise Development in Łódź. PRF Bulletin.

Chamier-Gliszczynski, N., Krzyzynski, T. (2004). *On modelling three-stage system of receipt and automotive recycling*. REWAS'04, Global Symposium on Recycling, Waste Treatment and Clean Technology 2005, Madrid, Spain, 26-29 September 2004, Conference Paper, ISBN: 8495520060, 2813-2814.

Chamier-Gliszczyński, N. (2010). Optimal Design for the Environment of the Means Transportation: a Case Study of Reuse and Recycling Materials. *Sold State Phenomena, 165*, 244-249.

Chamier-Gliszczyński, N. (2011). Environmental aspects of maintenance of transport means, end-of life stage of transport means. *Eksploatacja i Niezawodnosc-Maintenance and Reliability, 2*, 59-71.

Chamier-Gliszczyński, N., Staniuk, M. (2018). *Logistics audit 9A in the assessment of supply chain efficiency of companies operating in the industry 4.0*. CLC 2018: Carpathian Logistics Congress Conference Proceedings, 03-05 December 2018, Prague, Czech Republic, 482-487.

Deja, A., Matuszak, Z., Stempień, M. (2017). *Assessment of the functioning of the selected transport company in terms of preventing damage to the transported cargo.* Radom: Buses.

Directive of the European Parliament and UE Council from 27 March 2019 about the reduction of the environmental impact of certain plastic products (2019): Document 52018PC0340.

Directive 2014/47/EU (2014): Document 32014L0047.

EN 12195-1 (2011). Standard for Load restraining on road vehicles.

EN 12642 (2006). Tests of Vehicle Bodies.

EUMOS 40509 (2012). Safe Load Testing Technologies.

https://ami.international (date 24.09.2020).

CDS (2020). CDS Odszkodowania, https://www.cds-odszkodowania.info (date 25.08.2020).

Ergis (2020). Ergis Load Stability Academy, ELSA: https://ergis.eu (date 24.09.2020).

https://www.eurologistics.pl/eurologistics/newsy/autorskie-rozwiazania logistyczne (date 12.08.2020).

https://www.europarl.europa.eu (date 24.09.2020).

https://its.waw.pl (date 25.08.2020).

https://lab4pack (date 10.09.2020).

http://www.nowafolia.pl/certyfikaty-eumos.html (date 24.09.2020).

https://opakowania.com.pl/news/folie-z-tworzyw-proba-opisania-rynku-26459.html 2007.

https://tworzywa.org (date 24.09.2020).

https://pzpts.pl (date 05.08.2020).

IRU (2015). International guidelines for the safe securing of loads in road. IRU I-0323. IRU_CIT-2014 version 01.

Kielec, R., Sąsiadek, M., Woźniak, W. (2018). *Adoption of the Evolutionary Algorithm to Automate the Scheduling of the Production Processes.* Proceedings of the 31st International Business Information Management Association (IBIMA), Milan, Italy, ISBN: 978-0-9998551-0-2. 5039-5046.

Kostrzewski, M. (2013). *Loads Analysing In Pallet Racks Storage Elevation.* CLC 2013: Carpathian Logistics Congress Proceedings, 260-265.

Kostrzewski, M. (2020). Sensitivity Analysis of Selected Parameters in the Order Picking Process Simulation Model, with Randomly Generated Orders. *Entropy, 22(*423), 1-21. DOI: https://doi.org/10.3390/e22040423

Lenort, R., Baran, J., Wysokiński, M., Gołasa, P., Bieńkowska-Gołasa, W., Golonko, M., Chamier-Gliszczyński, N. (2019). Economic and Environmental Efficiency of the Chemical Industry in Europe in 2010-2016. *Rocznik Ochrona Środowiska, 21*, 1394-1404.

Mroziński, A. (2009). *Recirculation of plastics in Poland and Europe*. Bydgoszcz: TOP-garn Science Circle. Technological and Natural Inverternity in Bydgoszcz.

PlasticsEurope, 2019. *Plastics – the Facts 2019.* An analysis of European plastics production, demand and waste data: https://www.plasticseurope.org/application/files/1115/7236/4388/FINAL_web_version_Plastics_the_facts2019_14102019.pdf.

Regulation of the Minister of Infrastructure of 25 January 2018 on the method of cargo transportation. (2018). Warszawa: Document 20180361.

Regulation of the Minister of Infrastructure of 24 December 2019 amending the Regulation on technical conditions of vehicles and the scope of their necessary equipment. (2019). Warszawa: Document 20192560.

Rucińska, M., Kędzior-Laskowska, M. (2015). *Safety and Timeliness – quality Attributes in Road Transport of Goods*. Scientific Papers of the University of Gdańsk. Transport Economics and Logistics. 57 Contemporary problems of transport development = Present Problems of the Transport Development, 129-144.

Salomon, A. (2017). Cargo stacking as an important element in modeling multimodal transport chains (on the example of the Port of Gdynia). *Materials Management and Logistics, 12*, 988-1007.

Stachurek, I. (2012). *Problems with biodegradation of plastics in the environment*. Katowice: Scientific Journals of the University of Labour Protection Management in Katowice.

Szpotański, M. (2010). Shelf-ready packaging. Technical and Economic Monthly. *Opakowanie, 11-2010*.

Szpotański, M. (2013). Outsourcing as a chance for development. Technical and Economic Monthly. *Opakowanie, 11-2013*.

Szydełko, M., Jagieła, A. (2015). *Selected elements of plastic packaging distribution system – theoretical and practical aspects*. Poznań: Logistics.

Świeboda, J., Zając, M. (2017). *Information System as a Cause of Cargo Handling Process Disruption in Intermodal Terminal.* in: Advances in Dependability Engineering of Complex Systems. Springer, Cham, 418-427.

Świeboda, J., Zając, M. (2016). *Analysis of Reshuffling Cost at a Container Terminal*. In: International Conference on Dependability and Complex Systems. Springer, Cham. 491-503.

Tkaczyk, S. (2016). *Selection of means of transport for the implementation of technological processes*. Warszawa OWPW.

Tkaczyk, S., Ambroziak, T. (2016). *The method of optimal allocation of technical means and means of transport for the implementation of technological processes*. OWPW 2016, Pracy Naukowe Transport, 111, 555-572.

Woźniak, W., Sąsiadek, M., Stryjski, R., Mielniczuk, J., Wojnarowski, T. (2016). *An algorithmic concept for optimising the number of handling operations in an intermodal terminal node*. Proceeding of the 28th International Business-Information-Management-Association (IBIMA), Seville, Spain, ISBN: 978-0-9860419-8-3, 1-7, 1490-1500.

Zajac, P. (2015). *Evaluation of automatic identification systems according to ISO 50001: 2011*. International Conference on Automation. Springer, Cham.

Abstract

Damage to cargo in transport occurs as a result of improper securing of cargo, which causes not only material losses due to partial or complete damage to cargo, but may threaten the safety of participants in the distribution of cargo in the distribution chain. Dangers, difficulties and costs caused by human errors in packing and securing cargo in all modes of transport can be remedied and certainly significantly reduced. The best way to achieve this goal is to build the awareness of the great need for proper packaging and securing the cargo in a way that ensures the safety of all participants in the distribution chain among producers, distributors and carriers. The article discusses the problem of rational use of stretch film as the most frequently used method of securing loads. Author indicated necessity to develop methods and procedures for the proper protection of palletized loads with the use of stretch film to reduce the amount of stretch film used while ensuring proper load security, increase the safety and better protection to the environment of the planet and its natural resources.

Keywords:
stretch film, cargo, cargo damage, cargo securing, cargo securing methods

Problem ograniczenia zużycia foli stretch wykorzystywanej do zabezpieczania ładunków spaletyzowanych

Streszczenie

Uszkodzenia ładunków w transporcie powstają w wyniku niewłaściwego zabezpieczenie ładunku co powoduje nie tylko straty materialne, spowodowane częściowym lub całkowitym uszkodzenia ładunków, ale może zagrażać bezpieczeństwu uczestnikom dystrybucji ładunku w łańcuchu dystrybucyjnym. Takim niebezpieczeństwom i utrudnieniom a w konsekwencji kosztom spowodowanymi błędami ludzkimi przy pakowaniu i zabezpieczaniu ładunku na środkach transportu można zaradzić, a z pewnością znacznie je ograniczyć. Drogą do tego celu jest uświadomienie producentów, dystrybutorów i przewoźników o konieczność prawidłowego opakowania i zabezpieczania ładunku w sposób zapewniający bezpieczeństwo wszystkim uczestnikom łańcucha dystrybucji. W artykule omówiono problem racjonalnego zastosowania folii stretch, jako najczęściej stosowanego sposobu zabezpieczania ładunków. Wskazano na konieczność opracowania metody i procedur prawidłowego zabezpieczania ładunków spaletyzowanych przy zastosowaniu folii stretch co pozwoli na ograniczenie ilości zużywanej folii stretch przy jednoczesnym zapewnieniu prawidłowego zabezpieczania ładunku, a w konsekwencji pozwoli zwiększyć bezpieczeństwo oraz lepiej chronić środowisko naturalne planety i jej zasoby.

Słowa kluczowe:
folia stretch, ładunek, uszkodzenie ładunku, zabezpieczenie ładunku,
metody zabezpieczania ładunku

MIDDLE POMERANIAN SCIENTIFIC SOCIETY OF THE ENVIRONMENT PROTECTION

Rocznik Ochrona Środowiska

Volume 22. Year 2020 ISSN 1506-218X 376-390

The Method of Nitrogen Oxide Emission Reduction During the Combustion of Gaseous Fuel in Municipal Thermal Power Boilers

Sylwia Janta-Lipińska

Koszalin University of Technology, Poland

corresponding author's e-mail: sylwia.janta-lipinska@tu.koszalin.pl

1. Introduction

Currently, the Polish heat management works mainly on solid fuel (Konieczyński et al. 2017, Man et al. 2005, Park et al. 2013). Such a policy causes more and more technical, economic and ecological problems due to the conditions set for us by the European Union countries (Szyszlak-Bargłowicz et al. 2015, Szyszlak-Bargłowicz et al. 2017, Zając et al. 2017). Recently, the Polish government announced the country's heat policy program in the perspective of 2040. It assumes, among others transition of heat management from solid fuel to natural gas. Therefore, the challenge for Polish heating is the effective and environmentally friendly transition (switching) of thermal energy from solid fuel to gaseous fuel. These are devices called "Low energy" due to their age are characterized by low efficiency and a significant impact on the level of environmental pollution in the ground layers of the atmosphere (Zandeckis et al. 2010, Zang et al. 2015). The exhaust gas from these devices is discharged into urban development zones through small chimneys. The EU regulations obliging all European Union countries, including Poland, to reduce greenhouse gas emissions are not without significance here.

The combustion of organic fuel is accompanied by the formation and emission of toxic and carcinogenic substances into the atmosphere. In addition to nitric oxide, exhaust gases may contain carbon monoxide, aldehydes, organic acids and other carcinogenic compounds. The harmful importance of these pollutants for the natural environment is emphasized by the fact that they are legally limited. The emission of nitrogen oxides or dust depends on the type of fuel burned (Dal Secco et al. 2015, Xu et al. 1999, Wilk et al. 2010). Each of these substances has a different quantitative composition and poses a different danger

to man and the environment. During the combustion processes, the construction details and technological conditions affect the concentration of harmful components contained in the exhaust gas to varying degrees. For example, when burning gaseous fuel containing no sulfur, the emission levels of harmful substances contained in the exhaust gas are as follows (Sigal 1988):

- benzo(a)pyrene 0-20 μg/100 m^3,
- carbon monoxide 70-100 mg/m^3,
- sulphur dioxide 0 mg/m^3,
- nitrogen oxides 100-400 mg/m^3.

The above statement shows that mainly oxide and nitrogen dioxide (NO_x) determine the level of environmental performance of boiler equipment when burning gaseous fuel (Kromilitsyn & Ezhov 2013, Szkarowski & Janta-Lipińska 2011, Szkarowski & Janta-Lipińska 2013, Szkarowski & Janta-Lipińska 2015).

2. Formation mechanisms and methods for the suppression of nitrogen oxides

The concentration of nitrogen oxides in the exhaust gas depends on the maximum temperature of the combustion process, the concentration of oxygen in the combustion zone, the residence time of the reacting mixture in the maximum temperature zone, and on the nitrogen content in the fuel. Depending on the combination of these parameters, NO_x emissions in flue gas may oscillate from 0.1 to 2.0 g/m^3.

In the literature there are three mechanisms for the formation of nitrogen oxides in a flame of burning fuel distinguished (Gradoń 2003, Zeldovich 1946):

- thermal – which is formed as a result of high temperature oxidation of nitrogen from the air,
- prompt – formed in the initial combustion zone by chemical reactions with the participation of CH and CH_2 radicals. There is also a known in the literature hypothesis regarding another possible mechanism for the formation of nitrogen oxides in an organic fuel flame (the so-called "impact"), which otherwise explains the difference between the content of nitrogen oxides and the thermal mechanism of their formation (Szkarowski 2014),
- fuel – produced with the participation of chemical compounds containing nitrogen and included in the fuel.

Figure 1 shows a diagram of the formation of nitrogen oxides in the range of temperatures characteristic of boiler furnaces. In some cases, the formation of nitrogen oxides occurs predominantly by one of three mechanisms. For example,

when burning gas in low-power devices, the so-called "prompt" NO_x prevail, wheras in fluidized coal combustion the "fuel" ones. The combustion of gaseous fuel in the furnaces of boilers is accompanied by the formation of thermal and prompt nitrogen oxides.

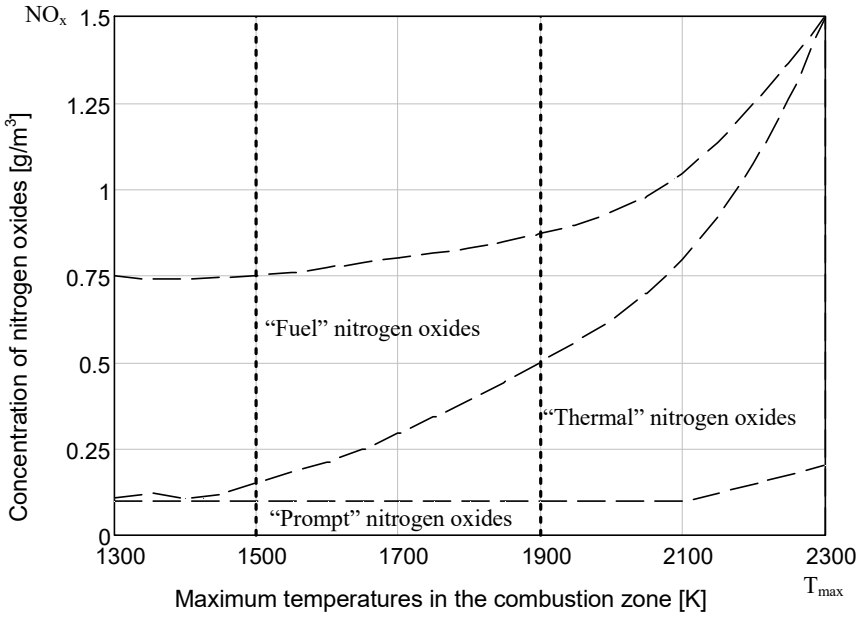

Fig. 1. Dependences of the concentration of nitrogen oxides, as a function of maximum temperatures in the combustion zone, divided into characteristic zones of the influence of NO_x formation mechanisms

The main directions of research in the field of suppressing nitrogen oxide emissions, taking into account the thermal mechanism of their formation, was the reduction of the maximum temperature and oxygen concentration in the combustion zone.

This can be achieved by:

- combustion with reduced α,
- exhaust gas recirculation,
- moisture injection (Janta-Lipińska &Shkarovskiy 2020a),
- multistage combustion.

Author in the composition of an international research team headed by prof. Szkarowski has been involved in the use of combustion methods with reduced α and moisture injection for many years. It should be emphasized that these two ways often complement each other. This article summarizes a number of experimental and theoretical studies in these two methods (Janta-Lipińska & Szkarowski 2018, Szkarowski 2002, Szkarowski & Janta-Lipińska 2009, Szkarowski & Janta-Lipińska 2011, Szkarowski & Janta-Lipińska 2013).

3. Theoretical research

The method of water ballast injection is considered one of the most promising scientific and technical solutions aimed at reducing atmospheric pollution by harmful products of organic fuel combustion (Szkarowski 2002, Szkarowski 2003, Szkarowski et al. 2016, Szkarowski et al. 2018, Janta-Lipińska & Shkarovskiy 2020a). Compared to other atmosphere protection technologies, the injection method is characterized by unique energy-ecological and technical-economic indicators (Jemieljanow 1992, Palenko et al. 2014).

As a result of the conducted research, the following two issues were analyzed. The first of these was to determine the detailed structure of the flame in terms of the processes of nitrogen oxides (NO_x) production that occur. This was to ensure optimal ballasting of the zones where the processes take place (Herdzik & Noch 2018). The second issue was to explore the possibility of intensifying processes within the flame to maximize the reduction of the excess air supplied for combustion and to reduce the value of heat loss with exhaust gases.

I.J. Sigal divided the combustion process into four temperature zones (Sigal 1988) that determine the formation of nitrogen oxides (Fig. 2). Zone I is the zone where the maximum temperature in the combustion zone reaches up to 750K. In turn, zone IV is the maximum temperature in the combustion zone reaching the limit above 2500K. The author of this division recognized that for the processes occurring in the furnaces of boilers, the temperature conditions of the zones occurring in the so-called III a and III b zone are characteristic.

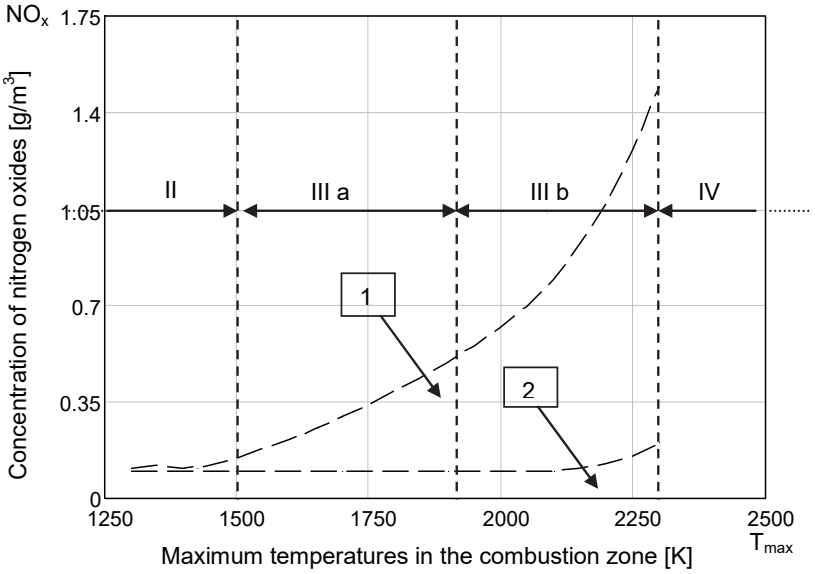

Fig. 2. Dependences of the concentration of nitrogen oxides as a function of maximum temperatures in the combustion zone, divided into zones of influence according to Sigal

Another division was proposed by L.M. Tsyrulnikow, namely the division of the flame structure into four zones depending on the relative length of the flame (Tsyrulnikow 1980) (Fig. 3):

- zone A_1 – from the place of flame outlet from the cross section of the burner to the cross section of the furnace where the temperature is 1650K (it is the temperature at which the concentration of thermal nitrogen oxides reaches the value of 1 mg/m^3),
- zone A_2 – from the above-mentioned section to the place where the maximum temperature in the flame is obtained, where the intensity of nitrogen oxidation from air reaches a maximum,
- zone B – from the cross-section with the maximum temperature in the combustion zone to the cross-section with the "critical" temperature of 1650K, where combustion of combustible components usually ends, and the concentration of "air" NO_x reaches its maximum value,
- zone C – from the section mentioned above to the exit from the furnace, where there are no significant changes in the concentration of nitrogen oxides.

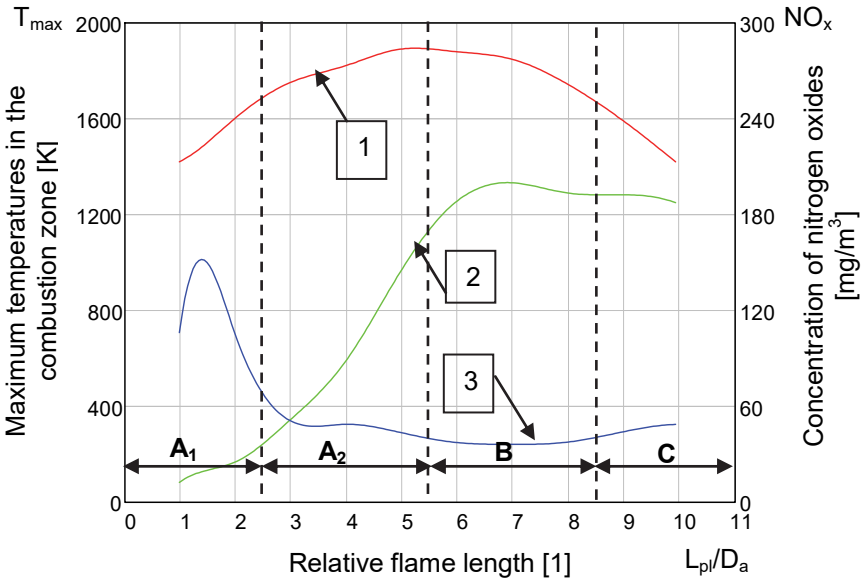

Fig. 3. Dependences of the maximum temperature in the combustion zone (1) and concentration of nitrogen oxides (2-thermal, 3-prompt) in flame as a function of relative flame length

On the other hand A.A. Jemieljanow distinguishes, in the resulting flame, the zones of intensive generation of nitrogen oxides (ZIG) (Jemieljanow 1992). The zones he separates are treated as intervals for achieving local temperature maxima.

The author has attempted to jointly consider and mutually enrich the flame structure analysis proposed by Sigal, Tsyrulnikow and Jemieljonow. This allowed to formulate the concept and separate two zones of decisive influence (ZDI), which determine the possibility of active influence on various processes occurring in the flame, also the mechanisms of nitrogen oxide formation:

- ZDI-I-, which includes a significant part of zone A_1, in which by introducing water ballast you can control the processes taking place in this flame zone in order to affect the conditions determining the intensity of further NO_x production by non-thermal mechanisms of its formation (i.e. prompt, impact).
- ZDI-II- is the zone of maximum temperatures at the junction of zones A_2 and B, in which both ballasting and controlling the excess air coefficient enables throttling of the thermal mechanism of nitrogen oxidation. An overview diagram of the flame as a result of such analysis is shown in Fig. 4.

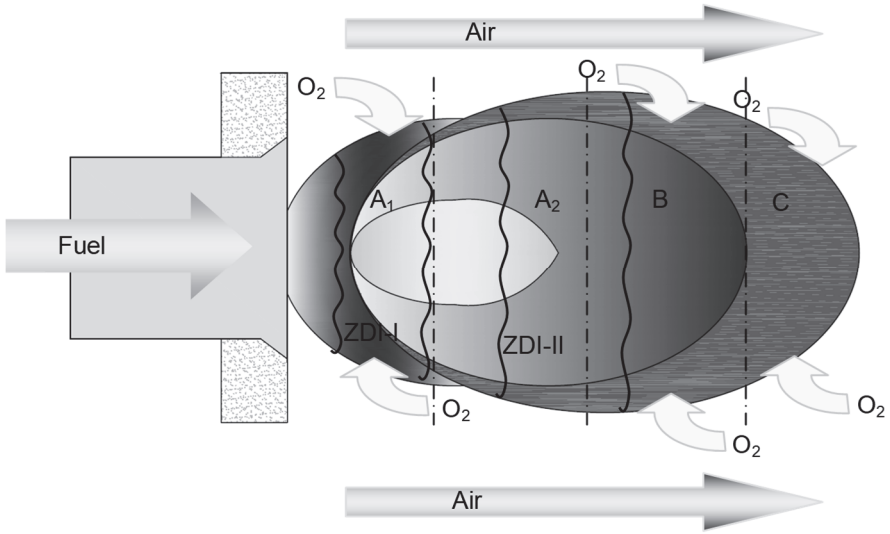

Fig. 4. Schematic diagram of the structure of the flame divided into zones of decisive influence

Studies on reducing NO_x emissions are usually based on the structure of the flame in its entirety (Sigal 1988, Tsyrulnikow 1980, Jemieljanow 1992) with the separation of the flame nucleus and other parts thereof. The measures taken to reduce the intensity of NO_x formation anticipate the effect on the entire flame. Known methods for reducing NO_x emissions (Krawczyk 2016, Kropka 2010, Lee et al. 2006, Janta-Lipińska & Szkarowski 2018, Xue et al. 2009) developed on this basis include: humidifying the entire air stream in front of the burner or ballasting it with exhaust gases. Some achievements of such methods are indisputable but limited.

However, the majority of the currently produced burners are characterized by turbulent-diffusion combustion organization (Gradoń 2003). The flame in the burner tunnel and then in the furnace is not uniform. It consists of many individual and in some sense isolated structures. Each fuel stream, mixing with the air flowing into it, creates such a structure (in aerodynamic and thermodynamic terms). The combination of mutually building up structures constituting molar masses of burning fuel can be defined as mono-flame, micro-flame, partial or component flames. Each mono flame is a fairly determinate structure that reacts only with the surrounding air stream. In a simplified form, not taking into account the turbulence of flame, Fig. 5 shows the aforementioned flame division zones and ZDI-s occurring in each monoflow (Szkarowski 2002).

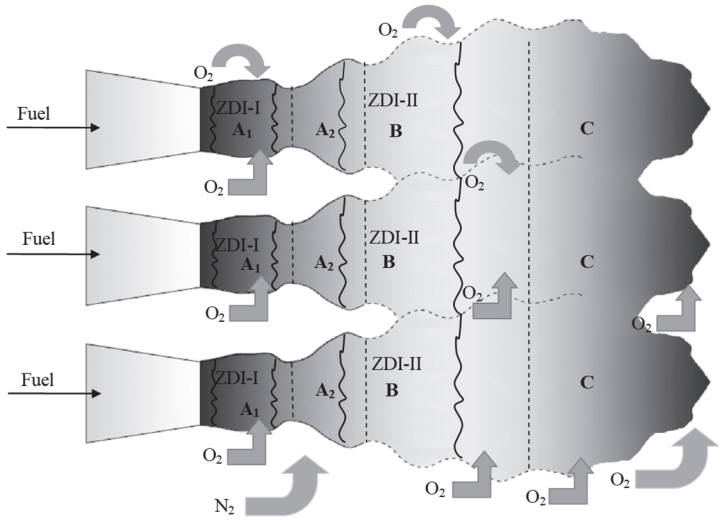

Fig. 5. Schematic diagram of the structure of a turbulent multi-stream flame

The mono-flames retain their seclusion until the beginning of zone B. That is in zones ZDI-I and ZDI-II. The end of zone B and the entire zone C are characterized by a quick connection of mono-flames and the formation of a more uniform structure of the entire flame. From this point of view, the generally accepted principle of examining the flame in its entirety is contrary to the complex structure of the flame described above. The course of the processes of formation and combustion of nitrogen oxides in each mono-flame is somewhat independent. Based on the above premises, a method of impact on the ZDI was proposed in each mono-flame. Experimental verification of these assumptions took place directly on steam boilers in operating boiler room conditions.

4. Research objects

The tests were carried out on four steam boilers of different power: DKVR 10-13, DKVR 20-13, DE 25-14 and PTVM-50 (Janta-Lipińska &Shkarovskiy 2020b). Each of the tested boilers was in a different industrial and heating boiler room located in the St.-Petersburg district. All tested boilers operated on gaseous fuel. Characteristics of individual boilers are presented in Table 1.

Table 1. List of boilers parameter values, on which investigations have been performed

Parameter	Boiler type			
	DKVR10-13	DKVR20-13	DE 25-14	PTVM-50
Boiler heat power [MW]	8.37	14.09	14.91	53.78
Type of burner	GMG-5.5	GMGB-5.6	GMP-16	DKZ
Number of burners	2	3	1	12
The fan and exhaust installation				
- Blow fan	VD-8	VD-10	VD-10	WC-14-46-8
- Exhaust fan	D-10	D-10	D-13.5	–

Based on the theoretical assumptions made above and the preliminary analysis of the flame structure by means of simulation and photography methods, individual constructions of moisture injection heads were developed for each boiler and burner. To ensure proper supply of water ballast to the ZDI-I and ZDI-II zones, the number of holes, their location and angle of inclination were subjected to each mono flame. During the tests, the pressure of injected steam was an additional factor. In the case of multi-burner boiler designs (i.e. PTVM-50 with 12 burners), parameters in different rows of burners were also differentiated. An example of such a head for the GMP-16 burner of the DE 25-14 boiler is shown in Fig. 6. The design of the head provided intensive mechanical and chemical interaction in the ZDI-I zone in the mono-flame of each gas stream. The rest of the water ballast provided interaction in ZDI-II by dissociation of water vapor. This principle of active impact on ZDI in each mono-flame has been referred to as directed dosed steam ballasting.

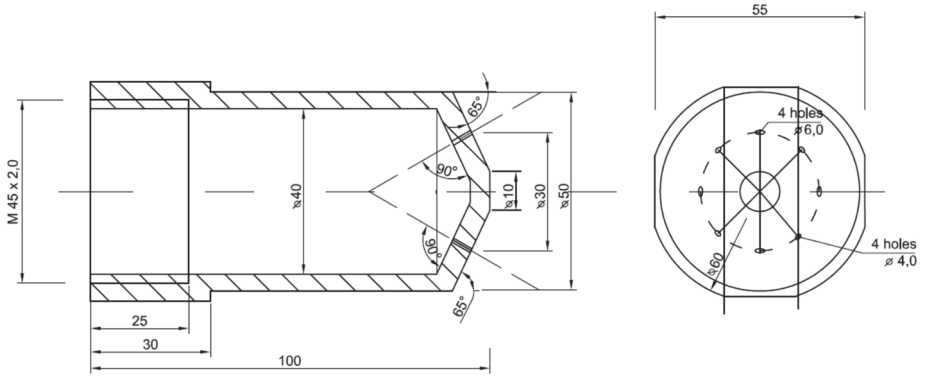

Fig. 6. Technical drawing of the exemplary design of the head for injecting moisture into the zones of decisive influence for the DE 25-14 boiler with the GMP-16 burner

5. Experimental results

The investigations have been performed on four gas-fired boilers. The performed investigations allowed to achieve the best results of the use of the proposed method with an inject of the moisture into zones of decisive influence (ZDI-I and ZDI-II).

In Fig. 7 the mass emission of nitrogen oxides as a function of boiler efficiency for two modes of its operation has been presented. The first mode relies on the measurements of mass emissions of nitrogen oxides during boiler work under its actual operating conditions, while the second one relies on the measurements with the additional suppression system of oxide emissions on (Shkarovskiy et al. 2016). In both cases, the value of the emission of nitrogen oxides depends on the boiler's steam capacity or its thermal power. The higher the steam output of the boiler or its heat output, the greater the mass emission of nitrogen oxides.

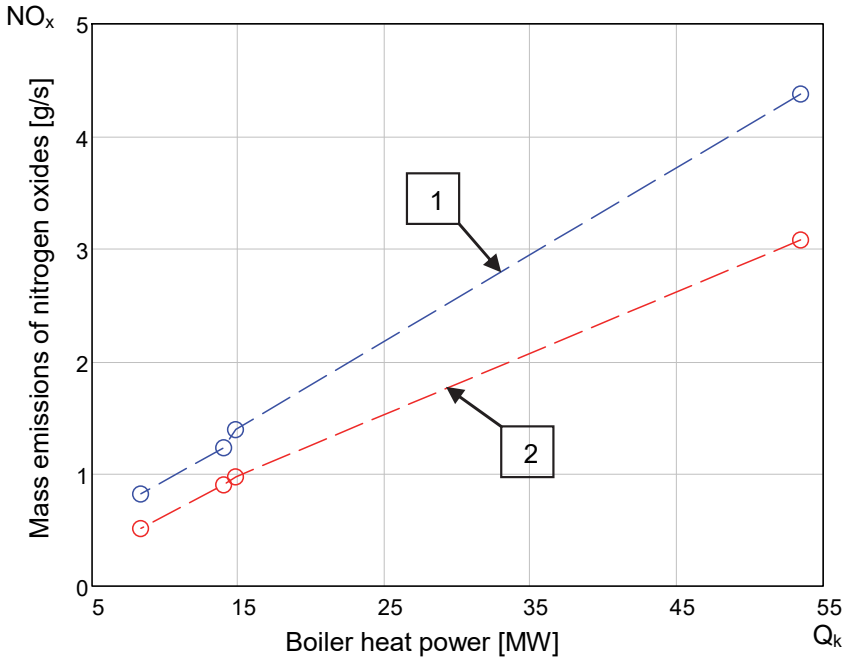

Fig. 7. The dependences of mass emission of nitrogen oxides as a function of boiler heat power (1 – boiler without additional systems activated; 2 – boiler with activated system of suppressing nitrogen oxides emission)

In Fig. 8 the obtained results of the mass value of nitrogen oxides emission, calculated to 1 MW heat power, for two boiler modes have been presented. This figure presents the effectiveness of the directed metered flame ballast method. The characteristics presents that the specific mass emissions of nitrogen oxides are lower for boilers with maximum power with the system turned on than for boilers with the minimum power in normal operating modes (without the NO_x suppression system switched on). The application of an automatic suppression system of nitrogen oxides emission on each of the boilers allowed reducing this emission by average 30%. In the case of the DKVR 10-13 boiler, compared to the value obtained for actual operating conditions, the reduction in nitrogen oxide emissions reached 37%. The steam consumption per flame injection for each of the investigated boilers has been presented in Fig. 9. In each case, the steam consumption per injection did not exceed 1% of the steam capacity of the boiler or its heat output (Janta-Lipińska & Shkarovskiy 2020a). The increase of boiler efficiency, being a result of the use of the proposed method, compensated the steam consumption per injection.

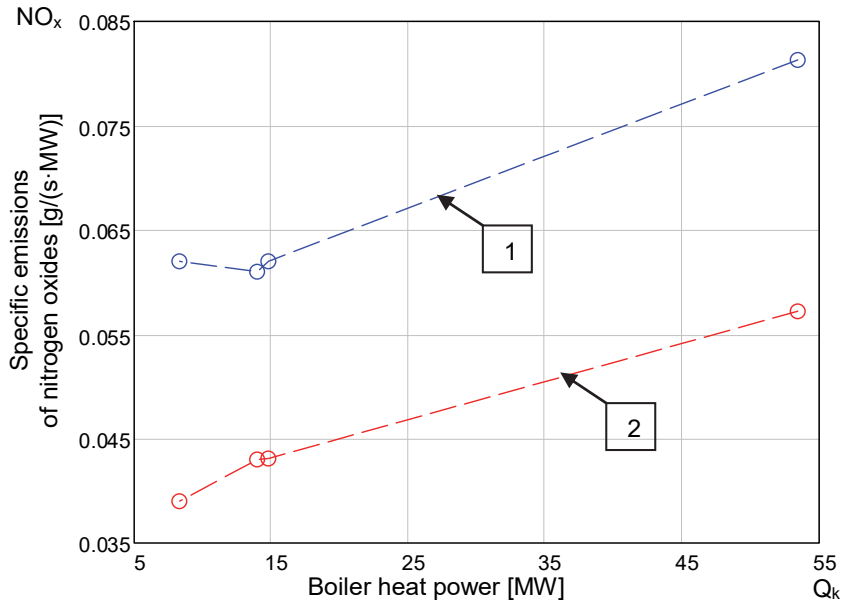

Fig. 8. Dependences of specific emissions of nitrogen oxides as a function of boiler heat power (1 – boiler without additional systems activated; 2 – boiler with activated system of suppressing nitrogen oxides emission)

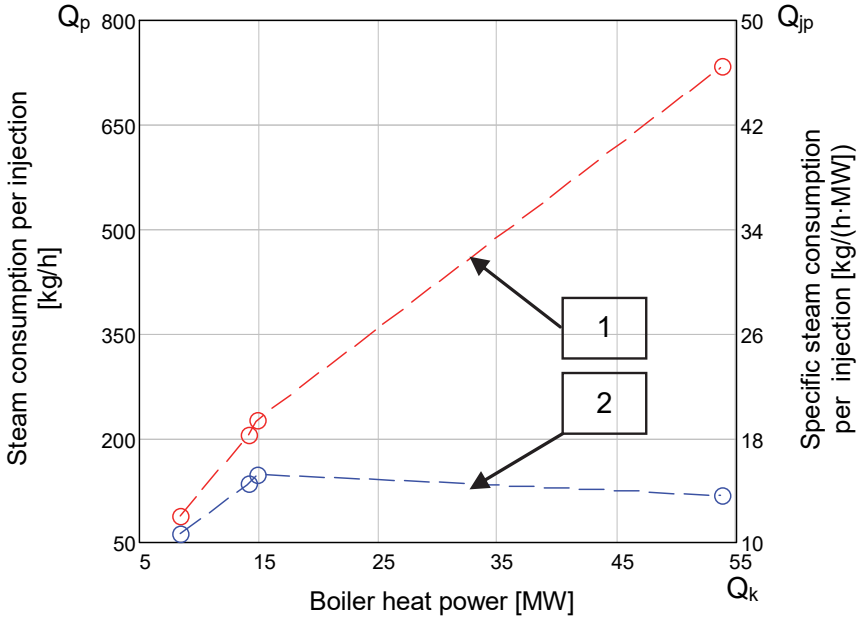

Fig. 9. The dependences of steam consumption (1 – absolute, 2 – unit) per injection as a function of boiler heat power (1 – absolute, 2 – unit)

6. Conclusions

1. A method for reducing nitrogen oxide emissions in city heat boilers has been developed and proposed. The method relies in directing the dosed moisture injection into the flame zone.
2. The method has been experimentally verified on steam and water thermal power boilers with capacities from 8.37 to 53.79 MW. The number of the burners in these boilers was form 1 to 12.
3. It has been proved that the proposed method allows a reduction of nitrogen oxides by 30-40% with moisture injection not exceeding 0.9% of the boiler efficiency. Due the work of a boiler with moisture injection is accompanied by an increase in its efficiency to 1%, the use of the proposed method does not reduce the efficiency of fuel consumption in the heat source.

ReferencesDal Secco, S., Juan, O., Louis-Louisy, M., Lucas, J.Y., Plion, P., Porcheron, L. (2015). Using a genetic algorithm and CFD to identify low NO_x configurations in an industrial boiler. *Fuel*, *158*, 672-683. DOI: 10.1016/j.fuel.2015.06.021.

Gradoń, B. (2003). *Rola podtlenku azotu w modelowaniu emisji NO z procesów spalania paliw gazowych w piecach wysokotemperaturowych*. Gliwice: Zeszyty Naukowe Politechniki Śląskiej.

Herdzik, J., & Noch, T. (2018). Ballast Water Management Systems on Vessels. The Water Cleanliness Requirements of New D-2 Standard Versus the Expectations. *Rocznik Ochrona Srodowiska*, *20*, 647-661.

Janta-Lipińska, S. & Shkarovskiy, A. (2018). The study on decreasing of nitrogen oxides emission carried out on DKVR 10-13 industrial heating boilers. *E3S Web of Conferences, 44*. DOI: 10.1051/e3sconf/20184400056.

Janta-Lipińska, S. & Shkarovskiy, A. (2020a). Investigations of nitric oxides reduction in industrial-heating boilers with the use of the steam injection method. *Archives of Environmental Protection*, *46*(2), 100-107. DOI: 10.24425/aep.2020.133480.

Janta-Lipińska, S. & Shkarovskiy, A. (2020b). Investigations of advantages of simultaneous combustion of natural gas and mazout in medium power steam boilers. *Journal of Engineering Thermophysics*, *29*(2), 331-337. DOI: 10.1134/S1810232820020149.

Jemieljanow, A. A. (1992). *Development of injection devices to suppress nitrogen oxides when burning gas and mazout in boiler hearths*. Sankt-Petersburg.

Kormilitsyn, V. I. & Ezhov, V. S. (2013). Studying the Removal of Nitrogen Oxides from Boiler Flue Gases in Firing Natural Gas. *Thermal Engineering*, *60*(2)*,* 147-152.

Konieczyński, J., Komosiński, B., Cieślik, E., Konieczny, T., Mathews, B., Rachwał, T., Rzońca, G.. (2017). Research into Properties of Dust from Domestic Central Heating Boiler Fired with Coal and Solid Biofuels. *Archives of Environmental Protection*, *43*(2)*,* 20-27. DOI: 10.1515/aep-2017-0019.

Krawczyk, P. (2016). Experimental investigation of N_2O formation in selective non-catalytic NO_x reduction processes performed in stoker boiler. *Polish Journal of Chemical Technology*, *18*(4), 104-109. DOI: 10.1515/pjct-2016-0078.

Kuropka, J. (2010). Reduction of Nitrogen Oxides from Boiler Flue Gases. *Environment Protection Engineering*, *36*(2), 111-122.

Lee, C., Jou, C.G., Tai, H., Wang, C., Hsieh, S., Wang, H.P. (2006). Reduction of Nitrogen Oxide Emission of a Medium-Pressure Boiler by Fuel Control. *Aerosol and Air Quality Research*, *6*(2), 123-133. DOI: 10.4209/aaqr.2006.06.0002.

Man, C. K., Gibbins, J. R., Witkamp, J. G.., Zhang, J. (2005). Coal characterization for NO_x prediction in air-staged combustion of pulverised coals, *Fuel*, *84*(17), 2190-2195. DOI: 10.1016/j.fuel.2005.06.011.

Park, H. Y., Baek, S. H., Kim, Y. J., Kim, T. H., Kang, D. S., Kim, D. W. (2013). Numerical and experimental investigations on the gas temperature deviation in a large scale, advanced low NO_x, tangentially fired pulverized coal boiler. *Fuel*, *104*, 641-646. DOI: 10.1016/j.fuel.2012.06.091.

Pavlenko, A., Szkarowski, A., Janta-Lipińska, S. (2014). Research on Burning of Water Black Oil Emulsions. *Rocznik Ochrona Środowiska*, *16*, 376-385.

Shkarovskiy, A.L., Novikov, O.N., Novikova, A.V., Polushhkin, V.I. (2016). Development of a new family of intelligent control systems of combustion quality. *Modern High Technologies*, *12,* 556-561.

Sigal, I.J. (1988). *Air protection during fuel combustion*. Leningrad: Nedra.

Szkarowski, A. (2002). Principles of Calculation at Suppression of NO_x Formation by a Method of the Dosed Directed Injection of a Water Ballast. *Rocznik Ochrona Środowiska*, *4*, 365-378.

Szkarowski, A. (2003). Detailed Problems of the Effective and Ecologically Clean Combustion of Fuel in the Pre-grates of the Furnaces. *Rocznik Ochrona Środowiska*, *5*, 67-78.

Szkarowski, A. & Janta- Lipińska, S. (2009). Automatic Control of Burning Quality of Solid Fuel in Industrial Heating Boilers. *Rocznik Ochrona Środowiska*, *11*, 241-255.

Szkarowski, A. & Janta-Lipińska, S. (2011). Modeling of Optimum Burning of Fuel in Industrial Heating Boilers. *Rocznik Ochrona Środowiska*, *13*, 511-524.

Szkarowski, A. & Janta-Lipińska, S. (2013). Examination of Boiler Operation Energy-ecological Indicators During Fuel Burning with Controlled Residual Chemical Underburn. *Rocznik Ochrona Środowiska*, *15*, 981-995.

Szkarowski, A. (2014). *Spalanie gazów. Teoria, praktyka, ekologia. WNT*

Szkarowski, A. & Janta-Lipińska, S. (2015). Experimental Research vs. Accuracy of the Elaborated Model. *Rocznik Ochrona Środowiska*, *17*, 576-584.

Szkarowski, A., Janta-Lipińska, S., Gawin, R. (2016). Reducing Emissions of Nitrogen Oxides from DKVR Boilers. *Rocznik Ochrona Środowiska*, *18*, 565-578.

Szkarowski, A., Janta-Lipińska, S., Dąbrowski, T. (2018). Research on Co-combustion of Gas and Oil Fuels. *Rocznik Ochrona Środowiska*, *20*, 1515-1529.

Szyszlak-Bargłowicz, J., Zając, G., Słowik, T. (2015). Hydrocarbon Emissions during Biomass Combustion. *Polish Journal of Environmental Studies*, *24*(3), 1349-1354. DOI: 10.15244/pjoes/37550.

Szyszlak-Bargłowicz, J., Zając, G.., Słowik, T. (2017). Research on Emissions from Combustion of Pellets in Agro Biomass Low Power Boiler. *Rocznik Ochrona Środowiska, 19*, 715-730.

Tsyrulnikow, L.M. (1980). *Methods for reducing the formation of toxic and corrosive combustion products of natural gas and fuel oil*. Overview information WNIIE Gazprom. Series: The most important scientific and technical problems of the gas industry.

Wilk, M., Magdziarz, A., Kuźnia, M., Jerzak, W. (2010). The reduction of the emission of NO_x in the heat-treating furnaces. *Metallurgy and Foundry Engineering*, *36*, 47-54.

Xu, H., Smoot, L. D., Hill, S. C. (1999). Computational model for NO_x reduction by advanced reburning. *Energy & Fuels*, *13*(2), 411-420. DOI: 10.1021/ef980090h.

Xue, S., Hui, S. E., Liu, T. S., Zhou, Q. L., Xu, T. M., Hu, H. L. (2009). Experimental investigation on NO_x emission and carbon burnout from a radially biased pulverized coal whirl burner. *Fuel Processing Technology*, *90*(9), 1142-1147. DOI: 10.1016/j.fuproc.2009.05.011.

Zając, G., Szyszlak-Bargłowicz, J., Słowik, T., Wasilewski, J., Kuranc, A. (2017). Emission Characteristics of Biomass Combustion in a Domestic Heating Boiler Fed with Wood and Virginia Mallow Pellets. *Fresenius Environmental Bulletin*, *26*(7), 4663-4670.

Zandeckis, A., Blumberga, D., Rochas, C., Veidenbergs, I., Silins, K. (2010). Methods of Nitrogen Oxide Reduction in Pellet Boilers, Scientific Journal of RTU, *Environmental and Climate Technologies*, *4*, 123-129.

Zeldovich, J. (1946). The oxidation of nitrogen in combustion and explosions. *European Physical Journal A. Hadrons and Nuclei*, *21*, 577-628.
Zhang, X., Zhou, J., Sun, S., Sun, R., Qin, M. (2015). Numerical investigation of low NO_x combustion strategies in tangentially-fired coal boilers. *Fuel*, *142*, 215-221. DOI: 10.1016/j.fuel.2014.11.026.

Abstract

The nitrogen oxides in a flame of burning fuel can be created by many mechanisms. The amount of NO_x concentration emitted to the ground atmosphere mainly depends on the type of fuel burned in the industrial and heating boilers. Changes in the country's thermal policy and requirements that are set for us by the European Union States are forcing us to reduce greenhouse gas emissions. Directed metered ballast method is one of the most attractive techniques for reducing NO_x emissions. In recent years, moisture injection technology is still investigated on low and medium power thermal power boilers operating on gaseous fuel. The goal of this work was to perform the investigations of the process of a moisture injection into the zones of decisive influence (ZDI-I and ZDI-II) on steam and water boilers: DKVR 10-13, DKVR 20-13, DE 25-14 and PTVM-50. The obtained results clearly show how the proposed method affects NO_x reduction and boiler efficiency.

Keywords:
emission, combustion, dosed directional ballasting method, mono flame, nitrogen oxides

Metoda zmniejszenia emisji tlenków azotu przy spalaniu paliwa gazowego w kotłach miejskiej energetyki cieplnej

Streszczenie

Tlenki azotu w płomieniu palącego się paliwa mogą powstawać na drodze wielu mechanizmów. Ilość emitowanego do przyziemnej warstwy atmosfery stężenia NO_x wynika przede wszystkim z rodzaju spalanego w kotłach przemysłowo-grzewczych paliwa. Zmiany w polityce cieplnej kraju oraz wymagania stawiane nam przez Państwa Unii Europejskiej zmuszają na do zmniejszenia emisji gazów cieplarnianych. Metoda skierowanego dozowanego balastowania jest jedną z najbardziej atrakcyjnych technik ograniczania emisji NO_x. W ostatnich kilku latach technologia wtrysku wilgoci badana jest na kotłach energetyki cieplnej małej i średniej mocy pracujących na paliwie gazowym. Celem pracy są badania eksperymentalne procesu wtrysku wilgoci do stref decydującego wpływu (ang. zone of decisive influence ZDI-I oraz ZDI-II) na kotłach parowych i wodnych: DKVR 10-13, DKVR 20-13, DE 25-14 oraz PTVM-50. Uzyskane wyniki pokazują, w jaki sposób proponowana metoda wpływa na redukcję NO_x oraz wydajność.

Słowa kluczowe:
emisja, spalanie, metoda skierowanego dozowanego balastowania, mono-płomień, tlenki azotu

MIDDLE POMERANIAN SCIENTIFIC SOCIETY OF THE ENVIRONMENT PROTECTION

Rocznik Ochrona Środowiska

Volume 22. Year 2020 ISSN 1506-218X 391-399

Economic Optimization of Medical Waste Treatment: A Case Study of Podlaskie Province

Maria J. Walery[*]*, Izabela Bartkowska, Izabela A. Tałalaj*

Bialystok University of Technology, Poland

[*]*corresponding author's e-mail: m.walery@pb.edu.pl*

1. Introduction

The term medical waste includes all the waste generated within health-care facilities, research centres and laboratories related to medical procedures. Between 75% and 90% of the waste produced by health-care providers is comparable to domestic waste and usually called "non-hazardous" or "general medical waste". It comes mostly from the administrative, kitchen and housekeeping functions at health-care facilities and may also include packaging waste and waste generated during maintenance of health-care buildings (Chartier et al. 2012, Kocak et al. 2017). The remaining 10-25% of health-care waste is regarded as "hazardous" and may pose a variety of environmental and health risks. Effective and efficient healthcare waste management is required to reduce the amount of hazardous and infectious wastes produced in the hospitals. Effective healthcare waste management not only helps the community and people, but also helps the hospitals and can bring in financial benefits along with health and environmental benefits (Marczak 2016, Michlowicz 2012, Teleszewski et al. 2018, Windfeld et al. 2015).

Medical waste management is a major challenge for cities of developing nations. Selecting the best treatment technology for medical waste can be regarded as a complex multi-criteria decision making issue involving a number of alternatives and multiple evaluation criteria. Minoglou et al. (Mingolou et al. 2017) developed the dependence of the healthcare waste (HCW) generation factor on several social-economic and environmental parameters. The statistical analysis included the examination of the normality of the data and the formation of linear multiple regression models to further investigate the correlation between those indices and HCW generation factors. Pearson and Spearman correlation coefficients were also calculated for all pairwise comparisons. Delmonico et al.

(Delmonico et al. 2018) has proposed to investigate the barriers in healthcare waste management and their relevance. For this purpose, this paper analyses waste management practices in two Brazilian hospitals by using case study and the Analytic Hierarchy Process method (AHP). The barriers were organized into three categories - human factors, management, infrastructure and the main findings suggest that cost and employee awareness were the most significant barriers. Shi et al. (Shi et al. 2009) has presented a Mixed Integer Linear Programming model with minimizing costs for medical waste reverse logistics networks. The total costs for reverse logistics include transportation cost, fixed cost of opening the collecting centers and processing centers and operation cost at these facilities over finite planning horizons. An improved genetic algorithm method with a hybrid encoding rule is used to solve the proposed model. Hu et al. (Hu et al. 2002) has presented a cost-minimization model for a multi-time-step, multi-type hazardous-waste reverse logistics system. A discrete-time linear analytical model is formulated that minimizes total reverse logistics operating costs subject to constraints that take into account such internal and external factors as business operating strategies and governmental regulations. Mantzaras et al. (Mantzaras et al. 2017) has presented an optimization model to minimize the cost of an accumulation, transport, treatment and disposal system for infectious medical waste (IMW). The model calculates the optimum locations of the treatment facilities and transport stations, their capabilities (Mg/d), the number and capacities of all waste accumulation, transport and their optimum transport path and the minimum IMW management system cost. For the execution of the optimization routine, two completely different software were used and the results were compared. The first software was Evolver, which is based on the use of genetic algorithms. The second one was Crystal Ball, which is based on Monte Carlo simulation. Lu et al. (Lu et al. 2016) has proposed a new hybrid decision making approach combining interval 2-tuple induced distance operators with the technique for order preference by similarity to an ideal solution (TOPSIS) for tackling HCW (Health-care waste) treatment technology selection problems with linguistic information. The proposed interval 2-tuple induced TOPSIS (ITI-TOPSIS) can not only model the uncertainty and diversity of the assessment information given by decision makers, but also reflect the complex attitudinal characters of decision makers and provide much more complete information for the selection of the optimum disposal alternative.

This paper describes the optimization studies aime dat analysing the impact of the parameter described by the discount factor on the cost of the system and its structure.

2. Case study

In this paper, the optimization model of the transport and disposal of medical waste is presented in the dynamic version, taking into account expected changes of input and output parameters of the waste management system as well as its status in given periods of time.

This paper usues the optimization model of disposal and treatment of municipal waste (Biedugnis et al. 2003), as well as a computer software MRGO+ (Model for Regional Waste Management), through which the model was implemented. It has been verified by the author and adapted to the needs of the proposed model to optimise the disposal and treatment of medical waste on the example of the Podlaskie Province.

The scope of operational research carried out under the optimization study was divided into two stages of optimization calculations with assumed technical and economic parameters of the system. In the first stage, the lowest cost of functioning of the analysed system was generated, whereas in the second one the influence of the input parameter of the system, i.e. the discount factor on the economic efficiency index (E) and the spatial structure of the system was determined.

The object of optimization studies were the influence of the input parameter of the system, i.e. the discount factor on the economic efficiency index (E) and the spatial structure of the medical waste system was determined.

18 sources of waste generation and accumulation (hospitals) within the studied area of the Podlaskie Province were selected for the analysis after taking into account the above mentioned assumptions and environmental conditions. The study also included: four intermediate objects (medical waste incinerators), respectively: IF1 (Suwalki), IF2 (Lomza), IF3 (Bialystok) and IF4 (Hajnowka), where pyrolytic decomposition process of waste will take place, and four end objects (respectively FF1, FF2, FF3, FF4) - areas for temporary storage of post-process waste from the incineration process located in the area of waste incineration facility. The model did not include restrictions on the capacity of intermediate and end objects (Walery 2017).

The scope of operational research carried out in the framework of the optimization study was divided into successive stages in order to present options of the proposed model:

Stage I – includes optimization calculations, assuming fixed technical and economic parameters. Sequence 1, made in this stage, was also a comparative course – a benchmark for other solutions and obtained results to compare.

Stage II – included a number of additional cours aimed at determining the impact of the model input parameters of the system on the indicator of expenses of economic efficiency index (E) and the spatial structure of the system (system location of objects and their associated waste disposal routes).

The following input data were taken into account:

- economic parameters describing the system (waste transport unitary costs, inflation and discount factor),
- economic parameters describing the objects of the system (capital and operating costs),
- the size reduction of medical waste in the system of indirect objects expressed in the form of the output factor of the process – wwp [%],
- the planned time horizon [t], (duration of model process) (Walery 2017).

The data relating to the costs of transport, investments and operation of the system objects, necessary for optimisation calculations, derived from existing plants, located in the model region. The calculation was performed by the unit cost of the work presented in Biedugnis et al. (Biedugnis et al. 2003) taking into account the current prices and fees. The cost of medical waste removal from the source unit to the disposal site, with the adopted technical and operational conditions is K_{ij} = 9.57 PLN, and when expressed in unit cost of 1 ton of transport per 1 minute (k) = PLN 1.33/t/min.

The economic efficiency calculations of the method were presented in the work by Biedugnis et al. (Biedugnis et al. 2003) whose dynamic model related to inflation and discounting of the annual capital and operating costs in each model period. Transport costs are also discounted and adjusted for inflation.

The discount factor and inflation factor of the capital cost (Z_N^t) and the current cost (Z_E^t) for the t model period can be expressed (Biedugnis et al. 2003):

$$Z_N^t, Z_E^t = \sum_{i=1}^{m_t} (d_t \cdot q_t)^i \tag{1}$$

where:
$d_t = 1/(1+r)^i$, discounting factor,
$q_t = 1/(1+e)^i$, inflation factor,
r – discount factor,
e – inflation factor.

Finding the best solution from the point of view of economic efficiency index was set as a priority. The above mentioned criterion takes into account both the selection of waste treatment technologies, as well as search for the best relationship between the location of objects used and the associated waste transport route network, depending on the amount of waste transported in each model periods.

3. Results and discussion

Calculations were carried out in the following courses:

Stage I – course 1 – the course like in the solution with the following parameters: duration of model period, respectively $t_1 = 5$ and $t_2 = 15$ years, the unitary cost of transportation of medical waste in the first and second model period, respectively, 1.33 and 0.44 PLN/Mg/min, the level of reduction of medical waste in the intermediate facilities expressed as a coefficient of the process output, wwp = 10%.

Stage II – in courses 2-5 – the impact of changes in the discount factor on the cost of the system and its spatial structure was examined. The discount factor has a significant impact on the cost of operating the system and, consequently, the change in the economic efficiency index (E).

As a result of optimization calculations for the course 1 (Stage I) of the pre-established model system of the 26 facilities (18 – the source of the medical waste, 4 – incineration, 4 – storage of hazardous waste, 55 – possible routes for waste transport), the was a number of facilities selected in model periods I and II: 3/3 incinerators, 3/3 of the landfills and 21/21 waste transport routes, in consequence minimizing the cost of the system. Process levels in intermediate and final facilities in each model period for Stage I are presented in Table 1.

Table 1. The level of processing activities of intermediate and final objects for the 1st course [Mg/year]

System facilities	Process	Processing activity level [Mg/year]	Duration of model studies I = 5 years, II = 15 years
IF1	incineration	140.400	I
IF1	incineration	148.800	II
IF2	incineration	210.400	I
IF2	incineration	222.400	II
IF3	incineration	434.400	I
IF3	incineration	450.900	II
FF1	storage	14.040	I
FF1	storage	14.880	II
FF2	storage	21.040	I
FF2	storage	22.240	II
FF3	storage	43.440	I
FF3	storage	45.090	II

For courses 2, 3, 4 and 5 – the impact of change of the discount factor on the final solution has been studied. This change was not accompanied by any modifications in the structure of the system or levels of processing activities in intermediate and final facilities in particular model periods.

The system layout of the system objects, the amount of transported waste and the related transport routes are shown in Fig. 1. The highest value of the economic efficiency index E = 2332.60 PLN/Mg was obtained (increase E by approx. 46% in relation to course 1) with the assumed discount factor = 0.980 (course 2), while for the discount factor = 0.909 (course 5) the lowest value of the economic efficiency index was E = 1164.20 PLN/Mg (E decrease by approx. 27% in relation to course 1).

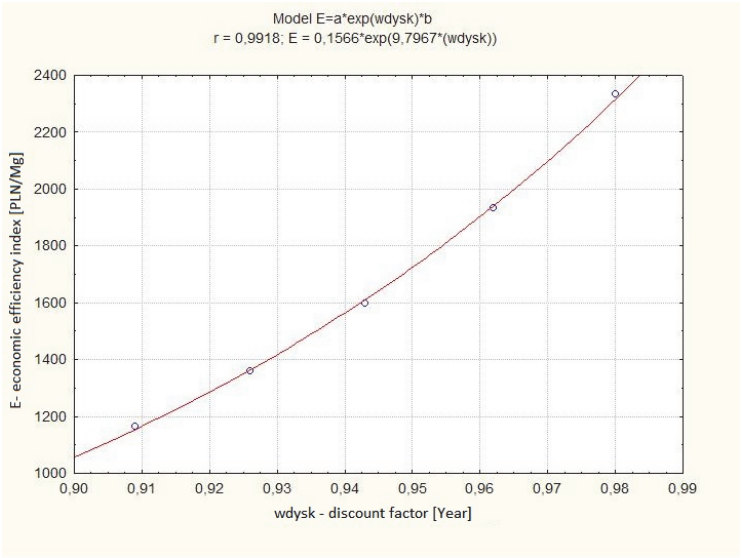

Fig. 1. Correlation of the economic efficiency index (E) and discount factor

4. Conclusions

This paper presents the optimisation model of the medical waste disposal and neutralisation system in the dynamic version, taking into account the expected changes in the input and output parameters of the waste management system and the status of the system at specific time intervals. This allows the system to be considered as an investment project, i.e. assuming the implementation of a system from scratch, modernisation or a project including modernisation of existing facilities as well as implementation of new system solutions, enabling application of the solution with the lowest total system cost.

The dynamic model includes inflation and discounting of annual capital expenditures and current costs. These costs are included in the model as time-varying values for subsequent model periods, i.e. with the assumed duration of the first and second model period respectively: t_1 = 5 years and t_2 = 15 years and *wwp* (input parameter) = 10%. Transport costs, like capital and current costs, are discounted and include inflation.

Taking into account the discount factor causes a significant change in the system's operating costs and consequently a change in the economic efficiency index (E). It does not, however change the spatial structure of the system, i.e. the location scheme of the system objects, the quantity of waste transported and the associated waste transport routes. With the assumed discount factor in the range of 0.980 to 0.909, the highest cost of the system was achieved at the level of E = 2332.60 PLN/Mg (increase of economic efficiency index E by ca. 46% in comparison with course 1, and discount factor = 0.980). The lowest cost of the system was achieved at the level of E = 1164.20 PLN/Mg (increase of economic efficiency index E by ca. 27% in comparison with course 1, and discount factor = 0.909).

The increase in the discount factor is accompanied by an increase in the economic efficiency index (E), which can be described by the following correlation:

$$E(wdysk) = 0.1566*\exp(9.7967*(wdysk)\ [PLN/Mg]$$

The final decision about choosing a variant of system operation does not have to coincide with the obtained solution being the result of modelling. The obtained results of optimisation studies should be treated as an aid in decision-making, taking into account a number of complex environmental conditions and the dynamics of economic factors and the socio-political conditions.

The research was conducted as a research project WZ/WBiIS/02/19 in Faculty of Building and Environmental Engineering of BUT and financed by the Ministry of Science and Higher Education.

References

Biedugnis, S., Podwójci, P., Smolarkiewicz, M. (2003). *Optimization of municipal waste management in micro and macro-region scale*. Warsaw, PAN.

Chartier, Y., Emmanuel, J., Pieper, U., Prüss, A., Rushbrook, P., Stringer, R., Townend, W., Wilbum, S., Zghondi, R. (2012). *Safe managemenet of wastes from health-care activities*. WHO.

Delmonico, D.V.G., Santos, H.H., Pinheiro, M.A.P., Castro, R., Souza, R.M. (2018). Waste management barriers in developing country hospitals: case study and AHP analysis. *Waste Management Resorces, 36*(1), 48-58.

Hu, T.L., Sheu, J.B., Huang, K.H. (2002). A reverse logistics cost minimization model for the treatment of hazardous wastes. *Transportation Research Part E, 38*, 457-473.

Kocak, O., Kurtuldu, H., Akpek, A., Kocoglu, A., Erogul, O. (2017). *A medicial waste management mdel for public private partnership hospitals*. Medical Technologies National Conference, TIPTEKNO.

Lu, C., You, J.X., Liu, H.C., Li, P. (2016). Health-care waste treatment technology selection using the interval 2-tuple induced TOPSIS method. *International Journal of Environmental Research and Public Health, 13*(6).

Mantzaras, G., Voudrias, E.A. (2017). An optimization model for collection, haul, transfer, treatment and siposal of infectious medical waste: Application to a Greek region. *Waste Management, 69*, 518-534.

Marczak, H. (2016). Logistics of waste management in healthcare institutions. *Journal of Ecological Engineering, 17*(3), 113-118.

Michlowicz, E. (2012). Optimization of nonlinear transport-production task of medical waste. *The Archives of Transport, 24*(3), 354-366.

Minoglou, M., Gerassimidou, S., Komilis, D. (2017). Healthcare waste generation worldwide and its dependence on socio-economic and environmental factors. *Sustainability, 9*(2), 220.

Shi, L., Fan, H., Gao, P., Zhang, H. (2009). *Network model and optimization of medical waste reverse logistics by improved genetic algorithm.* International Symposium on Intelligence Computation and Applications, ISICA 5821LNCS, 40-52.

Teleszewski, T.J., Zukowski, M. (2018). The influence of sludge on thermal performance of heat exchanger tubes inside in an anaerobic digester. *Journal of Ecological Engineering, 19*(4), 242-250.

Walery, M.J. (2017). The effect of inflation rate on the cost of medical waste management system. International Conference on Advances in Energy Systems and Environmental Engineering (ASEE17), *E3S Web of Conferences, 22*.

Windfeld, E.S., Brooks, M.S. (2015). Medical waste managaeent – a review. *Journal Environmental Management, 163*, 98-108.

Abstract

This paper describes the optimization studies aime dat analysing the impact of the parameter described by the discount factor on the cost of the system and its structure. The study was conducted on the example of the analysis of medical waste management system in north-eastern Poland, in the Podlaskie Province. The scope of operational research carried out under the optimization study was divided into two stages of optimization calculations with assumed technical and economic parameters of the system. In the first stage, the lowest cost of functioning of the analysed system was generated, whereas in the second one the influence of the input parameter of the system, i.e. the discount factor on the economic efficiency index (E) and the spatial structure of the medical waste management system was determined. With the assumed discount factor in the range of 0.980 to 0.909, the highest cost of the system was achieved at the level of 2332.60 PLN/Mg (increase of economic efficiency index E by ca. 46% in comparison with course 1, with discount factor = 0.980); furthermore, discount factor = 0.909 produced the lowest

value of the economic efficiency index, i.e. E = 1164.20 PLN/Mg (a decrease of E by ca. 27% in comparison with course 1).

Keywords:
medical waste, transport, disposal of medical waste, discount factor, economic efficiency index

Optymalizacja ekonomiczna systemu przetwarzania odpadów medycznych: studium przypadku województwa podlaskiego

Streszczenie

W artykule opisano badania optymalizacyjne, których celem była analiza wpływu parametru opisanego poprzez współczynnik dyskontowy na koszt funkcjonowania systemu i jego strukturę. Badania przeprowadzono na przykładzie analizy systemu gospodarki odpadami medycznymi w północno-wschodniej Polsce, w województwie podlaskim. Zakres badań operacyjnych, wykonany w ramach studium optymalizacji został podzielony na dwa etapy obliczeń optymalizacyjnych z założonymi parametrami techniczno-ekonomicznymi systemu. W pierwszym etapie wygenerowano najniższy koszt funkcjonowania analizowanego systemu, natomiast w drugim określono wpływ parametru wejściowego systemu, tj. współczynnika dyskontowego (wdysk) na wskaźnik efektywności kosztowej (E) oraz strukturę przestrzenną systemu gospodarowania odpadami medycznymi. Przy założonym współczynniku dyskonta w przedziale od 0,980 do 0,909, najwyższy koszt systemu został osiągnięty na poziomie 2332,60 zł/Mg (wzrost wskaźnika efektywności kosztowej E o ok. 46% w porównaniu z przebiegiem 1, przy założonym wdysk= 0,980), natomiast przy wdysk = 0,909 osiągnięto najniższą wartość wskaźnika efektywności kosztowej E = 1164,20 zł/Mg (spadek E o ok. 27% w stosunku do przebiegu 1).

Słowa kluczowe:
odpady medyczne, transport, unieszkodliwianie odpadów medycznych, współczynnik dyskontowy, wskaźnik efektywności kosztowej

MIDDLE POMERANIAN SCIENTIFIC SOCIETY OF THE ENVIRONMENT PROTECTION

Rocznik Ochrona Środowiska

Volume 22. Year 2020 ISSN 1506-218X 400-416

Applicability of the Multiple-Criteria Decision-Making Method to Assess Potential for Watercourse Revitalisation in Urbanised Areas Based on the Wierzbak Watercourse

*Tomasz Kałuża, Mateusz Hämmerling**

University of Life Sciences, Poznan, Poland

**corresponding author's e-mail: mateusz.hammerling@up.poznan.pl*

1. Review of literature

It is increasingly accepted that revitalisation of rivers, including also headwaters and small watercourses flowing through urbanised areas, not only consists in the protection and generation of natural resources and quality space, but it is also a response to climate change (SMURF 2003, Janauer 2005, Boitsidis & Gurnell 2006, Kasperek et al. 2013, Mazur et al. 2015, Walczak et al. 2018). Revitalisation in the literal sense refers to "revival, restoration to life". This term is most frequently used in relation to objects or areas, which in view of various transformations (e.g. economic) have lost their original functions (Kaluza et al. 2014, Brandyk & Majewski 2013). In contrast to renaturisation, revitalisation covers a narrower scope of actions (Gurnell 2007, Schueler et al. 2005). In relation to rivers its role is to resolve the crisis and restore ecological functions of the river. Measures promoting revitalisation of small urban watercourses facilitate an improvement in the ecological status or potential of waters as stipulated in the Water Framework Directive (Directive 2000/60/EC). All enterprises aiming at watercourse revitalisation contribute to an improved ecological potential of waters and quality of urbanised areas (Janauer 2005, Houriet 2006, Laks et al. 2013, Kaluza et al 2015, Tomczyk et al. 2019). Unfortunately, very few revitalisation projects have been successfully implemented in urbanised areas. This results e.g. from many strong revitalisation barriers (Zalewski & Wagner-Lotkowska 2004, Trząski & Mana 2007). Among them social as well as scientific and information barriers are of greatest importance (Schueler 2004, Trząski et al. 2006, Trząski et al. 2010). Scientific and information barriers stem from the fact that scientific knowledge is not adequately used and adapted to the specific character of a given investment project. The number of advisory institutions and the amount of

information available as guidelines for managing organs are insufficient. In turn, social barriers result mainly from the fact that the general public is not aware of the importance and need for revitalisation. People frequently underestimate the role of urban watercourses and neglect the problem of water deficits in the urban space, periodical flooding or improvement of environmental quality (Januchta-Szostak 2009, Tymiński & Kałuza 2012, Trząski et al. 2010).

When selecting the optimal solution we need to refer to multiple-criteria methods, which in turn may be divided in terms of the solution applied to the analysed problem. The first group comprises deterministic methods, in which decision variants are assessed based on criteria, the second group consists of stochastic methods, in which every decision variant is investigated in terms of individual criteria as a random variable, while the third group is composed of fuzzy logic methods, in which each solution is described by ordered fuzzy numbers (Trzaskalik 2014). The second significant criterion is connected with the time when factors are specified for multiple-criteria assessment. In the first group of factors the assessment criteria are defined only after the analysis has been completed. In the other group of methods factors are identified at the very beginning of the assessment process. The data envelopment analysis (DEA) belongs to the former group, while the latter group of factors includes the ELECTRE and SMART methods (Stypka & Flaga-Maryańczyk 2016). The AHP and REMBRANDT methods are most popular and used within a very wide range of applications in such areas as management, sociology, transport and logistics (Downarowicz et al. 2000) as well as environmental engineering (Stoltmann 2015, Kubicz et al. 2015, Stypka & Flaga-Maryańczyk 2016, Hämmerling 2019).

Search for the best solution to a given problem is a complicated task. Frequently problem solving decisions are expressed using one criterion, which does not present all parameters affecting a given problem. In such a case we deal with a single-criterion analysis, in which each variant is assessed in relation to one selected criterion, e.g. costs, operation parameters, etc. Such single criteria are not reliable. For this reason decisions should be made based on multiple criteria. Among other things, this requires comprehensive evaluation of solution variants, taking into consideration many characteristics (Adamus & Łasak 2010). This is provided by multiple-criteria methods, which facilitate thorough analyses of a given problem (Schueler & Brown 2004).

Taking into account the number of barriers and the need to search for an optimal solution, this paper analyses the application of the multiple-criteria decision-making method based on the analytic hierarchy process (AHP) for the revitalisation potential of watercourses in urbanised areas. The analyses were conducted on the Wierzbak watercourse flowing in the northern part of the city of Poznań, which segment as a storm sewer flows through the grounds of the Poznan University of Life Sciences and further (still as a storm sewer) discharges into the

Bogdanka River (a left-bank tributary of the Warta). Based on collected information and data the most advantageous solution for potential revitalisation of the Wierzbak watercourse was selected.

2. Description of object of study

The Wierzbak watercourse is the left-bank and the largest tributary to the Bogdanka River, to which it is discharged at Nad Wierzbakiem street downstream of the Stawy Sołackie ponds. Its total length is 7.85 km, of which 7.07 km lie within the administrative limits of Poznań (Biprowodmel 1998). As a result of progressing urbanisation within the Wierzbak watercourse catchment more than 1/2 of the Wierzbak length has been channeled and flows in a storm sewer under streets and housing districts. The total area of the watercourse catchment is 14.72 km^2 and it is an element of the Bogdanka catchment, which covers the north-western part of Poznań (i.e. the Podolany, Winiary, Sołacz, Piątkowo and Suchy Las districts). The Wierzbak originates from the headwater near Góra Moraska and next the channeled watercourse flows through housing districts. It reappears on the ground surface in the area of a water reservoir at Omańkowska street. In the vicinity of the Druskienicka and Strzeszyńska intersection another retention reservoir was built on the watercourse. Further the Wierzbak flows south through housing and industrial areas. Near Rabczańska street it flows under the Poznań-Piła rail tracks. In the southern part of the Literackie housing district two connected retention reservoirs with the total area of approx. 5110 m^2 were constructed on the Wierzbak. In its further course the Wierzbak flows through allotment gardens located between Lutycka and Dojazd streets. Towards the end of its course as a storm sewer it flows through two housing districts of Poznań, i.e. Sołacz and Winiary. Under Nad Wierzbakiem street it discharges into the Bogdanka (Hydroprojekt 1998). The course of the Wierzbak is presented in Fig. 1. A broken blue line denotes these segments of the watercourse, in which it flows in a storm sewer.

The Wierzbak collects precipitation waters from numerous areas, e.g. the Piątkow or Podolany districts. These waters are mostly polluted and need to be treated. Some of them are pre-treated in retention reservoirs built in the watercourse. Based on a study by the Institute of Meteorology and Water Management (1996), characteristic flows in the Wierzbak watercourse were estimated at the section of Szczawnicka street (for catchment area of 9.55 km^2). The figures are presented in Table 1. Design and control flows are given in Table 2. The design flow is the flow with the probability of occurrence p = 10%, while the control flow has p = 5%.

Fig. 1. The course of the Wierzbak in the city of Poznań

Table 1. Characteristic flows of the Wierzbak River at the cross-section of Szczawnicka Street

P.o.	Type of flow	Discharge [m^3/s]		
		Year	Summer	Winter
1	SNQ	0.007	0.005	0.011
2	SSQ	0.024	0.015	0.034
3	SWQ	0.420	0.160	0.390

Table 2. Design and control flows for different cross-sections of the Wierzbak River (IMiGW 1996)

No.	Cross-section location [km]	Catchment [km^2]	Discharge	
			$Q_{10\%}$ [m^3/s]	$Q_{5\%}$ [m^3/s]
1.	7+000	3.95	0.738	0.943
2.	4+560	5.86	0.961	1.228
3.	4+200	7.03	1.085	1.368
4.	3+240	9.55	1.330	1.700

In the northern part of the city the areas with high intensity housing and industrial development predominate, which has an effect on the quality of waters in the Wierzbak. The river also collects most precipitation waters in that area. Analyses of various flow variants in the Wierzbak river bed (Biprowodmel 1998) facilitates an assessment of flood risk. They showed that the watercourse in the area from Straży Ludowej street km 7+000 to the nearby water reservoir and in the stretch from Druskienicka street km 4+200 to Szczawnicka street km 3+240 may cause overflows and inundation of adjacent areas (which was recently the case in 2009, 2010 and 2017 due to further sealing of this part of the Wierzbak catchment). Thanks to restoration of the watercourse bed and the operation of the water reservoirs the mean maximum flow SWQ could be relatively safely discharged. However, discharge of the design flow $Q_{10\%}$, increased by design rainfall is connected with the risk of water overflow and inundation of adjacent areas.

In view of the fact that in many segments the watercourse flows through housing development areas and private plots currently the watercourse bed may not be expanded. Thus the present condition of the watercourse bed might be improved by such measures as e.g. reduction of direct inflow of precipitation waters to the watercourse and to its two tributaries, or greater utilisation of existing water reservoirs and their retention potential, as well as revitalisation of channeled segments and construction of new water reservoirs. There are segments in the Wierzbak catchment (between Dojazd and Urbanowska streets), where the channeled watercourse flows through green areas and garage facilities located in

artificial depressions, found to have considerable potential related to revitalisation of this watercourse. This potential is indicated by the existing land development around the previously constructed water reservoirs on the Wierzbak (Fig. 2).

Fig. 2. View of the water reservoir on the Wierzbak near Strzeszyńska and Druskiennicka streets

3. Methodology

Considering the number of barriers and the need to search for the optimal solution to potential revitalisation of the Wierzbak watercourse, this paper analyses the applicability of the multiple-criteria decision-making method using AHP. Such methods are particularly suitable when solving such problems, in which selection criteria include both qualitative and quantitative factors. The method created by Saaty (Saaty 1994, Saaty 1996) has been further developed by many researchers (Sun et al. 2019, Wang et al. 2009), facilitating solution of deterministic, stochastic and fuzzy problems.

In view of the fact that comparisons of individual factors and solutions may be biased, literature sources present parameters, which verify cohesion of comparisons. One of the most important values determined in AHP and a measure of cohesion of comparisons reflecting proportionality of preferences is provided by the eigenvalue of a matrix (Stoltmann 2015). The maximum eigenvalue of matrix λ_{max} is calculated from the formula:

$$\lambda_{\max} = \frac{1}{n}\sum_{=1}^{n}\lambda_i \tag{1}$$

where:
n – matrix size,
λ_i – eigenvalue of matrix for i-th row.

Due to partial bias in the case of these assessments, the Indeterminant Rate *IR* was calculated.

$$IR = \frac{CI}{RI} \tag{2}$$

where:
IR – Indeterminant Rate,
CI – consequence index,
RI – value of random index.

The value of the random index *RI* depends on the size of the comparison matrix. Validity assessment is considered convergent if the calculated *IR* value does not exceed 0.2 (Tułecki & Król 2007). The consequence index *CI* is determined following the formula:

$$CI = \frac{(\lambda_{śr} - n)}{(n-1)} \tag{3}$$

where:
n – matrix size,
$\lambda_{śr}$ – mean eigenvalue of matrix.

Analysis applying the AHP approach consisted in the decomposition of the problem, i.e. preparation of a hierarchical tree, which describes the aim, general factors, with increasingly more specific factors presented on the successive levels. The number of hierarchical tree levels in the AHP method may be unlimited, but solutions will always be found at the last level. Figure 3 presents a hierarchical tree for the selection of the most advantageous solution to the reconstruction of the Wierzbak watercourse. For the purpose of a detailed analysis of the problem several different barriers were considered, e.g. ecological, planning, social, economic and technological.

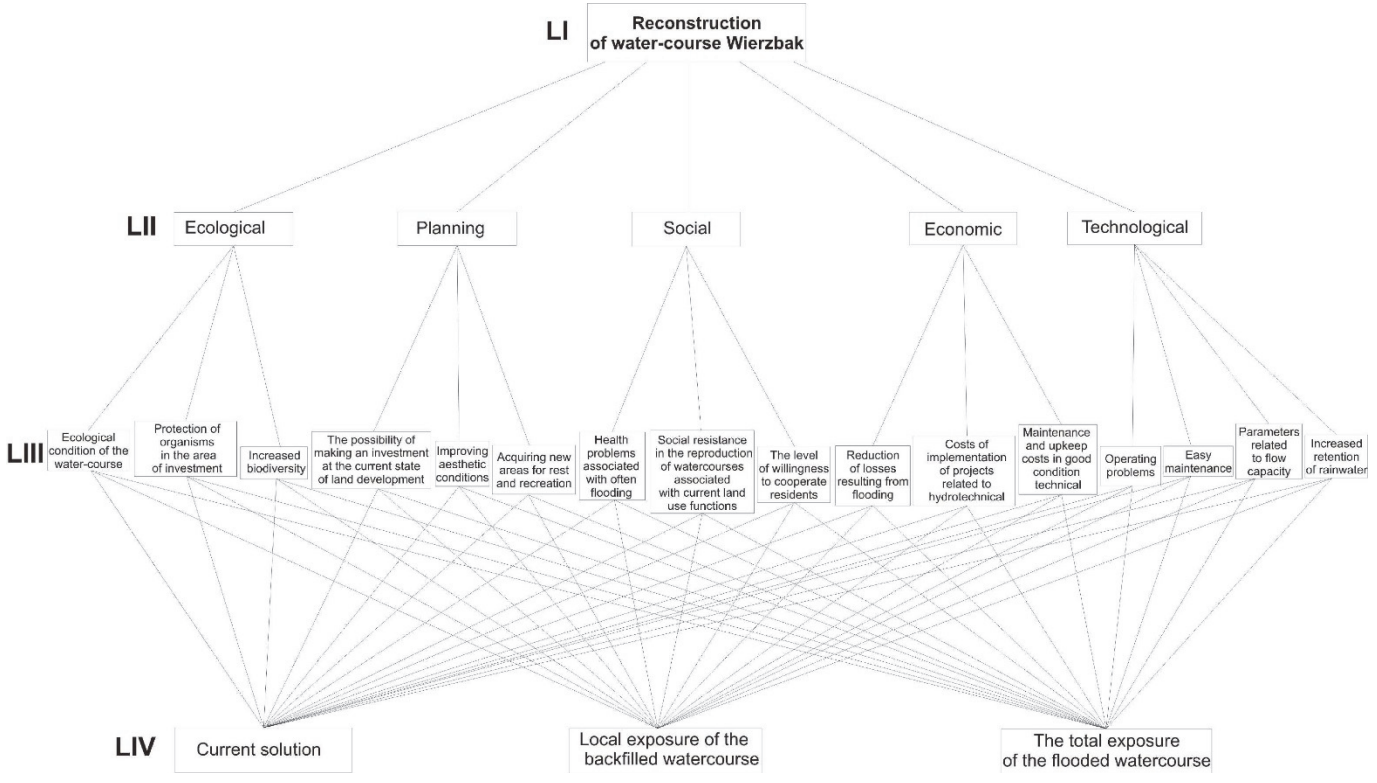

Fig. 3. Structure showing a hierarchical tree using the AHP method

In the next step the factors were compared pair-wise at levels LII and LIII creating matrices, which were next solved obtaining local and global vectors. Next a matrix was constructed for individual solutions from level LIV, which was analysed 16 times in terms of each factor from level LIII. Pair-wise comparisons in all the matrices were performed using a 9-point scale according to Saaty (Saaty 1994).

Since values in the Saaty scale ascribed to individual factors at level LII are highly subjective, several variants of their attribution were analysed. In variant A equal priorities were assumed for all factors at level LII, in variant B a very strong advantage was observed for ecological factors, in variant C a very strong advantage was found for planning factors, in variant D a very strong advantage was recorded for social factors, in variant E a very strong advantage was reported for economic factors, while in variant F a very strong advantage was presented for technological factors. Next the obtained global solution vectors were compared and those, which according to most variants were most advantageous, were selected.

4. Results

First analyses concerned the results obtained based on the assumptions of variant A, which assumed equal priorities of all factors at level LII. Figure 4 presents results of solutions for 5 matrices for factors from level LIII (local vector) and considering the priorities from level LII (global vector).

Analyses of local vectors from level LIII indicate that for each main factor from level LII we may find one specifying factor, which gained significant advantage over the others. For ecological factors it was an increase in biodiversity (0.68), for planning factors it was the possibility to execute the investment at the current land use (0.68), for social factors it was health problems resulting from continuous inundations (0.67), for economic factors it was the reduction of losses resulting from flooding (0.64), while for technological factors it was increased retention of precipitation waters (0.51). Figure 5 presents values of the hierarchical tree solution for variant A, in which all the factors at level LII were equivalent.

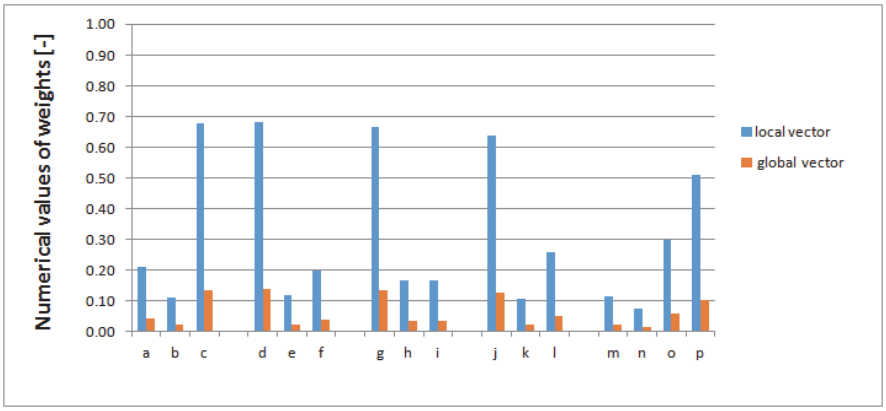

Fig. 4. Values of matrix solutions for level LIII hierarchical tree in variant A, including the division into local and global vectors; a – Ecological condition of the watercourse, b – Protection of organisms in the area of investment, c – Increased biodiversity, d – Potential for investment at the current state of land development, e – Improving aesthetic value, f – Acquiring new leisure and recreation areas, g – Health problems associated with frequent flooding, h – Social opposition to restoration of watercourses associated with current land use functions, i – Residents' willingness to cooperate, j – Reduction of losses resulting from flooding, k – Costs of implementation of hydrotechnical structure projects, l – Maintenance and upkeep costs, m – Operating problems, n – Easy maintenance, o – Parameters related to flow capacity, p – Increased rainwater retention

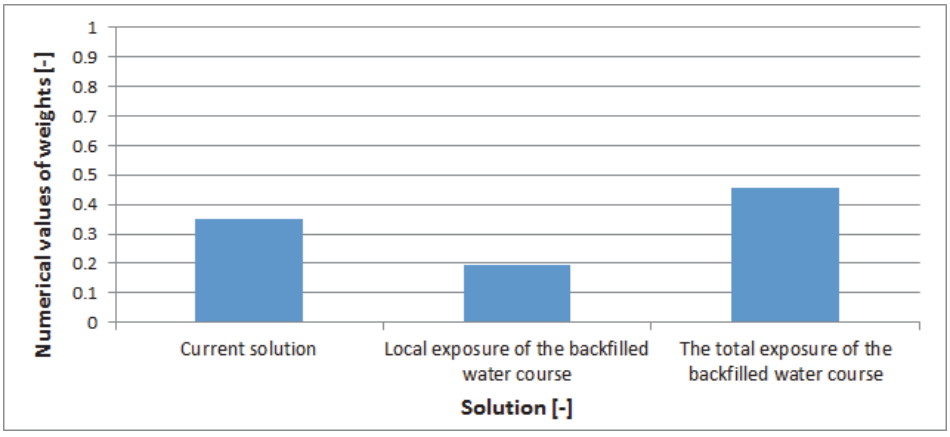

Fig. 5. Results of the analyzed problem solution for variant A

According to variant A the most advantageous solution was provided by complete exposure of the backfilled watercourse (0.46), while the least advantageous local exposure of the backfilled watercourse (0.18). The hierarchical tree was analysed in terms of individual variants (A – F), which results are presented in Table 3. Using such an approach a solution was searched for, which was most frequently the most advantageous solution.

Table 3. Results of level LIV matrix solutions for different variants (global vectors)

Variant	Priorities of selection at level LII of the hierarchical tree	Current solution	Local exposure of backfilled watercourse	Complete exposure of flood watercourse
		–	–	–
A	Equal priorities of all factors	0.35	0.19	0.46
B	Ecological	0.21	0.21	0.58
C	Planning	0.46	0.20	0.34
D	Social	0.33	0.25	0.43
E	Economic	0.56	0.14	0.30
F	Technological	0.20	0.17	0.63

Analysis of results showed that for the 4 variants (A, B, D, F) complete exposure of the watercourse was the most advantageous solution. The value greater than 0.5 for the complete exposure of the watercourse was obtained for variants B and F.

The current solution received a value greater than 0.5 for variant E including economic factors. In turn, the solution with local exposure of the backfilled watercourse did not receive any values of the solution greater than 0.5. Based on the multiple-criteria analysis it may be concluded that the most advantageous solution is to reconstruct the watercourse consisting in its complete exposure.

5. Discussion

The analysed revitalisation barriers may be divided according to (Trząski & Mana 2007) into six categories. These were economic, social, information, political, legislative and organisational barriers. Sources of decisive barriers are found in the social and scientific and information spheres. The most important aspect is connected with a lack of practical application of scientific information in the social sphere, determining prospects for revitalisation of rivers. Both the scientific and information sphere, as well as legislative and legal, economic and organisational spheres are sources of barriers directly affecting the practice. At

the same time, a lack of good practical experience – resulting also from the existing barriers – contribute to the reinforcement of the barriers already in existence (Tymiński et al. 2017).

The division of barriers presented in this study in relation to the proposal by Trząski and Mana (2007) more effectively reflects the specific nature of problems connected with the revitalisation of rivers in urbanised areas is also more comprehensible for the general public. This paper also shows the justification for the application of the AHP method to solve decision-making problems of such complexity and connected with watercourse revitalisation. To date the AHP method has been used within a very wide range of problems such as management, sociology, transport and logistics (Downarowicz 2000) as well as environmental engineering. Górski et al. (2015) presented e.g. applicability of the AHP method when designing microtunnel chambers. The AHP approach was also applied by Chmist and Hämmerling (2016), who stated that the best method of lake reclamation is connected with inactivation of phosphorus. In a study Kubicz et al. (2015) verified the most advantageous solution with barrage damming using the AHP method. This approach is becoming increasingly popular as a useful tool in the process of making difficult environmental decisions.

Obtained results indicate that for most variants the most advantageous solution would be to completely expose the analysed watercourse. Such a solution indicates both the adoption of equivalent priorities for all factors at level II (variant A – 0.46), as well as adoption at level II for the absolute advantage for ecological factors (variant B – 0.58), social factors (variant D – 0.43) and technological factors (variant F – 0.63). For the other variants, in which advantage was observed for planning and economic factors, the most advantageous solution was to leave the analysed watercourse with no changes introduced.

Literature sources may provide many examples for the analyses concerning methods eliminating revitalisation barriers (e.g. Schueler 2004, Trząski et al. 2006, Trząski et al. 2010, Tymiński & Kałuża 2013). Nevertheless, the authors would like to stress that currently the basic direction of activity is to develop and implement local projects. For example, in several towns of the Czech Republic some local projects have been implemented (Trząski & Mana 2007). It may be concluded on this basis that despite all indicated obstacles it is feasible also in Poland. Execution and adequate promotion of one or several local projects may lead to weakening of the scientific and information barriers. A logical consequence of such a change may be related with an increased interest of the local communities and local decision-makers in revitalisation of urban rivers, particularly if the general public becomes aware of the relationship between improved quality of rivers and improved quality of urban space and comfort of life. Additionally, this would also result in a reduced risk of flooding and increased local

retention of precipitation waters. This in turn may lead to weakening of social barriers. When selecting an optimal solution we may refer to tools of the multiple-criteria analysis, including the AHP approach.

6. Concluding remarks

The decision making process, in which many parameters and variables need to be considered, is complicated. This study showed justification for the application of the decision-making method using the AHP approach, which has not been used previously to identify the best watercourse reconstruction method. Application of such a method made it possible to take into consideration factors related with economics, ecology, technology, planning as well as social factors. In this study analyses were conducted on the effect of changes in the significance of individual factors at level LII on the obtained results (variants A-F). Thus the analysis of results obtained for most of the investigated variants (A, B, D, F) indicated the complete exposure of the watercourse as the most advantageous solution. It shows that despite differences in values obtained for global vectors at level LIV, a key role for the solution of the studied problem was played by specific factors, which were described at level LIII of the hierarchical tree.

The proposal presented in this study for analyses related with the potential revitalisation of the Wierzbak river valley in Poznań is a response to considerable interest in such solutions observed in Poland in recent years. The set of principles and criteria included ecological, planning, social, economic and technological aspects, since all of them need to be considered when making local revitalisation initiatives. The scope of analyses should comprise possibly the largest number of elements reflecting the target status of the watercourse and its valley. The proposed method to evaluate revitalisation with the properly selected assessment criteria seems to be feasible in the case of other valleys of small urban rivers also in other regions of Poland and Central Europe.

References

Adamus, W., & Łasak, P. (2010). Zastosowanie metody AHP do wyboru umiejscowienia nadzoru nad rynkiem finansowym. *Bank i kredyt*, *41*(4), 73-100.

Biprowodmel (1998). Studium programowo – przestrzenne Biura Projektów Wodnych Melioracji i Inżynierii Środowiska "BIPROWODMEL" Sp. z o.o. pt. "Biologiczna odnowa wód rzeki Bogdanki - Zadanie nr 6 Wierzbak" wyk. w 1998 r.

Boitsidis, A., & Gurnell, A. (2006). Environmental Sustainability Indicators For Urban River Management (http://www.smurf-project.info).

Brandyk, A., & Majewski G. (2013). Modeling of Hydrological Conditions for the Restoration of Przemkowsko-Przecławskie Wetlands. *Rocznik Ochrona Środowiska. 15,* 371-391.

Chmist, J., & Hämmerling, M. (2016). Wybór najskuteczniejszej metody rekultywacji zbiorników wodnych z wykorzystaniem metody AHP. *Acta Scientiarum Polonorum. Formatio Circumiectus*, *15*(2).

Directive 2000/60/EC of the European Parliament and of the Council of 23 October 2000 establishing a framework for Community action in the field of water policy. Official Journal of the European Communities L 327/1, 22.12.2000.

Downarowicz, O., Krause, J., Sikorski, M., & Stachowski, W. (2000). Zastosowanie metody AHP do oceny i sterowania poziomem bezpieczeństwa złożonego obiektu technicznego. *Wybrane metody ergonomii i nauki o eksploatacji. Gdańsk, Wydaw. Politechniki Gdańskiej*, 7-42.

Górski, K., Ignatowicz, L. R., & Bykowski, J. (2015). Zastosowanie metody AHP do projektowania komór mikrotunelowych. Przegląd Naukowy. *Inżynieria i Kształtowanie Środowiska, 24*(4(70)).

Gurnell, A. (2007). Urban River Survey Manual 2007. Centre for Environmental Assessment, Management & Policy. http://www.kcl.ac.uk/ceamp.

Hämmerling, M. (2019). Selection of the optimal type of fish pass using the Rembrandt method. *Acta Sci. Pol. Formatio Circumiectus*, *18*(1), 51-61.

Houriet, J.P. (2006). *Der Gewässerschutz ist eine Daueraufgabe*. Wege des Wassers. Umwelt No 4.

Hydroprojekt (1998). *Koncepcja programowa kanalizacji deszczowej Kolektora Wierzbak w Poznaniu.* BSiPBW, HYDROPROJEKT Poznań.

IMGW (1996). Charakterystyka cieków m. Poznania – Przepływy Maksymalne.

Janauer, G.A. (2005). *Aquatic Habitats in Vienna*. Integrating Ecology and Urban Water Management. UNESCO-Workshop, Lodz.

Januchta-Szostak, A. (2009). *Study existing best practice in the Northern Poland*. Ekspertyza w ramach projektu REURIS na zlecenie Urzędu Miasta w Bydgoszczy (materiał niepublikowany).

Kaluza, T., Szoszkiewicz, K., Radecki-Pawlik, A., Walczak, N., Plesinski, K. (2015). *Impact of River Restoration on Hydromorphological Processes: the Flinta River as a Case Study*. In: GeoPlanet. Earth and Planetary Sciences, XXXIV. Springer.

Kaluza, T., Pietruczuk, K., Szoszkiewicz, K. & Tyminski, T. (2014). Assessment and Classification of the Ecological Status of Rivers in Poland According to the Requirements of the Water Framework Directive. *Wasserwirtschaft, 104(12),* 24-29.

Kasperek, R., Mokwa, M. & Wiatkowski, M. (2013). Modelling of pollution transport with sediment on the example of the Widawa river. *Archives of Environmental Protection, 39*(2), 29-43.

Kubicz, J., Hämmerling, M., & Walczak, N. (2015). The Use of AHP Method for the Determination of the Most Environmentally Beneficial Variants of Barrages. *Journal of Ecological Engineering, 16*(4), 36-43.

Laks, I. Kałuża, T., Sojka, M. & Wróżyński, R. (2013). Problems with Modelling Water Distribution in Open Channels with Hydraulic Engineering Structures. *Rocz. Ochrona Środ., 15*(1), 245-257.

Mazur, R., Kałuża, T., Chmist, J., Walczak, N., Laks, I., & Strzeliński, P. (2015). Influence of deposition of fine plant debris in river floodplain shrubs on flood flow conditionse – The Warta River case study. *Phys. Chem. Earth, 94*, 106-113.

Saaty, T. (1994). *Fundamentals of Decision Making and Priority Theory with the Analytic Hierarchy Process*, Pitssburgh, PA: RWS Publications.

Saaty, T.L. (1996). Decision Making for Leaders: The Analytical Hierarchy Process for Decisions in a Complex World. *The Analytical Hierarchy Process Series, 2*, 71-74.

Schueler, T. (2004). *An Integrated Framework to Restore Small Urban Watersheds*. CWP Urban Subwatershed Restoration Manual Series. No 1. Version 1.0. March 2004.

Schueler, T. & Brown, K. (2004). *Urban Stream Repair Practices*. Urban Subwatershed Restoration Manual No 4, CWP-USEPA.

Schueler, T. & Kitchell A. (2005). Methods to Develop Restoration Plans for Small Urban Watersheds. *Urban Subwatershed Restoration Manual. 2*. CWP-USEPA.

SMURF, (2003). SMURF Project Methodology and Techniques. Produced by Environment Agency King's College London, University of Birmingham and HR Wallingford Ltd, in association with Wallingford Software Ltd. July 2003 (http://www.smurf-project.info/ methodologyreport.pdf).

Stoltmann, A. (2015). *Zastosowanie metody ahp do porównania kryteriów wyboru lokalizacji budowy farmy wiatrowej*. Zeszyty Naukowe Wydziału Elektrotechniki i Automatyki Politechniki Gdańskiej, 42, 187-190.

Stypka, T. & Flaga-Maryańczyk, A. (2016). Możliwości stosowania zmodyfikowanej metody AHP w problemach inżynierii środowiska. *Ekonomia i Środowisko, 2*, 37-53.

Sun, B., Tang, J., Yu, D., Song, Z. & Wang, P. (2019). Ecosystem health assessment: A PSR analysis combining AHP and FCE methods for Jiaozhou Bay, China1. *Ocean & Coastal Management, 168*, 41-50.

Tomczyk, P., Wiatkowski, M. & Gruss, Ł. (2019). Application of Macrophytes to the Assessment and Classification of Ecological Status above and below the Barrage with Hydroelectric Buildings. *Water 11*(5), 1028.

Trzaskalik, T. (2014). *Wielokryterialne wspomaganie decyzji. Przegląd metod i zastosowań*. Zeszyty Naukowe. Organizacja i Zarządzanie/Politechnika Śląska.

Trząski, L., Korczak, K., Bondaruk, J. & Łabaj, P. (2006). Użytkowe funkcje zasobów wodnych oraz uszczelnienie zlewni – kryteria nowego podejścia do gospodarowania ciekami miejskimi. Prace Naukowe GIG. *Górnictwo i Środowisko, 1*, 63-72.

Trząski, L. & Mana V. (2007). Bariery rewitalizacji niewielkich cieków wodnych na terenach zurbanizowanych regionu górnośląsko-ostrawskiego. *Research Reports Mining and Environment Quarterly, 4*.

Trząski, T., Polaczek A., Kopernik M., Łabaj P. & Szendera W. (2010). Rewitalizacja miejskich przestrzeni nadrzecznych w Polsce – ocena planowania i wdrożeń w południowej części kraju. Prace Naukowe GIG. *Górnictwo i Środowisko, 1*, 59-71.

Trząski, L., Szendera, W. & Mana, V., (2010). Propozycja ogólnych zasad rewitalizacji doliny potoku miejskiego i kryteriów wyboru inwestycji pilotowej na przykładzie projektu REURIS w Katowicach. *Research Reports Mining and Environment Quarterly, 4.*

Tułecki, A. & Król, S. (2007). Modele decyzyjne z wykorzystaniem metody Analytic Hierarchy Process (AHP) w obszarze transportu. *Probl. Eksploatacji, 2*, 171-179.

Tymiński, T. & Kałuża, T. (2012). Investigation of Mechanical Properties and Flow Resistance of Flexible Riverbank Vegetation. *Polish Journal of Environmental Studies, 21*(1), 201-207.

Tymiński, T., Mumot, J., Karpowicz, D. & XiaJianxin (2017). Sedimentation of river load in a step-pool rock ramp fishway with biotechnical embedded elements. Meteorology. *Hydrology and Water Management – Research and Operational Applications, 5*(2), 35-42.

Tymiński T. & Kałuża, T. (2013). Effect of vegetation on flow conditions in the "nature-like" fishways. *Rocznik Ochrona Środowiska, 15*, 348-436.

Walczak, N., Walczak, Z., Kałuża, T., Hämmerling, M.& Stachowski, P. (2018). The Impact of Shrubby Floodplain Vegetation Growth on the Discharge Capacity of River Valleys. *Water, 10*, 556.

Wang, J. J., Jing, Y. Y., Zhang, C. F., & Zhao, J. H. (2009). Review on multi-criteria decision analysis aid in sustainable energy decision-making. *Renewable and sustainable energy reviews, 13*(9), 2263-2278.

Zalewski, M. & Wagner-Lotkowska, I. (eds) (2004). *Integrated Watershed Management – Ecohydrology and Phytotechnology-Manual*. UNESCO IHP, UNEP IETC.

Abstract

Revitalisation of even small watercourses in urbanised areas improves water retention conditions, while at the same time reducing the risk of flooding. It also contributes to improved condition or ecological potential of waters. Measures implemented to revitalise small urban watercourses are hindered by many obstacles. When selecting an optimal solution we need to refer to multiple-criteria methods. Considering the number of barriers and the need to search for the optimal solution this paper analyses the applicability of multiple-criteria decision-making method involving analytic hierarchy process (AHP) to assess potential for revitalisation of watercourses in urbanised areas. The investigations were conducted on the Wierzbak watercourse flowing in the northern part of the city of Poznań, which has been channeled in over 60% of its course and is discharged into the Bogdanka River (a left-bank tributary of the Warta) in an ouflow sewer. In order to analyse the problem in detail various barriers were investigated, e.g. ecological, planning, social, economic and engineering. The analyses were conducted for 6 variants. Based on the collected information and data the AHP method was applied to select the most advantageous solution to potential revitalisation of the watercourse. Analysis of the results showed that for 4 out of the 6 tested variants complete exposure of the watercourse would be the most advantageous option. In turn, ecological and social barriers were deemed to be the most important. The study confirmed applicability of the AHP method to solve such complicated decision-making problems.

Keywords:
watercourse revitalisation, the multiple-criteria decision-making method

Wykorzystanie metody wielokryterialnego wspomagania decyzji do oceny możliwości rewitalizacji cieków na terenach zurbanizowanych na przykładzie cieku Wierzbak

Streszczenie

Rewitalizacja nawet niewielkich cieków na terenach zurbanizowanych poprawia warunki retencjonowania wody, wpływa także na zmniejszanie ryzyka powodzi. Przyczynia się również do poprawy stanu lub potencjału ekologicznego wód. Działania na rzecz rewitalizacji małych miejskich cieków napotykają na wiele barier. W wyborze optymalnego rozwiązania należy odwołać się do metod wielokryterialnych. Uwzględniając ilość barier i konieczność szukania rozwiązania optymalnego, w pracy przedstawiono analizę wykorzystania metody wielokryterialnego wspomagania decyzji AHP do oceny możliwości rewitalizacji cieków na terenach zurbanizowanych. Jako przykład wskazano ciek Wierzbak płynący w północnej części Poznania, który w ponad 60% został skanalizowany i w postaci kolektora uchodzi do rzeki Bogdanki (lewobrzeżnego dopływu Warty). W celu szczegółowego przeanalizowania problemu uwzględniono szereg różnych barier takich jak: ekologiczne, planistyczne, społeczne, ekonomiczne, technologiczne. Badania przeprowadzono dla 6 wariantów. Na podstawie zebranych informacji i danych wykorzystując metodę AHP został wykonany wybór najbardziej korzystnego rozwiązania potencjalnej rewitalizacji cieku. Analiza wyników wykazała, że dla 4 z 6 badanych wariantów całkowite odsłonięcie cieku było rozwiązaniem najbardziej korzystnym. Za najważniejsze uznano bariery ekologiczne i społeczne. Wykazano celowość wykorzystania metody AHP do rozwiązywania tego rodzaju skomplikowanych problemów decyzyjnych.

Słowa kluczowe:
rewitalizacja cieków, metody wielokryterialnego wspomagania decyzji

MIDDLE POMERANIAN SCIENTIFIC SOCIETY OF THE ENVIRONMENT PROTECTION

Rocznik Ochrona Środowiska

Volume 22. Year 2020 ISSN 1506-218X 417-430

Effective Impervious Area Mapping in Modeling Runoff from Urban Catchment

Karolina Mazurkiewicz, Marcin Skotnicki, Zbysław Dymaczewski*

Poznań University of Technology, Poland

corresponding author's e-mail: marcin.skotnicki@put.poznan.pl

1. Introduction

The effective impervious area (EIA) is a part of the total impervious area (TIA), from which the runoff goes directly to the storm water sewer system. Determination of the effective impervious area (EIA) is one of the main stages of building the storm water sewer systems simulation models for urban areas (Lee & Heaney 2003, Seo et al. 2013, Yao et al. 2016, Ebrahimian et al. 2018). TIA for a specific catchment can be estimated according to the information about land use, such as maps, aerial and satellite images, data from laser scanning (Mostrales et al. 2018). The EIA can be calculated on basis of a model calibration or with the use of empirical formulas based on TIA (Sahoo & Sreeja 2013, Gulliver et al. 2015, Ebrahimian et al. 2016, Zhuk et al. 2018).

Regardless of the method of determining the EIA, the value of EIA as an input data to the simulation model is necessary. This issue is connected with the method of reduction of impervious area and is particularly important when using one-dimensional (1D) runoff models. Despite the increasing popularity of two-dimensional (2D) models, the calculation of surface runoff using them is limited, mainly by data availability and long calculation time (Pina et al. 2016, Bermúdez et al. 2018). The most common use of 2D runoff models is the analysis of the flooded areas when storm water sewers are overloaded (Son et al. 2016). In this case, the surface runoff is determined using the 1D runoff model and the 2D model is used only to calculate the flow which occurs above ground level as a result of the storm water system overload. It means that the simulation result depends on the parameters of the one-dimensional surface runoff model.

In one-dimensional surface runoff models, such as SWMM5 (Rossman 2015, Nowogoński 2018), the catchment area is represented by impervious and pervious areas. The contribution of impervious area in the total catchment area

determines the imperviousness degree of a catchment area. The easiest way to put information about the EIA into the model is to use the imperviousness degree as a parameter used during the model calibration (Niazi et al. 2017). The reduction in the value of impervious area with the use of imperviousness degree eliminates the impervious area that is the difference between TIA and EIA from the model. It is replaced by a pervious area. Another option to include information about the EIA in the model is also available, e.g. in SWMM5 there is a possibility to redirect a part of the runoff from the impervious area to the pervious area. This is a situation that is definitely more relevant to real conditions. In case of reducing the imperviousness degree, a part of impervious area is removed from the catchment. In fact, this part of area does not disappear – the runoff from this surface is not discharged directly into the storm water sewer system. In other words, reduction of the imperviousness degree results in replacing an impervious area by a pervious area. Then the runoff is indirect – through the permeable surface.

Surface runoff from pervious areas is generated by heavy rainfalls and largely depends on the parameters characterizing soil infiltration capabilities. In that case in sewers the outflow generated by a runoff from pervious area takes place under hydraulic overload conditions and may be accompanied by a flooding. Such runoff conditions are the basis for flood risk assessment (PN-EN 752). If the storm water sewer system works under hydraulic overload conditions when flooding occurs, it is practically impossible to determine model parameters (especially infiltration) while model calibration based on the volume balance of registered and calculated outflow. Infiltration parameters can be determined mainly on the basis of analysis of soil conditions and land cover. In that case the infiltration parameters can be taken from the literature. However it may cause that the reliability of the simulation results of the runoff from pervious areas is lower than for the runoff from impervious areas, as the values selected from literature might not represent real conditions.

From a practical point of view, it is therefore important to know the influence of parameters characterizing the pervious part of the catchment area, including the EIA mapping in the model, on the simulation results. This gives rise to a rational selection of the values of these parameters, ensuring the reliability of the simulation results as high as possible. The easiest way to determine the influence of the model parameters on calculation results is sensitivity analysis (James 2003, Barco et al. 2008). It is based on assessing the impact of changes in values of model parameters on calculated values.

The publication presents the results of the sensitivity analysis used to assess the impact of the method of mapping the EIA in the model on the calculated runoff volume in case of runoff from the previous areas.

2. Catchment

2.1. Catchment characteristic

Presented analysis was performed for existing urban catchment located in Bydgoszcz (Fig. 1). The total area of the catchment was 78.3 ha. The predominant types of land use were single-family housing and multi-family buildings. The value of TIA for chosen catchment, which includes the surfaces of roofs and roads, was determined by Miejskie Wodociągi i Kanalizacja company (MWiK) in Bydgoszcz (the operator of storm water sewer system in the city) on the basis of the digital maps and aerial photographs. The size of the TIA for the catchment area was assessed as 35.4 ha.

The simulation model was performed with the use of SWMM program, widely used in urban catchments analysis (Zawilski & Dziedziela 2018, Nowogoński 2020). The model consist of 156 subcatchments and 171 conduits. Only sewers with diameter above 300 mm were considered. The areas of subcatchments (except two cases) were below 2 ha. The accuracy of storm water sewer system structure represented in a model is sufficient according to the requirements from the literature (Zawilski 2010, Krebs et al. 2014, UDG 2017). The model was provided and made available by MWiK company in Bydgoszcz.

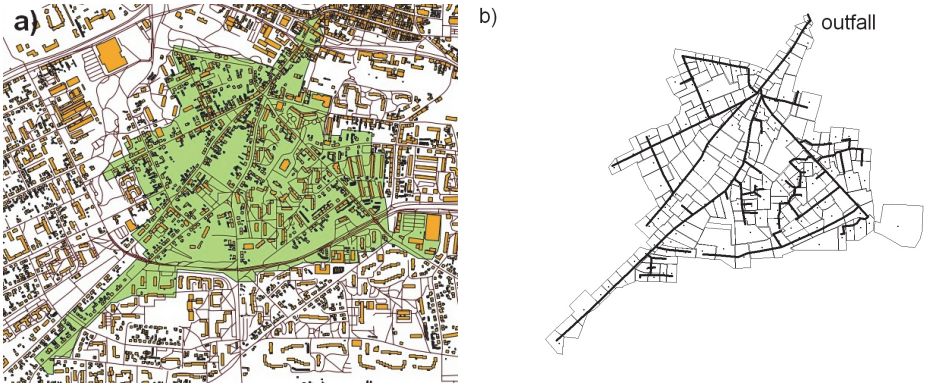

Fig. 1. Catchment area (a) and its model (b)

2.2. Assessment of EIA

Due to the lack of measurement data to determine the EIA on basis of the balance of rainfall-runoff volume for analyzed catchment, the EIA value was calculated according to the empirical formula (Alley & Veenhuis 1983, Sutherland 1995) represented by the equation:

$$EIA = a \cdot TIA^{b} \text{ [ha]} \tag{1}$$

The values of coefficients (a) and (b) depend on the catchment characteristic, interpreted as a part of impervious area that can be connected to the storm water sewer system. As the impervious area connected to the sewer system decreases, the values of coefficient (a) decrease and the values of coefficient (b) increase (Table 1).

Equation 1.1 concerns conditions for which the most of impervious area of the catchment is connected to a drainage system, a rainwater is not harvested and the roofs of single-family houses are connected to a storm water sewer system. Average conditions described by equation 1.2 are similar to the previously described - the difference is that the most of roofs of single-family houses are not directly connected to a drainage system. The catchment characteristics described by equations 1.3 and 1.4 represent the situation where only part of the catchment is connected to a drainage system and a rainwater is locally harvested. For equation 1.5 no specific conditions were given. The only information was that the values of coefficients (a) and (b) were determined for typical urban buildings (Alley & Veenhuis 1983).

Table 1. EIA values calculated by equation (1) for different coefficients a and b

Eq. number	a	b	EIA [ha]	RC [%]	Catchment characteristic (*)
1.1	0.4	1.2	28.85	18.4	highly connected
1.2	0.1	1.5	21.02	40.5	Average
1.3	0.04	1.7	17.15	51.5	somewhat disconnected
1.4	0.01	2.0	12.50	64.7	extremely disconnected
1.5	0.15	1.41	22.87	35.3	lack of data//information

(*) explanation in text

The change of an impervious area was expressed by a reduction coefficient RC (Table 1):

$$RC = \left(1 - \frac{EIA}{TIA}\right) \cdot 100 \ [\%] \tag{2}$$

The basic value RC = 40% which corresponds to the average characteristic of the catchment (equation 1.2) was assumed. Taking into account the characteristics of given catchment, this value was the most probable. Nevertheless, the possibility that the real value of EIA might be greater as described in equations 1.1 or 1.5 cannot be excluded. Due to the lack of information about local rainwater harvesting systems for analyzed catchment areas, the values of EIA calculated by equations 1.3 and 1.4 were rejected as not very probable.

3. Scope of analysis

3.1. Determining the EIA – variants

Two variants of the EIA mapping in a simulation model were considered. In variant A a decrease of imperviousness degree by a reduction coefficient RC (equation 2) was assumed. For each subcatchment the reduction in the impervious area causes an increase of the pervious area in order to remain the constant value of the total catchment area. In other words, the part of impervious area from which the runoff is not directed into the storm sewer system is converted into the pervious area in the model.

In variant B the SWMM option which allows to direct a part of runoff from the impervious area to the pervious area was used. The value for a part of the impervious area, from which the runoff was directed to the pervious area was considered similar to variant A – as a reduction coefficient RC. For the purpose of the analysis, an equal change in the impervious area for all subcatchments in both variants was assumed.

When the runoff occurs only from the impervious area, what can takes place for rainfalls with low intensity or in the case of very high infiltration capacity of pervious areas, both simulation variants generate the same runoff volumes. The impact of the EIA mapping method is significant during the runoff from pervious areas. In presented analysis this runoff was generated by a synthetic rainfall of high intensity and chosen parameters describing infiltration.

In the analysis four values of the reduction coefficient RC (equal to 10%, 20%, 30% and 40%) were taken into account. The values of assumed reduction coefficient RC corresponds to the values of the impervious area calculated according to the empirical formulas for the analyzed catchment (Table 1).

3.2. Rainfall

The Chicago hyetograph (Keifer & Chu 1957, Yao et al. 2016) with a peak intensity located at the centre was used to describe the variability of the rainfall intensity over time. In the analysis the synthetic rainfall with a frequency of occurrence c = 20 years was used. Rainfalls of such frequency of occurrence are considered to cause a significant runoff from pervious areas (Stall & Terstriep 1972). The duration of assumed rainfall T_D was equal to 60 min. The time that corresponds to the peak location (30 min) is longer than the longest flow time through the analyzed sewer system, which was calculated as equal to 27 min. Such rainfall should generate the largest instantaneous outflow in sewers (Mazurkiewicz & Skotnicki 2018), what is important while determining the flood volume V_F as a result of sewers overloading. The greatest outflow should also generate a maximum flood volume.

The rainfall depth was calculated with the use of Bogdanowicz and Stachy formula, which is the form of DDF curve for Polish conditions (Bogdanowicz & Stachý 1998). The value of rainfall depth for assumed rainfall was calculated as 39.7 mm.

3.3. Infiltration

The infiltration for pervious areas in the simulation model was computed according to the Horton equation (Rossman & Huber 2016). It was assumed that the soil in analyzed catchment had a good permeability. The values of initial infiltration rate F_{MAX} varied from 100 mm/h to 200 mm/h, while final infiltration rate F_{MIN} changed from 20 mm/h to 35 mm/h. The decay constant k for the Horton infiltration curve ranged from 2 h^{-1} to 8 h^{-1}.

Parameter	Values
F_{MAX} [mm/h]	100; 125; 150; 175; 200
F_{MIN} [mm/h]	20; 25; 30; 35
k [h^{-1}]	2; 4; 6; 8

Table 2. Assumed ranges of infiltration parameters for the Horton equation

In further analysis a cumulative effect of infiltration parameters on the volume of infiltrating rainwater was considered. The infiltration was expressed in a unit form with regard to the total pervious area of the catchment and described as UI [m^3/ha].

The UI values were calculated with the use of SWMM5 for assumed rainfall with total depth equal to 39.7 mm. In SWMM5 the infiltration process is connected with surface retention on the pervious area. For analyzed sets of the parameters of Horton equation and assumed rainfall (Table 2), the unit infiltration varied from 305 to 397 m^3/ha. The maximum value of calculated unit infiltration of 397 m^3/ha means that the entire rainfall infiltrated into the ground. Therefore, selected infiltration parameters of the Horton equation (Table 2) allowed to analyze the runoff from pervious areas from a threshold value equal to zero. It should be noted that the determined unit infiltration values do not represent the maximum soil infiltration capabilities. In case of an increase of a rainfall intensity, the volume of infiltrated rainwater may increase.

4. Results and discussion

The influence of mapping the EIA in simulation model on two basic characteristics – total runoff volume V and flood volume V_F was analyzed. The total runoff volume is the basic value that shows the impact of EIA mapping. The results represented by a runoff volume V are more universal as they depend only on the parameters of the catchment. The value of V is not influenced by the individual properties of the storm water sewer system, as it is calculated as the sum of the volume of runoff from individual subcatchments. The flood volume of V_F is influenced by the sewer parameters (e.g. diameters, slopes, lengths, roughness, etc.), therefore the results obtained for V_F are largely dependent on the specific storm water sewer system characteristics. However, according to the flood risk for storm water sewer system, the volume of V_F is of greater importance for maintenance these kinds of systems and, therefore, was also chosen with the runoff volume for the further analysis.

For all analyzed values of infiltration parameters (F_{MAX}, F_{MIN}, k) and reduction coefficient RC, the runoff volume V and the flood volume V_F were greater for variant B, which assumed the directing the runoff from the impervious area to the pervious one, than for variant A, which assumed the decrease of reduction coefficient RC (Fig. 2). It suggests that using the imperviousness degree as a parameter for EIA mapping can lead to underestimation of runoff simulation results.

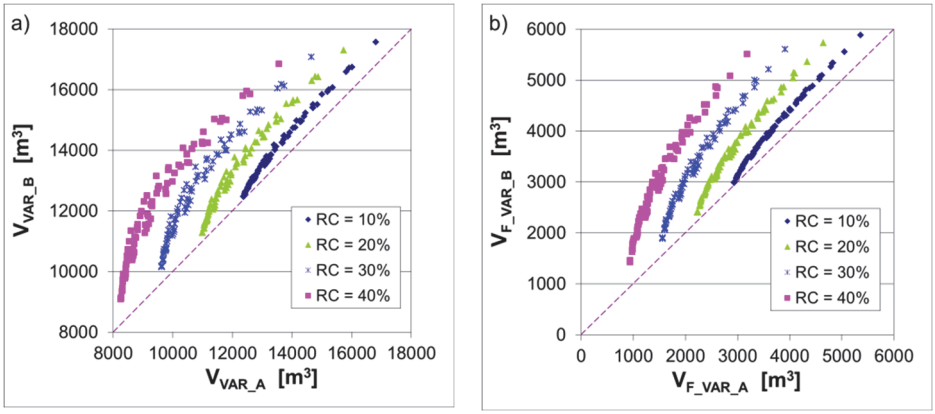

Fig. 2. The comparison of runoff volume V (a) and flood volume V_F (b) calculated for variants A and B

The volume increments ΔV and ΔV_F were used to compare the differences between variants A and B. These increments were calculated for each analyzed value of the reduction coefficient and were described by the equations:

$$\Delta V = V_{VAR\_B} - V_{VAR\_A} \ [m^3] \quad (3.1)$$

$$\Delta V_F = V_{F\_VAR\_B} - V_{F\_VAR\_A} \ [m^3] \quad (3.2)$$

where:

V_{VAR} – the runoff volume for variant A or B of EIA mapping [m^3]

V_{F_VAR} – the flood volume for variant A or B of EIA mapping [m^3]

Such defined volume increments ΔV and ΔV_F can be interpreted as a vertical difference in the location of the points regarding to the line with slope 45° presented in charts shown in Figure 2.

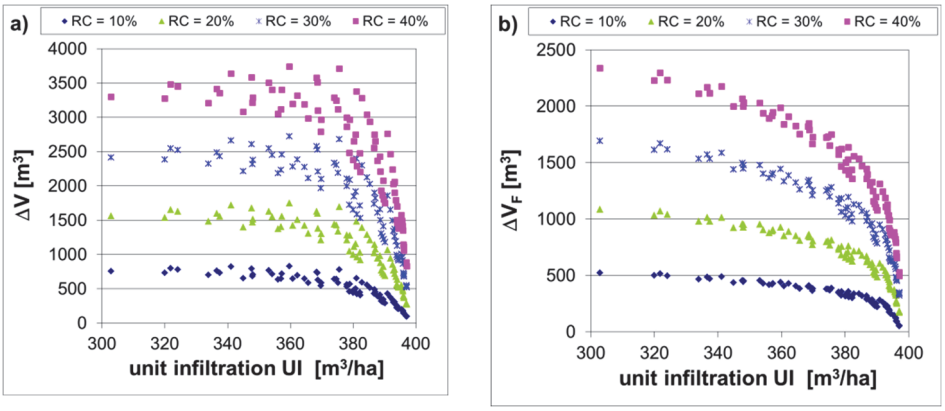

Fig. 3. The comparison of runoff volume increments ΔV (a) and flood volume increments ΔV_F (b) as a function of unit infiltration UI

The runoff volume increments ΔV had the lowest values for maximum values of a unit infiltration (Fig. 3a). With the decrease of unit infiltration, the runoff volume increments initially increased. The maximum value of ΔV was calculated for unit infiltration of approximately 360 m^3/ha. Further decrease of unit infiltration caused the decrease of the ΔV increments. This trend occurs for all analyzed values of reduction coefficient RC. With the increase of reduction coefficient RC, the range of variability in increments ΔV also increases.

For the flood volume increments the decrease of values ΔV_F with the increase of a unit infiltration was noticed (Fig. 3b). Similar to runoff volume increments ΔV, the range of ΔV_F variability was greater for higher values of

reduction coefficient RC. The relation between the variability of increments ΔV and ΔV_F and unit infiltration had met the expectations. The higher the infiltration values, the smaller the runoff from the pervious areas and thus the less impact of the EIA mapping in the model.

In order to find the average values of increments ΔV and ΔV_F, a probability distribution describing the variability of those increments was determined. The best fitting was achieved for the Beta distribution. For known probability distribution parameters the mean and standard deviation (Table 3) were specified.

Table 3. Mean values and standard deviations of increments ΔV i ΔV_F

Value	Reduction coefficient RC [%]			
	10	20	30	40
mean ΔV [m^3]	473	1073	1764	2521
std. deviation ΔV [m^3]	219	436	644	843
mean ΔV_F [m^3]	305	654	1033	1422
std. deviation ΔV_F [m^3]	126	243	359	484

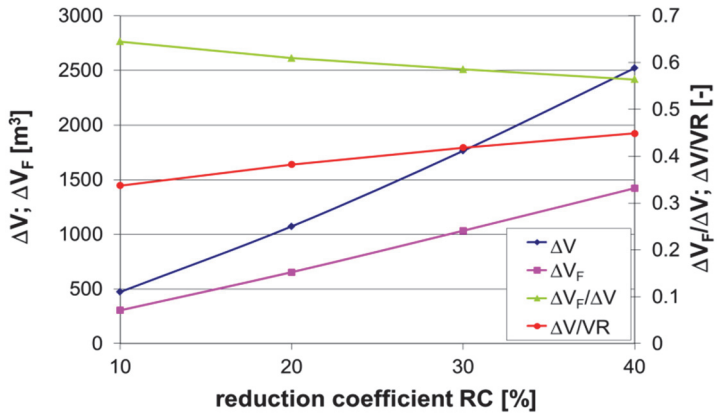

Fig. 4. Mean values of increments ΔV and ΔV_F and ratios $\Delta V/\Delta V_F$ and $\Delta V/VR$ as the function of reduction coefficient RC

Functions that describe the relations between mean values of increments ΔV and ΔV_F and reduction coefficient RC were close to linear (Fig. 4). The differences in the runoff volume or flood volume calculated for different EIA mapping variants increased directly proportional to the difference between EIA and TIA.

The mean values of increments ΔV were compared with the volume of runoff from the impervious area VR, which is directed to the pervious area in variant B. For the rainfall depth equal to 39.7 mm and TIA equal to 35.4 ha, the total volume of runoff from impervious area was approximately 14000 m^3. Therefore, each 10% of reduction coefficient corresponds to the volume approximately 1400 m^3 of runoff from impervious area that was directed to the pervious area. The runoff volume increments varied from 34% to 45% of this value (Fig. 4).

According to the European Requirements 752 in order to assess the operating conditions of the storm water sewer system, in particular with regard to flood risk, the relation between increments ΔV_F and ΔV was consider as important. With the increase of the reduction coefficient RC from 10% to 40%, the value of runoff increment ΔV that was converted into the flood volume ΔV_F decreased from 64% to 56% (Fig. 4). Therefore, the method of the EIA mapping can have significant impact on the flood risk assessment results.

5. Conclusions and summary

On basis of results of analysis presented in the publication, the following conclusions were formulated:

1. Directing a part of runoff from impervious area to pervious area instead of reduction in imperviousness degree results in greater calculated value of runoff volume and flood volume.
2. Increments of runoff volume and flood volume between two analyzed variants of EIA mapping decrease as infiltration increases.
3. The mean values of increments of runoff volume and flood volume increase almost linearly with the increase of reduction coefficient.
4. The value of increment of the runoff volume is approximately 40% of the volume of the runoff from impervious area that was directed to the pervious area.
5. The increment of the runoff volume is in approximately 60% converted into flood volume.

It should be made clear that at this stage of the analysis there are no grounds for generalization the relations presented in the paper. Obtained relations between the reduction of the impervious area and the increments of runoff volume ΔV can be expected to be similar for other catchments. For presented calculations only surface runoff was considered, so the results are not dependent on the storm water sewer system characteristic.

The relations between the increments of flood volume ΔV_F and the reduction of the impervious area or the increments of runoff volume ΔV may be characteristic only of the analyzed catchment. The flood volume is a function of

the sewers parameters that are individual of each urban catchment. In addition, the results may depend on assumed infiltration parameters and used method for calculating the infiltration in SWMM5.

The authors wish to thank the Miejskie Wodociągi i Kanalizacja company in Bydgoszcz for sharing their catchment models and measurement data.

This work was supported by the Poznan University of Technology under Grants (01/13/SBAD/0912 and 01/13/SBAD/0913).

No potential conflict of interest was reported by the authors.

References

Alley, W. M., Veenhuis, J. E. (1983). Effective impervious area in urban runoff modeling. *Journal of Hydraulic Engineering, 109*(2)*,* 313-319.

Barco, J., Wong, K. M., Stenstrom, M. K. (2008). Automatic Calibration of the U.S. EPA SWMM Model for a Large Urban Catchment. *Journal of Hydraulic Engineering, 134*(4)*,* 466-474, DOI: https://doi.org/10.1061/(ASCE)0733-9429(2008) 134:4(466).

Bermúdez, P. M., Ntegeka, V., Wolfs, V., Willems, P. (2018). Development and comparison of two fast surrogate models for urban pluvial flood simulations. *Water Resources Management, 32*(8), 2801-2815, DOI: https://doi.org/10.1007/s11269-018-1959-8

Bogdanowicz, E., Stachý, J. (1998). *Maksymalne opady deszczu w Polsce*. Warszawa: IMGW.

Ebrahimian, A., Wilson, B. N., Gulliver, J. S. (2016). Improved methods to estimate the effective impervious area in urban catchments using rainfall-runoff data. *Journal of Hydrology 536,* 109-118, DOI: https://doi.org/10.1016/j.jhydrol.2016.02.023

Ebrahimian, A., Gulliver, J.S., Wilson, B.N. (2018): Eestimating effective impervious area in urban watersheds using land cover, soil character and asymptotic curve number. *Hydrological Sciences Journal, 63*(4), 513-526.

EN 752:2017. *Drain and sewer systems outside buildings – Sewer systems management*. Warszawa: PKN

James, W. (2003). *Rules for responsible modeling*. Ontario: CHI.

Gulliver, J. S., Ebrahimian, A., Wilson, B. N. (2015). *Determination of Effective Impervious Area in Urban Watersheds.* Research Project, Final Report 2015-41, Minnesota Department of Transportation Research Services & Library.

Keifer, C. J., Chu, H. H. (1957). Synthetic rainfall pattern for drainage design. *ASCE Journal of the Hydraulics Division 83 (HY4)*, 1-25.

Krebs, G., Kokkonen, T., Valtanen, M., Setälä, H., Koivusalo, H. (2014). Spatial resolution considerations for urban hydrological modelling. *Journal of Hydrology, 512,* 482-497, DOI: https://doi.org/10.1016/j.jhydrol.2014.03.013

Lee, J. G., Heaney, J. P. (2003). Estimation of Urban Imperviousness and its Impacts on Storm Water Systems. *Journal of Water Resources Planning and Management, 129*(5)*,* 419-426, DOI: https://doi.org/10.1061/(ASCE)0733-9496(2003)129:5(419)

Mazurkiewicz, K., Skotnicki, M. (2018). A determination of the synthetic hyetograph parameters for flow capacity assessment concerning stormwater systems. *E3S Web of Conferences, 45, 00053* DOI: https://doi.org/10.1051/e3sconf/20184500053

Mostrales, D., Sanchez, K., Tudio, R., Malales, V., Ignacio, Ma. T. (2018). GIS-based Estimation of Catchment Basin Parameters and Maximum Discharge Calculation Using Rational Method of Luinab Catchment in Iligan City. *Philippine Journal of Science, 147*(2)*,* 327-342.

Niazi, M., Nietch, C., Maghrebi, M., Jackson, N., Bennett, B. R., Tryby, M., Massoudieh, A. (2017). Storm Water Management Model: Performance Review and Gap Analysis. *Journal of Sustainable Water in the Built Environment, 3*(2), DOI: https://doi.org/10.1061/JSWBAY.0000817

Nowogoński, I. (2018). *Epa SWMM 5.1. Wykorzystanie i rozbudowa modelu sieci Kanalizacyjnej. 2018-04-25*. www.iis.uz.zgora.pl/files/SWMM-instr.pdf

Nowogoński, I. (2020). Low impact development modeling to manage urbanstormwater runoff: case study of Gorzów Wielkopolski. *Journal of Environmental Engineering and Landscape Management, 28*(3), 105-115, DOI: https://doi.org/10.3846/jeelm.2020.12670

Pina, R. D., Ochoa-Rodriguez, S., Simões, N. E., Mijic, A., Marques, A., Maksimović, Č. (2016). Semi- vs. Fully-Distributed Urban Stormwater Models: Model Set Up and Comparison with Two Real Case Studies. *Water, 8*, 58, DOI: https://doi.org/10.3390/w8020058

Rossman, L. A. (2015). *Storm Water Management Model User's Manual Version 5.1*. www.epa.gov/water-research/storm-water-management-model-swmm

Rossman, L. A., Huber, W. C. (2016). *Storm Water Management Model Reference Manual Volume I – Hydrology (Revised).* U.S. Environmental Protection Agency https://www.epa.gov/water-research/storm-water-management-model-swmm

Sahoo, S. N., Sreeja, P. (2013). Role of rainfall events and imperviousness parameters on urban runoff modelling, *ISH Journal of Hydraulic Engineering, 19*(3), 329-334, DOI: https://doi.org/10.1080/09715010.2013.819706

Seo, Y., Choi, N.-J., Schmidt, A. R. (2013). Contribution of directly connected and isolated impervious areas to urban drainage network hydrographs. *Hydrology and Earth System Sciences, 17,* 3473-3483, DOI: https://doi.org/10.5194/hess-17-3473-2013

Son, A.L., Kim, B, Han, K. -Y. (2016). A Simple and Robust Method for Simultaneous Consideration of Overland and Underground Space in Urban Flood Modeling. *Water, 8,* 494, DOI: https://doi.org/10.3390/w8110494

Stall, J. B., Terstriep, M. L. (1972). *Storm sewer design – an evaluation of the RRL method*. Office of Research and Monitoring US EPA, Washington

Sutherland, R. C. (1995). Methods for estimating the effective impervious area of urban watersheds. *Watershed Protection Techniques, 2*(1)*.*

UDG (2017). *Code of Practice for the Hydraulic Modelling of Urban Drainage Systems* Version 01. CIWEM. www.ciwem.org/assets/pdf/

Yao, L., Wei, W., Chen, L. (2016). How does imperviousness impact the urban rainfall – runoff process under various storm cases? *Ecological Indicators, 60,* 893-905, DOI: https://doi.org/10.1016/j.ecolind.2015.08.041

Zawilski, M. (2010). Integracja zlewni zurbanizowanej w symulacji spływu ścieków opadowych. *Gaz, Woda i Technika Sanitarna, 6.*

Zawilski, M., Dziedziela, B. (2018). Stormwater quality modeling in urbanized areas. *E3S Web of Conferences, 45, 00104*, DOI: https://doi.org/10.1051/e3sconf/20184500104

Zhuk, V., Vovk, L., Matlai, I., Popadiuk, I., Mysak, I., Fasuliak, V. (2020). Dependency Between the Total and Effective Imperviousness for Residential Quarters of the Lviv City. *Journal of Ecological Engineering*, *21*(5), 56-62, DOI: https://doi.org/10.12911/22998993/122191

Abstract

The publication presents the results of an analysis concerning the impact of the method of an effective impervious area (EIA) mapping in the simulation model on the runoff from urban catchment. The runoff volumes and flood volumes generated by heavy rainfall, causing the runoff from pervious area, were compared. Two EIA mapping variants were taken into account – first one, concerning reduction in imperviousness degree and, second one, directing the runoff from impervious to pervious area. The runoff calculations were made on basis of simulation results in SWMM5. For building the catchment model data of existing catchment with the area of nearly 80 hectares in Bydgoszcz was used. The value of the EIA was estimated on the basis of empirical formulas. The reduction in impervious area connected directly to the storm water sewer system from 40% to 10% of the total impervious area were considered. It has been shown that using the reduction in imperviousness degree for EIA mapping can lead to underestimation of runoff volume. The difference in runoff calculated for analyzed EIA mapping variants increases with the decrease in infiltration capacity of pervious area and is in large part transformed into a flood volume.

Keywords:
effective impervious area, hydrodynamic modeling, SWMM5, urban catchment

Odwzorowanie efektywnej powierzchni szczelnej w modelowaniu odpływu ze zlewni miejskiej

Streszczenie

W publikacji przedstawiono wyniki analizy wpływu sposobu wprowadzenia danych o efektywnej powierzchni szczelnej (EIA) do modelu symulacyjnego zlewni miejskiej na odpływ. Porównywano objętości odpływu oraz objętości wypływu na powierzchnię terenu generowane przez opad o znacznym natężeniu, skutkujący formowaniem spływu z powierzchni przepuszczalnych. Uwzględniono dwa warianty odwzorowania EIA – redukcję stopnia uszczelnienia i skierowanie spływu z powierzchni szczelnej na przepuszczalną.

Obliczenia odpływu wykonano przy użyciu modelu symulacyjnego wykonanego w programie SWMM5. Wykorzystano dane rzeczywistej zlewni miejskiej o powierzchni blisko 80 ha znajdującej się w Bydgoszczy. Wielkość EIA oszacowano na podstawie formuł empirycznych. Rozpatrywano zmniejszenie powierzchni szczelnej podłączonej bezpośrednio do systemu kanalizacyjnego w zakresie od 10% do 40% łącznej powierzchni szczelnej (TIA). Wykazano, że wykorzystanie do odwzorowania EIA redukcji stopnia uszczelnienia może powadzić do zaniżenia objętości obliczonego odpływu. Różnica odpływu obliczonego dla analizowanych wariantów odwzorowania EIA rośnie wraz ze spadkiem zdolności infiltracyjnych powierzchni przepuszczalnych i w znacznej części jest transformowana w wypływ na powierzchnię terenu.

Słowa kluczowe:
efektywna powierzchnia szczelna, modelowanie hydrodynamiczne, SWMM5, zlewnia miejska

MIDDLE POMERANIAN SCIENTIFIC SOCIETY OF THE ENVIRONMENT PROTECTION

Rocznik Ochrona Środowiska

Volume 22. Year 2020 ISSN 1506-218X 431-443

Use of Quantitative and Qualitative Wastewater Monitoring in Water Protection on the Example of Lodz

Agnieszka Brzezińska[*], *Grażyna Sakson*

Lodz University of Technology, Poland

[*]*corresponding author's e-mail: agnieszka.brzezinska@p.lodz.pl*

1. Introduction

In recent decades surface water protection has become particularly essential among others due to the decreasing world drinking water resources and simultaneously the growing population and its requirements for water quality. Water protection largely depends on the functioning of sewage systems, which should not only ensure the safe functioning of the city, but also determine the ecological safety of the receiver. Urban development, and therefore an increase of urbanized areas in the total catchment area, additionally highlights the impact of sewerage systems on water reservoirs. In the last two decades, both methods and devices used for monitoring wastewater systems have significantly progressed (Lvovaa et al. 2016, Di Lecce et al. 2017). It should be noted, however, that the functioning of sewage systems carried out wastewater from urban areas is associated with the occurrence and character of rainfall, which should therefore also be constantly monitored (Langeveld et al. 2013, Zawilski & Brzezińska 2014). In addition to changes in the character of precipitation as a consequence of climate variations, changes in air temperature are also observed. This affects in some way the temperature of rainwater directed to the sewage system and the temperature in the wastewater receivers. This may alter, among other things, the morphology of the receiver as well as the kinetics of the chemical reactions taking place in it.

Pollutants introduced by wastewater sewer systems largely affect the chemical and ecological state of reservoirs (Casadio et al. 2010, Caissie et al. 2014). Monitoring of sewer systems should therefore be carried out in terms of both the quantity and composition of transported sewage (Brzezińska et al. 2016). This is particularly important for the assessment of pollution load in surface waters pollution load coming from the sewage system, including the effect of cobined sewer overflows activation (Phillips et al. 2012, Bi et al. 2015), and

wastewater treatment plant (WWTP). Only comprehensive knowledge of pollutant emissions allows to fully control and effectively counteract the pollution of water receivers and promotes the proper functioning of the sewage system, even in conditions of variable flows caused by precipitation events.

The aim of this article is to present the needs and benefits of different forms of monitoring in order to widely understood protection of surface waters on the example of Lodz.

2. Analysis of needs, tasks and benefits resulting from the application of quantitative and qualitative monitoring

Urban development and the increasing incidence of extreme rainfall events leads to sewage systems, including WWTPs, being increasingly overloaded, which reduces their operational safety. The condition of optimal use of their technical capabilities and determining the necessary scope of modernization and expansion is knowledge of the hydraulic conditions of the network operation and the composition of flowing wastewater. The database required for this is facilitated by on-line devices. Until recently, on-line monitoring was most often carried out mainly in WWTPs to control treatment processes and its use in sewage disposal systems was sporadic and rarely de-scribe (Torres & Bertrand-Krajewski 2008).

Currently, on-line monitoring can be carried out using, among other things:

- rain gauges that allow determining rainfall characteristics,
- filling sensors and flow meters in channels,
- on-line sensors measuring one or several indicators of wastewater pollution simultaneously (multi-parameter sensors).

For effective control of the impact of wastewater sewer systems on receiver waters, it is important to define criteria for the selection of monitoring points (Thompson et al. 2011). Depending on the applied solutions a lot of information can be obtain, among others, for:

- recognition of the dynamics of flow variabilities in the sewers,
- composition of wastewater flowing through the sewage network both in dry and wet weather,
- monitoring of wastewater inflow to the treatment plant,
- calibration of computer programs used for network modeling,
- analysis of the "first flush" phenomenon of pollution in the sewage system,
- assessment of the functioning of sewage systems in the hydraulic aspect, as well as pollutant emission,
- Real Time Control system implementation (RTC) in sewer networks (Campisano et al. 2013).

In accordance with PN-EN 752: 2017 "External sewage systems", when conducting research and analyses relating to the functioning of sewage systems and determining the needs for their modernization, should be used simulation models that require accurate data from measurement campaigns. The use of on-line sensors measuring the concentrations of selected wastewater pollution indicators, especially in the case of combined sewer system (CSS), allows for a significant cost reduction of sampling, their transport and laboratory tests.

The use of quantitative and qualitative monitoring of wastewater sewer systems is extremely important for the functioning of WWTPs. Variations of quantity and composition of inflowing wastewater, sewer system modernization and changes within the catchment area may reflected in the inflow characteristic to the WWTP and influence on hydraulic and pollution load.

3. Methods and tools used in Lodz

3.1. Characteristics of Lodz wastewater sewer system and the scope of its monitoring

Lodz is equipped with mixed sewer system. A CSS (43 km^2) exist in the central districts and a separated system in the rest of the city. There are 18 combined sewer overflows (CSOs), which discharge excess raw wastewater directly to Lodz rivers during heavy rainfall. The main receiver of all wastewater from the city, both the treated wastewater from the Lodz treatment plant and the raw wastewater coming from heavy rainfall, which is directed to the receiver from CSOs is the Ner River. Currently, all overflows are equipped with flow meters, which allow to monitor the functioning of these facilities, determine the frequency of their activity and the volume of discharged wastewater (Fig. 1a).

In addition the measurements mentioned above carried out by the network operator, the monitoring of the sewer system in Lodz is also carried out by the Institute of Environmental Engineering and Building Installations at the Lodz University of Technology at two research stations:

- the station on the J1 overflow equipped with a flow meter and on-line sensors (Solitax and UVvis) for measuring the wastewater composition and a sampler for the automatic collection of wastewater samples,
- a station at the outlet from the stormwater drainage system of the "Liściasta" district with a rainwater settler, equipped at its inlet with a sampler for collecting wastewater, a wastewater fill sensor and flow velocity sensor in the sewer and at its outlet equipped with a sampler and a wastewater fill sensor in the settler.

a) b)

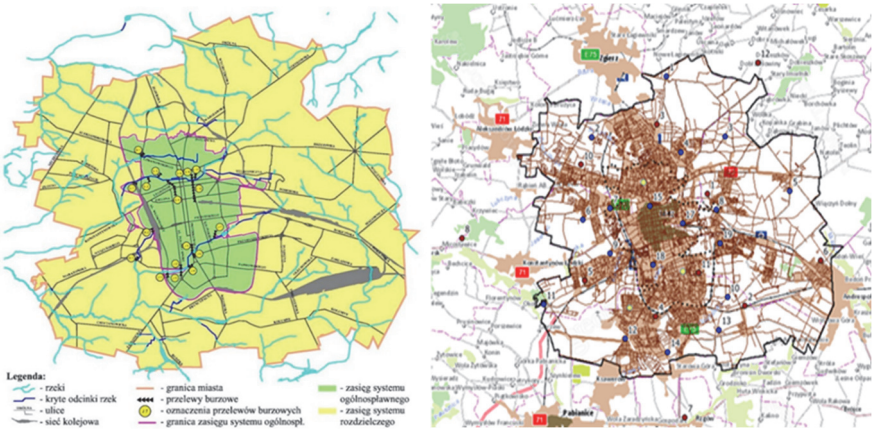

Fig. 1a. Location of combined sewer overflows in Lodz (Wierzbicki et al. 2010)
Fig. 1b. Location of rain gauges in Lodz (blue – Lodz Infrastructure Company rain gauges, red – University of Lodz, yellow – Lodz University of Technology)

3.2. Rainfall monitoring and its use

Lodz has an urban rain gauges network (18 devices) belonging to the Lodz Infrastructure Company. Additionally, three rain gauges belonging to the Lodz University of Technology and 12 rain gauges owned by the University of Lodz are located in the city (Fig. 1b). This type of data allows not only to determine the character of precipitation, but also to indicate the direction of precipitation and its spatial unevenness, which has a significant impact on the functioning of the sewage system. Much more favourable for the operation of the sewer system is opposite direction of rainfall movement in relation to the direction of wastewater flow (Zawilski & Brzezińska 2014). According to observations, during the year the air masses come to Lodz from the west (20% of observations), south-west (15%) and from the east (14%) (Kożuchowski 2011), which in some way helps in removal of excess stormwater from the city area.

Currently, cities increasingly need to have digital models of sewer networks. Thanks to them it is possible to assess their functioning, as well as determine the needs for modernization and design guidelines. According to the current requirements contained in the Regulation of the Minister of Maritime Economy and Inland Navigation of 12 July 2019 on substances particularly harmful to the aquatic environment and the conditions to be met when discharging sewage into waters or ground, as well as when discharging rainwater or meltwater into waters or into water devices to assess the functioning of sewer systems in the case of lack of data from observation of their functioning over longer period of time, it is

recommended to use verified computer models. However, for these models to be useful and generate reliable results, it is required to correctly map the net-work and have accurate input data, including precipitation data, needed to calibrate the combined sewage and rainwater drainage network. Currently, many Polish cities do not yet have a pluviometric network, and have only, for example, one rain gauge (or only a few) for the entire city. In this case, it is difficult to determine the spatio-temporal characteristics of precipitation, which is especially important for large catchments area. That model calibration based only on one rain gauge usually causes over-statement of results (Zawilski 2012). Examples of the results of simulation flow rate in the sewage system in comparison with the actual rainfall data (spatial precipitation, point precipitation) conducted in the use of the US EPA SWMM program at the outlet from the Bałutka catchment (609 ha) are shown in Figure 2. Results of the simulation of flow in the combined network for this catchment showed a better fit in the case of spatial precipitation, which confirms the usefulness of using extensive rainfall monitoring in the city.

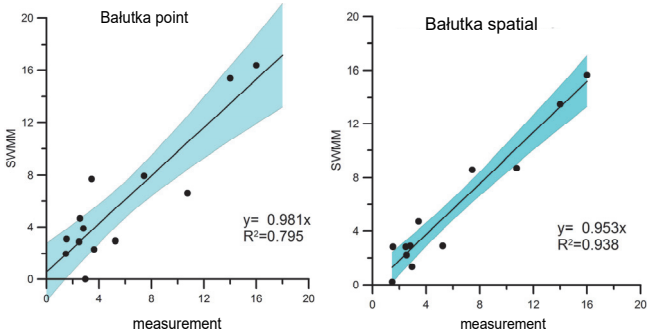

Fig. 2. Comparison of modeling results with real data of wastewater flow at the outlet of the Bałutka catchment area (flow stream in [m^3/s]) (Zawilski 2012)

3.3. Network flow monitoring

In most major cities in Poland, CSSs with overflows function in the central districts. Operation of these systems creates many problems, especially during the rainfall due to hydraulic over-load of sewers and with the pollution load discharged to the receiver. The flow meters located in the area of CSOs in Lodz, allow to determine both the frequency of their activity and the volume of discharged wastewater, which is particularly important in the case of surface water protection. According to RME, the number of activations of these facilities should not exceed 10 per year. Therefore, quantitative monitoring allows to determine the correct operation of overflows or, if necessary, to indicate exceedances in their functioning (Fig. 3).

Based on the measured data, the frequency of CSOs can be analysed at various time intervals. In Lodz, most CSOs usually operate in the summer months, and the volume of dis-charged wastewater is greatly varied. In example the B1 overflow in both June and July, works on average around 3.5 times, but the volume of wastewater emitted to the receiver is several times higher in June. Without quantitative monitoring, obtaining such information would be very difficult.

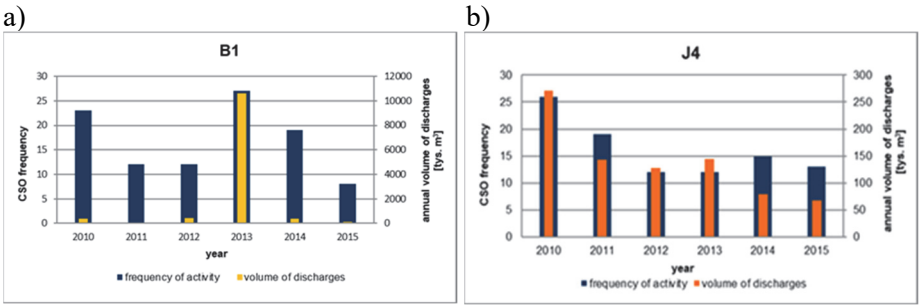

Fig. 3. Annual average frequency and volume of wastewater discharged by combined sewer overflow in the years 2010-2015, a) B1, b) J4 (Brzezińska 2019)

With this type of data, it is possible to determine the parameters relevant to the functioning of the network: flow variability (Fig. 4), hourly and daily unevenness coefficients, etc. The use of this data together with precipitation data in modeling systems enables their calibration. This allows, among others, to identify overloads and establish the required storage capacity of the system and the possible channel retention capacity.

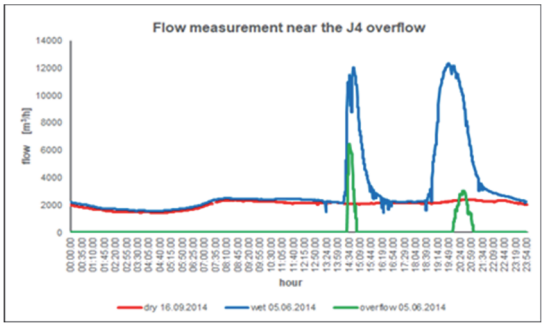

Fig. 4. Dynamics of flow variabilities during the day with dry and wet weather and an example of PB J4 functioning

3.4. Qualitative monitoring of wastewater in the sewage system

During measurements of the first tested indicator a method of measuring UV absorption with a wavelength of 254 nm (according to DIN 38402 C2) is used, while the measurement of the second one is carried out in a combination of the absorption process and infrared rays dispersion (according to DIN 27027). The probes are calibrated using the results of laboratory tests on the composition of the wastewater collected with the sampler installed on the bench. The data obtained from the monitoring also allow for the analysis of the concentrations of the measured indicators in dry and wet weather, as well as their changes depending on the day of the week, month, season, etc.

Data from quantitative and qualitative monitoring allow to assess pollution loads transported through the network and their variability during rainfall events (e.g. occurrence of the "first flush" of pollution). For example, the J1 transfer on 27-28.04.2013 caused the discharge of 2598 m^3 of untreated wastewater transporting 992 kg of total suspended solids and 658 kg of organic substances expressed as COD. Data analysis obtained from qualitative monitoring confirmed the occurrence of the first flush phenomenon (Fig. 5), whose capture to the retention tank and subsequent referral to the WWTP would significantly protect the receiver against the pollution inflow.

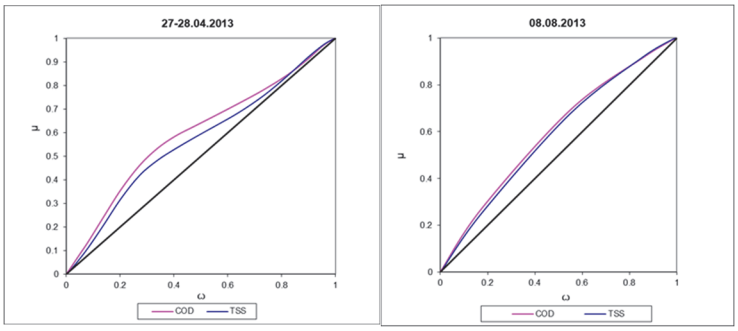

Fig. 5. An example of the occurrence of the first flush pollution phenomenon on the J1 overflow

The inflow of a large amount of pollutants in very short time, even if there are no toxic substances among them, can cause significant difficulties in the treatment process. Changes in the quality and quantity of sewage flowing into WWTP are not repeatable, they depend primarily on rainfall characteristic and the length of the dry weather period before precipitation, which determines the amount of pollution built-up on the catchment and wash-off during rainfall. Even

on the same catchment, in the case of different precipitation, the first flush phenomenon may not be observed, it may be pronounced or the so-called the last wave phenomenon may occur, moreover, the flow of pollutants may be different for basic quality parameters of sewage (Fig. 5).

3.5. The use of monitoring data for pollutant load prediction

Continuous monitoring of CSOs and storm water drainage outlets is costly, labour-intensive and sometimes complicated for technical reasons. That is why simpler, less expensive, but equally accurate methods for estimating the quantity and composition of wastewater emitted to the receiver are increasingly being sought (Hannouche et al. 2017, Montserrat et al. 2017). For this aim mathematical models are used, which allow to know and predict pollutant emissions and simultaneously limit the range of measurement campaigns. Based on the monitoring data, among others models for pollutant emissions from combined overflows and storm water drainage were developed for the Lodz catchment area. The predictive model of pollutant emissions from CSOs was based on three variables: height and maximum rainfall intensity and volume of wastewater discharged from CSO. These parameters were selected after a series of analyses using the Principal Component Analysis method (PCA) and multiple regression. On their basis, a mathematical formula to forecast the load of emitted pollutants for total suspended solids (TSS) and COD was developed (Brzezinska et.al. 2018). In addition to the parameters included in the model, other parameters such as the rainfall duration, its average intensity and the time of dry weather before precipitation were taken into account for the analysis. The results of the conducted analyses indicated that the above-mentioned parameters turned out to be less important. Pearson correlations between rainfall parameters and concentration as well as the load of TSS and COD were also made. The results showed practically no relationship between the concentration of the studied indicators and rainfall parameters, while strongly marked the dependence of the load on the height and maximum intensity of precipitation as well as volume of discharge, which was confirmed by the formula of the model.

$$L_{TSS} = 1.8 \cdot R_{depth}^{-0.37} \cdot i_{max}^{0.21} \cdot V_{CSO}^{0.97} \quad (1)$$

$$L_{COD} = 1.6 \cdot H_{op}^{-0.3} \cdot i_{max}^{0.22} \cdot V_{CSO}^{0.95} \quad (2)$$

where:
R_{depth} – rainfall height [mm],
i_{max} – maximum rainfall intensity [mm/h],
V_{CSO} – volume of discharged wastewater [m^3].

According to the developed model, the prediction of pollutant load emitted by a CSO depends mainly on the volume of wastewater in power close to 1. It should be remembered that for a single CSO event, the volume of wastewater has a various importance relative to the load of emitted pollutants. This is due to the fact that precipitation parameters and the "first flush" phenome-non significantly influance the concentration of pollutants in surface runoff and CSO. The proposed model provides reliable results on pollutant emissions ($R^2 = 0.79$ for TSS, and for COD $R^2 = 0.80$) in the case of the catchment area belong to J1 CSO for which it was developed (Fig. 6).

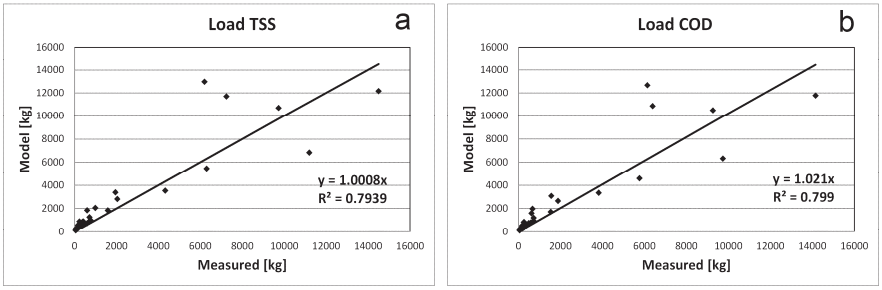

Fig. 6. Relationships between the measured values and model for J1 CSO: a) for TSS, b) for COD (Brzezinska at al. 2018)

For other catchments, this model can be used after adjusting the proporcional coefficient, which depends, among others, on the catchment characteristics, the way it is managed, sources of pollution, and the characteristics of the wastewater system and the overflow itself.

4. Advantages and disadvantages

On-line quantitative and qualitative monitoring used in sewage systems allows, among others, for:

- limitation of measurement campaigns,
- limitation of costs of wastewater laboratory tests,
- creating a large measurement database for analyzing of the functioning network,
- capturing all occurring variabilities of amount and composition of wastewater in both dry and wet weather.

These advantages are particularly important in the case of storm water drainage and CSS due to the unpredictability of precipitation phenomena and high dynamics of changes in the composition of wastewater and rainwater in these systems. The large advantage of using measurements directly in the medium

is the high quality of the obtained data and the possibility of their transmission directly to e.g. a dispatcher, which allows making quick decisions regarding the operation of the system. It should be added that the simultaneous possession of rainfall monitoring gives the possibility of earlier network preparation and sewage treatment plant for sudden rainwater inflows. Despite the many benefits resulting form the use a such monitoring, some disadvantages should also be noted. Belong to them:

- still relatively high price, despite the dynamic development of measuring methods and technical solutions,
- sensors susceptibility to dirt, clogging and mechanical damage,
- lack of power supply or other factors preventing the measurement or causing erroneous data (e.g. indication of the instantaneous concentration value exceeding the repeatedly measured average minute concentration persistent for a very short time of the order of a minute or 2 minutes, most likely due to hanging up around the sensor of large things like rag, foil, etc),
- the need for periodic calibration for some types of equipment,
- in case of on-line sensors for measuring the pollution concentration indicators, limited range of indicators measured and the need to select it,
- location difficulties (e.g. lack of technical possibilities for mounting the sensor due to hydraulic conditions, no possibility of power supply, operational difficulties, difficulties with data transmission),
- difficulties associated with these installation (sewer condition, hydraulic conditions,sewer deposits),
- the need for periodic inspections and repairs.

Despite the possible operational problems and significant purchase costs, monitoring is already becoming the basis for suitable network management, especially in unforeseen situations, e.g. during heavy rainfalls. The benefits of having quantitative-qualitative monitoring (or even quantitative in the initial phase of its creation) are definitely higher than the potential disadvantages.

5. Conclusions

The examples of the on-line monitoring application included in the article have shown its great usefulness in determining rainfall characteristics, assessing of the wastewater sewer system functioning, and pollutant emissions directed to the receiver. Presented in this article the possibility of forecasting pollutant load (TSS and COD) directed to the surface waters e.g. form CSO's based on the data of rainfall and volume discharges can be a useful tool in the selection of effective methods of reducing emissions of pollutants getting into surface waters. On-line

measurements allow to build a wide base for these purposes. The city's monitoring gives the possibility to observate changes taking place in the sewer system in real time and to reduce the costs associated with the wastewater analysis process. Despite the presented operational problems, having quantitative and qualitative monitoring is cost-effective and increasingly necessary due to the protection of surface waters. Sustainable development of city drainage systems will require the use of various forms of monitoring, interrelated to one another (rainfalls, flows in the network as well as to wastewater composition).

References

Bi E.G., Monette F., Gachon P., Gaspéri J., Perrodin Y. (2015). Quantitative and qualitative assessment of the impact of climate change on a combined sewer overflow and its receiving water body, *Environmental Science and Pollution Research, 22,* 11905-11921.

Brzezińska, A., Sakson, G., Zawilski, M. (2016). Assessment of pollutant load emission from combined sewer overflows based on the online monitoring, *Environmental Monitoring and Assessment, 188(9)*, 502.

Brzezińska, A., Sakson, G., Zawilski, M. (2018). Predictive model of pollutant loads discharged by combined sewer overflows, *Water Science and Technology, 77*(7-8), 1819-1828.

Brzezińska, A. (2019). *Emission of pollutants from combined sewer ovelflows*. Monographs of the Lodz University of Technology, No. 2279.

Casadio, A., Maglionico, M., Bolognesi, A., Artina, S. (2010). Toxicity and pollutant impact analysis in an urban river due to combined sewer overflows loads, *Water Science and Technology, 61*(1), 207-221.

Campisano, A., Cabot, J., Muschalla, D., Pleau, M., Vanrolleghem, P.A. (2013). Potential and limitations of modern equipment for real time control of urban wastewater system, *Urban Water Journal, 10*, 300-331.

Caissie, D., Kurylyk, B.L., St-Hilaire, A., El-Jabi, N., MacQuarrie, K.T. (2014). Streambed temperature dynamics and corresponding heat fluxes in small streams experiencing seasonal, ice cover, *Journal of Hydrology, 519,* 1441-1452.

Di Lecce, V., Petruzzelli, D., Guaragnella, C., Cardellicchio A., Dentamaro, G., Quarto, A., Soldo, D., Dario, R. (2017). Real-time monitoring system for urban wastewater, July 2017, *Conference: 2017 IEEE Workshop on Environmental, Energy, and Structural Monitoring Systems (EESMS).*

Hannouche, A., Joannis, C. & Chebbo, G. (2017). Assessment of total suspended solids (TSS) event load and its uncertainties in combined sewer system from continuous turbidity measurements. *Urban Water Journal, 17*(8), 789-796.

Keupers, I., Willems, P. (2013). Impact of urban WWTP and CSO fluxes on river peak flow extremes under current and future climate conditions, *Water Science and Technology, 67*(12), 2670-2676.

Kożuchowski, K. (2011). *Polish climate: a new look*. PWN Scientific Publisher, Warsaw, 1-292.

Langeveld, J.G., Schilperoort, R.P.S., Weijers, S.R. (2013). Climate change and urban wastewater infrastructure: there is more to explore, *Journal of Hydrolology, 476,* 112-119.

Lvovaa, L., Guanais, Gonçalvesa, C., Petropoulosa, K., Michelia, L., Volpea, G., Kirsanovb, D., Leginb, A., Viaggiud, E., Congestrid, R., Guzzellae, L., Pozzonie, F., Palleschia, G., Di Nataleb, C., Paolesse, R. (2016). Electronic tongue for microcystin screening in waters, *Biosensors and Bioelectronics, 80,* 154-160.

Montserrat, A., Hofer, T., Poch, M., Muschalla, D., Corominas, L. (2017). Using the duration of combined sewer overflow events for the calibration of sewer hydrodynamic models. *Urban Water Journal, 14*(8), 782-788.

Phillips, P.J., Chalmers, A.T., Gray, J.L., Kolpin, D.W., Foreman, W.T., Wall, G.R. (2012). Combined sewer overflows: an environmental source of hormones and wastewater micropollutants, *Environmental Science and Technology, 46*(10), 5336-5343.

Regulation of the Minister of the Environment of November 18, 2014 on the conditions which must be met during discharging wastewater into water or into the ground,, and on substances that are particularly harmful to the aquatic environment.

Thompson, K.E., Vamvakeridou-Lyroudia, L., Kapelan, Z., Savic, D. (2011). Optimal macrolocation methods for sensor placement in urban water systems," Exeter, UK.

Torres, A. & Bertrand-Krajewski, J.L. (2008). Partial Least Squares local calibration of a UV–visible spectrometer used for in situ measurements of COD and TSS concentrations in urban drainage systems, *Water Science and Technology, 57*(4), 581-588.

Wierzbicki, P., Waack-Zając, A., Koska, T. (2010). Hydrographic system of the city of Lodz, Scientific Notebooks of the Lodz University of Technology, *Civil Engineering, 1066*(61), 1-13.

Zawilski, M., Brzezińska, A. (2014). Areal rainfall intensity distribution over an urban area and its effect on a combined sewerage system, *Urban Water Journal, 11*(7), 532-542.

Zawilski, M. (2012). Analysis of the hydraulic load of the sewage system on a large urban catchment scale, Scientific Papers of Rzeszów University of Technology, *Civil and Environmental Engineering, 59*(2) / I, 237-247.

Abstract

Widely understood protection of water, and in particular surface waters, most exposed to direct pollution, requires many operations carried out both in the catchment area and in sewage systems as well as WWTPs. Due to its character and working conditions, it should be monitored not only in terms of hydraulics, but also in terms of the quality of transported wastewater. During atmospheric precipitation, large volumes of domestic and industrial wastewater as well as rainwater in various proportions flow through the canals, changing not only their quantity but also their composition. In such cases, the issue of monitoring becomes particularly vital. The article presents an analysis of the needs and tasks resulting from the application of quantitative and qualitative monitoring in the assessment of the functioning of sewage systems. Methods and tools used in Lodz that may be useful in water protection are presented. The benefits of using this type of solutions as well as the limitations and difficulties are discussed.

Keywords:
sewer system, wastewater monitoring, rainfall monitoring, predictive model

Stosowanie ilościowego i jakościowego monitorowania ścieków w ochronie wód na przykładzie Łodzi

Streszczenie

Szeroko rozumiana ochrona wód, a zwłaszcza wód powierzchniowych, najbardziej narażonych na bezpośrednie zanieczyszczenie, wymaga wielu działań przeprowadzanych zarówno w zlewni, jak i w systemach kanalizacyjnych oraz w oczyszczalniach ścieków. Ze względu na swój charakter i warunki pracy system kanalizacji należy monitorować nie tylko pod względem hydraulicznym, ale także pod względem składu transportowanych ścieków. Podczas opadów atmosferycznych przez kanały, w różnych proporcjach, przepływają znaczne ilości ścieków bytowych, przemysłowych oraz deszczowych, zmieniając przy tym także swój skład. W takich przypadkach kwestia monitorowania staje się szczególnie istotna. W artykule przedstawiono analizę potrzeb i zadań wynikających z zastosowania monitorowania ilościowego i jakościowego w ocenie funkcjonowania systemów kanalizacyjnych oraz metody i narzędzia stosowane w Łodzi, które mogą być przydatne w ochronie wód. Omówiono zalety korzystania z tego typu rozwiązań, a także ograniczenia i trudności.

Słowa klucze:
system kanalizacyjny, monitoring ścieków, monitoring opadów, model predykcyjny

MIDDLE POMERANIAN SCIENTIFIC SOCIETY OF THE ENVIRONMENT PROTECTION

Rocznik Ochrona Środowiska

Volume 22. Year 2020 ISSN 1506-218X 444-455

Reducing the Use of Electrochemical Sources of Electricity Through the Use of Wireless Power Supply

Jarosław Jajczyk[1], Michał Filipiak[1], Tomasz Dąbrowski[2]*

[1]Poznan University of Technology, Poland

[2]Koszalin University of Technology, Poland

[*]corresponding author's e-mail: jaroslaw.jajczyk@put.poznan.pl

1. Introduction

Ongoing technical developments are causing a continuous increase in the demand for more and more electrical devices. Because of the comfort of use, great emphasis is placed on the mobility of these devices. This has resulted in many electrical devices being equipped with energy storages (batteries or accumulators). Because of the elements used for their production, batteries and accumulators become hazardous to human health and natural environment at the end of their lives. Their proper management is necessary. A reduction in the negative impact of waste batteries and accumulators is obtained through recycling, which is enforced by law (Korkozowicz 2009, 2010). At this stage, we can follow the process of recycling end-of-life vehicles, which was presented in detail in the works of Chamier-Gliszczyński (Chamier-Gliszczyński 2010, 2011a, 2011b). Recycling, however, entails costs and is not neutral to the environment. Among other things, it requires energy, which results in the additional emission of CO_2 into the atmosphere. On top of this, it is still impossible to recycle 100% of the batteries and accumulators that are introduced into the market.

One optional solution may be to resign from electrochemical energy sources presented in the works Kasprzyk (2019), Tomczewski et al. (2019) and Burzyński et al. (2019) by using a different type of energy storage such as the supercapacitor. Supercapacitors have a number of advantages, though obviously they are not without certain disadvantages (Głuchy & Kasprzyk 2017, Głuchy et al. 2017, Kasprzyk et al. 2017). One of the most important features is their lifespans which may even extend to over 10 years (up to a million charge and discharge cycles), high efficiency (up to 95%), high current capacity, low environmental impact and low weight. With regards to their disadvantages, one can

mention the relatively low operating voltage of a single cell (2-3 V) as well as the possibility of self-discharge (up to 25% in 48 hours) and also the large size in relation to chemical energy storages of a comparable capacity. The relatively low energy capacity of supercapacitors (in comparison to accumulators or batteries) does not allow for their common use in devices in lieu of accumulators or batteries (because of the necessity of frequent charging) (Jajczyk & Słomczyński 2019). Such a solution is inconvenient and limits the use of supercapacitors as a source of power for devices which are operated frequently, but for a short time, and which consume a relatively low amount of energy. Examples of devices used in such a manner include remote controls for radios or TV sets, keyless car keys, etc. These devices are usually put away in the same place after a short period of use. Sometimes, devices are equipped with a battery, which may be recharged (e.g. smartphones, toothbrushes). The replacement of a battery by a supercapacitor also results in an increase in the size of the device. As well as this, its mobility parameter will also be worse, as more frequent connection of the power (charging) cable will be required. This, as such, is inconvenient and limits the possibility of operating the device while it is charging, and in certain conditions, the galvanic connection is even dangerous (there is the possibility of short-circuits or dirtying the connector).

In the case of some devices, it is possible to stop using electric energy storages and, instead, use a wireless power supply which does not require the galvanic connection. Power may be supplied "through the enclosure"; it only suffices to place a device in the right location. In recent years, this method of supplying power has gained popularity owing to, among other things, the optimisation of devices, improvement of their performance and the introduction of standardisation. Owing to the implementation of a wireless power supply, in the case of devices operated continuously in the area of impact of the power supply system, it is possible to resign from energy storages completely. One example of such a device is a computer mouse, whose operating range is usually limited to the area of a mouse-pad.

2. Consumption of batteries and accumulators in Poland

Low power electrical devices, specifically portable devices, use a power source in the form of an electrochemical battery. Their biggest disadvantage during operation is the loss of their initial ability to discharge energy, which leads to the necessity of their replacement. Because many elements which are harmful to humans and the natural environment are used to construct them, they must necessarily be subjected to the recycling process (Legal act 2020, Nowacki & Mroziński 2012). Poisonous elements are released by waste batteries into the soil and ground waters which cause pollution of the natural environment. As

a consequence of this – in the closed Earth's ecosystem – living organisms are poisoned leading to many diseases and illnesses.

Based on statistics, it is assumed that 1 tonne of batteries contains the following elements (Kozakiewicz 2009, 2010):

- manganese dioxide 270 kg (27%),
- iron 210 kg (21%),
- zinc 160 kg (16%),
- graphite 60 kg (6%),
- ammonium chloride 35 kg (3.5%),
- copper 20 kg (2%),
- potassium hydroxide 10 kg (1%),
- mercury (mercury oxide) 3 kg (0.3%),
- a few kilograms of nickel and lithium (0.4%),
- cadmium 0.5 kg (0.05%),
- silver (silver oxide) 0.3 kg (0.03%),
- small amounts of cobalt.

At present, due to the dynamically developing market of electrical vehicles, and thus, their accumulators, the percentage value of the elements used is changing (as more efficient and cheaper solutions are sought).

The Batteries and Accumulators Act adopted on 24.04.2009 (Legal act 2020) provided for an obligation to collect waste energy sources as described in art. 27 and art. 33. In accordance with the objectives, the required rate of collected batteries for the year 2016 was 45%. For the year 2016, the objectives of the Act were not accomplished. According to the reports of the Chief Inspectorate of Environmental Protection (CIEP), the actual battery collection rate on the Polish market in the year 2016 was only 39%, although nowadays, the situation has improved. According to the recent report of the CIEP for the year 2018 (Raporty GIOŚ 2019), the battery collection rate in Poland was 80% (Table 1).

The collection rate, increasing from year to year, has resulted in a decrease in the mass of recycled batteries and accumulators. An important aspect for the analysed level is also the organized process of collection and processing of end-of-life vehicles (Chamier-Gliszczyński 2011c), where the battery is an important element. Despite exceeding the collection threshold in the year 2017, which was at a level of 45%, and despite the achievement of a value of 80%, still a significant part (20% of batteries and accumulators) is not subject to processing, which constitutes a mass of over 2638 tonnes (Fig. 1).

Table 1. Batteries introduced into and collected from the Polish market in the years 2010-2018 (Raporty GIOŚ 2019)

Year	Mass of introduced portable batteries and accumulators [kg]	Mass of collected waste portable batteries and accumulators [kg]	Accomplished collection rate [%]	Predicted collection rate [%]
2010	9 866 370.92	1 774 838.76	17.99	18.00
2011	9 818 740.44	2 230 889.23	22.72	22.00
2012	10 078 906.07	2 933 105.21	29.10	25.00
2013	10 544 747.99	3 170 109.92	30.06	30.00
2014	11 220 634.34	3 710 034.47	33.06	35.00
2015	11 755 981.53	4 508 589.04	38.35	40.00
2016	12 196 457.76	4 756 258.77	39.00	45.00
2017	12 795 706.75	8 411 931.21	65.74	45.00
2018	13 192 347.62	10 554 051.37	80.00	45.00

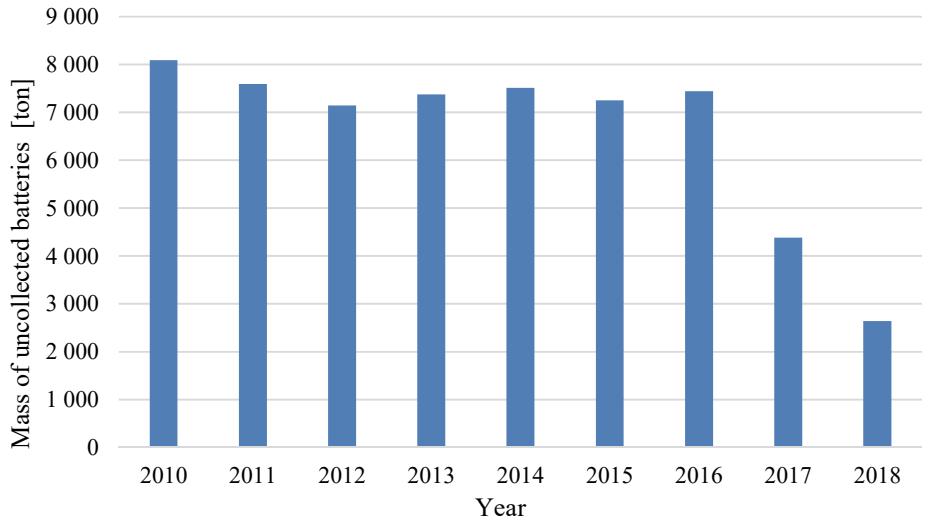

Fig. 1. Mass of uncollected waste portable batteries and accumulators in the years 2010-2018 (Raporty GIOŚ 2019)

A part of the mass of batteries and accumulators which were not subjected to recycling, includes batteries which were a source of power supply for electronic devices. A reduction in the number of batteries used is the simplest way to reduce the mass of batteries and accumulators which must be recycled.

3. A wireless power supply instead of electrochemical sources

The use of portable devices usually requires the use of energy sources such as batteries or accumulators to power these devices. Sometimes these sources can be replaced by capacitors. Specifically, this refers to devices which are characterised by low power consumption. These devices must be provided with the possibility of replenishing energy on a continuous basis, which creates certain inconveniences. However, it would then be possible to stop using energy storages owing to the use of wireless power supply systems.

Wireless power supply systems are based on the principle of electromagnetic induction. They transfer energy through the electromagnetic field just as is the case with transformers. The system consists of an energy transmitter and a receiver, that is, the primary winding side and the secondary winding side of the transformer. Unlike in transformers, the windings are separated (they are located in different devices). The transmitter may be provided with an air-core coil or coil wound onto a ferromagnetic core. However, on the side of the receiver, ferromagnetic core coils are implemented to avoid the accompanying increase in the mass of the powered device. With the assumption that the system is powered from a power network, the system comprises several converter blocks and a control system. At the input of each transmitter circuit, there is an AC/DC converter (rectifier), whose task is to convert the mains AC voltage into DC voltage. Then, there is the DC/AC converter, which converts DC voltage into high-frequency AC voltage (from several kHz to several MHz). The generated AC voltage is applied to the coil serially connected with the capacitor, with a capacity selected in such a way as to contribute to the occurrence of voltage resonance in the circuit. The receiver is provided with a passive power compensation system with a converter which converts AC voltage into DC voltage and a pulse system, used to power the receiver (Fig. 2).

The construction of a system which transmits energy in the form of an electromagnetic field is complicated, mainly due to the DC-AC converters used to match the appropriate operating frequency. To a great extent, the effective use of the wireless transmission of electricity depends on the performance of the circuit, i.e. the lowest possible energy losses. The greatest impact on losses is exerted by the stream of the dispersed electromagnetic field.

The year 2009 marked the development of the “Qi Wireless Charging” standard. This determined the parameters of devices which use a wireless power supply. Work on the standard was conducted by the Wireless Power Consortium, established by over one hundred companies interested in this technology. The first receiver which used the Qi Standard was presented in 2011.

Two groups of chargers were identified in the standard (Van Wageningen & Staring 2010, Hui 2013, Filipiak et al. 2019):

- the first one, low power – up to 5 W,
- the second one, medium power – up to 120 W.

In order to maintain maximum performance of the devices, the possibility of mechanical positioning of the receiver in relation to the base station was indicated, i.e. the use of a dock which enables the placement of the device only in one position. Another method is the automatic adaptation of the base station to the position of the mobile device, that is, the use of many coils in the transmitter which are switched on by the controller that searches for the configuration of the system that ensures its highest efficiency. The standard also determines the permissible frequency ranges for low power devices – from 110 to 205 kHz, and for medium power devices – from 80 to 300 kHz. The standard determines the maximum distance between the base device and the receiver, which is 40 mm. This means that the device is capable of transferring electricity to the receiver through an obstacle with a maximum thickness of 40 mm, if it is made of a material with relative magnetic permeability (Van Wageningen & Staring 2010, Hui 2013, Filipiak et al. 2019).

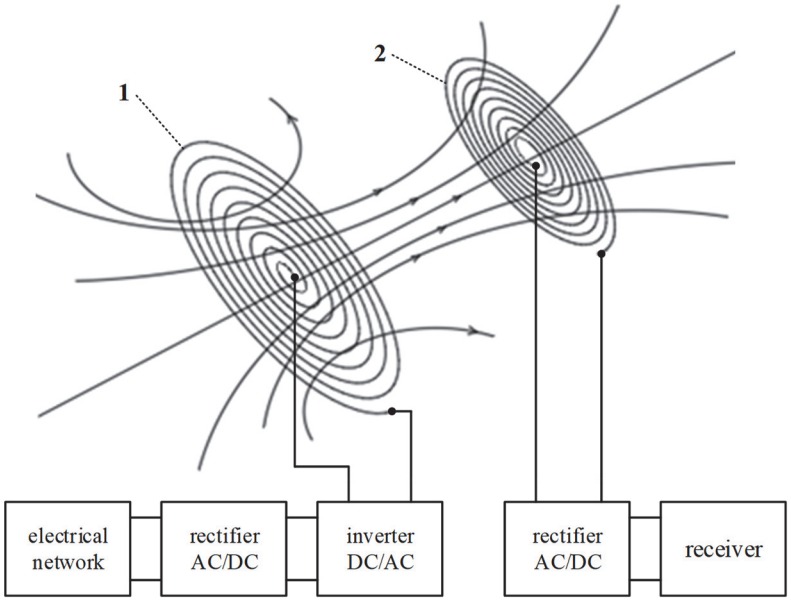

Fig. 2. Block diagram of the system for wireless energy transmission:
1 – coil of the transmitter of the power supply system, 2 – receiver inductor

4. An example of a device with a wireless power supply

Modern computer systems require the use of indicator systems such as e.g. a mouse. Among the offers presented by manufacturers of such equipment, we can distinguish trackball and optical devices, both wired and wireless. Out of those listed above, the most complicated devices, in terms of the processing of the real position into the virtual position on the computer screen, are the wireless mice. In most cases, they are powered with a battery (type: AA or AAA) with a 1.5 V rated voltage. It is also possible to encounter solutions which do not have their own power source, but use a wireless power supply. In this paper we tested an exemplary device which used a wireless power supply, that is, the A4Tech EVO Battery Free computer mouse (Fig. 3).

Fig. 3. Wireless mouse with a mouse pad for inductive power supply (A4Tech EVO Battery Free)

The tested device consists of an inductive pad and an optical mouse. The mouse pad is powered from a USB port (5 V DC). Transmission of power to the receiver is possible owing to the phenomenon of electromagnetic induction and the generation of electromotive force in the receiver coil (mouse) The electronic system located in the mouse pad converts the DC voltage coming from a USB port into AC voltage which allows for the induction of the alternating electromagnetic field with a frequency of approximately 122 kHz. A coil without a ferromagnetic core, in the shape of a rectangle measuring 14.5 cm by 18.5 cm, is mounted in the pad. There are 13 windings of copper wire on it. The mouse includes an air-core coil measuring 9.5 cm by 4.5 cm. The transmission of information about the position of the mouse cursor takes place through RFID technologies (Kostrzewski et al. 2019).

This paper verifies the practical aspects of the operation of such a type of power supply system. For this purpose, the value of the wirelessly induced voltage was measured depending on the position of the mouse on the power pad and

the distance of the mouse from the pad. Fig. 4 presents the shape and position of the air-core coil in the mouse pad and the areas in which the tested receiver was placed during measurements. The transmitter coil consists of a wound copper wire, in the shape of a rectangle, and its intrinsic inductance amounts to 62 μH. The receiver coil is smaller, however, it has more windings. Its intrinsic inductance is 76.6 μH (inductances were measured with a METERMAN LCR55). The voltage signal generated in the transmitter and the one induced in the receiver coil have forms, which approximate those of sinusoidal waves and their frequency is about 122 kHz.

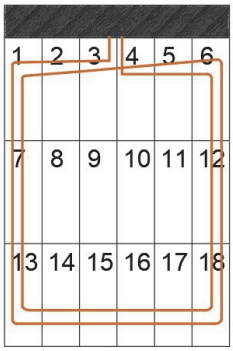

Fig. 4. Division of the power pad into sectors

During tests, the mouse (receiver) was placed in sectors defined in Fig. 4, and the effective value of the voltage induced on the receiver coil terminals was determined using the INSTEK GDS-82C oscilloscope. The values of the measured voltages are presented in Fig. 5. It was observed that the placement of the device powered in any place of the power pad ensures a voltage value that is sufficient for its correct operation.

It was verified in this paper whether the device met the requirements set by the Qi standard. For this purpose, the correctness of operation of the mouse was tested at a distance of 40 mm from the power pad. It was found that in each of 18 points (Fig. 4), the mouse works correctly after placing it 40 mm away from the power pad. The voltage measured at each point was less than 4 V.

5. Remarks and conclusions

This article has brought issues related to the use of electrochemical energy sources in mobile electrical devices to attention. Based on the reports of the Chief Inspectorate of Environmental Protection, the mass of portable batteries and accumulators introduced into the Polish market and collected from it in the years 2010-

2018 was analysed. It was demonstrated that the recycling system for this type of devices is more and more effective from year to year. However, attention has also been paid to the problem of energy sources which are still not collected. It was demonstrated that the batteries and accumulators which were not subjected to disposal because of their chemical composition are an environmental hazard.

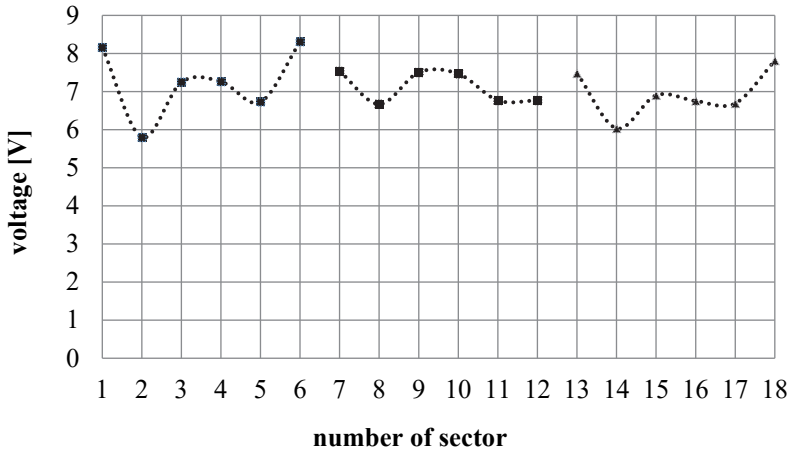

Fig. 5. Values of the induced voltage in the respective sectors of the power pad

The authors paid attention to the existing mobile solutions on the market, which do not require a power source in the form of a battery or accumulator. The paper discusses a wireless power supply system which takes advantage of the phenomenon of electromagnetic induction. A wireless mouse was given as an example of the device. The mouse uses an inductive power supply after it is placed on a special power pad and this mouse and power pad were subjected to insightful analysis with regards to their operation. As a result of the tests, it was found that the mouse works correctly irrespective of its place on the power pad. The tested device complies with the Qi Wireless Power standard and meets the requirements for operation set by this standard. It can be said that the wireless power supply successfully replaces a power supply obtained from batteries.

In devices which are used within a limited area (similarly to computer mice), it is possible to stop using power supplies dependent on batteries in order to switch to wireless inductive power supplies. As a solution which can help popularise this type of technology, there are suggestions to use inductive charging pads built into the table surface, with an area drawn to mark its location. The integration of a power supply system with a piece of office furniture will allow additional pads to be excluded, thus increasing the comfort of use of the mouse

and the aesthetics of a computer workstation. The production of these devices can also be improved, e.g. by applying the methods presented in Szajna et al. (Szajna et al. 2020, 2018).

Owing to the continuous development of wireless power supply technologies, these systems are achieving ever better parameters (efficiency and range). In the case of certain devices and systems, in addition to ensuring similar mobility, the necessity of using power supplies based on batteries is eliminated, thus the number of batteries is reduced, which, in turn has a positive effect on environmental protection.

References

Burzyński, D., Pietracho, R.. Kasprzyk, L., Tomczewski, A. (2019). Analysis and Modeling of the Wear-Out Process of a Lithium-Nickel-Manganese-Cobalt Cell during Cycling Operation under Constant Load Conditions. *Energies*, *12*, 3899.

Chamier-Gliszczyński, N. (2010). Optimal Design for the Environment of the Means Transportation: a Case Study of Reuse and Recycling Materials. *Sold State Phenomena*, *165*, 244-249.

Chamier-Gliszczyński, N. (2011a). Recycling Aspect of End-of Life Vehicles. Recovery of Components and Materials from ELVs. *Key Engineering Materials*, *450*, 421-424.

Chamier-Gliszczyński, N. (2011b). Reuse, Recovery and Recycling System of End-of Life Vehicles. *Key Engineering Materials*, *450*, 425-428.

Chamier-Gliszczyński, N. (2011c). Environmental aspects of maintenance of transport means. End-of life stage of transport means. *Eksploatacja i Niezawodnosc-Maintenance and Reliability*, *2*, 59-71,

Filipiak, M., Głuchy, D., Godek, M. (2019). Wpływ technologii stosowanych w ładowarkach bezprzewodowych na proces ładowania urządzeń mobilnych. *Poznan University of Technology Academic Journals. Electrical Engineering*, *99*, 41-51.

Głuchy, D., Kasprzyk, L. (2017). Modelowanie pracy superkondensatora zasilającego układ poprawiający bezpieczeństwo drogowe. *Przegląd Elektrotechniczny*, *93*(12), 99-102.

Głuchy, D., Kasprzyk, L., Tomczewski, A. (2017). Modelowanie superkondensatorów na potrzeby współpracy z OZE. *Poznan University of Technology Academic Journals. Electrical Engineering*, *89*, 335-345.

Hui, S.Y. (2013). Planar wireless charging technology for portable electronic products and Qi. *Proceedings of the IEEE*, *101*(6), 1290-1301.

Jajczyk, J., Słomczynski, K. (2019). A dedicated battery for an electric bike. *ITM Web of Conferences. Computer Applications in Electrical Engineering, 28*, 01033.

Kasprzyk, L. (2019). Selected issues of modelling degradation of the lithium-ion batteries in electric vehicles, *Przegląd Elektrotechniczny*, *95*(3), 70-73.

Kostrzewski, M., Varjan, P., Gnap, J. (2020). *Solutions Dedicated to Internal Logistics 4.0.* In: Grzybowska K., Awasthi A., Sawhney R. (eds) Sustainable Logistics and Production in Industry 4.0. EcoProduction (Environmental Issues in Logistics and Manufacturing). Springer, Cham, 243-262.

Korkozowicz, M. (2010). Co dalej z recyklingiem baterii? *Odpady i Środowisko*, *5*, 63-65.
Korkozowicz, M. (2009). Baterie-nowe prawo i obowiązki. *Recykling*, *6*, 18-19.
Legal act, Act of April 24, 2009 on batteries and accumulators in Poland, Dz. U. 2009, 79.
Nowacki, M., Mroziński, A. (2012). Przykłady procesów recyklingu baterii w Polsce. *Inżynieria i Aparatura Chemiczna*, *51*(5), 239-241.
Raporty o funkcjonowaniu gospodarki bateriami i akumulatorami oraz zużytymi bateriami i zużytymi akumulatorami za lata 2010-2018 (2011-2019), *GIOŚ*.
Szajna, A., Stryjski, R., Woźniak, W., Chamier-Gliszczyński, N., Kostrzewski, M. (2020). Assessment of Augmented Reality in Manual Wiring Production Process with Use of Mobile AR Glasses. *Sensors, 20*(17)*,* 4755, 1-26.
Szajna, A., Szajna, J., Stryjski, R., Sąsiadek, M., Woźniak, W. (2019). *The Application of Augmented Reality Technology in the Production Processes, Intelligent Systems in Production Engineering and Maintenance: conference proceedings ISPEM 2018, 2019*. / eds. A. Burduk, E. Chlebus, T. Nowakowski, A. Tubis, Cham: Springer Nature Switzerland (Advances in Intelligent Systems and Computing 835), 316-324.
Van Wageningen, D., Staring, T. (2010). The Qi wireless power standard. In *Proceedings of 14th International Power Electronics and Motion Control Conference EPE-PEMC 2010,* 15-25).

Abstract

The paper discusses issues related to the recycling of electrochemical sources of electricity such as portable batteries and accumulators. Based on the reports of the Chief Inspectorate of Environmental Protection, the collection rate of waste batteries and accumulators in Poland for the years 2010-2018 was subjected to analysis. Despite the increasing year-to-year percentage value of the collection rate, it has been demonstrated that a significant mass of batteries and accumulators is still not recycled.

This article presents a method of reducing the amount of waste electrochemical energy storages, through the use of inductive power supplies. The idea of the operation of such circuits has been discussed and the Qi Wireless Charging standard, applicable since 2011, has been characterised. As an example of a device with wireless power supply, a computer indicator system has been provided. Tests have been carried out and the correctness of operation of this solution has been verified. It has been demonstrated that in some cases it is possible to resign from power supplies based on batteries or accumulators, and use wireless power supplies instead, without degrading the functional properties of devices. Solutions of this type may contribute to the protection of the natural environment.

Keywords:
electrochemical energy storages, recycling of batteries and accumulators,
wireless power supply, Qi Wireless Charging standard

Ograniczenie wykorzystania elektrochemicznych źródeł energii elektrycznej poprzez zastosowanie zasilania bezprzewodowego

Streszczenie

W pracy omówiono problematykę recyklingu elektrochemicznych źródeł energii elektrycznej takich jak baterie i akumulatory przenośnie. Na podstawie raportów Głównego Inspektoratu Ochrony Środowiska przeanalizowano zbieralność zużytych baterii i akumulatorów w Polsce w latach 2010-2018. Pomimo rosnącego z roku na rok procentowego wskaźnika zbieralności wykazano, że znaczna masa baterii i akumulatorów wciąż nie jest poddawana recyklingowi.

W artykule przedstawiono metodę ograniczenia ilości zużywanych elektrochemicznych zasobników energii elektrycznej poprzez zastosowanie zasilania indukcyjnego. Omówiono ideę działania tego typu układów oraz scharakteryzowano obowiązujący od 2011 roku standard Qi Wireless Charging. Jako przykład urządzenia zasilanego bezprzewodowo podano układ wskaźnika komputerowego. Wykonano badania i zweryfikowano poprawność działania tego rozwiązania. Wykazano, że w niektórych przypadkach możliwe jest zrezygnowanie z zasilania bateryjnego lub akumulatorowego na rzecz zasilania bezprzewodowego bez pogorszenia własności funkcjonalnych urządzeń. Rozwiązania tego typu mogą przysłużyć się ochronie środowiska.

Słowa kluczowe:
elektrochemiczne zasobniki energii, recykling baterii i akumulatorów,
zasilanie bezprzewodowe, standard Qi Wireless Charging

MIDDLE POMERANIAN SCIENTIFIC SOCIETY OF THE ENVIRONMENT PROTECTION

Rocznik Ochrona Środowiska

Volume 22. Year 2020 ISSN 1506-218X 456-474

Model Investigations of Flow Rate and Efficiency of Air Lift Pump with PM 50 Mixer and Circumferential Mixer

Marek Kalenik[*]*, Marek Chalecki*

Warsaw University of Life Sciences – SGGW, Poland

[*]*corresponding author's e-mail: marek_kalenik@sggw.edu.pl*

1. Introduction

An air lift pump does not have any movable parts and it is used to lift liquids (Kujawiak et al. 2018, Kalenik 2015a) or liquid-solid mixes (Kalenik 2017). The device is built of a vertical pipe, partly submerged in liquid, where air under pressure is introduced into its lower part. During air introduction, a two-phase (liquid-air) or three-phase (liquid-air-solid) mix arises inside the vertical pipe, having lower density than the liquid (Kalenik & Chalecki 2018). As the mix within the vertical pipe becomes lighter than the surrounding liquid, the mix is pushed up by the air.

Due the simple construction and high reliability, air lift pumps are used in various applications. The air lift pumps were usually used to transport liquid both in water supply and sewage systems. Nowadays in Poland, these devices are used to lift sewage and sewage sediments in small near-home container sewage-treatment plants and big group sewage-treatment plants, i.a. in grit chambers (Sawicki 2004, Sawicki & Pawłowska 1999), as well as in high-rate filters with self-regenerating bed or for renovation of bored wells (Kalenik 2017).

The air lift pumps are also used to aerate and mix water, to remove carbon dioxide from water in industrial fish farming (Barrut et al. 2012) as well as to mix water in deep lakes and to aerate it by means of transport of water from the lake bed onto its surface (Fan et al. 2013, Qiang et al. 2018). Due to their simple construction and high reliability, the air lift pumps are applied in various branches of industry, especially in the petrochemical industry to raise oil from dead wells (Hanafizadeh et al. 2011), in the chemical industry to transport corrosive, radioactive, arid or toxic fluids (De Cachard & Delhaye 1996, Kassab et al. 2007) as well as to pump boiling fluids, where the change of liquid phase into gas phase occurs (Khalil et al. 1999). They are also used to transport suspensions in mining

industry and to lift manganese concretions from deep seabed up to ca. 4000-6000 m (Kassab et al. 2007). The air lift pumps can be also used to lift leachate from drainage wells in waste disposals (Koda et al. 2017). The performed investigations (Kujawiak et al. 2020) show that domestic sewage in near-home hybrid sewage-treatment plants with moving bed are also sufficiently aerated by the air lift pump.

A two-phase (liquid-gas) or three-phase (liquid-gas-solid) flow exists in the air lift pumps which is very difficult for mathematical modeling (Kalenik & Chalecki 2018, Kalenik 2017, Ahmed et al. 2016, Kalenik 2015a, Kalenik 2015b, Nicklin 1963). Multi-phase flows occurring in various systems applied for transport of mixes are characterized by high variability of the flow rate of individual phases and depend on many factors and hydraulic variables (Kujawiak et al. 2020, Qiang et al. 2018, Kalenik 2015c, Kalenik 2014, Hu et al. 2012). The hydraulic operating conditions of two- and three-phase flow in the air lift pumps are very poorly identified. Some attempts are made to describe flow structures, occurring in various conditions of liquid-gas flow or liquid-gas-solid flow, and to work out so-called flow structure maps for them and mathematical models for simulation of flows occurring in the air lift pumps (Kalenik & Chalecki 2018, Kalenik 2017, Kalenik 2015a, Kalenik 2015b, Kim et al. 2014, Mahrous 2014, Wahba et al. 2014, Meng et al. 2013, Mahrous 2013a, Mahrous 2013b, Mahrous 2012, Kassab et al. 2009, Yoshinaga & Sato 1996, Sawicki 2004, Sawicki & Pawłowska 1999).

Tests of air lift pumps built of rectangular (Esen 2010) and curved pipes (Fujimoto et al. 2004) have been also carried out. The performed investigations of the air lift pumps with the curved pipes behind the air mixer show that the pumping efficiency for solid bodies significantly falls in such air lift pumps. However, if only liquid is being pumped then the air lift pump pipe curvature does not affect its efficiency (Mahrous 2013a). The performed investigations show that the air lift pumps are characterized by small working efficiency if compared to conventional pumps (Kujawiak et al. 2018, Kalenik 2015a, Kalenik 2015b, Tighzert et al. 2013, Kassab et al. 2009, Kassab et al. 2007).

There is little information in the technical and scientific literature on principles of calculations of water flow rate Q_w in air lift pumps for a given mixer type (Kujawiak et al. 2018, Ahmed et al. 2016, Kalenik 2015a, Kalenik 2015b). Moreover, there is no information how to design mixers so as to obtain the best operating parameters of the air lift pump. From the investigations to date it arises that the mixer type and the diameter of a pressure pipe applied in a given air lift pump affect its efficiency and hydraulic operating conditions (Ahmed et al. 2016, Kalenik 2015b, Fan et al. 2013, Khalil et al. 1999). The number, diameter and distribution of holes in mixers significantly affect the type of structure of two-phase and three phase flow in the air lift pumps.

In aim to determine the efficiency of the tested air lift pump equipped with the PM 50 mixer with perforated rubber membrane as well as the circumferential mixer, the following formula has been applied (Nicklin 1963):

$$\eta = \left(\frac{\rho_w g Q_w \cdot (L - h)}{p_b Q_a \ln\left(\frac{p_a}{p_b}\right)} \right) 100 \tag{1}$$

where:
η – efficiency of the air lift pump [%],
Q_w – water flow rate [$m^3 \cdot s^{-1}$],
Q_a – air flow rate [$m^3 \cdot s^{-1}$],
p_a – air pressure [$N \cdot m^{-2}$],
ρ_w – water density [$kg \cdot m^{-3}$],
p_b – barometric pressure [$N \cdot m^{-2}$],
h – pressure pipe submergence length [m],
L – length of the pressure pipe till the outlet [m],
g – gravitational acceleration [$m \cdot s^{-2}$].

The paper presents the analysis of results of investigations concerning an influence of the applied constructive solutions on hydraulic operating conditions of a water-pumping air lift pump. The scope of the investigations encompassed the determination of flow rate and efficiency characteristics of an air lift pump having the discharge pipe with the internal diameter d = 0.04 m. The PM 50 mixer with a perforated rubber membrane, available on the market, as well as a mixer of own design, called circumferential mixer, were tested. The investigations were performed for three air-water mix delivery heads H: 0.40, 0.80, 1.20 m, for the specified pressure pipe submergence length h = 0.80 m.

2. Description of test rig

Figure 1 shows the construction and operating principle of a test rig for investigations of hydraulic operating conditions of air lift pumps. After the opening of a ball valve (2), a pipeline (1) delivered water to a tank (3). During the tests the tank (3) was permanently filled with water up to the height of 1.0 m. After the opening of another ball valve (8), the excess of the water being delivered to the tank (3) was carried by an overfall (7) to the sewerage through a floor inlet (12). A draining pipeline (10) served to empty the tank (3) from water after the ball valve (8) opening. Inside of the tank (3), at the height of 0.20 m upon its bottom,

a transparent PVC discharge pipe (4) with the internal diameter of 0.04 m was mounted. The measurements of the air lift pump delivery rate were carried out for the three sand-water mix delivery heads (H): 0.40 m, 0.80 m, 1.2 m, measured over the water level in the tank (3). In the discharge pipe (4), at the height of 0.30 m over its lower edge, an air mixer (9) was mounted. In aim to measure water temperature in the tank (3), an electronic resistance thermometer (17) was applied.

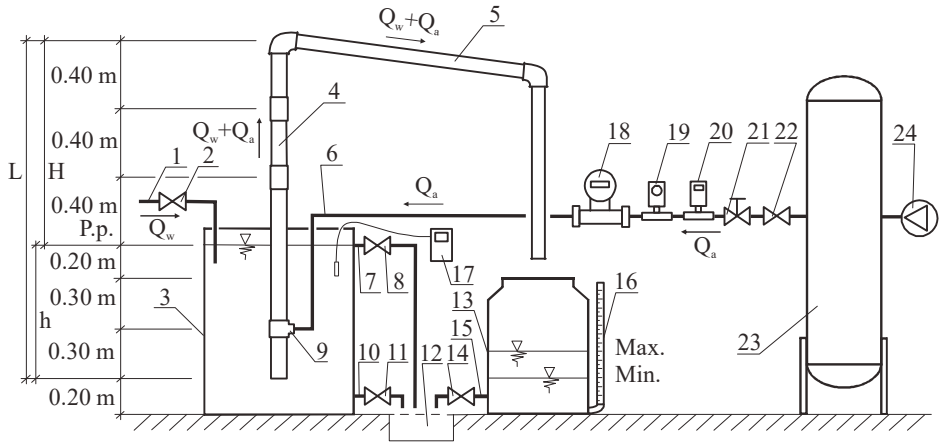

Fig. 1. Scheme of the air lift pump test rig: 1 – water supplying pipe, 2, 8, 11, 14, 22 – ball cut-off valve, 3 – tank with water, 4 – discharge pipe, 5 – water and air channeling pipe, 6 – air supplying pipe, 7 – overfall, 9 – mixer, 10, 15 – draining pipe, 12 – floor inlet, 13 – measuring container, 16 – scaled water level gauge, 17, 20 – electronic resistance thermometer, 18 – electromagnetic air flow meter, 19 – piezoelectric pressure sensor, 21 – needle valve, 23 – compressed air container, 24 – compressor, h – discharge pipe submergence length, L – discharge pipe length-to-outlet, H – water-air mix delivery head

Figures 2a, b show a constructive solution of the tested Aquatech PM 50 mixer equipped with a perforated rubber membrane (4), denoted hereinafter as M1, whereas Figures 2c, d – a circumferential mixer of own design, denoted hereinafter as M2. The M1 mixer had n = 8 holes having the total area A = 25.12 mm^2, the M1 mixer – n = 8 holes with the total area A = 25.12 mm^2. An elastic pipe (6) with the internal diameter of 0.013 m supplied air to the mixer (9, Fig. 1) from a compressed air container (23) where the air was pressured by a compressor (24). At the air supplying pipe (6) an electromagnetic air flow meter (18), piezoelectric pressure sensor (19), electronic resistance thermometer (20) measuring air temperature as well as a needle valve (21) and ball cut-off valve (22) were mounted.

The investigations were performed with use of Endress & Hauser devices. The measurement range of the electromagnetic air flow meter (18) was 0.0 to 30.0 $m^3 \cdot h^{-1}$ and the measurement range of the piezoelectric pressure sensor (20) – 0.0 to 400 kPa. According to the Endress & Hauser catalogue, the measurement error of the applied electromagnetic air flow meter and piezoelectric pressure sensor is lower than 1% and the output current signal falls into the range 4-20 mA. The measurement accuracy of the applied thermometer, however, was ±1°C and its measurement resolution – 0.1°C.

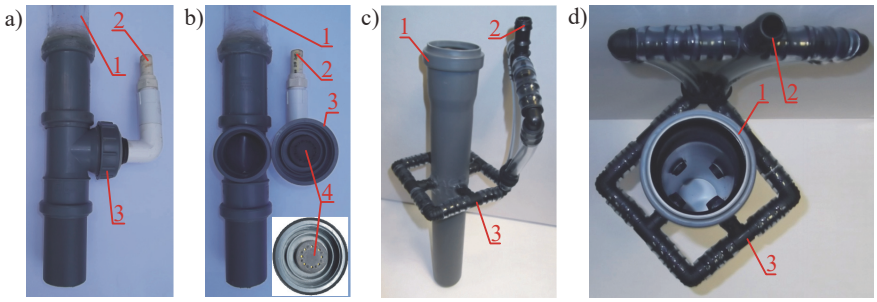

Fig. 2. Designs of mixers: a), b) PM 50 mixer with perforated rubber membrane (M1), c), d) circumferential mixer (M2), 1 – discharge pipe, 2 – air supplying pipe connecting tip, 3 – mixer, 4 – perforated rubber membrane

The measurements concerned water and air temperature, air pressure, barometric pressure, air flow rate, water volume and air lift pump operating time. The needle valve (21) was used to regulate the air pressure.

In aim to measure the water flow rate Q_w in the air lift pump delivery rate, the measuring vessel method was applied, i.e. a plastic measuring container (13), scaled at each 1 dm^3, was used. The measuring container (13) capacity scale was put on the transparent water-level gauge (16), mounted at the side of the measuring container. Such solution allowed very precise reading of the volume of the water lifted by the air lift pump per time unit. For a specified delivery head H, the pumped water flew down through the channeling pipe (5) with the internal diameter d = 0.04 m to the measuring container (13). The water flow in the channeling pipe (5) was pressure-less (gravitational). In this aim, little holes serving to discharge the pumped air outside the pipe (5) were drilled in the upper wall of the channeling pipe (5). Table 1 presents assumptions for the performed experiments.

Table 1. Assumptions for the performed experiments

Type of mixer	d [m]	H [m]	h [m]	L [m]	h/L = S_r* [–]	n [–]	A [mm^2]
M1	0.04	0.4 0.8 1.2	0.8	1.2 1.6 2.0	0.7 0.5 0.4	8	25.12
M2	0.04	0.4 0.8 1.2	0.8	1.2 1.6 2.0	0.7 0.5 0.4	4	254.34

*S_r – submergence ratio

3. Methodology of investigations

Before the beginning of each measurement series on the test rig (Figure 1), an actual barometric pressure (p_b) was measured with use of the piezoelectric pressure sensor (19). Then, on the water-level gauge (16) connected to the measuring container (13), it was marked the minimum level of a water free surface in the measuring container (13) by which the stop-watch was switched on as well as the maximum level of free surface of water by which the stop-watch was switched off. The level marked on the water-level gauge (16) scale referred to a certain water volume (V_w).

The measurement of the water flow rate (Q_w) was started from the opening the valves (2, 8), filling the tank (3) with water, turning on the compressor (24) and opening the valve (22) on the pipeline (6) supplying the mixer (9) with air. Then a demanded value of the air pressure (p_a) was fixed on the piezoelectric pressure sensor (19) using the needle valve (21). As the determined air pressure had been fixed, some quantity of water – depending on the air lift pump flow rate – flew out from the tank (3). In aim to make the measurement reliable, the water level in the tank (3) had to be kept constant. Changes of the submergence of the mixer (9) or water level changes in the tank (3) evoke significant changes in the air lift pump flow rate. The constant water level in the tank (3) was kept with use of the valve (2) placed on the discharge pipe (1) supplying water to the tank (3). Each time the valve (2) was set in the position which balanced the water flux through the channeling pipe (5) for a given value of the air pressure. Observations and regulations of the water level in the tank (3) were performed relatively to the level in the overfall (7) channeling the water excess. As these actions were completed and the working conditions of the air lift pump stabilized, the measurement started. At first, for a specified value of the air pressure, the air flow rate (Q_a) was being read from the electromagnetic air flow meter (18) and the air and water temperatures – from the electronic resistance thermometers (17 – water, 20 – air). As the water-level gauge (16) showed that the water free surface in the measuring

container (13) reached the marked minimum level, then, during the measurement of the water flow rate Q_w, the stop-watch was switched on and measured a container (13) filling time (t) till the moment when the water free surface reached the marked maximum level – then the stop-watch was switched off and the needle valve (21), cutting off the air from the mixer (9), was turned off.

Then the measuring container (13) was emptied, a next value of the air pressure was set on the piezoelectric pressure sensor (19) and a next measurement started. The measurements were carried out for specified values of the air pressure (p_a), established between 105 and 200 kPa with intervals 5 kPa. The water flow rate (Q_w) was calculated by dividing the volume (V_w) of the water being in the measuring container (13) for the filling time (*t*). During the tests, five measurement series were carried out – each of them for each established value of the air pressure (p_a) and for all three water delivery heads (H): 0.40 m, 0.80 m, 1.20 m measured relatively to the water free surface in the tank (3).

4. Results and discussion

During the operation of the air lift pump (Fig. 1) with the perforated rubber membrane mixer M1 (Fig. 2a, b), the air flow observed in the transparent discharge pipe had a form of very fine air bubbles creating air-water emulsion with water in the whole cross section of the discharge pipe (Fig. 3a). The stream of water flowing out from the air lift pump was almost continuous, with small pulsation visible. However, during the operation of the air lift pump with the circumferential mixer M2 (Fig. 2c, d), the air flow observed in the transparent discharge pipe had a form of fine irregular bubbles which filled only a part of the discharge pipe cross section and almost evenly lifted water up (Fig. 3b). The stream of water flowing out from the air lift pump was not continuous but broken and had a pulsating character.

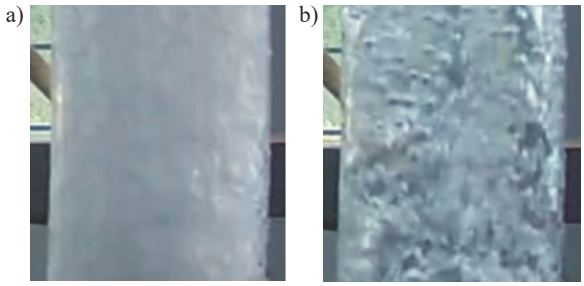

Fig. 3. Flow structures of air-water mix in the discharge pipe during operations of the air lift pump with: a) PM 50 mixer with perforated rubber membrane (M1), b) circumferential mixer (M2)

Figure 4 presents the distribution of the air flow rate Q_a in the mixer M1 with perforated rubber membrane and circumferential mixer M2 as a function of the established air pressure value p_a and the air-water mix delivery head H. Analysis of the obtained results allows to state that the air flow rate increased along with the increase of the air pressure in both of the mixer types in the air lift pump. Moreover, for a constant submergence of the mixer and specified values of the air pressure, the increase of the air-water mix delivery head had very small influence on the fall of the air pressure in these two types of mixers. Regardless the air-water mix delivery head, the values of the air flow rate by the specified air pressure were comparable for both of the mixer types what resulted from big amount of air. For the circumferential mixer, however, when the value of the air pressure was lower than $p_a = 170$ kPa, then the air flow rate Q_a values were higher, whereas for the perforated rubber membrane mixer they were lower. When, in turn, the value of the air pressure exceeded $p_a = 170$ kPa, the situation was opposite. It was caused by hydraulic resistance occurring during the air flow through the mixer – higher for the perforated rubber membrane mixer than for the circumferential mixer.

A statistical analysis was also performed in aim to check whether the differences between the mean values in the results of the air flow rate Q_a for the perforated rubber membrane mixer M1 and for the circumferential mixer M2 (Fig. 4) are statistically significant. Firstly, the normality of distribution was checked with use of the Shapiro-Wilk test and then the homogeneity of variance with use of the Levene test. Calculations of normality of distributions and homogeneity of variances were made with the STATISTICA software. In both tests for individual groups the value of calculated probability $p_{cal.}$ is greater than the assumed significance level $\alpha = 0.05$, which means that the conditions of normal distribution and homogeneity of variance in the examined groups are satisfied. Then, the t-Student test was used for two populations; a zero hypothesis (H_0: $n_1 = n_2$) stated that the mean values are statistically equal, an alternative hypothesis (H_1: $n_1 \neq n_2$) stated that the mean values are statistically different. Calculations of the t-Student statistics value $|t_{cal.}|$ were performed with the computer software STATISTICA; obtained results are gathered in Table 2.

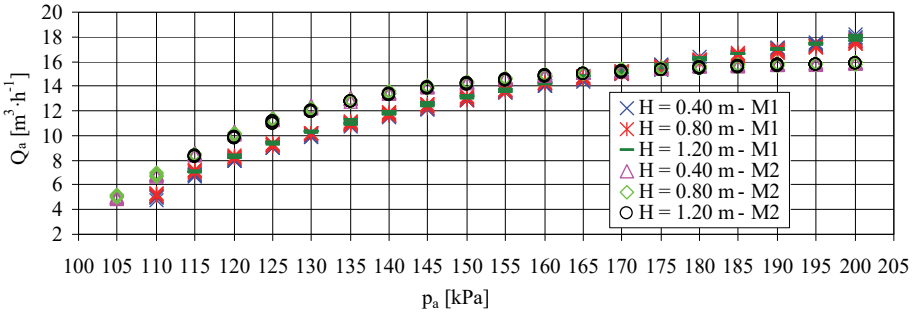

Fig. 4. Dependence of air flow rate Q_a in the air lift pump on air pressure p_a and water delivery head H for the perforated rubber membrane mixer M1 and the circumferential mixer M2

For the alternative hypothesis, it was determined a critical region $|t_{cal.}| \geq t_{\alpha=0.05}$ and, for $v = n_1 + n_2 - 2 = 36$ degrees of freedom and $\alpha = 0.05$, i.e. selected 5-percentage risk of error (significance level), the critical value $t_{\alpha=0.05} = 2.028$ was read from the tables. Analysis of Table 1 allows to state that $|t_{cal.}| \leq t_{\alpha=0.05}$, i.e. the zero hypothesis cannot be rejected, thus the differences between the mean values in the results of the air flow rate Q_a for the perforated rubber membrane mixer M1 and for the circumferential mixer M2 are statistically insignificant, hence the mean values are statistically equal to each other. This is also confirmed by the calculated probability value – $p_{cal.}$ is greater than 0.05 (assumed significance level, Table 2).

Table 2. Results of calculations of the statistics from the t-Student test for Q_a. Differences between the mean values are significant with the probability $p < 0.05$

Parameter	Mean	Standard deviation	Calculated value of the t-Student test $\|t_{cal.}\|$	Calculated probability value $p_{cal.}$	Value of the t-Student test read from the tables for $p = 0.05$ i $v = 36$ $t_{\alpha = 0.05}$
Q_a for M1*	12.92	3.69	0.144	0.89	2.028
Q_a for M2*	12.95	3.23			

* M1 – perforated rubber membrane mixer, M2 – circumferential mixer

Figure 5 presents results of measurements of the water flow rate Q_w in relation to the air flow rate Q_a and air-water mix delivery head H over the submergence ratio S_r for both of the mixer types. Analysis of these results allows to state that the water flow rate Q_w in the air lift pump decreased when the air-water mix delivery head increased, whereas Q_w increased when the air flow rate Q_a, i.e. the specified value of the air pressure p_a, increased. In aim to enable the water outflow from the air lift pump on a demanded delivery head, it must be provided an appropriate minimum air flow rate $Q_{amin.}$ what forces an appropriate air pressure $p_{amin.}$. When the air-water mix delivery head increased, the minimum demanded air pressure in the discharge pipe grew for both of the mixer types. In the air lift pump with the perforated rubber membrane mixer (Figs. 1 and 2a, b), for the delivery head H = 0.40 m, the demanded average minimum air flow rate $Q_{amin.}$ was equal to 5.00 $m^3 \cdot h^{-1}$, what corresponded to the average minimum air pressure $p_{amin.}$ = 110 kPa. For the delivery head H = 0.8 m: $Q_{amin.}$ = 5.24 $m^3 \cdot h^{-1}$ and $p_{amin.}$ = 110 kPa; for H = 1.2 m: $Q_{amin.}$ = 7.01 $m^3 \cdot h^{-1}$ and $p_{amin.}$ = 115 kPa. For the circumferential mixer, however (Figs. 1 and 2c, d), for the delivery head H = 0.40 m, the demanded average minimum air flow rate $Q_{amin.}$ was equal 5.00 $m^3 \cdot h^{-1}$, what corresponded to the average minimum air pressure $p_{amin.}$ = 105 kPa. For the delivery head H = 0.8 m: $Q_{amin.}$ = 5.11 $m^3 \cdot h^{-1}$ and $p_{amin.}$ = 105 kPa; for H = 1.2 m: $Q_{amin.}$ = 8.28 $m^3 \cdot h^{-1}$ and $p_{amin.}$ = 115 kPa.

If the perforated rubber membrane mixer was applied in the investigated air lift pump and, for the specified air-water mix delivery heads H: 0.40, 0.80, 1.20 m, if the average air flow rate exceeded the value Q_a = 16.0 $m^3 \cdot h^{-1}$ what corresponded to the specified air pressure p_a = 180 kPa, then the water flow rate Q_w in the air lift pump decreased instead of growing. The same behavior of the water flow rate Q_w in the air lift pump was observed for the circumferential mixer when the average air flow rate exceeded the value Q_a = 15.0 $m^3 \cdot h^{-1}$ what corresponded to the specified air pressure p_a = 165 kPa. This phenomenon is well known and described both for the two-phase flow (air-water) and three-phase flow (water-sand-air) (Kassab et al. 2009, Hanafizadeh et al. 2011, Meng et al. 2013, Kalenik 2015b, Kalenik 2015c, Kalenik 2017, Ahmed et al. 2016, Kalenik & Chalecki 2018). It means that if the discharge pipe submergence length h for the investigated air lift pump is equal to 0.80 m (Fig. 1), then the maximum air flow rate Q_a required for water pumping should not exceed 16.0 $m^3 \cdot h^{-1}$ if the perforated rubber membrane mixer M1 (Fig. 2a, b) is applied and 15.0 $m^3 \cdot h^{-1}$ if the circumferential mixer M2 (Fig. 2cd) is applied.

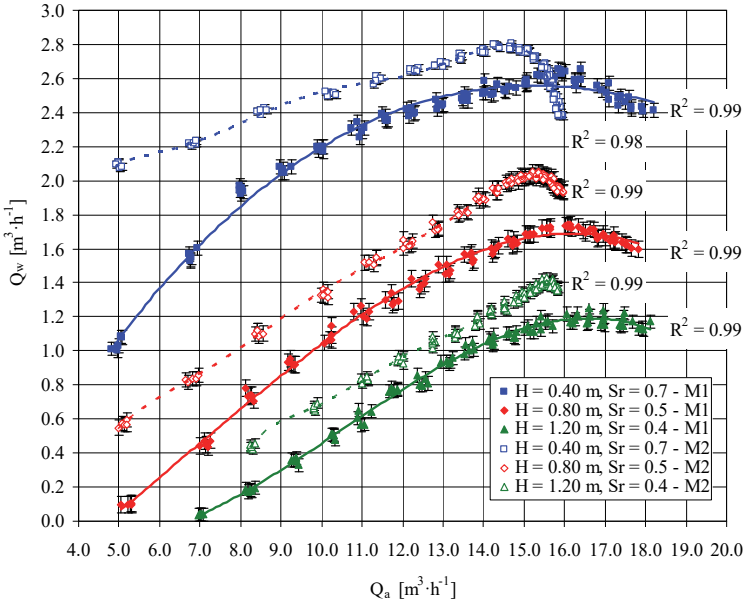

Fig. 5. Dependence of the water flow rate Q_w on the air flow rate Q_a for the perforated rubber membrane mixer M1 and the circumferential mixer M2

An abrupt fall of curves of the water flow rate Q_w for the M2 mixer, visible in Fig. 5, was evoked by a significant growth in the air slip velocity in the discharge pipe of the air mixer. Due to differences between the volume and viscosity of air and water, the air in the air mixer discharge pipe flew with much higher velocity than the water what evoked a phenomenon of phase slip which is characterized by the air slip velocity. The phase slip phenomenon causes the abrupt fall of the water flow rate if the air flow rate grows (Tighzert et al. 2013).

Figure 5 presents also the trend lines, standard error bars as well as determination coefficients R^2 for the values of Q_w. The functional relation between the water flow rate and air flow rate for both of the mixer types presented a nonlinear trend and the regression (trend) type was a 6^{th} degree polynomial within the range of the values of Q_w obtained from the measurements. The trend lines for the values of Q_w placed parallel to each other along with the increase of the air-water mix delivery head H. The values of the coefficient R^2 were over 0.98, what suggests that the water flow rate in the air lift pump at least in 98% depended mainly on the air flow rate, hence the specified air pressure and air-water mix delivery head, and only in 2% on remaining factors, e.g. air and water density, discharge pipe roughness or gravitational acceleration.

The standard error bars, marked in Fig. 5 for the values of Q_w, are very small. In case of the perforated rubber membrane mixer M1, the standard error for the values of Q_w fluctuated between 0.2% and 6.7% (1.8% in average). In case of the circumferential mixer M2, however, it fluctuated between 0.1% and 3.6% (0.9% in average). The standard error was also calculated with use of the computer software STATISTICA.

Using Form. (1) and the results of measurements of the air-water mix flow rate Q_w+Q_a, the efficiency of the investigated air lift pump (Fig. 1) was calculated for the perforated rubber membrane mixer (Fig. 2a, b) and the circumferential mixer (Fig. 2c, d).

Analysis of these results (Fig. 6) obtained for the perforated rubber membrane mixer M1 allows to state that the efficiency η of the air lift pump for the air-water mix delivery head H = 0.40 m decreased if the air flow rate Q_a, i.e. the established value of the air pressure p_a, increased.

For the air-water mix delivery head H equal to 0.80 m and 1.20 m, however, the efficiency η increased at the beginning, reaching a maximum value, then decreased. In the case of the air-water mix delivery head H = 0.40 m, the investigated air lift pump achieved the highest efficiency for the average air flow rate Q_a = 5.0 $m^3 \cdot h^{-1}$, i.e. for the air pressure specified as p_a = 110 kPa, and this efficiency amounted η = 9%. For the air-water mix delivery head H = 0.80 m, however, the respective values amounted Q_a = 8.23 $m^3 \cdot h^{-1}$, p_a = 120 kPa and η = 3.9% and for H = 1.20 m – Q_a = 11.77 $m^3 \cdot h^{-1}$, p_a = 135 kPa and η = 2.3%.

For the circumferential mixer M2, in turn, analysis of the obtained results (Fig. 6) allows to state that the efficiency η of the air lift pump decreased along with the increase of the air flow rate Q_a, i.e. the specified air pressure p_a, for all the air-water mix delivery heads H (0.40 m, 0.80 m, 1.20 m). In case of the air-water mix delivery heads H equal to 0.40 m and 0.80 m, the investigated air lift pump achieved the highest efficiency for the average air flow rate Q_a = 5.0 $m^3 \cdot h^{-1}$, hence the specified air pressure p_a = 105 kPa, and this efficiency was equal to η = 37% for H = 0.40 m and η = 21% for H = 0.80 m. For the air-water mix delivery heads H = 1.20 m, however, the investigated air lift pump achieved the highest efficiency for the average air flow rate Q_a = 8.28 $m^3 \cdot h^{-1}$, hence the specified air pressure p_a = 120 kPa, and this efficiency was equal to η = 4.4%.

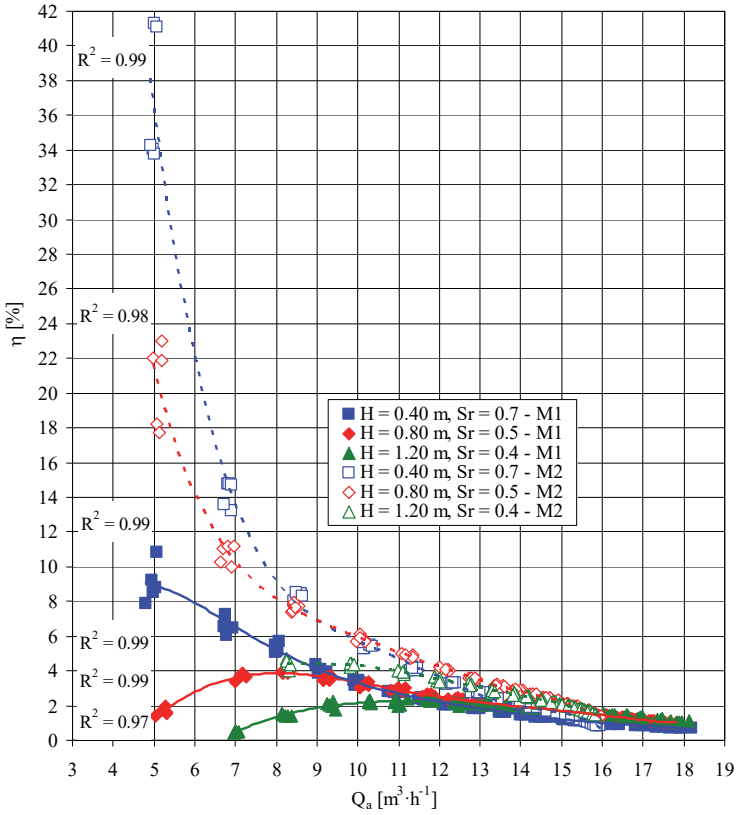

Fig. 6. Efficiency η of the air lift pump vs. air flow rate Q_a for the perforated rubber membrane mixer M1 and the circumferential mixer M2

For the analyzed air-water mix delivery heads H, the efficiency fall was evoked by the fact that when the air flow rate Q_a grew then more air bubbles appeared in the air lift pump discharge pipe occupying more space within the discharge pipe cross section and thus reducing the space occupied by water. The air flow rate increase in the discharge pipe evoked the water flow rate increase what, in turn, evoked the friction increase and fall in the efficiency of the investigated air lift pump. The efficiency η of the air lift pump for both of the mixer types decreased as well when the air-water mix delivery head H increased because the water flow rate Q_w decreased. For the air lift pump with the circumferential mixer, however, higher operational efficiency η was achieved than for the air lift pump with the perforated rubber membrane mixer.

As the differences between the mean values of the results of the air flow rate Q_a in case of the perforated rubber membrane mixer M1 and the air flow rate Q_a in case of the circumferential mixer M2 are statistically insignificant (Table 1), i.e. the mean values are statistically equal to each other, a statistical analysis was performed in aim to check whether the differences between the mean values of the water flow rate Q_w (Fig. 5) as well as the mean values of the efficiency η (Fig. 6) for the perforated rubber membrane mixer M1 and the mean values of the water flow rate Q_w as well as the efficiency η for the circumferential mixer M2 are statistically significant for the specified air-water mix delivery heads H equal to 0.40 m, 0.80 m, 1.20 m. Firstly, as earlier, the normality of distribution was checked with use of the Shapiro-Wilk test and then the homogeneity of variance with use of the Levene test. Calculations of normality of distributions and homogeneity of variances were made with the STATISTICA software. In both tests for individual groups the value of calculated probability $p_{cal.}$ is greater than the assumed significance level $\alpha = 0.05$, which means that the conditions of normal distribution and homogeneity of variance in the examined groups are satisfied. Then, the t-Student test for two populations was applied as well and a zero hypothesis was posed (H_0: $n_1 = n_2$) that the mean values of Q_w and the mean values of η are statistically equal, as well as an alternative hypothesis (H_1: $n_1 \neq n_2$) that the mean values of Q_w and the mean values of η are statistically different. Calculations of the t-Student statistics value $|t_{cal.}|$ were also performed with use of the computer software STATISTICA and the obtained results for the water flow rate are gathered in Table 3, whereas for the efficiency η – in Table 4.

Table 3. Results of calculations of the statistics for the t-Student test for Q_w. Differences between the mean values are significant with the probability $p < 0.05$

Parameter	H [m]	Mean	Standard deviation	Calculated value of the t-Student test $\|t_{cal.}\|$	Calculated probability value $p_{cal.}$	Value of the t-Student test read from the tables for $p = 0.05$ and $v = 36$ $t_{\alpha = 0.05}$
Q_w for M1	0.40	2.30	0.41	-4.998	$9.33 \cdot 10^{-5}$	2.028
Q_w for M2		2.60	0.19			
Q_w for M1	0.80	1.33	0.47	-31.899	$2.71 \cdot 10^{-17}$	
Q_w for M2		1.71	0.44			
Q_w for M1	1.20	0.87	0.37	-27,058	$1.00 \cdot 10^{-3}$	
Q_w for M2		1.17	0.28			

* M1 – perforated rubber membrane mixer, M2 – circumferential mixer

Table 4. Results of calculations of the statistics for the t-Student test for η. Differences between the mean values are significant with the probability $p < 0.05$

Parameter	H [m]	Mean	Standard deviation	Calculated value of the t-Student test $\|t_{cal.}\|$	Calculated probability value $p_{cal.}$	Value of the t-Student test read from the tables for $p = 0.05$ and $v = 36$ $t_{\alpha = 0.05}$
η for M1*	0.40	2.56	2.21	-3.562	$5.79 \cdot 10^{-4}$	2.028
η for M2*		4.87	8.27			
η for M1*	0.80	2.17	0.91	-2.200	$4.11 \cdot 10^{-2}$	
η for M2*		4.37	4.59			
η for M1*	1.20	1.68	0.48	-3.655	$1.96 \cdot 10^{-3}$	
η for M2*		2.57	0.96			

* M1 – perforated rubber membrane mixer, M2 – circumferential mixer

For the alternative hypothesis, a critical region $|t_{cal.}| \geq t_{\alpha=0.05}$ was determined and for $v = n_1 + n_2 - 2 = 36$ degrees of freedom and $\alpha = 0.05$, i.e. selected 5-percentage risk of error (significance level), the critical value $t_{\alpha=0.05} = 2.028$ was read from the *t*-Student distribution tables. Analysis of Tables 3 and 4 allows to state that $|t_{cal.}| \geq t_{\alpha=0.05}$, i.e. the zero hypothesis must be rejected, thus the differences between the mean values in the results of the air flow rate Q_w as well as the efficiency η for the perforated rubber membrane mixer M1 and the air flow rate Q_w as well as the efficiency η for the circumferential mixer M2 are statistically significant for the specified air-water mix delivery heads 0.40 m, 0.80 m and 1.20 m. This is also confirmed by the calculated probability value – $p_{cal.}$ is lower than 0.05 (assumed significance level, Tables 3 and 4).

The obtained results show that the type of an applied mixer strongly affects the flow rate and efficiency of the air lift pump – it is confirmed also by other scientists (Qiang et al. 2018, Ahmed et al. 2016).

5. Summary

In the investigated air lift pump, for both of the mixer types (perforated rubber membrane mixer and circumferential mixer), the air flow rate Q_a increased when the value of the air pressure p_a was specified on a higher level. When the air flow rate Q_a increased, the water flow rate Q_w also increased reaching maximum, then felt. For both of the mixer types, however, the water flow rate Q_w decreased when the air-water mix delivery head H increased.

In the investigated air lift pump with the discharge pipe with the internal diameter $d = 0.04$ m and constant discharge pipe submergence length $h = 0.80$ m,

for both of the mixer types, the water flow rate increased along with the increase of the air flow rate and it amounted between 5.0 $m^3 \cdot h^{-1}$ and 16.0 $m^3 \cdot h^{-1}$ in average for the perforated rubber membrane mixer and between 5.0 $m^3 \cdot h^{-1}$ and 15.0 $m^3 \cdot h^{-1}$ in average for the circumferential mixer. For higher air flow rates, however, the water flow rate decreased for both of the mixer types. In this respect, it is recommended that, during pumping in such a device, the air flow rate is no lower than 5.0 $m^3 \cdot h^{-1}$ and no higher than 16.0 $m^3 \cdot h^{-1}$ for the perforated rubber membrane mixer, whereas it is no lower than 5.0 $m^3 \cdot h^{-1}$ and no higher than 15.0 $m^3 \cdot h^{-1}$ for the circumferential mixer.

The efficiency η of the air lift pump for both of the mixer types decreased if the air-water mix delivery head H increased. For the air lift pump with the circumferential mixer, however, a higher efficiency η was achieved than for the air lift pump with the perforated rubber membrane mixer.

References

Ahmed, W.H., Aman, A.M., Badr, H.M., Al-Qutub, A.M. (2016). Air injection methods: The key to a better performance of airlift pumps. *Experimental Thermal and Fluid Science, 70*, 354-365.

Barrut, B., Blancheton, J-P., Champagne, J-Y., Grasmick, A. (2012). Mass transfer efficiency of a vacuum air lift – application to water recycling in aquaculture systems. *Aquacultural Engineering*, *46*, 18-26.

De Cachard, F., Delhaye, J. M. (1996). A slug-churn flow model for small-diameter airlift pumps. *International Journal Multiphase Flow*, *22(4)*, 627-649.

Esen, I. I. (2010). Experimental investigation of a rectangular airlift pump. *Advances in Civil Engineering*, ID 789547, 5, doi:10.1155/2010/789547.

Fan, W., Chen, J., Pan, Y., Huang, H., Chen, C-T. A., Chen, Y. (2013). Experimental study on the performance of air-lift pump for artificial upwelling. *Ocean Engineering*, *59*, 47-57.

Fujimoto, H., Murakami, S., Amura, A., Takuda, H. (2004). Effect of local pipe bends on pump performance of a small air-lift system in transporting solid particles. *International Journal of Heat and Fluid Flow, 25*, 996-1005.

Hanafizadeh, P., Ghanbarzadeh, S., Saidi, M. H. (2011). Visual technique for detection of gas–liquid two-phase flow regime in the air lift pump. *Journal of Petroleum Science and Engineering*, *75*, 327-335.

Hu, D., Tang, Ch., Ca, S., Zhang, F. (2012): The Effect of Air Injection Method on the Airlift Pump Performance. *Journal of Fluids Engineering*, *134*(11), 111302, DOI: 10.1115/1.4007592.

Kujawiak, S., Makowska, M., Matz, R. (2018). Hydraulic characteristics of the air lift pump. *Acta Scientiarium Polonorum, Formatio Circumiectus*, *17*(4), 85-95.

Kujawiak, S., Makowska, M., Mazurkiewicz, J. (2020). The Effect of Hydraulic Conditions in Barbotage Reactors on Aeration Effciency. *Water, 12*(3), 724-747.

Kalenik, M. (2014). Experimental investigations of interface valve flow capacity in the RoeVac type vacuum sewage system. *Environment Protection Engineering*, *40*(3), 127-138.

Kalenik, M. (2015a). Badania modelowe sprawności powietrznego podnośnika cieczy. *Ochrona Środowiska*, *37*(4), 39-46.

Kalenik, M. (2015b). Investigations of hydraulic operating conditions of air lift pump with three types of air-water mixers. *Annals of Warsaw University of Life Sciences – SGGW, Land Reclamation, 47*(1), 69-85.

Kalenik, M. (2015c). Empirical formulas for calculation of negative pressure difference in vacuum pipelines. *Water*, *7*(10), 5284-5304.

Kalenik, M. (2017). Badania modelowe strumienia objętości piasku i wody w podnośniku powietrznym. *Ochrona Środowiska*, *39*(1), 45-52.

Kalenik, M., Chalecki, M. (2018). Experimental Study of Air Lift Pump Delivery Rate. *Rocznik Ochrona Środowiska*, *20*, 221-240.

Kassab, S. Z., Kandil, H. A., Warda, H. A., Ahmedb, W. H. (2007). Experimental and analytical investigations of airlift pumps operating in three-phase flow. *Chemical Engineering Journal*, *131*, 273-281.

Kassab, S. Z., Kandil, H. A., Warda, H. A., Ahmed, W. H. (2009). Air-lift pumps characteristics under two-phase flow conditions. *International Journal of Heat and Fluid Flow*, *30*, 88-98.

Khalil, M. F.; Elshorbagy, K. A.; Kassab, S. Z.; Fahmy, R. I. (1999). Effect of air injection method on the performance of an air lift pump. *International Journal of Heat and Fluid Flow*, *20*, 598-604.

Kim, S. H., Sohn, C. H., Hwang, J. Y. (2014). Effects of tube diameter and submergence ratio on bubble pattern and performance of air-lift pump. *International Journal of Multiphase Flow*, *58*, 195-204.

Koda, E., Miszkowska, A., Sieczka, A. (2017). Levels of Organic Pollution Indicators in Groundwater at the Old Landfill and Waste Management Site. *Applied Sciences*, *7*(6), 638-660.

Mahrous, A.-F. (2014). Performance of airlift pumps: single-stage vs. multistage air injection. *American Journal of Mechanical Engineering*, *2*(1), 28-33.

Mahrous, A-F. (2013a). Experimental study of airlift pump performance with s-shaped riser tube bend. *International Journal Engineering and Manufacturing*, *1*, 1-12.

Mahrous, A.-F. (2013b). Performance study of an air-lift pump with bent riser tube. *Wseas Transactions on Applied and Theoretical Mechanics*, *8*(2), 136-145.

Mahrous, A.-F. (2012). Numerical Study of Solid Particles-Based Airlift Pump Performance. *Wseas Transactions on Applied and Theoretical Mechanics*, *7*(3), 221-230.

Meng, Q., Wang, C., Chen, Y., Chen, J. (2013). A simplified CFD model for air-lift artificial upwelling. *Ocean Engineering*, *72*, 267-276.

Nicklin, D.J. (1963). The air lift pump: theory and optimization. *Transactions of the Institution of Chemical Engineers*, *41*, 29-39.

Qiang, Y., Fan, W., Xiao, C., Pan, Y., Chen, Y. (2018). Effects of operating parameters and injection method on the performance of an artificial upwelling by using airlift pump. *Applied Ocean Research, 78*, 212-222.

Sawicki, J.M. (2004). Aerated grit chambers hydraulic design equations. *Journal Environmental Engineering*, *130*(9), 1050-1058.

Sawicki, J., Pawłowska, A. (1999). Energy balance for air lifting pumps. *Archives of Hydro-Engineering and Environmental Mechanics*, *46*(1-4), 63-72.

Tighzert, H., Brahimi, M., Kechroud, N., Benabbas, F. (2013). Effect of submergence ratio on the liquid phase velocity, efficiency and void fraction in an air-lift pump. *Journal of Petroleum Science and Engineering*, *110*, 155-161.

Wahba, E.M., Gadalla, M.A., Abueidda, D., Dalaq, A., Hafiz, H., Elawadi, K., Issa, R. (2014). On the performance of air-lift pumps: from analytical models to large eddy simulation. *Journal of Fluids Engineering*, *136*(11), 1-7.

Yoshinaga, T., Sato, Y. (1996). Performance of an air-lift pump for conveying coarse particles. *International Journal Multiphase Flow*, *22*(2), 223-238.

Abstract

The paper presents the analysis of results of investigations concerning an influence of applied constructive solutions on hydraulic operating conditions of a water-pumping air lift pump. The scope of the investigations encompassed the determination of flow rate and efficiency characteristics of an air lift pump having the discharge pipe with the internal diameter d = 0.04 m. The PM 50 mixer with a perforated rubber membrane, available on the market, as well as a mixer of own design, called circumferential mixer, were tested (the name origins from the fact that the mixer has the shape of a ring which encloses the discharge pipe on its whole circumference). The investigations were performed for three air-water mix delivery heads H: 0.40, 0.80, 1.20 m, for the specified pressure pipe submergence length h = 0.80 m. It has been stated that for both types of the applied mixers the water flow rate Q_w increased along with the increase of the air flow rate Q_a, reaching maximum, then decreased. However, in both of the applied mixers, the water flow rate Q_w permanently decreased as the air-water mix delivery head H increased. The air lift pump achieved higher water flow rate Q_w if the circumferential mixer was applied instead of that with perforated rubber membrane. It has been proved that for both of the applied types of mixers the air flow rate Q_a in the air lift pump cannot be lower during water pumping than 5.0 $m^3 \cdot h^{-1}$ and should not exceed 15.0 $m^3 \cdot h^{-1}$ in case of the circumferential mixer and 16.0 $m^3 \cdot h^{-1}$ for the perforated rubber membrane mixer. The efficiency η of the tested air lift pump for both of the applied types of mixers decreased when the air-water mix delivery head H increased. The higher efficiency η, however, was obtained for the air lift pump with the circumferential mixer than for the perforated rubber membrane mixer.

Keywords:
air lift pump, perforated rubber membrane mixer, circumferential mixer, two-phase flow

Badania modelowe wydajności i sprawności pracy powietrznego podnośnika z mieszaczem typu PM 50 i z mieszaczem obwodowym

Streszczenie

W artykule przedstawiono analizę wyników badań, dotyczących wpływu stosowanych rozwiązań konstrukcyjnych mieszaczy na hydrauliczne warunki pracy powietrznego podnośnika do tłoczenia wody. Zakres badań obejmował wyznaczenie charakterystyk wydajności i sprawności pracy powietrznego podnośnika o średnicy wewnętrznej rurociągu tłocznego d = 0,04 m. Do badań wykorzystano mieszacz dostępny na rynku typu PM 50 z perforowaną gumową membraną i mieszacz własnej konstrukcji, który nazwano mieszaczem obwodowym (nazwa pochodzi stąd, że ma on kształt pierścienia, który obejmuje rurociąg tłoczny na całym jego obwodzie). Badania wykonano dla trzech wysokości podnoszenia mieszaniny wody i powietrza H: 0,40, 0,80, 1,20 m, przy stałej długość zanurzenia rurociągu tłocznego h = 0,80 m. Stwierdzono, że dla obu zastosowanych typów mieszaczy natężenie przepływu wody Q_w rosło wraz ze wzrostem natężenia przepływu powietrza Q_a osiągając maksimum, a następnie malało. Natomiast w obu zastosowanych typach mieszaczy wraz ze wzrostem wysokości podnoszenia mieszaniny wody i powietrza H, natężenie przepływu wody Q_w tylko malało. Większą wydajność natężenia przepływu wody Q_w powietrzny podnośnik uzyskał z mieszaczem obwodowym niż z mieszaczem z perforowaną gumową membraną. Wykazano, że dla obu zastosowanych typów mieszaczy natężenie przepływu powietrza Q_a w powietrznym podnośniku podczas tłoczenia wody nie może być mniejsze niż 5,0 $m^3 \cdot h^{-1}$ i nie powinno przekraczać dla mieszacza obwodowego 15,0 $m^3 \cdot h^{-1}$, a dla mieszacza z perforowaną gumową membraną 16,0 $m^3 \cdot h^{-1}$. Sprawność pracy η badanego powietrznego podnośnika dla obu zastosowanych mieszaczy malała wraz ze wzrostem wysokości podnoszenia mieszaniny wody i powietrza H. Natomiast dla powietrznego podnośnika z mieszaczem obwodowym uzyskano większą sprawność pracy η, niż dla powietrznego podnośnika z mieszaczem z perforowaną gumową membraną.

Słowa kluczowe:
powietrzny podnośnik, mieszacz z perforowaną gumową membraną,
mieszacz obwodowy, przepływ dwufazowy

MIDDLE POMERANIAN SCIENTIFIC SOCIETY OF THE ENVIRONMENT PROTECTION

Rocznik Ochrona Środowiska

Volume 22. Year 2020 ISSN 1506-218X 475-487

Reducing Energy Demand in Liquefied Petroleum Gas Evaporation Processes

Sebastian Englart[*]*, Andrzej Jedlikowski,*
Wojciech Cepiński, Maciej Skrzycki
Wrocław University of Science and Technology, Poland
[*]*corresponding author's e-mail: sebastian.englart@pwr.edu.pl*

1. Introduction

Gaseous fuel remains a tremendously significant part of the traditional economy. Gas consumption can sufficiently satisfy many municipal, domestic, technological and industrial needs. Currently, this type of energy carrier can be divided into a group of natural and liquefied gases. Natural gas is traditionally a mixture of vapors and gases containing predominant amounts of methane (71–98%, for groups LS–E). Liquefied gas, however, contains primarily hydrocarbon compounds like propane and butane, the mixture of which is typically stored under pressure, usually in liquid form. Natural gas is typically used in areas with gas networks. On the other hand, in areas without access to this type of medium, it is possible to use liquid gas. Regardless of how the gas is stored, this type of energy carrier is considered as an environmentally-friendly, because it allows for the reduction of greenhouse gases, including CO_2 (Ekorynek.com 2018). In addition, there are no sulfur dioxide emissions during combustion, as it is with coal, coke and oil. For these energy carriers, gaseous fuels have significantly lowered emissions of nitrogen dioxide, carbon monoxide and PM10 particulate matter. Much attention has been paid to aspects related to the emission of pollutant in literature. Jerzak (Jerzak 2014) properly analyzed the effect of the CO_2 injection distance on the emissions of NO_X and CO during the combustion of natural gas in air enriched with oxygen up to 25%. Pathak et al. (Pathak et al. 2017) discussed the use of solar energy through seamless integration with existing heat source for a few processes involved in automobile industries. Wójcik et al. (Wójcik et al. 2017) presented an innovative mathematical model for the distribution of emissions from vehicles. Noch et al. (Noch et al. 2018) analyzed the emission of pollution to the atmosphere during the thermal energy production. Piątkowski and

Bohdal (Piątkowski & Bohdal 2011) investigated the influence of ecological properties of a spark-ignition engine powered by a propane-butane mixture.

It is also worth noting that gas is mainly used by various companies that care about sustainable development. This raw material is becoming increasingly popular due to the current limits of emission of pollution and penalties for exceeding them. The use of gas as an ecological fuel intentionally allows industrial plants to meet the requirements of specific regulations and concurrently to create an image of a socially responsible organization. In addition, it additionally allows for a significant reduction in the operating costs of heating systems. Modern gas appliances enable easy regulation and automation of the combustion process, which allows to obtain a high-energy effectiveness and uniform combustion parameters. Industrial plants often use a lot of energy. Its production with the use of conventional fuels (coal, coke, fuel oil) may have a negative impact not only on the environment, but also on the health of employees. This is a further argument in favor of replacing them with a gaseous fuel (Eko-rynek.com 2018).

2. Literature review

A standard form of using gaseous fuel is to deliver it via a gas distribution network (Englart et al. 2019). However, it is also possible to use liquid gas in its liquefied form. It is a product of a different kind than traditional fuels. At European level, it has been recognized as an alternative fuel and as a low-carbon, accessible and efficient energy carrier. The use of LPG should be promoted in order to ensure better air quality in Poland. It is also recommended to use this energy source more for heating purposes (POGP 2019). Liquefied form allows for storing large amounts of gas in smaller storage tanks, while allowing for its free transport. In the literature there are many possible solutions based on the practical use of liquefied gaseous fuel. Williams and Larson (Williams & Larson 2003) compared different direct and indirect liquefaction technologies for making fluid fuels from coal. Zakaria and Mustafa (Zakaria & Mustafa 2011) presented LPG characteristics in the cylinder during the exhaust process via modification of the existing composition design. Qeshta et al. (Qeshta et al. 2015) analyzed the effect of LPG sweetening process using tertiary alkanolamine. Barrera et al. (Barrera et al. 2012) performed the experimental analysis using absorption refrigeration advanced Solar cooperated with Generator Absorber eXchanger system. Dai et al. (Dai et al. 2018) presented a detailed investigation of an air-source liquefied petroleum gas – solar driven absorption heat pump using also Generator Absorber heat eXchanger. Shi (Shi 2012) presented an original model for the proper selection of LPG vaporization stations for storage tanks. Dolna and Mikielewicz (Dolna & Mikielewicz 2017) presented the numerical research on the ground coupled compressor heat pump operates under quasi-steady mode. The authors

analyzed the direct influence of a single field type vertical ground heat exchanger on the surrounding ground. Shi et al. (Shi et al. 2008) described a novel LPG gas supply system utilizing solar thermal energy. This authors system manages hot water produced by a solar water heating system as vaporization heat source and uses an electric heater as assisted heat source. Żuchowicki and Żuchowicki (Żuchowicki & Żuchowicki 2009) presented the selected problems of the gas systems reliability operation. Shi et al. (Shi et al. 2018) presented the transient behaviors of liquefied petroleum gas (LPG) natural vaporization in a cylinder using an experimentally validated model. Shi et al. (Shi et al. 2019) investigated a new LPG vaporization system utilizing direct-expansion solar-assisted heat pump for residential gas supply. In another paper, these authors (Shi et al. 2019) focused on the advancements and the current status of this system (DX-SAHPs). Han et al. (Han et al. 2017) performed thermal design optimization analysis for intermediate fluid vaporizer using liquefied natural gas. Shi et al. (Shi et al. 2019) claimed that integrating solar collector-evaporators with some modern technologies, such as photovoltaic, phase change material thermal storage and heat pipe, makes DX-SAHPs perform better under different climates and applications. Suslov et al. (Suslov et al. 2015) described an experimental heat pump unit for water thermal preparation in the closed water supply units.

This paper focuses on the more efficient use of renewable energy sources in the LPG vaporizer systems in moderate climate conditions. This process is typically used when the natural evaporation of gas in the storage tank is insufficient in relation to its demand. The use of such systems enables more efficient use of a low-emission and efficient energy carrier to supply gas systems with relatively high gas demand.

3. Operating principle of LPG vaporizer

The following method is commonly used to evaporate LPG: the gas in the liquid phase is supplied to the vaporizer, which raises its temperature and heats up the liquid phase above the boiling point at the discharge pressure. The liquefied gas is evaporated by indirect heating using hot water at a temperature from 40 to 85°C. (Pathak et al. 2017, Kowalczyk 2004). To ensure the precise interpretation of this process, the temperature range is shown in the diagram as evaporation temperature curves for propane, butane and their mixtures (Fig. 1). It is also worth noticing that the temperature range is directly related to the pressure range in the system components (tank, vaporizer, etc.). For example, the maximum overpressure in the above-ground storage tanks is 16 bar.

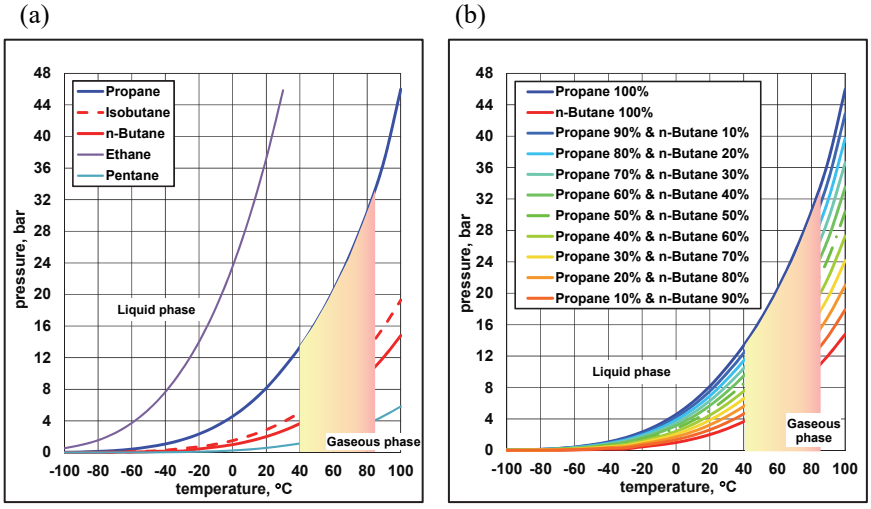

Fig. 1. Vapor pressure of selected Liquefied Petroleum Gases (Zajda & Tymiński 1999): (a) Propane, n-Butane and Isobutane, (b) mixtures of Propane and n-Butane

Depending on the method and the type of supply of the receivers, vaporizers are divided into two types: Feed-Back and Feed-Out. The first operates on the principle of gas-phase transmission through the vaporizer to the storage tank from where the gas is supplied to the gas system and the receiver. In the Feed-Out system, the gas from the vaporizer flows directly to the system and the receiver. The main advantage of the Feed-Back system is that it eliminates the direct consumption of gas in its liquid phase by the system by redirecting the gas from the vaporizer back to the gas storage tank. Also, the liquefied gas evaporation in the storage tank can be used to the maximum in this system. In Poland's climatic conditions, the Feed-Back system seems to be economically unjustified. At low outdoor temperatures, there will be large heat losses in the storage tank causing increased energy demand for gas heating. In Polish climatic conditions, the use of vaporizers in the Feed-Out system is recommended.

4. Requirements for the operating configuration of LPG vaporizers

Standard LPG systems provide an adequate amount of gas from natural evaporation through heat extraction from the wetted surface of the storage tank. Shi and others discussed a detailed description of the process of natural evaporation of gaseous fuel (Shi et al. 2018). The authors also pointed out the appropriate adjustment of the number of storage tanks to the liquid gas system. In their opinion, in the case of many storage tanks, a system with liquid phase consumption

and forced gas evaporation in the evaporator should be designed. This variant allows for a reduction the storage area of tanks. In addition to the technical factors, economic factors should also be considered (Shi et al. 2012). For this reason, electrical and water equipment solutions are available on the market. The first of them is typically used in systems with a lower power output and performance not exceeding 200 kg/h. Water devices are used in systems with a performance greater than 200 kg/h and whenever it is not possible to provide sufficient electrical power to supply the electrical vaporizer.

The vaporizers can be combined in a parallel arrangement. However, the fewer vaporizers work in a single battery, the easier it is to achieve a stable operation and the possibility of adjusting individual system parameters. For many industrial plants where there is no possibility of gas supply interruptions (e.g. glass factories, poultry farms) a more efficient solution is to use two smaller LPG vaporizers with less power than one more powerful vaporizer. Therefore, it is possible to use the power reserve to guarantee reliable operation of the system in case of a failure, malfunction or defect of the second vaporizer. The condition for proper operation of a system consisting of several vaporizers represents the selection of devices with the same power or effectiveness. Another necessary condition for the devices of this type working in a one system is to maintain the symmetry of the position of supply collectors and consumption of gas after the vaporizers. Moreover, the performance of vaporizer (in kg/h) should be 20-30% higher than the capacity of the receiver. The approx. 30% reserve guarantees more stable operation of both electric and water vaporizers and also is a safe reserve of energy in case of a sudden and unexpected high gas consumption, e.g. during the system start-up (Gasconcept Kurpińscy 2019).

5. Vaporizer supply options

Based on the analysis of vaporizer supply systems operation, solutions based on a conventional energy source (CES) were proposed. Vaporization of gaseous fuel taken from the gas storage tank takes place in a vaporizer supplied by a traditional high-temperature gas boiler (GB) (Fig. 2 (a)). This energy source can be replaced by a low-temperature gas boiler or a more efficient low-temperature condensing boiler or by a gas absorption heat pump (Fig 2 (b)). In this way, a system based on renewable energy source (RES) such as Ground Air Heat Exchanger (GAHE), Horizontal Heat Exchanger (HHE) or a Vertical Heat Exchanger (VHE) can be created (Fig. 2 (b)–(e)). Moreover, a solution using two cooperating lower heat sources (outside air and ground) allows creating a Multi-RES system (Fig. 2 (b)+(c)). The proposed solutions should be based on a vaporizer with an adequately larger heat exchange area and a design that ensures effective heating and effective gas evaporation.

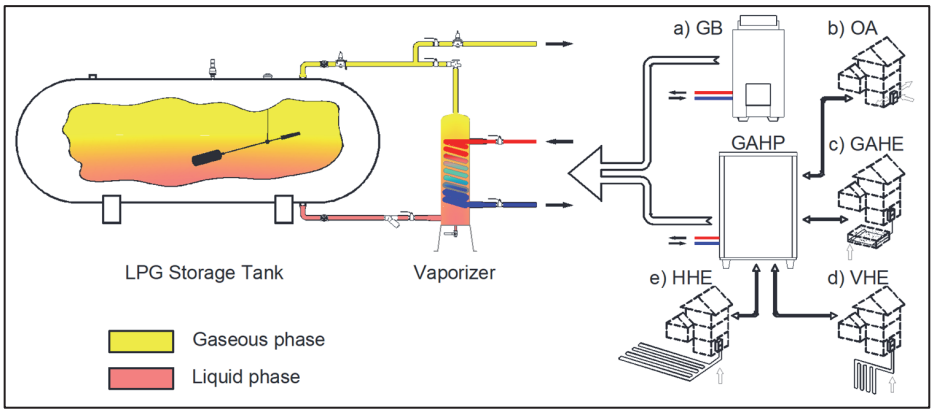

Fig. 2. Diagrams of considered gas vaporization systems equipped with: conventional energy source (a) GB, renewable energy sources: GAHP assisted by: (b) OA, (c) GAHE, (d) HHE, (e) VHE, (Abbreviations: GB – Gas Boiler, GAHP – Gas Absorption Heat Pump, GAHE – Ground Air Heat Exchanger, HHE – Horizontal Heat Exchanger, OA – Outdoor Air, VHE – Vertical Heat Exchanger)

6. Calculation results

The analysis was prepared as a variant for liquid gas evaporation systems using a vaporizer with a calculated performance 200 kg/h, which was supplied by the particular devices shown in Fig. 2. In the considerations, the parameters of the actual devices using only gaseous fuel were used, discussed in detail in the previous chapter. It was assumed that the tank is filled with propane, for which it was also assumed that it is necessary to heat the liquid phase in the vaporizer at outdoor air temperatures lower than 6°C. Because of the heat losses at low outdoor air temperature, it was assumed that the gas phase is heated to 20°C.

The calculations assume two modes of all-year-round operation:

- constant effectiveness for industrial applications,
- variable effectiveness for domestic needs (preparation of meals, heating and domestic hot water preparation).

The gas utilization effectiveness is expressed as the ratio of the heating performance of a whole device to the heat taken from the gas burner (calorific value of the gas). Fig. 3 shows the relation between the device's effectiveness for various system operating temperatures and outdoor air temperature for the considered types of gas devices cooperating with the vaporizer. In the analysis of all-year-round operation, the average times of occurrence of particular outdoor air temperatures at averaged relative air humidity for the city of Wrocław were also

used (Fig. 4). Next, the operation of gas vaporization systems for various assumed operation parameters (gas boiler, gas condensing boiler, absorption heat pump using energy from outdoor air or the ground – heat exchanger in three configurations: air and a system of horizontal and vertical heat exchangers) was compared (Fig. 2).

The following formula (1) was used to determine the annual gas consumption of individual devices $\dot{V}_a$ (m^3/h):

$$\dot{V}_a = \sum_{i=1}^{n} \frac{\tau_i \left[Q_V\left(t_o\right) + Q_P\left(t_o\right) \right] v_g}{\varepsilon_i\left(t_o\right)} \tag{1}$$

where:

$\varepsilon_i(t_o)$ – effectiveness of the device under outdoor air temperature conditions (according to Fig. 3); dimensionless,
τ_i – time of occurrence the outdoor air temperature (acc. to Fig. 4); h,
$Q_P(t_o)$ – heat of gas preheating at outdoor air temperature conditions; W,
$Q_V(t_o)$ – heat of gas vaporization at outdoor air temperature conditions; W,
ν_g – specific gas consumption coefficient; m^3/(h·W).

Heat of gas vaporization (2) can be expressed as follows:

$$Q_V\left(t_o\right) = \dot{m}_g \left[h_{Lp}\left(t_o\right) - h_{Gp}\left(t_o\right) \right] \tag{2}$$

where:

$\dot{m}_g$ – gas mass flow rate; kg/s,
$h_{Lp}(t_o)$ – specific enthalpy of liquid phase; J/(kg·K),
$h_{Gp}(t_o)$ – specific enthalpy of gaseous phase; J/(kg·K).

Heat of gas preheating (3) can be calculated as:

$$Q_P\left(t_o\right) = \dot{m}_g \left[h_{Gp}\left(20°\mathrm{C}\right) - h_{Gp}\left(t_o\right) \right] \tag{3}$$

where:

$\dot{m}_g$ – gas mass flow rate; kg/s,
$h_{Gp}(20°C)$ – specific enthalpy of gaseous phase at an outdoor air temperature of 20°C; J/(kg·K),
$h_{Gp}(t_o)$ – specific enthalpy of gaseous phase; J/(kg·K).

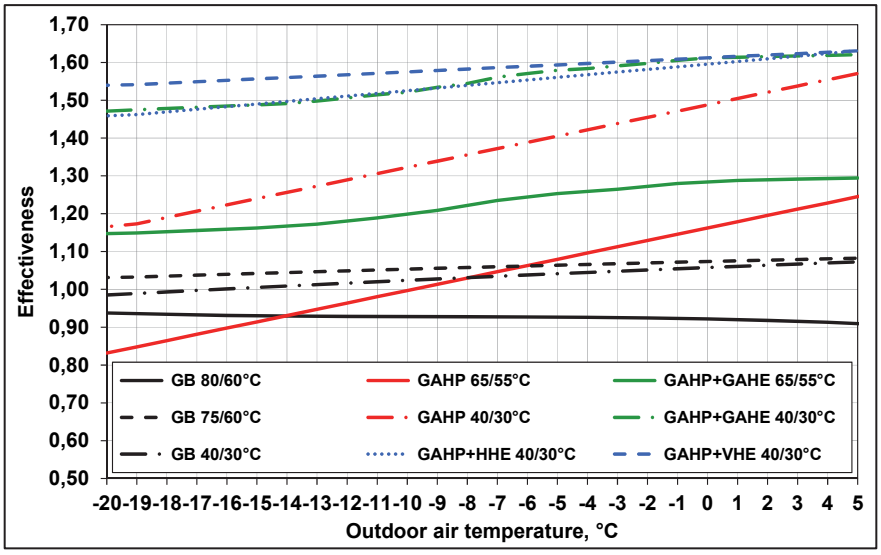

Fig. 3. Effectiveness of the considered gas vaporization systems expressed as a function of the outdoor air temperature, (Abbreviations: GB – Gas Boiler, GAHP – Gas Absorption Heat Pump, GAHE – Ground Air Heat Exchanger, HHE – Horizontal Heat Exchanger, OA – Outdoor Air, VHE – Vertical Heat Exchanger)

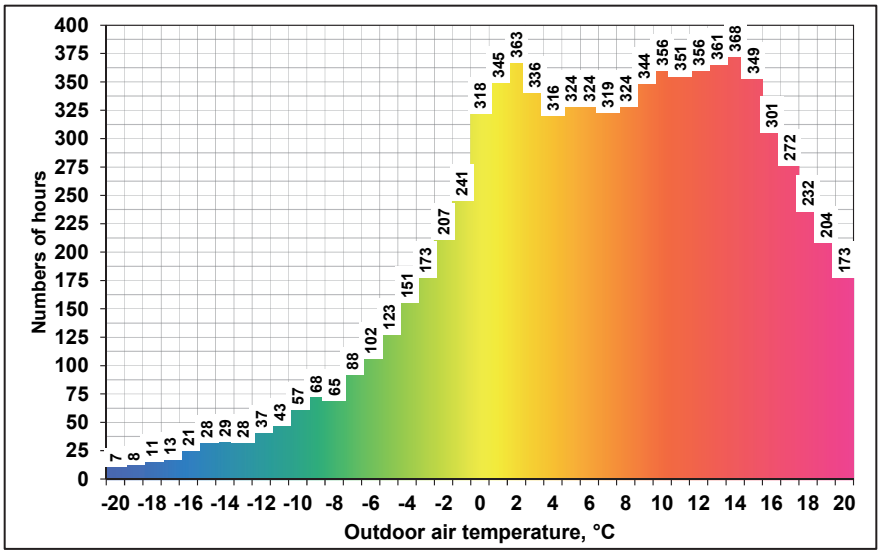

Fig. 4. Annual number of hours of occurrence of outdoor air temperature

It can be seen in Fig. 3 a simple replacement of the conventional energy source (gas boiler) with a condensing appliance increases the effectiveness of the entire system (from 0.90 to 1.10). Moreover, it is worth noting that the use of each of the renewable energy sources allows a noticeable increase in the effectiveness of the whole system (from 0.90 to 1.60).

Fig. 5 shows the results of a comparative analysis of the considered gas supply systems. The analysis was carried out in relation to a system based on a conventional gas boiler operating at standard parameters (80/60°C).

As can be seen, the use of proposed systems: GB (condensing boiler), GAHP or GAHP with GAHE, VHE or HHE can result in energy savings in gas consumption (from 14% to 42% per year, depending on the profile of gas consumption).

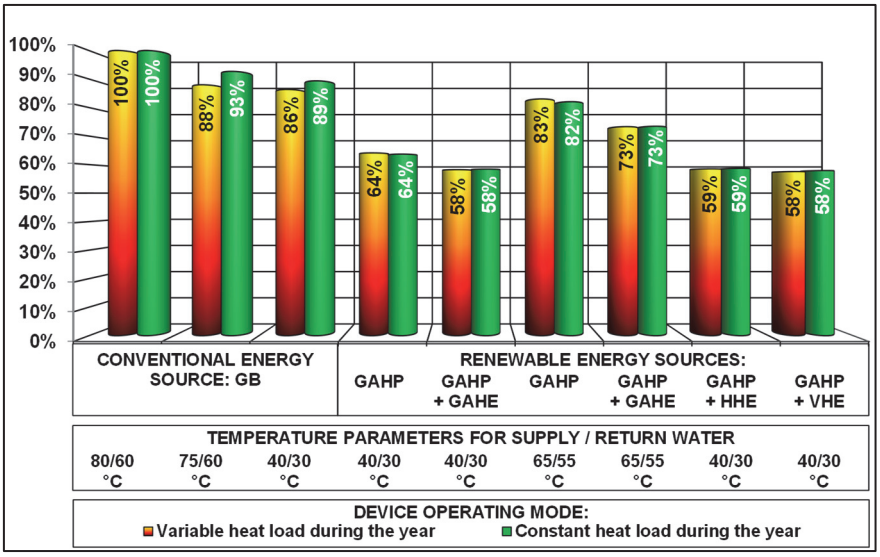

Fig. 5. Comparison of percentage gas demand of considered gas vaporization systems with respect to the conventional energy source (gas boiler operating under temperature parameters 80/60°C)

In terms of purchasing costs, the most effective solution is to use a condensing boiler operating at low temperature conditions (40/30°C), where gas consumption can be reduced by up to 14%. Otherwise, in the context of the gas demand, the most economic system is GAHP, which can work with GAHE with VHE or HHE. In this case, it is possible to reduce gas consumption by up to 42%.

7. Conclusions

In comparison to the classic and currently commonly used systems, the alternative solutions based on modern gas devices and renewable energy presented in the paper, show considerable potential for energy savings in liquid gas evaporation systems for the gas supply to various facilities.

The analysis of energy generation using low-temperature gas boilers, gas absorption heat pumps and heat pumps with combination with various lower heat sources convinces the advisability of undertaking the subject of research.

It has been demonstrated that the proposed solutions can significantly reduce the energy consumption for the evaporation of liquefied petroleum gas in an environmentally friendly way by exploiting the energy potential of its natural resources.

In addition, gas absorption heat pumps can be used to efficiently produce coolant for both production and social needs (e.g. for cooling of offices) during the summer when natural evaporation is sufficient and there is no need to start up the vaporizer. This allows for the purchase of smaller cooling devices and the reduction of electricity demand during warm periods throughout the year.

The analysis leads to the following conclusions:

- replacing the traditional gas boiler with a low-temperature gas boiler working with a larger heat exchanger (larger heat exchange area and higher heating power) allows reducing the energy demand from 7% to 14%,
- it is possible to reduce gas consumption to 36% by using gas heat pumps in comparison to the conventional energy sources,
- expansion of the heat pump system with ground heat exchanger, vertical or horizontal heat exchangers allows for gas savings of up to 42%,
- the analyses confirm the need for further research on other solutions based on renewable energy sources to achieve greater energy savings.

References

Barrera, M.A., Best, R., Gómez, V.H., Garcia-Valladares, O., Velázquez, N., Chan, J. (2012). Analysis of the Performance of a GAX Hybrid (Solar - LPG) Absorption Refrigeration System Operating with Temperatures from Solar Heating Sources. *Energy Procedia, 30*, 884-892.

Dai, E., Lin, M., Xia, J., Dai Y. (2018). Experimental investigation on a GAX based absorption heat pump driven by hybrid liquefied petroleum gas and solar energy. *Solar Energy, 169,* 167-178.

Dolna, O., & Mikielewicz, J. (2017). Studies on the Field Type Ground Heat Exchanger Coupled with the Compressor Heat Pump (Part 1). *Rocznik Ochrona Środowiska, 19,* 240-252.

Ekorynek.com. (2018). Ekologiczne paliwo XXI wieku. (Accessed 05.12.2019). http://www.ekorynek.com/index.php/eko-moto/236-ekologiczne-paliwo-xxi-wieku.

Englart, S., Jedlikowski, A., Cepiński, W., Badura, M. (2019). Renewable energy sources for gas preheating. *E3S Web of Conferences, 116, 00019*, 1-8.

Gasconcept Kurpińscy, Parowniki. (Accessed 05.12.2019) http://www.gasconcept.com/oferta/parowniki/parowniki-informacje-ogolne.html

Han, H., Yan, Y., Wang, S., Li Y.-X. (2017). Thermal design optimization analysis of an intermediate fluid vaporizer for liquefied natural gas. *Applied Thermal Engineering, 129,* 329-337.

Jerzak, W. (2014). Emissions of NO_x and CO from Natural Gas Combustion with Adding CO_2 at Varying Distances from the Burner. *Rocznik Ochrona Środowiska, 16*, 148-160.

Kowalczyk, M. (2004). *Gazowe i elektryczne promienniki podczerwieni*. Gdańsk: ZNTC Solaren.

Noch, T., Mikołajczewska, W., Wesołowska, A., Friedberg, A. (2018). Analiza emisji zanieczyszczeń w wyniku wytwarzania energii cieplnej. *Rocznik Ochrona Środowiska, 20*, 1181-1198.

Pathak, A., Deshpande, K., Jadkar, S. (2017) Application of Solar Thermal Energy for Medium Temperature Heating in Automobile Industry. *IRA-International Journal of Technology & Engineering, 7,* 19-33.

Piątkowski, P., & Bohdal, T. (2011). Badanie właściwości ekologicznych silnika samochodowego o zapłonie iskrowym zasilanego mieszanką propan-butan. *Rocznik Ochrona Środowiska, 13*, 607-618.

POGP Polska Organizacja Gazu Płynnego (2019). Raport roczny 2018, Warszawa.

Qeshta, H., Abuyahya, S., Pal, P., Banat, F. (2015). Sweetening liquefied petroleum gas (LPG): Parametric sensitivity analysis using Aspen HYSYS. *Journal of Natural Gas Science and Engineering, 26,* 1011-1017.

Shi, G. (2012). Cost Optimal Selection of Storage Tanks in LPG Vaporization Station. *Natural Resources, 03*, 164-169.

Shi, G., Jing, Y., Gao, Y. (2008). A liquefied petroleum gas gasification system utilizing solar thermal energy. *3rd IEEE Conference on Industrial Electronics and Applications. IEEE, Singapore*, 1668-1673.

Shi, G.H, Aye, L., Dai, R., Du, X.J., Wang, J.J. (2019). Dynamic modelling and performance evaluation of a direct-expansion solar-assisted heat pump for LPG vaporisation applications. *Applied Thermal Engineering, 149*, 757-771.

Shi, G.H,, Aye, L., Li, D., Du, X.J. (2019). Recent advances in direct expansion solar assisted heat pump systems: A review. *Renewable and Sustainable Energy Reviews, 109,* 349-366.

Shi, G.H., Aye, L., Liu, Y.C., Du, X.J. (2018). Dynamic simulation of liquefied petroleum gas vaporisation for burners, *Applied Thermal Engineering, 137*, 575-583.

Suslov, A., Fatychov, J., Ivanov, A. (2015). Energy Saving Technologies with the Use of Heat Pumps. *Annual Set The Environment Protection, 17*, 200-208.

Williams, R.H., & Larson, E.D. (2003). A comparison of direct and indirect liquefaction technologies for making fluid fuels from coal. *Energy for Sustainable Development, 7,* 103-129.

Wojcik, W., Adikanova, S., Malgazhdarov, Y.A., Madiyarov, M.N., Myrzagaliyeva, A.B., Temirbekov, N.M., Junisbekov, M., Pawłowski, L. (2017) Probabilistic and Statistical Modelling of the Harmful Transport Impurities in the Atmosphere from Motor Vehicles. *Rocznik Ochrona Środowiska, 19,* 795-808.

Zajda, R., & Tymiński, B. (1999). *Instalacje i urządzenia gazowe*, Warszawa: Centrum Szkolenia Gazownictwa.

Zakaria, Z., & Mustafa, A. (2011). The Influence of compositions on liquefied petroleum gas residue in storage. *International Journal of Research and Reviews in Applied Sciences, 7,* 360-367.

Żuchowicki, A.W., & Żuchowicki, J. (2009). Wybrane problemy zaopatrzenia w gaz jednostek osadniczych w Polsce. *Rocznik Ochrona Środowiska, 11,* 267-279.

Abstract

The paper discusses the use of renewable energy sources for the LPG vaporizer systems in a moderate climate. The presented alternative solutions based on modern gas devices and renewable energy show great potential for energy savings in liquid gas evaporation systems in comparison to classical and currently commonly used systems. It has been demonstrated that the proposed solutions can significantly reduce the consumption of energy used to evaporate LPG in an environmentally friendly manner. The use of gas heat pumps in relation to a traditional energy source enables gas consumption to be reduced to 36%. The extension of the heat pump system with ground air heat exchanger or with vertical or horizontal heat exchangers, allows savings in gas consumption up to 42%. Moreover, the application of such systems enables more effective use of low emission and efficient heating medium in gas systems. In addition, in summer, when there is no need to evaporate the liquefied gas, these devices can be used to cold-production for, social and living needs.

Keywords:
energy savings, LPG, vaporization technologies, heat pump, renewable energy

Obniżenie zapotrzebowania na energię w procesach odparowania skroplonego gazu

Streszczenie

W artykule omówiono wykorzystanie odnawialnych źródeł energii w układach parowników LPG w klimacie umiarkowanym. Przedstawione alternatywne rozwiązania oparte na nowoczesnych urządzeniach gazowych i energii odnawialnej wykazują duży potencjał oszczędności energii w instalacjach odparowania gazu płynnego w porównaniu z klasycznymi i obecnie powszechnie stosowanymi systemami. Wykazano, że proponowane rozwiązania mogą znacząco ograniczyć zużycie energii wykorzystywanej do odparowania LPG w sposób przyjazny dla środowiska. Zastosowanie gazowych pomp ciepła w stosunku do tradycyjnego źródła energii pozwala na redukcję zużycia gazu do 36%. Rozbudowa systemu pomp ciepła o pojedynczy gruntowy powietrzny wymiennik ciepła lub dodatkowo współpracujący z pionowymi, lub poziomymi systemami odwiertów

umożliwia uzyskanie oszczędności zużycia gazu sięgających nawet 42%. Ponadto zastosowanie takich systemów pozwala na bardziej efektywne wykorzystanie niskoemisyjnego i wydajniejszego czynnika grzewczego w systemach gazowych. Ponadto w okresie letnim, kiedy nie ma potrzeby odparowywania skroplonego gazu, urządzenia te mogą być wykorzystywane do produkcji „chłodu" przeznaczonego na potrzeby społeczne oraz bytowe.

Słowa kluczowe:
oszczędność energii, LPG, technologie odparowania, pompa ciepła, energia odnawialna

MIDDLE POMERANIAN SCIENTIFIC SOCIETY OF THE ENVIRONMENT PROTECTION

Rocznik Ochrona Środowiska

Volume 22. Year 2020 ISSN 1506-218X 488-513

Assessment of Different Doses of Sewage Sludge Application on Virginia Fanpetals Biomass Feedstock Production

Barbara Kołodziej[1], Jacek Antonkiewicz[2]*

[1]University of Life Sciences in Lublin, Poland

[2]Agricultural University in Kraków, Poland

[*]corresponding author's e-mail: barbara.kolodziej@up.lublin.pl

1. Introduction

Poland is a country where two-thirds of energy comes from coal mining, and the other energy sources are a.a. hydroelectric and wind plants and lately – solid biomass, liquid biofuels and biogas (Igliński et al. 2011). Biomass incineration or co-incineration makes above 80% of renewable energy. Technical potential of biomass in Poland is estimated at approximately 900 PJ year^{-1}, being the highest in the case of forest and agriculture origin biomass. Straw, cereal, rapeseed, wastes from agro-food and wood industries as well as dedicated energy plantations give the greatest potential for energy production. Agricultural and natural-environmental determinants permit energy crops cultivation at the area estimated from 1.6 to 2.0 million ha, which by 2020 could increase to approximately 2.9 million ha (Bartoszewicz-Burczy 2012). Thus, there is a need to enlargement the surface area by introducing the cultivation of new crops such as Virginia fanpetals (Slepetys et al. 2012, Matyka 2013, Szyszlak-Bargłowicz 2014, Nahm & Mohrat 2018, von Gehrena et al. 2019). However, it is worth mentioning that energy crops even though do not compete directly with food crops, use the same land resources, sometimes of high ecological value.

Virginia fanpetals (*Sida hermaphrodita* Rusby) is a perennial energy plant from Malvaceae family, originated from the southern states of the USA and occurring in the natural state in the North and South America, Africa and Asia (Borkowska 1991, Borkowska & Styk 2006, Borkowska & Molas 2012, Nahm & Mohrat 2018). It is classified as a highly endangered species in its original habitat (Spooner et al. 1985). *S. hermaphrodita* is a species with wide possibilities of use, however almost unknown outside of Europe (Borkowska & Molas 2013,

Matyka & Kuś 2018, Nahm & Mohrat 2018). Due to the considerable fiber content in the stems, originally it was used by Indians as a fiber plant, however, fiber is of poor quality (Spooner et al. 1985). It belongs to melliferous plants that is also suitable for covering slopes, soils exposed to erosion. Due to good performance and quality bleached cellulose can be used in the pulp and paper industry. Seeking is also as a raw material for the pharmaceutical industry and feed for animals (Borkowska 1991, Borkowska & Styk 2006, Matyka & Kuś 2018). Its stalks can be subjected also to direct combustion (the biomass can be granulated easily during pellets and briquettes production), conversion to bioethanol or as a substrate for biogas production (Borkowska & Molas 2013; Jasinskas et al. 2014, Szempliński et al. 2014, Šiaudinis et al. 2015). That species was introduced from the USA (via USSR) to Poland in the 1950s and now is cultivated at the area of about 300 hectares (Borkowska & Styk 2006, Borkowska & Molas 2012, Nahm & Mohrat 2018, von Gehrena et al. 2019), however potential area designated for cultivation of Virginia fanpetals for energy purposes is estimated at above 2.4 million ha (Jadczyszyn et al. 2008). Recently new plantations of this species arose in Germany, Romania and Lithuania (Jasinskas et al. 2014, Kurucz et al. 2014, Barbosa et al. 2014, Franzaring et al. 2014, Nahm & Mohrat 2018).

Virginia fanpetals is a plant having relatively low input requirements, great potential for C mitigation, drought tolerance and ability to maintain high yields under a wide range of environmental conditions. This species has low requirements for soil fertility and efficiently use water. It is a plant capable of generative (direct seeds sowing or by seedlings) and vegetative reproduction (through root sections, parts of the bush or rooted herbaceous stems), however so far there is no practical experience using *in vitro* biotechnology method (Borkowska & Styk, 2006, Borkowska & Molas 2012, Kurucz et al. 2014, Augustynowicz et al. 2008, Matyka & Kuś 2018, Nahm & Mohrat 2018).

Annual yields of *S. hermaphrodita* range from 10 to above 20 Mg ha^{-1} DM and over 220-400 GJ ha^{-1} a^{-1} and the similar yields of cellulose-ethanol per hectare as switchgrass (Borkowska & Molas 2012, 2013). The full establishment of *S. hermaphrodita* stand takes from 2 to 3 years, depending on the climatic conditions, but productive life span its estimated between 15 and 20 years (Borkowska & Styk 2006, Borkowska et al. 2009, Borkowska & Molas 2012, Nahm & Mohrat 2018).

Although Virginia fanpetals has many traits that make it ideal for biofuel production, environmental and management conditions can affect its productivity (Matyka 2013, Borkowska 1991, Borkowska & Molas 2012, Kalembasa & Wiśniewska 2006, Kuś & Matyka 2009, Strzelczyk 2013, Matyka & Kuś 2018, Nahm & Mohrat 2018). Virginia fanpetals can produce much higher biomass yield after applying fertilizer, e.g. municipal sewage sludge, which is the source of many valuable nutrients and has a value close to the manure, however contains

a number of potentially harmful constituents such as heavy metals (Borkowska & Wardzinska 2003, Singh & Agrawal 2008, Seleiman et al. 2013, Gondek et al. 2014). The use of sewage sludge could not only increase yields but also positively affects biological and physico-chemical properties of the soil profile (Singh & Agrawal 2008, Seleiman et al. 2013, Casado-Vela et al. 2006, Usman et al. 2012). Hence the interest in the use of sewage sludge in the cultivation of energy crops such as Virginia fanpetals has been studied by many authors (Augustynowicz et al. 2008, Strzelczyk 2013, Borkowska & Wardzińska 2003).

Thus, the main limiting factors in widespread production of this species are: low germination capacity, lack of plantlets or root cuttings mechanical system or large-scale technology, lack of chemical weed control or pests management and inadequate information about fertilization and ecological requirements (Kurucz et al. 2014). In order to expand and complete the missing information about *S. hermaphrodita* culture a six-year field experiment was established, aiming to determine the effect of increasing municipal sewage sludge doses on Virginia fanpetals yielding and biomass quality as well as indicate an optimal dose to minimize an environmental impact but guaranty sufficient yield. We assumed that due to the fact that this species is not used for food production, municipal sewage sludge could be used for its fertilization as a valuable source of minerals, preferably affecting plant growth and development. Additionally, efforts were made to assess sewage sludge impact on chemical composition and structure of the experimental plant yield and selected physico-chemical properties of the soil. The study also attempted to determine the best method of Virginia fanpetals plantation establishment (by roots sections or plantlets) in the conditions of south-eastern Poland and indicate the optimum harvest date of its biomass (autumn, winter and spring).

2. Materials and methods

This experiment is a part of long-term research on sewage sludge application in ten, different species of energy plants cultivation, aiming at finding the most suitable one for phytoremediation and at the same time characterizing by favorable energy parameters.

2.1. Experimental site and design

A six year (2008-2013) field studies were established at the landfill belonging to the Janów Lubelski Department of Public Utilities in south-eastern Poland (50°43'17.7"N 22°22'08.0"E). The soil was a clay loam belonging to Cambisols, which was characterized by slightly acidic pH (6.29), average humus content (1.45%), low phosphorus (30.09 $mg \cdot kg^{-1}$ DM), potassium (91.3 $mg \cdot kg^{-1}$ DM) and magnesium (27.6 $mg \cdot kg^{-1}$ DM) content and the heavy metal content remained at the natural level (Kabata-Pendias 2011). The average air temperature

recorded in sorghum vegetation period in 2008-2013 was higher than the average of long-term period by 1°C, while the total precipitation exceeded the average by 334 mm. However, each of the years of the experiment were characterized by considerable variability. The lowest rainfall and air temperature was marked by the first year of the experiment, while the best conditions for the growth and development of sorghum was recorded in 2010. The complete characteristic of soil and meteorological conditions were described in our previous papers (Kołodziej et al. 2015, 2016).

The experiment design was a split-split-plot based on randomized complete block design with three replications. Main plots were five doses of sewage sludge, two methods of plantation establishment were sub plots, while three harvest dates were arranged in sub-sub plots. Rows were 0.75 cm apart and each split-split plot was 4.8 m long for a harvest area of 14.4 m^2. Prior to the study the field was fallow, without conventional disk tillage. In September 2007 municipal sewage sludge was applied in doses according to experiment design and mixed with a topsoil. In spring 2008, several weeks before planting, the seedbed was prepared by tilling with a moldboard plow and disk harrow. The experiment was established as follows: 24 April 2008 by planting roots sections (vegetatively) and 15 May 2008 by planting the seedlings of Virginia fanpetals (generatively) at spacing of 0.75×0.4 m (33 325 units ha^{-1}). Seedlings of Virginia fanpetals were produced in multi-cell trays located in an unheated greenhouse from early April to mid-May and were transplanted to the field after the spring frost. The experiment comprised five levels of municipal sewage sludge (main plots), three dates of biomass harvesting (split-split plots) and two methods of plantation establishment – split plots – (from seeding of root stock (parts of roots) and the nurse-in-tray plantlets production). Roots used as a rootstock for vegetative propagation were 8-12 cm long with several buds, while in the case of generative propagation, seeds were sown in the multi-cell trays in the first decade of April (2-3 seeds per cell) and kept in an unheated greenhouse. After emergence, one plant per cell was left for further growth. Peat moss was the substrate for seedlings produced in multi-cell trays (cell dimension 4×4×6 cm). At the phase of 3-4 leaves (mid-May), they were transplanted into the field along with substrate clods. Single split-split plot (3.0×4.8 m) comprised 4 rows (interrows of 0.75 m) with 12 plants per row (0.4 m between plants in row).

Sewage sludge were applied only once, before experiment establishment at four rates: I – 60 Mg ha^{-1} DM; II – 40 Mg ha^{-1} DM; III – 20 Mg ha^{-1} DM; IV – 10 Mg ha^{-1} DM; control objects were not fertilized with sewage sludge: V – 0 Mg ha^{-1} DM. In the experiment, compressed and stored for 1 year in a lagoon municipal sewage sludge was used. Municipal sewage sludge characteristic: pH_{KCl} – 6.04; dry matter – 13.3%; organic matter – 59.4% DM; total N content – 7.45%; N ammonium content – 2.35%; available forms of: P –

2.25mg·kg^{-1} DM; Mg – 0.28 mg·kg^{-1} DM; Ca content – 0.29 mg·kg^{-1} DM; general forms of: Cd – 2.35 mg·kg^{-1} DM, Pb – 42.9 mg·kg^{-1} DM, Ni – 14.8 mg·kg^{-1} DM, Cr – 25.4 mg·kg^{-1} DM, Hg – 1.12 mg·kg^{-1} DM, Zn – 1005 mg·kg^{-1} DM, Cu – 111 mg·kg^{-1} DM. The sewage sludge was characterized by relatively low content of heavy metals compared to that found in the literature (Singh, Agrawal, 2008; Usman et al., 2012). Due to the high water content, it had been mixed with topsoil in the autumn of 2007. In addition, due to the low levels of potassium in the soil and in the sludge a supplemental fertilization with 100 kg K ha^{-1} was applied to all plots. A twice mechanical weeding were applied during the first growing season, while in the subsequent years plants covered the inter-rows and weeds were removed incidentally.

2.2 Sampling and analytical methods employed

In order to check the dynamics of dry matter content in the biomass and indicate the best date of biomass harvesting in terms of energy use (for combustion) there were used three harvest dates: autumn (beginning in November, after the first frost), winter (mid-January) and spring one (end of March following the growing season). Plants were harvested using hand implements at a stubble height of ca. 10 cm and stems were counted in the plots. During autumn biomass harvesting, two weeks before plants cutting, a biometric measurements were performed (height and diameter at the base of 10 stems per plant as well as weight of stems and leaves per single plant of five randomly selected plants in each plot). After that, dry biomass yield was determined and all aerial biomass from plot was chopped in a commercial chipper shredder Bear Cat 70080 s-8HP (Colorado, USA) and three subsamples (600 g, 1000 g and 2000 g) were taken. 600 g subsamples were collected in a paper bag and dried in an air force oven at 70°C for 48 h in order to adjust fresh mass to a dry matter basis, 2000 g subsamples of Virginia fanpetals feedstock obtained vegetatively (by roots sections) collected in autumn were used for its energy characteristics (placed in aplastic bags), whereas three 1000 g subsamples from each plot were taken for chemical analysis and dried at 70°C for 48 h in a paper bag. That subsamples was ground in a laboratory mill to pass a 1.0 mm (20 mesh) screen and analyzed for macronutrients by ICP-AES and total nitrogen content – by Kjeldahl method and phosphorus by spectrophotometer (Ostrowska et al. 1991, Nelson & Somers 1975, Jones & Case 1991). In order to assess the suitability of the test plants for disposal of sewage sludge an index of bioaccumulation (IBA) as a ratio of element concentration in Virginia fanpetals plants to element concentration in soil was calculated. For evaluation a four-scale bioaccumulation rate were adopted, where 0.001-0.01 was the lack of bioaccumulation, the bioaccumulation index 0.01-0.10 – a slight degree of bioaccumulation, 0.1-1.0 – a medium degree of bioaccumulation, the rate of 1.0-10.0 – an intensive degree of bioaccumulation (Kabata-Pendias 2011). In

the collected just after the autumn harvest and placed in a plastic bags 2000 g sample of raw material the moisture content (EN-14774-1), ash content (EN 14775), sulfur content (EN 15289) as well net calorific value (in a calorimetric bomb LECO AC 500) in accordance with the requirements of EN 14918 were also determined. Additionally, the primary energy yield was calculated as a product from the dry biomass yield and net calorific value.

Furthermore, soil samples were collected each autumn (acc. to ISO 10381-5:2005) from the layer of 0-20 cm, separately for each plot, dried and sieved (2 mm) for analytical purposes. In the soil were determined: pH by potentiometry, hydrolytic acidity by Kappen method, organic carbon by Tiurin method, total nitrogen by the Kjeldahl method, available phosphorus and potassium using the Egner-Riehm method, and magnesium absorbed by Schachtschabel method (Ostrowska et al. 1991, Jones & Case 1991).

2.3. Statistical analysis

Plant characteristics, macronutrient content, and yield changes due to the sludge dose, method of plantation establishment, harvesting date and their interactions over the course of the experiment were analyses were carried out using the Statistica 6.0 software programme. For soil characteristics and bioaccumulation index differences between means of treatments were compared by Tukey's test. Prior to the analysis, all data were tested for normality with the Shapiro-Wilk test. Homogeneity of variance was checked using Levene′s test. Statistical analysis (ANOVA at the 0.05 confidence limit followed by a Tukey post hoc test) were conducted with sewage sludge dose (as a whole plot effect), plantation establishment method (split effect) and harvest date (split-split effects).

3. Results and discussion

3.1. Virginia fanpetals yield and characteristic

Across the 6-year period, we observed a tendency of increasing plant size and weight in successive years of cultivation (Table 1). The average final height of Virginia fanpetals reached 2.8-3.0 m, which was in accordance with Borkowska et al. (2009), Kuś & Matyka (2009), Slepetys et al. (2012), Matyka (2013), Matyka & Kuś (2018) as well as Franzaring et al. (2014) indications. There was noted a clear trend to increase Virginia fanpetals height along with increasing sewage sludge dose (up to 288 cm across the 6-year period – Table 1). Plants reached maximum height in the fourth year, whereas the lowest ones were recorded in the first year of the experiment. In the fifth year of vegetation, plants created a big number of shorter and thinner stems than in the previous and next year, probably due to unfavorable weather conditions (water shortage in the soil, as a result of 39% lower rainfall during July and August). It is consistent with

Borkowska & Molas (2012) as well as Kuś & Matyka (2009) indications, who showed that Virginia fanpetals productivity significantly depended on the precipitation.

Average height of plants grown on plots where vegetative propagation (roots) were used for plantation establishment was significantly higher than those with generative propagation method (plantlets), likewise in Borkowska and Wardzińska (2003) research. Stem number per plant reached 11-17 units plant^{-1}, while basal stem diameter changed from 23 mm in the first year to 13-16 mm in subsequent years, and was larger than in Borkowska (1991) study with a frequent cutting as a fodder, but comparable to Matyka (2013) as well as Kuś & Matyka (2009) and Matyka & Kuś (2018) findings. Across the 6-year period, the average number of stems increased significantly, from approximately 3 stalks per plant in the first year, to about 14-17 stems per plant in the last two years of vegetation, which was in accordance with Borkowska & Wardzińska (2003), Borkowska et al. (2009) and Borkowska & Molas (2012) findings, but those latter authors noted a significantly higher number of stems per plant in the fifth and sixth years of vegetation. We observed a significantly higher number of stems in the case of plants grown on plots with root cuttings planting, which were better developed (higher, thicker and heavier) than on plots with seedlings planting and a tendency to increase stems number per plant along with increasing sewage sludge dose.

The average dry weight of aboveground parts of plant from a single plant comprised within the range of 176 in the first year of vegetation to 639 g plant^{-1} in the sixth year of culture, which was consistent with the results of Barbosa et al. (2014) studies. Total dry weight of single Virginia fanpetals plant increased significantly along with increasing sludge doses applied, being however significantly higher in objects with root cuttings used for Virginia fanpetals plantation establishment. Similar relationship of yields increasing along with increasing digestate doses observed also Nabel et al. (2014), however higher doses of digestate did not result in significantly higher biomass yields, but increased the risk of harmful effects with delayed plant development or even caused the loss of plants. It is worth to underline, that an increase in dry weight of single plant was a consequence of its stems weight increment (leaves share reached from 4 to 7%) (Table 1), which was in accordance with Franzaring et al. (2014) as well as Kalembasa & Wiśniewska (2006) findings. Moreover, higher sewage sludge doses promoted shoot development, like in Nabel et al. (2014) investigations with biogas-digestate.

Table 1. Characteristics of single Virginia fanpetals plant depending on the applied experimental factors

Treatment		Average height (cm)	Stem diameter (mm)	Stem number per plant	Leaves dry weight (g plant^{-1})	Stem dry weight (g plant^{-1})	Single plant dry weight (g plant^{-1})
Sewage sludge DM dose†	0 Mg ha^{-1}	234.0^{a}	12.97^{a}	10.0^{a}	12.2^{a}	251.5^{a}	263.7^{a}
	10 Mg ha^{-1}	260.0^{b}	15.70^{b}	11.2^{b}	19.0^{b}	404.3^{b}	423.3^{b}
	20 Mg ha^{-1}	275.3^{cd}	16.74^{c}	11.9^{b}	35.4^{c}	464.9^{c}	500.3^{c}
	40 Mg ha^{-1}	288.0^{c}	17.79^{d}	12.3^{c}	40.4^{d}	521.4^{c}	548.5^{c}
	60 Mg ha^{-1}	288.7^{c}	18.23^{d}	13.5^{d}	35.5^{c}	562.1^{d}	597.6^{cd}
	P	***	***	***	***	***	***
Plantation establishment method†	root cuttings	278.6^{b}	16.66^{b}	12.4^{b}	30.0^{b}	479.0^{a}	509.2^{b}
	plantlets	269.8^{a}	15.89^{a}	12.0^{a}	26.9^{a}	451.9^{b}	484.2^{a}
	P	***	***	***	*	***	***
Year	1st year	173.3^{a}	23.69^{c}	3.2^{a}	47.4^{f}	142.6^{a}	176.0^{a}
	2nd year	273.9^{b}	16.37^{b}	9.8^{b}	20.8^{c}	392.6^{b}	411.0^{b}
	3rd year	287.4^{c}	14.73^{a}	11.4^{c}	32.3^{d}	522.4^{d}	554.7^{e}
	4th year	300.7^{cd}	15.22^{a}	15.2^{d}	35.8^{e}	494.9^{b}	530.6^{d}
	5th year	292.8^{c}	13.90^{a}	17.0^{e}	19.9^{b}	468.7^{bc}	488.5^{c}
	6th year	296.2^{c}	13.75^{ad}	14.0^{c}	17.3^{a}	621.9^{e}	639.1^{e}
	P	***	***	***	***	***	***
sludge dose × establish. method		n.s.	**	*	n.s.	n.s.	n.s.
sludge dose × year		***	***	***	***	***	***
establishment method × year		***	n.s.	n.s.	***	***	***
sludge dose × establish. method × year		*	***	***	n.s.	n.s.	n.s.

The level of significance are indicated by an asterisk (*0.01< $P\leq$ 0.05; **0.001< $P\leq$ 0.01; *** $P\leq$ 0.001; n.s. - not significant) – results of multivariate Anova; the values designated by different lower case letters are significantly different (results of Tukey test); †Values presented for sewage sludge DM dose and plantation establishment method are the means across 6 years and other treatments

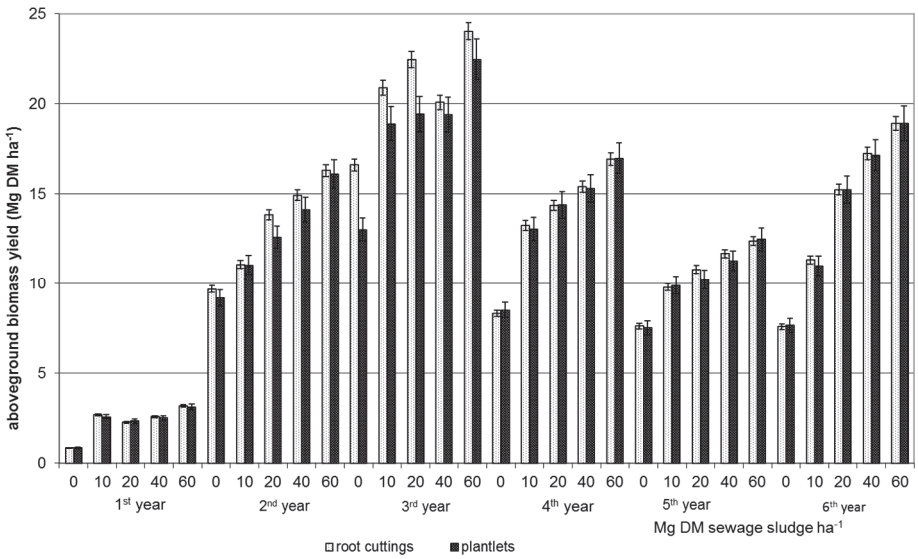

Fig. 1. Yields of dry weight of Virginia fanpetals biomass harvested in the autumn depending on the applied experimental factors (average from six following years of its vegetation). The vertical bars indicate the standard error of the mean values (n = 3)

Dry biomass yields of Virginia fanpetals over the following six years of cultivation are shown in Table 2, 3 as well as at Figure 1 (derived from the autumn harvesting only). In the first year of the field vegetation Virginia fanpetals productivity was negligible (Figure 1), similarly as in Borkowska & Wardzińska (2003), Borkowska (2005), Borkowska et al. (2009), Borkowska & Molas (2012, 2013) as well as von Gehrena et al. (2019) experiments. Hence, it should be taken into account that the yield from the first year caused a significant decrease in the 6-year average values – Table 2. Mean productivity of Virginia fanpetals harvested in autumn observed in this study (Figure 1) was close to the one reported by other researchers, who worked in the same area (Table 4). However, in Borkowska & Molas (2012, 2013) experiments, Virginia fanpetals yields reached about 20 Mg ha^{-1} DM in the fourth year of plant vegetation, whereas in our study similar 'ceiling' biomass yields were obtained already in the second year of plant vegetation. In the following year we observed an increases in Virginia fanpetals yielding (probably as a result of favorable weather conditions) but after that, the average dry biomass yields significantly decreased, remaining almost at the second year yield level (Figure 1, Table 2, 3). In Kuś & Matyka (2009) experiment however Virginia fanpetals yields increased progressively along with following

years of the experiment. That phenomenon could be explained by different soil type and fertilization in our and Kuś & Matyka (2009) as well as Matyka & Kuś (2018) experiments (in our study soil were enriched in sewage sludge only once, before plantation establishment), the exhaustion of crops after record-breaking yields in the previous year and the poor weather conditions. The confirmation of that explanation was the changes of autumn yielding on the object control (without fertilization) – Figure 1, where there was no such high reductions in yielding of plant as on the objects with sewage sludge application. Similar level of Virginia fanpetals yields noted also Slepetys et al. (2012) and Šiaudinis et al. (2015) in Lithuania. Dry biomass yield was significantly affected by the method of plantation establishment, sludge dose, year, harvest date and all their interactions (Table 2, 3). The plants propagated as seedlings produced 8% lower dry biomass yields over the six years of cultivation than those propagated through root cuttings ($P < 0.0001$). Research on Virginia fanpetals' cultivation under Central-East European growth and climate conditions has indicated the possibility of harvesting 9-17 Mg ha^{-1} DW yearly, from plantation established by seeds (Borkowska & Wardzińska 2003), and 20 Mg ha^{-1} DM oven dry, planted by root cuttings (Borkowska & Styk 2006). Differences in dry biomass yield due to method of plantation establishment of Virginia fanpetals have also been reported by other researchers (Borkowska & Wardzińska 2003). However, in our experiment such evident differences were obtained in the first three years of vegetation, probably due to the better growth of vegetatively propagated plants and the weather conditions (lower precipitation in June and July during seedlings establishing at the field, while plants from root cuttings benefited more from the stocks of water stored in the soil before planting). What is more, in the first year of vegetation plants from nurse-in-tray plantlets production stayed in the field shorter than plants propagated by roots. In the consecutive years of plant vegetation differences in Virginia fanpetals yielding caused by two compared methods of plantation establishment almost disappeared (Figure 1 – autumn harvesting), which was consistent with Borkowska & Styk (2006) as well Nahm & Mohrat (2018) results.

It was confirmed also by biometric measurements indicated significant differences between plants from the two compared methods of plantation establishment over the six year period (Table 1).

Table 2. Yields of dry weight (Mg ha^{-1}) of biomass as well as primary energy yields (MJ·Mg^{-1}·a^{-1}) of Virginia fanpetals depending on the applied experimental factors

Treatment		Yield of air dry weight of biomass (Mg ha^{-1})	Primary energy yields (MJ·Mg^{-1}·a^{-1})
Sewage sludge DM dose	0 Mg ha^{-1}	6.44^{a}	107.6^{a}
	10 Mg ha^{-1}	8.45^{b}	140.3^{b}
	20 Mg ha^{-1}	10.53^{c}	159.7^{c}
	40 Mg ha^{-1}	11.40^{d}	186.4^{d}
	60 Mg ha^{-1}	11.38^{d}	184.5^{d}
	P	***	***
Plantation esta-blishment	root cuttings	9.99^{b}	161.2^{b}
	plantlets	9.18^{a}	148.3^{a}
	P	***	***
Harvest date	autumn	12.13^{c}	196.0^{c}
	winter	9.19^{b}	148.4^{b}
	spring	7.42^{a}	119.7^{a}
	P	***	***
Year	1st year	1.83^{a}	29.7^{a}
	2nd year	11.06^{d}	178.8^{b}
	3rd year	14.53^{e}	235.0^{d}
	4th year	11.02^{d}	177.9^{c}
	5th year	8.39^{b}	135.5^{e}
	6th year	10.64^{c}	171.3^{f}
	P	***	***

*** significant at the 0.001 probability level; n.s. – not significant – results of multivariate Anova; the values designated by different lower case letters are significantly different (results of Tukey test)

Sewage sludge application significantly affected dry biomass yield across the methods of plantation establishment and the dates of harvesting. The highest average dry yields of biomass were collected from plots fertilized with the highest municipal sewage sludge doses, while lower sewage sludge doses (10 and 20 Mg ha^{-1} DM) introduced into the soil before the experiment establishment caused on average 31 and 63% yield increment compared to the control object, respectively. This could be due to the nutrients present in sewage sludge which might have enhanced plant growth even without the application of inorganic fertilizer as a source of plant nutrition (Singh & Agrawal 2008, Seleiman et al. 2013, Usman et al. 2012). It is worth to underline that higher sewage sludge application was connected with almost equal *S. hermaphrodita* yielding, without any significant differences (Table 2). Thus, an inversion point of the relationship between

the sewage sludge application and yield increases indicated that sludge supply beyond 40 Mg ha^{-1} DM is not reasonable.

Table 3. Analysis of variance of Virginia fanpetals dry weight yield and primary energy yields based on measurements from six following years of its vegetation

Effect	*DF*	Yield of air dry weight of biomass		Primary energy yields	
		F value	*P* value	*F* value	*P* value
Sludge dose	4	454.95	0.0001	454.95	0.0001
Establishment method	1	200.19	0.0001	200.19	0.0001
Harvest date	2	953.18	0.0001	953.18	0.0001
`Year	5	1493.88	0.0001	1493.88	0.0001
Sludge dose × establishment method	4	4.61	0.012	4.61	0.012
Sludge dose × harvest date	8	22.24	0.0001	22.24	0.0001
Establishment method × harvest date	2	8.93	0.002	8.93	0.002
Sludge dose × year	20	25.47	0.0001	25.47	0.0001
Establishment method × year	5	30.06	0.0001	30.06	0.0001
Harvest date × year	10	85.59	0.0001	85.59	0.0001
Sludge dose × establishment method × year	20	3.71	0.001	3.71	0.001
Sludge dose × harvest date × year	40	2.18	0.8889	2.18	0.8889
Establishment method × harvest date × year	10	4.30	0.0001	4.30	0.0001
Sludge dose × establishment method × harvest date	8	3.26	0.0013	3.26	0.0013

Similar relationship of yields increasing along with increasing sewage sludge dose observed also Nabel et al. (2014) after digestate application as well as Seleiman et al. (2013) – in other energy plants. Measurements of single Virginia fanpetals plant (Table 1) indicate that they perfectly use fertilization potential of sludge. Positive reaction of *S. hermaphrodita* plant for sludge application noted also Borkowska et al. (2001), Augustynowicz et al. (2008) and Strzelczyk (2013).

We also observed a significant effect ($P < 0.0001$) of year (age of plant and climatic conditions) on Virginia fanpetals productivity. We recorded a significant increase in yield up to the third year of vegetation, when the major minerals resources brought into the soil along with increasing doses of sludge applied were available for plants, and then a significant reduction of biomass yields. This confirms earlier observations of Szempliński et al. (2014), who reported yield

increase during first three years of *S. hermaphrodita* vegetation and after that yields naturally decreasing.

Table 4. Sample dry yields of Virginia fanpetals' biomass in the studies conducted in Poland

No. year after establishment	Borkowska and Wardzińska (2003)	Borkowska et al. (2009)	Borkowska and Molas (2013)	Szempliński et al. (2014)	Kuś and Matyka (2009)	Borkowska et al. (2001)
1	3.71	2.61	2.51	n.d.	n.d.	4.85
2	10.2	8.12	14.47	10.3	n.d.	3.93
3	7.99	11.98	15.52	11.6	9.0	9.28
4	n.d.	11.00	19.6	7.8	11.4	9.35
5	n.d.	n.d.	n.d.	n.d.	9.6	n.d.
6	n.d.	n.d.	n.d.	n.d.	6.9	n.d.

n.d. – no data

Delaying of biomass harvesting causes usually a reduction in energy crop yields and at the same time an increase of cellulose content in the dry matter and a water reduction (Lewandowski & Heinz, 2003). In the current study three dates of biomass harvesting (performed in late autumn, in winter and in the spring) were compared. An autumn harvesting, carried out immediately at the end of growing season, proved to be the most favorable. Virginia fanpetals plants harvested at that time produced significantly ($P < 0.0001$) the highest yield of dry biomass (Table 2, 3). During the winter average dry biomass yields were significantly lower (by 24.2%) compared to those obtained in the autumn. The lowest biomass yields were obtained at early spring – the reduction reached almost 38.8% compared to the autumn harvest. The mean daily loss observed in a current study was 0.25% day^{-1}. Thus, autumn harvest offers better yields than late harvesting, mainly due to a loss of harvestable biomass during winter, but on the

other side, in the spring a significant reduction of water and improvement of combustion quality was observed by Borkowska (2005) and was described by Nahm & Mohrat (2018). Similar relationship in experiments with delayed miscanthus harvesting observed Lewandowski & Heinz (2003). We also observed a significant interactions of sludge dose, year, and the harvest date in Virginia fanpetals biomass yields within 6-year study (Table 3).

3.2. Biomass characteristic

Moisture content in Virginia fanpetals biomass harvested in autumn reached up to 30% (Table 5) and was comparable to Borkowska (2005), Kuś & Matyka (2009), Szyszlak-Bargłowicz & Piekarski (2009) as well as Borkowska & Molas (2013) findings, but lower than that obtained in Slepetys et al. (2012) experiments. Borkowska (2005) as well as Borkowska & Molas (2013) studies indicated, that there is an advantage to the late harvest as it reduces the amount of drying that is required to obtain low moisture content. Lower moisture content in *S. hermaphrodita* biomass was achieved in objects with the lowest doses of sewage sludge, probably associated with smaller stems which tend to dry faster.

A very important indicator of biomass quality is also ash and sulphur content. Biomass ash has a relatively low melting point, which can lead to slagging and fouling the combustion chamber or boiler, while high sulfur content can pose corrosion problems (Obernberger et al. 1997). A positive feature of Virginia fanpetals biomass were significantly low ash (from 3.5 to 5.7%) and sulfur content (from 0.03 to 0.09%), which was comparable with Kalembasa & Wiśniewska (2008) as well as Slepetys et al. (2012) and von Gehrena et al. (2019) findings.

Table 5. The fuel characteristics of Virginia fanpetals biomass depending on the sewage sludge dose

Treatment		Moisture content (%)	Ash content (%)	Sulfur content (%)	Net calorific value ($MJ \cdot kg^{-1}$)
Sewage sludge DM dose	0 Mg ha^{-1}	24.6^{b}	3.5^{a}	0.03^{a}	16.61^{c}
	10 Mg ha^{-1}	25.6^{c}	4.7^{b}	0.09^{c}	16.59^{c}
	20 Mg ha^{-1}	23.1^{a}	3.9^{a}	0.03^{a}	16.71^{d}
	40 Mg ha^{-1}	25.1^{c}	5.1^{c}	0.05^{b}	16.35^{b}
	60 Mg ha^{-1}	30^{d}	5.7^{c}	0.06^{b}	16.22^{a}
	P	***	***	***	***

*** significant at the 0.001 probability level – results of one-way Anova; the values designated by different lower case letters are significantly different (results of Tukey test)

The thermal energy was assessed also on the basis of the net calorific values (lower heating values). The highest values of the net calorific value as well as the lowest ash and sulfur content were obtained on the control objects and after application lower doses of sludge. Similarly, in the case of other energy crops, there was noted an increase of lower heating value after sewage sludge was applied (Seleiman et al. 2013). The net calorific value was shaped by percentage of moisture content in the biomass. Obtained in the current study LHV levels were in accordance with Szyszlak-Bargłowicz & Piekarski (2009), whereas Jasinskas et al. (2014), Szempliński et al. (2014) and von Gehrena et al. (2019) stated slightly higher gross calorific value of *Sida*, but confirmed the differences between calorific values of biomass collected in the winter and spring.

In the case of energy crops a very important indicator of its quality is the energy value of yield (Table 2, 3). Significantly ($P < 0.001$) the highest value of the parameter was obtained for plantation established by roots (161.2 MJ Mg^{-1} a^{-1}). On average, about 8% less energy value was found in plants grown on plots with plantlets planting. However, regardless of the plantation establishment method and the harvest date, the highest average Virginia fanpetals biomass energy value was calculated for the objects fertilized with 40 and 60 Mg ha^{-1} sewage sludge (Table 2). Alike in the case of other energy crops, increasing gross energy yields were produced following sewage sludge application (Seleiman et al. 2013). Similar level of energy efficiency reported Szempliński et al. (2014) and Matyka (2013), while higher energy production from 1 ha of land by *S. hermaphrodita* noted Borkowska & Molas (2012), but those authors adopted for calculations the one, high value of the higher heat value of 18.74 MJ kg^{-1} of dry biomass, while comparable energy yields were obtained by Borkowska et al. (2009) in the experiment with different mineral fertilization doses. When it comes to identify the optimum date for biomass harvesting, an autumn date proved to be the most favorable, as the plants produced the highest yields of aboveground parts with a relatively high calorific value. Slightly less favorable seems to be a winter harvesting, when we recorded an average energy value yield lower by 24.3% compared to that obtained in the autumn. The lowest energy value of biomass (mainly due to significantly lower biomass yields) was obtained in the case of harvesting conducted in the early spring – on average by 38.9% lower in relation to the autumn one – Table 2. Observed trend of decreasing of total thermal energy potentially produced by combustion of Virginia fanpetals biomass during later harvesting was in accordance with Lewandowski & Heinz (2003) findings on miscanthus. The effect of date of harvesting interacted with sludge application ($P < 0.0001$) and plantation establishment method in primary energy yields within the study.

3.3. Plant nutrient concentration and accumulation

For biofuel purposes, high cellulose content and low lignin content, minimum moisture, ash and other mineral elements (N, P, K, S and to a lesser degree Ca, Mg) are desired biomass chemical characteristics to improve conversion efficiency (Obernberger et al. 1997). Excessive mineral nutrients levels within the harvested material can cause corrosion, slagging, fouling and environmentally harmful emissions (Szyszlak-Bargłowicz 2014).

In the current study, sewage sludge dose and morphological part of plant significantly affected macronutrients content by Virginia fanpetals plants (Table 6). Generally, *S. hermaphrodita* stalks contained significantly higher amounts of nitrogen, phosphorus, potassium, and magnesium, while its leaves accumulated more sodium and calcium (Table 7). An opposite tendency was obtained by Kalembasa & Wiśniewska (2006, 2008) and Szyszlak-Bargłowicz (2014), who noted higher content of all analyzed macroelements in *Sida* leaves, but their examination was performed in full plants vegetation phase, while our results were collected just before leaves dropping and plants harvesting in late autumn. What is more, content of all studied elements in *S. hermaphrodita* plants strictly depended on the dose of sewage sludge introduced before the establishment of the experiment (increasing the dose caused an increase in the content of elements studied in the aerial parts of plants). A similar tendency was observed in Strzelczyk (2013) studies, while the opposite trend was stated in the case of other energy plants by Seleiman et al. (2013). Wherein the content was not strictly proportional, because 6-fold increase in sludge dose caused a relatively small increase in the content of macronutrients in plant tissues. Independently of the plantation establishment method, significantly greater macronutrients concentrations were noted in *S. hermaphrodita* biomass obtained from plots fertilized with the maximum dose of sewage sludge, suggesting its important fertilizer role.

On the other side, the lowest macronutrients content was stated in the control object, which was characterized only by natural content of biogenic elements in the soil. The same tendency were reported in Strzelczyk (2013) experiments with Virginia fanpetals grown in soil irrigated with municipal wastewater, Barbosa et al. (2014) experiments with digestate fertilization, Kalembasa & Wiśniewska (2006) with increasing mineral fertilization level, while Kalembasa & Wiśniewska (2008), Szyszlak-Bargłowicz (2014) as well as Slepetys et al. (2012) did not observed significant changes in elements analyzed content on plots with increasing mineral fertilization. The effect of the sewage sludge dose interacted with morphological part of plant ($P < 0.001$) in macronutrients under study within six following years of *Sida* vegetation. However, despite slightly lower amount of N, P and K in generatively propagated tissues, we did not recorded a significant effect of the method of plantation establishment of *S. hermaphrodita*

on the content of N, Ca and Mg in plant biomass (Table 6). Minerals concentration in Virginia fanpetals tissues was comparable to Borkowska (1991), Krzywy-Gawrońska (2012), Barbosa et al. (2014) experiments, while the concentration of macronutrients occurring in the samples in this trail was higher than in Matyka (2013) study. The effect of the method of plantation establishment interacted with dose of sludge ($P < 0.001$) and morphological part in macronutrients under study within six following years of *Sida* vegetation.

Table 6. Macronutrients content (in g DM kg^{-1}) in aboveground parts of Virginia fanpetals plants depending on the applied experimental factors

Treatment		N	P	K	Na	Ca	Mg
Sewage sludge DM dose	0 Mg ha^{-1}	1.03^{a}	0.66^{a}	3.62^{a}	0.36^{a}	9.34^{a}	0.87^{a}
	10 Mg ha^{-1}	1.27^{b}	0.77^{b}	3.94^{b}	0.38^{b}	10.32^{b}	0.94^{b}
	20 Mg ha^{-1}	1.80^{c}	0.85^{c}	4.50^{b}	0.41^{c}	11.03^{c}	1.01^{b}
	40 Mg ha^{-1}	1.91^{c}	0.90^{c}	4.78^{c}	0.43^{d}	11.88^{a}	1.19^{c}
	60 Mg ha^{-1}	2.02^{d}	1.54^{d}	5.94^{d}	0.48^{e}	12.10^{e}	1.33^{d}
	P	***	***	***	***	***	***
Morphological part of plant	leaves	2.77^{b}	1.58^{b}	6.63^{b}	0.29^{a}	10.33^{a}	1.74^{b}
	stems	0.45^{a}	0.30^{a}	2.48^{a}	0.55^{b}	14.97^{b}	0.39^{a}
	P	***	***	***	***	***	***
Plantation establishment method	root cuttings	1.66	0.98^{b}	4.94^{b}	0.29^{a}	10.33	1.06
	plantlets	1.55	0.91^{a}	4.17^{a}	0.54^{b}	11.54	1.08
	P	n.s.	**	**	***	n.s.	n.s.
sludge dose × morphological part		***	***	***	***	***	***
sludge dose × establishment method		***	***	***	***	***	***
establishment method × morph. part		n.s.	**	**	***	*	n.s.
sludge dose × establ. meth. × morph. part		***	***	***	***	n.s.	*

The level of significance are indicated by an asterisk (*$0.01 < P \leq 0.05$; **$0.001 < P \leq 0.01$; *** $P \leq 0.001$; n.s. - not significant) – results of multivariate Anova; the values designated by different lower case letters are significantly different (results of Tukey test)

Table 7. Macronutrients uptake (in kg ha^{-1}) depending on the applied experimental factors

Treatment		N	P	K	Na	Ca	Mg
Sewage sludge DM dose	0 Mg ha^{-1}	24.61^{a}	18.97^{a}	183.15^{a}	22.24	288.04	28.20
	10 Mg ha^{-1}	30.03^{b}	24.65^{b}	219.95^{b}	24.02	349.30	33.91
	20 Mg ha^{-1}	52.50^{c}	34.62^{c}	285.94^{b}	30.29	420.47	43.49
	40 Mg ha^{-1}	71.73^{d}	39.55^{c}	342.84^{b}	34.15	474.14	52.61
	60 Mg ha^{-1}	90.02^{e}	59.24^{d}	399.31^{c}	42.27	544.45	67.36
	P	***	*	*	n.s.	n.s.	n.s.
Plantation establishment method	root cuttings	46.00	33.64	251.54	27.61	369.43	42.99
	plantlets	61.56	37.17	320.93	33.58	461.12	47.24
	P	n.s.	n.s.	n.s.	n.s.	n.s.	n.s.
sludge dose × establishment method *P*		**	***	*	*	n.s.	**

The level of significance are indicated by an asterisk (*0.01< $P \leq 0.05$; **0.001< $P \leq 0.01$; *** $P \leq 0.001$; n.s. - not significant) – results of two-way Anova; the values designated by different lower case letters are significantly different (results of Tukey test)

When energy crops are cultivated on the soil where sewage sludge is used, it is crucial to determine the uptake of individual minerals. Despite the significant effect of sewage sludge dose on macronutrients content in Virginia fanpetals tissues we did not observed the same relation in the case of macronutients uptake. Sludge dose significantly affected the uptake of N, P and K as in Kalembasa & Wiśniewska (2008) experiments, while despite a slightly higher macro-elements uptake by plants grown from plantlets, statistical analyses did not confirmed significance of such differences (Table 7). Like in the nutrients content, the smallest uptake of macro-elements were noted in the control objects, whereas all the doses of sewage sludge caused a significant increase in macronutrients uptake (the highest being after 60 Mg sewage sludge ha^{-1} application). Similar level of analyzed macronutrients uptake observed Kalembasa & Wiśniewska (2008), while Krzywy-Gawrońska (2012) noted higher N uptake increasing along with increasing fertilization. The reverse trend in N uptake, but similar in P uptake after sludge application in maize, hemp and oilseed rape was observed by Seleiman et al. (2013). Uptake of all studied elements by *S. hermaphrodita* tissues delivered from plants grown on plots with plantlets produced in multi-cell trays used for plantation establishment method were similar as that one from plots with roots cuttings planting (Table 7).

3.4. Soil characteristic

Soil pH and hydrolytic acidity was clearly modified by the use of experimental factors under study (Table 8). The highest pH_{KCl} was recorded on control plots, while increasing doses of sludge resulted in gradual decrease in soil pH. Similar observations have made also Casado-Vela et al. (2006). However, Singh and Agrawal (2008) pointed out that the use of biosolids may also result in increasing the acidity of the soil and changes in heavy metals binding. On the other side, the lowest hydrolytic acidity was recorded in control objects, and increasing doses of sewage sludge applied to the soil resulted in its significant increase.

We also observed a clear linear relationship between sludge dose and accumulation of C_{org} in the soil (Table 8), similarly as in Nabel et al. (2014) as well as Casado-Vela *et al*., (2006) experiments. The use of increasing doses of sludge resulted in a systematic increase in the content of organic carbon in the soil. A similar relationship was also observed in the total nitrogen content. Thus there was a build-up of a soil nitrogen and organic matter pool providing a longer lasting N reservoir for the plants. Similarly, the content of phosphorus, potassium and magnesium was positively correlated with increasing dose of sewage sludge and their content in the soil profile, which was consistent with the results of Casado-Vela et al. (2006), Singh & Agrawal (2008) and Usman *et al*., (2012). C_{org} and N_t in the soil was consistent with Nabel et al. (2014) results, while macronutrients contents were higher, probably as a result of their higher amounts applied to the soil with the municipal sewage sludge.

3.5. Index of bioaccumulation

Bioaccumulation index (IBA) is calculated as the quotient of the contents of the element in the plant to its content in the soil. This is a parameter that indicates the size and speed of movement of the elements contained in the soil profile to the interior of plant cells. It has been recognized that a high biomass and a high bioaccumulation factor are two key factors for successful phytoextraction (Zhao et al. 2003). Nitrogen was subjected to intensive bioaccumulation in the tissues of Virginia fanpetals (Table 9).

Table 8. Chosen physical and chemical parameters of soil under Virginia fanpetals culture depending on the sewage sludge dose

Sewage sludge DM dose	pH_{KCL}	Hydrolytic acidity (mmol(+) kg^{-1})	C_{org}	N_t	P	K	Mg
			(g kg^{-1} DM of soil)			(mg kg^{-1} DM of soil)	
0 Mg ha^{-1}	6.46^{a}	10.77^{a}	12.46^{a}	1.38^{a}	27.57^{a}	88.03^{a}	46.51^{a}
10 Mg ha^{-1}	5.56^{b}	13.46^{b}	12.89^{a}	1.42^{b}	29.36^{b}	98.15^{b}	50.42^{b}
20 Mg ha^{-1}	5.38^{c}	19.75^{c}	15.16^{b}	1.53^{b}	31.42^{c}	102.72^{c}	51.29^{b}
40 Mg ha^{-1}	5.35^{c}	24.88^{d}	17.62^{c}	1.67^{c}	42.73^{d}	126.83^{d}	51.52^{b}
60 Mg ha^{-1}	5.85^{d}	35.66^{e}	20.14^{d}	1.89^{d}	49.93^{e}	132.37^{e}	54.22^{c}
P	***	***	***	*	***	***	***

The level of significance are indicated by an asterisk (*$0.01 < P \leq 0.05$; *** $P \leq 0.001$) – results of one-way Anova; the values designated by different lower case letters are significantly different (results of Tukey test)

Table 9. Index of bioaccumulation (IBA) of chosen macronutrients in Virginia fanpetals plant depending on the sewage sludge dose

Treatment		N	P	K	Mg
Sewage sludge DM dose	0 Mg ha^{-1}	0.167^{a}	0.007	0.021	0.006^{a}
	10 Mg ha^{-1}	0.204^{b}	0.009	0.022	0.007^{b}
	20 Mg ha^{-1}	0.278^{c}	0.009	0.024	0.007^{b}
	40 Mg ha^{-1}	0.318^{d}	0.008	0.022	0.009^{c}
	60 Mg ha^{-1}	0.336^{e}	0.009	0.023	0.010^{d}
	P	***	n.s.	n.s.	***

*** significant at the 0.001 probability level; n.s. – not significant – results of one-way Anova; the values designated by different lower case letters are significantly different (results of Tukey test)

We observed that the highest ratio of the content of the element in the plant in relation to its amount in the soil was found in objects with the highest dose of sewage sludge application. IBA of phosphorus ranged from 0.007 to 0.009 – Table 9, which, according to Kabata-Pendias (2011) indicates lack of bioaccumulation. In the case of potassium bioconcentration factor was known to be a weak, reaching the highest value after lower doses of municipal sewage sludge application. The bioconcentration factor of Mg was also weak and ranged from 0.006 to 0.01. The highest values was recorded after the higher doses of sewage sludge application (Table 9).

4. Conclusions

Sida hermaphrodita (L.) Rusby is an energy plant achieving stable, 'ceiling' biomass yield in the second year after planting, exceeded 20 Mg ha^{-1} a^{1} in an optimized system within this study. Virginia fanpetals seems to be a species effectively using fertilization potential of sewage sludge. Increasing doses of municipal sewage sludge stimulated production of significantly more thicker, higher and heavier stems per plant and as a result dry yields biomass from the unit area. 40 Mg ha^{-1} DM municipal sewage sludge could be recommended in cultivation of Virginia fanpetals for energy purpose.

Under the influence of increasing doses of sewage sludge macronutrients content and uptake increased steadily, taking the highest value after its maximum dose application. Virginia fanpetals intensively bioaccumulated nitrogen, while potassium and magnesium bioaccumulation factors were weak. Sludge cause changes in the physico-chemical properties of the soil (ie. reducing of the pH value while increasing hydrolytic acidity, total nitrogen content as well as the content of available phosphorus, potassium and magnesium). Applied sewage sludge also contributed to increase the organic carbon content, which varied primarily due to different its doses.

Significantly higher dry biomass yield (especially in the first three years of plants vegetation) was obtained using root cuttings for plantation establishment in comparison to the nurse-in-tray plantlets.

During autumn harvesting *S. hermaphrodita* biomass intended for combustion was characterized by a relatively low moisture content (23-30%), high net calorific value (16.2-16.7 MJ kg^{-1}) as well as low ash and sulfur concentrations. The harvest window of Virginia fanpetals is between October and March. Delaying harvesting date, however, was connected with significant loss of biomass yield relative to the peak yield noted in the autumn.

Thus, Virginia fanpetals an important energy plant in Poland has a potential for the use of municipal sewage sludge, but the short-term advantage of sludge applying as a fertilizer requires continuous monitoring.

This study was performed partially with the financial support of the Ministry of Science and Higher Education (grant No. N N310080336), Poland.

References

Augustynowicz, J., Pietkiewicz, S., Kalaji, H.M., Russel, S. (2008). The effect of the EM technology on the physiological parameters of energetic plant Virginia mallow (*Sida hermaphrodita* (L.) Rusby) fertilized with sewage sludge. *Ecol. Techn*., *16*(5A), 11-19.

Barbosa, D., Nabel, M., Jablonowski, N. (2014). Biogas-digestate as nutrient souse for biomass production of *Sida hermaphrodita, Zea mays* L., and *Medicago sativa* L. *Energy Proc*., *59*, 120-126.

Bartoszewicz-Burczy, H. (2012). Biomass potential and its energy utilization in the Central European countries. *Energ., 12*, 860-866.

Borkowska, H., Jackowska, I., Piotrowski, J., Styk, B. (2001). Suitability of cultivation of some perennial plant species on sewage sludge. *Polish Journal of Environmental Studies, 10*(5), 379-381.

Borkowska, H., Molas, R., Kupczyk, A. (2009). Virginia fanpetals (*Sida hermaphrodita* Rusby) cultivated on light soil; Yield and biomass productivity. *Polish Journal of Environmental Studies, 18*, 563-568.

Borkowska, H., & Molas, R. (2012). Two extremely different crops, *Salix* and *Sida*, as sources of renewable energy. *Biomass and Bioenergy, 36*, 234-240.

Borkowska, H., & Molas, R. (2013). Yield comparison of four lignocellulosic perennial energy crop species. *Biomass and Bioenergy*, *51*, 145-153.

Borkowska, H., & Styk, B. (2006). Virginia fanpetals (*Sida hermaphrodita* L. Rusby) cultivation and utilization. *Monograp*h, WAR Lublin.

Borkowska, H., & Wardzińska, K. (2003). Some effects of *Sida hermaphrodita* R. cultivation on sewage sludge. *Polish Journal of Environmental Studies*, *12*, 119-122.

Borkowska, H. (2005). Changes of dry matter content in *Salix viminalis* and *Sida hermaphrodita* yields of biomass depending on harvest date. *Annales UMCS sec E*., *60*, 155-161.

Borkowska, H. (1991). *Study on chosen biology and agrotechnical elements of Virginia fanpetals (*Sida hermaphrodita Rusby*) as a fodder plant.* Rozpr. Nauk, WAR Lublin.

Casado-Vela, J., Sellés, Navarro, J., Bustamante, M.A., Mataix, J, Guerrero, C., Gomez, I. (2006). Evaluation of composted sewage sludge as nutritional source for horticultural soils. *Waste Manag*., *26*, 946-952.

CEN Solid biofuels. Determination of moisture content – Oven dry method. Part 1: Total moisture – Reference method, EN 14774-1. (2009). Brussels, Belgium: European Committee for Standarization.

Franzaring, J., Schmid, I., Bäuerle, L., Gensheimer, G., Fangmeier, A. (2014). Investigations on plant functional traits, epidermal structures and the ecophysiology of the novel bioenergy species *Sida hermaphrodita* Rusby and *Silphium perfoliatum* L. *J. Appl. Bot. Food Quality, 8*, 36-45. DOI: 10.5073/JABFQ.2014.087.006.

von Gehrena, P., Gansbergera, M., Pichlerb, W., Weiglb, M., Feldmeierc, S., Wopienkac, E., Bochmannd, G. (2019). A practical field trial to assess the potential of *Sida hermaphrodita* as a versatile, perennial bioenergy crop for Central Europe. *Biomass and Bioenergy*, *122*, 99-108. DOI: org/10.1016/j.biombioe.2019.01.004

Gondek, K., Mierzwa-Hersztek, M., Kopeć, M., Sikora, J., Lošák, T., Grzybowski, P. (2014). Sewage sludge biochar effects on phosphorus mobility in soil and accumulation in plant. *Ecological Chemistry and Engineering S., 26*, 367-381.

Igliński, B., Iglińska, A., Kujawski, W., Buczkowski, R., Cichosz, M. (2011). Bioenergy in Poland. *Ren. Sust. Energy Rev., 15*, 2999-3007.

IUSS Working Group WRB. (2007). World Reference Base for Soil Resources 2006, first update 2007. *World Soil Resources Reports No. 103*. FAO, Rome.

Jadczyszyn, J., Faber, A., Zaliwski, A. (2008). *Designation of areas in Poland potentially suitable for growing willow and Virginia mallow for energy purposes.* In*:* Studies and Reports ISSPC-SRI. 11, 55-65.

Jasinskas, A., Šarauskis, E., Domecka, R. (2014). Technological evaluation of non-traditional energy plant cultivation and utilization for energy purposes in Lithuania. *Proc. Int. Con. Agri. Engin, Zurich*. 6-10. July 2014, AngEng, Ref: C0281, www.eurageng.eu.

Jones, J.B., 7 Case, V.W. (1991). Soil testing and plant analysis. 3rd ed. *Soil Science Society of America SSSA*, 15.

Kabata-Pendias, A. (2011). *Trace Elements in Soils and Plants*. 4th ed. by Taylor and Francis Group, LL*C*.

Kalembasa D., Wiśniewska B. (2006). The influence of nitrogen doses on the *Sida* biomass (*Sida hermaphrodita* Rusby) and the content of soma macroelements. *Acta Agroph*., *8*(1), 127-138.

Kalembasa, D., Wiśniewska, B. (2008). The influence of nitrogen doses on the content of Ca, Mg, S and Na in biomass of Pensylwania mallow (*Sida hermaphrodita* Rusby). *Acta Agroph*., *11*(3), 667-675.

Kołodziej, B., Antonkiewicz, J., Stachyra, M., Bielińska, E., Wiśniewski, J., Luchowska, K., Kwiatkowski, C. (2015). Use of sewage sludge in bioenergy production – A case study on the effects on sorghum biomass production. *Europ. J. Agro*n., *269*, 63-74.

Kołodziej, B., Antonkiewicz, J., Sugier, D. (2016). *Miscanthus* × *giganteus* as a biomass feedstock grown on municipal sewage sludge. *Ind. Crops Prod*., *81*, 72-82

Krzywy-Gawrońska, E. (2012). The effect of industrial wastes and municipal sewage sludge compost on the quality of virginia fanpetals *(Sida hermaphrodita* Rusby) biomass. Part 1. Macroelements content and their uptake dynamics. *Pol. J. Chem. Techn*., *14*(2), 9-15.

Kurucz, E., Antal, G., Gábor, F., Popp, J. (2014). Cost-effective mass propagation of Virginia fanpetals (*Sida hermaphrodita* L. Rusby) from seeds. *Environ. Eng. Manag. J*., *13*(11), 2845-2852.

Kuś, J., & Matyka, M. (2009). Wydajność wybranych gatunków roślin uprawianych na cele energetyczne w zależności od jakości gleby. *Fragm. Agronom*., *26(*4), 103-110.

Lewandowski, I., & Heinz, A. (2003). Delayed harvest of miscanthus – influences on biomass quantity and quality and environmental impacts of energy production. *Europ. J. Agron*., *19*, 45-63.

Matyka, M. (2013). Production and economic aspects of cultivation of perennial plants for energy purposes. Ed. by Institute of Soil Science and Plant Cultivation. *State Research Institute in Puławy, 35*, 1-93.

Matyka, M, & Kuś, J. (2018). Influence of soil quality for yield and biometric features of *Sida hermaphrodita* L. Rusby. *Polish Journal of Environmental Studies*, *27*(6), 2669-2675. DOI: 10.15244/pjoes/80961

Nabel, M., Barbosa, D.P.B., Horsch, D., Jablonowski, N.D. (2014). Energy crop (*Sida hermaphrodita*) fertilization using digestate under marginal soil conditions: A dose-response experiment. *Energy Proc*., *59*, 127-133.

Nahm, M., & Mohrat, Ch. (2018). Virginia mallow (*Sida hermaphrodita* (L.) Rusby) as perennial multipurpose crop: biomass yields, energetic valorization, utilization potentials, and management perspectives. *GCB Bioenergy, 10*(6), 393-404. DOI: 10.1111/gcbb.12501

Nelson, D.W., & Sommers, L.E. (1975). Determination of total nitrogen in plant material. *Agron. J*., *65*, 109-115.

Obernberger, I., Bidermann, F., Widmann, W., Riedl, R. (1997). Concentrations of inorganic elements in biomass fuels and recovery in the different ash fractions. *Biomass and Bioenergy*, *12*(3), 211-224.

Ostrowska, A., Gawliński, S., Szczubiałka, Z. (1991). Methods of analysis and assessment of soil and plant properties. *A Catalgoue. Institute of Environmental Protection – National Research Institute*. Warsaw, 1-334.

Seleiman, M., Santanen, A., Jaakkola, S., Ekholm, P., Hartikainen, H., Stoddard, F., Mäkelä, P. (2013). Biomass yield and quality of bioenergy crops grown with synthetic and organic fertilizers. *Biomass and Bioenergy*, *59*, 477-485.

Singh, R.P., & Agrawal, M. (2008). Potential benefits and risks of land application of sewage sludge. *Waste Manag*., 28(2), 347-358.

Slepetys, J., Kadziuliene, Z., Sarunaite, L., Tilvikiene, V., Kryzeviciene, A. (2012). Biomass potential of plants grown for bioenergy production. *Proc. Intern. Sci. Conf*.: Renewable Energy and Energy Efficiency. Jelgava, Latvia, 66-72.

Soil quality - Sampling - Part 5: Guidance on the procedure for the investigation of urban and industrial sites with regard to soil contamination, (2005). ISO 10381-5. Brussels, Belgium: European Committee for Standarization.

Soild biofuels – Determination of total content of sulfur and chlorine, (2011). EN 15289. Determination of ash content, 2009. EN 14775. Determination of calorific value, 2009. EN 14918. Brussels, Belgium: European Committee for Standarization.

Spooner, D.M., Cusick, A.W., Hall, G.F., Baskin, J.M. (1985). Observations on the distribution and ecology of *Sida hermaphrodita* (L.) Rusby (Malvaceae). *Sida, 11*, 215-225.

Strzelczyk, M. (2013). Discharge of biogenic components (N, P) in the yield of biomass of *Sida hermaphrodita* Rusby irrigated by rural sewerage. *Inż. Ekol*., *32*, 181-186.

Szempliński, W., Parzonka, A., Sałek, T. (2014). Yield and energy efficiency of biomass production of some species of plants grown for biogas. *Acta Sci. Pol., Agricultura, 13*(3), 67-80.

Szyszlak-Bargłowicz, J., & Piekarski, W. (2009). Calorific value of biomass from Virginia fanpetals (*Sida hermaphrodita* Rusby) stems depending on humidity. *Inż. Roln*., *8*(117), 223-230.

Szyszlak-Bargłowicz, J. (2014). Content of chosen macroelements in biomass of Virginia mallow (*Sida hermaphrodita* Rusby). *J. Central Europ. Agric*., *14*(3), 263-272.

Šiaudinis, G., Jasinskas, A., Šarauskis, E., Steponavičius,E., Karčauskiené, D., Liaudanskiené, I. (2015). The assessment of Virginia mallow (*Sida hermaphrodita* Rusby) and cup plant (*Silphium perfoliatum* L.) productivity, physic-mechanical properties and energy expenses. *Energy*, *93*, 606-612. DOI: org/10.1016/j.energy. 2015.09.065

Usman, K., Khan, S., Ghulam, S., Khan, M.U., Khan, N., Khan, M.A., Khali, S.K. (2012). Sewage sludge: an important biological resource for sustainable agriculture and its environmental implications. *Am. J. Plant Sci., 3*, 1708-1721.

Zhao, F.J., Lombi, E., McGrath, S.P. (2003). Assessing the potential for zinc and cadmium phytoremediation with the hyperaccumulator *Thlaspi caerulescens. Plant Soil*., *249*(1), 37-4.

Abstract

The objective of this study was to determine the effect of increasing municipal sewage sludge doses on *Sida hermaphrodita* Rusby (Virginia fanpetals) yielding and bioenergy feedstock characteristics. In a six-year-lasting field experiment two methods of plantation establishment (by roots cuttings and nurse-in-tray plantlets) and three dates of biomass harvesting (autumn, winter and spring one) were additionally tested in climatic conditions of south-eastern Poland.

Virginia fanpetals dry yields increased each year and exceeded 20 Mg ha^{-1} in the second year of culture. Application of 40 Mg ha^{-1} sludge DM resulted in obtaining the highest yield. Similarly the content, uptake and index of bioaccumulation of macronutrients contained in the sludge increased along with increasing its dose. Biomass was characterized by a favorable parameters: net calorific values were in the range of 16.2-16.7 MJ kg^{-1}. The highest energy value of biomass yield was obtained with root cuttings use for plantation establishment, especially in objects with high dose of sludge during autumn harvest. Both, winter and spring harvesting significantly reduced yields, while using root cuttings for plantation establishment gave better yields only during the first three years of plant vegetation, than biomass yields equalized with the ones obtained by plantlets planting.

Keywords:
biomass yield, harvest date, municipal sewage sludge, propagation,
Sida hermaphrodita Rusby

Ocena efektów stosowania różnych dawek osadów ściekowych w produkcji biomasy ślazowca pensylwańskiego

Streszczenie

Celem badań było określenie wpływu zwiększających się dawek komunalnych osadów ściekowych na plonowanie i cechy jakościowe surowca energetycznego sidy-ślazowca pensylwańskiego (*Sida hermaphrodita* Rusby). W sześcioletnim doświadczeniu polowym przetestowano dodatkowo dwie metody zakładania plantacji (z sadzonek korzeniowych i rozsady wyprodukowanej w paletach wielokomórkowych) oraz trzy terminy zbioru biomasy (jesienny, zimowy i wiosenny) w warunkach klimatycznych południowo-wschodniej Polski.

Plony suchej masy ślazowca pensylwańskiego zwiększały się w kolejnych latach badań przekraczając 20 Mg ha^{-1} w drugim roku uprawy. Zastosowanie 40 Mg sm osadu ha^{-1} spowodowało uzyskanie najwyższych plonów biomasy. Notowano również zwiększenie zawartości, pobrania i wartości indeksu bioakumulacji makroelementów zawartych w osadach wraz ze zwiększaniem ich dawki. Biomasa ślazowca charakteryzowała się korzystnymi cechami: jej wartość opałowa mieściła się w przedziale 16,2-16,7 MJ kg^{-1}. Największą wartość energetyczną plonu biomasy uzyskano przy zastosowaniu sadzonek korzeniowych do zakładania plantacji, zwłaszcza na obiektach z aplikacją wysokich dawek osadu i podczas jesiennych zbiorów biomasy. Zarówno podczas zbioru zimowego, jak i wiosennego notowano istotne zmniejszenie plonów biomasy sidy, a wykorzystanie sadzonek korzeniowych do założenia plantacji wiązało się z lepszym plonowaniem tylko w pierwszych trzech latach wegetacji roślin, w okresie późniejszym plonowanie roślin było podobne jak na obiektach z wysadzaniem rozsady.

Słowa kluczowe:
plony biomasy, termin zbioru, komunalne osady ściekowe, rozmnażanie, *Sida hermaphrodita* Rusby

MIDDLE POMERANIAN SCIENTIFIC SOCIETY OF THE ENVIRONMENT PROTECTION

Rocznik Ochrona Środowiska

Volume 22. Year 2020 ISSN 1506-218X 514-525

Pool Boiling Heat Transfer from Rough and Microstructure Coated Surfaces

Łukasz J. Orman[1], Katarzyna Orman[2], Iwona Wojton[3]*

[1]Kielce University of Technology, Poland

[2]Pragmatic, Kielce, Poland

[3]Z.O.Z., Ostrowiec Świętokrzyski, Poland

[*]corresponding author's e-mail: orman@tu.kielce.pl

1. Introduction

Boiling heat transfer is affected by a number of factors related to the conditions of the process as well as material and geometrical parameters of the heater surface. These factors occur simultaneously and interact with each other. The value of the heat transfer coefficient depends significantly on, among others, saturation pressure, thermophysical properties of the working fluid as well as surface characteristics (material properties, dimensions, surface finish, thickness) (Pioro et al. 2004).

Surface microgeometry is an important parameter affecting thermal performance of the phase – change heat exchangers. Such surfaces are easy to produce, because in the most simple case emery paper could be used. In (Nishikawa et al. 1982) the test results of the impact of pressure and surface roughness on boiling of refrigerants R-11, R-21, R-113 and R-114 were presented. The experiments were performed on vertical smooth copper surfaces of diameter 20 mm and 40 mm. Roughness amounted to 0.022-4.310 μm. It was reported that the highest impact of roughness on the heat transfer coefficient could be observed under small pressures, while for higher ones this effect diminishes and disappears when pressure is critical. The paper (Kang 2000) contains research results of water boiling on tubes with different orientations – 0°, 45°, 90° (vertical) and mean roughness 60.9 nm and 15.1 nm. Tube diameters were 9.7 mm, 19.05 mm and 25.4 mm. Increased roughness enhanced heat transfer, which must be related to a higher density of active nucleation sites (locations were bubbles are generated). This effect was more evident for more inclined tubes. At high values of superheat (defined as the difference between surface and saturation temperatures) vapour

agglomeration decreased heat flux. The work (Ribatski & Saiz Jabardo 2003) analyses the effects of roughness and found that an increase in heat flux with surface roughness is related to a larger number of vapour producing nucleation sites. As a result, heat flux is enhanced on surfaces of higher roughness. In (Hosseini et al. 2011) experimental tests of boiling of R-113 on horizontal copper surfaces of different roughness: 0.901 μm, 0.735 μm, 0.65 μm and 0.09 μm were presented. It was found that the heat transfer coefficient improved with increasing roughness. The sample with roughness of 0.901 μm provided 38.5% higher value of the heat transfer coefficient than the smoothest surface of 0.09 μm.

Another method of surface modification is the application of additional coatings. Many such technologies are available, for example capillary – porous structures made from metal fibers, sintered powders, mesh structures and others. Typically, observations prove that they enhance boiling heat transfer. However, scientific reports found in literature are not entirely unanimous or even ambiguous and there is still discussion what impact such coatings have on the boiling phenomenon.

Most works considering pool boiling heat transfer on heaters with capillary – porous coatings state that the influence of their application is very favourable. In (Zaripov et al. 1989) boiling of water, nitrogen and acetone was tested. The microstructural layer was composed of copper, nickel and steel fibers. Its maximal porosity reached 93% and maximal height 10 mm. The authors found the optimal height of the layer, for which the thermal performance was highest. The work (Poniewski 2001) provides test results for boiling of water, ethanol and R-113 on horizontal isothermal surfaces with copper fibrous structures of fiber diameter 50 μm. The author confirmed the advantageous effect of this porous layer. For example the value of the heat transfer coefficient during boiling of water on a specimen of 85% porosity at the pressure of 0.1 MPa was 5.5 times higher than for the smooth surface at the same heat flux. In (Wójcik 2005) investigation of water boiling heat transfer on tubes covered with porous copper – fibrous layers of the heights in the range of 0.5 to 2.0 mm was presented. As in the earlier work of this author (Wójcik 2004) a large improvement of thermal performance was observed for the microstructural coverings. The paper (Kalawa et al. 2016) provides the test results of water boiling on heaters with porous structures from steel fibers. The authors observed enhancement of heat transfer in relation to the smooth surface (for example heat flux dissipated from the surface covered with the coating of fibers ϕ25 μm was about 3.5 larger than for the surface without any coating).

In all the presented references, the test of boiling heat transfer have been obtained on the isothermal surfaces – similarly to the author's own research for example (Orman 2016). Non – isothermal surfaces of fins are hardly ever tested

due to significant measurement complexities. Thus, in order to expend the knowledge in this area, the current paper is focused on the impact of the application of the porous microstructure and surface roughness on the thermal performance of the non – isothermal heaters.

2. Material and method

The test have been performed on the rough copper surface and the surface covered with a porous layer made of copper fibers of 50 μm diameter. The microstructure was attached to the base using the sintering process in the reduction atmosphere in order to prevent oxidation of the specimen. Figure 1 presents the image of the produced porous layer on the copper base in form of the fin. The volumetric porosity of the layer was 68%, while its height 1 mm.

Fig. 1. The fin with the microstructural covering

Another tested surface has been treated with emery paper in order to produce certain roughness. The emery paper number was 280. Details of the roughness profile has been presented in Figure 2a, while the generated surface morphology in Figure 2b.

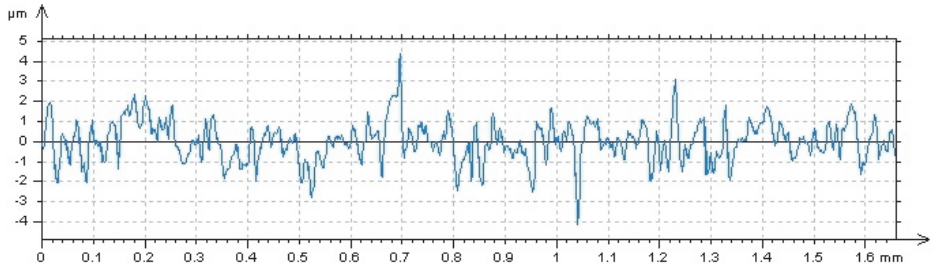

Fig. 2a. Surface roughness profile

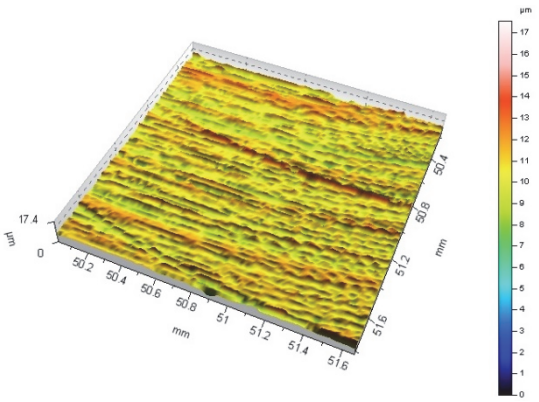

Fig. 2b. Rough surface morphology

Boiling heat transfer has been analysed at atmospheric pressure. The main component of the experimental set-up was a fin (as presented in Fig. 1). Its height was 12 mm, width 4 mm and length 90 mm. It is part of one side of the vessel, in which liquid was boiled (Fig. 3). The fin was in contact with the liquid on one side and on the other with the surroundings – this side was observed with a thermovision camera. Heat was supplied to the base of the fin by an electric cartridge heater. As a result, a temperature gradient was generated along this element. Measurements of temperature have been carried out with the infrared camera. The generated vapour was returned to the vessel so that the liquid level could have been kept constant during the experiments.

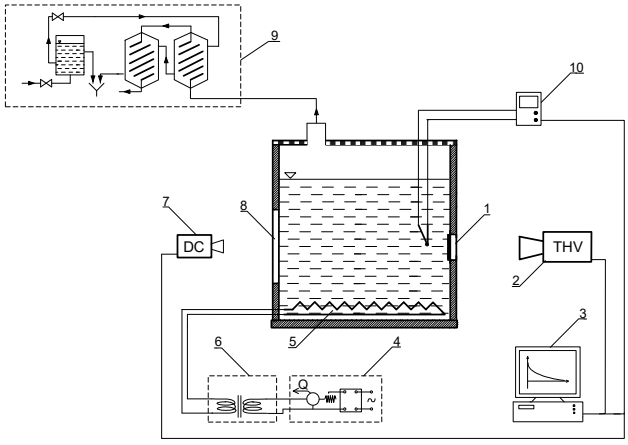

Fig. 3. Schematic of the experimental stand: 1 – fin, 2 – infrared camera, 3 – data acquisition unit, 4 – autotransformer, 5 – auxiliary heater, 6 – electrical current

separation unit, 7 – digital camera, 8 – window, 9 – cooling and condensate retrieval unit, 10 – temperature measurement device (Orzechowski & Orman 2006)

The use of the thermovision camera enables the determination of surface temperature at many points of the observed element. This number is determined by the resolution of the device. Local values of the heat transfer coefficient can be found using a method presented in (Orzechowski 2003) and described below. In this technique boiling heat transfer coefficient α is assumed to depend exponentially on superheat θ (the difference between the surface and saturation temperature):

$$\alpha = a\,\theta^{n} \tag{1}$$

where a, n are constants, whose experimental determination leads to a formula for the boiling curve. Having considered equation (1) together with other assumptions, the formula for temperature distribution in the fin equals:

$$\frac{d^2\theta}{dx^2} = m^2\,\theta^{n+1} \tag{2}$$

which was analysed in (Ünal 1985). Differentiation of (2) results in an equation for superheat gradient along the fin, which in logarithmic coordinates equals:

$$\ln\left(\frac{d\theta}{dx}\right)^2 = \ln\left(\frac{2m^2}{n+2}\right) + (n+2)\ln\theta \tag{3}$$

where $n \neq 2$, while m^2 is defined as:

$$m^2 = \frac{a\,P}{\lambda F} \tag{4}$$

P and F describe the circumference and surface area of the fin, respectively. λ is the thermal conductivity of the material. For long fins no heat transfer at the tip can be assumed. In this case C equals 0, as has been considered in (3).

Results from linear fitting lead to the determination of constants (a, n) and, consequently, boiling curves can be drawn as a function of local values of the heat transfer coefficient and wall superheat according to (1). In order to more precisely determine the heat transfer coefficients the measurement results can be analysed assuming the non-linear dependence for the heat transfer coefficient as proposed in (Orzechowski 2007).

3. Results and discussion

In the present study surface roughness produced with emery paper and the application of the copper porous microstructural coating have been considered

as factors affecting nucleate pool boiling heat transfer under ambient pressure. Figures 4 and 5 present the boiling performance of the microstructure coated surface (whose porosity was 68% and the height 1 mm) for distilled water and ethyl alcohol (purity 99.8%) as the dependence of the superheat gradient vs. wall superheat.

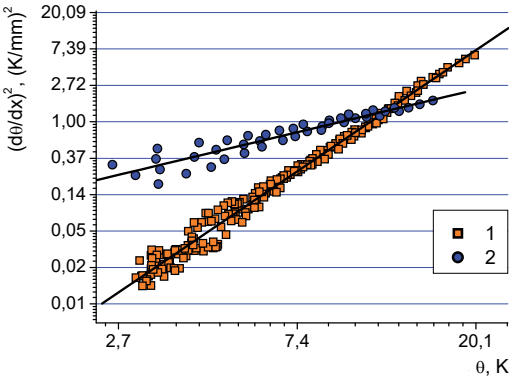

Fig. 4. Superheat gradient vs. wall superheat for distilled water: 1 – smooth surface, 2 – porous layer of porosity 68% and 1 mm height made of fine copper fibers

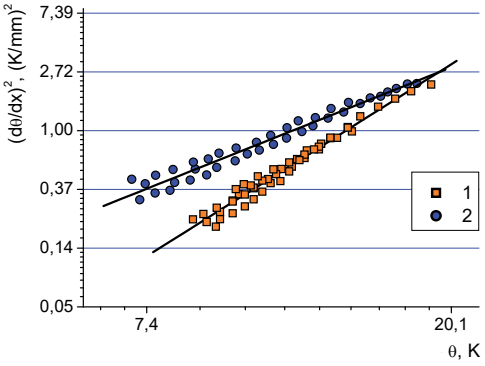

Fig. 5. Superheat gradient vs. wall superheat for ethyl alcohol: 1 – smooth surface, 2 – porous layer of porosity 68% and 1 mm height made of fine copper fibers

The application of the porous microstructure resulted in the enhancement of pool boiling heat transfer for both the working fluids in the area of low range of superheats. For higher temperature differences the performance of the capillary – fibrous heater is similar (or even worse in the case of water) to the one observed in the case of the smooth surface. It might be related to the fact that vapour

production is low at small superheats and vapour removal from the microstructure is easy for all the surfaces (including the porous layers). However, at high superheats more vapour is produced and permanent vapour blanket might be created inside the layer regardless of its porosity. Consequently, its performance diminishes. However, the porous layer provides more nucleation sites that are already active at low heat fluxes. This fact explains better thermal performance for low superheats – for both the boiling liquids.

In order to better visualize the obtained results and confront them with the rough surface tests, they have been presented in form of boiling curves as a dependence of heat flux vs. wall superheat. Figures 6 and 7 show the results for both the working fluids.

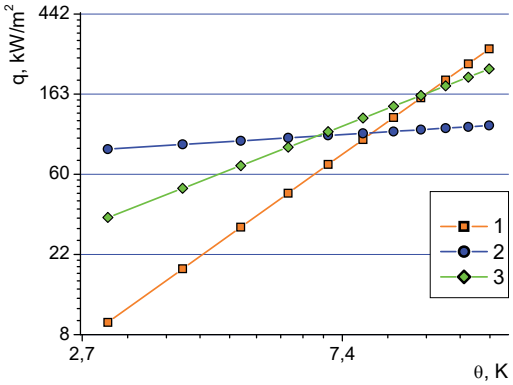

Fig. 6. Boiling curves for distilled water: 1 – smooth surface, 2 – copper fibrous microstructure, 3 – rough surface

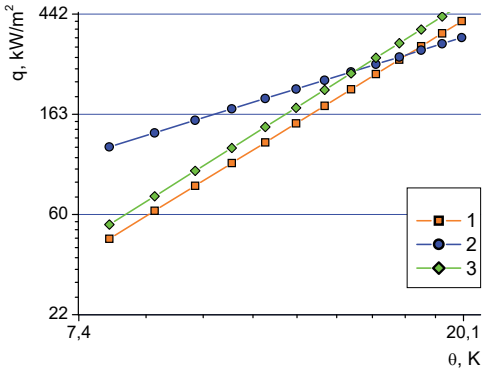

Fig. 7. Boiling curves for ethyl alcohol: 1 – smooth surface, 2 – copper fibrous microstructure, 3 – rough surface

Boiling heat transfer has been enhanced by roughening the surface in the wide range of superheats for ethyl alcohol and for lower superheats in the case of water. Roughness of the surface provides additional nucleation sites which are active at small superheats. This explains why the performance in the low superheats region is better. At higher heat fluxes more nucleation sites become active on the smooth surface, so the improvement of thermal performance becomes smaller and even diminishes. However, in the case of ethyl alcohol the diameter of bubbles is much smaller and even at high heat fluxes, when bubble coalescence occurs, the rough surface is very efficient. It is worth noting that the general trend is that the rough surface is able to provide heat transfer enhancement, however, the application of the porous covering is much more efficient in the range of small temperature differences. It is related to the fact that the microstructure traps the vapour bubbles at higher heat fluxes and an insulating vapour blanker is created within the porous layer.

The details of the enhancement possibilities have been presented in Figure 8 as the enhancement factor – the ratio of the heat flux for the microstructural heaters q_m (fibers or roughness) and for the smooth surface q_s.

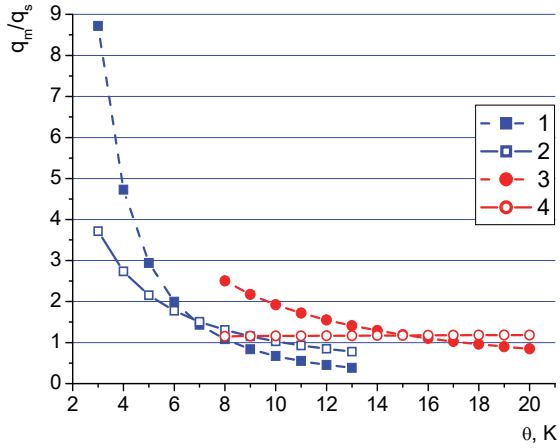

Fig. 8. Enhancement factor: 1 – distilled water, porous layer, 2 – distilled water, rough surface, 3 – ethyl alcohol, porous layer, 4 – ethyl alcohol, rough surface

As can be seen in the above figure, the largest enhancement is possible with the use of the porous layer and water as the boiling liquid. Here, the heat flux dissipated from the microstructural coating can be almost nine times higher than for the smooth surface. The rough surface provides lower improvement possibilities in the low range of superheat, however for higher ones it proves to be

better. The same phenomenon can be observed in the case of ethyl alcohol, but the enhancement ratios are much lower.

A different and quite complex problem is providing a reliable model of boiling on surfaces of modified morphology. Currently, there is no efficient correlation available in literature, which could successfully determine the boiling performance of heaters based on physical and chemical properties and parameters. In the current experiment, the obtained experimental test results of water boiling have been compared with correlations for pool boiling heat transfer available in literature and presented below in Figure 10. In the case of the metal fibrous layer, the model proposed in (Nishikawa et al. 1979) has been used. It was developed for the sintered porous coatings. While the calculations for the rough surface have been performed with the Cooper model (Cooper 1984).

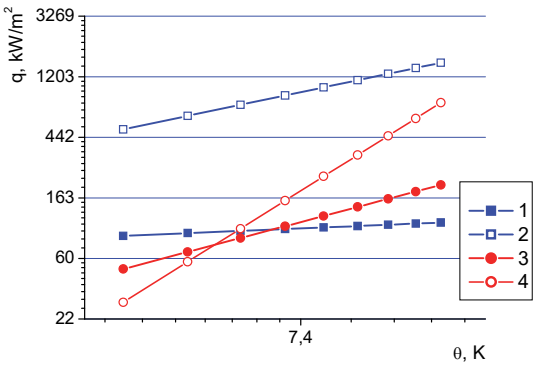

Fig. 9. Comparison of the test results and calculations according to selected correlations; microstructural surface: 1 – test results, 2 – calculation results according to Nishikawa et al. model; rough surface: 3 – test results, 4 – calculation results according to Cooper correlation

The simple model based on the assumption of the leading role of conduction (Nishikawa et al. 1979) provided much higher results than the experimental values. Although the Cooper model has been more accurate for the rough surface, still significant difference occur – especially as the superheat increased. The discrepancies in the results and calculations indicate that a new model or correlation of boiling heat transfer is necessary for surfaces of modified morphology. It needs to be noted that the results have been obtained on the non-isothermal surface of the analysed fin, while the considered correlations were developed based on the isothermal surface data.

4. Conclusions

Pool boiling heat transfer is enhanced by the application of porous and rough surfaces layers in comparison to the smooth surface. The heat flux values at the same superheat might be several times higher if additional microstructure is applied. Generally, roughening the heat exchanger surface improves the heat transfer performance in a larger range of superheats, however, the maximal enhancement is much lower than for the porous layers. The mechanism of heat transfer enhancement seems to be a combination of two factors. One is an increased number of nucleation sites (both for rough and porous surfaces) and the surface extension (only in the case of metal fibrous layer). The complexity of the phenomenon might be responsible for the fact that a successful model or a correlation for boiling heat transfer on microstructural coatings is still unavailable.

The project is supported by the program of the Minister of Science and Higher Education under the name: "Regional Initiative of Excellence" in 2019-2022 project number 025 / RID / 2018/19 financing amount PLN 12,000,000.

References

Cooper, M.G. (1984). Heat Flow Rates in Saturated Nucleate Pool Boiling-a Wide-Ranging Examination Using Reduced Properties. *Advances in Heat Transfer*, *16*, 157-239.

Hosseini, R., Gholaminejad, A., Jahandar, H. (2011). Roughness effects on nucleate pool boiling of R-113 on horizontal circular copper surfaces. *World Academy of Science, Engineering and Technology*, *55*, 679-684.

Kalawa, W., Wójcik, T.M., Piasecka, M. (2016). Heat transfer research on enhanced heating surfaces in pool boiling. Proc. of Int. Conf. Exp. Fluid Mechanics 2016, Mariánskè Lázně, Czech Republic, *EPJ Web of Conferences*, *143*, 02048.

Kang, M.G. (2000). Effect of surface roughness on pool boiling heat transfer. *Int. J. of Heat and Mass Transfer*, *43*, 4073-4085.

Koshlak, H. & Pavlenko A. (2019). Method of formation of thermophysical properties of porous materials. *Rocznik Ochrona Środowisk*a, *21*, 1253-1262.

Nishikawa, K., Fujita, Y., Ohta, H., Hidaka, S. (1982). Effect of the surface roughness on the nucleate boiling heat transfer over the wide range of pressure. *Proc. 7th Int. Heat Transfer Conf., Munchen, Germany*, *4*, 61-66.

Nishikawa, K., Ito, T., Tanaka, K. (1979). Enhanced heat transfer by nucleate boiling on a sintered metal layer. *Heat transfer – Japanese Research*, *8*, 65-81.

Orman, Ł.J. (2016). Enhancement of pool boiling heat transfer with pin-fin microstructures. *J. of Enhanced Heat Transfer*, *23*, 137-153.

Orzechowski, T. (2003). *Wymiana ciepła przy wrzeniu na żebrach z mikropowierzchnią strukturalną*. Kielce, Wydawnictwo Politechniki Świętokrzyskiej.

Orzechowski, T. (2007). Local values of heat transfer coefficient determination on fin's surface. *Experimental Thermal and Fluid Science*, *31*, 947-955.

Orzechowski, T. & Orman, Ł.J. (2006). Boiling heat transfer on surfaces covered with copper fibrous microstructures. *Proc. of XI Int. Symp. „Heat Transfer and Renewable Sources of Energy", Szczecin, Poland*, 613-619.

Pavlenko, A., & Koshlak, H. (2019). Heat and mass transfer during phase transitions in liquid mixtures. *Rocznik Ochrona Środowiska*, *21*, 234-249.

Pioro, I.L., Rohsenow, W., Doerffer, S.S. (2004). Nucleate pool boiling heat transfer. I: review of parametric effects of boiling surface. *Int. J. of Heat and Mass Transfer*, *47*, 5033-5044.

Poniewski, M.E. (2001). *Wrzenie pęcherzykowe na rozwiniętych mikropowierzchniach*, Kielce, Wydawnictwo Politechniki Świętokrzyskiej.

Ribatski, G., Saiz Jabardo, J.M. (2003). Experimental study of nucleate boiling of halocarbon refrigerants on cylindrical surfaces. *Int. J of Heat and Mass Transfer*, *46*, 4439-4451.

Ünal, H.C. (1985). Determination of the temperature distribution in an extended surface with non – uniform heat transfer coefficient. *Int. J. Heat Mass Transfer*, *28*, 2279-2283.

Wójcik, T.M. (2004). Boiling on cylindrical surfaces with thick-layered porous covering. *Proc. of X Int. Symp. Heat Transfer and Renewable Sources of Energy, Szczecin – Miedzyzdroje, Poland*, 653-660.

Wójcik, T.M. (2005). Pool boiling heat transfer on horizontal tubes with metal, fibrous porous coverings. *Proc. of 4th Int. Conf. on Transport Phenomena in Multiphase Systems HEAT2005, Gdansk, Poland*, 535-542.

Zaripov, V.K., Semena, M. G., Shapoval A.A., Levterov, A.I. (1989). Heat-transfer rate in boiling at a surface with porous coatings in conditions of free motion. *Journal of Engineering Physics*, *57*, 859-863.

Abstract

The paper presents the test results of pool boiling heat transfer on the rough surface and the surface covered with capillary – porous microstructure. The porous layer is made of copper fibers sintered in the reduction atmosphere. The volumetric porosity amounted to 68%, while its height 1 mm. Distilled water and ethyl alcohol were used as the working fluids. The experiments have been carried out under the atmospheric pressure. Enhancement of heat transfer in relation to the smooth reference surface has been recorded especially for the low range of superheats, which might be related to the density of active nucleation sites. Experimental results have been compared with selected models of boiling available in literature.

Keywords:
boiling heat transfer, porous coatings, rough surface

Wymiana ciepła przy wrzeniu na powierzchniach chropowatych i z pokryciem mikrostrukturalnym

Streszczenie

Artykuł przedstawia wyniki badań wymiany ciepła przy wrzeniu na powierzchniach chropowatych i z porowatym pokryciem metalowo-włóknistym. Mikrostruktura porowata została wykonana z włókien miedzianych spiekanych w atmosferze redukcyjnej. Porowatość objętościowa wynosi 68%, a wysokość warstwy 1 mm. Badania prowadzono dla wody destylowanej i alkoholu etylowego jako cieczy wrzących pod ciśnieniem atmosferycznym. Zaobserwowano intensyfikację wymiany ciepła w porównaniu do powierzchni gładkiej, szczególnie w zakresie małych przegrzań, co może być związane z gęstością aktywnych centrów nukleacji. Wyniki badań eksperymentalnych porównano z wybranymi modelami wrzenia dla danych powierzchni.

Słowa kluczowe:
wymiana ciepła przy wrzeniu, pokrycie porowate, chropowatość

MIDDLE POMERANIAN SCIENTIFIC SOCIETY OF THE ENVIRONMENT PROTECTION

Rocznik Ochrona Środowiska

Volume 22. Year 2020 ISSN 1506-218X 526-536

The Influence of an External Waste Carbon Source on the Rate of Changes in Pollutant Concentrations During Wastewater Treatment

Katarzyna Ignatowicz[1], Joanna Smyk[2], Jacek Piekarski[3]*

[1]Bialystok University of Technology, Poland

[2]Transition Technologies Managed Services, Poland

[3]Koszalin University of Technology, Poland

[*]corresponding author's e-mail: k.ignatowicz@pb.edu.pl

1. Indroduction

Carbon sources may come from wastewater flowing into the treatment plant or may be supplied as additional external carbon sources added to the treatment system. These sources are divided into internal (present in wastewater), endogenous (produced in activated sludge chambers as a result of biomass decomposition) and external (absent in wastewater) (Mąkinia et al. 2008, Smyk & Ignatowicz 2017, Cherchi et al. 2009). Internal carbon sources refer to organic carbon substrates obtained both in the sewage system (as an organic load of introduced sewage) or produced and stored in cells, also called endogenous carbon sources (Min et al. 2002, Elefsiciotis & Li 2006, Fernandeaz-Nava et al. 2010).

One of the initial stages of the activities related to the possibility of using alternative carbon sources in the denitrification process is the screening of available waste products due to the high COD/N ratio and high content of easily decomposable organic compounds. The main consideration is given to post-production wastewater, waste and semi-finished products such as starch syrup, glucose, molasses, beet pulp, raw spirit or Fusel alcohol (Mąkinia et al. 2008, Kalinowska 2006, Yang et al. 2012, Tora et al. 2011, Silva et al. 2009, Bernat et al. 2016 Dąbrowski & Puchlik 2010).

Molasses is produced as a by-product of the sugar industry and used in the distillery industry. Molasses is a malleable brown liquid. The substance has a characteristic smell and a bittersweet taste. Molasses contains about 48-50% sucrose (Arshad et al. 2008, Silva et al. 2009, Smyk & Ignatowicz 2017). The main component of molasses, i.e. polysaccharides, contains long chains that

prevent rapid use of this substrate by denitrifying bacteria, therefore it is recommended that molasses be hydrolysed to convert it into simpler compounds such as glucose, sucrose and fructose (Ignatowicz et al. 2011, Janczukowicz & Rodziewicz 2013, Janczukowicz et al. 2011).

The aim of the research was to confirm the effectiveness of the use of waste products, in the example of molasses, in the denitrification process, as well as to determine their influence on the rate of changes in pollutant concentrations during wastewater treatment.

2. Testing methodology

The research was carried out in two SBR reactors with activated sludge supplied by mechanically treated municipal wastewater. (Smyk & Ignatowicz 2017, Smyk et al. 2019) The active capacity was 13 dm^3, of which 8 dm^3 was activated sludge. A single reactor cycle lasted 6 hours and included the following phases: wastewater supply (2 min), mixing (anaerobic) (60 min), aeration (210 min), sedimentation (60 min) and decantation (30 min). During the aeration phase, compressed air was fed through a diffuser placed at the bottom of the rector. Depending on the phase of work, from 0.1 to 2.0 mg O_2 /dm^3, active sludge concentration 3.5 kg/m^3, sludge index ranged from 120-180 cm^3/g, hydraulic load of the chamber was 1.5 m^3/m^3d and load of organic pollutants 0.2-0.3 kg COD/m^3d.

An external source of carbon was added to one of the chambers twenty minutes after filling the sewage. The dose was calculated with the amount and composition of raw sewage taken into account, assuming the COD/N ratio was equal to 6. The sewage samples were subjected to filtration immediately after collection. During filtration, the samples were measured in accordance with the current methodology (Smyk et al. 2019, Puchlik et al. 2015, Ignatowicz & Puchlik 2011):

- COD – dichromate method as per PN-74/C-04578.03 standard,
- BOD – manometric method of OxiTop Standard system,
- $N\text{-}NH_4$ – spectrophotometric method according to PN-ISO 7150-1:2002,
- $N\text{-}NO_3$ – spectrophotometric method according to PN-82/C-04576/08,
- N tot. – Spectrophotometric method according to PN-EN ISO 6878:2006,
- P tot. – Spectrophotometric method according to PN-C-04576-00:1973P.

On the basis of the results obtained, the rate of removal of individual pollutants from waste water during the process phases of SBR reactors (anaerobic denitrification phase and aerobic nitrification phase) was determined using the formula:

$$r_v = \frac{A - B}{T} \left[\frac{mg}{dm^3 \cdot h}\right]$$

where:
A – value/concentration at the beginning of the process phase [mg/dm^3],
B – value/concentration at the end of the process phase [mg/dm^3],
T – process phase lengh [h].

The nitrate utilization rate NUR was also determined from the formula:

$$NUR = \frac{S_{N-NO3,t1} - S_{N-NO3,t2}}{\Delta t} \left[\frac{mg\ N - NO_3}{dm^3 \cdot h}\right]$$

where:
S_(N-NO3,t) – nitrate nitrogen concentration at t [mg N/dm^3],
Δt – measurement time [h].

The phosphorus release rate PRR was determined based on the formula:

$$PRR = \frac{S_{P,t2} - S_{P,t1}}{\Delta t} \left[\frac{mg\ P}{dm^3 \cdot h}\right]$$

The phosphorus uptake rate PUR based on the formula:

$$PUR = \frac{S_{P,t1} - S_{P,t2}}{\Delta t} \left[\frac{mg\ P}{dm^3 \cdot h}\right]$$

where:
S_(P,t) – concentration of phosphorus at time t [mg P/dm^3],
Δt – measurement time [h].

3. Results and Interpretation of tests

The COD/Nog ratio in municipal sewage was 7.2 on average (Fig. 1). Filling the reactors with sewage and a twenty-minute process of wastewater mixing resulted in a lower COD/Nog ratio - the value ranged from 4.2 to 4.4. According to the literature data, denitrification has been conducted when the COD/Nog ratio is from 5 to 10. A lower value indicates the necessity of introducing an external carbon source into the sewage (Elefsioris & Li 2006, Smyk et al. 2019, Janczukowicz & Rodziewicz 2013). The addition of external carbon sources to the SBR reactors increased the COD/Nog ratio – during the denitrification phase. The ratio gradually increased to its highest value of 6.3 in the reactor

with the addition of molasses at the end of the anaerobic phase. This ensured the correct course of denitrification. During the anaerobic phase, the COD/Nog relationship ranged from 2.0 to 4.7.

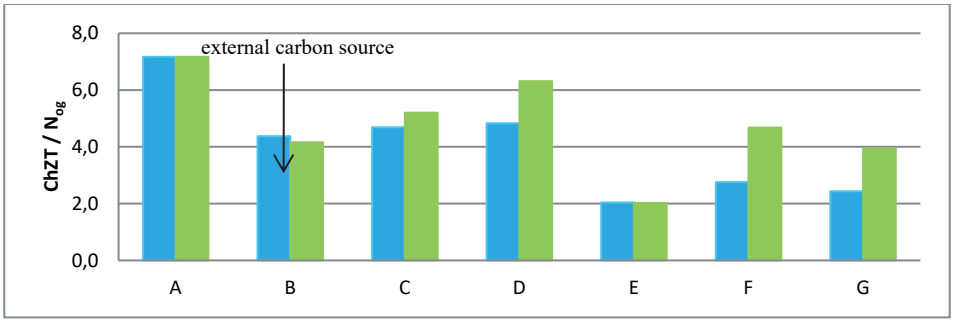

Fig. 1. Comparison of COD to total nitrogen at individual control points

During the anaerobic phase of wastewater treatment, the removal of organic compounds referred to as COD took place only in a control reactor (Fig. 2). The reason for this was the dosage of an external carbon source to a second reactor to increase the amount of organic compounds. During the processes of mixing and aeration of wastewater in the reactors, a decrease in the value of organic compounds referred to as COD was recorded (Fig. 3). In the reactor where molasses was introduced, the removal rate of organic matter measured as COD was found to be higher than in the control reactor. This rate was 61.43 mg COD/dm^{3}h (17.55 mg COD/g_{dm}h) and in the control reactor 54.86 mg COD/dm^{3}h (15.67 mg COD/g_{dm}h).

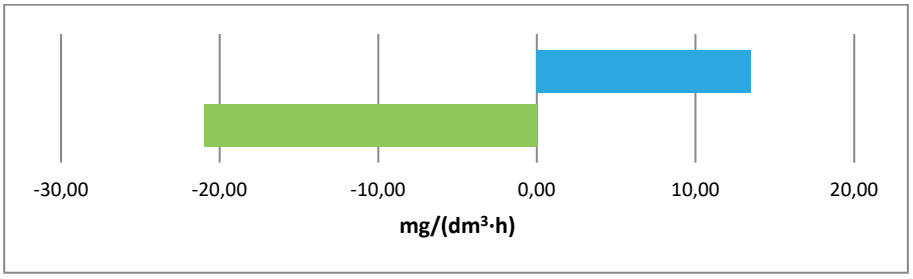

Fig. 2. Average removal rate of organic compounds, referred to as COD, during the anaerobic phase in SBRs

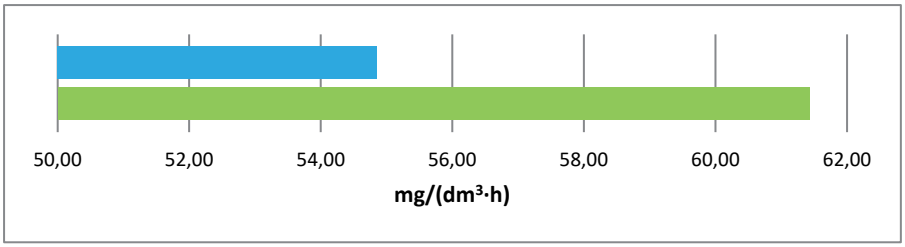

Fig. 3. Average removal rate of organic compounds, referred to as COD, during the mixing and aeration phase in SBRs

On the other hand, for both reactors, the same average removal rate of organic compounds ,defined as BOD_5, during the anaerobic phase of wastewater treatment was calculated – 22.50 mg BOD_5/dm^3h (6.43 mg $BOD/g_{dm}h$). (Fig. 4). The microorganisms absorbed the assimilable organic compounds at the same rate. During the process of mixing and aeration of wastewater, a decrease in the amount of organic compounds, defined as BOD_5, was recorded in all SBR reactors (Fig. 5). In the reactor where an external source of carbon was introduced, a slightly (by 1.43 mg BOD/dm^3h) faster process of organic matter removal, measured as BOD_5, was observed in comparison with the control reactor.

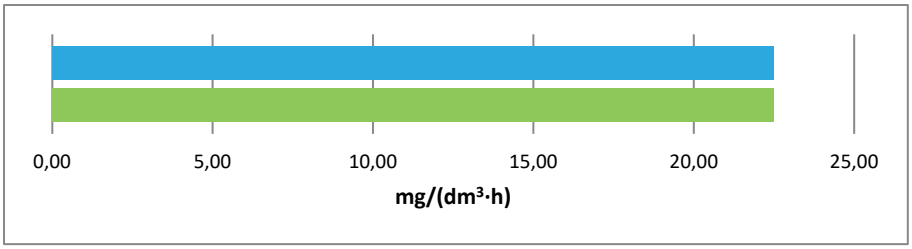

Fig. 4. Average removal rate of organic compounds, referred to as BOD_5, during the anaerobic phase in SBRs

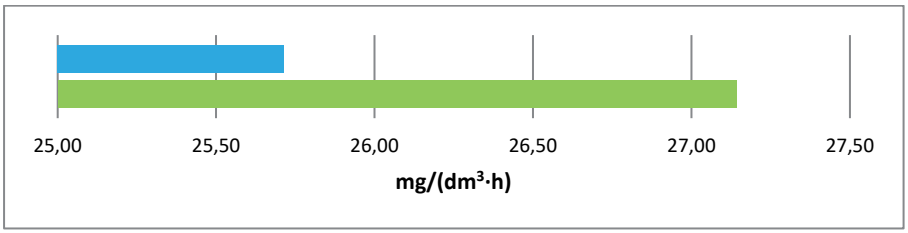

Fig. 5. Average removal rate of organic compounds, known as BOD_5, during the mixing and aeration phase of SBRs

During the anaerobic phase of wastewater treatment in the reactor with molasses, a much higher average rate of total nitrogen removal was found compared to the control reactor (Fig. 6). The removal of total nitrogen occurred here by 17.03 mg N/dm^{3}h faster than in the control reactor. During the process of mixing and aeration of wastewater in the reactor with molasses, the rate of removal of total nitrogen decreased from 28.58 to 8.81 mg N/dm^{3}h, but was still higher than in the control reactor (Fig. 7).

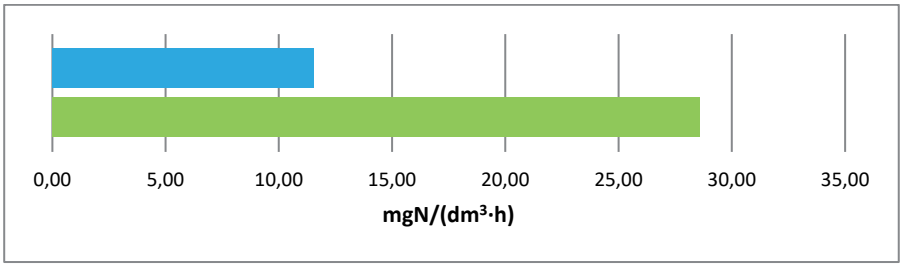

Fig. 6. Average removal rate of total nitrogen during anaerobic phase in SBRs

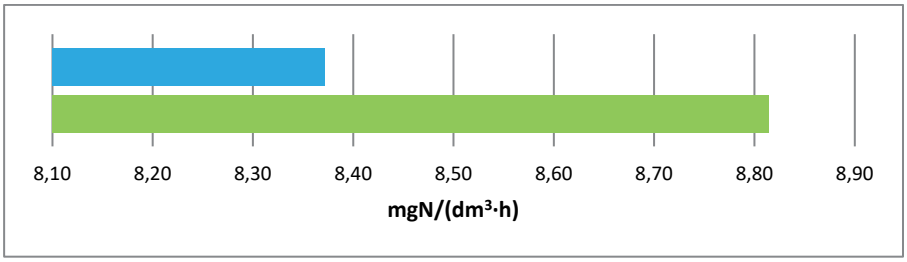

Fig. 7. Average removal rate of total nitrogen during the mixing and aeration phase in SBRs

The increased amount of easily assimilable carbon compounds in the form of molasses has also contributed to an increase in the NUR denitrification rate. Figure 8 shows the denitrification rate twenty minutes after the addition of the carbon source and the average rate of all denitrification. In the initial phase of denitrification with the addition of an external carbon source, no acceleration of nitrogen removal was observed. However, the average rate of the whole denitrification phase (Fig. 9) in a reactor without the addition of a carbon source was much lower, only 0.45 mg N/dm^3·h, while the difference in speed between reactors was 2.48 mg N/dm^3·h. The NUR rate in the molasses reactor was 2.93 mg N/dm^3·h (0.88 mg Nog/g_{dm}·h). Quan et al (2005) described the effect of hydrolysed molasses on the effectiveness of nitrogen removal in the SBR reactor treating synthetic

wastewater. The authors obtained denitrification rates of 2.9-3.6 mg N_{tot}/(gsmo-h). Bernat and others. (2016) studied the removal of nitrogen compounds from wastewater in SBR reactors using molasses as a carbon source. In the 22-hour process of wastewater mixing with COD/N = 5.5, the authors obtained a nitrate (V) removal rate of about 22 mg N/(dm^3·h) (5.2 mg N/(gsmo·h)) for the initial 3 hours of the cycle, while during the further part of the SBR reactor cycle the rate decreased to 3 mg N/(dm^3·h) (0.71 mg N/(g_{dm}·h)). The authors obtained much higher denitrification rates in comparison to the presented own research, however, in their research they used model sewage produced on liquid mineral substrate and the only source of nitrogen in the sewage were nitrates(V) and nitrates(III) in the form of KNO_3 and $NaNO_2$ solutions respectively.

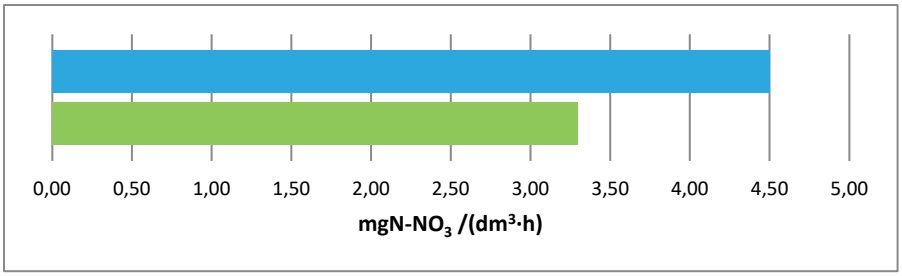

Fig. 8. NUR denitrification rate twenty minutes after the addition of a carbon source in an SBRs

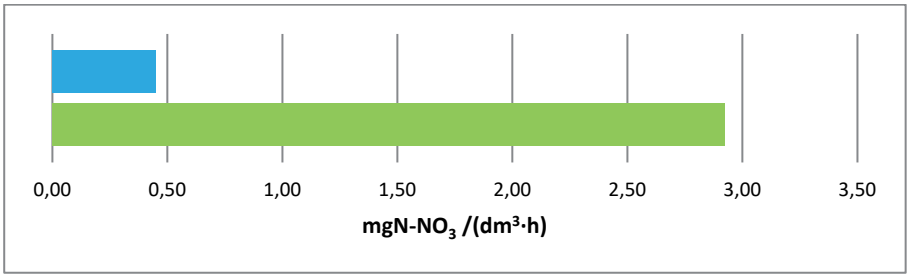

Fig. 9. Average rate of NUR denitrification in SBRs

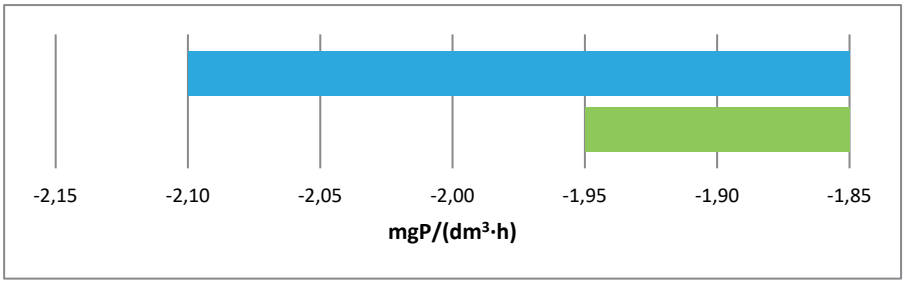

Fig. 10. Average release rate of total phosphorus PRR during anaerobic phase in SBRs

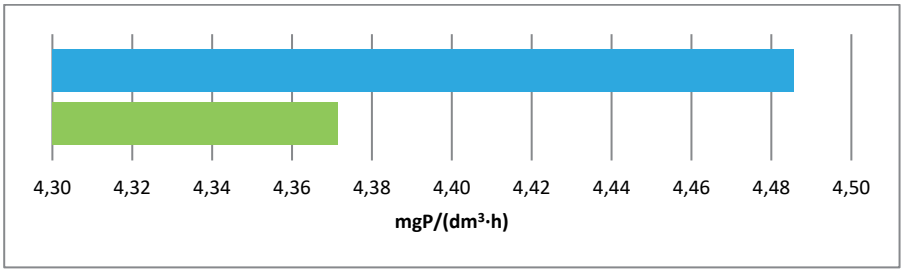

Fig. 11. Average PUR total phosphorus removal rate during the mixing and aeration phase in SBRs

During the anaerobic phase of wastewater treatment, an increase in total phosphorus concentration was observed in all reactors due to the secondary release of phosphorus from PAO phosphorus bacteria (Fig. 10), which translates into a negative value of phosphorus compounds removal rate. This phenomenon occurred much faster in the control reactor. Therefore, it can be concluded that an increased amount of easily assimilable organic compounds from molasses inhibited the release of phosphorus from PAO bacteria. During the process of mixing and aeration of wastewater, a decrease in total phosphorus concentration in all reactors was recorded (Fig. 11). The process speed was comparable in both reactors and was 4.40 and 4.37 mg P/dm^3 h respectively.

To sum up, the studies confirmed a high potential for the use of waste substances (molasses) as an alternative external carbon source in the process of municipal wastewater treatment. The use of waste substances contributed to an increase in the amount of easily assimilable organic compounds required by activated sludge microorganisms and to a higher removal efficiency of nitrogen forms than in the control reactor while maintaining a high efficiency of removing organic compounds.

4. Conclusions

1. The use of an external source of waste carbon in the treatment of municipal wastewater has resulted in a higher removal efficiency of nitrogen forms than in a control reactor while maintaining a high removal efficiency of organic compounds.
2. The use of molasses as an external source of carbon during wastewater treatment resulted in an increased removal rate during waste water treatment.
3. The rate of NUR denitrification in the molasses reactor increased by 2.48 mg $N/dm^3 \cdot h$ compared to the control SBR.
4. Molasses as a waste product can be successfully used as an external source of carbon in the denitrification process.

The research was funded by a Research Project conducted in the Department of Technology in Engineering and Environmental Protection (WZ/WBiIS/8/2019).

References

Arshad, M., Chan, Z.M., Khalil-ur-Rehman, M., Szach, F.A., Rajoka, M.I. (2008). Optimization of process variables for minimization of byproduct formation during fermentation of blackstrap molasses to ethanol at industrial scale. *Lett. Appl. Microbiol*., *47*(5), 410-414.

Bernat, K., Kulikowska, D., Kordel, A. (2016). Usuwanie związków azotu ze ścieków w procesach denitryfikacji i skróconej denitryfikacji z wykorzystaniem melasy jako źródła węgla organicznego. *Ochrona Środowiska*, *38*(2), 9-15.

Cherchi, C., Onnis-Hayden, A., El-Shawabkeh, I., Gu, A.Z. (2009). Implication of using different carbon sources for denitrification in wastewater treatments. *Water Environment Research*, *81*(8), 788-799.

Dąbrowski, W., Puchlik, M. (2010). Udział frakcji ChZT w ściekach mleczarskich w oczyszczalni stosującej intensywne usuwanie związków węgla, azotu i fosforu. *Rocznik Ochrona Środowiska*, *12*, 735-746.

Elefsiniotis, P., Li, D. (2006). The effect of temperature and carbon source on denitrification using volatile fatty acids. *Biochemical Engineering Journal*, *28*(2), 148-155.

Fernández-Nava, Y., Maranón, E., Soons, J., Castrillón, L. (2010). Denitrification of high nitrate concentration wastewater using alternative carbon sources. *Journal of Hazardous Materials*, 173, 682-688.

Ignatowicz, K. (2008). Sorption process for migration reduction of pesticides from graveyards. *Archives of Environmental Protection, 34*(3), 143-149.

Ignatowicz, K., Piekarski, J., Kozłowski, D. (2011). Intensification of the Denitrification Process by Using Brenntaplus VP1 Preparation, *Rocznik Ochrona Srodowiska, 17*(2), 1178-1195.

Ignatowicz, K., Puchlik, M. (2011). Rotary Biological Contactor as Alternative for Small Amount of Wastewater Treatment. *Rocznik Ochrona Środowiska*, *13*, 1385-1404.

Janczukowicz, W., Rodziewicz, J., Filipkowska, U. (2011). Ocena procesów biologicznego usuwania azotanów (V) i fosforanów w komorze SBR z zewnętrznym źródłem węgla. *Rocznik Ochrona Środowiska*, *13*, 453-470.

Janczukowicz, W., Rodziewicz, J. (2013). *Źródła węgla w procesach biologicznego usuwania związków azotu i fosforu,* Monografie Komitetu Inżynierii Środowiska Polskiej Akademii Nauk, 114, Lublin.

Kalinowska, E. (2006). Zewnętrzne źródło węgla do denitryfikacji. *Forum Eksploatatora, 3*, 41-42.

Mąkinia, J., Czerwionka, K., Drewnowski, J., Swinarski, M., Chrzanowska, M., Fordoński, W. (2008). Porównanie tradycyjnych i alternatywnych źródeł węgla zewnętrznego dla poprawy efektywności procesu denitryfikacji. *Forum Eksploatatora, 2,* 15-20.

Min, K., Park, K.-S., Jung, Y.-J., Khan, A.R. (2002) Acidogenic Fermentation: Utilization of Wasted Sludge as a Carbon Source in the Denitrification Process. *Environmental Technology, 23*(3), 293-302.

Puchlik, M., Ignatowicz, K., Dąbrowski, W. (2015). Influence of bio- preparation on wastewater purification process in constructed wetlands. *Journal of Ecological Engineering*, 16*(1)*. 159-163.

Quan, Z.X., Jin, Y.S., Yin, C.R., Lee, J., Lee, S.T. (2005). Hydrolyzed molasses as an external carbon source in biological nitrogen removal. *Bioresource Technology*, *96*(15), 1690-1695.

Silva, F., Nadais, H., Prates, A., Arroja, L., Capela, I. (2009). Molasses as an external carbon source for anaerobic treatment of sulphite evaporator condensate. *Bioresource Technology*, *100*, 1943-1950.

Smyk, J., Ignatowicz, K. (2017). The influence of molasses on nitrogen removal in wastewater treatment with activated sludge, *Journal of Ecological Engineering*, *18*, 199-203.

Torà, J.A., Baeza, J.A., Carrera, J., Oleszkiewicz, J.A. (2011). Denitritation of a high-strength nitrite wastewater in a sequencing batch reactor using different organic carbon sources. *Chemical Engineering Journal, 172(2-3)*, 994-998.

Yang, X., Wang, S., Zhou, L. (2012). Effect of carbon source, C/N ratio, nitrate and dissolved oxygen concentration on nitrite and ammonium production from denitrification process by *Pseudomonas stutzeri D6. Bioresource Technology*, *104*, 65-72.

Abstract

Providing external sources of carbon to the treated wastewater often becomes necessary to achieve high efficiencies of wastewater treatment plants. The use of conventional sources of carbon brings high operating costs for wastewater treatment plants. This has become a prerequisite for the exploration of other, alternative, sources of organic carbon. The aim of the research was to confirm the effectiveness of the use of waste products, for example molasses, in the denitrification process, as well as to determine their influence on the rate of changes in pollutant concentrations during wastewater treatment. The studies were carried out during the process of municipal sewage treatment in two independent SBR-type activated sludge chambers on a laboratory scale. A single reactor operating cycle lasted 6 hours and included the following phases: wastewater supply

(2 min), mixing (anaerobic) (60 min), aeration (210 min), sedimentation (60 min) and decantation (30 min). Molasses was added to one of the chambers in each cycle twenty minutes after filling the wastewater as a source of easily assimilable organic compounds. The use of a waste external carbon source during treatment of municipal wastewater resulted in a higher efficiency of removing nitrogen forms than in the control reactor while maintaining a high efficiency of removing organic compounds. The use of molasses during wastewater treatment resulted in an increased removal rate during waste water treatment. The rate of NUR denitrification in the molasses reactor increased by 2.48 mg $N/dm^3 \cdot h$ compared to the control SBR. Molasses as a waste product can be successfully used as an external carbon source in the denitrification process.

Keywords:
external carbon source, molasses, SBR reactor

Wpływ odpadowego zewnętrznego źródła węgla na szybkość zmian stężenia zanieczyszczeń podczas oczyszczania ścieków

Streszczenie

Dostarczanie do oczyszczanych ścieków zewnętrznych źródeł węgla często staje się niezbędne do osiągnięcia wysokiej wydajności oczyszczalni ścieków. Wykorzystywanie konwencjonalnych źródeł węgla niesie za sobą wysokie koszty eksploatacyjne oczyszczali ścieków. Stało się to przesłaną do poszukiwań do innych, alternatywnych źródeł węgla organicznego. Celem prowadzonych badań było potwierdzenie skuteczności stosowania produktów odpadowych na przykładzie melasy w procesie denitryfikacji, a także określenie ich wpływu na szybkość zmian stężenia zanieczyszczeń podczas oczyszczania ścieków. Badania prowadzono podczas procesu oczyszczania ścieków komunalnych w dwóch niezależnych komorach osadu czynnego typu SBR w skali laboratoryjnej. Pojedynczy cykl pracy reaktora trwał 6 godzin i obejmował fazy: doprowadzenia ścieków (2 min), mieszania (beztlenowa) (60 min), napowietrzania (210 min), sedymentacji (60 min) i dekantacji (30 min). Do jednej z komór w każdym cyklu po dwudziestu minutach od napełnienia ścieków dodawano melasę jako źródło łatwo przyswajalnych związków organicznych. Zastosowanie odpadowego zewnętrznego źródła węgla podczas oczyszczania ścieków komunalnych przyczyniło się do wyższej skuteczności usuwania form azotu niż w reaktorze kontrolnym przy zachowaniu wysokiej efektywności usuwania związków organicznych. Zastosowanie melasy podczas oczyszczania ścieków spowodowało zwiększenie szybkości usuwania zanieczyszczeń podczas oczyszczania ścieków. Szybkość denitryfikacji NUR w reaktorze z melasa wzrosła o 2,48 mg $N/dm^3 \cdot h$ w porównaniu do SBR kontrolnego. Melasa jako produkt odpadowy z powodzeniem może być stosowany jako zewnętrzne źródło węgla w procesie denitryfikacji.

Słowa kluczowe:
zewnętrzne źródło węgla, melasa, reaktor SBR

MIDDLE POMERANIAN SCIENTIFIC SOCIETY OF THE ENVIRONMENT PROTECTION

Rocznik Ochrona Środowiska

Volume 22. Year 2020 ISSN 1506-218X 537-548

The Investigation of Thermophysical Characteristics of Porous Insulation Materials Based on Burshtyn TPP Ash

Hanna Koshlak[*]*, Anna Kaczan*

Kielce University of Technologies, Poland

[*]*corresponding author's e-mail: kganna.777@gmail.com*

1. Introduction

Reducing heat emissions through the construction of buildings and structures, industrial equipment, heating networks and other facilities is the main goal of energy saving. Therefore, the production and use of thermal insulation materials in thermal technologies and construction is an important component in ensuring the sustainable development of society.

One of the most promising technologies to produce porous structures is the use of fly ash thermal power station as the base material. The authors of (Chudnovsky 1962) explored the possibility of using as solid mineral filler to obtain porous structures solid wastewater and coal ash. Study Dehghan (2016) presents a novel thermal plasma melting technique for neutralizing and recycling municipal solid waste incinerator (MSWI) ash residues. MSWI ash residues were converted to water-quenched vitrified slag using plasma vitrification, which is environmentally benign. Slag is produced as a raw material in producing porous materials for architectural and decorative applications, eliminating the problem of its disposal (Koshlak & Pavlenko 2019). Propose to use fly ash and silicon dioxide in the production of autoclaved aerated concrete. However, in this work, as in all of the above, the aim was not to carry out comprehensive studies aimed at selecting the composition of the raw material mixture based on cheap raw materials (in our case, the technogenic waste – TPP ash).

Thermophysical characteristics of porous thermal insulation materials are generally determined by the structure, size, type and shape of pores, as well as their relative arrangement in the material (Pavlenko & Koshlak 2019). The most important thermophysical properties of porous materials include three characteristics of heat transfer: thermal conductivity, thermal diffusivity and specific heat.

The thermal conductivity of materials depends on the following factors:

1) the physical state and structure, which are determined by the phase state of the substance; degree of crystallization and crystal size; anisotropy of thermal conductivity of crystals and direction of heat flux; the volume of porosity of the material and the characteristics of the porous structure,
2) the chemical composition and the presence of impurities, the latter especially affect the thermal conductivity of crystalline bodies,
3) operating conditions depending on the temperature, pressure, humidity of the material.

The most important of these characteristics is thermal conductivity. The thermal conductivity of porous materials with a constant composition of the solid phase depends on the porosity, type and characteristics of the porous structure.

Also thermophysical characteristics of porous materials will vary depending on the size and location of pores, chemical composition and molecular structure of the components, humidity. The specific heat of the materials depends on their nature and to a small extent on the volume of porosity. Average density is a value that is equal to the ratio of the mass of a substance to its volume, is measured in kg/m^3. It should be noted that the average density of thermal insulation materials is quite low compared to most building materials, because a considerable volume is occupied by pores. The density of thermal insulation materials used in construction ranges from 17 to 400 kg/m^3, depending on their purpose.

Humidity – adversely affects the thermophysical properties of thermal insulation products. As the moisture content of the insulating (and building) materials increases, their thermal conductivity dramatically increases. An important characteristic of a thermal insulation material is the sorption moisture, which is the equilibrium hygroscopic moisture of the material, at different temperatures and relative humidity.

Water absorption (hygroscopicity) – (the ability of a material to absorb and retain moisture in the pores in direct contact with water) has a negative effect on the thermal conductivity of the material, because with increasing humidity the thermal conductivity increases.

Temperature resistance is an important property of thermal insulation materials, especially when used to insulate industrial equipment operating at high temperatures. The application temperature of insulation materials should be slightly lower than their temperature resistance, since it is necessary to take into account destructive phenomena in products with prolonged heating (Muthtamilselvan et al. 2010, Kahveci 2017).

Frost resistance – the ability of a material in a saturated state to withstand repeated alternation of freezing and thawing without signs of destruction. The longevity of the whole structure depends on this indicator.

The mechanical properties of thermal insulation materials include strength (compression, bending, tensile, resistance to the formation of cracks).

Strength – the property of materials to resist the destruction of external forces that cause deformation and internal stresses in the material. The strength of thermal insulation products depends on the structure, strength of their solid component (skeleton) and porosity. Solid material with small pores is more durable than material with large uneven pores.

2. Purpose of work and research methods

Conducting a study of raw material mixture based on TPP Bursthyn ash to identify patterns of change in the thermophysical characteristics of porous materials. Thermal conductivity in porous material is due to various physical processes that can be reduced to three types: conduction, convection, and radiation. Literature sources indicate that the dependence of thermal conductivity has the character of an exponential function (Nield & Bejan 2013). These dependencies are not sufficiently clear and expressive in nature, which makes it impossible to offer an analytical expression to describe this function, especially at large values of material density. In our experiments, the coefficient of thermal conductivity was determined in the dry state and in the state of sorption moisture, which did not exceed 20%.

The thermal conductivity of porous insulation materials was investigated using an IT-λ-400 instrument. The test specimens of cylindrical shape with a thickness of 5 mm and a diameter of 15 mm were placed in the device and subjected to heating to 800°C. In this temperature range, the thermal conductivity of the material was determined according to the standard procedure outlined in the operating instructions of the device.

The thermal conductivity of the samples was calculated by the formula:

$$\lambda = \frac{h}{R_S} \tag{1}$$

where:
λ – thermal conductivity, h – sample thickness, RS – thermal resistance.

To improve the measurement accuracy, the thermal conductivity of each sample was measured three times, followed by averaging. The measurement error was 4-5%. The experimental value of the thermal conductivity of the samples varied from 0.04 to 1.3 W/(mK).

Investigation of the compressive strength of the specimens. The compressive strength of materials was determined by standard methods (Tarasov 2016). To determine the compressive strength, the cubes with rib sizes of 5 and 10 cm were cut. The samples were dried to constant weight at a temperature of 105-110°C. Cubes tested on the press. The maximum effort obtained during the test was taken as the value of the destructive load, such as the compressive strength was in the range of 0.3-8.0 MPa.

Water absorption. To determine the water absorption was made samples of dimensions 100×100 mm with a thickness of the product. The sample was dried to constant weight and immersed in water at 20°C, covered with a mesh and mounted on top of the sample and kept for twenty-four hours. For the first three hours, half the thickness of the specimen was under water, and then completely in water after all the time. After the experiment, the sample was wiped with a cloth, weighed on scales. Water absorption W, % was calculated by the formula:

$$W = \frac{m_1 - m}{m} \cdot 100 \tag{2}$$

where:
m – dry sample mass, g; m_1 – mass of water saturated with the sample, g.

Water absorption in the experiments varied from 1 to 18%.

3. Experimental research

The experimental data were processed using the planned experiment method. As the objective function (Y, W/(mK)), thermal conductivity is accepted. The experiment was based on the program of the central composite rotatable plan of the second order of Box-Hunter (Pian 2016). The kernel of the plan is represented by the semicolon 2^{5-1} ($1 = X_1X_2X_3X_4X_5$). Controlled factors are those investigated in the previous series of experiments. The selected factors satisfy the requirements of controllability, interdependence, uniqueness, which must be satisfied by variational factors when planning the experiment. 16 experiments were implemented at the basic levels, supplemented by another 10 experiments at the star points (the magnitude of the star shoulder in our case is 2) and six experiments at the center of the plan. The main levels, factor variation intervals, and boundaries of the study area were selected from previous experiments and based on information (Table 1).

The feedback function is approximated by a second-order polynomial:

$$Y = b_0 + \sum_{1<i<k} b_i X_i + \sum_{1<i<k} b_i X^2{}_i + \sum_{1<i,l<k} b_{i,l} X_i X_l \tag{3}$$

where:
k – number of independent variables.

Table 1. Basic levels, intervals of variation of factors and boundaries

Factor	Code	Value					Change interval
		-2	-1	0	+1	+2	Δ
Ash content, part of weight	X_1	0	30	60	90	120	30
Clay content, part of weight	X_2	0	20	40	60	80	20
Water content, part of weight	X_3	10	30	50	70	90	20
Temperature, °C	X_4	100	150	300	450	600	150
Content Na_2SO_4, part of weight	X_5	0	3	6	9	12	3

The processing of the experimental results and the analysis of the regression model were performed using the "Experiment Planning" module of the Statgraphics 5.0 Plus statistical program. The significance of the coefficients of the model was determined with the help of the P-level and shown on a standardized Pareto graph (Fig. 1). The vertical line in Fig. 1 corresponds to 95% of the statistical significance of the coefficients. According to Fig. 1, the coefficients for the linear terms of the regression equation for the ash, water and temperature contents are statistically significant. In this case, the coefficients for pair interactions are statistically insignificant and may not be taken into account when calculating the obtained model.

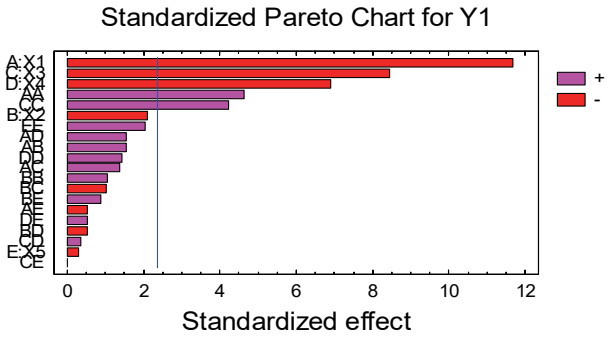

Fig. 1. Significance of model coefficients (Pareto graph)

The regression equation, given the significance of the coefficients, is:

$$Y1 = 0{,}978724 - 0{,}00966389 \cdot X_1 - 0{,}00824062 \cdot X_3 + \\ + 0{,}000705556 \cdot X_4 + 0{,}0000322917 \cdot X^2_1 + 0{,}0000664062 \cdot X_3{}^2 \quad (4)$$

The adequacy of the model of the studied process is confirmed by the high value (about 100%) of the coefficient of determination $R_2 = 99{,}44\%$, as well as the small value of the standard error of the estimate SE = 0,1598.

As can be seen in many cases, the difference between these data is negligible. Most of the experimental points are near the straight line.

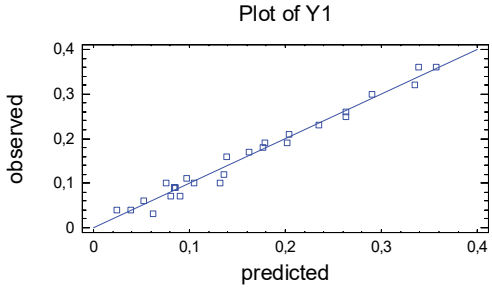

Fig. 2. Comparison of experimental (observed) and estimated (predicted) model data (2)

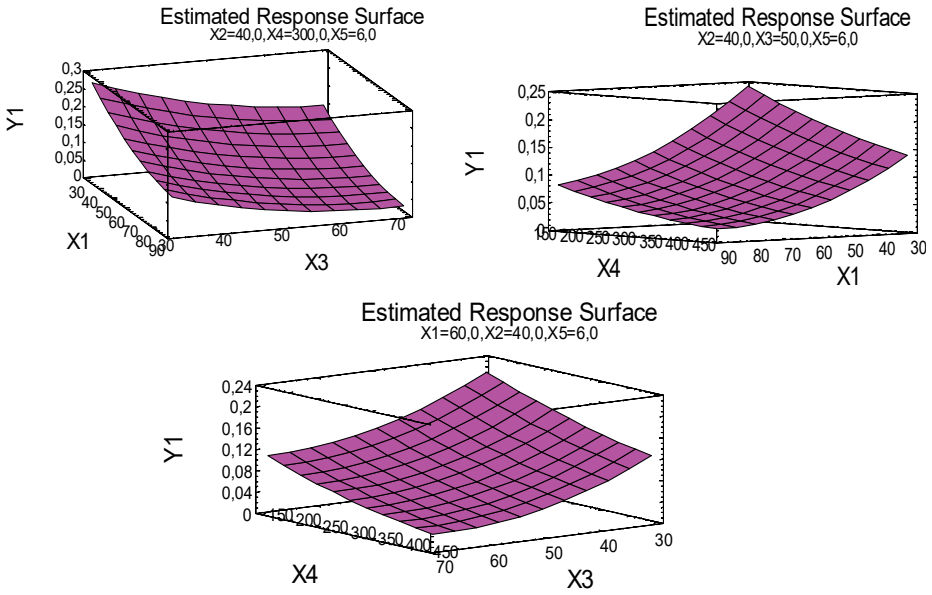

Fig. 3. Surfaces of the influence of paired factors on thermal conductivity of porous materials

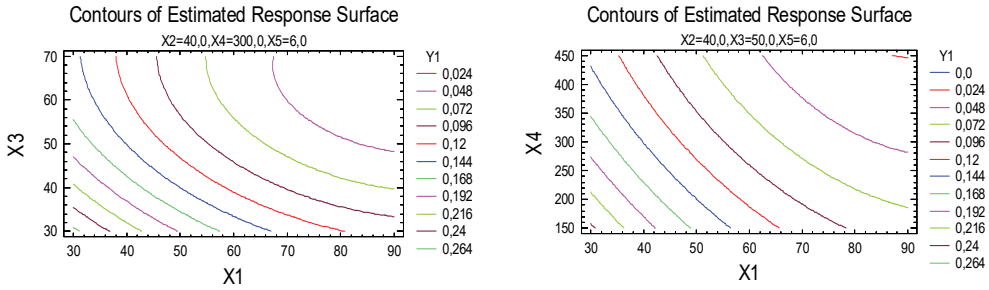

Fig. 4. Surfaces of the influence of paired factors on the thermal conductivity of porous materials

As can be seen from the three-dimensional cross sections of the hypersurface Y_1 (X_i) and the contour curves of these surfaces, the thermal conductivity of the porous thermal insulation materials increases as the mass fraction of amber ash (X_1) and the water content (X_3) decrease and the swelling temperature (X_4) decreases. This is consistent with our understanding of the influence of these factors on thermal conductivity. Another indicator that was investigated under the conditions indicated in table 1 is the strength of porous compression materials (Y_2). As can be seen from the figures in Fig. 5 data, statistically significant are the coefficients for the linear terms of the regression equation for the water content (X_3), clay (X_2), ash (X_1), temperature (X_4) and interaction X_3X_4, X_4X_5.

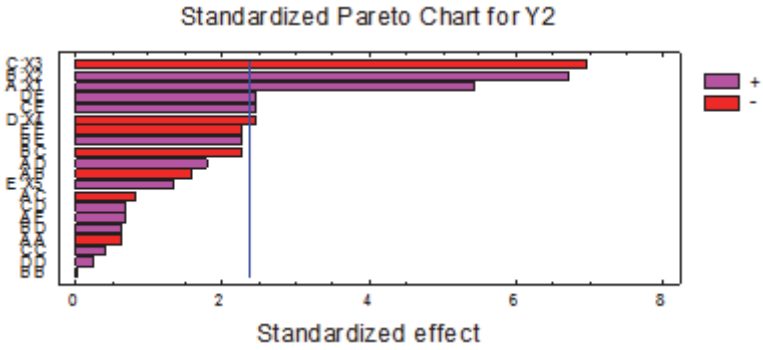

Fig. 5. Significance of model coefficients (Pareto graph)

The regression equation, given the significance of the coefficients, is:

$$Y_2 = 7{,}91641 + 0{,}0415278 \cdot X_1 - 0{,}0693229\ X_2 + 0{,}0771875 \cdot X_3 - \\ - 0{,}0174444 \cdot X_4 + 0{,}0075 \cdot X_3 \cdot X_5 + 0{,}001 \cdot X_4 \cdot X_5. \quad (5)$$

The model was found to be adequate to the process under study (coefficient of determination R_2 = 96.9%, standard error of estimate SE = 0.29).

Figure 6 shows a comparison of experimental and predicted data. The difference between these data is small.

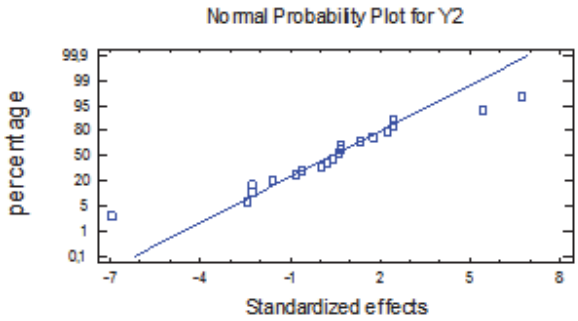

Fig. 6. Comparison of experimental (observed) and estimated (predicted) model data (5)

In Fig. 7 shows the surfaces of the influence of paired factors on the strength of porous materials based on the ash of a thermal power plant.

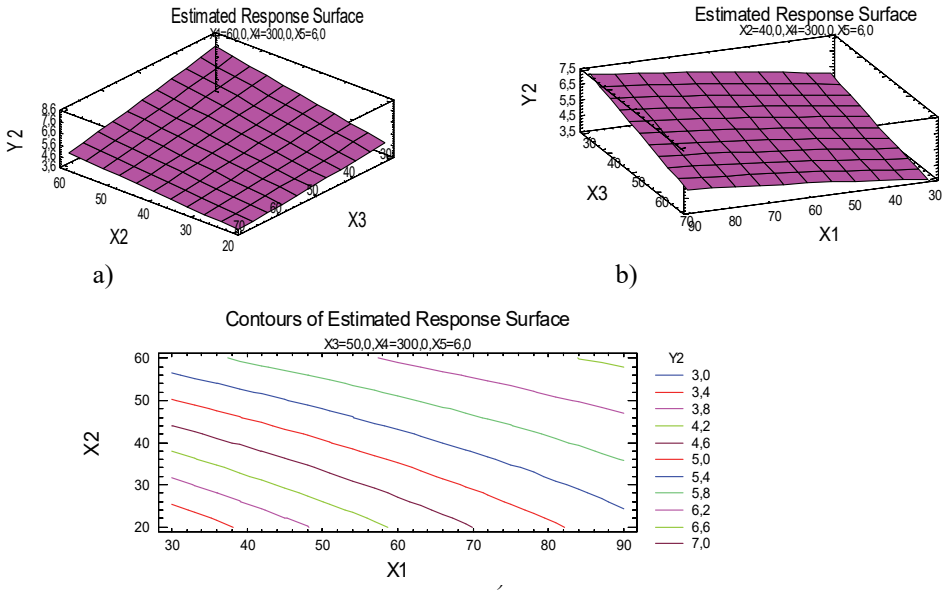

Fig. 7. Surfaces of influence of factors on the strength of porous ash-based materials: a) $Y_2 = f(X_1,X_3)$; b) $Y_2 = f(X_2,X_3)$; c) $Y_2 = f(X_1,X_2)$

The water absorption (Y_3) of porous materials depends, first of all, on the presence of open porosity of the material. The conditions of the experiments did not change (Table 1). Water absorption was assessed by controlling the change in mass of the test samples of the porous materials. Water absorption in the experiments varied from 1 to 18%.

In Fig. 8, we can distinguish statistically significant coefficients for the terms of the regression equation for Y_3: temperature (X_4, X^2_4), ash (X_1), water (X_3), clay (X_2, X^2_2) and interaction X_1X_4.

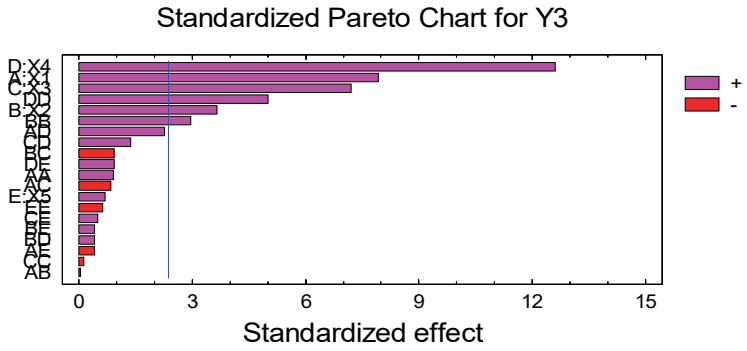

Fig. 8. Significance of model coefficients (Pareto graph)

The regression equation, given the significance of the coefficients, is:

$$Y_3 = 3{,}94297 + 0{,}016875 \cdot X_1 - 0{,}00907292 \cdot X_2 + 0{,}0874479 \cdot X_3 - 0{,}0331528 \cdot X_4 + \\ + 0{,}000141667 \cdot X_1 \cdot X_4 + 0{,}00180469 \cdot X^2_2 + 0{,}0000543056 \cdot X^2_4 \quad (6)$$

The model proved to be adequate to the process under study (coefficient of determination $R_2 = 97.9\%$, standard error of estimate SE = 0.2).

Fig. 9 show the surfaces of the influence of paired factors on the water absorption of porous ash-based materials.

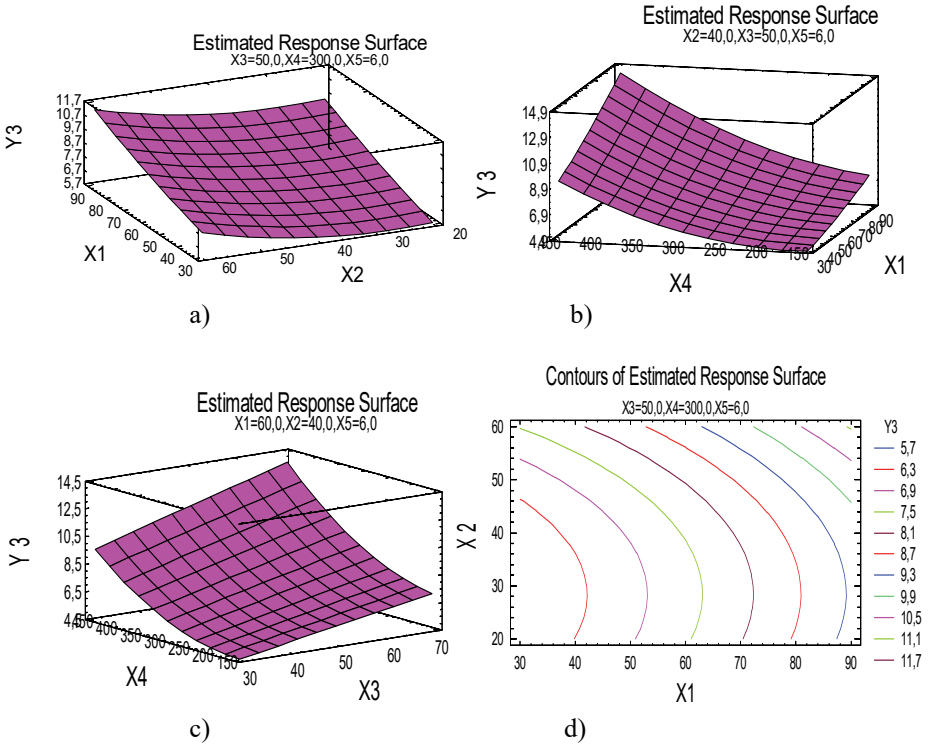

Fig. 9. Surfaces of influence of factors on water absorption of porous materials based on ash of thermal power stations: a) $Y_3 = f(X_1,X_2)$; b) $Y_3 = f(X_1,X_4)$; c) $Y_3 = f(X_3,X_4)$; d) $Y_3 = f(X_1,X_2)$

From the graphs, for example, Figs. 7, 9, it follows that by increasing the ash content and, thus, replacing it with clay and Na_2SO_4, the same desirable values of thermal conductivity, durability and water absorption can be achieved, which is actually to be proved.

4. Conclusions

The results obtained give a qualitative and quantitative assessment of the components of the raw material mixture based on ash with structural indicators of materials. The very structure of the material affects the thermophysical characteristics in a certain quantitative dimension. The proposed dependencies determine the influence of the studied factors on the thermophysical properties of the obtained samples of porous materials. The proposed methods and solutions allow us to predict the values of thermal conductivity, strength and water absorption,

and with the help of variables X_1, X_2, X_3, X_4, X_5 it is possible to control the swelling process to achieve optimal values of these thermophysical parameters. The results obtained suggest that the parameter Y_i can be optimized by selecting the investigated factors.

The project is supported by the program of the Minister of Science and Higher Education under the name: "Regional Initiative of Excellence" in 2019-2022 project number 025 / RID / 2018/19 financing amount PLN 12,000,000.

References

Chudnovsky, A.F. (1962). *Thermophysical characteristics of dispersed materials*. State Publishing House of Physical and Mathematical Literature. 456.

Dehghan, M., Valipour, M. S., Saedodin, S. (2016). Microchannels enhanced by porous materials: Heat transfer enhancement or pressure drop increment? *Energy Conversion and Management*, *110*, 22-32.

Kahveci, K. (2017). Modeling and numerical simulation of simultaneous heat and mass transfer during convective drying of porous materials. *Textile Research Journal*, 0040517516635998.

Koshlak, H., Pavlenko, A. (2019) Method of formation of thermophysical properties of porous materials | [Metoda formowania właściwości termofizycznych materiałów porowatych] *Rocznik Ochrona Srodowiska, 2*, 1253-1262.

Muthtamilselvan, M., Kandaswamy P. K., and Jinho Lee, (2010). Hydromagnetic Mixed Convection in a Two-Sided LidDriven Porous Enclosure, *Int. J. Fluid Mech. Res*., *37*, 406-423.

Nield, D. A., Bejan, A. (2013) Heat transfer through a porous medium // Convection in Porous Media. *Springer New York*, 31-46.

Pavlenko, A., Koshlak, H. (2019). Heat and mass transfer during phase transitions in liquid mixtures | [Przenoszenie ciepła i masy podczas przemian fazowych w mieszaninach ciekłych], *Rocznik Ochrona Srodowiska, 21*(1), 234-249.

Pian, G. (2016). Porosity and pore size distribution of influenza on thermal conductivity of yttria-stabilized zirconia: Experimental findings and model predictions. *Ceramics International, 42*, 5802-5809.

Tarasov, V.E. (2016). Heat transfer in fractal materials. *International Journal of Heat and Mass Transfer, 93*, 427-430.

Abstract

Thermophysical characteristics of porous thermal insulation materials (PTM) are generally determined by the structure, size, type and shape of pores, as well as by their mutual arrangement in the material. Thermal conductivity is one of the most important among these characteristics, is caused by different physical processes and can be reduced to three types: conduction, convection and radiation. Literature sources imply that thermal conductivity dependence is represented as an exponential function. These dependencies fail to have a sufficiently clear and pronounced nature and do not allow developing an analytical expression to describe this function, especially at high values of material density. In our

experiments, the thermal conductivity coefficient was determined in the dry and sorption humidity states, not exceeding 20%. The thermal conductivity of porous thermal insulation materials was studied using an IT-λ-400 device. Cylindrical test specimens, 5 mm thick and 15 mm in diameter, were placed in the device and heated to 800°C. Within this temperature range, the material thermal conductivity was determined according to the standard procedure described in the device operating instructions. The observed data were processed using the designed experiment approach. Thermal conductivity is considered as the target function (Y, W/(m K)). The experiment was conducted according to the program of the central composite rotatable second-order design by Box-Hunter. The factors, studied in the previous series of experiments, are considered as controllable ones. Variable factors shall meet these criteria during experiment design process. 16 experiments were conducted at basic levels and supplemented by another 10 experiments at star points.

Keywords:
porous thermal insulation materials, thermal conductivity, convection, radiation, Burshtyn TPP ash, Box-Hunter

Badanie właściwości termofizycznych porowatych materiałów izolacyjnych na bazie popiołu TPP Burshtyn

Streszczenie

Właściwości termofizyczne porowatych materiałów termoizolacyjnych (PTM) są ogólnie określone przez strukturę, wielkość, rodzaj i kształt porów, a także przez ich wzajemne rozmieszczenie w materiale. Przewodność cieplna jest jedną z najważniejszych spośród tych cech, jest spowodowana różnymi procesami fizycznymi i może być zredukowana do trzech rodzajów: przewodzenia, konwekcji i promieniowania. Źródła literatury sugerują, że zależność przewodności cieplnej jest reprezentowana jako funkcja wykładnicza. Zależności te nie mają wystarczająco wyraźnego charakteru i nie pozwalają na opracowanie analitycznego wyrażenia opisującego tę funkcję, szczególnie przy wysokich wartościach gęstości materiału. W naszych eksperymentach współczynnik przewodności cieplnej został określony w stanie suchym i wilgotności sorpcji, nie przekraczając 20%. Przewodność cieplną porowatych materiałów termoizolacyjnych badano za pomocą urządzenia IT-λ-400. Próbki cylindryczne o grubości 5 mm i średnicy 15 mm umieszczono w urządzeniu i ogrzano do 800°C. W tym zakresie temperatur przewodność cieplna materiału została określona zgodnie ze standardową procedurą opisaną w instrukcji obsługi urządzenia. Obserwowane dane zostały przetworzone przy użyciu zaprojektowanego podejścia eksperymentalnego. Przewodność cieplna jest uwzględniana jako funkcja celu (Y, W/(m K)). Eksperyment przeprowadzono zgodnie z programem centralnego obrotowego kompozytowego projektu drugiego rzędu firmy Box-Hunter. Zmienne czynniki muszą spełniać te kryteria podczas procesu projektowania eksperymentu. Przeprowadzono 16 eksperymentów na poziomach podstawowych i uzupełniono o kolejne 10 eksperymentów w punktach gwiazdowych.

Słowa kluczowe:
porowate materiały termoizolacyjne, przewodnictwo cieplne, konwekcja, promieniowanie, popiół Bursthyn TPP, Box-Hunter

MIDDLE POMERANIAN SCIENTIFIC SOCIETY OF THE ENVIRONMENT PROTECTION

Rocznik Ochrona Środowiska

Volume 22. Year 2020 ISSN 1506-218X 549-560

Energy Efficiency Operational Indicator as an Index of Carbon Dioxide Emission from Marine Transport

Jerzy Herdzik

Gdynia Maritime University, Poland

corresponding author's e-mail: j.herdzik@wm.umg.edu.pl

1. Introduction

International shipping is the reason of emission about 2.5-3.0% of the carbon dioxides (CO_2) in the worldwide pollution. In 2015, it was 932 million tons and percentage of 2.6%. Transport accounts for 24% of global emission. CO_2 emission depends on total fuel consumption and carbon concentration in used fuel. CO_2 is one of green-house gases (GHG) (Olmer et al. 2017). Due to emission other GHGs like: black carbon, nitrogen and sulfur oxides from marine diesel engines, equivalent CO_2 (CO_{2e}) emission is sometimes used. The difference between CO_2 and CO_{2e} is rather small, about 7-9% more for CO_{2e} and is quite stable.

There are 223 flag states in the world. The most CO_2 emission can be attributed to ships flying six flags: Panama (15%), China (11%), Liberia (9%), Marshall Islands (7%), Singapore (6%) and Malta (5%). About 66% of the global shipping fleets' deadweight tonnage is registered to them (Olmer et al. 2017).

To ensure that shipping is cleaner and greener, International Maritime Organization (IMO) has adopted regulations to reduce the emission. The aim is zero-carbon shipping. In that aim, by adding a new Chapter 4 to Annex VI of the International Convention for the Prevention of Pollution from Ships (MARPOL 73/78 Convention) on the regulation of energy efficiency of ships, it was introduced making mandatory from 1st January 2013 the energy efficiency design index (EEDI) for new built ships and the Ship Energy Efficiency Management Plan (SEEMP) for all ships (IMO 2012a, IMO 2012c). The required EEDI is determined by equations (IMO 2012d, IMO 2012e) include several factors to suit specific types of vessels, their configurations and operating conditions. The level of CO_2 emission is to be tightened every 5 years (about 10% less, going to next number of required EEDI Phase) from 1st January 2015 (IMO 2012e, Polish Register 2019, Polish Register 2020). It is expected to stimulate continued innovation

and technical development of all the components influencing the engine fuel consumption and hull resistance from its design phase.

The EEOI is the total carbon dioxide emission (in g CO_2) in a given time period per unit of transport effect (ton-km or ton-mile). A lower EEOI means a ship more efficient in its operation (IMO 2009, Acomi et al. 2013). An application of Ship Energy Efficiency Management Plan (SEEMP) requires to perform some actions. As an example, the calculating of EEOI is voluntary but from 1st January 2018 the ship-owners of large vessels over 5,000 gross tonnage loading or unloading cargo or passengers at ports in the European Economic Area (EEA) should monitor and report their related CO_2 emission and other relevant information (Directive 2015, Directive 2018). From 30th April 2019 of each year, ship-owners shall submit first to States in which those ships are registered and after approving to the European Commission, a satisfactory verified emissions report for each ship that has performed activities in the EEA in the previous reporting period (last calendar year). It shall be done through a THETIS MRV platform (a special basis prepared by European Maritime Safety Agency for Paris Memorandum of Understanding) (Elliot 2009).

Total consumption reports of each type of fuel and emissions reports in marine transport allow to recognize the possibility for formulation new regulations for efficiency increasing and emissions restrictions.

Advantages and disadvantages from enforcing emission restrictions within emission control areas is analyzed in (Dulebenets 2016) and an evaluating the effects of speed reduce for shipping costs and CO_2 emission is presented in (Chang & Wang 2014).

2. Energy Efficiency Design Index as the primary requirement

EEDI is a first step of IMO's drive to reduce the CO_2 emission from shipping and a benchmarking scheme aiming to provide an indication of a merchant ship's CO_2 output in relation to its transport work.

EEDI is provided by formula (1) where in the numerator is CO_2 emission from main engines and auxiliaries (calculating as a product of fuel factor c_{Fi}, engine load P_i and specific fuel consumption SFC_i at this load) and the denominator is a product of ship's deadweight DWT and the ship's reference speed V_s (IMO 2012e):

$$EEDI_i = (\sum_i c_{Fi} \cdot P_i \cdot SFC_i)/(DWT \cdot V_s) \quad (1)$$

The reference speed means ship's speed at 75% Maximum Continuous Rating of main engine. The units used for EEDI are: g CO_2/(ton-mile).

The EEDI is an estimated measure of transport energy efficiency of a ship, which is currently under the design stage. It should be estimated for

designed vessel and it is an important index for designers and builders of ships (IMO 2012b, IMO 2012d).

Goal of EEDI:

- mitigate CO_2 emissions,
- increase cargo carrying capacity to maximal possible ship's deadweight,
- enhance ship's speed performance,
- design and use the most efficient equipment,
- design the ship's hull with the lowest resistance,
- design the marine power plant as much efficient as possible.

3. EEOI calculation

The calculation of EEOI needs to measure some parameters during vessel operation, like:

- the distance sailed as recorded in ship's Bridge Log Book,
- the cargo mass as per Bill of Lading and Deck Log Book,
- the total fuel consumption as recorded in Engine Log Book.

It should be known the fuel coefficient c_F depending on the type of used fuel. The c_F is presented in Table 1 (Elliot 2009, on base: Acomi & Acomi 2014).

Table 1. Fuel coefficient for different types of fuel

Type of fuel		Reference	Carbon content	c_F [kg-CO_2/kg-fuel]
1	Diesel/gas oil	ISO 8217 grades DMX through DMC	0.875	3.20600
2	Light fuel oil	ISO 8217 grades RMA through RMD	0.860	3.15104
3	Heavy fuel oil	ISO 8217 grades RME through RMK	0.850	3.11440
4	Liquefied Petroleum Gas (LPG)	propane butane	0.819 0.827	3.00000 3.03000
5	Liquefied Natural Gas (LNG)	methane	0.750	2.75000
6	Hydrogen	hydrogen	0	0.0
7	Biofuels	Biodiesel, renewable diesel, F-T diesel, FP bio-oil	different	0.0

An equation (2) for *EEOI* calculation shows the idea of index term.

$$EEOI = \frac{actual\_CO2\_emission}{performed\_transport\_work} \tag{2}$$

EEOI is provided by other formulas for ships being into operation. The examples are presented in formulas (3) and (4).
The EEOI for a voyage is calculated as follows:

$$EEOI = \frac{\sum_{j=1}^{j} FC_j \times c_{Fj}}{m_{cargo} \times D} \tag{3}$$

For a number of voyages the index *Average_EEOI* is expressed by formula (4):

$$Average\_EEOI = \frac{\sum_{i=1}^{i}\sum_{j=1}^{j} FC_{ij} \times c_{Fj}}{\sum_{i=1}^{i} m_{cargo,i} \times D_i} \tag{4}$$

where:
j – is the fuel type,
i – is the voyage number,
FC_i – is the mass of consumed fuel at voyage i,
c_{Fj} – is the fuel mass to CO_2 mass conversion factor for fuel j (fuel factor),
$m_{cargo,i}$ – is mass cargo carried (in tons) or work done (number of TEU or passengers) or gross tons for passenger ships,
D_i – is the distance (in nautical miles) corresponding to the cargo carried or work done.

The EEOI depends strongly on vessel capacity. At the same speed and type of a vessel, EEOI will decrease about twice when the capacity increases four times. So the EEDI is determined among others by ship capacity (IMO 2012b, Polish Register 2014). It is presumable that the EEOI will be smaller during operation than required EEDI in design phase.

Approximate EEOI for different types of ships is presented in Table 2 (on base: Acomi & Acomi 2014).

Table 2. Comparison of EEOI for chosen different types of vessels

Type of vessel	EEOI [g-CO_2/ton-km]	EEOI [g-CO_2/ton-mile]
Ro-ro	33	18
Container ship	18	9.8
General cargo	14	7.6
Product tanker	11	5.9
Bulk carrier	4.5	2.4
VLCC tanker	4.2	2.3

The EEOI reaches different values depending on type and size of vessel, cargo capacity, area of sailing etc. For definite vessel the comparison between individual voyages in different condition may be done. The aim is minimizing the index. This is a task for crew members and shipowners.

4. Expected effects of EEDI and EEOI introduction

A wide variety of design, operational and economic solutions is presented in Fig.1.

Looking at Fig.1 it may be seen that we have many possibilities to decrease the EEOI near zero. If we cannot do it till now means it will exist many troubles for introducing those solutions. Of course, the best solution is using hydrogen, other synthetic fuels and bio-fuels (till c_F will be calculated as zero).

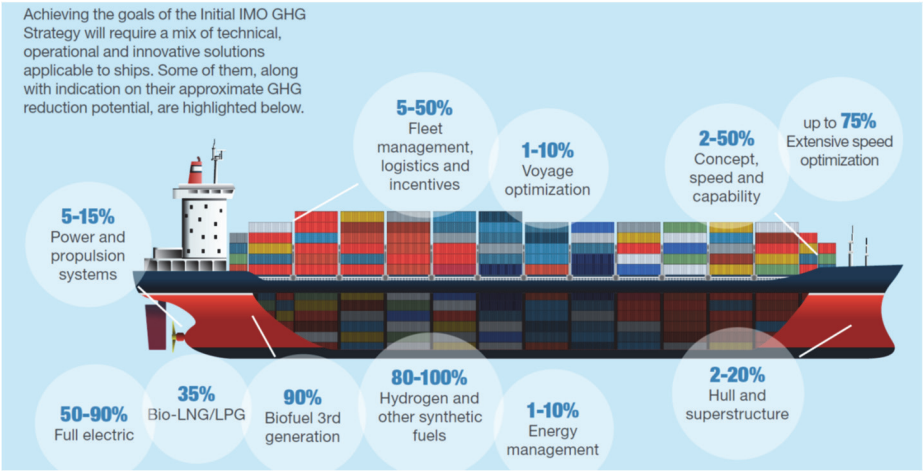

Fig. 1. A wide variety of design, operational and economic solutions (IMO Action 2018)

In reality into ship's operation there are much less possibilities. Methods like: energy or power management systems (EMS, PMS), voyage optimization (special computer programs, improved voyage planning) and extensive speed optimization (conducive for slow steaming) (MAN 2012) are still into consideration.

The IMO idea "zero carbon" in shipping in 2050 (and as soon as possible in this century) is the target for next steps. The timetable of IMO Action to reduce GHG emissions from ships is (IMO Action 2018):

- 2020 – EEDI phase 2: up to 20% reduction in carbon intensity of the ship,
- 2023-2030 – mid-term measures to reduce carbon intensity of the fleet by at least 40%,
- 2025 – EEDI phase 3: up to 30% reduction in carbon intensity of the ship. Note: early entry into effect (2022) for several ships types with up to 50% carbon intensity reduction for largest containerships,
- 2030-2050 – long term measures to reduce carbon intensity of the fleet by at least 70%,
- 2050 – at least 50% reduction of total annual GHG emissions (requires approximately 85% CO_2 reduction per ship).

The EEDI introduction in 2013 has an influence on all design processes. Better designed and equipped vessel allows to reach lower EEOI (Polish Register 2014). Due to IMO Action program (phases of decreasing required EEDI) the EEOI will have a possibility to decrease it for vessels built later. But the index is more complicated. It requires a co-operation between technical superintendent office and crew members, depends on mass cargo and other operational conditions like: estimated time of arrival, route of voyage (distance), hull resistance, sea conditions, wind force and direction, sea current etc. (Elliot 2009, Herdzik 2017). Analyzing the variation of EEOI with respect to different voyage parameters it could be noticed that the most preferred parameters that result in major beneficial changes decreasing that factor are: increasing the quantity of mass cargo maintaining the same route (optimization the route and speed in time constraint) and decreasing the fuel consumption maintaining a medium vessel speed or using waste heat recovery systems (WHRS) (Herdzik 2014b, IMO 2018, IMO 2019).

The Life Cycle Assessment (LCA) is the other point of view on EEOI. There are four main phases in whole life of a ship: building, operation, maintenance and scrapping. The CO_2 emission during design phase is negligible. During three main phases the CO_2 is emitted due to consuming a large of electricity and other forms of energy. Only during scrapping process the balance of CO_2 emission may be different (possible less than zero) because a part of materials would be recycled. The ship produce benefits only in operation phase. Knowing the

benefits (total work transport) it may be estimated the real EEOI or as a correction factor introduces to the *Average_EEOI*.

The other proposition is Energy Efficiency Technical Indicator (EETI) (UCL Energy 2015) defined as the energy efficiency (g-CO_2/(ton-mile) of a ship in a reference operating condition (speed and draught). It seems to be a better indicator for comparison different voyages of the same vessel because disposing the changing operating conditions.

We should try to adopt for shipping other ideas (e.g. from ashore transport) (Jachimowski et al. 2018) for improving the all transport cycle of cargo.

5. Slow steaming of a vessel as the primary method of EEOI decreasing. Main engine operational problems

Slow steaming of a vessel decreases the fuel consumption. The main engine load (and fuel consumption) depends on the third power (cubic dependency) of vessel speed (propeller characteristics) but the vessel speed is in linear dependency to propeller rotational speed (Faber et al. 2012, Herdzik 2017). So the overwhelming reason for adopting slow steaming is the promise of fuel savings and decreasing the EEOI. Slow steaming practices introduced after a slowdown in global trade in 2008. Between 2013 and 2015 there has been an increase in speed for some of the largest vessels. The observed vessel speed decreasing after 2015 and respectively the main engine (ME) load has an effect on the its operation. ME are designed to work at 70-85% of maximum continuous rating (MCR). Now the ME load is in a range of 10-50% MCR (see Table 3).

Table 3. Typical engine load in slow steaming vessels (percentages) (MAN 2012)

Type of vessel/ME load	10-30%	20-40%	30-50%
Container	17.8	25.8	56.4
Bulk/Tank/others	5.9	11.9	82.2

There are the following concerns with regards to slow steaming (Faber et al. 2012, Herdzik 2014a, MAN 2012):

- frequent and thorough scavenge system and under piston inspections must be carried out,
- till the engine has a load dependent cylinder lubrication system which is suited for slow steaming it may work properly, unless the engine has not such system the cylinder lubrication rate must be adjusted to optimal value as per manufacturer's advice,

- slow steaming causes fouling of the turbochargers and loss of efficiency of turbochargers and engines, requires more often washing processes,
- turbochargers operating outside their designed range produce less air flow leading to more deposits,
- increased carbon deposits on the injectors compromises with their performance,
- causes fouling of the exhaust gas economizer resulting in reduction of capacity as well as increased danger of soot fire,
- causes reduction in scavenge air pressure resulting in improper combustion,
- leads to improper atomization of the fuel as well as leads to knock combustion or misfire,
- maintenance intervals have to be modified,
- causes low temperature corrosion of cylinder liners,
- increases the risk of scavenge fires and needs extra scavenge and under piston draining,
- cause loss of heat transfer due to carbon deposits and failure of components due to thermal stresses, etc.

When main engine is run at full load (periodically, according to manufacturer's advice, as an example: four hours of slow steaming and one hour of full load) after long periods of slow steaming the risk of engine damage becomes imminent. But this is infeasible in many cases.

To overcome the mentioned concerns it requires performing many actions like: proactive on-board servicing, manual cleaning, manual adjustments, fuel adjustments, enhanced engine room staff training, engine upgrade kits etc. It means additional works and competencies for engine room staff.

The approach for long-term slow steaming requires the preparedness of main engine like: engine retrofit, derating and upgrade measures taken to minimize the return on slow steaming (MAN 2012).

A ship can be designed to have an optimal hull form, rudder and propeller to sail in a certain speed, while it may redundant power in order to manoeuvre safely in adverse conditions.

When ships are designed to sail at lower speed, their design may change. In (Faber et al 2012), it has presented the Germanisher Lloyd (GL) example for comparison of the designs of an typical existing post panama container ship (6500 TEU) with a design speed of 26 knots and a ship with a design speed of 22.5 knots. The latter ship is shorter and broader and has a higher block coefficient. Due to introduced changes its water resistance increases but its main engine power decreased by 21.5% (but less than square).

6. EEOI as carbon dioxide emission index

The EEOI may perform a role of carbon dioxide emission index from shipping. A basic problem is its proper understanding and application. It should be used all possibilities for decreasing that indicator but only reasonable. One simple example: during voyage knowing the estimated time of arrival (ETA) and a distance to sail, it is easy to calculate the required medium speed of a vessel to reach the ETA – it is a reasonable method. In other case, if we will sail with bigger speed and the saved time we will spend in standing in a drift or sail in a circulation with low speed (the distance will be longer and the EEOI lower) is unreasonable.

Knowing the mass cargo, distance to sail, types of vessels and their capacity it is possible to estimate the total carbon dioxide emission to the atmosphere from shipping due to monitor, report and verification (MRV) systems.

Introducing the EEDI and EEOI, IMO has an aim to decrease the total CO_2 emission from shipping to zero. This is a laudable goal. But it must be remembered that all imposed limitations, requirements and regulations provide to increasing the cost of transport and shipping.

7. Final remarks

Total shipping fuel consumption is on a level of 300-330 million tons yearly with CO_2 emission about 0.9-1.0 billion tons.

The expectation is minimizing the CO_2 emission from shipping. A limitation of other GHG emission from marine diesel engines provides to increasing the specific fuel consumption (according to IMO about 2%, but probably more) and respectively to increasing the CO_2 emission.

Slow steaming method is the most perspective but required to research preferable solutions and propositions to minimize its effects.

Energy storage through use the batteries and cold ironing (shoreside electrical power to a ship at berth) are still under development.

Introducing through IMO the regulations of EEDI and EEOI is reasonable but should be the first step to other actions.

The decarbonization process in global shipping was started. The supreme hope is marine fuel switch to lower (up to zero) carbon in fuel for propulsion.

References

Acomi, N. et al. (2013). The Energy Efficiency Operational Index - An instrument for the marine pollution control. *Recent Advances in Energy, Environment, Economics and Technological Innovation.* 177-180, DECO, Paryż.

Acomi, N., Acomi, O.C. (2014). The influence of different types of marine fuel over the energy efficiency operational index. *Energy Procedia. 59*, 243-248.

Chang, C. & Wang, C. (2014). Evaluating the effects of speed reduce for shipping costs and CO_2 emission. *Transportation Research Part D: Transport and Environment. 31*, 110-115.

Directive (2015). 2015/757 of the European Parliament and of the Council of 29 April 2015, as amended by Delegated Regulation 2016/2071 *on monitoring, reporting and verification of carbon dioxide emissions from maritime transport*, and amended Directive 2009/16/EC.

Directive (2018). 2018/410 of the European Parliament and of the Council of 14 March 2018 amending Directive 2003/87/EC *to enhance cost-effective emission reductions and low-carbon investments*, and Decision (EU) 2015/1814.

Dulebenets, M.A. (2016). Advantages and disadvantages from enforcing emission restrictions within emission control areas. *Maritime Business Review, 1*(2), 107-132.

Elliot, B. (2009). The Energy Efficiency Operational Index and Voluntary Measures for Improving Energy Efficiency, EMSA.

Faber, J. et al. (2012). *Regulated Slow Steaming in Maritime Transport, An Assessment of Options, Costs and Benefits*, Delft, 2012.

Herdzik, J. (2014a). (in Polish). Modyfikacja wskaźników efektywności energetycznej statków różnych typów i konstrukcji. *Logistyka, 6*, 706-711.

Herdzik, J. (2014b). Remarks on Implementation of Ship Energy Efficiency Management Plan. *Scientific Journal of Gdynia Maritime University, 3,* 81-88.

Herdzik, J. (2017). *U*wagi do eksploatacyjnego wskaźnika efektywności energetycznej statku. (in Polish). *Autobusy, Technika, Eksploatacja, Systemy Transportowe, 6*, 209-213.

Jachimowski, R. et al. (2018). Selection of a Container Storage Strategy at the Rail-road Intermodal Terminal as a Function of Minimization of the Energy Expenditure of Transshipment Devices and CO_2 Emissions. *Rocznik Ochrona Środowiska, 20*, 965-988.

IMO, (2009). *Guidelines for voluntary use of ship energy efficiency operational indicator, EEOI,* MEPC.1/Circ.684, 2009.

IMO, (2012a). *Guidance for the development of a ship energy efficiency management plan, SEEMP,* MEPC 59/24/Add.1, Annex 19, 2012.

IMO (2012b) Resolution MEPC.2012.(63). *Guidelines on the method of calculation of the attained Energy Efficiency Design Index for new ships*.

IMO (2012c) Resolution MEPC.2013(63). *Guidelines for the development of a Ship Energy Efficiency Management Plan*.

IMO (2012d) Resolution MEPC.2014(63). *Guidelines on survey and certification of the Energy Efficiency Design Index*.

IMO (2012e) Resolution MEPC.2015(63). *Guidelines for calculation of reference lines for use with EEDI.*

IMO (2018) MEPC 72/INF.5, *Reduction of GHG from ships. Understanding CO_2 emissions and challenges in assessing the operational efficiency for ships*.

IMO (2019). http://www.imo.org/en/OurWork/Environment/PollutionPrevention/AirPollution/Pages/GHG-Emissions.aspx (accessed: 15th March, 2019).

IMO Action (2018). *To Reduce Greenhouse Gas Emission From International Shipping*, IMO 2018.

MAN (2012). *Slow Steaming Practices in the Global Shipping Industry*, Report, MAN PrimeServ 2012.
Olmer, N. et al. (2017). Greenhouse Gas Emission from Global Shipping 2013-2015. *The International Council on Clean Transportation*, ICCT, Washington, USA.
Polish Register of Shipping (2014). *Przepisy, Wytyczne dotyczące efektywności energetycznej statków*, (in Polish). Polski Rejestr Statków, Publication No. 103/P.
Polish Register of Shipping (2019). *Przepisy nadzoru konwencyjnego statków morskich, część IX, ochrona środowiska,* (in Polish). Gdańsk, January 2019.
Polish Register of Shipping (2020). *Rules for Statutory Survey of Sea-going Ships, Part IX, Environment Protection*, January 2020.
UCL Energy (2015). *Understanding the Energy Efficiency Operational Indicator,* UCL Energy Institute*,* Final Report and Appendices*,* Royal Belgium Shipowners' Association, May 2015.

Abstract

The paper presents Energy Efficiency Operational Index (EEOI) introduced through International Maritime Organization (IMO) which defined the carbon dioxide emission as a result of transport specific cargo mass on specific distance. The total fuel consumption from all elements of vessel energetic system causes the carbon dioxide emission. Ship-owners should inform the marine administration about the fuel consumption from all vessels of 5000 tons of gross tonnage or more from 1st January 2018. In marine transport about 85% of carbon dioxide emission comes from such vessels. The calculating of EEOI is voluntary now but it is indicated to do it. It allows on an assessment the differences between the Energy Efficiency Design Index (EEDI) obligatory during design process of a vessel and its power plant and EEOI. Due to it may be estimated the correctness of vessel and power plant operation in exploitational conditions.

The basic way of EEOI decreasing is slow steaming of a vessel. The power demand for propulsion (and fuel consumption) is proportional to the third power of vessel velocity (according to the propeller characteristics) on the other hand the hull resistance (the demand for thrust by propeller) is proportional to the second power of vessel velocity. As a result it causes the decreasing of total fuel consumption for covering the same distance but increasing the time of voyage. It is for acceptance during a bad economic situation. Although it will be no acceptable during a good economic situation when it will be required the increasing of vessel velocity (decreasing the time of voyage).

The other effective methods are under research which allows to reach the same aim. It is known such methods of vessel operation which leading to the decreasing of that index. The paper shows these methods with their characteristics.

Keywords:
marine transport, emission to atmosphere, carbon dioxide, energy efficiency operational indicator, ship operation, shipping

Eksploatacyjny indeks efektywności energetycznej statku jako wskaźnik emisji dwutlenku węgla w transporcie morskim

Streszczenie

W artykule omówiono wprowadzony przez Międzynarodową Organizację Morską (IMO) wskaźnik zwany eksploatacyjnym indeksem efektywności energetycznej statku (EEOI), który określa emisję dwutlenku węgla w wyniku transportu jednostki masy ładunku na jednostkową odległość. Za emisję CO_2 odpowiada zużycie paliwa przez wszystkie elementy okrętowego układu energetycznego. Od 1 stycznia 2018 r. armatorzy muszą zgłaszać do administracji morskiej ilość zużytego paliwa przez poszczególne statki o tonażu od 5000, które odpowiadają za 85% zużycia paliwa w transporcie morskim. Wyznaczanie wskaźnika EEOI jest obecnie dobrowolne, ale wskazane, aby go wyznaczać. Pozwala to na określenie różnic między projektowym indeksem efektywności energetycznej statku (EEDI), który jest obligatoryjny w procesie projektowania statku i elementów układu energetycznego, a eksploatacyjnym. Dzięki temu można oszacować poprawność eksploatacji siłowni i statku w warunkach rzeczywistych.

Podstawowym sposobem zmniejszenia wskaźnika EEOI jest zmniejszenie prędkości eksploatacyjnej statku. Zapotrzebowanie na moc napędu (i zużycie paliwa) jest proporcjonalne do trzeciej potęgi prędkości statku (wg tzw. charakterystyki śrubowej), natomiast opór kadłuba (zapotrzebowanie na siłę naporu przez śrubę okrętową) jest proporcjonalny do potęgi drugiej prędkości statku. Skutkuje to zmniejszeniem zużycia paliwa na pokonanie tej samej drogi, ale wydłuża czas podróży. W okresie dekoniunktury na rynku żeglugowym jest to do przyjęcia. Jednak wraz z pojawieniem się oznak koniunktury, które będą wymagać wzrostu prędkości statku (skrócenia czasu podróży) będzie to niemożliwe.

Poszukuje się więc innych skutecznych metod, które pozwolą osiągnąć ten sam cel. Znane są możliwości takich sposobów eksploatacji statku, które prowadzą do zmniejszenia tego wskaźnika. W artykule wskazano na te metody wraz z ich charakterystyką.

Słowa kluczowe:
transport morski, emisja do atmosfery, dwutlenek węgla, eksploatacyjny wskaźnik efektywności energetycznej, eksploatacja statku, żegluga

MIDDLE POMERANIAN SCIENTIFIC SOCIETY OF THE ENVIRONMENT PROTECTION

Rocznik Ochrona Środowiska

Volume 22. Year 2020 ISSN 1506-218X 561-588

Life Cycle Assessment of Eco-Innovative Organo-Mineral Granulated Fertilizer's Production Technology

Maria Bałazińska[*], *Małgorzata Markowska,*
Agata Blaut, Marcin Głodniok
Central Mining Institute; Katowice, Poland
[*]*corresponding author's e-mail: mbalazinska@gig.eu*

1. Introduction

A number of legal acts, both at the level of the European Union and Polish legislation, as well as the obligations arising from international agreements impose on water and sewage treatment plants the obligation to carry out activities that minimize the negative environmental effect. The most important legal act regulating activities in sewage management is the Council Directive of 21 May 1991 concerning urban wastewater treatment 91/271/EEC (the so-called sewage directive), which aims to protect the environment against the adverse effects of municipal wastewater (EUR-Lex 1991, Rauba 2015). Tailoring actions in the field of processing and use of sewage sludge to the requirements of the Directive (EUR-Lex 1991) is one of the priority tasks in the field of sewage management for Poland (Biegańska 2010). Changes in the perception of the place and role of sewage sludge in water and sewage management began in Poland in the early 2000s, when EU pre-accession funds became available, which were then an important instrument of EU structural policy (Smuda 2014). According to Polish legislation, sewage sludge resulting from wastewater treatment processes is waste code 19 08 05 (Regulation 2014, Regulation 2020). Unlike other waste fractions, their production cannot be prevented and the increase in sewage sludge production in treatment plants is estimated at about 2% per year (Bagreev et.al. 2001). In accordance to statistical data, about 500-600 thousand tonnes of dry matter of sewage sludge is generated annually in Polish wastewater treatment plants (Statistics Poland 2019) with an upward trend.

Therefore, the importance of choosing an ecologically safe and economically and environmentally justified method of sewage sludge management increases.

In accordance to Polish Law, in activities relating to municipal sewage sludge MSS, it is necessary to follow the waste hierarchy – depending on the form in which it appears and its quality, it is required to: 1) prevent the formation of sewage sludge by (among other things) subjecting the sludge to disintegration processes, deep stabilization, hygienization and dehydration or other measures to enable it to lose its waste status; 2) recycle MSS – by organic recycling and mineral recycling with recovery of phosphorus; 3) use MSS recovery methods (including recovery in composting plants, biogas plants or cement kilns), including energy recovery; 4) dispose MSS – sludge in this process may be incinerated in waste incineration plants or waste co-incineration plants, without energy recovery, or landfilled, after treatment, if it meets the requirements specified by law (National Waste Management Plan 2016), which make it practically impossible to store sewage sludge without prior treatment.

Also statistical data about different methods of MSS management confirm that the amount (and percentage) of landfilled sludge has significantly decreased in the last 10 years, while thermal processing and use in agriculture have an upward trend (Fig. 1).

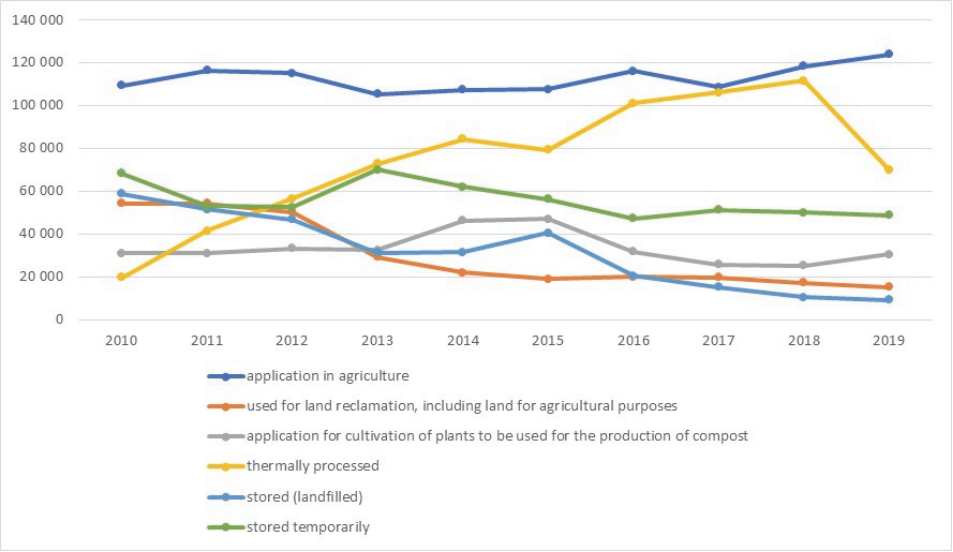

Fig. 1. Management of MSS by different methods in the years 2010-2019 in Poland; Source: own elaboration, based on data from Statistics Poland

Although methods based on incineration and co-incineration are effective and condition a significant reduction in the volume of sewage sludge, its by-product are ashes which can be characterized by a high content of heavy metals

(Wójcik & Masłoń 2019). The presence of heavy metals, as well as other physical and chemical properties largely determine the possibilities and subsequently the choice of an appropriate and effective method of sewage sludge processing and disposal (Act 2007, Regulation 2009, Gawdzik 2013), especially its application in agriculture.

For sludge where the heavy metal content in mg/kg of dry matter of the sludge is no more than the permissible amount (Regulation 2015), their agricultural use is recommended (Kulikowski et.al. 2019).

The need to look for new methods of sludge utilization has led to the development of research in the field of sludge management, which has recently led to municipal sewage sludge being increasingly seen as a raw material or resource, not just waste (Masłoń 2015, Naukawpolsce 2017). Due to the content of protein in its composition, sewage sludge can be used in the production of chelate fertilizers containing trace metals (Liu et. al. 2009). At the same time, the specific characteristics of sludge, in particular the presence of harmful substances and pathogenic organisms, determine the need for an appropriate selection of the method of its management, which will ensure the maximization of the use of valuable components contained in it while minimizing harmful effects on the environment (Wójcik & Masłoń 2019). From the point of view of the circulation of organic matter in nature, enabling the return of sewage sludge to the environment after processing is very valuable. Therefore, developing and implementing more and more modern and eco-innovative solutions for its processing and disposal is necessary.

Eco-innovative solutions (or also eco-innovations) is a term used to describe all forms of innovative activities that contribute to environmental protection, especially those aimed at preventing or reducing adverse environmental impacts and misuse of natural resources (Rennings 2000, European Commission 2007, European Commission 2011). Despite the fact that eco-innovations became the subject of research already in the 1970s, and the term eco-innovations became common in the late 1990s (Jasiński 1997, Bartoszczuk 2016), there are still ongoing discussions in the literature regarding the full definition of this phenomenon and strict criteria explaining its essence (e.g. Rennings 2000, Reid & Miedzinski 2008, Oslo Manual 2008, Kemp & Pearson 2008, Woźniak et al. 2008, Cheng & Shiu 2012, Peng & Liu 2016). There is also a lack of agreement in the scientific literature on whether environmental benefits can be an additional effect of the implemented innovative solution (Carillo-Hermosilla et al. 2010, Urbaniec 2015) or whether they must be the main goal of implementing ecological innovations (Little 2005), as it is the case with the optimization of organic-mineral granular fertilizer.

The implementation of eco-innovation in agriculture is favoured by the European Union's environmentally friendly policy contained in the Europe 2020 strategy, which is based on the premise of intelligent development, based on knowledge and innovation, but also sustainable, consisting in supporting an economy that uses resources efficiently and a more environmentally friendly (Europe 2020, 2010). Since the priority research directions currently carried out in the European Union and in the world are both food security and rational management of natural resources, as well as counteracting climate change, the importance of eco-innovation in the food economy and in the broadly understood agriculture is constantly increasing (Dziedzic &Woźniak 2013).

The paper presents an eco-innovative technological solution for the production of organic-mineral granular fertilizer and its environmental assessment. The scientific aim of the research was to determine the environmental impact of manufactured fertilizer products in the developed technology. The practical aim of the research focused on comparison and selection of the most environmentally friendly fertiliser product.

2. Technology

Organo-mineral granulated fertilizer developed by Central Mining Institute is a mixture of municipal dewatered sewage sludge collected from municipal waste water treatment plant, complying with Polish law requirement, dolomite (50% $CaCO_3$ and 40% $MgCO_3$) provided by JSKM Zielona Góra, lime (96% CaO) from Lhoist, gypsum, ammonium carbonate and microcrystalline cellulose from Rettenmeier–Arbocel. Sewage sludge for fertilizer production contained heavy metals at levels less than: chromium (Cr) 100 mg/kg, cadmium (Cd) 5 mg/kg, nickel (Ni) 60 mg/kg, lead (Pb) 140 mg/kg and mercury (Hg) 2 mg/kg, so well within amount permissible for application in agriculture and for land reclamation for agricultural purposes by Polish Law (Regulation 2015). They were also free from live eggs of intestinal parasites *Ascaria sp. Trichuris sp.*, *Toxacara sp.* bacteria of the genus *Salmonella*. Sewage sludge after dewatering in centrifuges contained 19-20% of dry mass. The final product was in the form of irregular shape non-dusting granulate with diameter 1-6 mm.

Granulation of materials is one of the most significant unit operations applied in many manufacturing processes. It means of forming of grains or granules from a powdery or solid substance of appropriate physicochemical properties, shape and dimensions. The most important advantages of the former include suppression of dusting, avoidance of caking, better behaviour during transport or prevention of segregation in multicomponent materials (Heim 2012). The technology of granulating was applied to produce granular organic fertilizers from dewatered sewage sludge and a few chemicals.

The application for the method was covered by patent protection by the Polish Patent Office as an invention (Głodniok et al. 2017). The planned process of production of the granulate is presented in block scheme at Fig. 2.

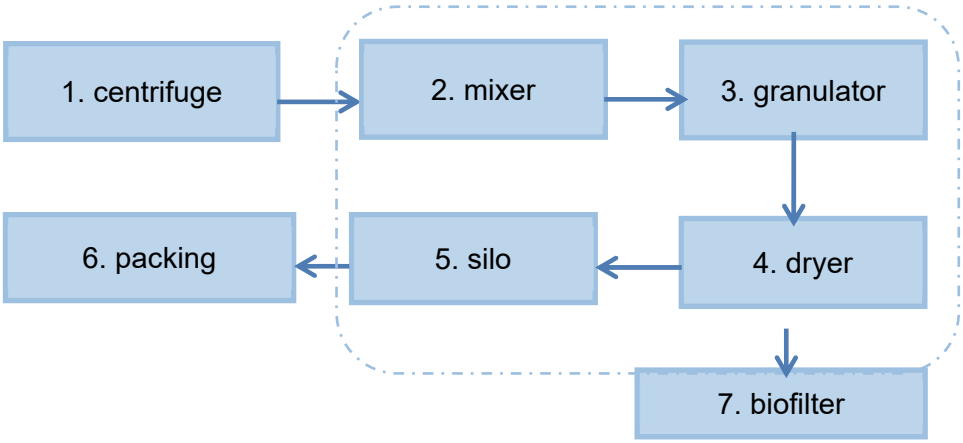

Fig. 2. Block scheme of granulated fertilizer production; Source: own elaboration

Fermented and mechanically dewatered, with a filter press or a centrifuge (1), sewage sludge is gravitationally fed onto a belt conveyor, which transports it to the mixer (2). At the same time, screw conveyors transport proper doses of other components of the granulate: lime, microcrystalline cellulose and dolomite from three separate silos directly to the same mixer. The components are transported to the silos pneumatically from road tankers equipped with compressors.

When the components are mixed in the mixer, a chemical reaction between sewage sludge and lime occurs. From the mixer the product is gravitationally fed into the granulator (3). After granulating, the produced granules of dry matter content of approximately 40-45% are transported to the dryer (4), where, at the temperature 50-80°C they are desiccated until they reach dry matter content of approximately 75-80%. As a result of the reaction, large quantity of ammonia is released, which, together with odours, is exhausted to the biofilter (7). The granules, after desiccation in the dryer, are taken to the silo (5) to cool them before bagger packaging (6). After packaging the fertilizer is stored.

3. Method

The assessment of eco-innovative fertilizer production technology was carried out using the Life Cycle Assessment (LCA) technique, which is the most acceptable method for assessing environmental impact due to the holistic approach, although its complexity is a certain limitation (Kleiber 2011, Heijungs & Guinée, 2012). This technique is known and appreciated by scientific centres around the world (Burchart-Korol et al. 2017a, Burchart-Korol et al. 2017b, Hollberg et al. 2020, Jullien et al. 2019, Morales et al. 2019, Khoo et al. 2019, Zhang et al. 2019, Chen et al. 2019, Fiala et al. 2020, Dal Pozzo et al. 2019, Guinee (Ed.) 2002, Curran (Ed.) 2012, Warshay et al. 2017, Di Maria et al. 2018, Velandia Vargas et al. 2019, Croft et al. 2018). It is also promoted for use by political centres (Federal LCA Commons 2019, EPA 2019, Recommendation 2013/179/EU). The LCA method is a valuable environmental impact assessment tool also applicable in the field of wastewater treatment (Guest et al. 2009, EPA, 2014, Machado et al. 2007, Mouri et al. 2013, Garrido-Baserba et al. 2014, Pintilie et al. 2016, Zawartka 2016).

The LCA collects data and assesses its environmental impact for the analysed product system. The product system is the whole of processes that describe the subject of the study. The quantitative effect of the product system is the so-called functional unit (FU), which is the reference unit in the analysis. According to the methodology (EN ISO 14040: 2006, EN ISO 14044: 2006) LCA analysis is carried out within four stages:

1. Determining the purpose and scope of research,
2. Inventory analysis (Life Cycle Inventory – LCI),
3. Impact Assessment (Life Cycle Impact Assessment – LCIA),
4. Interpretation.

Determining the purpose and scope clearly defines the subject of the study, indicating the product system, its boundaries, as well as the functional unit. LCI collects input and output data describing the product system. Within this stage, calculations are also performed to determine them. Impact Assessment transforms the results of the LCI stage into a unit of impact categories under consideration. Impact categories are selected environmental problems considered in the analysis. The LCIA stage is the heart of the LCA analysis, as it allows us to determine to what extent the product system affects a specific environmental problem. In practice, by entering the LCIA stage, the appropriate method is chosen that guides the user through this stage. On the other hand, conclusions, restrictions and recommendations are formulated as part of the interpretation stage.

The subject analysis was carried out as a comparative analysis, for which, according to the guidelines, system boundaries as well as the functional unit are

required to match each other. As part of the research, four cases of mineral-organic fertilizer production technology were compared, which were developed at the Central Mining Institute at the Department of Water Protection. The analysis aims to indicate which technological variant is the most environmentally friendly so that it could be developed in the future and eventually introduced to the fertilizer market. Environmentally friendly should be understood as having the least negative impact on the environment. 1 Mg of fertilizer product was selected as the functional unit.

Material and Energy Flow Analysis – MEFA was used to carry out the LCI stage. MEFA allows establishing an inventory for LCA (Korol et al. 2016, Burchart-Korol et al. 2013, Golak et al. 2011). MEFA collates the flow of materials as well as energy for the analysed system, thus helping to achieve high levels of efficiency. Sankey diagrams are often used to illustrate MEFA. The arrow thickness indicates the size of the material/energy flow. This allows locating particularly large streams, which in turn allows system modification and reduction of energy and materials consumption, and, consequently, also reduction of pollutant emissions (Korol et al. 2016). The MEFA performed for the purposes of this analysis was carried out in the Umberto NXT Universal program.

The method used during the Impact Assessment stage was the ReCiPe 2016 method, both ReCiPe Midpoint and Endpoint (Huijbregts et al. 2016). This method allows the assessment of the environmental impact of the analysed product systems within 18 impact categories, which are then grouped into three damage categories to finally express the overall environmental burden in the form of the so-called ecopoints (Pt). One ecopoint, in turn, expresses the thousandth part of the damage caused by one inhabitant of Europe during a year (Huijbregts et al. 2016, RIVM 2018).

4. Results and discussion

The MEFA analysis was carried out for four alternative solutions for the production of organic and mineral fertilizers. The flow of materials and energy for each of the options is shown in Fig. 3 and Fig. 4. For each production process, the process substrates are located on the left, and the resulting products on the right. This collation also constitutes the results of the LCI stage as input data for the life cycle impact assessment (LCIA).

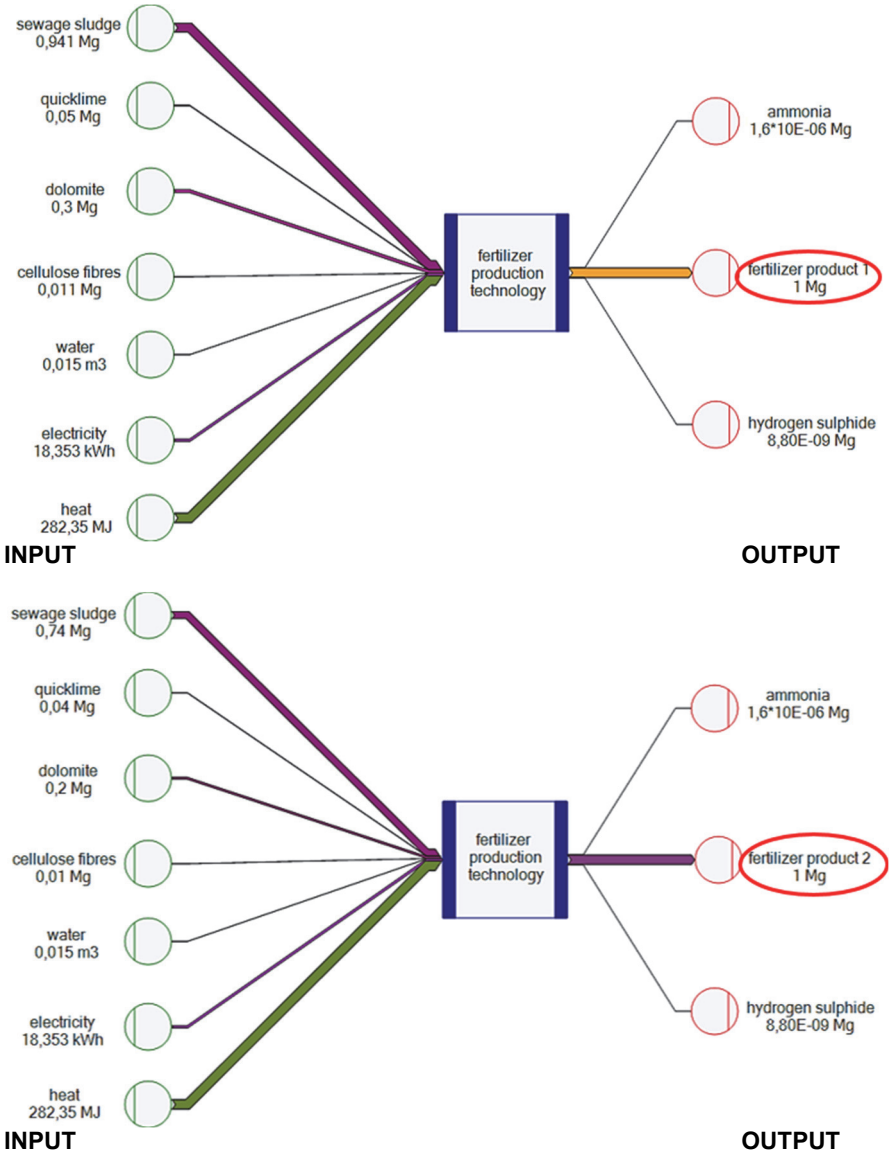

Fig. 3. Material and Energy Flow Analysis (MEFA) of production technology of fertilizer no. 1-2; Source: own elaboration in Umberto NXT Universal

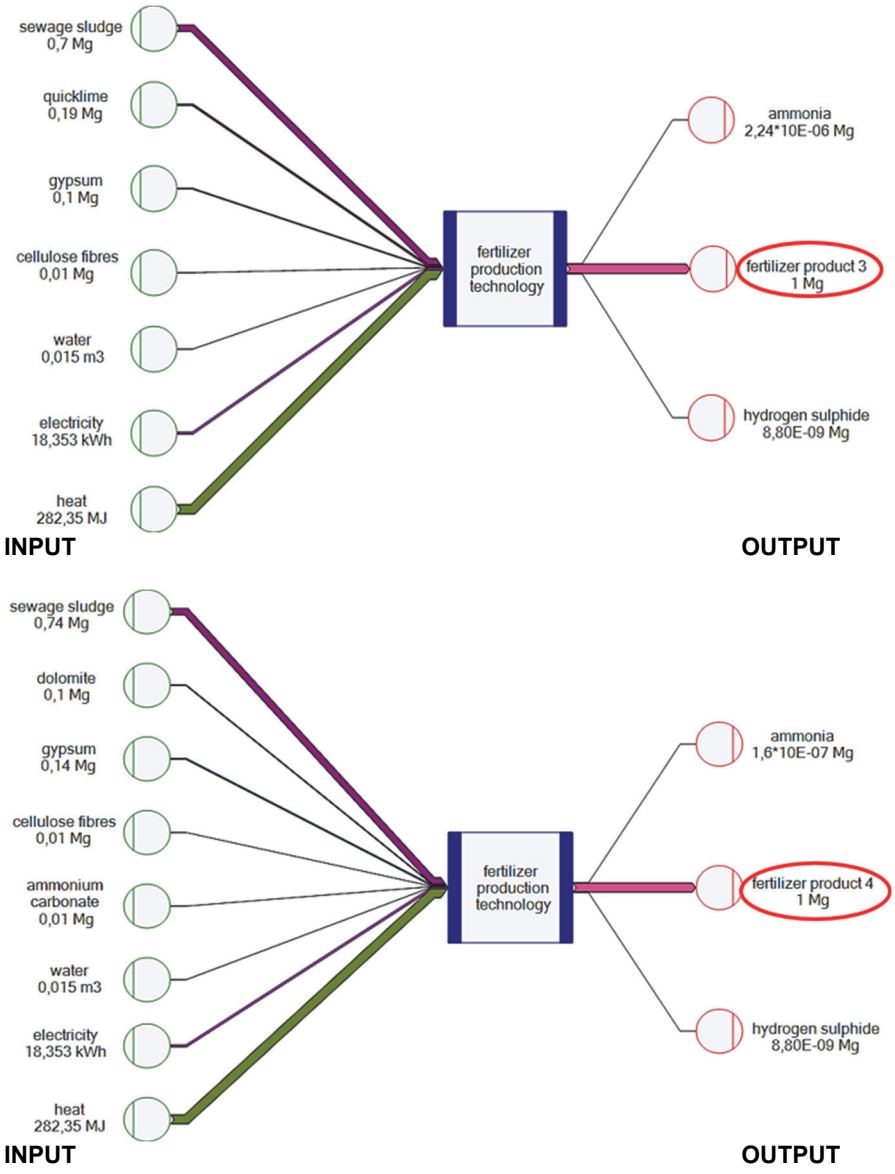

Fig. 4. Material and Energy Flow Analysis (MEFA) of production technology of fertilizer no. 3-4; Source: own elaboration in Umberto NXT Universal

Each of the fertilizer production options considered has the largest mass and energy flow for the sewage sludge used and for heat consumption for the drying process. For each of the analysed alternatives, the amount of heat used is the same. Consequently, there is no less environmental burden resulting from heat consumption for any production technology. In the case of sewage sludge, the thicker arrow in Fig. 3 and Fig.4 means a more environmentally friendly solution, which results from the fact that the sludge is waste which in this system finds useful management. This premise is part of the concepts of the circular economy promoted by the European Union (Circular Economy 2019). According to it, whenever possible, waste should be recycled to minimize the extraction of raw materials from the environment. Therefore, comparing the analysed solutions of the fertilizer production process, the most advantageous option in the field of effective use of sewage sludge is proposal No. 1.

Turning to an actual assessment of the environmental effects of fertilizer production technology presenting the impact on subsequent environmental problems, the results obtained are summarized in Tables 1 and Fig 5-9.

In terms of impact on global warming, the production of fertilizer product No. 4 is the most environmentally friendly. This product is also beneficial in the case of terrestrial acidification or fossil resource scarcity. In the case of marine eutrophication, freshwater and marine ecotoxicity, human non-carcinogenic toxicity, mineral resource scarcity, as well as water consumption, it shows the greatest environmental burden. In turn, the most beneficial fertilizer with regard to the impact on marine eutrophisation is product No. 1. This fertilizer, in turn, generates the largest environmental effect in relation to ionizing radiation, freshwater eutrophisation, or land use. The most environmentally friendly fertilizer in the field of fine particular matter formation, freshwater and marine eutrophication, terrestrial, freshwater as well as marine ecotoxicity, human cancerogenic and non-cancerogenic toxicity, land use and mineral resource scarcity is fertilizer product No. 2. For the largest number of categories, the product Fertilizer No. 3 has the most adverse effect. These categories are: global warming, stratospheric ozone depletion, ozone formation (in terms of impact on both human health and terrestrial ecosystems), fine particular matter formation, terrestrial acidification, terrestrial ecotoxicity, human carcinogenic toxicity and fossil resource scarcity.

Table 1. Impact category indices for fertilizer production technology per functional unit ($kg_{fertilizer\ product}$) – characterization stage according to ReCiPe 2016 Midpoint H/H

Impact category	Unit	Product no.1	Product no.2	Product no.3	Product no.4
Global warming	kg CO_{2eq}	1,16E-01	9,90E-02	2,69E-01	6,38E-02
Stratospheric ozone depletion	kg $CFC11_{eq}$	2,70E-08	2,29E-08	4,18E-08	2,17E-08
Ionizing radiation	kBq $Co\text{-}60_{eq}$	6,15E-02	5,56E-02	5,63E-02	5,64E-02
Ozone formation, Human health	kg NO_{Xeq}	1,67E-04	1,40E-04	2,29E-04	1,25E-04
Fine particulate matter formation	kg $PM2.5_{eq}$	1,10E-04	9,36E-05	1,49E-04	9,77E-05
Ozone formation, Terrestrial ecosystems	kg NO_{Xeq}	1,70E-04	1,43E-04	2,34E-04	1,27E-04
Terrestrial acidification	kg SO_{2eq}	2,74E-04	2,39E-04	3,70E-04	2,35E-04
Freshwater eutrophication	kg P_{eq}	3,71E-05	3,45E-05	3,59E-05	3,63E-05
Marine eutrophication	kg N_{eq}	3,32E-06	3,06E-06	3,19E-06	2,51E-05
Terrestrial ecotoxicity	kg 1,4-DCB	2,26E-01	1,88E-01	4,50E-01	2,02E-01
Freshwater ecotoxicity	kg 1,4-DCB	1,94E-03	1,75E-03	1,85E-03	2,04E-03
Marine ecotoxicity	kg 1,4-DCB	2,79E-03	2,51E-03	2,83E-03	2,90E-03
Human carcinogenic toxicity	kg 1,4-DCB	2,87E-03	2,59E-03	2,91E-03	2,70E-03
Human non-carcinogenic toxicity	kg 1,4-DCB	5,52E-02	4,97E-02	5,51E-02	5,90E-02
Land use	$m^2a\ crop_{eq}$	6,47E-03	5,86E-03	5,88E-03	5,99E-03
Mineral resource scarcity	kg Cu_{eq}	3,78E-04	3,39E-04	6,35E-04	7,78E-04
Fossil resource scarcity	kg oil_{eq}	2,31E-02	2,06E-02	3,77E-02	2,00E-02
Water consumption	m^3	5,41E-03	5,14E-03	5,25E-03	5,44E-03

(Units: kg CO_{2eq} – kilograms of carbon dioxide equivalents, kg $CFC\text{-}11_{eq}$ – kilograms of trichlorofluoromethane equivalents, kg $Co\text{-}60_{eq}$ – kilograms of cobalt-60 equivalents, kg NO_{Xeq} – kilograms of oxides of nitrogen equivalents, kg $PM2.5_{eq}$ – kilograms of particulate matter 2.5 micrometer equivalents, kg SO_{2eq} – kilograms of sulfur dioxide equivalents, kg P_{eq} – kilograms of phosphorus equivalents, kg $N_{eq,}$ – kilograms of nitrogen equivalents, kg 1,4-DCB – kilograms of 1,4 dichlorobenzene equivalents, $m^2a\ crop_{eq}$ – square meters x years of agricultural land use equivalents, kg Cu_{eq} – kilograms of copper equivalents, kg oil_{eq} – kilograms of oil equivalents, m^3 – cubic meters of freshwater)

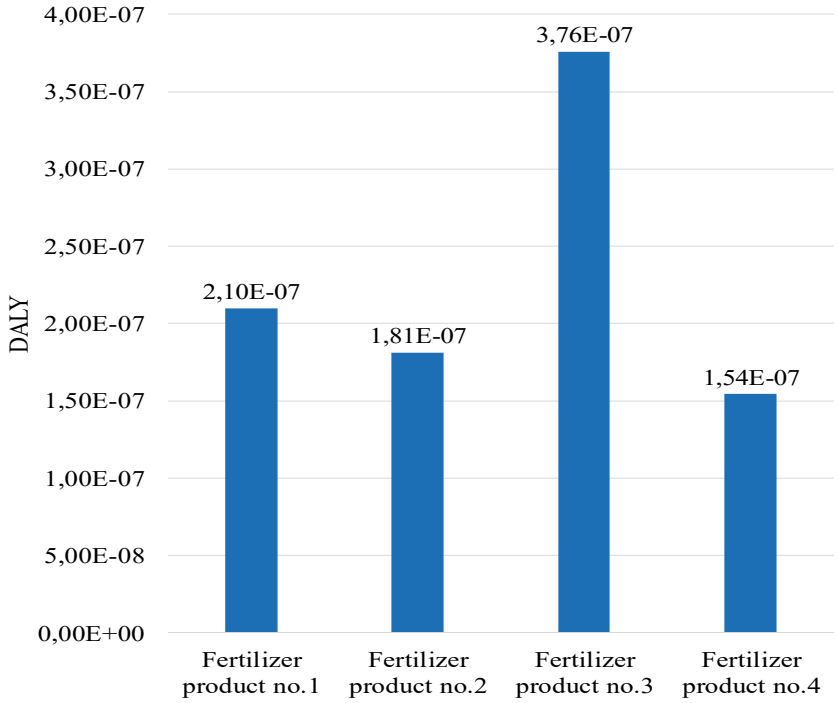

Fig. 5. Human health category indices for fertilizer production technology per functional unit ($kg_{fertilizer\ product}$) – characterization stage according to ReCiPe 2016 Endpoint H/A (Unit: DALY express the sum of shortened years of human life and years of reduced quality as a result of disability)

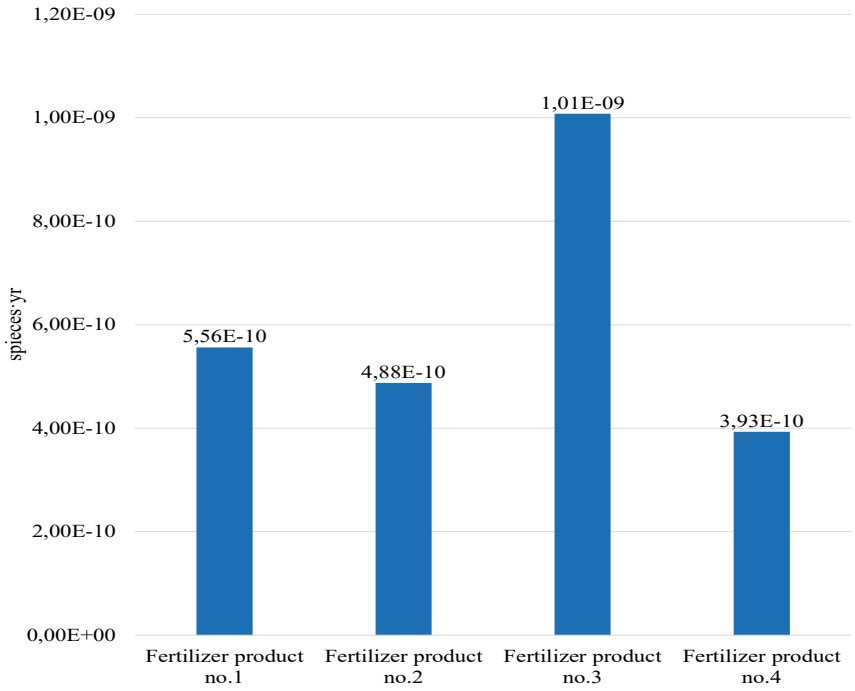

Fig. 6. Ecosystems category indices for fertilizer production technology per functional unit ($kg_{fertilizer\ product}$) – characterization stage according to ReCiPe 2016 Endpoint H/A (Unit: species · yr express loss of species throughout the year)

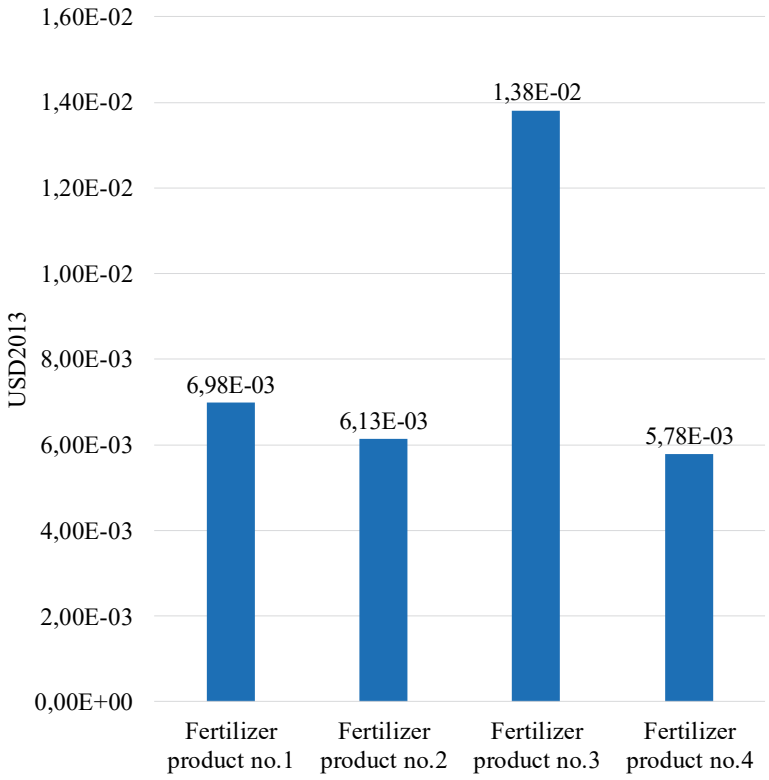

Fig. 7. Resources category indices for fertilizer production technology per functional unit ($kg_{fertilizer\ product}$) – characterization stage according to ReCiPe 2016 Endpoint H/A (Unit: USD2013 – dollars understood as an increase in costs as a result of the need to obtain raw materials from hard-to-reach deposits as a result of using resources from readily available deposits)

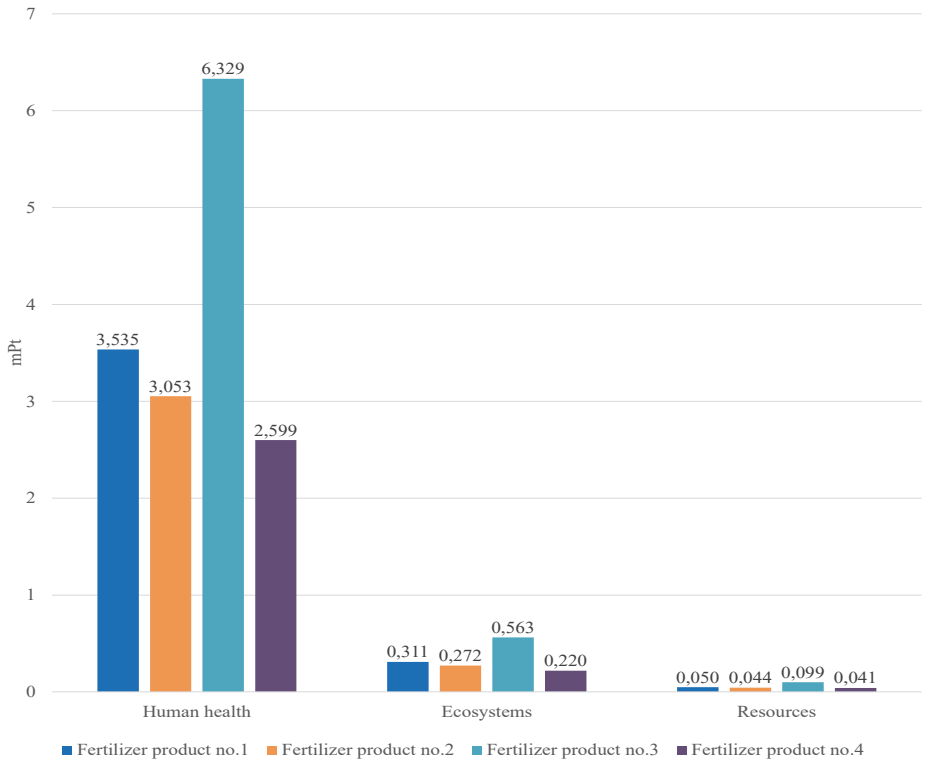

Fig. 8. Damage category indices for fertilizer production technology per functional unit ($kg_{fertizer\ product}$) – weighing stage according to ReCiPe 2016 Endpoint H/A (Unit: mPt – miliekopoint understood as a millionth of the annual environmental damage caused by one inhabitant)

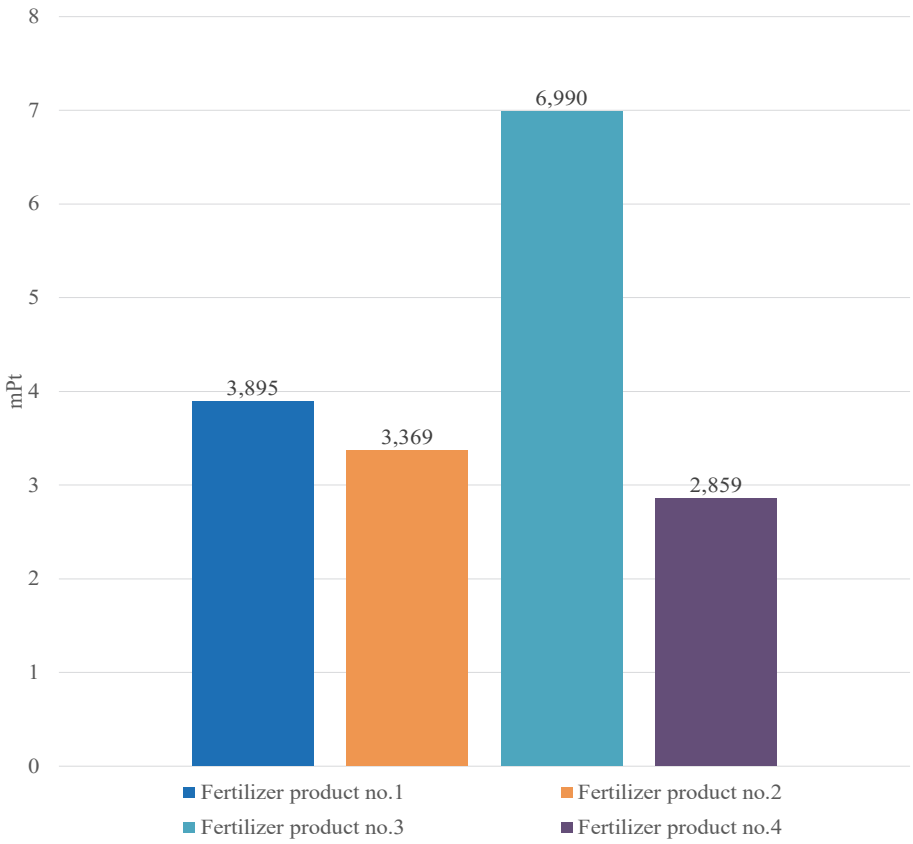

Fig. 9. Total environmental burden for fertilizer production technology per functional unit ($kg_{fertizer\ product}$) – weighing stage according to ReCiPe 2016 Endpoint H/A (Unit: mPt – miliekopoint understood as a millionth of the annual environmental damage caused by one inhabitant)

In the next step, the impact categories were grouped into three damage categories, i.e. human health, ecosystems and resources. Impact category units were converted into general damage category units and then added up. As a result, fertilizer product No. 3 proved to be the most adverse solution in terms of impact on both human health, ecosystems and resources. In turn, the most advantageous solution turned out to be fertilizer product No. 4, which showed the lowest environmental load for each category of damage analysed. After converting the damage category units into ecopoints, the indicator values within each product were summarized to obtain the total load attributed to the specific fertilizer. Product no. 4 was the most environmentally friendly fertilizer, with a total environmental load of 2.859 mPt/$kg_{fretilizer\ product}$. This value is almost two and a half times lower than the value attributed to fertilizer product No. 3, which turned out to be the most environmentally friendly fertilizer. Its total environmental effect was as much as 6.990 mPt/$kg_{fretilizer\ product}$.

With a view to comparing the results obtained with scientific literature data characterizing the fertilizers available on the market, a literature review was carried out. In order for the results of the research presented in this paper to be compared to the results of analyses carried out for other fertilizer products, it is necessary that the assumptions are consistent. The same functional unit, system boundaries and LCIA method are required. Detailed guidelines in this respect are included in EN ISO 14044 (2006). Among the publications, it is problematic to find items presenting the environmental effects of fertilizer products that collectively meet the listed requirements. It is also recommended that the fertilizer be of the same type, and therefore mineral-organic.

J. Lammel (2000) focused his research on mineral fertilizers (urea and ammonium nitrate fertilizers). He led the system boundaries in such a way that it covered both the production process and the use of products. 1 Mg of nitrogen was selected as the functional unit. Consequently, the different functional unit included in the presented paper and in (Lammel 2000) makes it impossible to compare the results. In addition, a fertilizer that is of a different type than the product presented in this paper is analysed.

R. Charles et al. (2006) analysed the wheat production system for bread production, taking into account emissions from fields, but also the production and transport of fertilizers. In this study the intensity of nitrogen, phosphorus and potassium fertilization was optimized using LCA analysis. 1 ha of land, 1 Mg of wheat produced and 1 Mg of wheat containing 13% protein was selected as the functional unit. Various assumptions adopted by the authors in relation to this paper also in this case result in the inability to compare the results.

In turn, T. Nemecek (2011) assessed the impact of agriculture using fertilizers on the natural environment. The system boundaries included both the production process and the use of fertilizers. The functional unit stood for 1 kg of dry matter of cultivated product per 1 ha of land within one year. As a result, a different functional unit makes it impossible to compare the test results with the subject analysis.

However, in the case of Quirós et al. (2015), the impact on the environment of fertilizers was studied, for which the system boundaries included the stage of production, transport to their place of application and cultivation of plants on fertilized land. ReCiPe was chosen as the method for the LCIA stage. Therefore, if the results were presented as unit processes, i.e. listing the environmental effects for the production stage and assuming that the functional unit would correspond to the size selected for analysis presented in this paper, it would be possible to compare the results. Unfortunately, the results of the analysis were not presented as unit processes by the authors. In addition, the functional unit accepted for analysis in the publication is 1 m^2 of fertilized soil. Therefore, it is also a unit different from 1 kg of fertilizer product, the unit which was selected for the purpose of conducting the analysis presented in this paper. Therefore, it is not possible to compare the results to the results of the research presented in (Quirós et al. 2015).

Another publication presenting the results of LCA analyses for fertilizers is Vera-Acevedo et al. 2016. Unfortunately, the assumptions adopted for analysis in that paper also prevent comparison of the test results. In Vera-Acevedo et al. 2016, 1 kg of coffee crops grown on soil fertilized with the analysed fertilizer product was selected as a functional unit. On the other hand, the system boundaries do not take into account the environmental effects associated with growing vegetation in fertilized areas in that paper, which excludes the possibility of compiling results.

In the case of Chen et al. (2018), life cycle assessment of potash fertilizer production in China is presented. The authors selected 1 Mg K_2O production (1.67 KCl fertilizer with a K_2O content of 60.03%) as the functional unit, and the system boundaries covered only the fertilizer production stage. ReCiPe 2008 was used as the method of assessing the life cycle impact on the environment. Therefore, in terms of the direct requirements listed in EN ISO 14044 regarding the possibility of comparing the results of LCA analyses, they are met. Solely different versions of the ReCiPe method used in the calculations may raise doubts (Chen et al. 2018 – ReCiPe 2008, this work – ReCiPe 2016). Both versions, though one older and the other newer, are based on the same principles. The differences are associated with impact categories which do not always overlap or units assigned to them. It is therefore possible to combine results, but to a limited

extent. The problem, however, may be the fact that the subject of the study is potassium fertilizer, which does not belong to the group of mineral-organic fertilizers. Therefore, its composition, and thus the environmental effect associated with obtaining other fertilizer components will differ from the one analysed in this paper. For illustrative purposes, however, Table 2 summarizes the results.

In the case of the global warming fertilizer category, product No.3 significantly exceeds the range of values corresponding to the fertilizer described by W. Chen et al. (2018). Product No.4 assumed a value below the range, while fertilizers No.1 and 2 fitted in with the area defined in the literature. Regarding stratospheric ozone depletion and fine particular matter formation, each of the fertilizer products analysed in this paper has a greater negative impact in relation to potassium fertilizer. For terrestrial acidification and marine eutrophication, only product No. 3 exceeds the range of values specified in Chen et al. (2018). The other values correspond to the data area assigned to the potassium fertilizer. In the case of fossil resource scarcity, the range specified by W. Chen et al. (2018) is exceeded by fertilizers No.1 and 3. On the other hand, for water consumption, all data characterizing the analysed fertilizer products fall into the range of values corresponding to potassium fertilizer.

As it has already been mentioned, due to the different types of compared fertilizers, the presented statement is for reference only and cannot be the basis for taking specific environmental decisions.

Table 2. Summary of LCA analysis results for the production stage of fertilizer No. 4 for potassium fertilizer, according to Chen et al. 2018

Impact category	Unit	Fertilizer product no.1	Fertilizer product no.2	Fertilizer product no.3	Fertilizer product no.4	Range of values according to Chen et al.2018 after conversion into the functional unit taken into account in this application (FU=1 kg of fertiliser)	
						min	max
Global warming	kg CO2 eq	1,16E-01	9,90E-02	2,69E-01	6,38E-02	8,44E-02	1,53E-01
Stratospheric ozone depletion	kg CFC11 eq	2,70E-08	2,29E-08	4,18E-08	2,17E-08	2,03E-11	7,78E-11
Fine particulate matter formation	kg PM2.5 eq	1,10E-04	9,36E-05	1,49E-04	9,77E-05	2,19E-05	4,86E-05
Terrestrial acidification	kg SO2 eq	2,74E-04	2,39E-04	3,70E-04	2,35E-04	1,29E-04	2,43E-04
Marine eutrophication	kg N eq	3,32E-06	3,06E-06	3,19E-06	2,51E-05	2,21E-06	5,97E-06
Fossil resource scarcity	kg oil eq	2,31E-02	2,06E-02	3,77E-02	2,00E-02	1,11E-02	2,13E-02
Water consumption	m3	5,41E-03	5,14E-03	5,25E-03	5,44E-03	3,99E-03	5,94E-03

5. Conclusions

After converting the results of the analyses into the same unit (mPt), it was observed that for each damage category, the environmental burden of fertiliser product 4 is the lowest compared to other products. Consequently, the total environmental load of product 4 is also the lowest, and this results in fertilizer No. 4 is the most environmentally friendly among the products considered. This product is also consistent with the definition of eco-innovation adopted by the European Commission as 'innovations aimed at significant and visible progress towards achieving the goal of sustainable development, by limiting the impact on the environment or achieving greater efficiency and responsible use of natural resources, including energy'(European Commission 2007). In this fertilizer, the addition of quicklime was completely abandoned and replaced with gypsum, and as a result the greenhouse effect was significantly reduced. The use of ammonium carbonate in product No. 4 significantly increased its fertilizing properties in terms of nitrogen content. However, this significantly affected the increase in the impact on eutrophication, which is an unfavourable phenomenon for the environment. The addition of ammonium carbonate increased the requirement for easily absorbable nitrogen to the environment. Considering the collected test results, it can be concluded that the most environmentally beneficial product should contain sewage sludge, cellulose, dolomite flour and gypsum. The direction of further product optimization may be the abandonment of dolomite flour due to the fact that grinding dolomite rock is an energy-intensive process that also has a negative impact on the environment.

Refrences

Bagreev, A., Bashkova, S., Locke, D.C., Bandosz, T.J. (2001). Sewage sludge-derived materials as efficient adsorbents for removal of hydrogen sulfide. *Environmental Science & Technology, 35*, 1537-1543.

Bartoszczuk, P. (2016). Ekoinnowacje w gospodarce wodnej, *Gospodarka w praktyce i teorii [Eco-innovations in water management, Economy in practice and theory], 44,* 10, DOI: 10.18778/1429-3730.44.01 (in Polish)

Biegańska, M. (2010). Dyrektywa 91/271/EWG a prawo krajowe [Directive 91/271/EEC vs. national law], *Wodociągi i Kanalizacja, 11*(81), 24-29.

Burchart-Korol D. (2013). Life cycle assessment of steel production in Poland: a case study, *Journal of Cleaner Production, 54*, 235-243.

Burchart-Korol, D., Zawartka, P., Bondaruk, J. (2017a). Environmental assessment of wastewater treatment plant under Polish conditions. Part 1. Identification and data inventory in the life cycle of wastewater treatment plant, *Chemical Industry, 96*(10), 2081-2086, DOI: 10.15199/62.2017.10.9 (in Polish)

Burchart-Korol, D., Zawartka, P., Bondaruk, J. (2017b). Environmental assessment of wastewater treatment plant under Polish conditions. Part 2. Life cycle assessment of wastewater treatment plant, *Chemical Industry 96*(11), 2247-2252, DOI: 10.15199/62.2017.11.6 (in Polish)

Carrillo-Hermosilla, J., del Rio, P., Könnölä, T. (2010). Diversity of eco-innovations: reflections from selected case studies. *Journal of Cleaner Production, 18*(10-11)*,* 1073-1083

Charles, R., Jolliet, O., Gaillard, G., Pellet, D. (2006). Environmental analysis of intensity level in wheat crop production using life cycle assessment. Agric. *Ecosystems Environ., 113*, 216-225.

Chen, Z., Huang, L. (2019). Application review of LCA (Life Cycle Assessment) in circular economy: From the perspective of PSS (Product Service System), *Procedia CIRP, 83,* 210-217, DOI: https://doi.org/10.1016/j.procir.2019.04.141

Chen, W., Geng, Y., Hong, J., Yang, D., Ma, X. (2018). Life cycle assessment of potash fertilizer production in China, *Resources, Conservation & Recycling 138,* 238-245, DOI: https://doi.org/10.1016/j.resconrec.2018.07.028

Cheng, C.C., Shiu, E.C. (2012). Validation of a proposed instrument for measuring eco-innovation: An implementation perspective, *Technovation, 32*(6), 329-344.

Circular Economy (2019). https://ec.europa.eu/environment/circulareconomy/index-en.htm (21.10.2019)

Croft, J., Engelbrecht, S., Ladenika, A.O., MacGregor, O.S., Maepa, M., Bodunrin, M.O., Burman, N.W., Goga, T., Harding, K.G. (2018). Review: the availability of life-cycle studies in Sweden, *The International Journal of Life Cycle Assessment, 24*(1), 6-11. DOI: https://doi.org/10.1007/s11367-018-1510-4

Curran, M.A. (2012). *Life Cycle Assessment Handbook: A Guide for Environmentally Sustainable Products*, Scrivener Publishing, DOI:10.1002/9781118528372

Dal Pozzo, A., Carabba, L., Bignozzi, M.C., Tugnoli, A. (2019). Life cycle assessment of a geopolymer mixture for fireproofing applications, *The International Journal of Life cycle Assessment, 24*(10), 1743-1757, DOI: https://doi.org/10.1007/s11367-019-01603-z

Di Maria, A., Salman, M., Dubois, M., Van Acker, K. (2018). Life cycle assessment to evaluate the environmental performance of new construction material from stainless steel slag, *The International Journal of Life Cycle Assessment*, *23*(11), 2091-2109, DOI: https://doi.org/10.1007/s11367-018-1440-1

Dziedzic, S., Woźniak, L. (2013). *Ekoinnowacje w gospodarce żywnościowej – model rozwoju dla województwa podkarpackiego* [Eco-innovations in the food economy - a development model for the Podkarpackie Voivodeship], Politechnika Rzeszowska, Rzeszów, 1-140.

EN ISO 14040 (2006). Environmental management – Life cycle assessment – Principles and framework

EN ISO 14044 (2006). Environmental management – Life cycle assessment – Requirements and guidelines

EPA (2014): *Environmental and Cost Life Cycle Assessment of Disinfection Options for Municipal Wastewater Treatment*, United States Environmental Protection Agency.

EPA (2019). *Design for the Environment Life-Cycle Assessments*, United States Environmental Protection Agency, https://www.epa.gov/saferchoice/design-environment-life-cycle-assessments (date of access: 17.10.2019)

EUR-Lex (1991). *Council Directive 91/271/EEC of 21 May 1991 concerning urban waste water treatment,* http://eur-lex.europa.eu, (date of access 29.11.2019)

EUROPE 2020. A strategy for smart, sustainable and inclusive growth, COM(2010) 2020 final, Bruksela, 03.03.2010

European Commission (2007). *Competitiveness and Innovation Framework Programme (2007 to 2013),* Brussels

European Commission (2011). *Innovation for a sustainable Future – The Eco-innovation Action Plan (Eco-AP),* Brussels, COM (2011) 899 final, 2.

Federal LCA Commons (2019). Federal LCA Commons, https://www.lcacommons.gov/(date of access: 17.10.2019)

Fiala, M., Marveggio, D., Viganò, R., Damartini, E., Nonini, L., Gaviglio, A. (2020). LCA and wild animals: Results from wild deer culled in a northern Italy hunting district*, Journal of Cleaner Production, 244*, Article: 118667, DOI: https://doi.org/10.1016/j.jclepro.2019.118667

Garrido-Baserba, M., Molinos, M., Abelleira-Pereira, J., Fdez-Güelfo, L.A., Poch, M., Hernández-Sancho, F. (2014). Selecting sewage sludge treatment alternatives in modern wastewater treatment plants using environmental decision support systems. *Journal of Cleaner Production*. 107, DOI: 10.1016/ j.jclepro.2014.11.021.

Gawdzik, J. (2013). Mobilność wybranych metali ciężkich w osadach ściekowych (Mobility of selected heavy metals in sewage sludge). *Monografie, Studia, Rozprawy (M44).* Wydawnictwo Politechniki Świętokrzyskiej, Kielce.

Głodniok, M., Korol, J., Zawartka, P., Krawczyk, B., Deska, M. (2017). *Organic fertilizer and method for obtaining it. 420420.* Polish Pattent Office [in Polish]

Golak, S., Burchart-Korol, D., Czaplicka-Kolarz, K., Wieczorek, T. (2011). Application of Neural Network for the Prediction of Eco-efficiency, *Advances in Neural Networks, 6677*, 380-387.

Guest, J.S., Skerlos, S.J., Barnard, J.L., Beck, M.B., Daigger, G.T., Hilger, H., Jackson, S.J., Karvazy, K., Kelly, L., Macpherson, L., Mihelcic, J.R., Pramanik, A., Raskin, L., Van Loosdrecht, M.C.M., Yeh, D., Love, N.G. (2009). A new planning and design paradigm to achieve sustainable resource recovery from wastewater. *Environmental Science and Technology, 43*(16), 6121-6125.

Guinee, J.B. (ed.) (2002). *Handbook on Life Cycle Assessment. Operational Guide to the ISO Standards,* Springer Netherlands, DOI: 10.1007/0-306-48055-7

Heim, A., (2012). Granulation – still an important process. *Chemik 66*(5)*,* 358-359.

Hollberg, A., Genova, G., Habert, G. (2020). Evaluation of BIM-based LCA results for building design, *Automation in Construction, 109,* Article: 102972, DOI: https://doi.org/10.1016/j.autcon.2019.102972

Heijungs, R. & Guinée, J.B. (2012). An Overview of the Life Cycle Assessment Method – Past, Present, and Future. In: Curran M.A. (red.) *Life Cycle Assessment Handbook; A Guide for Environmentally Sustainable Products.* Beverly: Scrivener Publishing. 15-42.

Huijbregts, M.A.J., Steinmann, Z.J.N., Elshout, P.M.F., Stam, G., Verones, F., Vieira, M.D.M., Hollander, A., Zijp, M., van Zelm, R. (2016). *ReCiPe, 1.1. A harmonized life cycle impact assessment method at midpoint and endpoint level. Report I: Characterization.* RIVM Report 2016-0104a. National Institute for Public Health and the Environment of Netherlands

ISO/IEC 31010:2009 (2009). International standard. Risk management - Risk assessment techniques.

Jasiński, A.H. (1997). *Innowacje i polityka innowacyjna [Innovation and innovation policy],* Wydawnictwo Uniwersytetu w Białymstoku, Białystok, 12.

Jullien, A., Proust, C., Yazoghli-Marzouk, (2019). LCA of alternative granular materials – Assessment of ecotoxicity and toxicity for road case studies, *Construction and Building Materials,* 227, Article: 116737, DOI: https://doi.org/10.1016/j.conbuildmat.2019.116737

Kemp, R., Pearson, P. (2008). *Final report MEI project about measuring eco-innovation,* Maastricht.

Khoo, H.H., Eufrasio-Espinosa, R.M., Koh, L.S.C., Sharratt, P.N., Isoni, V. (2019). Sustainability assessment of biorefinery production chains: A combined LCA-supply chain approach, *Journal of Cleaner Production, 235,* 1116-1137, DOI: https://doi.org/10.1016/j.jclepro.2019.07.007

Kleiber, M., (red.) (2011). *Ekoefektywność technologii [Eco-efficiency of technology],* Główny Instytut Górnictwa, ISBN 978-83-7789-050-9

Korol, J., Kruczek, M., Pichlak, M. (2016). Material and Energy Flow Analysis (MEFA) – first step in eco-innovation approach to assessment of steel production, *METALURGIJA 55*(4), 818-820.

Kulikowski, Ł., Piętka, P., Kiepurski, J. (2019). Przetwarzanie osadów ściekowych w nawóz mineralno-organiczny na platformie mobilnej [Processing of sewage sludge into mineral-organic fertilizer on a mobile platform], *Inżynieria Ekologiczna (Ecological Engineering), 20*(1), 38-44, DOI: https://doi.org/10.12912/23920629/106205

Lammel, J. (2000). *Environmental aspects of fertilizer production and use – consequences for fertilizer types and use.* IFA Production and International Trade Conf., October 17-19, Shanghai, China.

Little, A.D. (2005). *How leading companies are using sustainability-driven innovation to win tomorrow's customers,* Innovation High Ground Report

Liu, Y., Kong, S., Li, Y., Zeng, H. (2009). Novel technology for sewage sludge utilization: Preparation of amino acids chelated trace elements (AACTE) fertilizer. *Journal of Hazardous Materials, 171*, 1159-1167.

Machado, A.P., Urbano, L., Brito, A.G., Janknecht, P., Salas, I.L., Nagueira, R. (2007). Life cycle assessment of wastewater treatment options for small and decentralized communities. *Water Science and Technology, 56*(3), 15-22.

Masłoń, A. (2015). Surowiec z osadów [Raw material from sewage sludge]. *Kierunek WODKAN*, *3*(613), 60-67.

Morales, M., Moraga, G., Kirchheim, A.P., Passuello, A. (2019). Regionalized inventory data in LCA of public housing: A comparison between two conventional typologies in southern Brazil, *Journal of Cleaner Production, 238,* Article: 117869, DOI: https://doi.org/10.1016/j.jclepro.2019.117869

Mouri, G., Takizawa, S., Fukushi, K., Oki, T. (2013). Estimation of the effects of chemically-enhanced treatment of urban sewage system based on life-cycle management, *Sustainable Cities and Society, 9,* 23-31.

National Waste Management Plan 2022, Annex to the Resolution No 88 of the Council of Ministers of 1 July 2016 (item 784), Warsaw 2016.

Naukawpolsce.pl (2017). *Innowacyjna technologia zamieni osady ściekowe w nawóz, który także nawodni glebę [Innovative technology will turn sewage sludge into fertilizer that also irrigates the soil],* http://naukawpolsce.pap.pl/aktualnosci/news%2C414037%2Cinnowacyjna-technologia-zamieni-osady-sciekowe-w-nawoz-ktory-takze-nawodni-glebe.html, date of access: 03.12.2019

Nemecek, T., Elie, O.H., Dubois, D., Gaillard, G., Schaller, B., Chervet, A. (2011). Life cycle assessment of Swiss farming systems: II. Extensive and intensive production. *Agricultural Systems, 104,* 233-245.

Oslo, Manual, 2008. *Guidelines for Collecting and Interpreting Innovation Data,* 3rd Edition. OECD, Eurostat, MNiSW, Warszawa, 48.

Quirós, R., Villalba, G., Gabarrell, X., Muñoz, P. (2015). Life cycle assessment of organic and mineral fertilizers in a crop sequence of cauliflower and tomato, *International Journal of Environmental Science and Technology 12*, 3299-3316, DOI: https://doi.org/10.1007/s13762-015-0756-7

Pintilie, L., Torres, C.M., Teodosiu, C., Castelles, F. (2016). Urban wastewater reclamation for industrial reuse: An LCA case study. *Journal of Cleaner Production, 139,* 1-14.

Peng, X., Liu, Y. (2016). Behind eco-innovation: Managerial environmental awareness and external resource acquisition. *Journal of Cleaner Production, 139*, 347-360.

Rauba, E. (2015). Kształtowanie gospodarki wodno-ściekowej w gminie na przykładzie gminy miejsko – wiejskiej Choroszcz Shaping water and wastewater management in the commune on the example of the urban and rural commune Choroszcz [Shaping water and wastewater management in the commune by the example of the urban and rural commune Choroszcz], *Studia i prace Wydziału Nauk Ekonomicznych i Zarządzania, 40*(2), Białystok.

Recommendation 2013/179/EU: Commission Recommendation of 9 April 2013 on the use of common methods to measure and communicate the life cycle environmental performance of products and organisations, *Official Journal of the European Union L 124, 56,* 1-210, ISSN 1977-0677, DOI:10.3000/19770677.L_2013.124.eng

Reid, A., Miedzinski, M. (2008). *Eco-innovation. Final Report for Sectoral Innovation Watch,* www.technopolis-group.com

Rennings, K. (2000). Redefining innovation – eco-innovation research and the contribution from ecological economics. *Ecological Economics, 32*(2). 319-332.

RIVM (2018). National Institute for Public Health and the Environment of Netherlands, https://www.rivm.nl/en/life-cycle-assessment-lca/downloads (date of access: 17.10.2019)

Rozporządzenie Ministra Klimatu z dnia 2 stycznia 2020 r. w sprawie katalogu odpadów [Regulation of the Minister of Climate of 2 January 2020 on the waste catalog] [Journal of Laws 2020, item 10].

Rozporządzenie Ministra Rolnictwa i Rozwoju Wsi z dnia 21 grudnia 2009 r. zmieniające rozporządzenie w sprawie wykonania niektórych przepisów ustawy o nawozach i nawożeniu [Regulation of the Minister of Agriculture and Rural Development of 21 December 2009 amending the Regulation on the implementation of certain provisions of the Act on Fertilizers and Fertilization] [Journal of Laws 2009, no 224, item 1804]

Rozporządzenie Ministra Środowiska z dnia 9 grudnia 2014 r. w sprawie katalogu odpadów [Regulation of the Minister of the Environment of December 9, 2014 regarding the waste catalog] [Journal of Laws 2014, item 1923].

Rozporządzenie Ministra Środowiska z dnia 6 lutego 2015 r. w sprawie komunalnych osadów ściekowych [Regulation of the Minister of the Environment of February 6, 2015 regarding the municipal sewage sludge] [Journal of Laws 2015, item 257].

Smuda, K. (2014). Trudny problem z osadami ściekowymi [Difficult problem with sewage sludge], Głos Pszczyński, https://www.glospszczynski.pl/ekoglos/152-trudny-problem-z-osadami-sciekowymi (access: 05.12.2019)

Urbaniec, M. (2015). Towards Sustainable Development through Eco-innovations: Drivers and Barriers in Poland, *Economics and Sociology, 8*(4), 179-190.

Ustawa z dnia 10 lipca 2007 r. o nawozach i nawożeniu [Act of 10 July 2007 on Fertilizers and Fertilization] [Journal of Laws 2020, item 726]

Velandia, Vargas, J., Falco, D.G., da Silva, Walter, A.C., Nakao, Cavaliero, C.K., Abel, Seabra, J.E. (2019). Life cycle assessment of electric vehicles and buses in Brazil: effects of local manufacturing, mass reduction, and energy consumption evolution, *Journal of Life Cycle Assessment*, *24*(10), 1878-1897, DOI: https://doi.org/10.1007/s11367-019-01615-9

Vera-Acevedo, L.D., Vélez-Henao, J.A., Marulanda-Grisales, N. (2016). Assessment of the environmental impact of three types of fertilizers on the cultivation of coffee at the Las Delicias indigenous reservation (Cauca) starting from the life cycle assessment, *Revista Facultad de Ingeniería,* Universidad de Antioquia, 80, 93-101.

Warshay, B., Brown, J.J., Sgouridis, S. (2017). Life cycle assessment of integrated seawater agriculture in the Arabian (Persian) Gulf as a potential food and aviation biofuel resource, *The International Journal of Life Cycle Assessment, 22(*7), 1017-1032 DOI: https://doi.org/10.1007/s11367-016-1215-5

Węgrzyn, G. (2013). Ekoinnowacje w Polsce na tle Krajów Unii Europejskiej [Eco-innovations in Poland against the background of European Union countries], *Ekonomia i Środowisko, 3*(46).

Woźniak, L., Ziółkowski, B., Warmińska, A., Dziedzic, S. (2008). *Przewodnik ekoinnowacji [Eco-innovation guide]. Diagnoza trendów i dobre praktyki*, Politechnika Rzeszowska, Rzeszów.

Wójcik, M., Masłoń, A. (2019). Nowe kierunki zagospodarowania komunalnych osadów ściekowych [New directions of municipal sewage sludge management], https://www.portalsamorzadowy.pl/gospodarka-komunalna/nowe-kierunki-zagospodarowania-komunalnych-osadow-sciekowych,121242.html (date of access: 30.11.2019)

Zawartka, P. (2016). *Determinanty środowiskowej oceny cyklu życia systemu zbierania, transportu i oczyszczania ścieków, [Determinants of environmental life cycle assessment of the waste water collection, transport and treatment system]* Rozprawa doktorska (PhD thesis), Główny Instytut Górnictwa, Katowice,

Zhang, Y., Yan, D., Hu, S., Guo, S. (2019). Modelling of energy consumption and carbon emission from the building construction sector in China, a process-based LCA approach, *Energy Policy, 134,* Article: 110949, DOI: https://doi.org/10.1016/j.enpol.2019.110949

Abstract

This paper presents the possibilities of waste management originating from municipal wastewater treatment through the production of mineral-organic fertilizers based on sewage sludge. The original method created for this purpose was used in the study together with the environmental assessment of this method. Therefore, the purpose of this publication is twofold. On the one hand, the first goal of the paper is to draw attention to the need to choose the appropriate method of utilization of sewage sludge, taking into account its characteristics and potentially harmful effects on the environment. The second goal of the paper is to assess the environmental impact of the selected method and demonstrate its eco-innovation.

The first part of the paper is a theoretical introduction to the issues of sewage sludge management, as well as theoretical considerations on the essence of eco-innovation. The second part of the paper presents practical issues of production and application of the organo-mineral granulated fertilizer subjected to research, while the third part – the methodology of the applied Life Cycle Analysis (LCA), including in particular the application of Material and Energy Flow Analysis (MEFA) at the Life Cycle Inventory stage. The fourth section presents the assumptions and results of the conducted research for four alternative solutions for the production of organic-mineral fertilizers. The fifth and final part summarizes the results and contains a number of conclusions and recommendations that should be considered in the context of the possibilities of further product optimization.

Keywords:
organic-mineral fertilizer, sewage sludge, Life Cycle Assessment (LCA), eco-innovation, granulate

Ocena cyklu życia eko-innowacyjnej technologii produkcji nawozu mineralno-organicznego

Streszczenie

W niniejszym artykule przedstawiono możliwości użytkowego wykorzystania odpadów z oczyszczania ścieków komunalnych, poprzez wytwarzanie nawozów mineralno-organicznych na bazie osadów ściekowych autorską metodą oraz ocenę środowiskową tej metody. Tak więc, cel niniejszej publikacji jest dwojaki. Z jednej strony, pierwszym celem artykułu jest zwrócenie uwagi na konieczność doboru odpowiedniej metody utylizacji osadów ściekowych z uwzględnieniem ich charakterystyki oraz potencjalnie szkodliwego oddziaływania na środowisko. Drugim celem artykuły jest ocena wpływu środowiskowego wybranej metody, celem wykazanie jej eko-innowacyjności.

Pierwsza część pracy stanowi wprowadzenie teoretyczne do problematyki zagospodarowania osadów ściekowych, jak również teoretyczne rozważania nad istotą eko-innowacyjności. Druga część pracy przedstawia praktyczne zagadnienia produkcji i zastosowania organo-mineral granulated fertilizer poddanego badaniom, podczas gdy trzecia – metodykę zastosowanej analizy cyklu życia LCA, w tym szczególnie zastosowania analizy Material and Energy Flow Analysis (MEFA) na etapie Life Cycle Inventory. Czwarta sekcja przedstawia założenia i wyniki prowadzonego badania dla czterech alternatywnych rozwiązań technologii produkcji nawozów organiczno-mineralnych. Część piąta i ostatnia podsumowuje wyniki i zawiera szereg wniosków i zaleceń, które należy rozważyć w kontekście możliwości dalszej optymalizacji produktu.

Słowa kluczowe:
nawóz mineralno-organiczny, osady ściekowe, ocena cyklu życia, eko-innowacje, granulat